The Determination of Geomorphologically Effective Flows for Selected Eastern Sea-Board Rivers in South Africa

THESIS
Submitted in fulfilment of the
requirements for the Degree of
DOCTOR OF PHILOSOPHY
of
RHODES UNIVERSITY

by

EVAN STEPHEN JOHN DOLLAR

November 2000

for S.M.G.

ABSTRACT

In South Africa the need to protect and manage the national water resource has led to the development of the Reserve as a basic right under the National Water Act (1998). The Ecological Reserve relates to the quality and quantity of water necessary to protect the sustainable functioning of aquatic ecosystems. The geomorphological contribution to setting the Reserve has focussed on three groups of information requirements: the spatial and temporal availability of habitat, the maintenance of substratum characteristics, and the maintenance of channel form. This thesis focusses on the second and third information requirements. The thesis has attempted to achieve this by adding value to the theoretical and applied understanding of the magnitude and frequency of channel forming discharge for selected southern African rivers. Many of the eastern sea-board rivers are strongly influenced by bed rock in the channel perimeter, and by a highly variable hydrological regime. This has resulted in characteristic channel forms, with an active channel incised into a larger macro-channel being a common feature of eastern seaboard rivers. Within the active channel inset channel benches commonly occur. This alluvial architecture is used to provide clues as to the types of flows necessary to meet the Reserve.

Three river basins are considered: the Mkomazi, Mhlathuze and Olifants. The Mkomazi is a relatively un-impacted perennial eastern-sea board river and forms the research component of the study. The Mhlathuze and Olifants rivers are highly regulated systems and form the application component of the study. Utilising synthesised daily hydrological data, bed material data, cross-sectional surveys, hydraulic data and relevant bed material transport equations, channel form was related to dominant discharge and effective discharge in an attempt to identify the magnitude and frequency of flows that can be considered to be 'effective'.

Results from the Mkomazi River indicate that no single effective discharge exists, but rather that there is a range of effective discharges in the 5-0.1% range on the 1-day daily flow duration curves that are responsible for the bulk (>80%) of the bed material transport. Only large floods (termed 'reset' discharges) with average return periods of around 20 years generate sufficient stream power and

shear stress to mobilise the entire bed. The macro-channel is thus maintained by the large 'reset' flood events, and the active channel is maintained both by the range of effective discharges and the 'reset' discharges. These are the geomorphologically 'effective' flows.

Results from the Mhlathuze River have indicated that the Goedertrouw Dam has had a considerable impact on the downstream channel morphology and bed material transport capacity and consequently the effective and dominant discharges. It has been suggested that the Mhlathuze River is now adjusting its channel geometry in sympathy with the regulated flow environment. Under present-day conditions it has been demonstrated that the total bed material load has been reduced by up to three times, but there has also been a clear change in the way in which the load has been distributed around the duration curve. Under present-day conditions, over 90% of the total bed material load is transported by the top 5% of the flows, whereas under virgin flow conditions 90% of the total bed material load was transported by the top 20% of the flows.

For the Olifants River there appears to be no relationship between the estimated bankfull discharge and any hydrological statistic. The effective discharge flow class is in the 5-0.01% range on the 1-day daily flow duration curve. It has also been pointed out that even the highest flows simulated for the Olifants River do not generate sufficient energy to mobilise the entire bed. It is useful to consider the Olifants River as being adapted to a highly variable flow regime. It is erroneous to think of one 'effective' discharge, but rather a range of effective discharges are of significance.

It has been argued that strong bed rock control and a highly variable flow regime in many southern African rivers accounts for the channel architecture, and that there is a need to develop an 'indigenous knowledge' in the management of southern African fluvial systems.

ACKNOWLEDGEMENTS

- To my supervisor Kate Rowntree for all her guidance over the last 11 years, and for teaching me much about fluvial geomorphology. Thanks for everything.

- To Denis Hughes who gave up a lot of his valuable time to assist in the hydrological modelling and bed material transport coding.

- To the Water Research Commission Steering Committee including: Steve Mitchell, Chris James, Bill Rowlston, Mark Chutter, Jackie King, Jay O'Keeffe and Jan Boelhouwers for all the useful input they had into this research.

- To all those who helped me in the field including: Kate Rowntree, Marinda Els, Anna van der Stok, Pete Illgner, Andrew Birkhead, Angelina Jordanova, Michael Dollar, Emily Cobern, Simone Meister, Mark Bantich and Ben Cobban.

- To Angelina Jordanova and Drew Birkhead for help with the hydraulics.

- To Disa Dollar and Rachel McDermott for proof reading.

- To Debbie Brody for her cartographic work.

- To all the staff of the Department of Geography at Rhodes University for all the help over the last three-and-a-half years.

- To Delana Louw for all the unsung work and the tremendous contribution that she has made to conserving South African rivers.

- To the Water Research Commission for financial support.

TABLE OF CONTENTS

Page

LIST OF FIGURES

Page

LIST OF TABLES

Page

LIST OF PLATES

Page

LIST OF EQUATIONS

Chapter 1: Introduction

1.1 Introduction

Newson (1995) defines fluvial geomorphology as the science that seeks to investigate the complexity of behaviour of river channels at a range of spatial scales from cross-sections to catchments. It also seeks to investigate process and response over a range of time scales. Fluvial geomorphology considers that river channels are a natural continuum, hard to separate, and that load, sediment supply and steamflow factors have a significant influence on form (Newson *et al.*, 1998). Rhoads (1994a) has argued that (p.588) "The most critical challenge confronting fluvial geomorphologists today is to devise strategies for integrating a diverse assortment of research that spans a broad range of spatial and temporal scales". Furthermore, Rhoads (1994a) suggested that if fluvial geomorphology is to grow as a science it must (p.601) "demonstrate its value by contributing either to fundamental scientific issues that transcend boundaries or to the solution of pressing societal problems".

One of the ways in which fluvial geomorphology has made a contribution is in the field of river management. In the past the dominant approach to river management has been an engineering one, the focus of which has been on controlling rivers rather than managing them in sympathy with their natural operation. Recently, however, given the current political climate and as river management time scales and perceptions change, it is now much easier to convince river managers of the need for geomorphological input in managing of fluvial systems (cf. Newson & Sear, 1998; Brizga & Finlayson, 2000). A major focus in this regard has been the relationship between fluvial geomorphology and ecology (Dollar, 2000). The basis of this relationship is that the channel boundary provides the physical habitat for lotic ecosystems, and hence channel habitat and associated biota (cf. Petts, 1985; Padmore, 1997; Mosley & Jowett, 1999; Rowntree & Wadeson, 1999). Substrate conditions, for example, have been shown to have a profound effect on the health of aquatic ecosystems (cf. Milhous, 1998a), while flow regime has been shown to have a significant impact on riparian vegetation (cf. Bendix, 1999).

Of particular interest to fluvial geomorphologists are the impacts of impoundments (Boon *et al.*, 1992). These impacts vary with function and management of reservoirs, but commonly include a decrease in flood magnitude and frequency, reduced sediment transport capacity and competence, and reduced downstream sediment supply due to trapping behind the dam. Attempts to minimise these impacts have resulted in scientists attempting to define a (regulated) flow regime that will mimic the significant effects of the natural pre-impoundment flow (King & Louw, 1998). These flows have been given the generic term 'environmental flows' (cf. Dollar, 2000). The underlying assumption is, however, that scientists know the range of flows which maintain the flood plain, macro-channel and active channel in a 'natural' or 'equilibrium state'. This requires identifying the magnitude and frequency of channel forming discharge and sediment-maintenance flushing flows.

The magnitude-frequency concept is based on the assumption that in alluvial systems, channel form (and/or morphological features) can be related to a specific magnitude (discharge) and frequency (return period or duration) of flow. Sediment-maintenance flushing flows refer to the magnitude and frequency of flows that perform a particular sediment-related task; moving gravel through a riffle for example. From a river management perspective, it is of great practical benefit to identify the flows that perform these tasks so that a regulated flow regime can be implemented that will result in minimal long-term disturbance to the channel. It is ironic that the search for these 'environmental flows' has led to the re-visiting of the classic magnitude-frequency debates of the 1960s and 1970s. The magnitude-frequency concept is central to this thesis and will be discussed in greater detail in Chapter 3.

1.2 Fluvial geomorphology and river management

The geomorphological approach to river management differs fundamentally from an ecological or engineering one in that:

- Fluvial geomorphologists adopt a catchment-scale approach to river management in which the link between the catchment and the channel is considered inseparable. By contrast, the engineering approach tends to be reach based, where solutions tend to deal with local symptoms of a problem, rather than its more fundamental causation (Knighton, 1998).

- The geomorphologist adopts a long-term strategy to fluvial system understanding, recognising that channel dynamics can be conceptualised over a wide range of spatial and temporal scales (see Section 1.3). Engineering and ecological approaches to management tend to ignore longer-term natural changes and variability.
- One of the fundamental causes of channel adjustment is the supply and movement of sediment through a fluvial system. A conceptual understanding of this requires a spatial and temporal approach. A catchment-wide audit of the source, supply, transport and sinks of this sediment is necessary for effective river management to take place (Newson, 1995).
- One of the bases of geomorphology is the assumption of dynamic change. Knighton (1998) argues that the regime assumptions favoured by river engineers need to be augmented by a more dynamic framework which involves the development, evaluation and application of methodologies for the analysis of change.

It is important to recognise that while the geomorphological approach is fundamentally different to an ecological or engineering one, the value that fluvial geomorphologists can add to managing fluvial systems is limited by their conceptual understanding of the physical functioning of the said systems. There is by no means consensus of opinion as to how fluvial systems function. A good illustration of this is the legal case in the United States of reserved water rights in the Platte River in Boulder, Park and Teller counties (Gordon, 1995). Two eminent fluvial geomorphologists, Luna B. Leopold and Stanley M. Schumm, differed fundamentally on a number of key issues pertaining to fluvial system functioning. These included theories of channel formation and maintenance, the interpretation of bankfull level, the definition of the term flood, the adjustability of stream channels, flushing flows, hydraulic geometry, geomorphic thresholds, stream geometry, the effects of vegetation on stream processes, sediment transport in mountain streams, pavement and armouring, incipient motion, the calculation of boundary shear stress and effective discharge. It is important in managing fluvial systems that the paradigm from which the management strategy is developed is clearly stated, as this will determine the planning and ultimately the implementation of the regulated flow regime.

1.3 Temporal scales and river management

It is instructive at this point to consider the importance of temporal scales in fluvial system understanding. This was first highlighted by Schumm & Lichty (1965) who have shown that the distinction between cause and effect in fluvial systems is a function of time and scale. The factors determining channel form and process can be viewed as either dependent or independent, depending on the temporal scale within which they are considered (Table 1.1). Furthermore, it is common knowledge that tectonic, climatic and environmental change have impacted on fluvial systems throughout geological time (cf. Arnell, 1992; Blum *et al.*, 1994; McCabe & Hay, 1995; Thomas & Thorp, 1995). Scientists need to bring this to the attention of river managers, as it is possible to misinterpret natural instability in fluvial systems as being a result of human impact (cf. Macklin & Lewin, 1992; Gilvear, 1994; Zhang, 1998), or to mis-diagnose cyclical changes as channel instability (cf. De Ploey, 1989; Moon *et al.*, 1997; Poesen & Hooke, 1997) or even to exaggerate human impact (cf. Grayson *et al.*, 1998). While the integrated management of catchments is implicitly contemporaneous, it should always be performed within a historical context (Davis *et al.*, 1999).

Despite this knowledge, temporal scales in fluvial systems are seldom accounted for in river management. Recently, however, larger time scales are becoming more politically acceptable given an era dominated by sustainable development and by the general scientific impression of impending rapid environmental change (cf. Brooks, 1995; Environmental Agency, 1998; Newson & Sear, 1998). It is within this context that the management of southern African fluvial systems should be undertaken.

Table 1.1: The status of river control variables considered in different temporal scales (after Schumm & Lichty, 1965).

River variables	**Status of variables during designated time span**		
	Geologic (10^3+ years)	**Geomorphological (10^1 to 10^2 years)**	**Ecological (10^0 to 10^1 years)**
Time	Independent	Not relevant	Not relevant
Geology	Independent	Independent	Independent
Climate	Independent	Independent	Independent
Vegetation	Dependent	Independent	Independent
Relief	Dependent	Independent	Independent
Palaeohydrology	Dependent	Independent	Independent
Valley dimensions	Dependent	Independent	Independent
Channel morphology	Indeterminate	Dependent	Independent
Observed discharge of water and sediment	Indeterminate	Indeterminate	Dependent
Observed flow characteristics	Indeterminate	Indeterminate	Dependent

1.4 The southern African management context

Human impact on fluvial systems in southern Africa takes two forms: direct and indirect. Direct impacts include the abstraction of water, gravel and sand, engineering structures such as impoundments, inter-basin water transfer schemes and canalisation. Indirect impacts occur through catchment land use and management practices which affect the delivery of sediment and water to the channel. It is expected that these impacts are likely to escalate given increased demands for water for domestic, industrial and agricultural use (Davies & Day, 1996). The need to protect and manage this important national resource has led to the development of the Reserve as a basic right under the South African National Water Act (1998).

The Reserve consists of two parts, the *Ecological Reserve* and the *Basic Human Needs Reserve*. The Ecological Reserve relates to the quality and quantity of water necessary to protect the sustainable functioning of aquatic ecosystems. At one level, the determination of the Reserve has been based on the Building Block Methodology (BBM) (cf. King *et al.*, 1993; King & Tharme, 1994; King & Louw, 1998). Setting the Reserve culminates in determining the Instream Flow Requirement (IFR) for a river. The basis of IFRs are the calculation of the range of flows necessary to maintain a river ecosystem at a specified Ecological Management Class (EMC). The modified in-stream flow should be a skeleton of the original flow regime, encompassing a range of flow types that have specific ecological and geomorphic significance.

The geomorphological contribution to the setting of IFRs has focussed on three groups of information requirements (Table 1.2): the spatial and temporal availability of habitat, the maintenance of substratum characteristics, and the maintenance of channel form. The first information requirement is at a smaller scale of resolution, where the geomorphologist is involved in determining the relationship between flow type and habitat. Rowntree & Wadeson (1999) have developed the hydraulic biotype to account for this. The second information requirement is the maintenance of substratum characteristics. This involves firstly, the seasonal flushing of fine materials from the surface matrix of the gravel-bed, and secondly, the over-turning and transport of the coarse matrix itself (Rowntree, 2000). These types of flows have been termed 'environmental flows' or 'sediment-maintenance flushing flows' elsewhere (Dollar, 2000). A review of these types of flows is provided in Chapter 3. The third information requirement is the maintenance of channel form, the ultimate determinant of the in-stream flow environment. This thesis will focus on the second and third information requirements; the maintenance of channel substratum characteristics and the maintenance of channel form. Given this context, the following aim and objectives are identified.

Table 1.2: A geomorphological framework for the assessment of Instream Flow Requirements: problems and information needs (after Rowntree & Wadeson, 1997).

Problem	Time scale	Spatial scale	Information needs
Spatial and temporal availability of habitats:	Short-term (<1-5 years)	Hydraulic biotype and morphological unit (<1-10m^2)	Distribution of hydraulic biotypes: channel cross-sections. substratum type. flood plain morphology
Maintenance of channel substratum characteristics:			
Seasonal flushing of substrate:	Short-term (<1-5 years)	Morphological unit (10 -100m^2)	Substratum particle size distribution. cross-section hydraulic geometry.
Modification to substrate:	Medium term (2-20 years)		channel gradient. rate of sediment supply from upstream
Maintenance of channel form:			
Channel plan and cross-section adjustment:	Long-term (10-100 years)	Reach (100m)	Channel cross-sections. gradients. bed and bank resistance. sediment supply. natural flow regime

1.5 Aim

The overall aim is to determine the magnitude and frequency of channel forming discharge for selected southern African rivers.

1.6 Objectives

Objective 1: To review the literature in order to assess the limitations of fluvial geomorphological knowledge in southern Africa.

This objective is achieved through a comprehensive literature review presented in Chapter 2. The review reveals the limitations of current fluvial knowledge in southern Africa. While considerable progress has been made in understanding the geological evolution of southern African fluvial systems, little progress has been made with regard to present-day processes.

Objective 2: To use cross-sectional data, bed material class, hydrology, hydraulics and relevant bed material transport equations to assess the relationship between channel form and bed material transport to flow discharge for selected rivers.

This objective is achieved through a field-based study in which three different river basins are analysed. The rivers are analysed in an attempt to create an understanding of the magnitude and frequency of channel forming discharge for selected southern African rivers.

Objective 3: To determine the magnitude and frequency of channel forming discharge by determining the natural bankfull discharge with respect to channel form for selected rivers.

To achieve this objective, channel cross-sections have been surveyed and related to hydrological data to explore the possible relationships between bankfull discharge, dominant discharge and effective discharge. This has been done in order to determine whether there is a particular stage, morphological feature, or transport index to which environmental flows can be pinned.

Objective 4: To develop a conceptual model of channel forming discharge for selected rivers.

It is necessary to develop at least a conceptual understanding of the importance of different flows for South African fluvial systems. The outcome of the research is therefore to make a contribution towards a better understanding of the discharges that are of 'significance' or 'importance' in selected South African rivers. This is of particular relevance in South Africa, as the rivers tend to distinct in that they are often controlled or semi-controlled by bedrock, have steep gradients with irregular long profiles, are often supply-limited and are subject to a highly variable hydrological regime. Furthermore, little attention has been paid to these sorts of fluvial systems in the literature, and they are therefore poorly understood. Chapter 3 discusses these issues in more detail.

1.7 Selection of representative rivers

To achieve the above objectives, three rivers in South Africa were selected for analysis. These were the Mkomazi River in KwaZulu-Natal, the Mhlathuze River in northern KwaZulu-Natal and the Olifants River in Mpumalanga. These will be discussed in detail in Chapter 5. Here, a short review will suffice.

The Mkomazi River is a cobble-bed river with strong bed rock control and remains one of South Africa's least disturbed rivers. As yet, there are no impoundments along the course of the river, but this is due to change soon (Louw, 1998a). The Mkomazi provides an opportunity to study a relatively un-impacted system and therefore forms the main research component of the study. The Mhlathuze and Olifants Rivers on the other hand are highly regulated systems. The Mhlathuze River is a regime sand-bed channel which flows over Quaternary alluvium. In contrast, the Olifants River is a highly impacted cobble-bed river, with strong bed rock control. The rivers also formed part of an Ecological Reserve assessment (Louw, 1998b; Louw, 2000). These rivers therefore provided an opportunity to test the methods developed for the un-impacted Mkomazi system on two regulated systems - the Mhlathuze and Olifants systems are therefore the application systems.

1.8 Research outline

1.8.1 Chapter 1: Introduction

Chapter 1 presents a motivation for the research, the aim and objectives of the study, a summary of the approach used and the chapter outline.

1.8.2 Chapter 2: Southern African fluvial systems

Chapter 2 provides a discussion on the present state of knowledge of southern African fluvial systems. It is argued that while palaeofluvial geomorphology has made important strides in reconstructing past fluvial forms and processes, modern channel process studies are limited and fragmentary.

1.8.3 Chapter 3: Magnitude and frequency of channel forming discharge

Chapter 3 outlines the major conceptual issues surrounding the magnitude and frequency of channel forming discharge. The discussion makes the point that in order for geomorphologists to provide useful information for managing fluvial systems, information requirements on the magnitude and frequency of flows and their impact on channel form, process and bed material transport must be met.

1.8.4 Chapter 4: Geomorphological approaches to bed material transport

Chapter 4 presents a discussion on the problems of bed material transport. Chapter 4 also provides the context within which the bed material transport equations used in this thesis were applied.

1.8.5 Chapter 5: The study area and research design

Chapter 5 provides an overview of the three rivers that were considered for this thesis. Information is presented on their general characteristics, geology, sediment yield and so on. Also provided are details regarding the impoundments on the Mhlathuze and Olifants Rivers. The research design is presented in this chapter.

1.8.6 Chapter 6: Hydrology

Chapter 6 describes the methods and techniques used to generate daily flow data for each of the sites for the three rivers. Also presented are historical flood data.

1.8.7 Chapter 7: Cross-sectional data, bed material and hydraulics

Chapter 7 presents the methods and techniques used to generate the cross-sectional data, bed material data and hydraulic computations for the three rivers. These were used to provide input to chapters 8, 9 and 10 where the bed material transport data and sediment-maintenance flushing flow methods and results are presented.

1.8.8 Chapter 8: Bed material transport and sediment-maintenance flushing flow methods

Chapter 8 discusses the methods and techniques used to generate the bed material transport data. It also presents information on the methods used to generate the dominant discharge, effective discharge and sediment-maintenance flushing flows.

1.8.9 Chapter 9: Results and discussion - the Mkomazi River

Chapter 9 presents the results and discussion on the relationship between morphological features and the dominant and effective discharge for the un-impacted Mkomazi River. Also presented are the results from the sediment-maintenance flushing flow analysis.

1.8.10 Chapter 10: Results and discussion - the Mhlathuze and Olifants Rivers

Chapter 10 applies the techniques developed for the Mkomazi River to the regulated Mhlathuze and Olifants Rivers. It is demonstrated in this chapter that these techniques provide a useful mechanism for identifying the impacts of flow regulation and in setting Instream Flow Requirements (IFRs).

1.8.11 Chapter 11: Discussion, synthesis and conclusions

Chapter 11 provides the discussion, synthesis and conclusions for the thesis. It discusses the results in the light of the research objectives set in Chapter 1. Also presented is a discussion on the implications of the findings of this thesis for river management in southern Africa. Recommendations for future research are presented.

Chapter 2: Southern African Fluvial Systems

2.1 Introduction

Research into southern African fluvial geomorphology has a long history (Dollar, 1998a). The environment, landscape and fluvial systems have played a central role in people's lives in southern Africa for thousands of years. However, it is only within the last hundred years that the scientific study of the environment, landscape and fluvial systems has evolved. This chapter will focus on fluvial research work in southern Africa in order to elucidate current knowledge in the sub-region and to identify potential areas of weakness. This is done to place the current research into a regional context.

The chapter is divided into three sections. The first section will consider ancient southern African fluvial systems (for a full discussion, see Dollar, 1998a). The second section will consider modern southern African fluvial systems, while the third section will provide an overview of the main characteristics of southern African fluvial systems.

2.2 Ancient southern African fluvial systems

Modern southern African fluvial systems owe their development to the geological template, Jurassic rifting of Gondwana and subsequent creation of new base-levels for erosion. There is an extensive literature dealing with pre-Gondwana fluvial systems. Details regarding ancient fluvial systems have been uncovered through deep mining operations. A good example of this is the Early Archaean (2885 Ma B.P.) Ventersdorp Contact Reef (VCR) which is a sedimentary layer that occurs at the base of the Ventersdorp lavas which rest on the Witwatersrand Supergroup (de Kock, 1941). The fossil river has been mined for gold since 1888 (de Kock, 1941; Chunnet, 1994). This ancient fluvial system shows evidence of successive terraces, cuesta ridges, theatre headed valleys, trellis drainage, strath terraces, wash terraces and concave bed rock ridges (cf. Krapez, 1985; Hall, 1994; Henning *et al.*, 1994; MacWha, 1994; Viljoen & Reimold, 1994). The sedimentary rocks of the Karoo Supergroup have also been extensively studied; these are best exposed in the Karoo basin. The basin fill consists of up to 9 000 metres of clastic sediments and lavas. The ages of these sediments range from around 300 Ma B.P. to c.190 Ma B.P. The depositional environments are well documented (cf. LeBlanc-Smith & Eriksson, 1979; Eriksson, 1986; Visser; 1989; Smith, 1995; Smith *et al.*, 1997).

An in-depth review of the post-rifting landscape and the associated fluvial landforms has been admirably achieved by other authors (cf. King, 1963; Fair, 1978; Partridge & Maud, 1987; Dardis *et al.*, 1988; De Wit, 1993; Hattingh, 1996; Maud, 1996). Here, a short review will suffice.

In southern Africa long periods of tectonic stability (African, Post-African I and Post African II erosion surfaces) have been interspersed with periods of tectonic uplift (Miocene and Pliocene) along clearly defined axes that have influenced the macro-level functioning of southern African rivers (Figure 2.1). The main denudational period was initiated shortly after the rifting of Gondwana (c. 180 Ma) and extended to the Late Cretaceous. Major sedimentation peaks in the Eocene, Miocene and Pliocene relate to these periods of maximum relief. Imprinted on these tectonic phases have been the impact of climatic change with associated periods of wetness and dryness and concomitant changes in vegetation cover, runoff, erosion, weathering rates and environmental change (Dollar & Goudie, 2000). After an extensive period of planation, the African erosion surface developed with flat meandering rivers dominating the southern African landscape (Partridge & Maud, 1987). Two periods of axial uplift in the Miocene and Pliocene rejuvenated many southern African rivers, hence the incised nature of many coastal rivers (Figure 2.1). The fluvial geomorphology of southern African must be seen within the context of these (polycyclic) macro-processes.

A general trend that emerges from the literature is to ascribe older (usually Mid to Early Pleistocene and older) fluvial changes to tectonic activity and more recent (usually Late Pleistocene to Holocene) fluvial changes to climatic oscillations. Worldwide advances in the study of the Quaternary glacial/interglacials leaves little doubt that climatic change has played a significant part in the evolution of fluvial systems worldwide and also in southern Africa (Maud & Partridge, 1988). Reviews of Late Pleistocene climate change in southern Africa by Partridge *et al.* (1990) and Tyson & Lindesay (1992) present clear evidence for climatic change. The impacts of climate change on landforms have been discussed elsewhere at length (cf. Maud & Partridge, 1988; Partridge, 1988; 1990). It is the contention of the author that the impact of these changes in climate has not been fully appreciated by the fluvial geomorphology community in southern Africa, notably those considering modern fluvial processes and landforms.

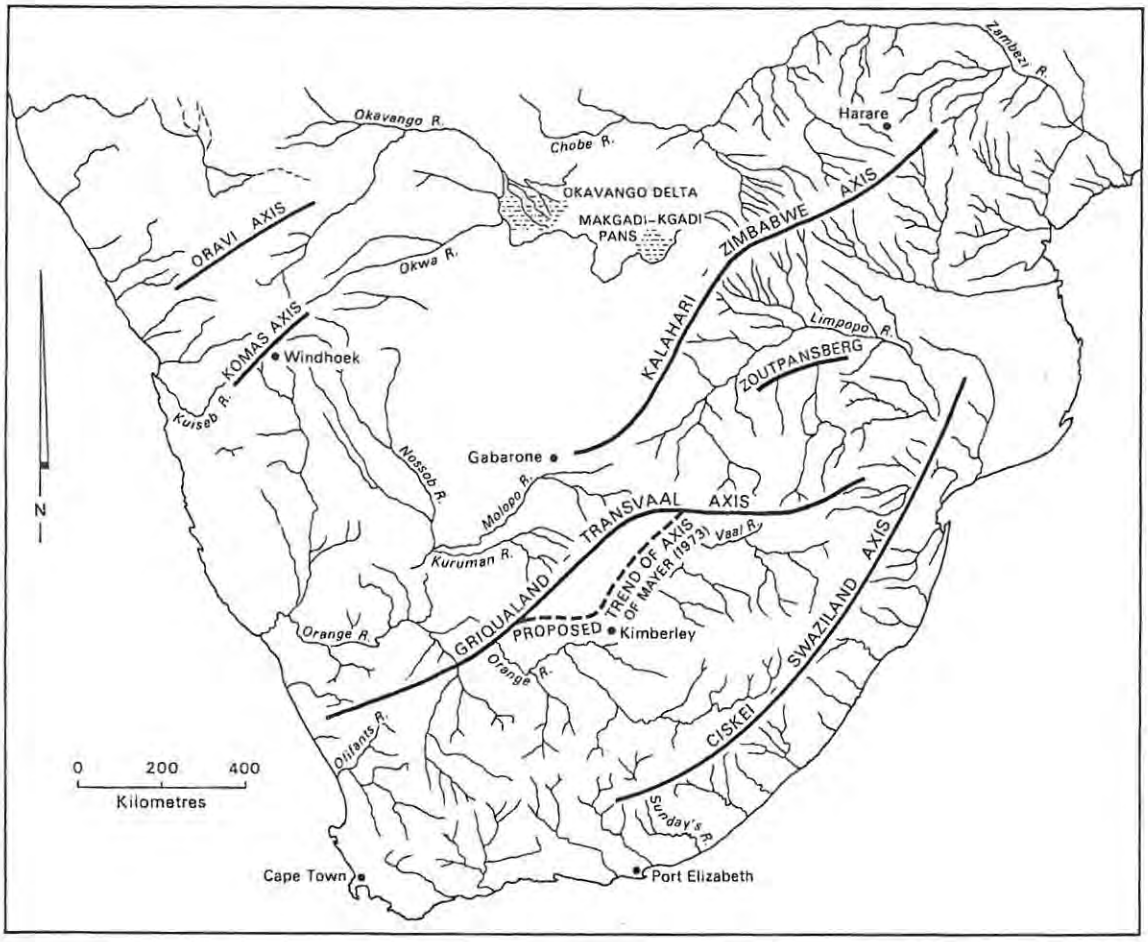

Figure 2.1: Fluvial systems of southern Africa (after Dollar, 1998a).

2.2.1 Palaeoflood hydrology

Of relevance to this study is the field of palaeoflood hydrology (PFH). Although this technique has been applied internationally since the 1970s (cf. Baker, 1973), limited attention has been given to the technique in southern Africa (Helgren, 1979; Turner, 1980). The basis of PFH is that certain empirical relationships can be defined between hydraulic and geomorphic variables and channel characteristics. By these means palaeohydraulic conditions can be reconstructed with relative estimates of palaeodischarge, palaeovelocity, palaeogeometry and palaeoform being made within certain confidence limits of the regression line.

Zawada *et al.* (1996) and Zawada (1996; 1997) provide comprehensive reviews of the techniques, methods, potential application and limitations of PFH. Zawada (1997) makes a strong case for the use of PFH to augment the somewhat limited flood record in southern Africa. PFH can provide magnitude and frequency data for floods of variable time scales ranging from 10s to 1000s of years, it augments the flood record and it makes prediction more accurate. Zawada (1994) made the point that the Laingsburg flood of 1981, which was the largest recorded flood (5680 m^3s^{-1}) in the Buffels River for the period of record, could be calculated as a 1 in 10 000-year flood using a log-Pearson distribution or a 1 in 100-400 year flood using a log-normal distribution. Using this as an example, Zawada (1994) points out that the variable predicted return periods using conventional flood-frequency techniques are unreliable, especially for high-magnitude floods, and that PFH provides a useful alternative to extend the record for flood frequency analysis (cf. Smith & Zawada 1990; Smith, 1992a; 1992b).

Zawada *et al.* (1996) provide evidence to show that the Orange River has experienced thirteen major floods with discharges in the range of 10 200 m^3s^{-1} to 14 660 m^3s^{-1} in the last 500 years, whereas the largest gauged flood in the Orange on record is 8 330 m^3s^{-1} at Vioolsdrift in 1974. Similarly, slack-water sediments indicate that a flood of 28 000 m^3s^{-1} occurred in the Late Holocene in the Mfolozi River, nearly twice the size of the largest recorded flood of 16 000 m^3s^{-1} in 1984. Clearly, PFH provides a significant source of information (Boshof *et al.*, 1993). Zawada *et al.* (1996) were able to show that the Orange could be divided into four palaeoflood periods (Table 2.1). They argue that there is a clear relationship between flood magnitude and climate change (cf. Partridge *et al.*, 1990; Tyson & Lindesay, 1992) and that there has been a gradual warming since the end of the Little Ice Age (A.D. 1850).

Table 2.1: Flood-magnitudes for the Orange River for the last 5000 years (after Zawada et al., 1996).

Period Number	Approximate Date	Flood Magnitude
1	5450 B.P. - 1800 B.P.	No flood exceeded 12 800 m^3s^{-1}
2	961 A.D. - 1332 A.D.	No flood exceeded 14 700 m^3s^{-1}
3	1453 A.D. - 1785 A.D.	No flood exceeded 28 000 m^3s^{-1}
4	1785 A.D. to present	No flood exceeded 9 500 m^3s^{-1}

2.2.2 Palaeosediment yields

A change in climate, drainage pattern or orientation will result in a change in the sediment yield of a river. It is therefore appropriate to provide a brief discussion on palaeosediment yields for southern African rivers. Table 2.2 presents evidence of a variable but overall declining rate of sediment yield in the Orange River. Dingle & Hendey (1984) suggest that declining sedimentation off the West Coast depocentres can be accounted for by increasing aridity associated with the upwelling of the Benguela Current in the Upper Miocene (Siesser, 1978). Modern values for the Orange's sediment load are 6.5 x $10^6 m^3$ per annum but are thought to have been declining since the 1930s (Rooseboom, 1978).

Table 2.2: Sediment yield for the Orange River since the Late Cretaceous (after Dingle & Hendey, 1984 and Rooseboom, 1978).

Period	**Drainage Area ($10^3 km^2$)**	**Mean Annual Sediment Yield ($10^6 m^3$)**
Late Cretaceous	969	10
Palaeogene	517	2.0
Neogene	969	0.3
Present	969	6.5

Martin (1987) has compared modern sediment yields from KwaZulu-Natal rivers to palaeoyields from the Natal Valley in the Indian Ocean. Using seismic profiles he determined that average modern rates of sediment yield (322 t $km^2 yr^1$) are 12-22 times higher than the geological average (14-27 t $km^2 yr^1$). It is tempting to explain this higher modern yield as anthropogenically induced, but Davies *et al.* (1977) have pointed out that sediment yields have varied by a factor of as much as fifteen between glacial and interglacial periods. Rates for the last 3 Ma are for example, twice as high as for the previous era of rapid sedimentation. The question is to what extent are the large increases in modern fluvial sediment yields anthropogenically forced, or do high modern yields form part of a natural fluctuation (cf. Murgatroyd, 1979) Bremner *et al.* (1991) indicated that the sediment yield from the 1988 Orange River floods [Swart *et al.* (1990) reported that the 1988 flood reached a peak of around 8 500 $m^3 s^{-1}$] were not nearly as impressive as the runoff values. They suggested that the modest discharges of sediment were related to limited sediment supply to the channel.

Illenberger (1992; 1993) suggests that for selected Eastern Cape rivers (Krom, Gamtoos, Van Stadens, Swartkops, Great Fish and Great Kei) modern sediment yields are eight times higher than the geological average of 12 t km^2yr^1, but that considerable variation in the geological rates also exist. High modern yields are attributed to poor catchment management practices. Milliman & Meade (1983), however, make the point that today's river sediment yields should not simply be extrapolated backwards in time, as present-day climates and erosional regimes do not resemble even those of a few thousand years ago.

What is clear from the above review is that the present-day fluvial regime is a recent one. The evidence presented suggests that a variable hydrological and sediment regime has occurred since the fragmentation of Gondwana. This has significant implications for our understanding of the functioning of modern fluvial systems as the past has left its imprint on modern channel. In order for southern African fluvial systems to be adequately understood, a broader temporal context is required. Untested assumptions about human-induced channel changes should therefore be avoided. Given this context, the following section deals with the current state of knowledge of modern southern African fluvial systems.

2.3 Modern southern African fluvial systems

2.3.1 Introduction

The previous section emphasised that southern African fluvial systems have undergone considerable changes due to tectonic and climatic influences. This section will review the current state of knowledge of modern southern African fluvial systems. While the field of fluvial geomorphology is well established in the Northern Hemisphere, knowledge of the physical functioning and processes operating in southern African fluvial systems is still fragmentary. It is only in the last ten years that a concerted effort has been made to elucidate modern channel processes. Ironically, this has been motivated not by knowledge for its own sake, but by ecology (cf. Pitman & Pullen, 1989; van Wyk, 1989; Looser, 1989; Bruwer & Ashton, 1989; Palmer & O'Keeffe, 1985; 1990; Davies, 1989; Vogt & Moon, 1989). Prior to the 1990s, comments on modern fluvial systems were only made in passing, usually with reference to catchment condition, or flooding (cf. Gevers, 1948; Weiss & Midgley, 1976; Wilson & Dincer, 1976; Alexander, 1979; Beckedahl & Moon, 1980; Beaumont, 1981; Garbharran, 1983; Dix, 1984; Perry, 1985; van Heerden & Swart, 1986).

2.3.2 Channel process studies

The first systematic study of a modern fluvial system in southern Africa was that of the Okavango Delta in Northern Botswana. McCarthy *et al.* (1986; 1987; 1988) were able to show that active channel migration in the Delta was the result of sediment accumulation in the channels, leading to channel aggradation, a reduction in hydraulic gradient and ultimately avulsion. Rates of accretion of up to 50 mm per annum were noted. Channels of the Okavango are thought to be inherently unstable, but these dynamic changes are necessary for the even distribution of sediment through the delta. Channel changes have been occurring throughout geological time, and may also be related to tectonics and changing climatic conditions (cf. Cooke, 1976; Shaw, 1984).

Recent evidence from the Okavango Delta stresses the significant role that vegetation plays in the geomorphic functioning of the system (cf. Ellery, 1988; Ellery *et al.*, 1990; 1993; van Coller *et al.*, 1997). Channel margin vegetation assemblages are related to, and impact on, sediment deposition and long-term and seasonal water levels. Erosion-resistant vegetated banks retard water velocities, so that all the sediment introduced into the system is retained. This results in channel aggradation, vegetation establishment and subsequent avulsion (McCarthy *et al.*, 1992). Channel switching is thought to relate to a two phase process of erosion and deposition. Channels that receive their water via seepage and overspill are erosion dominated channels, while channels that receive their water from a direct source (i.e. an active channel) are deposition dominated channels. Once critical thresholds have been attained, channel switching takes place. It is clear that channel avulsion forms part of the natural process of sediment distribution within the Okavango Delta, and that a dynamic relationship exists between discharge, sediment load and riparian and in-stream channel vegetation. McCarthy *et al.* (1991) argue that channel switching indicates that the present channels are attempting to attain an equilibrium condition and that the initial disequilibrium was probably caused by fault movements on the northwestern side of the graben. Without the constant channel switching within the Okavango Delta and the dynamic relationship between the water, sediment and vegetation, the Okavango system would probably become stagnant and moribund (McCarthy, 1992).

A systematic study of channel change in the Bell River in the North Eastern Cape was undertaken by Dollar (1992). He found that change in the form of channel straightening from a meandering to a braided channel (as evidenced by a series of recent meander cutoffs) could be accounted for by increased sediment production to the channel as a result of poor catchment management practices. Triggering mechanisms were argued to be major flow events following periods of extended dryness. This sequence of wet and dry cycles of approximately 18-years was thought to be comparable to Flood Dominated Regimes (FDRs) and Drought Dominated Regimes (DDRs) in Australia (cf. Warner, 1987). This issue is explored further in Section 3.8. Dollar & Rowntree (1995) pointed out that catchment and channel processes were clearly linked and that any disturbance in the catchment would have a concomitant impact on the channel. Rowntree (1991) and Rowntree & Dollar (1996a) also mention the significance of riparian vegetation in maintaining channel stability. Alien woody vegetation on the channel banks may stabilize the banks at low and intermediate flows, whereas at high flows they may aid the process of channel avulsion.

Spatial and temporal changes in the rivers of the Kruger National Park (KNP) have been widely investigated (cf. Venter & Bristow, 1986; Vogt & Moon, 1989; Chunnet *et al.*, 1990; Venter, 1991; Vogt, 1992; Cheshire, 1994; Heritage *et al.*, 1995). Vogt (1992) was able to show that the Sabie River has experienced a number of channel planform changes between the 1940s and the 1980s and that these changes could be related to rainfall periodicities in the catchment as well as changing rates of channel sedimentation and scour. By contrast sediment transport rates were thought to be controlled by antecedent catchment and channel conditions such as drought (Heritage & van Niekerk, 1994; Birkhead *et al.*, 1996). Channel vegetation was considered a major control on channel form. Vegetation density was shown to have increased progressively since the 1940s. Later, Heritage *et al.* (1995) made the point that sedimentation patterns (deposition and scour) in the Sabie River could be related to the 18-year rainfall periodicity in the summer rainfall region (linked to El Niño) which was translated to the flow pattern. Channel change was thought to be related to increased sedimentation in the channel as evidenced by catchment degradation.

2.3.3 Channel forming discharge

Conventional wisdom for alluvial channels is that moderate flow events with a return period of 1 to 2 years are responsible for the maintenance of channel form (cf. Wolman & Miller, 1960; Richards, 1982). Although southern African has an extensive literature on flooding, flood magnitude and flood frequency estimation (cf. Alexander, 1976; Kovacs, 1980; 1985; 1988; Kovacs *et al.*, 1985; Begg, 1988; Zawada, 1991), little attention has been paid to determining the magnitude and frequency of flow events responsible for channel form. It is clear that semi-arid rivers exhibit a markedly different flow regime to temperate systems (cf. Baker, 1977) and that the conventional 1 to 2 year channel forming discharge of temperate alluvial channels should not be applied universally to southern African rivers (Newson, 1996). This theme is expanded on in Chapter 3.

An extensive literature search revealed that other than work by Heritage *et al.* (1995) and Wadeson (1989), no work on channel forming discharge has thus far been attempted in southern Africa. Heritage *et al.* (1995) have shown that the macro-channel of the Sabie River is inundated once every 20 years. They suggested that the concept of bankfull discharge as applied to semi-arid rivers may be erroneous. The Sabie River is probably in a state of disequilibrium and hence the river may not have had time to adjust its morphology to the current flow regime.

2.3.4 Present-day sediment yield

Although Du Toit had mentioned the problem of siltation of South African reservoirs as early as 1910 (Du Toit, 1910), limited data is available on modern sediment yield for southern African rivers. Du Toit (1910) ascribed siltation to a combination of high natural levels of sediment load as well as poor agricultural practices. Van Warmelo (1922a; 1922b; 1922c); Mason (1924) and Lewis (1936) mention the problem of reservoir siltation in the Vaal and Orange Rivers, while Warren (1922, p.42) suggested that "... this evil is becoming so pronounced that it would appear that some form of legislation will have to be introduced". Early workers thus recognized the link between reservoir sedimentation and poor agricultural practices (cf. Roberts, 1952).

Rooseboom (1978) has shown that the annual sediment yield from South African rivers is between 100 and 150 x 10^6 tons per annum, but that this figure is declining. Rooseboom & Harmse (1979) indicated that between 1929 and 1969 the average load of the Orange River decreased by more than 50%, while flow reductions during the same period remained insignificant. They argue that these reductions cannot be ascribed to land use, reduction in flows or sediment capture by impoundments but (p.463) "... should be attributed to progressive change in extant material rather than land use."

Le Roux (1990) was able to show that the present-day rate of erosion in South Africa (as a whole) was at least two to three times the rate of replacement by weathering. Rooseboom *et al.* (1992) argue that (p.2.9) "...sediment concentrations and loads in rivers are determined by the availability of sediments rather than by the carrying capacities of the flows". Rooseboom (1992) concludes (p.4.1) "... after more than 20 years involvement with sediment load data for southern African rivers, the main impression which remains is the variability thereof". It is clear that there is extreme variability in the daily, annual and seasonal sediment yields of southern African rivers and that it is risky to draw simple conclusions from limited records. Very little knowledge exists on the impact of 'sediment pulses' through southern African rivers. To the best knowledge of the author, there are no measured bed load data available for southern African rivers. Bed material is significant, as channel pattern and form has long been associated with bed load and calibre (cf. Schumm, 1977; Church *et al.*, 1987; Ferguson, 1987). This lack of information serves as a major gap in the understanding of the functioning of modern southern African fluvial systems.

2.3.5 Flow regulation and channel processes

The late 1980s and early 1990s saw a growing recognition in southern Africa of the impact of engineering structures on fluvial systems. These related specifically to channel impoundments and inter-basin transfer schemes (IBTs). Initially the focus of research on these regulated rivers was ecological. However, it became clear to ecologists that the physical template for habitats was determined by the flow, channel substrate and banks of the river - the realm of the fluvial geomorphologist. Geomorphologists were increasingly being called on to aid in the process of river conservation and management.

Early work on the geomorphological effects of regulated rivers was undertaken by Dollar (1990) who showed that the building of the Isandile Dam on the Keiskamma River attenuated flood peaks resulting in the build-up of tributary bars at channel junctions and general sedimentation problems immediately downstream of the dam. Work by McGregor (1999) has confirmed this finding. The impact of introducing water from the Wriggleswade Dam to the Nahoon River in the Eastern Cape was shown to have a significant scouring impact on the upper reaches of the receiving channel (Hughes, 1994). Du Plessis (2000) has shown how the Skoenmakers River in the semi-arid Karoo region, which is used as a conduit for water transferred from the Orange-Fish-Sundays River IBT, has altered its channel morphology and riparian vegetation structure in response to the imposed flow regime. Other than these four studies, no other published information is available on the impact of flow regulation on channel processes in southern Africa.

2.3.6 River classification and channel processes

Two major bodies of work on river classification have emerged out of the southern African literature since the early 1990s (Figure 2.2). Both systems were borne out of the requirements of ecologists for a physical desription for aquatic ecosystem management. The first is the hierarchical classification system of Rowntree & Wadeson (1997), the second is the classification system of van Niekerk *et al.* (1995). These have been extensively reported on elsewhere (cf. van Coller, 1993; van Niekerk & Heritage, 1993; Wadeson & Rowntree, 1994; Wadeson, 1994; 1995; van Coller *et al.*, 1995; van Niekerk *et al.*, 1995; Rowntree & Wadeson, 1996; 1997; 1999; Heritage *et al.*, 1997). Here a short review will suffice.

Rowntree & Wadeson (1997) stress the need for a stream classification system that can provide a scale-based link between the channel and the catchment, and that will allow a structural description of the spatial variation in stream habitat. The idea of classification assumes that distinct boundaries can be defined for fluvial systems, and that these boundaries can be isolated by means of a set of discrete variables. Wadeson & Rowntree (1994) modified the stream classification system of Frissel *et al.* (1986). Their classification system can be regarded as a cascading system, in which each level provides input into the lower one. The system therefore allows a link between the catchment and channel (Figure 2.2).

Rowntree & Wadeson, 1993	van Niekerk *et al*, 1995
CATCHMENT	CATCHMENT
	RIVER SYSTEM
ZONE	
SEGMENT	ZONE
REACH	MACRO-REACH
	REACH
	CHANNEL TYPE
MORPHOLOGICAL UNIT	MORPHOLOGICAL UNIT

Figure 2.2 Hierarchical classification systems of Rowntree & Wadeson (1997) and van Niekerk et al. (1995).

The second major attempt at river classification was developed by van Niekerk *et al.* (1995). Working contemporaneously with Rowntree and Wadeson, they produced a bottom-up hierarchical classification system based on an extensive study of the rivers of the KNP. Van Niekerk & Heritage (1993) focussed on the Sabie River drawing on earlier work by Vogt (1992), Venter (1991) and Chunnet *et al.* (1990). The Sabie River consists of a macro-channel extending across the width of an incised valley, cut into the macro-channel are one or more active channels (see Figure 2.3). The active channels are determined by normal flow conditions (i.e. non-flood conditions) while the macro-channel is controlled by high magnitude, low frequency events.

Van Niekerk & Heritage (1993) point out that the geomorphology of the Sabie system reflects the response of the system to a highly variable water and sediment discharge superimposed on a macro-channel controlled by the underlying geology. The implicit assumption is that there are various spatial and temporal levels at which fluvial systems operate, and that these can be 'separated-out' into distinct temporal scales. They suggest that rigid sub-division of rivers using some pre-determined classification system may result in important fluvial processes being ignored. They argue that for a full understanding of the dynamic interrelationships of fluvial systems, a classification system should be built from the bottom-up. In this way, implicit assumptions about the river are not imposed from the top and made to fit a rigid classification system.

Moon *et al.* (1997) were able to show that this approach to stream classification resulted in the ability to predict morphological change in the Sabie River, as well as to identify which channel types were likely to undergo habitat changes with altered discharge and sediment loads. They also suggest that this approach should be able to predict the direction of longer-term change which may become ecologically significant.

2.4 Overview of southern African fluvial systems

It is useful at this point to provide an overview of the main characteristics of southern African fluvial systems. As mentioned previously, the rivers of southern African reflect the tectonic and climatic history of the region since the breakup of Gondwana some 180 million years ago. This, together with a variable climate, has created the template within which modern southern African fluvial systems function. Tectonic uplift during the Miocene and Pliocene have rejuvenated many of the eastern sea-board rivers which drain the escarpment. Consequently many of these rivers are incised onto bed rock and have steep and often irregular long profiles. These irregular long profiles consist of sections that are morphologically uniform, these have been termed macro-reaches (Rowntree, 2000). Macro-reach breaks are usually due to changes in lithology, but can also be the result of Miocene and Pliocene tectonic activity. This situation has disrupted the classic downstream gradation bed material sequence of boulder to cobble to gravel and ultimately to sand. Consequently, sand-bed channels in the lower reaches may often be replaced by bed rock, boulder or cobble.

Many rivers draining the eastern sea-board of South African display complex cross-sections. An active channel which is formed within a larger macro-channel bordered by high terraces commonly occurs (Figure 2.3). The macro-channel has been described in a number of publications (cf. van Niekerk *et al.*, 1995; Rowntree & Wadeson, 1999). Macro-channels develop as a result of incision by the active channel into former terraces that mark the outer boundary of all but the most extreme flood flows. The active channel is the channel which by definition is inundated most frequently and is geomorphologically the most active (Rowntree & Wadeson, 1999). Within the active channel a distinct in-channel bench commonly occurs. There is often no clear flood plain. It is suggested that this channel architecture is a response to the geological template and the variable hydrological regime. This issue will be explored later in the thesis.

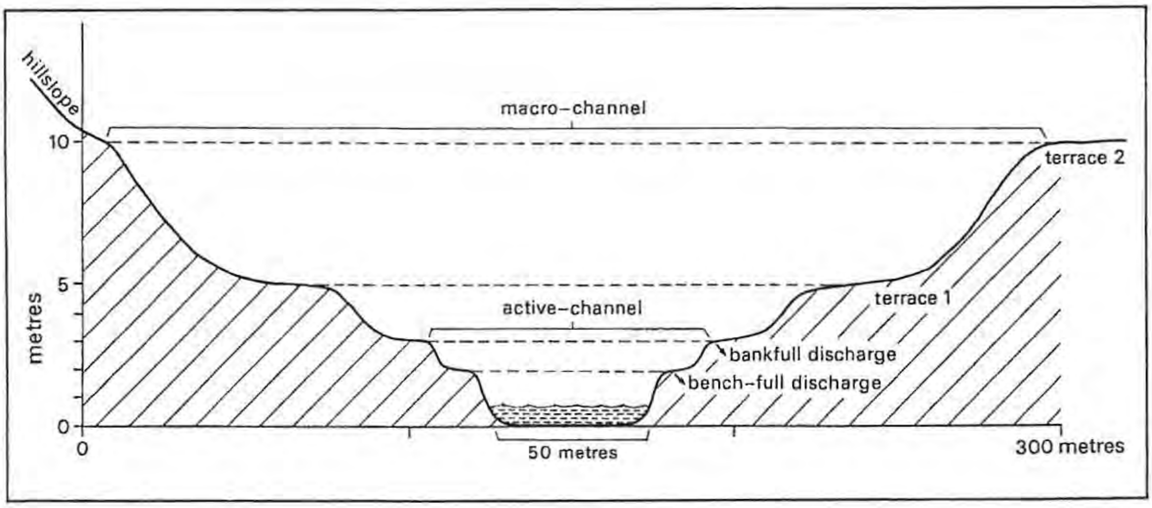

Figure 2.3: Diagrammatic representation of the macro-channel, active channel, benches, estimated bankfull discharge and terraces

As mentioned earlier, present-day southern African fluvial systems display a highly variable hydrological regime. Walling (1996) has shown that the rivers of southern Africa have the highest coefficient of variation of mean annual runoff, the highest average storage requirement for flow regulation, the highest average annual flood variability and the highest extreme flood index [defined as the standard deviation of the logarithms of the annual peak discharge (Figure 2.4)]. Görgens & Hughes (1982) have shown that the average inter-annual variability of runoff in South African fluvial systems is extremely high. The coefficient of variation (CV) of annual runoff is around 1.13, which is higher than the CV for Australian rivers of 0.7 (cf. McMahon *et al.*, 1992;

McMahon & Finlayson, 1995; Brizga & Finlayson, 2000) and considerably higher than the world average of between 0.25 and 0.4. Furthermore, the 18-year periodicity in rainfall characteristic of much of the eastern half of the country is translated to the flow regime, resulting in highly variable short- and medium-term flow regimes.

It is clear from the above discussion that southern African fluvial systems differ from alluvial systems in temperate climes from whence much of the conventional wisdom in fluvial geomorphology has been developed. [Recently, however, work from the dryland areas in the United States (cf. Graf, 1988) and a focus on bed rock systems (cf. Tinkler & Wohl, 1998) has gone some way to balance this perspective]. Fluvial form is a function of the geological template, channel boundary resistance, climatic inheritance, vegetation and observed discharge of water and sediment. It is inconceivable that all fluvial systems will therefore conform to conventional theory derived from a particular region. Consequently, there is an urgent need to develop appropriate local knowledge.

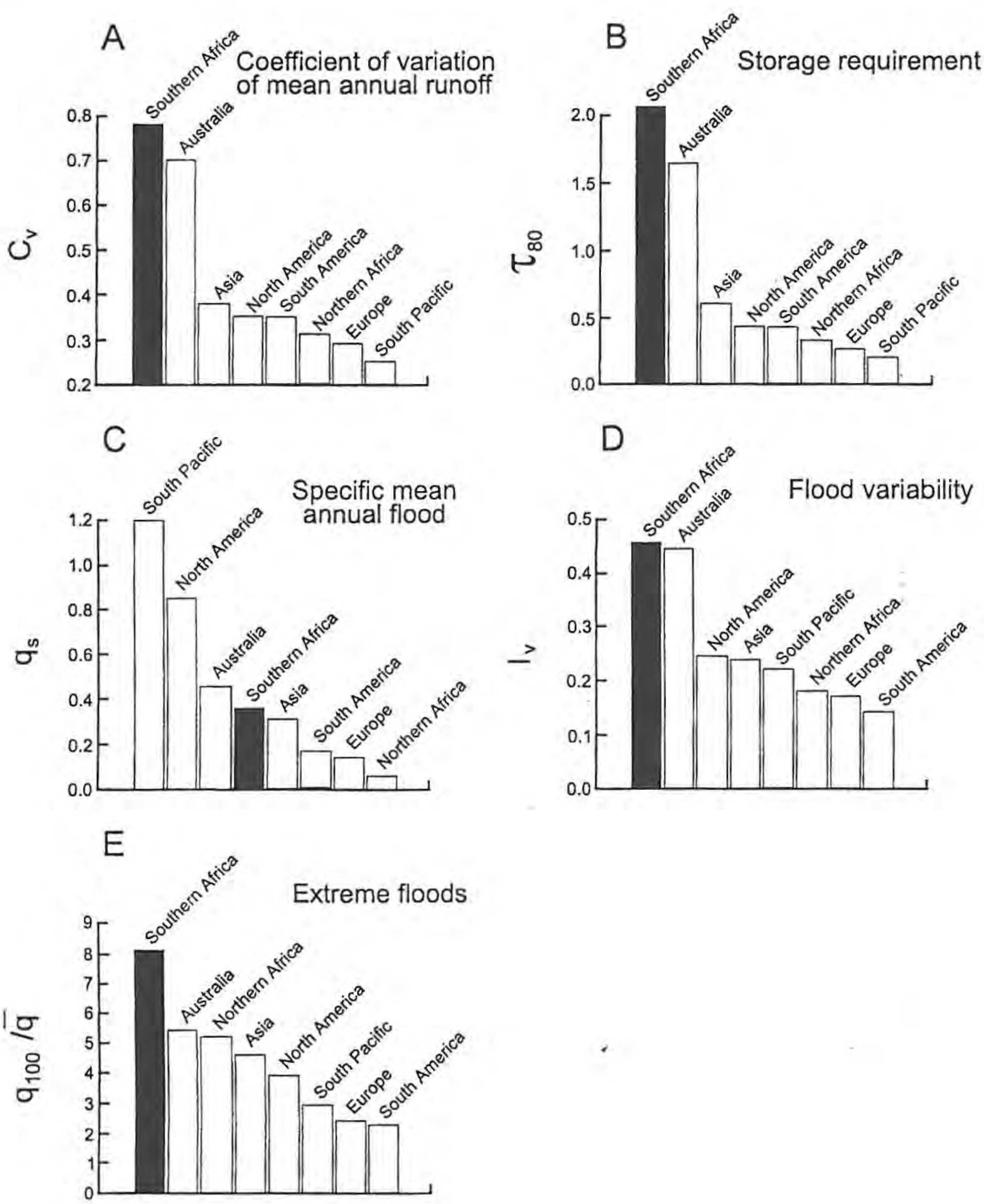

Figure 2.4: A comparison of the runoff characteristics of rivers of southern Africa with those of other continents (after Walling, 1996). Where a) C_v is the ratio of the standard deviation and the mean, b) τ_{80} is the storage for a constant draughts at 80% of the mean annual flow with a variability of 95% expressed as a ratio of the mean annual flood, c) q_s is the 2.33 year return period flood, d) I_v is the standard deviation of the logarithms of the annual peak discharge, e) q_{100}/q is the ratio between the 100 year flood and the mean annual flood.

2.5 Discussion and conclusion

The review has highlighted two important points. First, while the study of palaeofluvial geomorphology in southern Africa is well documented, modern fluvial process studies are limited, and the understanding of modern fluvial systems is fragmentary. In terms of the focus of this thesis, there is a paucity of information regarding the magnitude and frequency of channel forming discharge and bed material transport in southern African rivers. This is of concern, as effective river management requires information in this regard. Second, southern African fluvial systems differ fundamentally from temperate alluvial systems. If effective river management is to occur, there is a need to develop appropriate local knowledge. This thesis attempts to contribute to that local knowledge in southern Africa.

Chapter 3: Magnitude and Frequency of Channel Forming Discharge

3.1 Introduction

Three sets of information are necessary in providing a geomorphological assessment for in-stream flow requirements (Rowntree & Wadeson, 1997). These are the flows that maintain the spatial and temporal availability of habitat; the substratum characteristics; and the channel form. Rowntree & Wadeson (1997) have suggested the use of the hydraulic biotype to provide the information requirements for the maintenance of aquatic habitat. The latter two information requirements (the maintenance of substratum characteristics and the maintenance of channel form) are fundamentally linked to the magnitude-frequency debate. The aim of this chapter is to provide a theoretical framework within which the flows necessary for the maintenance of channel form can be appraised. The chapter is divided into two sections, the first section considers the magnitude-frequency debate, while the second section reviews environmental flows with specific reference to sediment-maintenance flushing flows.

3.2 The origins of the magnitude-frequency debate

The origins of the magnitude-frequency debate dates back to the late 1800s when British hydraulic engineers attempted to develop stable irrigation canals in India. They noted that canals could adjust their boundaries until a stable configuration was attained (the regime channel), and that the geometry of the channel was related to its discharge of sediment and water (Kennedy, 1895; Lacey, 1930). The equations that were developed became known as regime equations (Nixon, 1959; Ackers, 1972; Osterkamp & Hedman, 1977). Later, regime equations were related to 'natural channels'. The thinking behind this was that, in principle, the morphology and dynamics of rivers should be explicable in terms of the laws of physics.

This line of thought was later to emerge in the magnitude-frequency debate. This debate, as mentioned in Chapter 1, centred on the assumption that in alluvial systems, channel form (and/or morphological features) can be related to a specific magnitude (discharge) and frequency (return period or duration) of flow (cf. Leopold & Maddock, 1953; Blench, 1957; Lane, 1957; Leopold & Wolman, 1957; Dury, 1959; Dury *et al.*, 1963; Leopold *et al.*, 1964; Woodyer, 1968; Osterkamp *et al.*, 1983). Early researchers sought a physical expression of this flow. Initially, it was argued that the flood plain, shape and pattern of the channel are related to the bankfull condition - the stage at which overtopping onto the flood plain occurs. The literature came to equate the bankfull discharge with dominant discharge and effective discharge (cf. Ackers & Charlton, 1970; Gregory, 1976; Pickup & Warner, 1976). These three discharges will be discussed in turn.

3.3 Dominant discharge

By the 1970s, the term 'dominant discharge' had become firmly entrenched in fluvial geomorphology and hydraulic engineering literature (cf. Neill, 1968; Bray, 1975; Gill, 1965). The term 'dominant discharge' was introduced by Inglis (1941) as a discharge and gradient to which a channel returns annually. At this discharge, equilibrium is most closely approached and the tendency to change is least. This was regarded as a constant flow rate that would produce the same channel morphology as a sequence of naturally varying flows. Thus dominant discharge was defined by its product.

There are a number of problems with the dominant discharge concept. Pickup & Rieger (1979) argue, as does Kennedy (1972), that to assign a single dominant discharge to a channel is an oversimplification, for to accept the idea of a 'dominant discharge' is to imply that the river is in regime (equilibrium). They argue that instead of a single channel forming discharge, a channel is much more likely to be adjusted to a whole range of flows as well as to the sequential nature of the flows.

Prins & de Vries (1971) suggest that a distinction must be made between dominant discharge as a concept and the determination of dominant discharge. It is clear that the simplified regime can never replace the real regime as far as the reproduction of the morphological characteristics of a river are concerned (Prins & de Vries, 1971). Furthermore, they point out that there could be a number of dominant discharges each related to a different channel characteristic, for example the steady flow that would yield an observed meander length. Thus the accepted notion of dominant discharge is for a particular channel morphology, despite the fact that the channel morphology is made-up of a collection of channel properties. Each of these properties will have their own response to the variability of flow and therefore their own dominant discharge. The concept of dominant discharge can only hold true if each one of the channel properties responds similarly to the variability of flow, i.e. the dominant discharge for each of the properties of the channel is the same.

A further problem with the dominant discharge concept is that dominant discharge is not a property of the flow sequence itself, but a property of the response that the flow sequence generates in a particular channel characteristic - the same channel characteristic that defines the dominant discharge in the first place. Dominant discharge thus refers to a conceptual parameter without a unique statistical or physical interpretation.

Marlette & Walker (1968) developed a computational method for defining dominant discharge. To avoid confusion, this thesis adopts the term dominant discharge when referring specifically to Marlette & Walker's (1968) computational method rather than when referring to the broader conceptualisation of dominant discharge. Marlette & Walker (1968) argued that if the bed sediment transport was the dominant factor in determining the channel size and shape, then a channel designed to carry the dominant discharge (see Equation 3.1) would be the most stable configuration. The Netherlands Engineering Development Consultants (NEDCO)(Prins & De Vries, 1971) adopted Marlette and Walker's (1968) approach and developed a method for determining dominant discharge using bed load discharge, flow duration data and the stage-discharge curve. The concept was that the dominant water level is that water stage above which half the bed sediment transport takes place - this was termed the bed-boundary level. A three step computational system was used. First, the monthly river flows were arrayed in ascending order, second, the bed load discharges corresponding to each monthly flows were computed, and third, the bed load discharges were subdivided into class intervals. The dominant discharge (Q_d) is calculated by:

$$Q_d = \frac{\sum_{h=1}^{k} Q_h \; T_h \; n}{\sum_{h=1}^{k} T_h \; n} \qquad (3.1)$$

where

k total number of class intervals

b specific class interval

Q_h mean monthly or daily water discharge (m^3s^{-1})

T_h bed load discharge for a given month or day corresponding to Q_h in tonnes per day

n number of events in each class interval

This model was tested on the Platte and Missouri Rivers. It was found that, before flow regulation, the dominant discharge of the Missouri River below the confluence was 67 000 cfs. This decreased to 38 000 cfs after regulation. Using a similar procedure, Komura and Gill (1968) calculated the dominant discharge for the Nagara River in Japan. The dominant discharge was calculated as 3000 m^3s^{-1}, this equated to a recurrence interval of 1.43 years on the annual series and a probability of excedence of 70% for the annual peak discharge. Komura (1968) found that the dominant discharge depended on the type of bed material present. Where bed load was predominant, a dominant discharge of 2030 m^3s^{-1} with a recurrence interval of 1.04 years occurred. Where bed and suspended load were equal, a dominant discharge of 3000 m^3s^{-1} with a recurrence interval of 1.43 years occurred, and where suspended load was dominant, a dominant discharge of 3985 m^3s^{-1} with a recurrence interval of 2.78 years occurred.

3.4 Bankfull discharge

The notion of bankfull discharge has existed in the literature for some time (cf. Inglis, 1947), but its use as an independent variable controlling channel form became popular in the late 1950s and 1960s. Wolman & Miller (1960) argued that the flood plain and the shape and pattern of the channel are related to discharges that approximate the bankfull condition. Harvey (1969, p.82) defined bankfull discharge as "... the discharge which just fills the natural stream channel and above which spilling onto the floodplain occurs". The bankfull stage was thus taken as the elevation of the active floodplain, and is a physical measure of the flow capacity of the channel.

Dury (1959; 1961) has shown that on many English and American rivers, bankfull discharge has a recurrence interval of somewhere between 1 and 2 years. This became conventional wisdom (cf. Brusch, 1961; Leopold *et al.*, 1964). Dury *et al.* (1963), however, argued that many rivers in Queensland, Australia, are incised to such an extent that the bankfull stage is well above the mean annual flood and that some sites had not experienced a bankfull stage during the period of record. This suggested that the rivers were still adjusting to a recent climate or tectonic event and may not reach a bankfull stage. It is also possible that Dury was inappropriately applying concepts developed for the British and American context. Hickin (1967) similarly argued that the rivers of New South Wales, Australia, had become deeply incised due to climatic, tectonic and eustatic events, and that for this reason bank top at many sites do not correspond to the natural bankfull stage. Dury (1976) suggested that due to the widespread evidence that streams have incised their flood plains in the mid-latitudes, the feasibility of using the present flood plain level to identify the bankfull stage in these regions should be avoided. Woodyer (1968) suggests that, for this reason, many flood plains may in fact be terraces and argues that channel benches should be used as an alternative.

A consistent definition of what can be considered the bankfull stage is problematic (cf. Kilpatrick & Barnes, 1964; Riley, 1972; Williams, 1978). Although definitions of bankfull discharge have included morphometric, sedimentary or discharge criteria, more often than not morphometric criteria are used to define the bankfull condition. Rosgen (1996) described bankfull discharge as the single most important parameter in morphological classification. He used bankfull discharge to relate dimensions such as width, meander length, radius of curvature, belt width, meander width ratio and amplitude to. He argued that the most consistent bankfull stage determination is obtained from the top of the flood plain. This is the elevation where incipient flooding begins for those flows that extend above the bankfull stage. He argued that it is important that the physical and morphological differences between a low terrace and a flood plain are recognized, since alluvial channels can often have low-level terraces adjacent to the flood plain, easily confused with the bankfull stage.

3.5 Effective discharge

In temperate alluvial channels, the term effective discharge has been used interchangeably with bankfull discharge and dominant discharge. Effective discharge can be defined as the discharge that transports the most sediment over time (Orndorf & Whiting, 1999). Leopold (1994) argues that although the largest flows have the greatest stream power and can do work on the channel boundaries at the greatest rate, they occur only rarely. At the other end of the scale, low flows have such low stream powers that they are incapable of altering channel boundaries, regardless of how often they occur. Moderate flows with moderate stream power can do more work over time and are therefore more efficient than rare high flows (Andrews & Nankervis, 1995). The definition of effective discharge in terms of sediment transport introduces substantial difficulties, as the rate of sediment discharge is difficult to determine. This will be discussed further in Chapter 4.

Pickup & Warner (1976) considered three separate variations of 'dominant discharge':

- *Effective discharge* - the range of flows that over a period of time transports the most bed load or bed material load (cf. Prins & de Vries, 1971).
- *Statistical bankfull discharge* - the 1.58 year flood on the annual series (cf. Dury *et al.*, 1963; Harvey, 1969)
- *Natural bankfull discharge* - the discharge that fills the channel banks (cf. Dury, 1961; Harvey, 1969; Pickup, 1976).

Using data from the Cumberland basin in New South Wales, Australia, Pickup & Warner (1976) attempted to determine which of the three 'types' of flows could be classified as 'dominant discharge'. Different techniques were used to estimate each 'dominant discharge'. For the estimation of *effective discharge*, Pickup & Warner (1976) divided the flow into classes, determined the flow duration within each class, and calculated the mean bed load discharge within the class and multiplied it by the duration. A histogram showing the amount of load transported by each class was then constructed. The most effective discharge was taken as the mid-point of the class which transported the most bed load.

Results indicated that a limited range of discharges were responsible for the transportation of much of the bed load. Below it, the flow was not competent to move the bed load. Above it, the reduced flow duration more than offset the higher rate of transport. The return periods for the *effective discharge* lay within the range of 1.15 to 1.45 years on the annual series, while for the partial series the return period lay between 0.20 to 0.40 years. The effective discharge was exceeded or equalled 3 to 5 times a year. This finding was in general agreement with Wolman & Miller's (1960) assertion that a large proportion of the sediment transport is accomplished at flows of low to moderate magnitude, but high frequency. Thus the channel form of streams in the Cumberland basin of New South Wales, Australia, were related to the optimum flow for bed load transport. Pickup (1976) therefore suggested that a bed load channel adjusts its slope so that it tends towards the optimum or bed load transport maximum form at the discharge which over time transports the most bed load.

Analysis of bankfull discharge yielded interesting results. In the Cumberland basin, bankfull discharge did not fall into the typical 1 to 2 year return period. Pickup & Warner (1976) argue that due to a bipolar flood frequency curve, the channel capacity is related to the large floods described by the upper limb of the flood frequency curve - a capacity equal to a peak discharge with a return period of around 4 to 7 years. They suggest two possible reasons for this situation. First, that channel capacities are equivalent to the 1 to 2 year flood, and that greater capacities reflect incision. They do however stress that channel resistance to erosion may completely modify the role of the hydrological regime depending on the strength of the channel perimeter material. Second, rivers with a highly variable hydrological regime may be related to less frequent events, as suggested by Harvey (1969). They therefore propose that many of the channels may be in a non-equilibrium state and conclude that in the Cumberland basin the capacity of the channel is related to high magnitude, low frequency events. It is only under these conditions that bank erosion, flood plain destruction and construction can occur. They suggest that the bed is shaped by high frequency, low magnitude events that occur on average 2 to 5 times a year. These small discharges are capable of transporting bed material, but are not competent to erode the banks. Thus Pickup and Warner (1976) identified two 'dominant discharges' - a major group determining the basic size and shape of the channel and a minor group determining transport capacity and the slope.

Working in the Yampa River basin, Andrews (1980) found that the most effective discharge occurred on average for a few days a year. He also found that the effective discharge and the bankfull discharge were almost identical, while the mean annual discharge was about 12% of the bankfull and effective discharges. He therefore argued that the close agreement between the effective and bankfull discharge would suggest that the channel is adjusted to the flows that transport the largest part of the annual sediment load, this was on average between 1.5 days per year and 11 days per year for the 15 sites in the Yampa River basin.

Pitlick & Van Steeter (1998) used duration data and sediment transport relations to determine the effective discharge for the upper Colorado River using the Parker *et al.* (1982) equation. At high discharges, they calculated unit bed load transport rates of between 3 to 4 kg m^{-1} s^{-1}. These compare well with other rates measured in other active gravel-bed rivers (cf. Reid & Laronne, 1995). The most effective discharges were found to occur at daily discharges in the range of 500 to 600 m^3s^{-1}, which occur on average about 2% of the time or on average 7 days per year, transporting approximately 30% of the annual load. More than 80% of the annual sediment load is carried by the highest 10% of the flows. This is in agreement with information presented by Ashmore & Day (1988) and Nash (1994) who have shown that the duration of the effective discharge increases with drainage area. (Data presented by these authors suggest that for rivers with drainage areas greater than 100 000 km^2 the effective discharge is exceeded about 10% of the time). The effective discharges for the upper Colorado were found to be slightly less than the bankfull discharge.

Pitlick & Van Steeter (1998) thus argue that aquatic habitats in the upper Colorado River are maintained by flows ranging from about half bankfull up to about the bankfull stage. At the half bankfull stage, gravel transport on a widespread basis is initiated, which is important for flushing fine sediment from the bed. Flows at the bankfull stage carry the majority of the sediment load and erode fine sediment from the side channels. These flows are therefore important for maintaining backwater habitats. Furthermore, these high flows define the upper limit for the onset of bank erosion and the formation of bars and side channels.

3.6 Dominant discharge, bankfull discharge and effective discharge in controlled and semi-controlled systems

Carling (1988) argues that the Wolman-Miller principle cannot be sustained in non-alluvial streams that are out of equilibrium or are unable to adjust their form freely. He was able to show that the concept could be applied to a sand-bed stream close to the steady state in the sense that, of a range of flows capable of transporting bed material, one class is the most effective in terms of the total mass transported, this being the bankfull condition. This relationship cannot be applied to a gravel-bed stream as high entrainment thresholds are required for bed movement. Overbank flows are often simply not competent to mobilize the bed completely.

Baker (1988), like Carling (1988), therefore argued that the Wolman-Miller principle needs to be adapted for different river types. In resistant bed rock rivers, adjustment cannot occur as easily as in alluvial channels (Harvey, 1984). Such systems are often sediment limited and the excess energy is often dissipated as remarkable intense turbulent phenomena (cf. Baker & Kali, 1998). Often the only flows capable of significant channel alteration in bed rock streams are high magnitude events.

Furthermore, Carling (1988) has argued that most channels probably have some slight 'system memory' of past events recorded in the channel form. He argues that for alluvial channels, negative feedback systems and short relaxation times (cf. Allen, 1974) ensure that the system memory is short and that the preferred channel morphology is largely invariant. Thus the concept of a unique discharge that fills the channel and transports the most bed load (usually the bankfull discharge) has been seen as morphologically significant and equated with 'dominant discharge' (Carling, 1988). It remains untested whether 'system memory' is as short in semi-controlled or controlled bed rock channels or in arid and semi-arid regions.

Gupta (1995) has shown that rivers in the seasonal tropics fall somewhere in-between the arid and temperate categories. Seasonal variability in discharge significantly alters the width-depth ratio and stream power. He argues that the seasonality of the flow produces a nested channel pattern, a large channel for the storm and a small channel for the high discharge of inter-storm periods. This channel architecture is similar to that reported in central Australia (Pickup, 1991) and South Africa (see Section 2.4), and suggests activity at a widely different and discrete scales. The tropics, located between two anticyclonic belts at about 30° north and south of the equator, are characterised by marked concentration of rainfall within a few months. This seasonality is transferred to the streamflow, and the hydraulic geometry of the river changes dramatically between the wet and dry seasons. Rivers of the seasonal tropics have to adjust to distinct separate periods of high and low flows. Equilibrium of river form requires adjustments to multi-scale discharges. This would suggest that channels in these landscapes cannot be related to a single dominant discharge, rather that they are related to a series of discharges.

3.7 Summary and management implications of the dominant discharge, bankfull discharge and effective discharge concepts

It is clear from the above discussion that the literature freely interchanges the terms dominant discharge, bankfull discharge and effective discharge. This leads to much confusion as the concepts are not interchangeable. The two key questions for geomorphologists are as follows: first, is the dominant discharge, bankfull discharge and effective discharge also the channel forming discharge? Second, are the frequencies of the dominant, effective and bankfull discharges the same as those measured using some recurrence interval or probability of exceedence? It is possible to argue that the characteristics of the channel dictate the dominant discharge rather than vice versa. This may be related to the imprint of past climates, or the resistance of the channel boundary to deformation. The resolution of these questions offers the potential to predict channel response to hydrologic regime.

It would appear that the usefulness of the dominant discharge approach is probably related to different climatic and channel boundary conditions. Alluvial channels that are free to alter their boundaries may respond to a dominant discharge. There is a case for arguing that there could be different dominant discharges for any characteristic of the channel, for example, a dominant discharge for width, slope, point bars and so on. It may only be appropriate to talk about dominant discharge in terms of maintaining overall channel form if the in-channel characteristics all respond similarly to the said discharge. This is unlikely to be the case, especially in southern African rivers where the hydrological regime is highly variable and structural control on the channel is considerable.

In terms of management implications, it is apparent that the magnitude-frequency debate forms the context within which an understanding of the flows necessary to maintain the channel form and the channel bed can be understood (given the limitations mentioned in the previous paragraph). The use of terms such as dominant discharge, bankfull discharge and effective discharge provides concepts around which the magnitude-frequency debate can move forward. Terms need to be clearly defined and concepts that were developed for certain types of channels should not be applied to others. While it is useful to use the bankfull discharge as a surrogate for effective discharge in alluvial channels, this should not be applied to a river responding to a variable hydrological regime, or a channel that is in disequilibrium or is structurally controlled. For the purpose of this thesis, the terms bankfull discharge, dominant discharge and effective discharge are defined as follows:

Dominant discharge usually refers to a conceptual discharge without a specific statistical, physical or sediment transport interpretation. For the purposes of this thesis, however, the definition as used by Marlette & Walker (1968) will be applied.

Bankfull discharge refers to a unique and measurable physical characteristic of the channel at a particular cross-section. For the purposes of this thesis, it refers to the boundary between the active channel and the macro-channel.

Effective discharge refers to the discharge that over a period of time transports the most bed material load.

3.8 Magnitude-frequency and floods

The concept of geomorphic effectiveness refers to the ability of an event to alter landforms and to the relative persistence of the altered landforms under the influence of processes tending to restore the landscape to its previous condition (Wolman & Gerson, 1978; Hugget, 1994). Miller (1990) has shown that large floods may not be 'effective', and that in order for a flood to be effective, it (p.132) "requires the coincidence of sufficiently large peak flows with a physiographic setting where large values of unit stream power can be applied to valley reaches with erodible alluvial bottomlands". In certain river systems, however, the only flows capable of significant channel modification are rare high magnitude events. The main reason for this is that high levels of applied stress are required to scour perimeter material. In order for modifications to occur, thresholds must be achieved that prevent low to moderate magnitude events from reconstructing the system (cf. Carling & Beven, 1989; Magilligan *et al.*, 1998).

The role of post-flood adjustment is of great significance (cf. McPherson & Rannie, 1969; Beaumont & Oberlander, 1971; Schwarz *et al.*, 1975; Anderson & Calver, 1977; Thornes, 1977; Moss & Kochel, 1978; Harvey *et al.*, 1979), especially the role of re-vegetation. If re-vegetation is rapid, and given a sufficient supply of sediment, the reconstructive process will be rapid. In semi-arid and arid regions, where vegetation growth is limited, high magnitude events may produce irreparable and therefore progressive changes in the channel (cf. Hack & Goodlett, 1960; Schumm & Lichty, 1963; Stuckman, 1969; Cleaves *et al.*, 1970; Burkham, 1972; Clarke, 1973; Costa, 1974; Gupta & Fox, 1974; Stevens *et al.*, 1975; Walsh *et al.*, 1994). In some instances, thresholds of non-recovery may be attained (Tricart, 1961; Brykowicz *et al.*, 1973).

In arid and semi-arid regions, large floods can have significant effects on channel form, both in terms of geomorphological work (sediment transported) and geomorphological effectiveness (landscape impact). Clearly then, climate and hydrology are important parameters determining the effectiveness of floods of differing magnitude and frequencies (Harvey, 1984). Kochel (1988) cites the example of dramatic channel and flood plain modification by large floods in Virginia (cf. Hack & Goodlett, 1960; Williams & Guy, 1973; Johnson, 1983), while hurricane Agnes floods (cf. Moss & Kochel, 1978) produced insignificant change. The response and recovery time from extreme events is of particular significance (cf. Baker, 1973; Thornes, 1976; Baker, 1977; Schumm, 1977; Dietrich & Dunne, 1978; Patton *et al.*, 1979; Hickin, 1983; Meade, 1983; Harvey, 1984; Nanson, 1986; Baker & Pickup, 1987; Schumm *et al.*, 1987; Lewin, 1989; McEwan, 1989; Baker & Kali, 1998).

Costa & O'Connor (1995) have argued that the recognition that some really large floods may not have long lasting effects or cause long-term changes in channel and valley morphology led to the realisation that the absolute magnitude of the event is not the sole factor responsible for the resulting landforms or their perseverence. They have argued that by generating a time stream power curve, it is possible to integrate the area under the curve to derive the total amount of energy that a flood expends per unit area, thus adding the duration dimension to the effectiveness (Figure 3.1). Using this method, they argue that there are three types of floods that are represented by three types of curves. Curve A (Figure 3.1) represents a flood on a low-gradient river that generates low stream power per unit area. Curve B represents a flood that generates high values of peak stream power per unit area and has a moderate to long duration. Curve C represents a flood which also generates high values of instantaneous peak stream power per unit area, but is short-lived. The floods that are the most effective are those floods that generate high stream power per unit area, but also expend considerable energy.

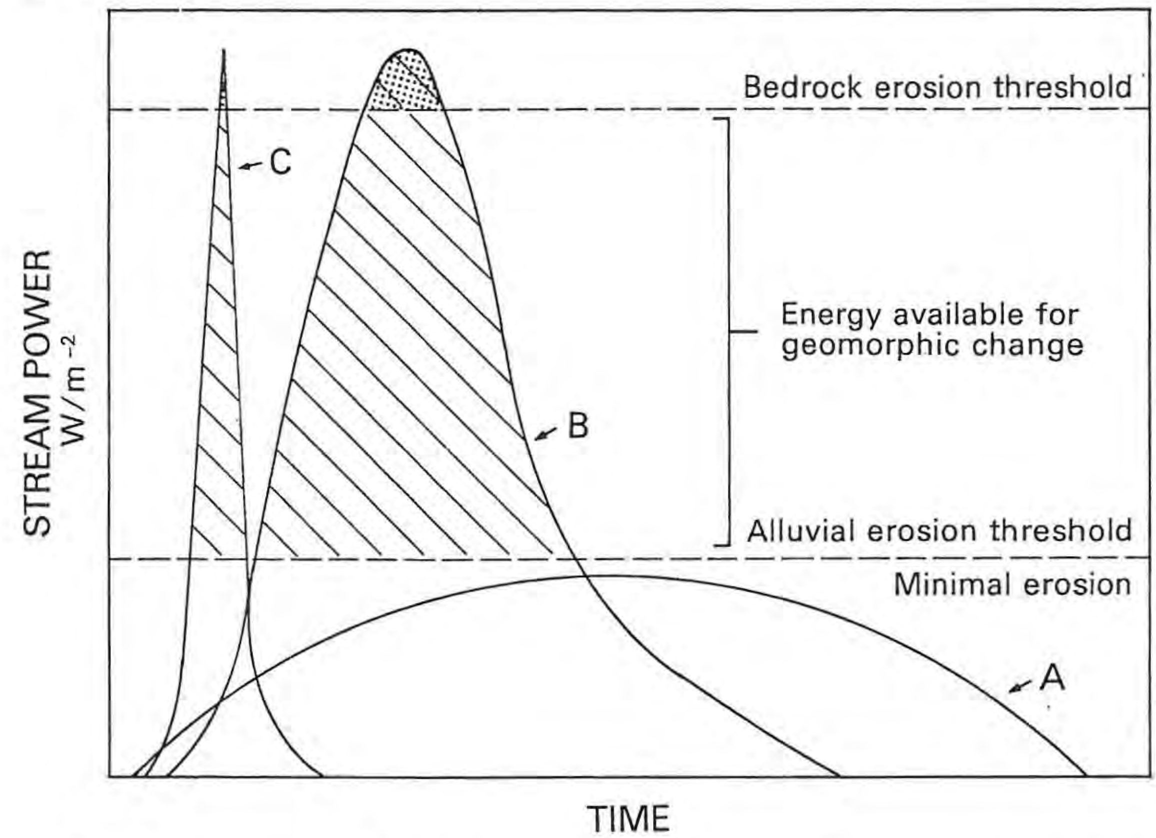

Figure 3.1: Conceptual stream power graphs used to determine geomorphic effectiveness of different types of floods (after Costa & O'Connor, 1995).

Of interest to the magnitude-frequency question, particularly in the Southern Hemisphere, is the debate that emerged in Australia about Flood and Drought Dominated Regimes (FDRs/DDRs). The concept was developed to explain the large-scale cyclical channel changes that occurred in many Australian rivers that were out of phase with well documented land use changes (Rutherfurd, 2000). FDRs are periods characterised by episodic catastrophic floods and persistent flood activity with runs of large floods for up to eleven years in a row separated by shorter periods of smaller floods. DDRs are relatively long periods of low flood activity when runs of floods occur for up to six years in a row separated by longer periods of little flood activity. Erskine & Warner (1998) argue that the alternating flood regimes appear to be caused by cyclical medium-term shifts in the location of the summer rainfall belt, with FDRs corresponding to a southerly incursion and DDRs to a northerly retreat. They have argued that rivers respond to the alternating flood regime by bank erosion, channel widening and chute cutting during FDRs, and deposition, channel contraction and chute infilling during DDRs. Erskine & Warner (1998) have pointed out that the alternating flood regime has important implications for understanding the physical functioning of Australian fluvial systems and has considerable management implications.

Kirkup *et al.* (1998) reject the FDR/DDR hypothesis, arguing that the notion has been overstated and that managing rivers on the basis of FDRs and DDRs, as had occurred in the past, was likely to be ineffective. They argue that the FDR/DDR hypothesis had seriously underplayed the significance of European disturbance on river channels and catchments, while overplaying the significance of climate-driven controls on river channel changes. Brooks & Brierley (1998) have shown that the massive sedimentation that resulted from European disturbance in the Bega catchment in New South Wales (which resulted in significant channel changes) was out of phase with FDR/DDRs. Brooks & Brierley (2000) thus argue that human alteration of channel and catchment conditions and increased geomorphic effectiveness of floods are the principal reasons for changes in channel morphology in NSW. The similarity in climate between southern Africa and Australia brings into question the possible significance of FRDs and DDRs in southern Africa. This has been argued for the Bell River in South Africa (cf. Rowntree & Dollar, 1996b).

3.9 Environmental flows in geomorphology

The final section of this chapter will consider the concept of environmental flows. For a full review see Dollar (2000). The ecological diversity and productivity of channels and flood plains are directly related to the areal extent, complexity and variety of physical habitats. This includes the channel bed, side channels and related habitats, as well as irregularities in the channel that provide cover and refugia from high velocity flows. This variety is dependent on the full range of natural flows, both high and low. Where rivers are impounded, reduced magnitude and frequency of flooding may lead to the accumulation of finer sediment on the channel bed. Where this occurs over long periods of time, the channel may narrow, resulting in increased flood risk and reducing the variety and areal extent of aquatic habitat (cf. Finlayson *et al.*, 1994; Gippel & Stewardson, 1995). The determination of the magnitude and frequency of regulated flows necessary to maintain the aquatic environment in a 'natural condition' is known as *environmental flow determination*. Environmental flows thus fall within the broad magnitude-frequency debate. Determining environmental flows is a complex endeavour. Methods range from simple abstraction of stream flow records to more complex techniques such as the Instream Flow Incremental Methodology (IFIM) (Milhous *et al.*, 1989). Traditionally, there are four main methods for determining environmental flows (Reiser *et al.*, 1989):

- *self-adjusted channel methods* base flows on a statistic determined from the pre-dam flow regime, the assumption being that the pre-dam channel has achieved a form of equilibrium;
- *statistical methods* recommend flows based on a flow duration or flood frequency curve;
- *sediment entrainment methods* recommend flows based on the discharges at the threshold of particle motion; and
- *direct calibration methods* involve the observation of bed movement, sediment transport or changes in fine sediment content by bed gravels.

There is much debate in the literature as to the goals of environmental flows. This is partly a result of the lack of consistency in the terminology employed. The objectives of the recommended flows need to be clearly stated. Terminology such as maintaining the river in a 'natural state' is too broad and can serve no real purpose. The goals must be stated in a manner that permit the identification of a particular discharge and water volume to achieve certain objectives, while accepting that in all cases there will be uncertainty associated with estimates of sediment transport.

Kondolf & Wilcock (1996) argue that when determining an environmental flow a distinction must be made between the ages of impoundments. For recently built impoundments, objectives may be stated in terms of maintaining certain aspects of the existing channel. In such cases, it is prudent to use flows based on the natural hydrograph. For old impoundments, the channel may already have adjusted to the regulated flow regime. Thus, methods for determining a flushing flow, such as using the natural hydrograph or channel geometry, may not be appropriate as they implicitly assume a mutual adjustment between hydrology, channel geometry and sediment transport. Furthermore, the range of flushing objectives are limited by the dam operating rules, release capacity of the reservoir, degree of post-dam adjustment, public safety and legal constraints (McMahon & Finlayson, 1995). In this case, it may only be possible to specify flows that perform some of the objectives, such as removal of fines. Other objectives such as maintaining natural channel geometry cannot be met (Kondolf & Wilcock, 1996; Wilcock *et al.*, 1996a).

Despite these inherent difficulties, the holistic management of rivers requires that an environmentally acceptable flow regime is based on sound scientific principles (Petts, 1996). Traditionally, environmental flows have been based on a minimum flow requirement, but the conservation or maintenance of a system requires a full range of flows. Petts (1996) established that the primary need in environmental flows is underpinned by five scientific principles: longitudinal connectivity, vertical exchanges, flood plain flows, minimum flows and optimum flows. The determination of all of these principles is complex, and requires an in-depth study of the river basin. This in-depth analysis is often lacking and, consequently, models used for determining instream flow requirements are imprecise. Furthermore, Petts (1996) makes the point that ecosystem response to flow regulation, physical habitat alteration and manipulation of biological communities is as yet indeterminate, and the models remain qualitative. Nevertheless, the ecologically sound allocation of instream flow requirements remains a fundamental component of environmentally sound river management. For the geomorphologist, this is essentially embodied in the magnitude-frequency debate.

3.10 Summary and conclusions

The aim of this chapter was to provide a conceptual framework for the magnitude-frequency debate. It has been pointed out that dominant discharge is primarily a concept, while the bankfull discharge and effective discharge are practical ways of determining or defining dominant discharge. Dominant discharge, bankfull discharge and effective discharge cannot, however, be used interchangeably. It has also been demonstrated that these concepts need to be applied with caution in different climatic and geomorphic regions. Nevertheless, they provide a useful means of moving the magnitude-frequency debate forward.

Furthermore, it has been pointed out that the role of floods is of great significance in arid and semi-arid rivers and in rivers that are strong controlled by bed rock. In these rivers, large floods are often the only flows that can be considered to be effective. This is of particular significance in southern Africa which has a highly variable hydrological regime and strong bed rock influence in the channel boundary. These issues will be taken up in Chapters 9 and 10.

Given the literature just reviewed, the aim of this thesis is to achieve the following: to examine the relationship between bankfull discharge, effective discharge and dominant discharge for three South African rivers.

Chapter 4: Geomorphological Approaches to Bed Material Transport

"Researchers have already cast much darkness on the subject, and if they continue their investigations we shall soon know nothing at all about it."
Mark Twain

4.1 Introduction

Schumm (1971) has shown that one of the major factors determining the shape and pattern of a river is its sediment regime. Although bed load constitutes a small fraction of the total sediment transported by a river, the movement of bed load is often responsible for the problems associated with shifting channels, loss of reservoir capacity and with local difficulties that arise in water abstraction (Reid *et al.*, 1985; Kondolf, 1995). Morisawa (1985) argues that a river will maintain a channel morphology that is most suited to the transportation of its bed load. Channel pattern has traditionally been seen in part as a function of bed load and calibre. The classification of channels according their bed load characteristics is common (cf. Schumm & Khan, 1972; Schumm, 1977; Miller, 1984; Church *et al.*, 1989). Reid & Frostick (1997) argue that a thorough knowledge of bed load transport in a river is essential, as the movement of bed load acts as a regulator of a river's character, geometry, planform, cross-section and long profile.

By inference then, any change in sediment supply or transport will have an impact on the fluvial system. Changes in sediment supply may be in response to tectonic movement, climatic change, major floods, land use change or human modification of the fluvial system (e.g. impoundments, water abstraction). If these changes are transient, they may cause sediment slugs or pulses to move through the system, marked by sedimentation zones in which changes in form and pattern are common (Church & Jones, 1982; Church, 1983). Changes in supply make the situation extremely complex, as supply events may be both spatially and temporally episodic (cf. Nordin, 1963; Ferguson, 1987; Simons & Simons, 1987). Temporal and spatial storage are therefore important determinants of potential channel form and pattern.

Clearly, bed material load in rivers plays an important part in understanding the functioning of fluvial systems, but there are also numerous other factors to consider. These include channel and valley slope, these are often functions of tectonic history (Gregory & Schumm, 1987); perimeter conditions, including vegetation (Thorne, 1991; Rowntree & Dollar, 1999); percentage of silt and clay in the channel banks (Knighton, 1987); human impacts, both direct and indirect (Park, 1981) and, channel forming discharge as discussed earlier. The focus of this chapter will be on bed material transport.

4.2 Basic terminology

The term *load*, as used in sediment transport, refers to the sediment in motion in a river. It is also used to denote the *rate* at which sediment is moved, for example, kilograms per second or tonnes per day. The *load* is further divided into two categories, *bed load* and *suspended load*. *Bed load* is defined as that part of the load moving on or near the bed by rolling, saltating or sliding. Bagnold (1973) defines bed load as those grains that are dispersed upwards from the stationary bed by occasional grain-to-grain and grain-to-bed impacts as the prevailing fluid drag causes them to shear over each other. Upward dispersive stress is balanced entirely by the immersed weight of the moving grain, implying that no net upward-directed fluid stress affects the bed load. Lift on bed grains due to fluid pressure variation around them is described by the Bernoulli equation. Table 4.1 presents a classification of sediment transport.

Of significance to this discussion is the issue of sediment supply. A hydraulically-controlled stream is one that is capable of moving virtually all sizes of material on the streambed. The amount transported is a function of the water's energy. For example, in a sand-bed stream there is virtually an unlimited supply of transportable material on the bed and it can be assumed that whatever is being carried is only limited by the energy of the water. A supply-limited stream is one in which there is a limited supply of transportable material on the bed, and the stream is able to transport more sediment than it is presently carrying. The impact of flow regulation may therefore be different in hydraulically-controlled and supply-limited streams. In a hydraulically-controlled stream if flows were reduced, aggradation would be expected because sediment supply would not change. In a supply-limited stream the capacity to carry sediment is much higher than the amount being delivered to the system, the flows could therefore be reduced and it would still be competent to transport the delivered material without aggradation occurring.

Table 4.1: Classification and measurement of sediment transport.

Movement classification	Source classification
Suspended load: is suspended in the flowing water by turbulent eddies. It moves faster than bed load.	*Bed material load:* is the material contributed by the streambed. Can be calculated by hydraulic calculations.
Bed load: moves by rolling, saltation or hopping along the stream bed. It is 'pushed' by the water. This pushing force is correlated with velocity and can be expressed as shear stress.	*Washload:* is always carried in suspension and washes through the system. It is not found in appreciable quantities on the bed. It cannot be determined by hydraulic calculations.

4.3 Particle entrainment

Part of the problem in predicting bed load transport is predicting the initial entrainment and movement of particles (Carling, 1983). Considerable effort has been expended on microscale studies of flow resistance, incipient motion of bed material and bed load transport (Johnston *et al.*, 1998). A particle generally starts to move when the force of the column of moving fluid that intercepts it generates a moment equal to the oppositely directed moment of the immersed particle weight. This is the balance between the fluid forces of drag and hydrodynamic lift, which turns a particle, and the resisting forces of the immersed-particle weight, which keeps the particle at rest (Helley, 1969). When the two opposing forces are just in balance, the fluid is competent to move its bed particles and critical or threshold conditions exist (Andrews, 1983). This assumes that the particle is available for entrainment. The conditions necessary to initiate motion depend on particle size, slope, specific gravity, shape, density, surface roughness, orientation angle, surface packing, exposure to flow and so on (cf. Beaumont & Oberlander, 1971; Miller *et al.*, 1977; Morisawa, 1985).

Reid *et al.* (1997) make the point that most transport equations incorporate a term that defines the critical flow condition for transport. The reliable application of these equations therefore depends on the appropriate specification of these conditions. The conditions under which particle movement ceases is equally important, and are not necessarily the same as those conditions that initiated motion. Most researchers make use of critical shear stress, or critical average velocity (cf. Shields, 1936), while some advocate the use of unit stream power rather than shear stress (cf. Yang, 1973).

Andrews (1983) reports on an investigation to determine the threshold conditions necessary to entrain gravel and cobbles from a river bed composed of heterogenous material. In sand-bed rivers, bed forms have a major impact on transport rates (Bradley *et al.*, 1972; Dietrich *et al.*, 1979). Andrews (1983) was able to show that the presence of bed forms in all types of rivers considerably increases the shear stress necessary to initiate particle motion compared to the critical value for a flat bed. Leopold *et al.* (1964) had already noted that particle spacing exerted more control over movement than did particle size, and they were able to show that little relationship existed between the size of the gravel and the distance moved.

Wilcock (1992) has suggested that where a bed has coarse, mixed-size sediments, all sizes may begin moving over a range of flow conditions that is relatively narrow. A number of authors (cf. Komar, 1987; Wiberg & Smith, 1987) have shown that in the size range of medium sands through to gravel, larger particles of a size distribution are moved at flow stresses less than those required to entrain that size from a uniform bed. This issue will be discussed further in Section 4.4. In the opposite direction, the finer-sized fractions require greater flow stresses than if they had formed under uniform deposits. The complexity of entrainment is infinitely greater under non-uniform bed conditions. It would appear that the bed condition acts as a major controlling factor in determining incipient motion, especially in gravel- and cobble-bed rivers. This is particularly so after a prolonged period of no sediment transport, where the bed material has had time to become consolidated (Reid *et al.*, 1997). The infiltration of fine, cohesive sediments into a framework of coarser sizes can create a powerful cementing effect. Reid *et al.* (1997) have demonstrated from field measurements that negligible transport may occur during the rising stage of the first flood after a long period of stasis. Once the armour layer or bed structure has been broken, transport on the falling stage of the hydrograph may be considerable, thus the conditions for the initiation and cessation of motion can be substantially different. Where floods are closely spaced, however, the bed material remains comparatively loose and offers less resistance to entrainment, such that considerable transport will occur on the rising limb of the hydrograph (Reid *et al.*, 1997). The critical conditions are, thus, to some extent dependent on flow history so that it is possible for bed load transport rates to vary widely, even at the same river stage, or during the same flood event.

Baker & Costa (1987) have attempted to determine the impact of flooding on sediment entrainment and bed load transport and have found that the highest shear stresses (Equation 4.1) and stream power per unit area (Equation 4.2) are not necessarily associated with the largest discharges. High values of stress and power occur mainly in bed rock channels. Large rivers like the Mississippi and Amazon that experience major floods in fact experience relatively low unit stream power as the increase in discharge is accommodated by width adjustments as opposed to depth and velocity adjustments in bed rock rivers (Baker & Costa, 1987). Magilligan (1992) has shown that major morphological adjustments in alluvial rivers do not occur unless mean bed shear stresses exceed 100 Nm^{-2} or stream power per unit area exceeds 300 Wm^{-2}. In bed rock rivers Wohl (1992) has demonstrated that boulder bars only become mobilised at unit stream powers of around 1000 Wm^{-2}. Floods that generate these levels of stream power are thought to have a return period of around 200 years in bed rock rivers.

$$\tau = \gamma RS \quad \text{.......} \quad (4.1)$$

where

τ is shear stress (Nm^{-2})

γ is specific weight of the fluid (9800 Nm^{-3})

R is the hydraulic radius (m)

S is the energy slope (m/m)

$$\omega = \left(\frac{\gamma Q s}{w}\right) \qquad (4.2)$$

where

ω is unit stream power (Wm^{-2})

w is the channel width (m)

Pitlick & Van Steeter (1998) propose that the key factor in estimating thresholds for sediment transport and channel change is developing appropriate methods of determining boundary shear stress (τ) and critical shear stress (τ_c). Average boundary shear stress is given by

$$\tau = \rho g D S \qquad (4.3)$$

where

ρ is the density of the water (kg m^{-3})

g is the gravitational acceleration (m s^{-1})

D is the flow depth (m)

In the absence of direct observations of particle entrainment the only practical means of estimating τ_c is to use the Shields criterion where

$$\tau_{critical} = \tau_{ci} = \tau^*_{ci}(\rho_s - \rho) g D_i \qquad (4.4)$$

where

τ_{ci}^* is the dimensionless shear stress

ρ_s is the density of the sediment (kg m^{-3})

D is the particle diameter (m)

There has been considerable discussion (cf. Parker *et al.*, 1982; Gomez, 1995) as to the minimum value of τ_{ci}. It is now fairly well recognised that significant motion of the bed, which is characterised by continuous movement of particles and much higher transport rates, occurs at τ_{c50}^* (where τ_{c50}^* is the critical dimensionless shear stress for the particle size where 50% of the bed material is finer) in the range of $0.045 < \tau_{c50}^* < 0.06$ (Wilcock & Southard, 1989; Andrews, 1994; Pitlick & Van Steeter, 1998). At discharges higher than this ($\tau_{c50}^* < 0.09$) the transport is so rigorous that gravel-bed forms begin to develop. The impact of bed forms on bed material transport is discussed in Section 4.4. Minimum values of $\tau_{c50}^* \sim 0.03$ are required for initiation of transport, but at these levels very few particles of any size are moving and bed material transport rates are very low (Pitlick & Van Steeter, 1998).

Carling & Tinkler (1998) have shown that where large boulders are of the same magnitude in terms of vertical dimension to the depths of normal floods (recurrence intervals in the range of 1 to 5 years), it is questionable whether flow magnitudes experienced over decades or centuries are competent to move them. It is therefore difficult to determine an initial motion criteria for large boulders in shallow, non-uniform and unsteady flow conditions. In bed rock systems, flow is frequently not only non-uniform, but the mode of boulder movement may be by sliding as well as rolling. It is thus clear that empirical and theoretical relationships between the entrainment force and the force resisting motion commonly involve coefficients that are substitutes for the imperfect knowledge of critical parameter values in the force balance. The result of this is that a single coefficient subsumes various physically distinct effects. These findings beg the question whether the classic concept of competence is of relevance in gravel-bed rivers with complex bed forms. The present state of knowledge is certainly incomplete and, as Carling (1983) has stated, insufficient data presently exists for defining a threshold of motion for (large) particles in natural stream flows.

4.4 Bed heterogeneity

The structure of the channel bed has been shown to have a major impact on bed load transport (Brayshaw *et al.*, 1983; Rhoads, 1994b). Where sand-beds occur, most if not all of the bed is available for transport (Ferguson *et al.*, 1989). In gravel-bed rivers where there is a complex bed structure as well as a variable assemblage of grain sizes, the availability of particles for entrainment is complex. Gravel-bed rivers are defined as those in which hydraulic processes are controlled by material coarser than 2 mm in diameter. Gravel-bed rivers are characterised by macro bed forms, pools and riffles and the general absence of smaller scale ripple, dune and antidune features (Hey & Thorne, 1983).

Gravel-bed rivers are commonly armoured (Klingeman & Emmett, 1982; Dunkerley, 1990). Armour refers to a bed where coarse grains have been concentrated over the original sediment mix (Kuhnle & Southard, 1988). The presence of an armoured layer poses a problem in the calculation of bed load transport (Nanson, 1974). It has been mentioned in Section 4.3 that heterogenous beds can affect the forces acting on a given particle in two significant ways. First, the relatively smaller particles in a mixture are hidden in the turbulent wake of the relatively larger particles and, second, the forces needed to start a larger particle rolling over smaller particles is less than that required to start a smaller particle rolling over larger particles (Bathurst, 1987a). This would suggest that less shear stress is required to entrain a given size particle if that particle is surrounded by smaller particles rather than larger particles (White & Day, 1982; Andrews, 1983; Proffitt & Sutherland, 1983). For bimodal sediments, transport may consist of sand and fine gravel moving in threads between cobbles and boulders.

In many cases, the clast shapes and sizes allow for the consolidation of the clasts into tightly interlocking structures during periods of low flow (Bathurst, 1987b). As noted earlier in Section 4.3, critical tractive forces may be increased by up to three times in this regard. Conversely, on the falling limb of a flood, transport may continue to a value up to six times lower than that corresponding to initiation of motion on the rising stage. Thus Bathurst (1987b) suggests that due to these factors, transport during storm events can occur at relatively high rates for up to several days after a storm. There may also be an aftermath of relatively high transport rates in subsequent storms (Tacconi & Billi, 1987).

Rhoads (1994b) has shown that flow resistance varies significantly not only between pools and riffles, but also within these distinct morphological features. Rhoads (1994b) has also shown that these differences in terms of shear stress, near-bed velocity and profile averaged velocity can be greater at single locales than the differences between pool and riffles. These differences can also vary with stage. Sediment transport for a river as a whole may be accomplished by a large number of disconnected zones of moving sediment, associated with areas of flowing water with depth and velocity sufficient to entrain and move bed material (which are termed jet zones) (Mosley & Jowett, 1999).

The acknowledgement of the significance of bed microforms and the changing integrity of the armour-layer appears to provide some explanation as to why bed load discharge is often out of phase with changing hydraulic conditions (Reid & Frostick, 1987; Hassan & Reid, 1990; Hoey & Sutherland, 1991). Reid & Frostick (1987) argue that most bed load transport equations are based on the assumption that the bed of a stream will respond to the applied stress in the same way, and that bed load begins and ends at the same threshold value of applied force. Both these assumptions have been shown to be inappropriate (cf. Brayshaw, 1985; Reid & Frostick, 1987). Furthermore, bed load transport equations assume that bed load transport rates will continue to rise as a function of increasing stream energy (stream power or shear stress).

Reid & Frostick (1987) argue that the mismatch between the flood hydrograph and sediment transport rates can be ascribed to the effects of bed microforms and pebble clusters, and the fact that there are significant differences between traction thresholds at the beginning and ending of sediment motion. Pebble clusters are the most common microform in gravel-bed rivers (Reid *et al.*, 1997). In sand-bed rivers these are usually ripples and dunes. Pebble clusters are groups of interlocking clasts formed around exceptionally large bed particles and standing above an otherwise planar gravel-bed. The principal components of clusters have been shown to be an obstacle clast, around which is developed an upstream stoss deposit and a downstream wake deposit (Brayshaw, 1985) (Figure 4.1). Grains in the lee of an obstructing particle suffer considerable reduction in lift and drag forces. Accordingly wake-side clasts are far less susceptible to entrainment than are their exposed counterparts (Brayshaw, 1985). Brayshaw (1985) has further shown that in a number of gravel-bed streams, only 29% of the particles can be considered to occupy reasonably exposed positions - the implicit assumption in treatment of initial motion and bed load transport equations. Furthermore, Brayshaw (1985) argues that between 50% and 70% of bed particles can experience a delay in predicted incipient motion beyond that predicted for more exposed equivalents of like size and shape. Rooseboom & le Grange (1992) have shown that these microforms can increase roughness to such an extent in sand-bed rivers that negligible transport may occur, even during flood conditions.

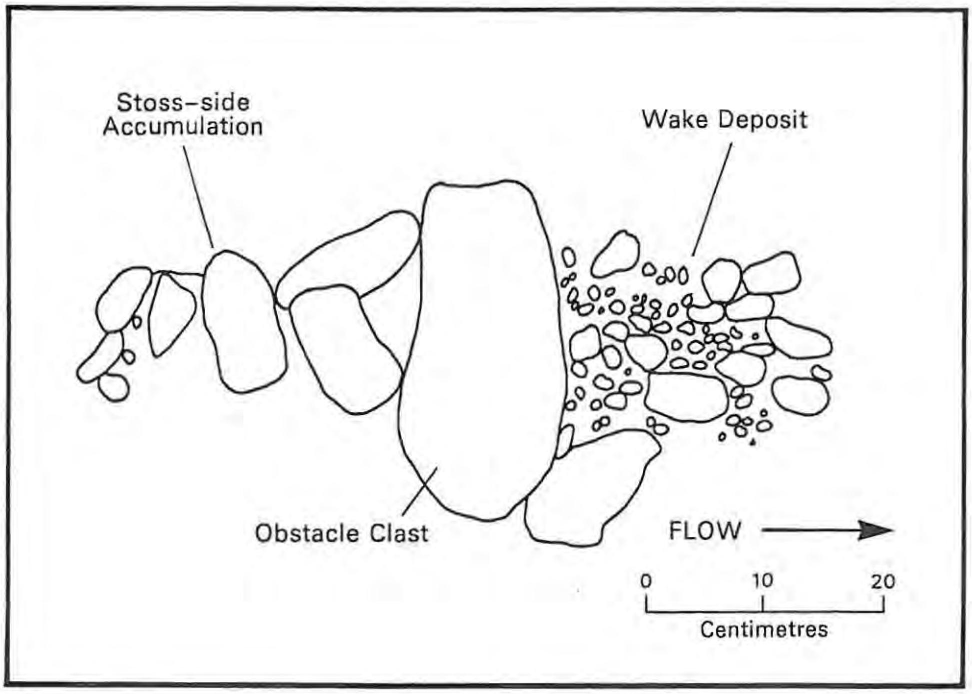

Figure 4.1: Obstacle clasts (after Brayshaw, 1985).

4.5 Temporal variations in bed load transport rates

Temporal variability in bed load transport rates under quasi-steady flow conditions were first identified in the 1930s (Carey, 1985; Hoey, 1992). As mentioned in Section 4.3, transient bed load transport conditions are commonly found in many different environments in the field (cf. Lekach & Schick, 1983; Proffitt & Sutherland, 1983; Ashworth & Ferguson, 1989; Ashmore, 1991; Schmidt & Ergenzinger, 1992; Wharburton, 1992; Reid *et al.*, 1998). Short-term variations in bed load transport have been observed in gravel-bed rivers at times of steady streamflow (cf. Klingeman &

Emmett, 1982; Carling *et al.*, 1998), while longer-term pulses at uniform flow have also been shown to exist (cf. Pickup *et al.*, 1983; Nicholas *et al.*, 1995). As mentioned earlier, at a given discharge, bed load transport rates for the rising and falling limb of the hydrograph can differ by an order of magnitude, with the rising limb rate being less than the falling limb rate or vice versa (Kuhnle, 1992; Moog & Whiting, 1998).

During the rising limb, availability and mobility of bed material for transport appear to be controlled by the armour layer. These conditions may exist well beyond those producing critical tractive forces. During the falling limb there is generally a reduction in bed load transport as the armour layer is re-established during the waning limb of the flood flow (Gomez, 1983). Reid *et al.* (1985) have suggested that one of the factors that may help explain the confusion surrounding hysteresis effect with the passage of a flood wave is the availability of sediment from one flood to another. This availability need not necessarily be due to the temporal exhaustion of supply (cf. Leopold & Emmett, 1976), but may be due to temporal differences in the resistance of the bed material to movement. Long periods between floods may allow for particle interlocking, thus adding strength to the bed. As a result, the first flood generates significant coarse bed load during the recession limb, only after the rising limb has loosened the structure and winnowed out the fines.

Reid & Frostick (1987) have shown at Turkey Brook, north of London, that the incidence of bed load transport in relation to floods is highly variable. At times bed load may be initiated on the rising limb of the hydrograph, at other times no movement occurs until after the flood peak on the recession limb of the hydrograph. It is clear from the international literature that transport rates do not follow a simple pattern mimicking the flood hydrograph. From a river management perspective, the occurrence of large-scale bed load pulses presents considerable difficulties for any attempt to sample or predict mean bed load transport rates (Goff & Ashmore, 1994). The movement of macropulses has been argued as being a major factor in controlling channel change (cf. Lane *et al.*, 1996). Where bed load moves in the form of pulses, actual transport rates may be considerably lower than predicted rates.

A further complication in bed load transport is that of velocity reversal. Sidle (1988) has shown that during moderate flows, transport competence is greater in the riffle than in the pool and largely sand-sized particles are transported. As flow increases, the hydraulic gradient of the pool-riffle sequence tends to even out and coarse particles become entrained and are subsequently deposited on downstream riffles. Keller (1971) suggested that this phenomenon accounted for the areal sorting of sediments and the maintenance of pool-riffle sequences. Jackson & Beschta (1982) similarly suggest that this results in a 'leap frogging' effect where bed material is moved from riffle to riffle. New evidence has shown that this situation is not necessarily found in all pool-riffle sequences (cf. Knighton, 1998).

A conceptual approach is needed that takes account of the two phase transport process that may occur in coarse-bedded rivers (cf. Beschta, 1981; Jackson & Beschta, 1982; Klingeman & Emmett; 1982; Bathurst, 1987a; Knighton, 1987). *Phase I transport* occurs when the flow is below a threshold for the breakup of the armour layer and bed load consists of the finer fraction of the bed material moving between the coarser fraction (Gomez, 1983; Knighton, 1987). The fractions are small and, consequently, bed load transport equations based on the assumption of a uniform sediment size will necessarily over-predict the observed volume as they assume that all size fractions are mobile when transport begins. In boulder-bed streams, where most transport is Phase I type, Knighton (1987) suggests that over-prediction may be several orders of magnitude.

Phase II transport occurs when the flow exceeds a critical value for the movement of the coarse or armour layer, or bed macroforms. Under these conditions, it is possible for all size fractions to be moved, and therefore sediment supply is unlimited. Parts of the coarse surface layer may be maintained and as a result of the subtle balance derived from the coarse surface material and from the exposure/hiding effect, there is approximately equal mobility for all size fractions. The effect of the non-uniform size distribution is then minimal and predictions of bed load transport can be based on one size diameter without serious error (Knighton, 1987). Phase II type transport equations occur where there is a restricted range of bed material sizes (1-100 mm) and in which sediment moves in events much greater than the thresholds needed for bed load transport (Knighton, 1987). These are likely to be gravel-bed rivers and have slopes of less than 1%.

Much of the research into bed load transport has been conducted in sand- or gravel-bed rivers with a permanent flow. Research into bed load transport rates in ephemeral arid systems has only recently made progress. Laronne & Reid (1993) have reported on data from a bed load trap in Israel which shows that ephemeral rivers can on average transport bed load up to 400 times more efficiently than perennial counterparts. They argue that this increased efficiency is due to the different vertical structure of the stream bed. While perennial gravel-bed rivers have a well-developed armour layer, ephemeral rivers have poorly developed or no armour layers. The lack of an armour layer results in a reduction in size-selective transport, and consequently ephemeral rivers may be more effective bulk sediment carriers (Reid & Laronne, 1995). This leads to the problem of predicting bed load transport in ephemeral streams, as most sediment transport equations are calibrated and designed for sand- and gravel-bed rivers (Reid *et al.*, 1996).

4.6 Approaches to predicting bed load transport

There are a number of approaches to predicting bed load transport. These include formulae based on shear stress (e.g. DuBoys, 1879), discharge (e.g. Schoklitsch, 1934), stochastic functions for sediment movement (e.g. Einstein, 1950) and those based on stream power (e.g. Bagnold, 1980). The development of these models are based on certain theoretical considerations that attempt to link bed load transport rates to hydraulic and sedimentological properties, empirical observation and testing to determine the coefficients and constants on the basis of the available data (Gomez & Church, 1989).

The theory behind most bed load transport equations is that there is always a determinant relationship between sediment discharge and a dominant independent variable such as flow discharge, flow velocity, energy slope or shear stress (cf. Yang, 1973; Bathurst, 1987b; Karin, 1998). The preceding discussion has demonstrated that this is not always the case. Part of the problem of relating bed load equations to field conditions is that most bed load equations were developed in the laboratory with uniform sized sediments (Yalin, 1963; Bathurst, 1987a). Rhoads (1994a) has pointed to the significance of the type of flume in determining incipient motion. In a sediment-feed flume, the final equilibrium state is determined by flow and sediment input and is independent of initial conditions. In a recirculating flume, the upstream sediment input depends in part on the initial composition of the bed material. Thus the equilibrium state is not independent of initial conditions. Further important considerations are that all available sizes are assumed to begin to move at the same critical flow conditions, that sediment density is uniform, and that negligible movement occurs below this critical condition.

Furthermore, many field based studies of sediment transport are directed towards assessing sediment related problems, rather than seeking to evaluate theory. Bagnold (1966) states that the dilemma is that no established branch of physics has interested itself in the two-phase flow (fluid-solid) that is involved in sediment transport. It follows that the complexity of two-phase flow cannot properly be tackled until the intricacies of fluid-flow are mastered, fluid turbulence in particular. The complex nature of sediment transport simply cannot be recreated in a flume environment, thus all equations developed for sediment transport estimation remain at best estimates.

Ackers & White (1973) rejected the early preference for using shear stress as the main parameter defining a rivers transporting power. They suggested that the total shear on a deformed bed is in part composed of along-stream components of the normal pressures on the irregular bed profile. Although these pressures may contribute indirectly to sediment motion through suspension, many sediment transport equations separate the bed shear into non-transporting form loss, and shear on the grains. The rate of transport is sensitive to transporting power, and as such inaccuracy in the separation procedure gives rise to large prediction errors. Ackers & White (1973) argue that this factor is important, as very few natural streams have a plane bed. They suggest that because shear stress is not the most rational basis of sediment transport function, stream power should be used instead.

An alternative approach to predicting bed load transport is to use the virtual velocity method. This method uses data of the virtual velocity of the particle movement, dimensions of the active channel layer, and the porosity and density of the bed material (Haschenburger & Church, 1998). Virtual velocity is defined as the total distance travelled by individual grains divided by the measurement interval - typically the total time of competent flow during a flood event. The fundamental equation for the mass transport of bed material is given by:

$$G_b = v_b d_s w_s (1-p) \rho_s \qquad (4.5)$$

where

v_b is the mean travel rate of the bed material (m h^{-1})

d_s is the active depth of the stream bed (m)

w_s is the active width of the stream bed (m)

p is the fractional porosity of the channel sediment

ρ_s is the mineral density of the sediment (kg m^{-3})

Haschenburger & Church (1998) were able to show that the virtual velocity method provided good results and in general, replicated what is known about sediment transport-flow relations in gravel-bed rivers derived from conventional sampling approaches. In particular, they found that the virtual velocity approach confirmed the sensitivity of transport to stream power that is typical for gravel transport near the threshold for significant transport. Results showed the often quoted disproportionate importance of the highest flows in transport which arises from the non-linear increase in transport with flow magnitude (Haschenburger & Church, 1998).

4.7 Limitations of bed load transport equations

Despite over a century of work on bed load transport, a satisfactory, universal formula has yet to be developed. Gomez & Church (1989) note that there are more transport formulae than there are reliable data sets by which to test them. Reid & Frostick (1987) have stated that even the best known predictive equations have not yet been sufficiently developed for universal application to rivers outside the one from which they were derived. They ascribe this to two factors. First, each river has a unique hydraulic and sedimentological character. Second, even where complicated bed arrangements have been acknowledged (cf. Einstein, 1950; Proffitt & Sutherland, 1983), there has been a tendency to seek an *average* response of particles to applied stress. A number of assumptions are made when using bed load transport equations. These include:

- that the flow and sediment properties for the period in question are invariant and can be described with reference to a steady state;
- that the bed load transport is a unique function of tangible and comprehensive flow and sediment parameters; and
- that the maximum possible amount of bed load is being transported. In other words, that the formulae describe an equilibrium state.

Computed results are susceptible to error stemming from uncertainties in the exact values of the hydraulic variables, in particular velocity, depth and slope, which affect calculations of critical shear stress and stream power (McLean, 1985). Gomez & Church (1989) have shown that sampling errors and conceptual errors may produce errors of up to an order or two of magnitude. Most bed material is transported by runoff events in which flows are very unsteady in nature, yet the effect of flow unsteadiness on the rate at which sediment is transported remains poorly understood. Despite this, all bed load transport equations assume steady uniform flow. Furthermore, formulae are derived from a restricted data base. This has resulted in a proliferation of bed load formulae rather than a consolidation of existing knowledge. The traditional approach has been to calculate the transport rate for a single characteristic grain size, for example, the median. This can lead to poor results in bimodal bed rivers (Wilcock, 1998).

As mentioned previously, where a heterogenous bed occurs, only the highest flows are capable of moving the entire bed. Even where moderate events occur, only partial sediment transport occurs with some sizes in motion and others not. Under these conditions the transport rate for the moving size fraction is not directly comparable with the rate for a uniform bed material of the same mean size as those fractions within the bed material. As a result, equations assuming a uniform bed material size will overestimate the observed rate since they assume that once any transport begins, all size fractions are in motion. One way of overcoming this problem is to apply the transport equation separately to each bed material size fraction and sum the resulting partial transport rates to give the total rate. Additional problems are then encountered as the relative effects of the different size fractions in impeding or promoting each others' movement and for the effect of bed armouring need to be taken into account (Reid *et al.*, 1997). Little progress has been made in this regard.

4.8 Comparison of bed load transport equations

Yang (1973) applied the following criteria for evaluating sediment transport equations: the equation should be theoretically sound; it should be dimensionally homogenous; it should be thoroughly verified by both laboratory and field measurements that cover a wide range of variations in both flow and sediment conditions; the parameters used in the equation can be obtained from both laboratory flumes and natural streams without much difficulty; and the computations should be simple and straightforward. Due to the large number of sediment transport formulae available, it is instructive to select a formula most appropriate to the physical conditions of the bed. The suitability of the formulae should be judged on the generality of the basic assumptions used and, most importantly, by comparison of the bed load discharge prediction with measurement. A number of comparisons for accuracy of different formulae have been made. These include White *et al.* (1975); Alonso (1980) and Yang (1984). Most bed load transport formulae were developed for sand-bed rivers and as such should not be applied outside of these conditions (Vanoni, 1964; Graf, 1971; Simons & Şentürk, 1977). Fewer equations have been developed for gravel- and boulder-beds, those that exist have been reviewed in White *et al.* (1975); Bathurst *et al.* (1987) and Gomez & Church (1989). The modification of popular sediment transport models to fit local conditions is common (cf. Misri *et al.*, 1984; Smart, 1984; Bathurst, 1987a; Diplas, 1987; Phillips & Sutherland, 1989; Shih & Komar, 1990).

Many attempts have been made to verify bed load transport equations. However, one of the problems is that the various approaches can only be tested in relation to one another (Reid *et al.*, 1997). Three major problems with verification were identified by Gomez & Church (1989):

- Most attempts at verification have been based on comparing the calculated bed load transport rate with the bed load transport rate measured in a flume or a natural stream (Carson & Griffiths, 1989). Relatively few verifications refer to channels outside the sand- to fine-gravel range. The performance of these formulae has therefore not been assessed with respect to the range of grain sizes for which they were ostensibly derived.
- There is considerable overlap of data employed in the development of many subsequent evaluations (cf. Ackers & White, 1973; White *et al.*, 1975; Yang, 1973). The formulae which are most reliable were developed on the basis of relatively extensive data.
- There has been little attempt to select test data which refer consistently to the hydraulic and sedimentological conditions that the data specifically purport to describe (i.e. steady flow and equilibrium transport conditions).

Gomez & Church (1989) selected ten formulae for testing. These were divided into two categories, those applicable to sand-bed and those applicable to sand- and gravel-bed rivers. The sand-bed river equations tested included Schoklitsch (1934; 1950) and Meyer-Peter & Müller (1948). The sand- and gravel-bed equations included DuBoys-Straub formula (Straub, 1935), Einstein (1950), Ackers & White (1973), Bagnold (1980) and Proffit & Sutherland (1983). Gomez & Church (1989) found that the equations of Bagnold, Einstein and Ackers & White perform best. (For the purposes of this thesis, the Yang, Ackers & White and Engelund & Hansen equations were used. Justification for the use of these equations are given in Chapter 8). Only the Einstein equation consistently under-predicts the river data. Most of the formulae over-predict, possibly as a result of the failure to account for surface coarsening in reducing the rate of transport of fine material in gravel-bed rivers with low, overall rates of transport. Similarly, they fail to take account of the fact that the whole discharge may not be available or utilised for sediment transport (Gomez & Church, 1989). This effect is realised in two ways. First, no account is taken of the resistance afforded by bed forms. Second, the use of average hydraulic variables (e.g. average velocity) which relate to the entire cross-section, fail to take into account the fact that only a portion of the bed may be active at any given time.

The complexity of the bed load transport process is such that little real progress has been made in the field (Carling *et al.*, 1998). Part of the reason for this is that modellers have not taken sufficient notice of the role of process in bed load transport. Ashworth *et al.* (1992) make a plea for (p.1895) "the need for larger research teams, pooled equipment and expertise, and a focus on taking intensive and representative spatial and temporal hydraulic and bed load measurements using a rigorous research design".

4.9 Bed material transport and river management

Many of the problems associated with river management are related to an inadequate understanding of the role of bed material transport in rivers. Changes in the sediment load and/or bed type in rivers usually have complex, long-lasting biological consequences (Kondolf & Wolman, 1993; Trimble, 1997). Surficial bed-material size is often the primary influence on benthic invertebrate community composition and density. Bed sediment influences habitat suitability for fish, and to a lesser extent for invertebrates that live on or in the bed (ASCE, 1992).

Human impacts may change the relationship between channel hydraulics and bed sediment size. While short-term temporal variations in bed-material type are common, longer-term temporal variations in bed type occur infrequently. If sediment loading is greater than capacity, channel morphology or bed type may change. In coarse-bedded channels, such as boulder-cobble or cobble-gravel-bed streams, interstitial voids provide important habitat - the hyporheic zone. If these interstitial voids are filled or covered by finer material, such as sands and silts, their habitat value is greatly reduced. Human activity has been shown to result in hyporheic interstitial sedimentation (ASCE, 1992). It is clear that sediment management is an important component of river management. It is only recently, however, that sediment management has been considered a part of an environmental flow (Milhous *et al.*, 1994).

Van Steeter & Pitlick (1998) have shown that flow reductions in the Colorado River have resulted in significant channel narrowing, as well as reductions in side-channel areas. Discharges that approximate the bankfull stage are necessary for a clean loose substrate, critical to the reproductive success of Colorado squawfish. Narrowing of the channel represents significant losses in potential fish habitat. They found that sediment accumulation on the bed can degrade the quality of the spawning bars and fill the interstices in the bed where organisms live. These can only be winnowed out by moving the protective gravels around them (Pitlick & Van Steeter, 1998).

Wilcock *et al.* (1996a; 1996b) have shown how flow regulation in the Trinity River has reduced the mean annual flood from 525 to 73 m^3s^{-1} and the 2 year flood from 484 to 30 m^3s^{-1}. Concurrent increases in sediment yield from tributaries as a result of road construction and timber harvesting have created a sedimentation problem. Little transport of the bed material occurs in the river at flows less that 85 m^3s^{-1}, and no transport of bed material coarser than 1 mm occurs at typical post-dam minimum flows of 4 m^3s^{-1} (1961-1978) and 8.5 m^3s^{-1} (1978 onwards). This has resulted in the encroachment of riparian vegetation and a narrowing of the active channel. The active channel has narrowed by 20 to 60% of its pre-dam width, resulting in a straightened channel and reduced topographic variability (Wilcock *et al.*, 1996b).

4.10 Conclusions

The preceding discussion has demonstrated the significance of bed material and bed material transport in fluvial systems. It has been shown that bed material transport is a complex process which is difficult to model accurately, particularly in coarse grained, heterogenous beds under unsteady flow conditions. Very little real progress has been made either in gaining an understanding of the process itself, or in the development of realistic sediment transport models that can be applied to natural systems (Carling *et al.*, 1998). Furthermore, as long as the physics of bed load transport remains incompletely understood, there is no reason to believe that any of the available bed load transport formulae will result in accurate results (Gomez & Church, 1989).

Nonetheless, when faced with a practical geomorphological problem such as recommending flows that will perform a specific sediment transport task (e.g. entraining gravel or maintaining a riffle), the application of highly simplified, imprecise sediment transport models calibrated using empirical data is often the only practical path forward. The transport equations should therefore be seen for what they are, an approximation of the truth over a limited range of conditions, within the bounds of professional practice. It is within this context that the bed load transport equations were utilised in this research.

Chapter 5: The Study Area and Research Design

5.1 Introduction

Three rivers were selected for study, the Mkomazi and Mhlathuze in KwaZulu-Natal and the Olifants in Mpumalanga. These rivers all drain the eastern sea-board of South Africa and the dominant processes are vertical accretion and incision. No true meandering occurs in these systems. The Mkomazi was selected on scientific grounds because it is one of the few large un-impacted rivers in South Africa with a perennial flow. [A dam is to be built on the river within the next few years (Louw, 1998a)]. The Mkomazi is a cobble-bed river with strong bed rock control. It represents the eastern sea-board summer rainfall rivers, many of which are threatened with further developments. The other two rivers selected are both impounded rivers with highly regulated flow environments. These rivers were the subject of a Ecological Reserve assessment in which the author was involved. The selection of sites was constrained by the terms of reference of the Reserve study. Although not directly comparable with the Mkomazi River, they nonetheless provided additional rivers and an applied context within which the concepts could be further tested. The Mhlathuze is a sand-bed river in northern KwaZulu-Natal. It is impacted by the Goedertrouw Dam. Downstream of the dam the river flows over Quaternary alluvium and, as such, can be viewed as an alluvial channel quite distinct from the Mkomazi. The Olifants River in Mpumalanga is a semi-confined highveld river with strong bed rock control and a coarse cobble-bed. It is impacted by a number of dams, including the Witbank, Doornpoort, Bronkhorstspruit, Premier and Middelburg Dams. Both the Mhlathuze and Olifants Rivers formed part of a Reserve assessment.

5.2 The Mkomazi River

5.2.1 Regional setting

The Mkomazi River drains an area of approximately 4387 km^2 in KwaZulu-Natal (Figure 5.1). The Great Escarpment forms the headwaters of the Mkomazi, and it exits into the Indian Ocean at the town of Umkomaas. The upper catchment geology is fairly simple, with Karoo sequence Elliot and

Clarens sandstones capped by Drakensberg lavas. The upper-middle catchment is dominated by Tarkastad mudstones and dolerite, while the Ecca and Beaufort Group dominate the middle catchment. The lithology produces clay and clay loam soils, which are only moderately erodible (Midgley *et al.*, 1994). According to the Surface Water Resources of South Africa (WR90) (Midgley *et al.*, 1994) the estimated sediment yield from the catchment is around 155 t/km^2/yr for the upper, middle and lower-middle catchment. The lower catchment produces an estimated 175-190 t/km^2/yr. The middle and lower parts of the catchment display a more complex geology. The catchment lithology here forms part of the Natal structural and metamorphic province, consisting of granites and gneiss. The terrain is faulted, and structural control on the channel is considerable. The geology has produced an upper catchment with steep relief, while the middle catchment can be classified as undulating. Steep relief in the lower catchment is a function of the underlying lithology.

The distribution of rainfall is reasonably consistent throughout the catchment, ranging from nearly 1300 mm per annum at the headwaters to around 1000 mm per annum in the middle and 900 mm per annum in the lower parts of the catchment. Catchment land use is mainly grazing and commercial forestry (wattle, pine and eucalyptus). Under natural conditions, the catchment vegetation would be dominated by pure grassveld and temperate and transitional forest and scrub, with false grassveld and coastal tropical forest dominating the middle and lower catchment. Overgrazing and high population densities in the upper-middle and lower parts of the catchment probably produces an increased sediment yield, although this remains untested.

The Mean Annual Runoff (MAR) of the Mkomazi is 1089 million cubic metres (WR90). Most of the runoff is generated in the upper part of the catchment, with the lowest 33% of the catchment contributing only 14% of the total MAR (WR90). The Mkomazi catchment is in the summer rainfall region of South Africa, and consequently most of the discharge occurs during the summer months (December to March). The winter is characterised by low flows (April to October/November). The average coefficient of variation (CV) for the catchment is 0.41 (WR90). The upper parts of the river has a more variable regime, with a CV of up to 0.74 (WR90). The Mkomazi has experienced a number of large floods. These are usually related to cut-off low pressure systems and appear to have an average return period of 20 to 50 years. Section 5.3.1 provides more information in this regard.

5.2.2 Identification of macro-reaches

The long profiles of many South African rivers display a diverse form (Rowntree & Dollar, 1996a). The long profiles very seldom display a uniform convex or concave profile. This is in part a function of tectonic history and climate change, but also of variable lithology. Major breaks of slope are often coincident with changes in channel type, bed material and reach type (Rowntree & Wadeson, 1999). It is therefore instructive to subdivide the long profile into morphologically uniform reaches - these have been termed macro-reaches (Rowntree, 2000). This provides the basis for site selection and for extrapolation of sites from one reach to another (Rowntree, 2000). Two methods for delineating macro-reaches have commonly been used for South African rivers. The first is a technique developed by Rowntree & Wadeson (1999) which delineates reaches based on the percentage gradient change as measured off a 1:50 000 topographical map - generally, where gradient changes of greater than 50% occur, a reach break is denoted. A second technique is to use the CUSUM plot to identify major breaks of slope. This technique is similar to the previous technique in that it sums the cumulative percentage slopes thus making the major breaks of slope easily identifiable. For the purposes of this report, both techniques were used to identify the breaks of slope and good agreement was found between the two. Four macro-reaches (Figure 5.2) were identified for the Mkomazi River. Table 5.1 presents the characteristics of each macro-reach.

5.2.3 Identification of sites

Within each macro-reach, sites were selected that were considered to best represent the reach morphology. Access to the river proved a major problem, and site selection was thus constrained by access. Thirteen sites were selected for analysis and where possible each site was surveyed using at least three fixed-point cross-sections. At a number of sites, only one or two cross-sections were surveyed. This was done where it was considered that one or two cross-sections were sufficient to characterise the site. It was not practical to represent each site by a greater number of cross-sections, as it was necessary to generate a stage-discharge relationship for each cross-section. This was achieved by repeated calibration surveys. The bed material transport modelling for each site relied on hydraulic information, and could not be started before the stage-discharge curves were computed. It was therefore necessary to limit the amount of cross-sections at each site to maximise efficiency. It is considered that the surveyed cross-sections adequately represent the sites, and in total twenty-eight cross-sections were surveyed for the Mkomazi. Chapter 7 will discuss the site surveys in more detail. Appendix A presents the cross-sectional data, sketch map and photograph of each site.

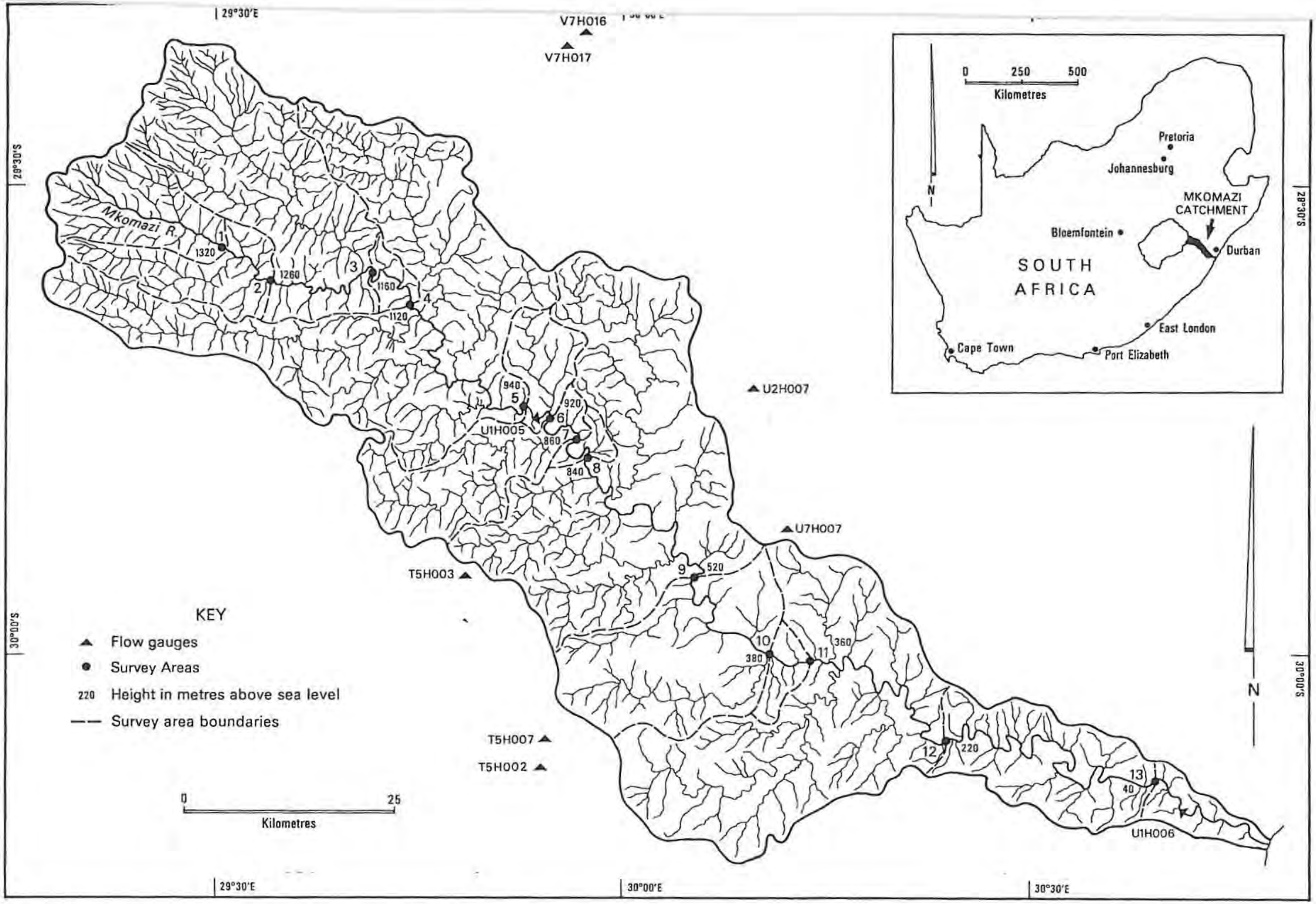

Figure 5.1: The Mkomazi catchment.

Table 5.1: Characteristics of the Mkomazi River.

Macro-reach	Characteristics	Average Gradient	Geology	Site numbers
1 (2850m to 1020m)	Confined valley. Low population density. Cobble-bed foothills to mountain stream zone with cobble-bed channel characterised by plane beds, step pool morphology, rapids and pools. Floodplains generally absent, but lateral depositional bench features occur.	0.0073	Shales and mudstones with dolerite intrusions	1, 2, 3, 4
2 (1020m to 840m)	Confined to semi-confined valley. Moderate population density with extensive cultivation. Irregular channels with infrequent islands, cobble-bed foothills zone with gravel- and cobble-bed river. Pool-riffle or pool-rapid morphology, locally bed rock controlled. Narrow floodplain of sand and gravel may be present.	0.0046	Shales and mudstones with dolerite intrusions	5,6,7
3 (840m to 400m)	Confined to semi-confined valley, cultivation on floodplain areas. Commercial farming of timber and livestock. Mainly single channel with well developed lateral bars. From 620 metres the channel goes into a gorge with an anabranching channel. Mixed pool-riffle or pool-rapid morphologies in lower gradient reaches, bed rock or boulder/large cobble dominated channels in steeper sections. Rapids, cascades and bed rock controlled pools common.	0.0213	Shales and mudstones with extensive dolerite intrusions	8,9
4 (400m to sea level)	Confined to semi-confined valley. Many small 1st and 2nd order tributaries. High rural population densities. Anabranching channels common, foothill zone has mixed alluvial bed rock channel, pool-riffle morphology, sand or gravel bars.	0.0037	Instrusive granites with sedimentary sequences	10,11,12,13

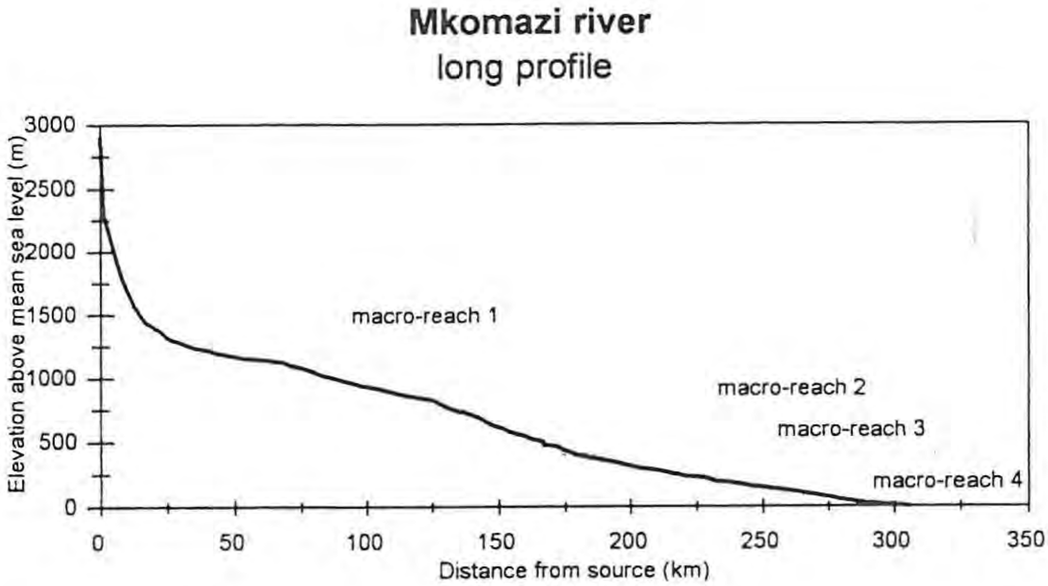

Figure 5.2: Long profile of the Mkomazi River.

5.3 The Mhlathuze River

5.3.1 Regional setting

The Mhlathuze River drains an area of approximately 4209 km^2 in northern KwaZulu-Natal (Figure 5.3). The Mhlathuze rises at about 1280 metres around Babanango and discharges into Richards Bay harbour. The geology of the area is complex, with faulting and thrust faulting impacting on the traverse of the river. The upper catchment geology is dominated by Dwyka tillite. The lower part of the upper catchment consists mainly of Natal Structural and Metamorphic province rocks such as granite, quartzite and basaltic lava. The middle catchment consists mainly of sedimentary rocks of the Ecca group, with Vryheid, Volksrust and Pietermartizburg formations occurring. The lower catchment is dominated by Quaternary sands. Weathering of the quartzites, tillites and granite produces mainly sand-sized material, resulting in a predominantly sand-bed channel. Estimated sediment yield from the sub-catchments range from 27 $t/km^2/yr$ to 216 $t/km^2/yr$ with an estimated average sediment yield of 160 $t/km^2/yr$ (WR 90). Catchment land use includes commercial wattle, pine, eucalyptus and sugar cane production. The highly faulted middle terrain affects considerable structural control on the channel. The impact of this can be seen in the numerous orthogonal turns on the river. Mean annual rainfall distribution in the catchment varies from 870 mm in the upper and middle catchment to around 1100 mm in the lower catchment. The Mhlathuze forms part of the summer rainfall region of South Africa. Most of the rainfall (and hence discharge) occurs during the summer months (December to April), however the seasonal distribution of flow is not as marked as it is for the Mkomazi River.

The Mhlathuze has been impounded by the Goedertrouw Dam which was completed in 1979. The Goedertrouw Dam is an 81-metre high earthfill embankment dam with a maximum surface area of 12 km^2 and a maximum storage capacity of $321 x 10^6 m^3$. This dam has had a significant impact on the flow regime of the Mhlathuze River. The virgin MAR of the Mhlathuze River has been estimated to be 362 million cubic metres (Hughes & Smakthin, 1998). The Mhlathuze has a very high CV of 0.934 (WR90). This is due to the geographical location of the Mhlathuze catchment in northern KwaZulu-Natal, an area subject to heavy and prolonged rains due to the frequent (once every 20 years or so) occurrence of cut-off lows which result in large floods. These cut-off lows are specific types of low-pressure systems which are strongest in the upper troposphere and are associated with strong uplift and the occurrence of widespread rain on their eastern sides (Tyson, 1986). The northern parts of KwaZulu-Natal are particularly prone to this meteorological phenomenon. The Mkomazi catchment which is further south, is also impacted on by cut-off lows, but not as frequently. The construction of the Goedertrouw Dam has reduced the virgin MAR to around 217 million cubic metres per annum (Hughes & Smakthin, 1998). It has also resulted in the attenuation of flood peaks and higher flows (van Bladeren, 1992). This will be discussed in greater detail in Chapters 6 and 10.

5.3.2 Identification of macro-reaches

Four macro-reaches were identified using a combination of the CUSUM plot and the percentage gradient change. Table 5.2 displays the characteristics of each macro-reach. Figure 5.4 displays the long profile of the Mhlathuze River.

5.3.3 Identification of sites

Four sites were selected to represent the macro-reaches. The terms of reference of the Ecological Reserve assessment were that all the sites should be located below Goedertrouw Dam (Louw, 1998b) (Figure 5.3). Site 1 is approximately 25 kilometres below the dam. No major tributaries join the Mhlathuze between the dam wall and Site 1. Site 2 occurs some 35 kilometres downstream of Site 1. Between Site 1 and Site 2, a major tributary, the Mfule River joins the Mhlathuze. The Mfule is also a sand-bed channel. Site 3 is a further 35 kilometres downstream of Site 2. No major tributaries join the Mhlathuze between these two sites. Site 4 is approximately 15 kilometres downstream of Site 3, just upstream of a major tributary input, the Nseleni. It is important to point out that Site 4 is an artificial channel that was cut by the Port authorities at Richards Bay to accommodate the development of Richards Bay harbour (Dollar, 1998b). Site 1 has multiple channels with different water elevations. This necessitated the surveying of six cross-sections to ensure accurate hydraulic calculations. Sites 2, 3 and 4 were simple sand-bed channels, and were therefore only represented by one cross-section at each site. Appendix A presents the cross-sectional data, sketch map and photograph of each site.

Table 5.2: Characteristics of the Mhlathuze River.

Macro-reach	Characteristics	Average gradient	Geology	Site numbers
1 (1280m to 1080m)	Confined valley with a mountain stream and a bed rock and cobble-bed channel. No floodplain is present but lateral depositional features occur in a few places.	0.0373	Dwyka tillite	0
2 (1080m to 820m)	Confined valley with no floodplain present. The topography is undulating.	0.0126	Natal structural and metamorphic province rocks including granite, quartzite and basaltic lavas	0
3 (820m to 180m)	The boundary between macro-reach 2 and 3 is coincident with the faulting of the sedimentary and volcanic rocks. The gradient is generally steep and is associated with resistant lithologies and periods of tectonic re-adjustment. The reach, although steep, displays a remarkable number of depositional features.	0.0215	Sedimentary rocks of the Ecca Group, including Vryheid, Volksrust and Pietermaritzburg formations	0
4 (180m to sea level)	The boundary between macro-reach 3 and 4 is coincident with thrust faulting of sedimentary rocks associated with the Natal structural and metamorphic province. Rapid gradient changes are common in this macro-reach as a result. Below the Goedertrouw Dam, remarkable changes occur in channel type from a pool-rapid channel type to a sinuous single thread channel. Channel narrowing and vegetation encroachment is evident. The depositional features that are common in macro-reach 3 are no longer evident.	0.0096	Sedimentary and intrusive rocks associated with the Natal structural and metamorphic province	1,2,3,4

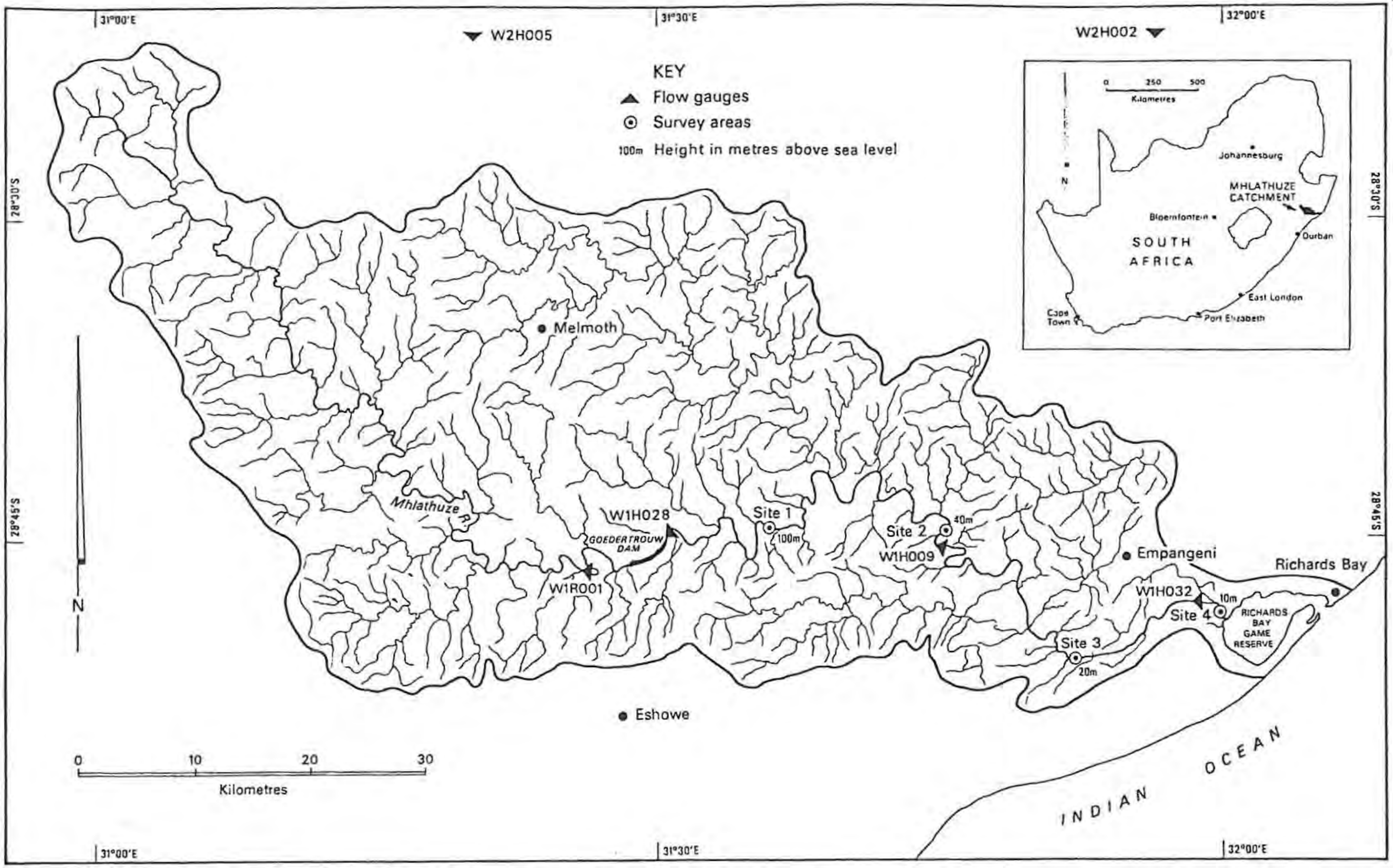

Figure 5.3: The Mhlathuze catchment.

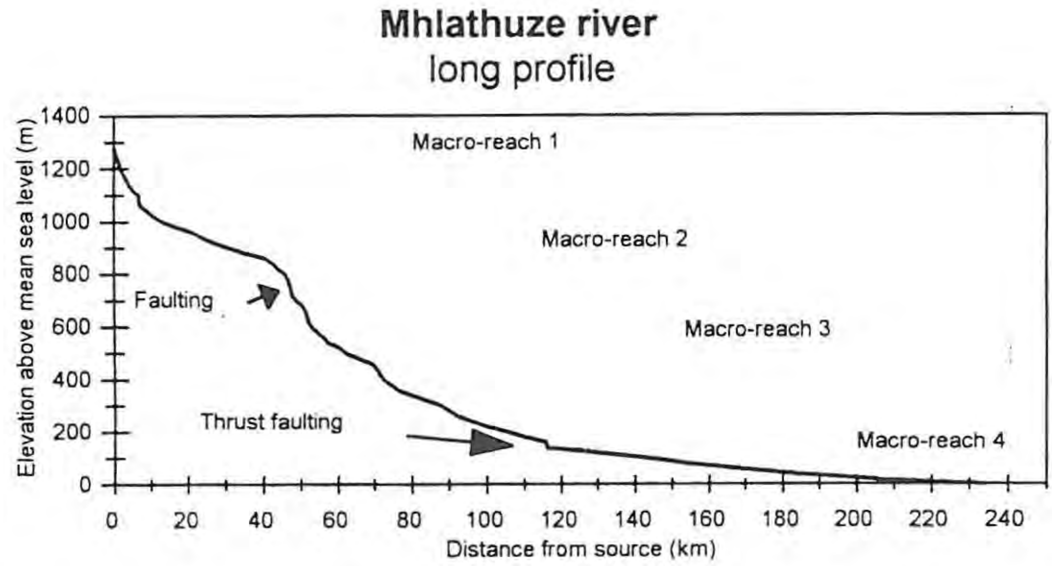

Figure 5.4: Long profile of the Mhlathuze River.

5.4 The Olifants River

5.4.1 Regional setting

The Olifants River is a highveld river that drains the Gauteng and Mpumalanga provinces of South Africa before entering Mozambique to the east and exiting into the Indian Ocean (Figure 5.5). For the purposes of this thesis only the upper Olifants catchment will be considered. The upper Olifants River above Loskop Dam drains an area of approximately 10 841 km^2. The upper Olifants catchment has three main stems, the Wilge to the west (4356 km^2), the Klein Olifants to the east (2391 km^2) and the Olifants proper (4094 km^2). The upper Wilge, Olifants and Klein Olifants drain a flat, gentle relief plateau underlain by Vryheid formation Karoo sequence rocks. In the middle parts of the catchment, the channels are incised into the ancient basement rocks of the Transvaal sequence (mainly Pretoria group quartzite, shales and granite, Rooiberg group rhyolite and sandstones) and the Bushveld Igneous Complex (BIC). The geology of the area has a considerable impact on the structure and flow direction of the river. The country rocks are intruded by dolerite and diabase dykes and sills. The flat relief and basement geology in the upper parts of the catchment are associated with shallow, sandy soils, while the undulating relief in the lower parts of the catchment is associated with moderate to deep clayey loam soils. The soils are only moderately erodible. The grassveld and false grassveld produces a good vegetation cover. This results in moderate to low estimated annual sediment yield for the catchment of approximately 45 t/km^2yr^1(WR90).

The gross channel structure and planform is to a large extent determined by bed rock. A number of lineaments and faults cross the river, forming local gradient changes. Where the river is incised onto the more resistant lithologies, significant structural changes occur in the channel and in the long profile. Resistant bed rock outcrops create local downstream steepening, but also result in an upstream decrease in gradient, reducing channel energy and creating areas for sediment accumulation. A number of knick-points and abandoned plunge pools along the course of the Olifants attest to the incised nature of the channel. Mean annual rainfall in the catchment varies between 600 and 700 mm, with mean annual potential evapotranspiration ranging from 1500 mm in the east of the catchment to around 1700 mm in the west.

The hydrology of the Olifants River is described in terms of the three main-stem tributaries for virgin conditions. This is because there is insufficient information on the operation of the dams, water abstraction for irrigation, return flow from effluent treatment works and land use change impacts to model the present-day conditions. The Wilge River (Site 4) has an MAR of 167 million cubic metres, with a CV of 0.73. The Klein Olifants (Site 3) has an MAR of 81.6 million cubic metres, with a CV of 0.72. The Olifants proper (Sites 1 and 2) has an MAR of 449 million cubic metres, with a CV of 0.70. The Olifants system falls in the summer rainfall area of South Africa. Consequently, most of the discharge occurs during the summer months (November to February). The high CV indicates that the Olifants is a highly variable system, with high magnitude, short duration storm events which are concentrated in rapidly rising and receding flow events (Hughes, 2000).

The Wilge River is impounded by two major dams, the Bronkhorstspruit Dam and the Premier Dam. The Bronkhorstspruit Dam is a 30-metre high arch/earthfill combination dam nearly 80 kilometres upstream of Site 4. It was completed in 1950 and has a surface area of nearly 9 km^2 and a capacity of $59.4x10^6m^3$. Downstream of the Bronkhorstspruit Dam is the 9-metre high Premier Dam. It is a concrete gravity dam which was completed in 1909 with a surface area of 0.60 km^2 and a capacity of $5.036x10^6m^3$. Site 4 is approximately 40 kilometres downstream of Premier Dam. The main Olifants stem is regulated by two dams, the Witbank Dam and the Doornpoort Dam. The Witbank Dam is a 9-metre high earthfill dam with a very small capacity and surface area. Just downstream of the Witbank Dam is a much larger dam, the 9-metre high earthfill Doornpoort Dam, with a capacity of $5.7x10^6m^3$ and a surface area of 0.10 km^2. The Doornpoort Dam was completed in 1924. Site 1 is 15 kilometres downstream of Doornpoort Dam. The Klein Olifants River is impounded by the 27-metre high concrete buttress Middelburg Dam. The dam has a surface area of 4.7 km^2 and a maximum capacity of $48.4x10^6m^3$. Site 3 is approximately 45 kilometres downstream of Middelburg Dam. Site 2, which is the lowest site on the Olifants system is thus regulated by five impoundments. These impoundments have been in place for some time (over 50 years) and have had a major impact on the flow regime of the Olifants system.

5.4.2 Identification of macro-reaches

Four macro-reaches have been determined for each of the three main-stem tributaries of the upper Olifants catchment (Figures 5.6 to 5.8). The macro-reaches were determined from an analysis of the long profile, geology and gradients from the 1:50 000 topographical sheets and the 1:250 000 geological maps. A CUSUM plot was used to determine the major breaks of slope for each of the three main-stem rivers of the upper Olifants. Tables 5.3 to 5.5 display the characteristics of each macro-reach.

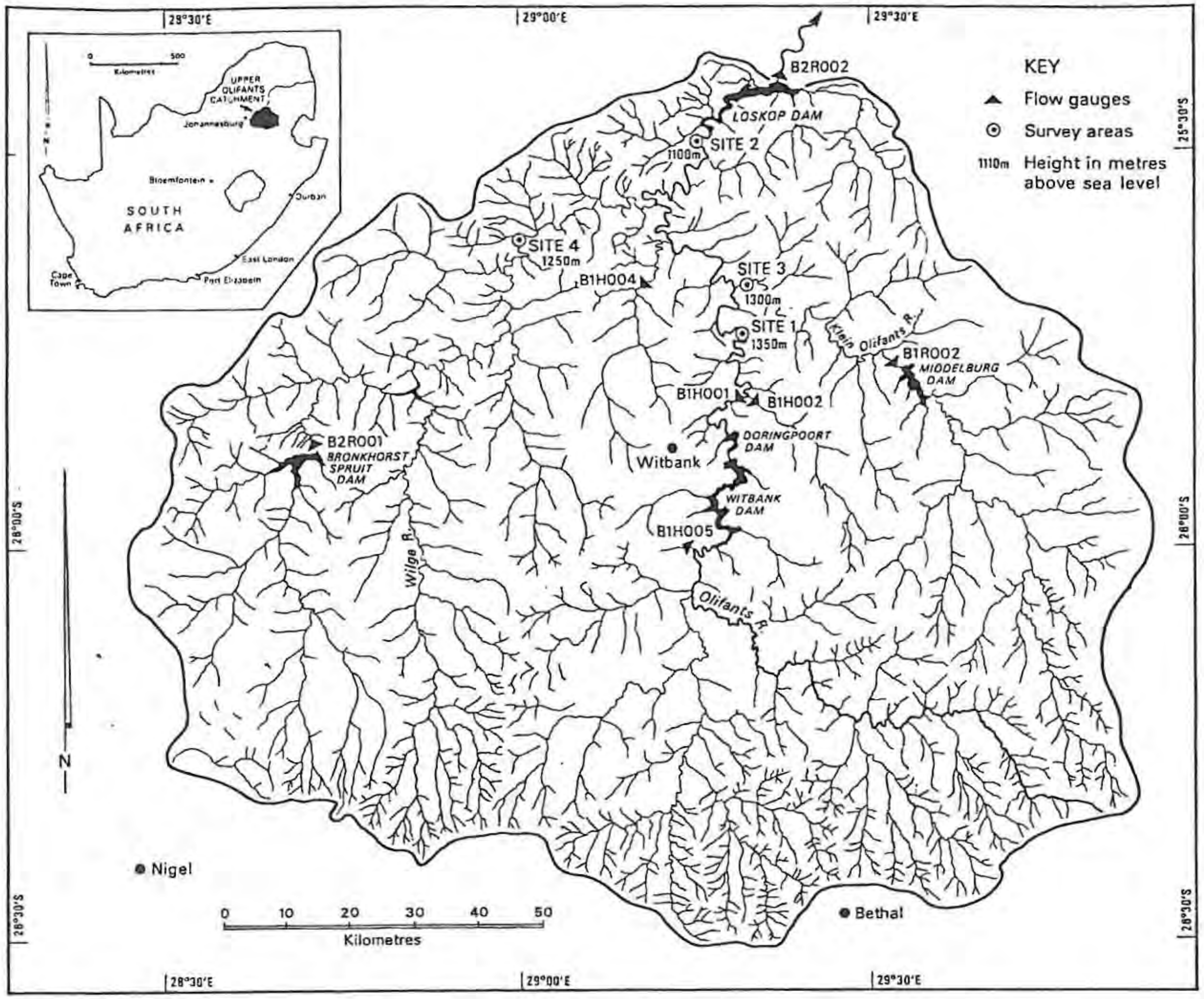

Figure 5.5: The Olifants catchment.

Table 5.3: Characteristics of the Olifants River.

Macro-reach	Characteristics	Average gradient	Geology	Site numbers
1 (1780m to 1670m)	No information is available.	0.0223		0
2 (1670m to 1570m)	The reach has low relief, and this is reflected in the channel type which is mainly sinuous single thread. At the lower end of the reach, the Doornpoort and Witbank Dams are underlain by Selonsrivier formation sandstone and quartzite. The channel is partially controlled by bed rock. Bank erosion is a significant source of sediment.	0.0026	Permian age Vryheid formation interbedded sandstones and shales	0
3 (1570m to 1230m)	The country rock is intruded by diabase (metamorphosed dolerite) and diabase dykes and sills which strike across the Olifants resulting in significant gradient adjustments. These sandstones have been deformed. There are numerous structural controls on channel form and pattern, including faults and joints. The Olifants has exploited lines of weakness which has determined the traverse of the channel. Variable rock hardness has resulted in a pool-rapid channel type. The more resistant lithologies producing rapids and creating hydraulically controlled upstream pools.	0.0098	Mogolian age Wilgerivier formation sandstone, dolerites and diabase	1
4 (1230m to 1000m)	There are a number of knick-points along this stretch (one being Kanongat). These are likely structural knick-points (rather than tectonic or cyclical knick-points), but have served to allow the Olifants to adjust to different base-levels. The boundary between macro-reach 3 and macro-reach 4 is probably such a knick-point. Given the nature of the bed rock, the channel type is pool-rapid.	0.0047	Mogolian age Wilgerivier formation sandstone, dolerites and diabase	2

Table 5.4: Characteristics of the Wilge River.

Macro-reach	Characteristics	Average gradient	Geology	Site numbers
1 (1770m to 1430m)	The channel structure of the Wilge River is controlled by the underlying bed rock, and its post-depositional formation such as faulting and weathering along joints. The gorges are incised into Wilgerivier sandstone and quartzite.	0.0223	Wilgerivier sandstone and quartzite	0
2 (1430m to 1360m)	This reach is underlain by Vaalian age Pretoria group sediments consisting of quartzite, shales and subgraywackes. Also present is diabase. This is reflected in the channel type for the reach which is sinuous single thread.	0.0004	Pretoria group quartzite, shales and subgraywackes and diabase	0
3 (1360m to 1170m)	This reach is underlain by Mogolian age Waterberg group sediments consisting of Wilgerivier sandstones. There are numerous structural controls on the channel form and pattern, including faults and joints. As the river traverses the Wilgerivier sandstones, lines of weakness have been exploited which have determined the direction of the channel. Structural control of the channel in this macro-reach is considerable. Variable rock hardness has resulted in a pool-rapid channel type. The more resistant lithologies producing rapids and creating hydraulically controlled upstream pools.	0.0003	Wilgerivier sandstones	4
4 (1170m to 1090m)	This reach is underlain by Waterberg group Lebowa granites. Granite is extremely resistant to weathering and very little jointing occurs, hence the flatter topography. Sinuous single thread channels dominate together with mixed anabranching channels.	0.0001	Lebowa granites	0

Table 5.5: Characteristics of the Klein Olifants River.

Macro-reach	Characteristics	Average gradient	Geology	Site numbers
1 (1700m to 1630m)	No information is available.	0.0117		0
2 (1630m to 1585m)	No information is available.	0.0037		0
3 (1585m to 1440m)	The reach is one of low relief and strong bed rock control. The channel type is mixed, ranging from sinuous single thread to pool-rapid. Bank erosion is an important source of bed material.	0.0035	Selonsrivier sandstone and quartzite as well as diabase	0
4 (1440m to 1250m)	Macro-reach 4 is underlain by Wilgerivier sandstones and quartzite as well as diabase and diabase dykes and sills. This has resulted in a pool-rapid channel type.	0.0049	Wilgerivier sandstones and quartzite as well as diabase dykes and sills	3

5.4.3 Identification of sites

The analysis of the Olifants formed part of an Ecological Reserve assessment (Louw, 2000). The terms of reference of the Reserve assessment were that one site be located on the Wilge River, one site be located on the Klein Olifants and two sites be located on the Olifants River (Figure 5.5). The four sites were surveyed with a minimum of three cross-sections per site. All the chosen sites are located at the lower end of the upper Olifants catchment, and hence represent mainly pool-rapid channel types. Site 1 and Site 2 are in transitional zones, with Site 1 representing a reach that constitutes mainly a single thread sinuous channel. Site 2 is in a reach classified as pool-rapid but is transitional to single thread sinuous. Site 3 and Site 4 are pool-rapid channel types. Appendix A presents the cross-sectional data, sketch map and photograph of each site.

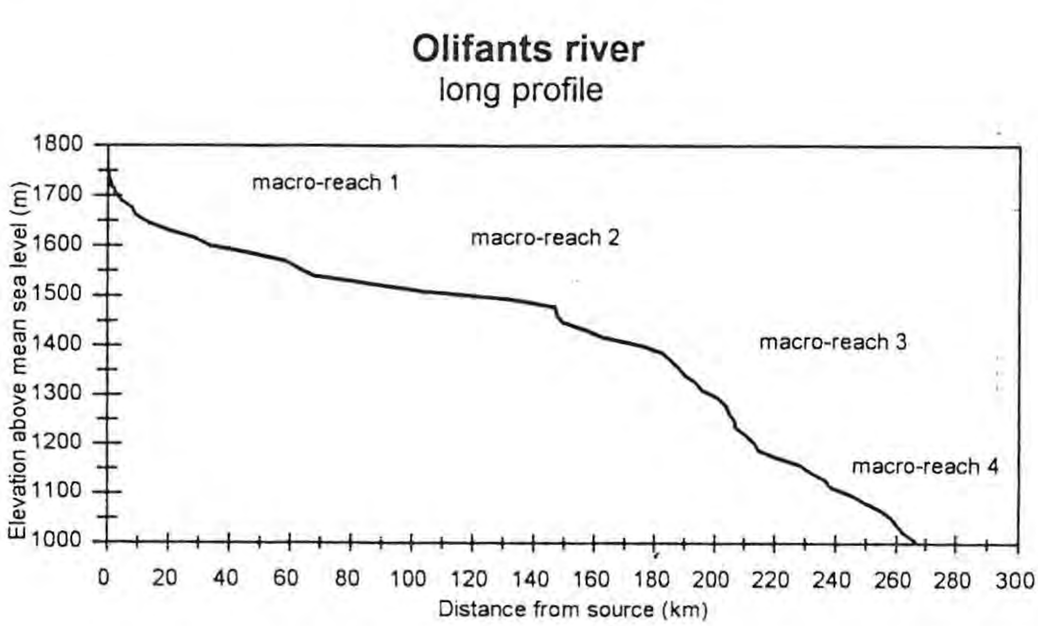

Figure 5.6: Long profile of the Olifants River to Loskop Dam.

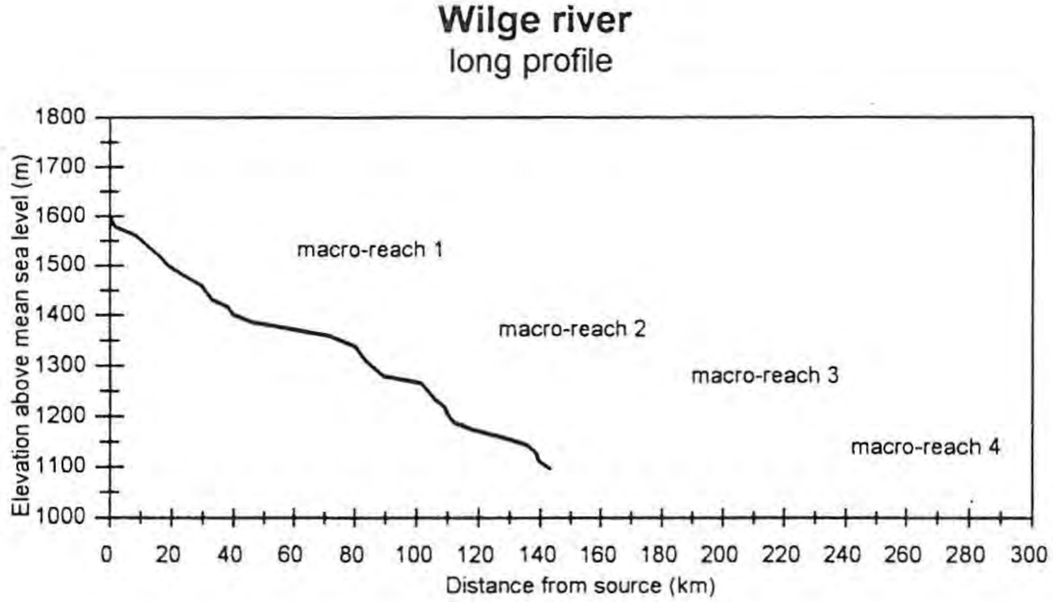

Figure 5.7: Long profile of the Wilge River.

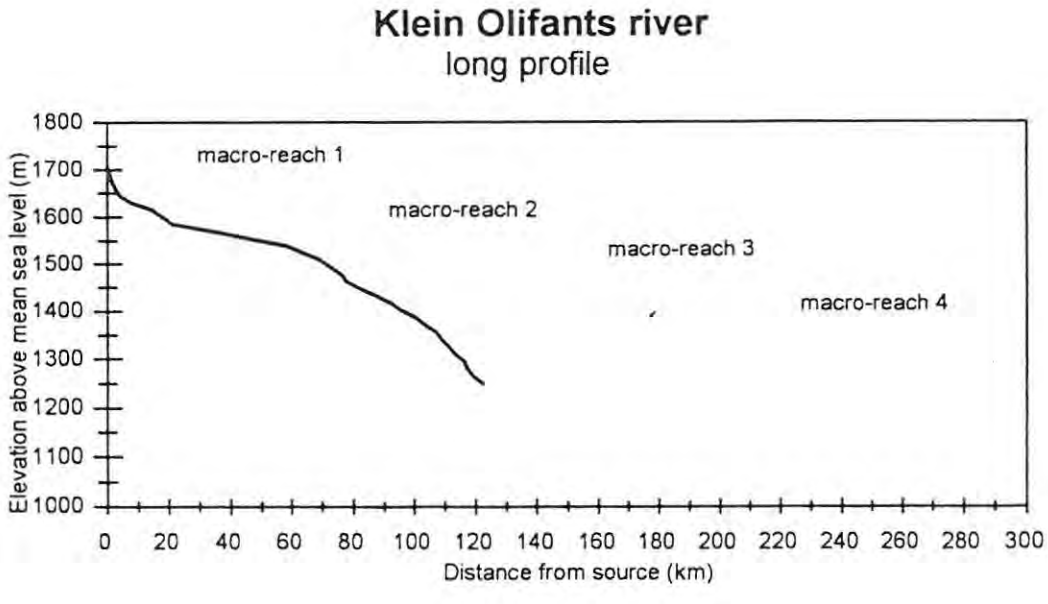

Figure 5.8: Long profile of the Klein Olifants River.

5.5 Research design

The thesis has two major foci: the research system (the Mkomazi River) and the application systems (the Mhlathuze and Olifants Rivers). The method and results sections are presented in this context. Figure 5.9 presents a flow diagram which illustrates the project research design. As mentioned previously the Mkomazi River was used as the main study river, where the techniques to determine the magnitude and frequency of channel forming flows were developed. The Mhlathuze and Olifants Rivers were selected for pragmatic reasons, but also to test the methods developed for the Mkomazi on two impounded systems.

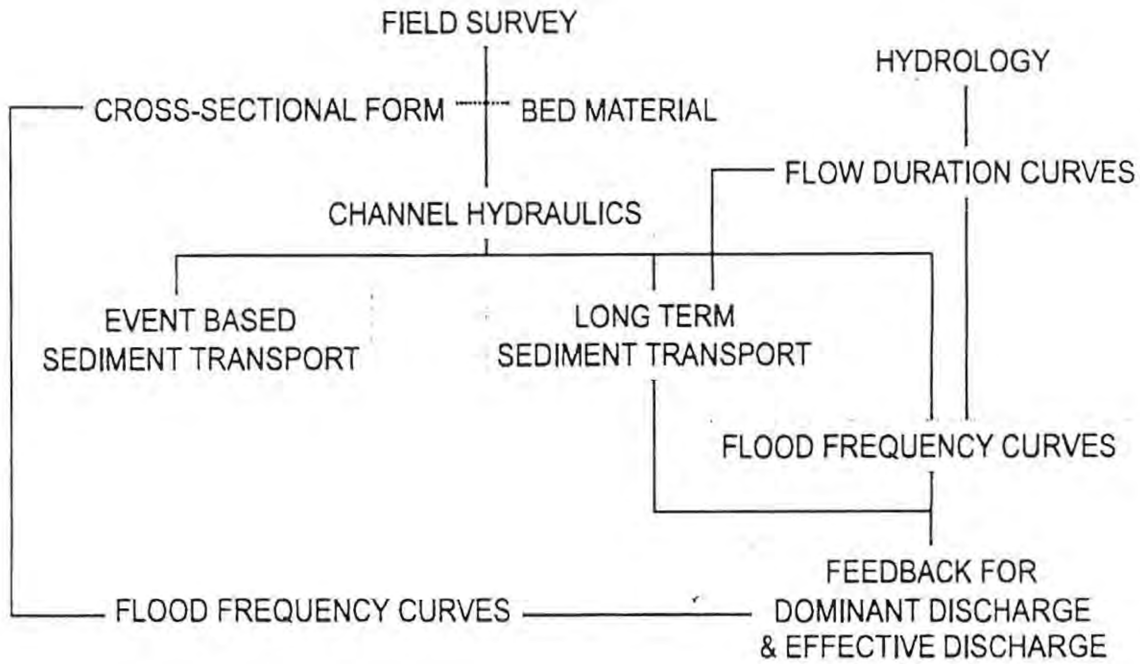

Figure 5.9: Flow diagram indicating the structure of the research.

The remainder of the thesis is structured as follows and illustrates the research design. Chapter 6 presents the methods and results of the hydrological data that were used in this research. Daily time series were required at each site to generate flow duration curves and flood frequency curves (Chapter 6). These were used in conjunction with the information from the field survey of channel cross-sections, bed material characteristics and hydraulic computations for each of the rivers (Chapter 7) to generate bed material transport rates (Chapters 8, 9 and 10). The generation of bed material transport rates allowed for the determination of effective and dominant discharge for each cross-section for each site for each river. This was then related back to cross-sectional form and hydrology. This information was synthesised to develop an understanding of the magnitude and frequency of channel forming flows and environmental flows for selected southern African rivers (Chapter 11).

5.6 Summary and conclusions

The preceding discussion has presented an overview of the rivers that were selected for analysis. The rivers represent examples of different channel types that occur in the southern African landscape. These channels reflect a range of rivers, from an un-impacted semi-confined cobble-bed channel (Mkomazi), to a highly impacted alluvial single thread channel (Mhlathuze) to a semi-confined bed rock controlled channel (Olifants). The sites selected within each river were systematically chosen to be representative of different channel types associated with particular macro-reaches. The rivers were surveyed and studied in a manner that would achieve the research objectives as outlined in Chapter 1. The following four chapters present the methods and results of the research.

Chapter 6: Hydrology

6.1 Introduction

The main aim of the hydrological analysis is to generate representative daily time series for each of the selected sites on the Mkomazi, Mhlathuze and Olifants Rivers. Daily time series were necessary as the bed material transport modelling presented in Chapters 9 and 10 is based on the 1-day daily flow duration curve. This chapter will present the methods, techniques and results of the hydrological analysis for the three rivers concerned. As a large volume of daily data was generated for 21 sites, it is impractical to display all the information. Much of the data is thus presented in Appendices B to D which are available at the back of the thesis.

There are two main sources of hydrological data in South Africa. The first is primary data from the Department of Water Affairs and Forestry (DWAF), and the second is secondary data from the Surface Water Resources of South Africa 1990 (WR90) (Midgley *et al.*, 1994). WR90 provides virgin monthly modelled data based on the Pitman model for quaternary catchments and therefore serves as a useful reference for total flow volume and monthly flows. However, it is not useful for daily flow data.

6.2 The Mkomazi River

6.2.1 Data availability

The Mkomazi River in KwaZulu-Natal has its source in the southern Drakensberg. There are two streamflow gauges for the Mkomazi with flow records dating from 1960: an upper gauging station, U1H005, gauging 1744 km^2 and a station close to the mouth, U1H006, gauging 4349 km^2. These records are stationary and are of good quality. The data used in all cases can be considered to represent natural flow conditions in the catchment. There is a problem with extreme high flows, especially at the lower station which has a very low Discharge Table Limit (DTL). U1H005 has a DTL of 637.8 m^3s^{-1} and has been overtopped only once since 1960. U1H006 has a DTL of 226 m^3s^{-1}

and has been overtopped 35 times since 1962. The high flows must therefore be treated with circumspection. Monthly flow data for virgin flow conditions are available for a 70 year period (1920-1990) from WR90. WR90 has divided the Mkomazi catchment into 12 quaternary sub-catchments. These quaternary catchments were used to check and calibrate the daily data generated for each of the sites. These details will be discussed later in the chapter.

The 1-day daily flow duration curves for U1H005 and U1H006 clearly indicate the similarity in the hydrological regime of the two sites (Figure 6.1). However, U1H006 demonstrates a slight increase in the maintenance of low flows during drought periods compared to U1H005 (flows equalled or exceeded more than 90% of the time). Analysis of the seasonality of the flows demonstrates that these differences are more pronounced during the dry months of the year. This is an indication that, at the lower end of the Mkomazi, the regime is more base-flow driven. By inference then, the upper end of the Mkomazi is probably more flashy. This assumption was used to estimate the shape of the target daily flow duration curves.

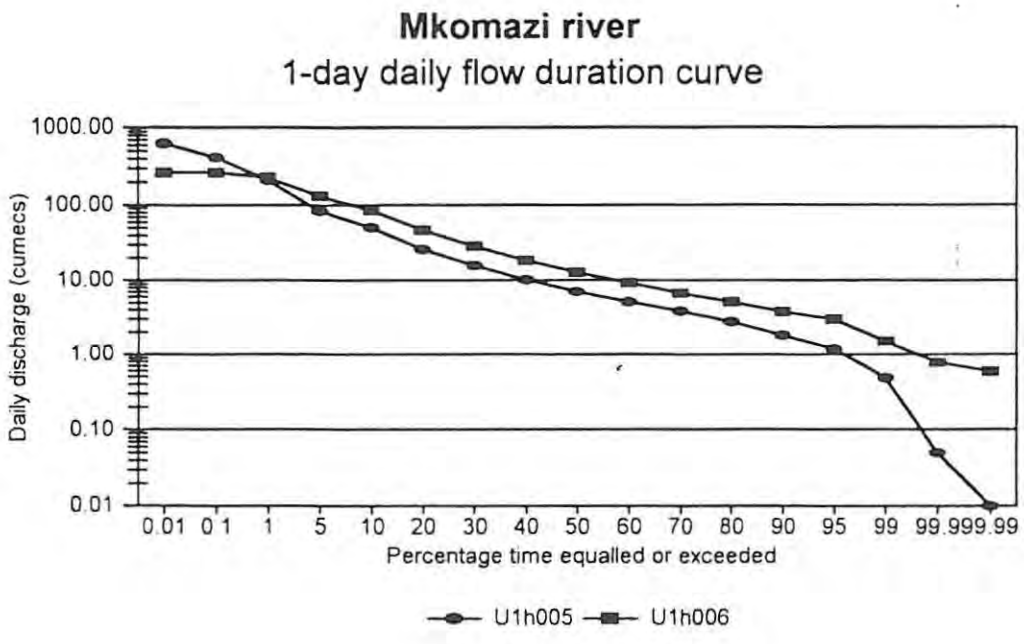

Figure 6.1: 1-day daily flow duration curves for U1H005 and U1H006.

6.2.2 Selection of appropriate calibration stations

This section describes the data and techniques used to generate the representative daily streamflow time series at each of the thirteen selected sites for the Mkomazi River. Figure 5.1 shows the location of the flow gauging stations in relation to the sites selected for analysis. There are a number of ways to generate at-a-station daily time series, these include stochastic and deterministic modelling. However, these models require detailed information on catchment soils, vegetation, antecedent soil moisture indices and so on. This level of information is not available for the Mkomazi catchment and for this reason, a different approach was adopted.

The technique used is an adaptation of the one used to generate flow data for Ecological Reserve assessments. The model uses an algorithm to patch and extend (if necessary) observed time series of daily streamflow. A full description of the model has been published (Hughes & Smakthin, 1996). The technique is based on typical flow duration curves and on the assumption that flows occurring simultaneously at sites in reasonably close proximity to each other correspond to similar percentage points on their respective flow duration curves. Figure 6.2 displays the technique in graphical form. The technique involves identifying the percentage point position of the source site's streamflow (Figure 6.2b) on the source site's flow duration curve (Figure 6.2d), and then reading off the flow value for the equivalent percentage point from the target site's flow duration curve (Figure 6.2d). The weighted average of the target site flow value is then assumed to be the target site's flow value. The technique is based on two steps:

- the generation of source flow duration curve tables for source and target sites;
- the simulation of the time series using target flow duration curves for each site.

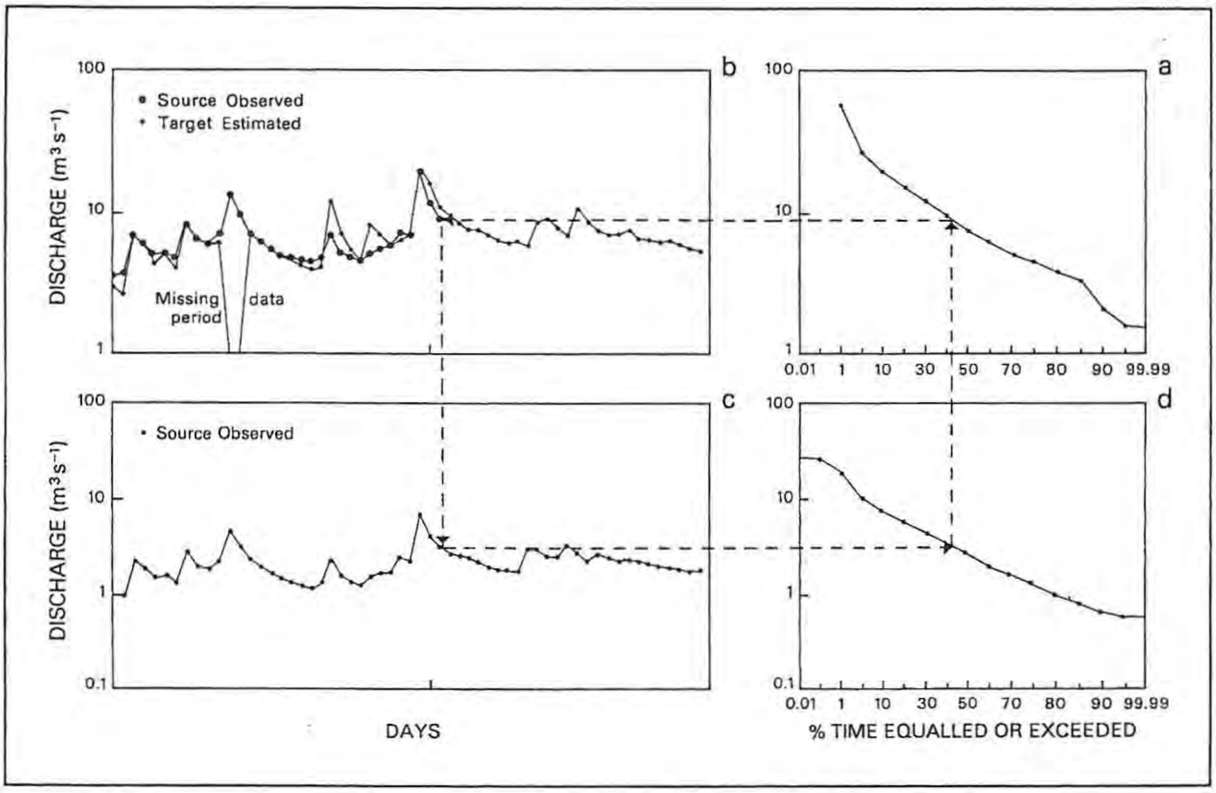

Figure 6.2: Method used for generating daily time series from flow duration curves (after Hughes & Smakthin, 1996).

6.2.3 Generating target flow duration curves

6.2.3.1 Regionalising the flow data

In order to run the model, source daily time series and target daily flow duration curves were required. The daily time series for U1H005 and U1h006 were used as the source daily time series. The target daily flow duration curves were more problematic. The following technique was used to generate them. Twelve stations in and around the Mkomazi were selected for analysis. These stations were chosen on the basis of their length and reliability of record, and proximity to the target sites. Daily flow data were obtained from DWAF and were imported into a hydrological package *HYMAS* (Hughes & Smakthin, 1996). For each of the twelve stations, a 1-day daily flow duration curve was generated. The flow duration curves were then regionalised to compare the shape of the 1-day curve with the shape of the 1-day curves for the Mkomazi gauging stations. The procedure used was as follows: the average daily flow (in cubic metres per second) was calculated:

$$Average\ daily\ flow\ (ADF) = \frac{(MAR*1000)}{(365*24*3.6)} \quad \text{(6.1)}$$

where

MAR is the Mean Annual Runoff in million cubic metres

and regionalised

$$\frac{Q}{ADF} \quad \text{(6.2)}$$

where

Q is the discharge for a given point on the flow duration curve in cubic metres per second

Using this method it was possible to determine which flow stations produced similar shaped flow duration curves to the Mkomazi River. Figure 6.3 demonstrates that the curves generated for stations U7H007, V2H007, V2H005, V7H016, V7H017, T5H002 and T5H007 all plot very close to U1H005 and U1H006, i.e. between the 1% equalled or exceeded and the 90% equalled or exceeded flows. Those stations that plotted with a different shape (T5H003 and T5H005) to the two stations for the Mkomazi were excluded from further analysis. For the purpose of this study, the low flows (those flows equalled or exceeded 90% of the time or more) are of little consequence, as these do not generate sufficient stream power or shear stress to have any impact on channel form or bed material transport. The high flows are of greater significance. Simulating high flows in South Africa is problematic as South African flow gauging stations are very poorly calibrated for high flows and are often overtopped, resulting in poor flood peak estimates.

Table 6.1: Flow gauging stations around the Mkomazi catchment.

Station	River	Years	MAR (10^6m^3)	ADF (m^3/s)	Coefficient of variation	Area (km^2)
U7H007 (Beaulieu Estate)	Lovu	1964-1999	23.18	0.74	0.598	114
V2H007 (Broadmoor)	Hlatikulu	1972-1999	32.27	1.02	0.538	109
V7H016 (Drakensberg)	Ncibidwane	1976-1999	48.30	1.53	0.442	121
V2H005 (The Bend)	Mooi	1972-1999	115.25	3.65	0.461	260
V7H017 (Drakensberg)	Boesmans	1972-1999	137.90	4.37	0.428	276
T5H002 (Nooitgedacht)	Bisi	1960-1974	153.8	4.88	0.383	867
U1H005 (Camden)	Mkomazi	1960-1999	635.58	20.15	0.468	1744
T5H007 (Bezweni)	Mzimkulu	1956-1978	957.1	30.35	0.360	3586
U1H006 (Delos Estate)	Mkomazi	1962-1999	1033.17	32.76	0.446	4349

6.2.4 Generating target daily flow duration curves

Once the percentage points of the 1-day daily flow duration curve were determined for each of the regional stations, the ratio between each percentage point and the lower percentage point was calculated. For example, for station U7H007, the 0.10% q/adf is 19.86, and the 0.01% q/adf is 57.96. This gives a ratio of 2.92, i.e. the flow equalled or exceeded 0.01% of the time is 2.92 times the size of the flow equalled or exceeded 0.10% of the time (Table 6.2). This gave an indication of the relative sizes of the flows in relation to one another. However, it is clear from the evidence presented in Figure 6.3 that although the curves from each of the flow stations overlap between the 1st and 90th percentile, the two stations that gauge the smaller catchments and have a lower mean daily flow, also have a 'flashier' hydrological regime as measured by the coefficient of variation (CV) (Table 6.1). This is also reflected in the ratios between the percentage points between the 1% and 0.1% and the 0.1% and 0.01% equalled or exceeded range. This would suggest that in this region, smaller catchments in the upper parts of the drainage basin have a 'flashier' type hydrological regime, while the lower parts of the systems tend to be more base flow dominated with a less 'flashy' high flow regime.

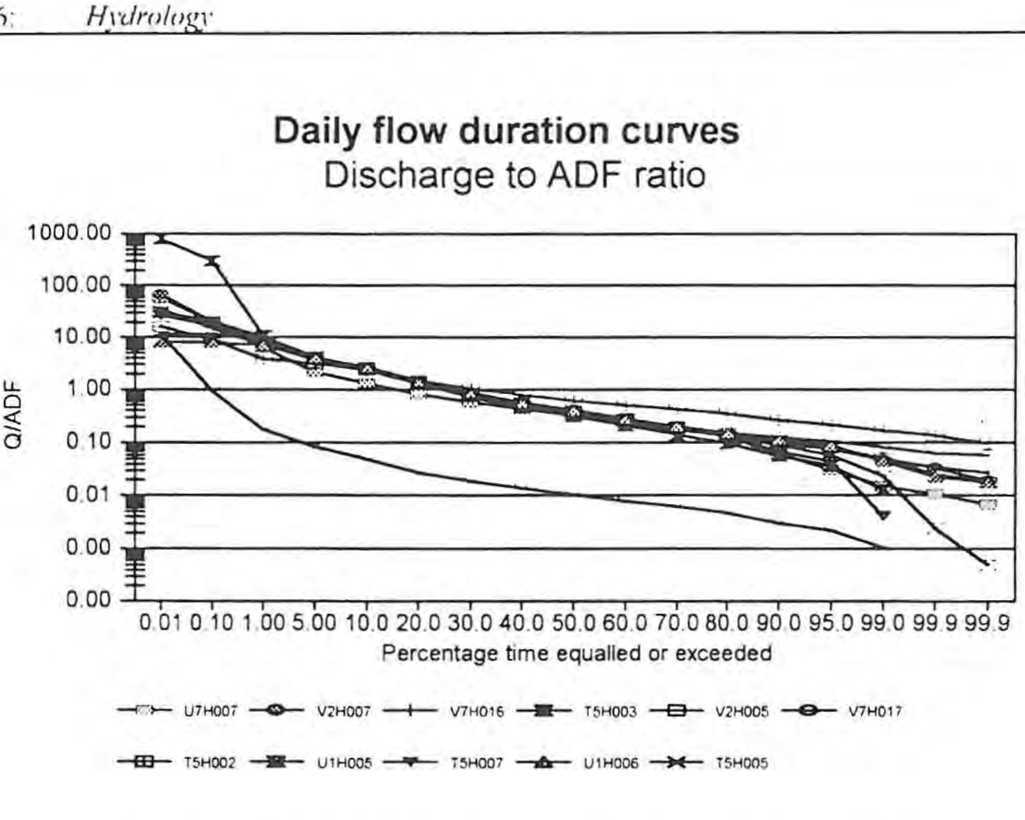

Figure 6.3: Daily flow discharge to average daily flow for 11 gauging stations.

6.2.4.1 Generating the scaling factor for the target daily flow duration curves for sites 1 to 10

The target daily flow duration curves needed to be adjusted to accommodate the flashier nature of the upper catchment as well as the base-flow driven nature of the lower catchment. In the *HYMAS* model, the target daily time series is accommodated by utilising a scaling factor. To generate the daily time series for sites 1 to 10, the source flow data was taken to be the daily series for U1H005, as these sites were closer to U1H005 than U1H006. For sites with an MAR less than 70, the average of the ratios for U7H007, V2H007, V7H016 and U1H005 were used to downscale (sites 1 to 4) the target daily flow duration curve for the 0.1 and 0.01 percentiles. For the 1 to 99.99 percentiles, the target daily flow duration curve was downscaled using the ratio of the site's MAR to the MAR of U1H005. The MAR of each site was calculated using the available data from the quaternary catchments from WR90 and the catchment area for each site (measured using the 1:50 000 topographical map).

To generate the daily time series for sites 5 and 6, the source flow data was taken to be the daily series for U1H005, as U1H005 is within two kilometres of each of these sites. The ratios for U1H005 were used to downscale the target daily flow duration curve for the 0.1 and 0.01 percentiles. For the 1 to 99.99 percentiles, the target daily flow duration curve was downscaled using the ratio of the site's MAR to the MAR of U1H005. The MAR of each site was calculated using the available data from the quaternary catchments from WR90. For sites 7, 8, 9 and 10 the same technique was used, but the scaling was in the upward direction. In this way, daily time series were generated for sites 1 to 10 for the Mkomazi River. The daily time series are available in Appendix B at the back of the thesis. Figure 6.4 displays two examples of the daily time series for the Mkomazi River. Figure 6.5 displays examples of the 1-day daily flow duration curves for four sites for the Mkomazi River.

6.2.4.2 Generating the scaling factor for the target daily flow duration curves for sites 11 to 13

To generate the daily time series for sites 11 to 13, the source flow data was taken to be the daily series for U1H006, as these sites are closer to U1H006 than U1H005. For sites draining greater than 70 MAR, the average of the ratios for V2H005, V7H017, T5H002, T5H007 and U1H006 were used to downscale the target daily flow duration curve for the 0.1 and 0.01 percentiles. For the 1 to 99.99 percentiles, the target daily flow duration curve was downscaled using the ratio of the site's MAR to the MAR of U1H006. The MAR of each site was calculated using the available data from the quaternary catchments from WR90. In this manner, daily time series were generated for sites 11 to 13 for the Mkomazi River. (Table 6.3 presents the flows for the 1-day daily duration curves that were used to generate the daily time series for each site. The daily time series for all sites are presented in Appendix B at the back of the thesis).

Table 6.2: Regional flow gauging stations around the Mkomazi catchment.

Station	U7H007		V2H007		V7H016		V2H005		V7H017		T5H002		U1H005		T5H007		U1H006	
MAR	23.18		32.27		48.30		115.25		137.90		153.8		635.58		957.1		1033.17	
ADF	0.71		1.02		1.53		3.65		1.37		4.88		20.15		30.35		32.76	
CV	0.598		0.538		0.442		0.461		0.128		0.383		0.168		0.360		0.116	
%	Q/adf	Ratio*	Q/adf	Ratio*	Q/adf	Ratio*	Q/adf	Ratio*	Q/adf	Ratio*	Q/adf	Ratio*	Q/adf	Ratio*	Q/adf	Ratio*	Q/adf	Ratio*
0.01	57.96	2.92	66.79	3.25			29.18	1.53	35.77	2.37	16.41	1.79	31.22	1.53	57.37	3.47		
0.10	19.86	3.10	20.54	2.42	11.71	1.38	19.11	2.38	15.07	2.07	9.16	2.38	20.39	1.95	16.53	2.44	8.03	1.16
1.00	6.41	3.01	8.49	2.11	8.49	2.25	8.02	2.09	7.28	1.98	3.84	1.27	10.471	2.50	6.76	1.64	6.92	1.74
5.00	2.13	1.59	4.04	1.61	3.78	1.58	3.84	1.55	3.67	1.56	3.04	1.32	4.18	1.67	4.13	1.56	3.98	1.54
10.00	1.34	1.65	2.50	1.95	2.39	1.86	2.48	1.80	2.35	1.77	2.31	1.58	2.51	1.94	2.65	1.79	2.59	1.83
20.00	0.82	1.41	1.28	1.76	1.29	1.65	1.38	1.59	1.33	1.56	1.46	1.38	1.29	1.65	1.48	1.68	1.42	1.64
30.00	0.58	1.38	0.73	1.52	0.78	1.57	0.87	1.52	0.85	1.48	1.06	1.33	0.78	1.56	0.89	1.53	0.86	1.56
40.00	0.42	1.33	0.48	1.51	0.50	1.45	0.57	1.48	0.57	1.42	0.79	1.29	0.50	1.45	0.58	1.44	0.56	1.42
50.00	0.32	1.35	0.32	1.44	0.34	1.45	0.38	1.41	0.41	1.40	0.62	1.23	0.35	1.38	0.40	1.42	0.39	1.38
60.00	0.23	1.32	0.22	1.31	0.24	1.33	0.27	1.33	0.29	1.45	0.51	1.18	0.25	1.35	0.28	1.49	0.28	1.38
70.00	0.18	1.31	0.17	1.29	0.18	1.33	0.20	1.33	0.20	1.31	0.43	1.24	0.18	1.36	0.19	1.43	0.20	1.32
80.00	0.13	2.20	0.13	1.36	0.13	1.36	0.15	1.41	0.15	1.22	0.34	1.33	0.14	1.51	0.13	1.93	0.15	1.36
90.00	0.06	1.96	0.10	1.28	0.10	1.31	0.11	1.37	0.12	1.16	0.26	1.19	0.09	1.51	0.07	1.55	0.11	1.26
95.00	0.03	2.09	0.08	1.59	0.08	1.51	0.08	1.57	0.11	1.32	0.22	1.30	0.06	2.48	0.05	11.02	0.09	1.96
99.00	0.01	1.38	0.05	1.40	0.05	1.43	0.05	2.01	0.08	1.28	0.17	1.22	0.02	9.60	0.004	-	0.05	1.96
99.90	0.01	1.60	0.03	1.75	0.04	1.29	0.02	1.37	0.06	1.11	0.14	1.31	0.002	5.00			0.02	1.33
99.99	0.01	-	0.02	-	0.03	-	0.01	-	0.06	-	0.09	-	0.001	-			0.01	-

* Ratio refers to the ratio between the upper flow class and the lower flow class. For example, for U7H007, the Q/adf for flow class 0.10 is 19.86 and the Q/adf for the 0.01 flow class is 57.96. Thus 57.96/19.86 is 2.92.

6.2.5 Flood frequency analysis

The daily time series generated for each site were used to generate flood frequency curves using the annual and partial series. Standard techniques were applied (cf. Dunne & Leopold, 1978; Gordon *et al.*, 1992). The cutoff for the partial series was taken as the smallest annual flood for the period of record. It must be noted that the flood frequency analysis was based on mean daily flows and not the peak flows. Instantaneous peak flows are simply not available as these flows often exceed the Discharge Table Limit (DTL) of the flow gauging stations, as previously explained. However, it is argued that given the focus of the research and the importance of modelling bed material transport, average flow conditions better represent long-term sediment transport patterns. This does not negate the significance of instantaneous peak discharges, these will be dealt with in Section 6.2.6. It is not practical to display all the data for the flood frequency analysis. Examples of the analysis are provided in Figures 6.6 and 6.7. The bulk of the data are presented in Appendices C and D.

6.2.6 Historical flood records

Historical flood records for the Mkomazi River have been compiled by van Bladeren & Burger (1989) and van Bladeren (1992). These records were compiled using a combination of historical records, hydraulic modelling using the slope-area method and cross-sectional data. Table 6.4 presents the data in summary form. Van Bladeren (1992) demonstrated that the inclusion of the historical record has a significant impact on the frequency distribution of the gauged data. Results indicate that calculating historical flood data may provide more realistic flood estimates. These records serve as useful information and will be utilised in the discussion of results.

Table 6.3: Flows for the 1-day daily flow duration curves generated for the daily time series.

MAR	635.6	1033.2	67.15	121.81	355.6	374.56	633.63	640.39	681.31	698.31	910.25	949.63	975.63	1026.88	1032.00
%	**U1H005**	**U1H006**	**Site 1**	**Site 2**	**Site 3**	**Site 4**	**Site 5**	**Site 6**	**Site 7**	**Site 8**	**Site 9**	**Site 10**	**Site 11**	**Site 12**	**Site 13**
0.01	629.4	263	102.772	183.404	436.522	459.907	622.337	634.909	672.627	691.485	900.230	939.010	964.890	1015.570	1021.130
0.1	411.07	263	47.143	84.130	216.100	227.677	406.756	414.973	439.625	451.951	588.380	613.740	630.640	663.770	667.410
1	211.04	226.605	19.561	34.909	99.585	104.920	208.593	212.907	225.449	231.77	301.740	314.740	323.410	340.400	342.260
5	84.28	130.502	9.271	16.013	47.197	49.725	83.437	85.123	90.180	92.708	114.842	120.062	122.672	129.197	130.502
10	50.57	85.006	5.563	9.608	28.319	29.836	50.064	51.076	54.11	55.627	74.805	78.206	79.906	84.156	85.006
20	26.03	46.501	2.863	4.946	14.577	15.358	25.770	26.290	27.852	28.633	40.921	42.781	43.711	46.036	46.201
30	15.79	28.418	1.737	3.000	8.842	9.316	15.632	15.948	16.895	17.369	25.008	26.145	26.713	28.134	28.418
40	10.12	18.227	1.113	1.923	5.667	5.971	10.019	10.221	10.828	11.132	16.040	16.769	17.133	18.045	18.227
50	7.00	12.810	0.770	1.330	3.920	4.130	6.930	7.070	7.490	7.700	11.273	11.785	12.041	12.682	12.810
60	5.07	9.250	0.558	0.963	2.839	2.991	5.019	5.121	5.425	5.577	8.140	8.510	8.695	9.158	9.250
70	3.76	6.692	0.414	0.714	2.106	2.218	3.722	3.798	4.023	4.136	5.889	6.157	6.290	6.625	6.692
80	2.77	5.051	0.305	0.526	1.551	1.634	2.742	2.798	2.964	3.047	4.445	4.647	4.748	5.000	5.051
90	1.80	3.718	0.198	0.342	1.008	1.062	1.782	1.818	1.926	1.980	3.272	3.421	3.495	3.681	3.718
95	1.19	2.947	0.131	0.226	0.666	0.702	1.178	1.202	1.273	1.309	2.593	2.711	2.770	2.918	2.947
99	0.48	1.501	0.053	0.091	0.269	0.283	0.475	0.485	0.514	0.528	1.321	1.381	1.411	1.486	1.501
99.9	0.05	0.766	0.006	0.101	0.028	0.030	0.050	0.051	0.054	0.055	0.674	0.705	0.720	0.758	0.766
99.99	0.01	0.578	0.001	0.002	0.006	0.006	0.010	0.010	0.011	0.011	0.509	0.532	0.543	0.572	0.578

Table 6.4: Highest extreme flood peaks on record for the Mkomazi River (modified after van Bladeren & Burger, 1989 and van Bladeren, 1992).

Year	Catchment area (km^2)	Equivalent current research site	Discharge (m^3s^{-1})	Period under review	Maximum depth (m)	Return period (years)
1959	1744	5 and 6	1490	1931-1990		20-50
1975	1744	5 and 6	2010	1931-1990		
1987	1744	5 and 6	2770	1931-1990	5.28	50-100
1988	1744	5 and 6	1230	1931-1990		
1959	3177	9	2470	1931-1990	3.55	20-50
1959	3339	11	3480	1931-1990	8.79	50-100
1987	3339	11	6030	1931-1990	11.42	>200
1989	4349	12 and 13	2618	1931-1990	4.31	10-20
1856	4375	12 and 13	7250	1856-1990	11.91	>200
1868	4375	12 and 13	5820	1856-1990	11.01	100
1917	4375	12 and 13	3570	1856-1990	8.55	20-50
1925	4375	12 and 13	6100	1856-1990	10.61	100-200
1959	4375	12 and 13	5510	1856-1990	10.69	50-100
1976	4375	12 and 13	2880	1856-1990	8.99	
1987	4375	12 and 13	6830	1856-1990	10.78	

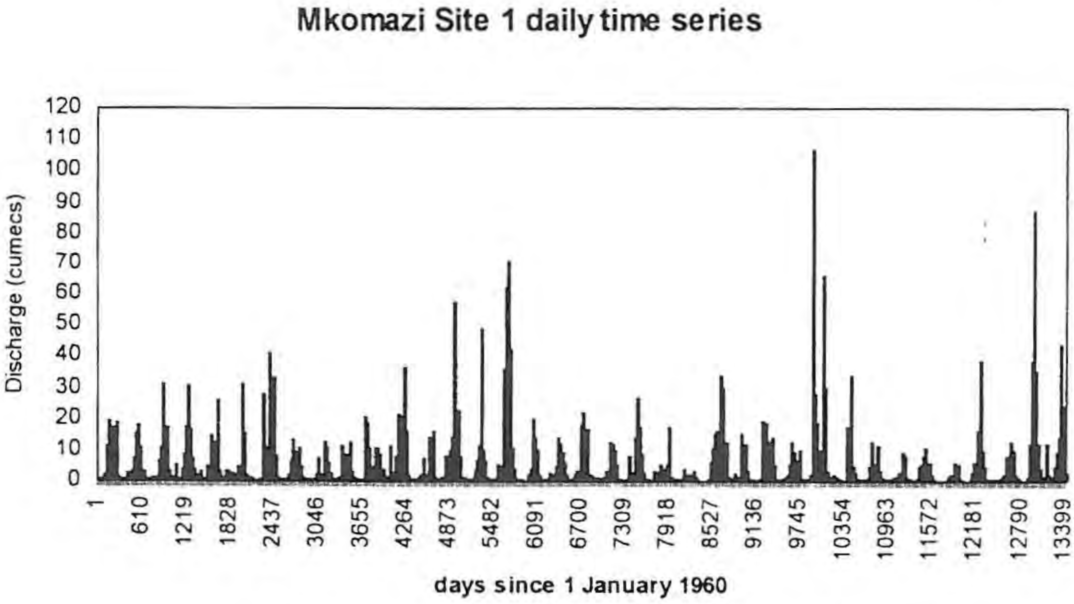

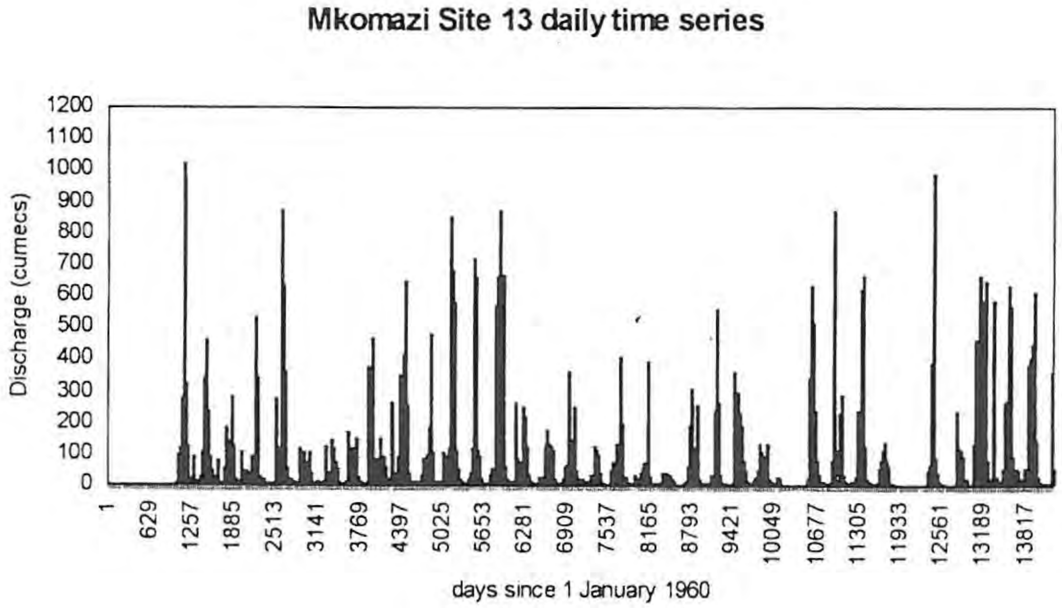

Figure 6.4: Synthesised daily time series for sites 1 and 13 for the Mkomazi River.

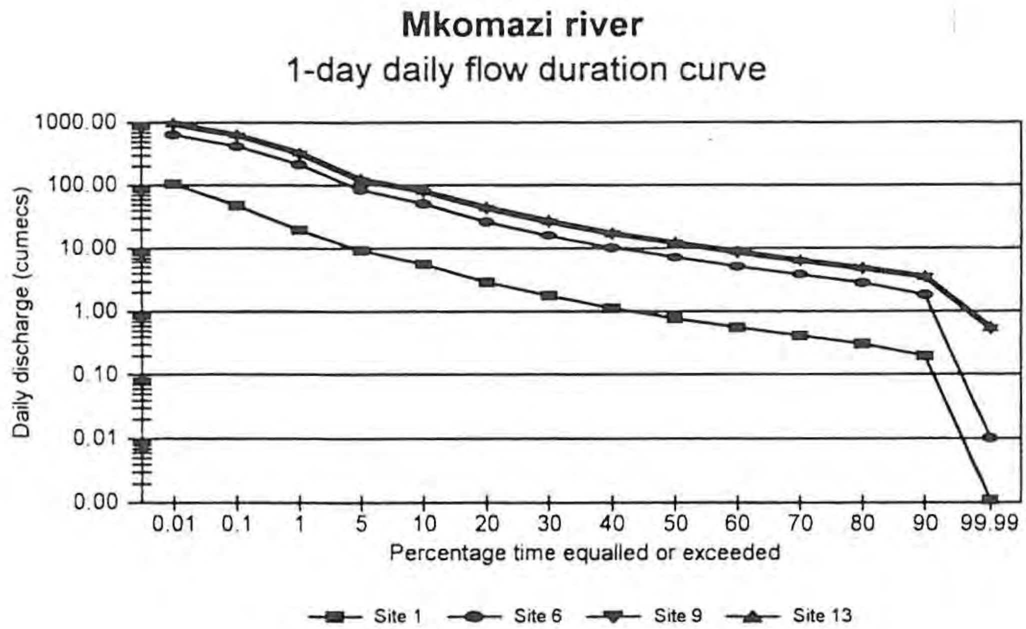

Figure 6.5: Synthesised 1-day daily flow duration curves for sites 1, 6, 9 and 13 for the Mkomazi River.

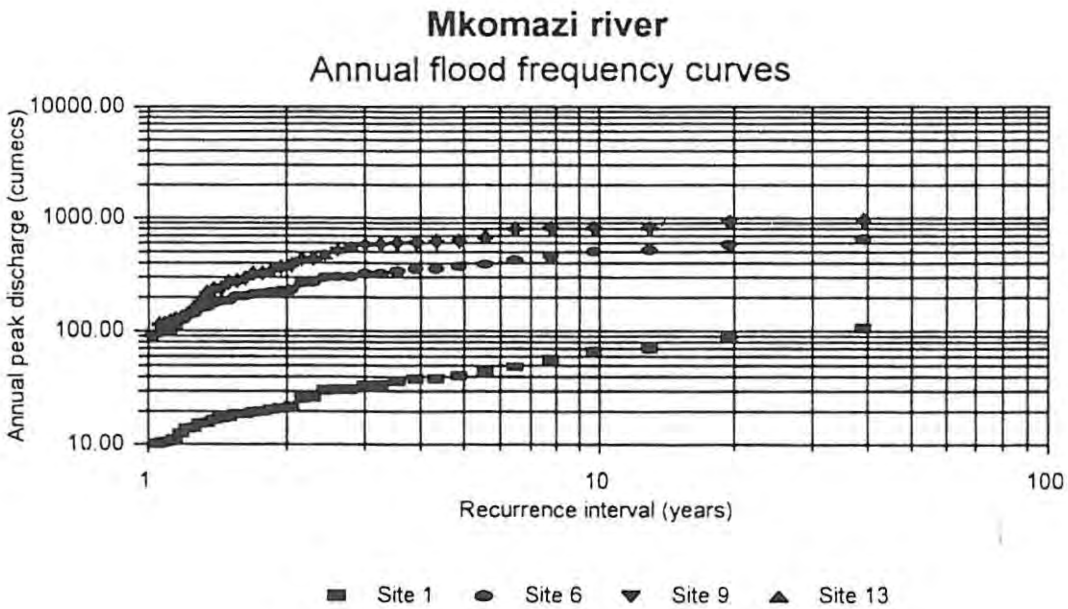

Figure 6.6: Annual flood frequency curves for sites 1, 6, 9 and 13 for the Mkomazi River.

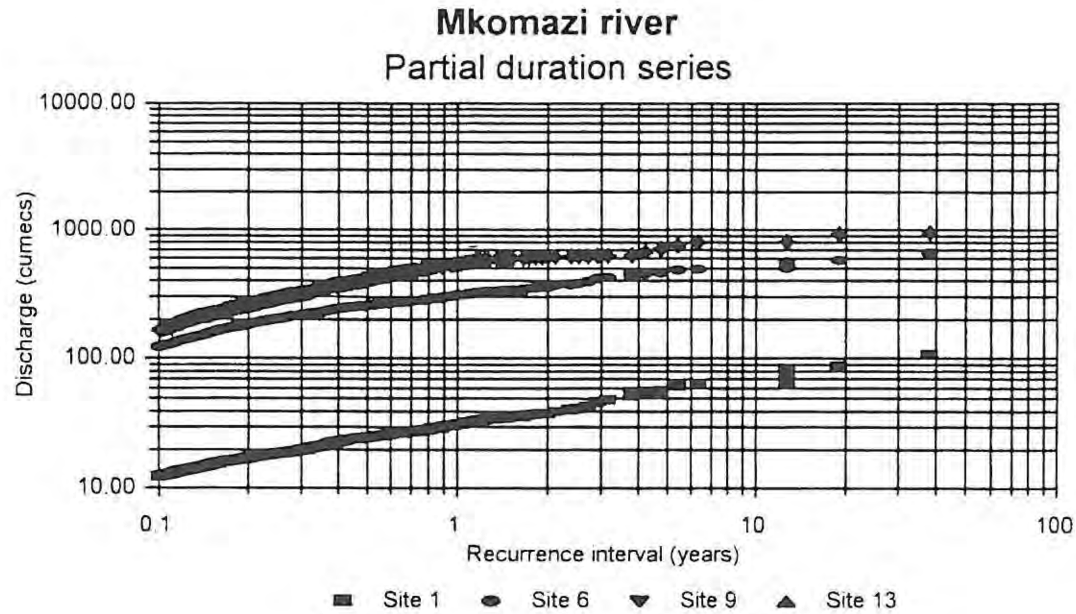

Figure 6.7: Partial duration series flood frequency curves for sites 1, 6, 9 and 13 for the Mkomazi River.

6.3 The Mhlathuze River

6.3.1 Data availability

Synthesised daily hydrological data was available for the Mhlathuze River. The data was generated by Hughes & Smakthin (1998). Here, a short review of the context of the data is provided. There are two streamflow gauging stations available for the Mhlathuze River, the first is at the site of the Goedertrouw Dam which was completed in 1979. Prior to the building of the dam, a flow gauging station, W1H006 (Normanhurst), had data ranging from 1964 to 1973, but also contained long periods of missing data. After the construction of Goedertrouw Dam, the present gauging station, W1H028, was re-opened. This has data from 1980 to the present-day. A second gauging station, W1H009 (Riverview) has data from 1963-1991 (Figure 5.3). These latter two stations were used by Hughes & Smakthin (1998) to generate virgin and present-day daily time series for the four sites identified for the Mhlathuze River.

To generate the virgin time series, Hughes & Smakthin (1998) calibrated the model to achieve mean annual volumes and monthly distributions that were similar to those presented in WR90 and the pattern of daily flow variation to the station W1H009. To simulate present-day conditions, the model was calibrated against water use data supplied by the local water authority, Mhlathuze Water.

6.3.2 Hydrological regime of the four Mhlathuze sites

Eight daily time series were generated for the four Mhlathuze sites, four daily time series for the virgin conditions and four daily time series for the present-day conditions. This information is available in Appendix B. Examples of the virgin daily time series data are given in Figure 6.8 and examples of the present-day daily time series in Figure 6.9. The virgin 1-day daily flow duration curves are presented in Figure 6.10, while Figure 6.11 displays the present-day 1-day daily flow duration curves.

6.3.3 Flood frequency analysis

Results of the analysis of the virgin time series and present-day time series for the annual series are presented in Figures 6.12 and 6.13 respectively. The results of the analysis of the virgin time series and present-day time series for the partial duration series are given in Figures 6.14 and 6.15 respectively.

6.3.4 Historical flood records

The Goedertrouw Dam has been shown to have a significant effect on flood peaks downstream of the dam. Van Bladeren (1992) has shown that the September 1987 inflow flood to Goedertrouw Dam was 3760 m^3s^{-1}, while the outflow was 550 m^3s^{-1}. A similar flood in 1984 was also severely attenuated by the dam (Table 6.5). These records serve as useful information and will be utilised in the discussion of results.

Table 6.5: Highest extreme flood peaks on record for the Mhlathuze River (modified after van Bladeren & Burger, 1989 and van Bladeren, 1992).

Year	Catchment area (km^2)	Equivalent current research site	Discharge (m^3s^{-1})	Period under review	Maximum depth (m)	Return period (years)
1940	1273	-	4100	1940-1989	-	-
1963	1273	-	850	1940-1989	-	-
1984	1273	-	2620	1940-1989	-	-
1985	1273	-	540	1940-1989	-	-
1987	1273	-	3780	1940-1989	-	-
1988	1273	-	450	1940-1989	-	-
1940	1348	-	4100	1940-1989	11.98	50-100
1913	2409	1	2170	1913-1990	-	-
1917	2409	1	3290	1913-1990	7.68	20-50
1940	2409	1	3630	1913-1990	-	-
1984	2409	1	2420	1913-1990	-	-
1987	2409	1	3590	1913-1990	8.31	20-50
1984	2409 *	1	4790	1980-1990	-	-
1987	2409 *	1	6000	1980-1990	-	-
1913	2771	3	2330	1913-1987	6.01	10-20
1917	2771	3	3530	1913-1987	9.54	20-50
1918	2771	3	3500	1913-1918	10.04	20-50
1940	2771	3	3890	1913-1987	10.42	20-50
1971	2771	3	725	1913-1987	-	-
1977	2771	3	3540	1913-1987	8.70	20-50
1987	2771	3	4130	1913-1987	8.45	20-50

* Calculated as if the flood peak had not been attenuated by Goedertrouw Dam.

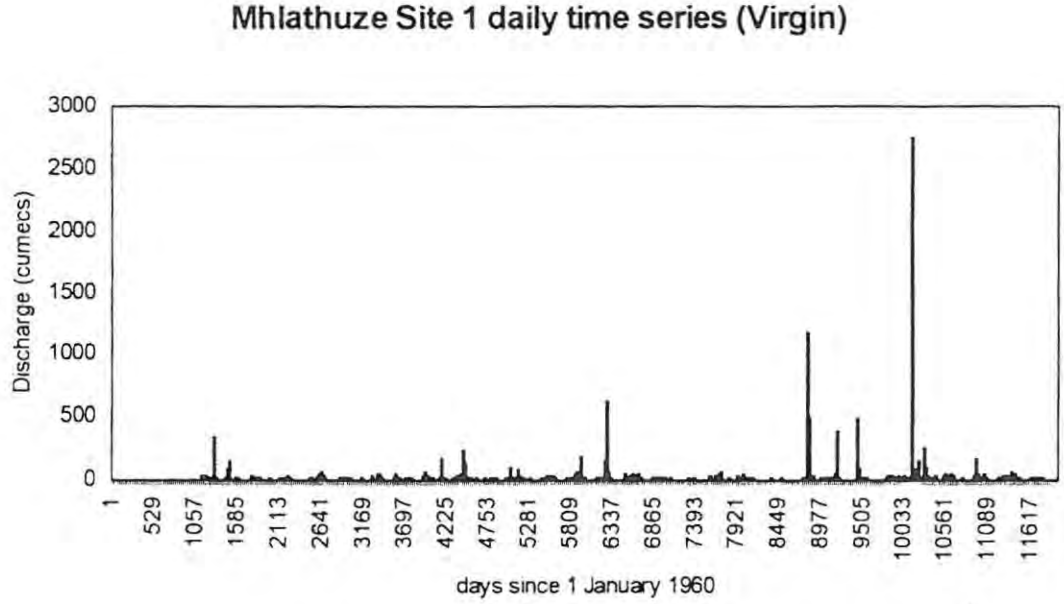

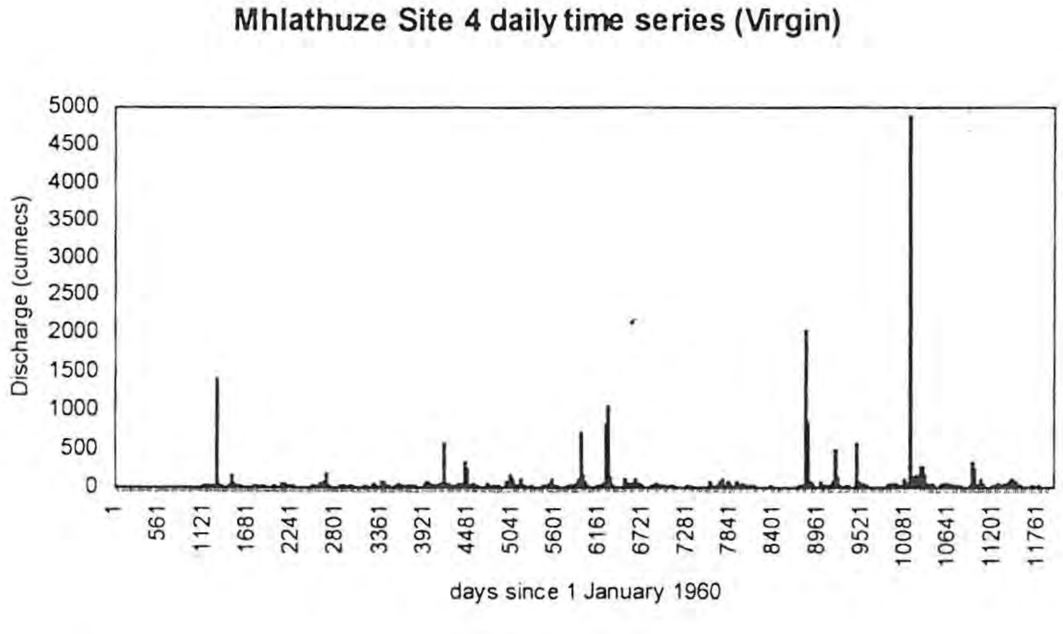

Figure 6.8: Virgin daily time series for two sites for the Mhlathuze River.

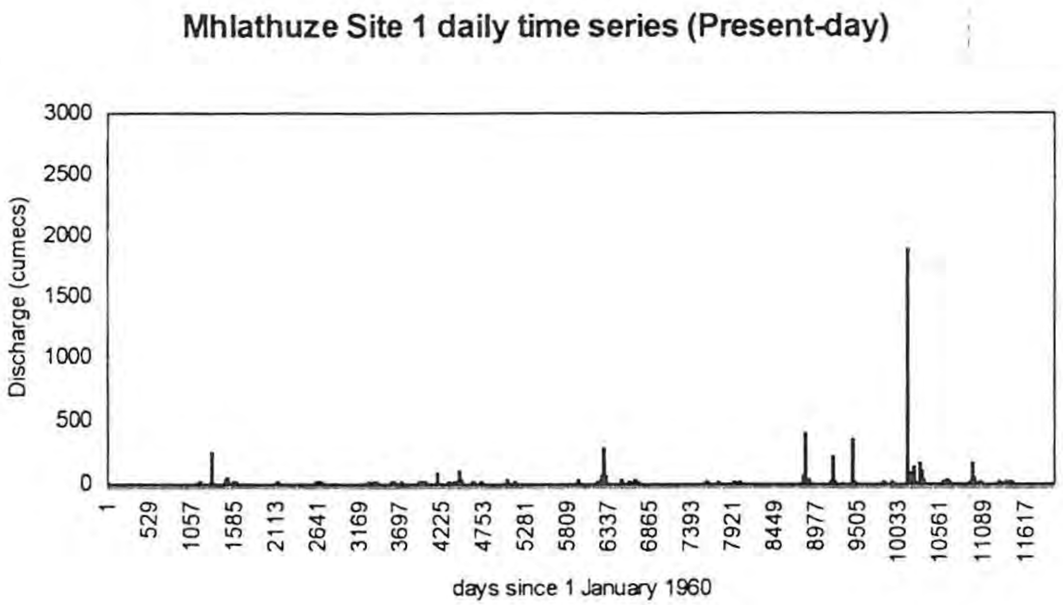

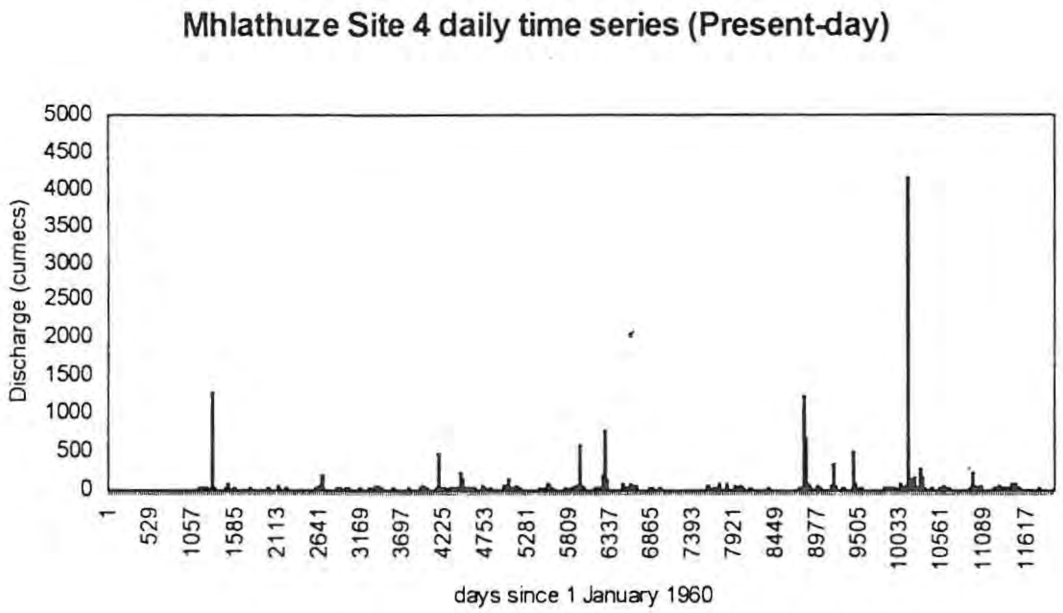

Figure 6.9: Present-day daily times series for two sites for the Mhlathuze River.

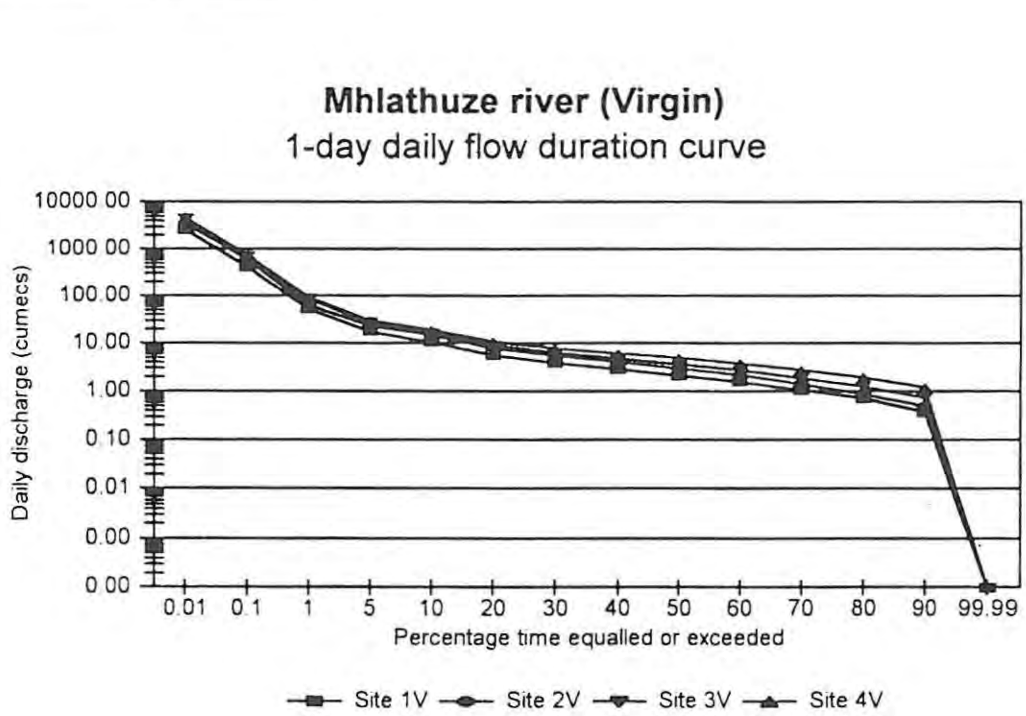

Figure 6.10: Virgin 1-day daily flow duration curves for four sites for the Mhlathuze River.

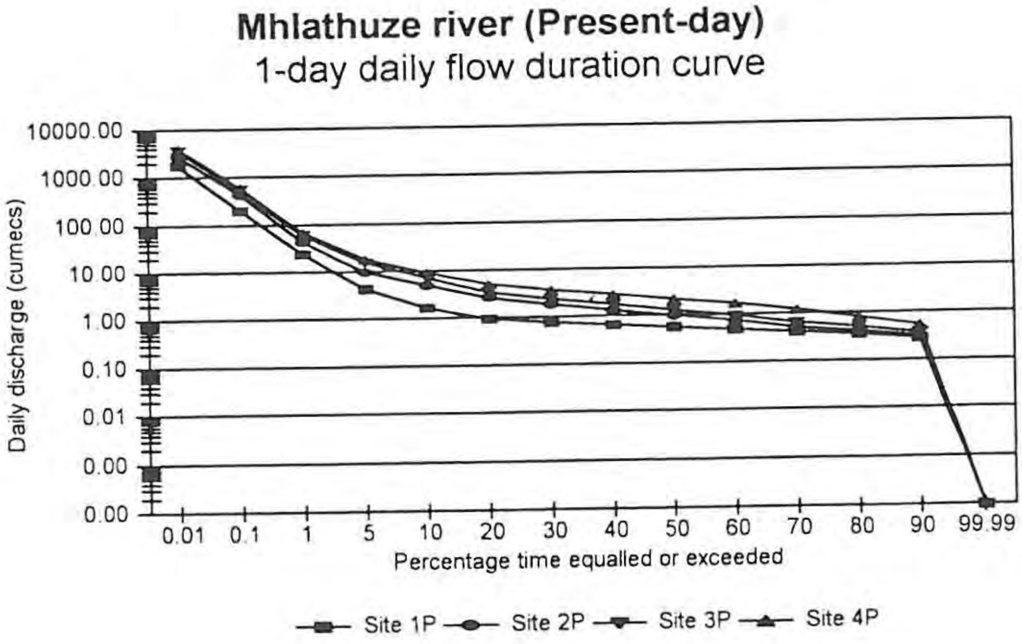

Figure 6.11: Present-day 1-day daily flow duration curves for four sites for the Mhlathuze River.

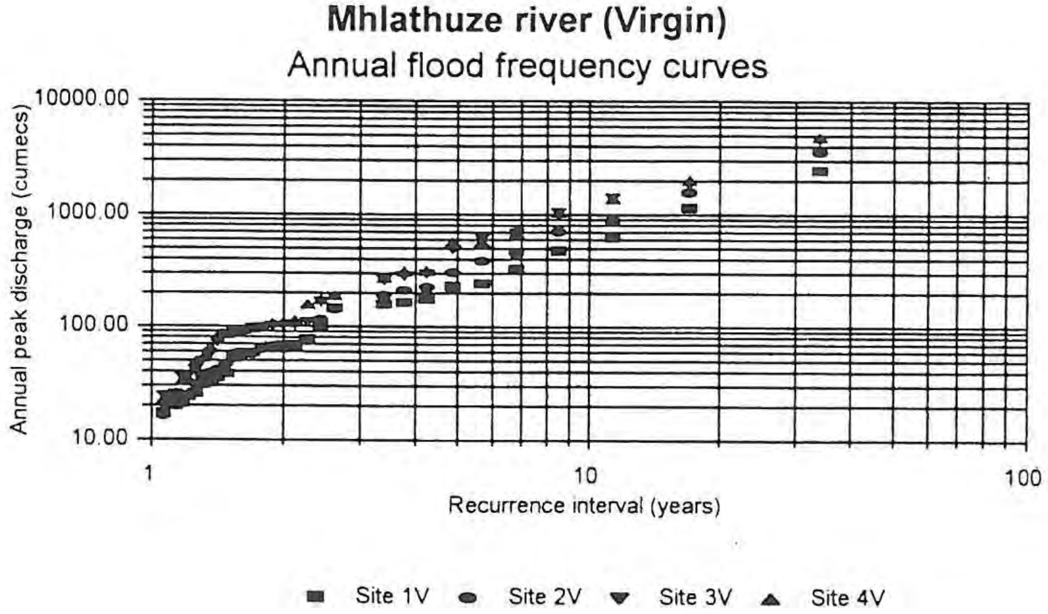

Figure 6.12: Virgin annual flood frequency curves for four sites for the Mhlathuze River.

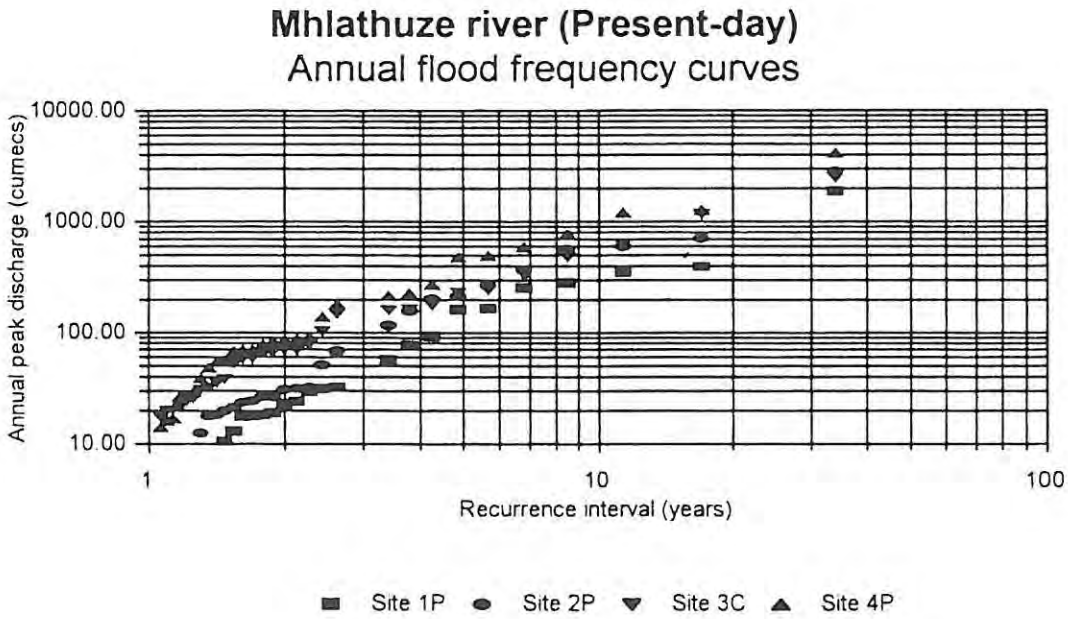

Figure 6.13: Present-day annual flood frequency curves for four sites for the Mhlathuze River.

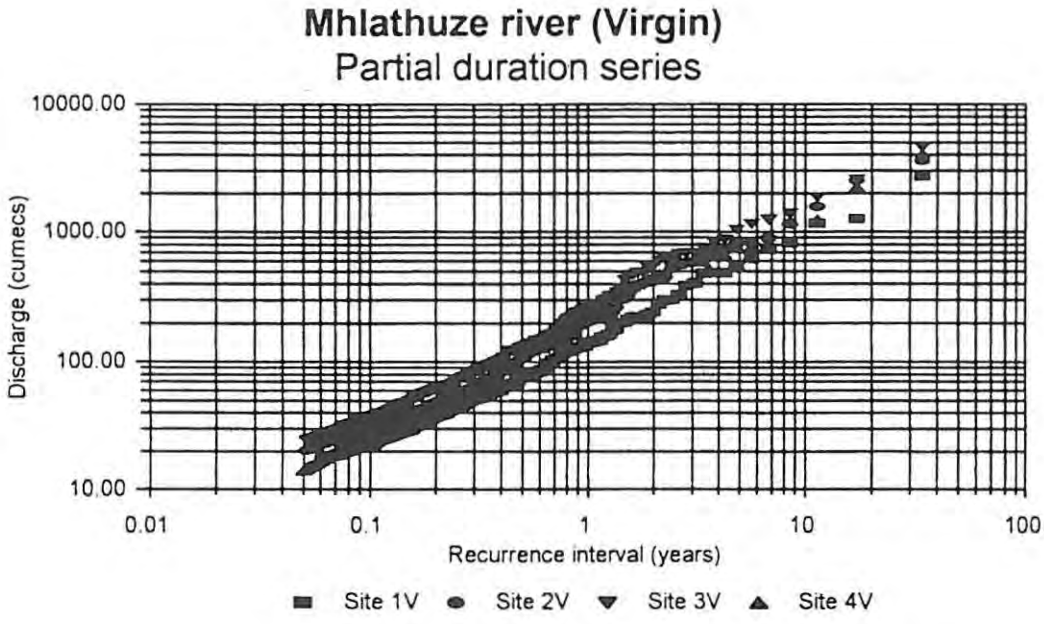

Figure 6.14: Virgin partial duration series flood frequency curves for four sites for the Mhlathuze River.

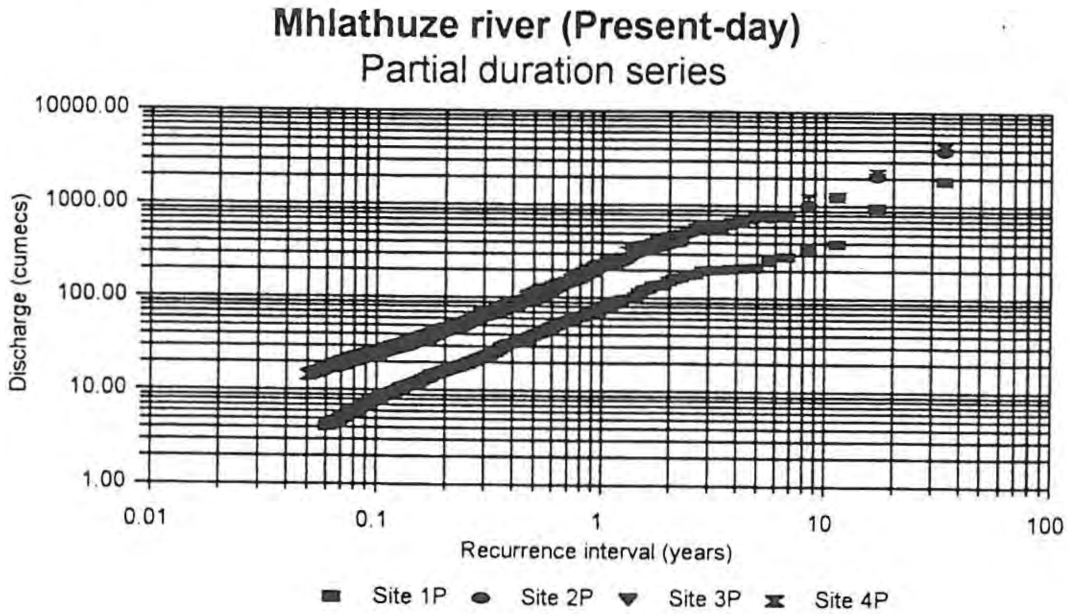

Figure 6.15: Present-day partial duration series flood frequency curves for four sites for the Mhlathuze River.

6.4 The Olifants River

6.4.1 Data availability

Synthesised hydrological data was available for the Olifants River. The data obtained was generated by Hughes (2000) for each of the four sites of the Olifants River using the VTI model. The use of this model was necessary due to the paucity of good quality data for the Olifants River, and due to the lack of information on the operating procedures of the dams that control streamflow in the upper Olifants River. The VTI model contains four basic functions for the generation of streamflow (Hughes, 2000):

- An infiltration excess function that is largely controlled by the surface soil characteristics and the intensity of rainfall.

- A saturation excess function that is controlled by soil depth, water holding capacity and drainage characteristics as well as the total rainfall amounts that can occur.

- A soil moisture drainage or base flow function that is controlled by topography, water holding capacity and the rate of drainage characteristics of the soil.

- A groundwater drainage function that can generate groundwater outflows as spring flows or through intersection of the regional groundwater table with the river channel system.

Hughes (2000) argues that the data from the DWAF gauging stations (B1H015 and B2H003) suggests that under virgin conditions, the upper Olifants is dominated by the runoff generation processes represented by the first function, but with a significant, slowly responding groundwater base flow contribution. The VTI model was run using this scenario and calibrated against an earlier yield assessment generated by consulting engineers BKS. Hughes (2000) suggests that the model output simulates larger events than appear in the DWAF observed records (flow gauging stations

B1H015 and B2H003). The daily time series that were generated for the four sites for the Olifants River can be assumed to be for virgin conditions.

6.4.2 Hydrological regime of the Olifants sites

Four daily time series were generated for the Olifants sites, representing virgin flow conditions. This information is available in Appendix B. Examples of the virgin daily time series data are given in Figure 6.16. The virgin 1-day daily flow duration curves are presented in Figure 6.17.

6.4.3 Flood frequency analysis

The annual duration series flood frequency curves are presented in Figure 6.18 and the partial duration series in Figure 6.19.

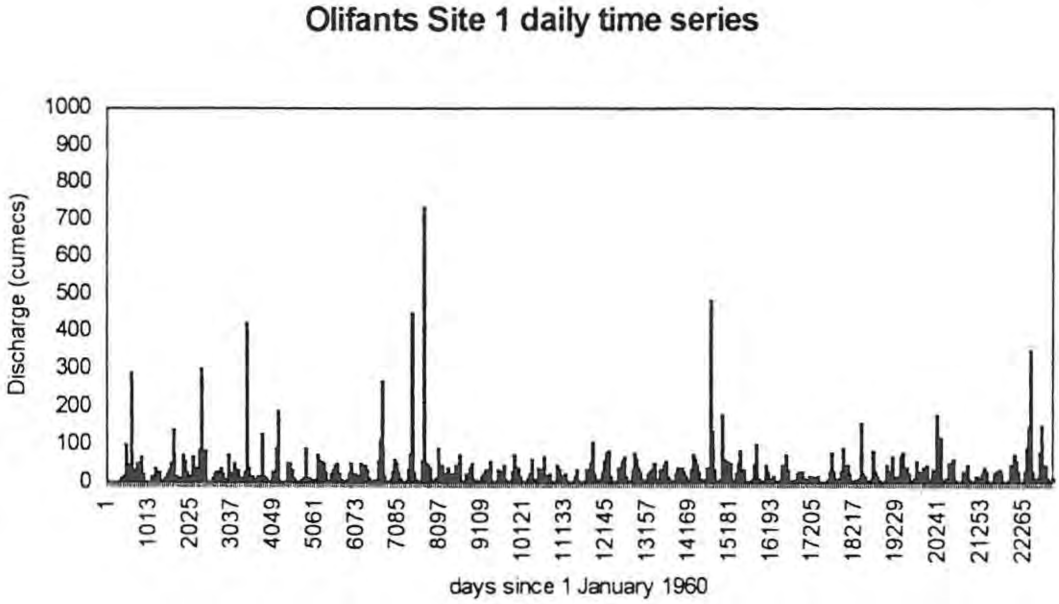

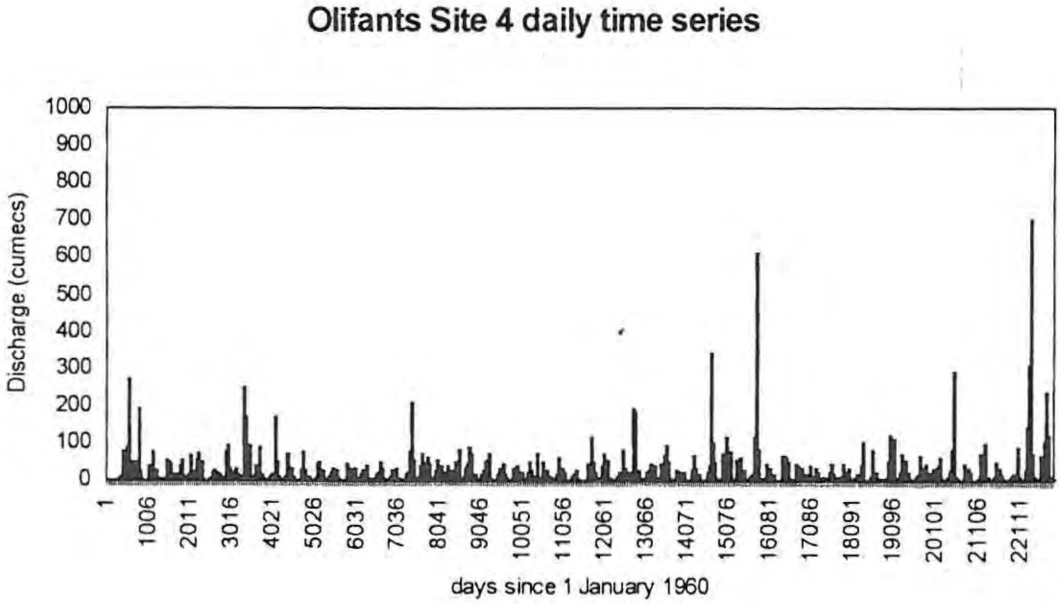

Figure 6.16: Virgin daily time series for two sites for the Olifants River.

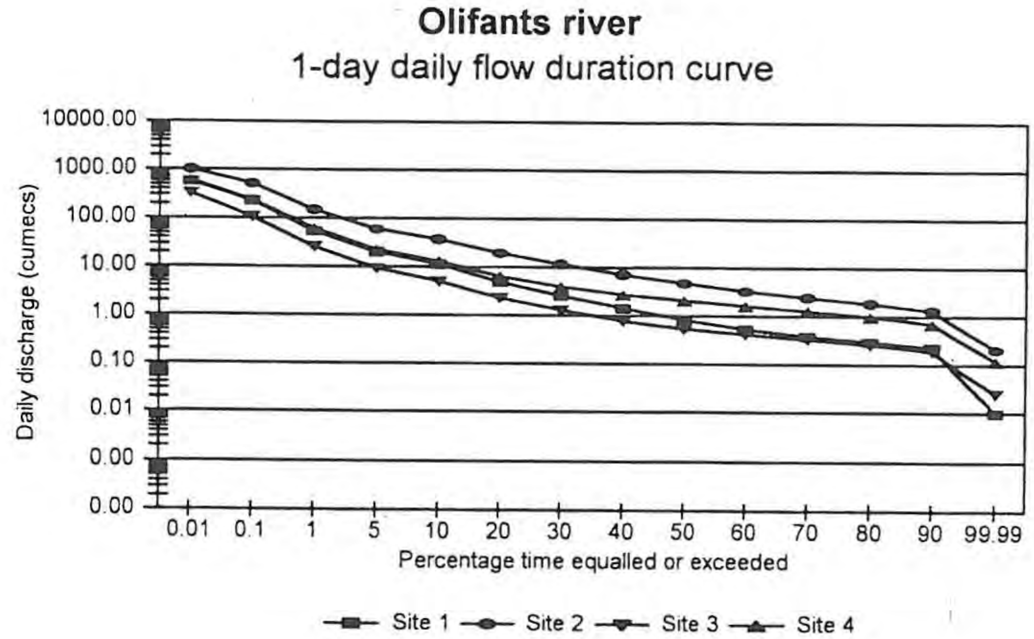

Figure 6.17: Virgin 1-day daily flow duration curves for four sites for the Olifants River.

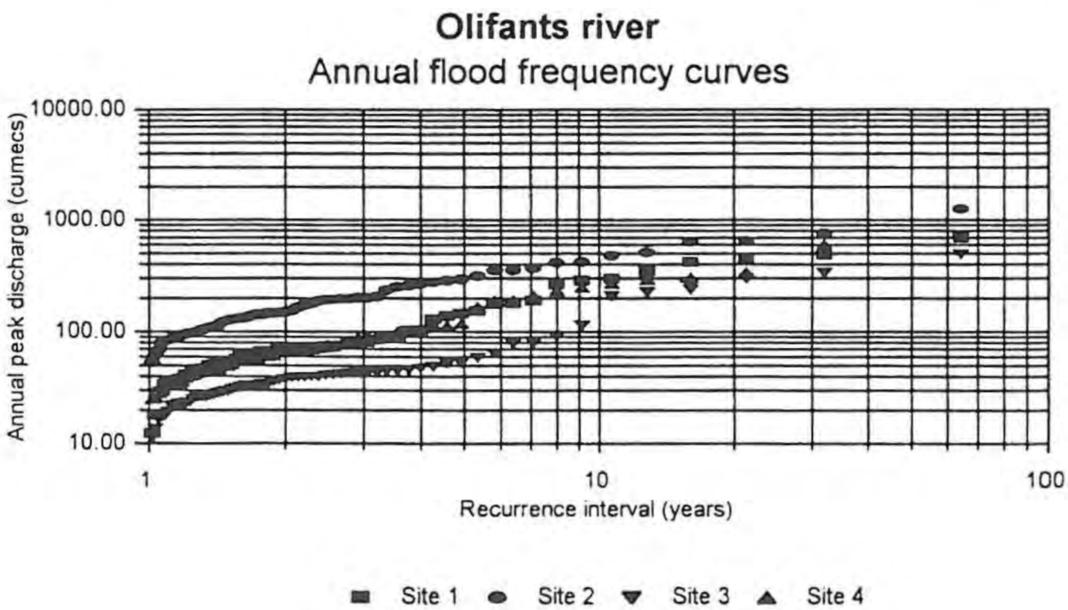

Figure 6.18: Virgin annual flood frequency curves for four sites for the Olifants River.

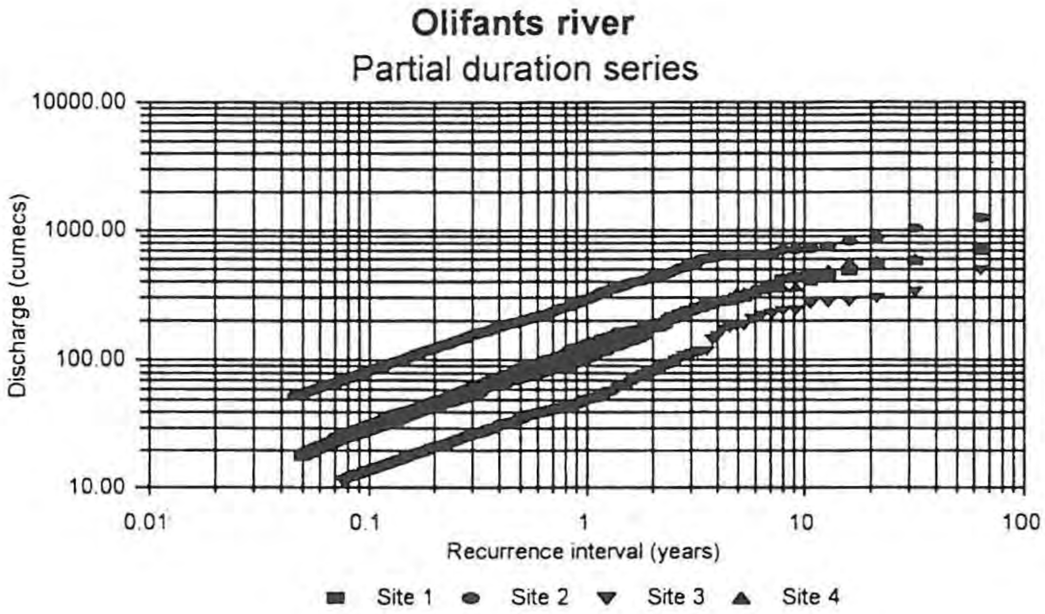

Figure 6.19: Virgin partial duration series flood frequency curves for four sites for the Olifants River.

6.5 Summary and conclusions

The primary objective of this chapter was to present the techniques used and hydrological data generated for use in the magnitude-frequency analysis. It is appropriate at this point to summarise and discuss the data that were generated. Table 6.6 presents the summarised hydrological data for the three systems.

Table 6.6: Summary hydrological data for the Mkomazi, Mhlathuze and Olifants Rivers.

Parameter	Mkomazi virgin	Mhlathuze virgin	Mhlathuze present-day	Olifants virgin
Area (km^2)	4387	4209	4209	10 891
MAR (million cubic metres)	1089	362	217	449
Wet season	Summer	Summer	Summer	Summer
CV	0.41	0.934	-	0.70
Highest modelled flow (m^3s^{-1})	1021.28	4896.09	4163.04	734.56
Highest flood record flow (m^3s^{-1})	7250	6000	4790	-

The Mkomazi generates the largest MAR of all the rivers considered for this research (Table 6.6). It also has the lowest CV. The data generated for the Mkomazi River was based on target flow duration curves generated on the basis of the source data and regionalised flow duration curves. For all intents and purposes, the synthesised data can be regarded as the natural flow regime as there is no impoundment (as yet) on the Mkomazi. It is difficult to assess the accuracy of the data, in that apart from the flow gauging stations in the catchments around the Mkomazi, there is nothing to calibrate the data against. What is clear from the historical flood record is that the method used does not accurately reflect the flood peaks (Table 6.6). Table 6.4 has shown that since 1856 there have been a number of floods in the middle and lower catchments that well exceed the Discharge Table Limits (DTL) of the gauging stations. In the upper catchment, there have been at least four major floods exceeding 1230 m^3s^{-1} since 1959. This would suggest that a flood of this magnitude or greater is fairly common (perhaps a 1 in 20 year flood). Van Bladeren (1992) has calculated the 1987 flood (2770 m^3s^{-1}) as being somewhere between and 50 and 100 year flood, while the flood in 1959 of 1490 m^3s^{-1} was calculated as a 20 to 50 year flood. In the lower catchment at least seven major floods exceeding 2880 m^3s^{-1} have occurred in the last 150 years. Again, this would suggest that on average every 20 years or so a major flood is likely to occur. Van Bladeren (1992) has calculated that floods in the range of 3500 m^3s^{-1} to 5000 m^3s^{-1} are likely to have a return period in the range of 20 to 50 years. The point is that large floods occur fairly frequently in the Mkomazi River. Their significance on channel form, maintenance and bed material transport will be discussed in Chapter 9.

The Mhlathuze has a lower MAR than the Mkomazi (virgin and present-day). However, it has the highest CV of all the rivers under consideration (Table 6.6). This is due to the cut-off lows that generate extreme floods in relation to the 'normal flow'. For the Mhlathuze River, synthesised records were generated for two scenarios - the pre-dam flow record and the post-dam flow record. Again, it is difficult to determine the accuracy of the flow record. In the case of the Mhlathuze however, the synthesised data sets are in good agreement with the historical flood data (Table 6.6). For the upper part of the Mhlathuze, six major flood events have been recorded since 1940 (Table 6.5). Again, this would suggest a return period of around 20 years. The flood discharge in the lower channel has however been severely attenuated by the construction of the Goedertrouw Dam in 1979. Since 1913 there have been at least seven major floods at the lower end of the Mhlathuze. These are reflected in the synthesised virgin flow record. As mentioned earlier this has been shown in the September 1987 flood where the inflow to the Goedertrouw Dam was 3760 m^3s^{-1} and the outflow was 550 m^3s^{-1}. The implications of these reduced flood peaks are considerable.

The data for the Olifants system indicates that the Olifants proper has an MAR between that of the Mkomazi and Mhlathuze (Table 6.6). It has a higher CV than the Mkomazi, but lower than the Mhlathuze (Table 6.6). The hydrological data generated for the Olifants River is based on the VTI model (Hughes, 2000). The data were calibrated against flow gauging stations B1H015 and B2H003. The data indicate that the synthesised data set probably over-predicts the present-day flow environment. Records from B1H015 and B2H003 indicate that there are now significant periods of no flow in the Olifants River (between 10% and 30% of the time). Unfortunately there are no historical flood records for the Olifants River against which to compare the synthesised record. It is thus difficult to assess the accuracy of the synthesised record.

The daily time series must be seen within the context of the historical flood records that were available for the Mkomazi and Mhlathuze Rivers. Furthermore, Zawada *et al.* (1996) and Smith (1991) have both suggested that the present flow environment in southern African fluvial systems probably came into being around 1850. It is possible that prior to this many southern African fluvial systems experienced higher mean annual runoff and larger flood peaks (see Chapter 2 for a discussion on this subject).

Chapter 7: Cross-sectional Data, Bed Material and Hydraulics

7.1 Introduction

This chapter presents the methods and results for the cross-sectional data analysis, bed material sampling and hydraulic computations for the Mkomazi, Mhlathuze and Olifants Rivers. The techniques that were applied to the Mkomazi River were also applied to the Mhlathuze and Olifants Rivers. To avoid repetition, the techniques and methods will only be described for the Mkomazi River. The large amount of data generated means that only a portion of it can be displayed. The bulk of the data is presented in the form of appendices at the back of the thesis. The cross-sectional data together with a sketch map and photograph of each site can be found in Appendix A, while the hydraulic data are presented in Appendix E.

7.2 Cross-sectional data

7.2.1 Mkomazi River

Figure 5.1 displays the location of the thirteen sites that were selected for analysis. The sites were selected on the basis of representivity of the macro-reaches, degree of disturbance, and accessibility. Sites that were avoided included those sites that were on a river bend, had a high degree of human impact (stock grazing or trampling for example), were close to an engineering construction (e.g. bridge or drift), or were immediately upstream or downstream of a major tributary input. Table 7.1 displays a summary of the characteristics for each of the sites for the Mkomazi River. The sites are classified either as pool-riffle, pool-rapid or boulder-rapid sites. Many of the sites are controlled or semi-controlled by bed rock in the channel perimeter.

Table 7.1: Channel characteristics for thirteen sites for the Mkomazi River.

Site	Latitude and Longitude	Catchment area (km^2)	Macro-reach	Regional Slope	Number of cross-sections	Reach type	Bed rock present
1 (1320m)	29° 34' 08 S 29° 31' 11 E	171	1	0.0135	3	Pool-riffle	No
2 (1260m)	29° 35' 52 S 29° 34' 15 E	304	1	0.0039	3	Pool-riffle	Yes
3 (1160m)	29° 35' 05 S 29° 41' 38 E	872	1	0.00285	3	Pool-riffle	Yes
4 (1120m)	29° 37' 25 S 29° 44' 26 E	901	1	0.0028	2	Pool-riffle	Yes
5 (940m)	29° 44' 56 S 29° 44' 26 E	1665	2	0.0028	2	Pool-riffle	Yes
6 (920m)	29° 44' 56 S 29° 54' 47 E	1741	2	0.0040	3	Pool-rapid	Yes
7 (860m)	29° 46' 20 S 30° 56' 43 E	1949	2	0.0028	2	Pool-riffle	Yes
8 (840m)	29° 47' 12 S 30° 57' 28 E	1965	3	0.0036	2	Boulder-rapid	Yes
9 (520m)	29° 55' 55 S 30° 05' 23 E	2931	3	0.0062	2	Boulder-rapid	Yes
10 (380m)	30° 00' 03 S 30° 10' 51 E	3436	4	0.00434	2	Pool-riffle	Yes
11 (360m)	30° 00' 43 S 30° 14' 05 E	3462	4	0.0036	1	Pool-riffle	Yes
12 (220m)	30° 05' 30 S 30° 24' 20 E	4177	4	0.00266	1	Pool-riffle	Yes
13 (40m)	30° 07' 50 S 30° 40' 00 E	4334	4	0.00266	1	Pool-rapid	Yes

7.2.1.1 Cross-sections

Where practical at each of the sites, a minimum of three cross-sections were surveyed using a Topcon Total Station. The cross-sections were spaced at an interval of one channel width apart. Cross-sections were chosen on the basis of their representivity of a reach, but also on local hydraulic conditions to ensure that the stage-discharge curves could be computed without too many complicating factors. Cross-sections were also chosen so that, where possible, pools, riffles and rapids were represented at each site. The cross-sections were marked using a fixed point in the form of a bench mark. The bench marks were constructed by digging holes in the ground, and filling them with concrete. Metal stakes were inserted into the concrete so that the fixed points could be used for re-surveying. At each cross-section, relevant morphological data were marked on the cross-section so that, for example, the top of a point bar or the estimated bankfull discharge could be related to stage. The estimated bankfull stage was based on a sharp change in topography (Table 7.2). This occurred where there was a clear break of slope between the active channel and the macro-channel (see Section 2.4). Figure 2.3 shows a diagrammatic representation of these features for the Mkomazi.

Benches and terraces were identified on the basis of their relationship to the bankfull stage as estimated in the field. The bench-full stage estimate criteria were based on two factors. The first was an obvious break in slope below the bankfull stage. This slope was characteristically concave. The break in slope had to be related to a clear bench-like feature, with a distinct flat surface parallel and adjacent to the active channel-bed, but raised above it. The second factor was a change in vegetation. In many cases, the flatter bench was covered by grass. In this manner, a consistent definition of the estimated bench-full stage was achieved (Table 7.2).

Major breaks in the cross-sectional profile above the estimated bankfull stage were designated *terraces*. The terraces were numbered in sequential order from the lowest to the highest. Figure 7.1 displays two examples of the types of cross-sections surveyed for the Mkomazi River. Table 7.3 displays the elevation of the benches and terraces above the lowest point in the bed together with their associated vegetation and sediment characteristics. It can be seen that the features above the low bench are all associated with sediment in the sand-sized range and finer. The vegetation is mainly grass and trees.

Table 7.2: Bankfull stage and bench-full stage characteristics for the Mkomazi River.

Site	Bench (m)	Bench-full estimate criteria	Estimated bankfull (m)	Bankfull estimate criteria
1a	2.48	Break in slope and start of the grassed vegetation	3.28	Change in topography
1b			3.05	Change in topography
1c			3.15	Change in topography
2a	2.76	Break in slope and start of the grassed vegetation	4.43	Change in topography
2b	2.81	Break in slope and start of the grassed vegetation	4.26	Change in topography
2c	2.05	Break in slope and start of the grassed vegetation	3.73	Change in topography
3a	1.74	Break in slope and start of the grassed vegetation	5.91	Change in topography
3b	2.15	Break in slope and start of the grassed vegetation	4.96	Change in topography
3c			5.00	Change in topography
4a	2.68	Break in slope and start of the grassed vegetation	4.06	Change in topography
4b	2.75	Break in slope and start of the grassed vegetation	4.78	Change in topography
5a	4.39	Break in slope and start of the grassed vegetation	4.79	Change in topography
5b			4.31	Change in topography
6a	2.53	Break in slope and start of the grassed vegetation	3.53	Change in topography

6b	2.92	Break in slope and start of the grassed vegetation	4.27	Change in topography
6c			4.66	Change in topography
7a			3.74	Change in topography
7b	2.21	Break in slope and start of the grassed vegetation	3.46	Change in topography
8a			2.55	Change in topography, top of lateral bar
8b			2.88	Change in topography, top of lateral bar
9a	2.13	Break in slope and start of the grassed vegetation	2.63	Change in topography
9b			3.11	Change in topography, deposition of sand
10a			2.48	Change in topography, start of grassed vegetation
10b			2.21	Change in topography, start of grassed vegetation
11	2.20	Break in slope and start of the grassed vegetation	3.38	Change in topography
12			2.80	Change in topography, start of grassed vegetation
13			2.32	Change in topography, start of grassed vegetation

Table 7.3: Morphological features for the Mkomazi River.

Site	Vegetation	Sediment	Terrace 1 (m)	Vegetation	Sediment	Terrace 2 (m)	Vegetation	Sediment
1a			4.03	grass and trees	sand and finer	5.47	grass	sand and finer
1b			3.49	grass and trees	sand and finer	5.42	grass	sand and finer
1c			3.78	grass and trees	sand and finer	4.37	grass	sand and finer
2a	grass	sand and finer	5.37	grass and trees	sand and finer	6.36	grass	sand and finer
2b			5.93	grass and trees	sand and finer			
2c			4.06	grass and trees	sand and finer	6.53	grass	sand and finer
3a	grass and trees	sand and finer	8.20	grass and trees	sand and finer			
3b			5.72	grass and trees	sand and finer	7.03	grass	sand and finer
3c								
4a	grass and trees	sand and finer	5.25	grass and trees	sand and finer	6.90	grass	sand and finer
4b			5.59	grass and trees	sand and finer	6.68	grass	sand and finer
5a			5.93	grass and reeds	sand and finer	8.08	grass and trees	sand and finer
5b			5.74	grass and reeds	sand and finer	7.13	grass and trees	sand and finer
6a			4.89	grass and trees	sand and finer	7.11	grass and trees	sand and finer
6b			5.10	grass and trees	sand and finer			
6c			6.54	grass	sand and finer	8.50	grass	sand and finer
7a			8.46	grass and trees	sand and finer			
7b			7.77	grass and trees	sand and finer			

Table 7.3 continued: Morphological features for the Mkomazi River.

Site	Vegetation	Sediment	Terrace 1 (m)	Vegetation	Sediment	Terrace 2 (m)	Vegetation	Sediment	Terrace 3 (m)	Vegetation	Sediment
8a			4.84	grass and trees	sand and finer	5.58	grass and trees	sand and finer	7.75	grass and trees	sand and finer
8b			5.00	grass and trees	sand and finer	6.84	grass and tress	sand and finer			
9a	grass	sand and finer	4.78	grass and trees	sand and finer						
9b			4.74	grass and trees	sand and finer						
10a			4.71	grass	sand and finer	7.49	grass and trees				
10b			4.44	grass	sand and finer	7.95	grass and trees				
11	grass	sand and finer	3.34	grass and trees	sand and finer	5.22	grass and trees				
12			4.15	grass and trees	sand and finer	6.75	grass and trees				
13			7.08	grass and trees	sand and finer	8.82	grass and tress	sand and finer	12.07	grass and trees	sand and finer

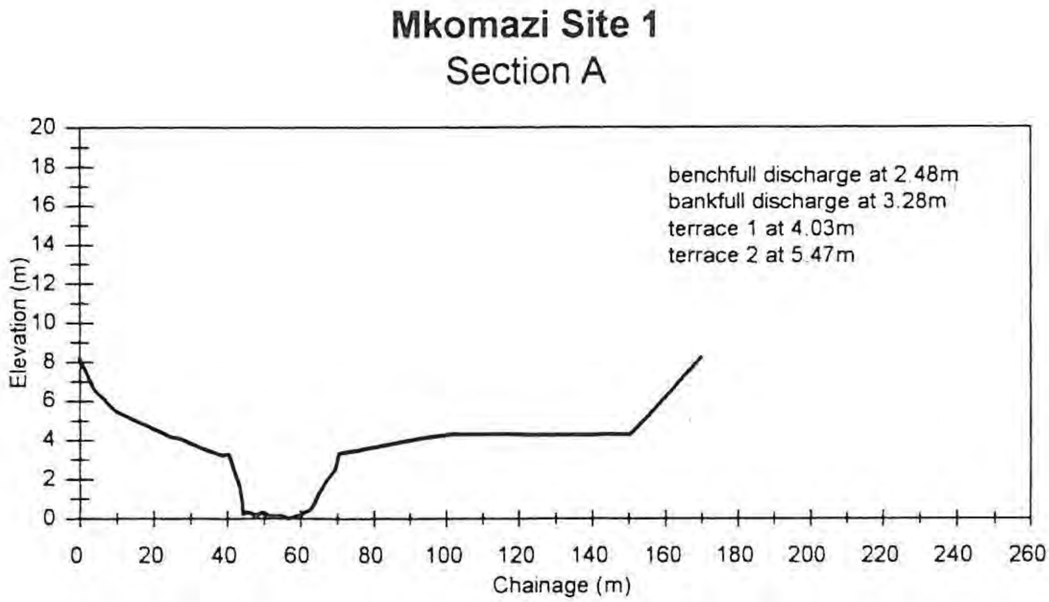

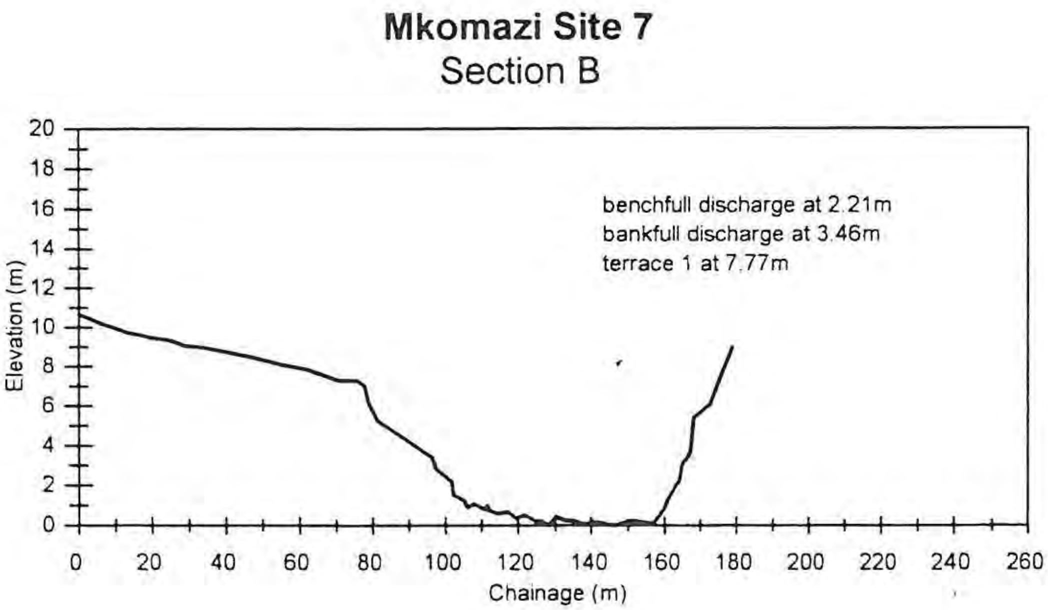

Figure 7.1: Cross-sections for sites 1a and 7b for the Mkomazi River.

Plate 7.1: Mkomazi Site 1 looking downstream.

Plate 7.2: Mkomazi Site 7 looking upstream.

7.2.2 Mhlathuze River

Four sites were chosen for the Mhlathuze River. Figure 5.3 displays the location of the sites that were selected for analysis. Table 7.4 displays a summary of the characteristics for each of the sites. Site 1 is just below the Goedertrouw Dam and as such has been affected by the regulated flow regime. This has resulted in the channel narrowing and deepening. Site 1 is semi-controlled by bed rock, as the right bank of the site contains a dyke that has intruded into the country rock. Site 1 consists of three distributary channels, each with a different flow level. The complexity of Site 1 was such that seven cross-sections were surveyed to ensure that the hydraulic calculations were accurate. Sites 2, 3 and 4 are wide, regime sand-bed channels.

Table 7.4: Channel characteristics for four sites for the Mhlathuze River.

Site	Latitude and Longitude	Catchment area (km²)	Macro-reach	Regional Slope	Number of cross-sections	Reach type	Bed rock present
1 (100 m)	28° 44' 31 S 31° 36' 20 E	1941	4	0.0015	7	Pool-riffle	Yes
2 (40 m)	28° 44' 50 S 31° 44' 50 E	2666	4	0.00282	2	Regime[1]	No
3 (20 m)	28° 50' 45 S 31° 52' 00 E	2860	4	0.00087	1	Regime	No
4 (10 m)	28° 37' 25 S 31° 44' 26 E	3608	4	0.00070	2	Regime	No

[1] A regime channel is defined by Rowntree & Wadeson (1999) as a channel with a mobile bed that adjusts rapidly to changes in imposed flow.

7.2.2.1 Cross-sections

The same cross-sectional survey technique used in the Mkomazi was used for the Mhlathuze River. Figure 7.2 displays two examples of the types of surveyed cross-sections. Plates 7.3 and 7.4 display a visual impression of sites 1 and 3. As in the Mkomazi River, a common feature in the Mhlathuze River is the occurrence of distinct benches and terraces. Employing the definitions mentioned earlier, the features were designated benches or terraces depending on their elevation relative to the bankfull stage. Table 7.5 displays the criteria used to define the bench-full and bankfull stage, while Table 7.6 displays the heights above the lowest point in the bed as well as the sediment and vegetation characteristics for each of these features for the Mhlathuze River.

Table 7.5: Bankfull discharge and bench-full discharge characteristics for the Mhlathuze River.

Site Number	Bench 1 (m)	Bench-full estimate criteria	Estimated bankfull (m)	Bankfull estimate criteria
1a	1.45	Break in slope and start of the reed vegetation	3.00	Change in topography
1b			2.16	Change in topography
2	1.19	Break in slope, top of grassed island and start of the reed vegetation	2.67	Change in topography
3			2.69	Change in topography
4			2.29	Change in topography

Table 7.6 Morphological features for the Mhlathuze River

Site	Vegetation	Sediment	Terrace 1 (m)	Vegetation	Sediment	Terrace 2 (m)	Vegetation	Sediment	Terrace 3 (m)	Vegetation	Sediment
1a	Reeds	sand and finer									
1b			3.86	reeds and trees	sand and finer	4.45	reeds and tress	sand and finer	6.61	trees	sand and finer
2	Reeds	sand and finer	4.47	reeds and trees	sand and finer	5.87					
3			4.54	reeds and trees	sand and finer	7.25					
4			3.41	reeds	sand and finer	5.78	reeds and trees	sand and finer			

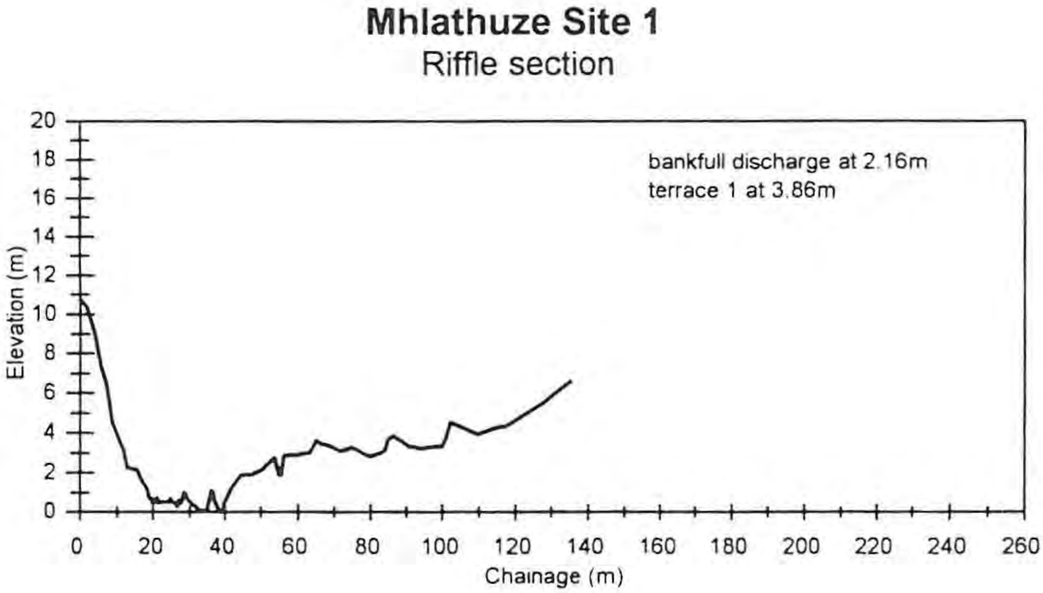

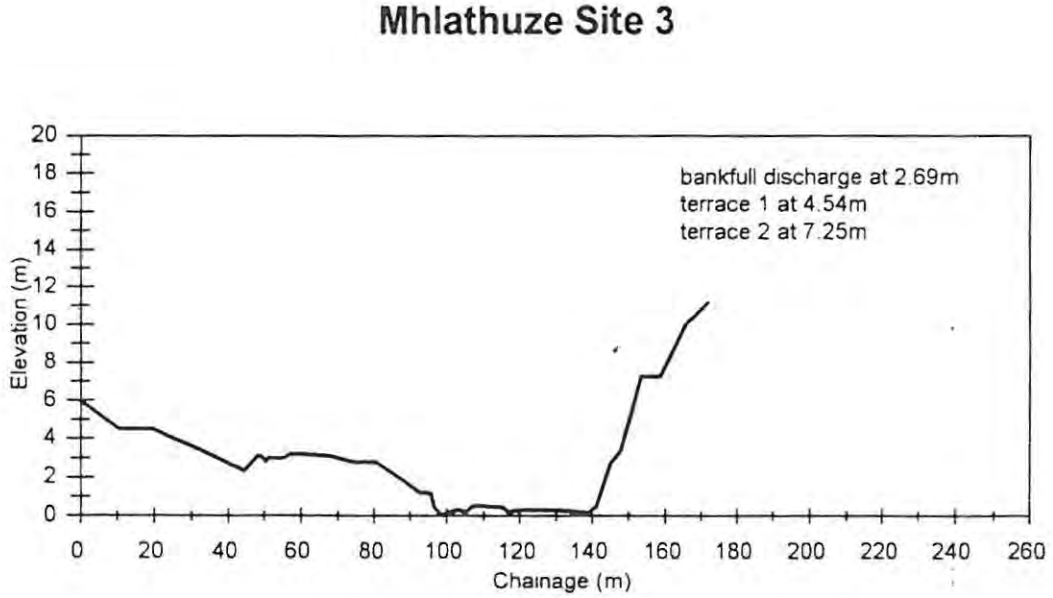

Figure 7.2: Cross-sections for sites 1 and 3 for the Mhlathuze River.

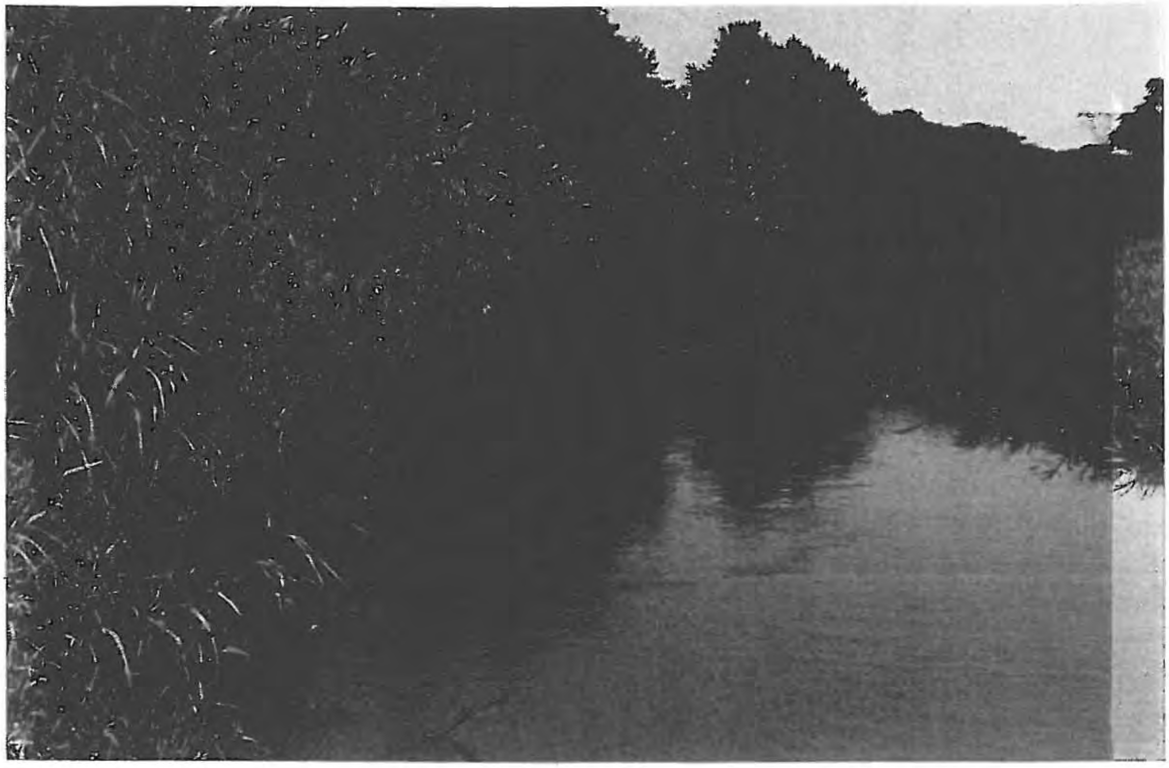

Plate 7.3: Mhlathuze Site 1 looking upstream.

Plate 7.4: Mhlathuze Site 3 looking downstream.

7.2.3 Olifants River

Four sites were chosen for the Olifants River. Figure 5.5 displays the location of the sites that were selected for analysis. Table 7.7 displays a summary of the characteristics for each of the sites. The Olifants River is a predominantly bed rock controlled system, and as such has little capacity for changing its overall channel morphology except by sediment deposition.

Table 7.7: Channel characteristics for four sites for the Olifants River.

Site	Latitude and Longitude	Catchment area (km²)	Macro-reach	Regional Slope	Number of cross-sections	Reach type	Bed rock present
1 (1380m)	25° 45' 31 S 29° 18' 46 E	2520	3	0.00366	7	Regime	No
2 (1030m)	25° 29' 44 S 29° 15' 18 E	10 820	4	0.00403	7	Pool-rapid	Yes
3 (1265m)	25° 40' 24 S 29° 18' 58 E	2350	4	0.00616	6	Pool-rapid	Yes
4 (1200m)	25° 37' 10 S 28° 59' 59 E	4300	3	0.00015	6	pool-riffle anabranching	Yes

7.2.3.1 Cross-sections

As with the Mkomazi and Mhlathuze Rivers, bench marks were constructed for re-surveying and hydraulic calibration for the Olifants River. Figure 7.3 displays two examples of the types of cross-sections surveyed for the Olifants River. At each of the sites for the Olifants River at least six cross-sections were surveyed. This was because the channels are complex with multiple distributaries. The water surface in the distributary channels was at different elevations due to strong upstream hydraulic control. Morphological features were noted and fixed onto the survey. Table 7.8 displays the criteria used to determine the bankfull discharges. Table 7.9 displays the height of each of these features above the lowest point in the bed as well as the sediment and vegetation characteristics of each site.

Table 7.8: Bench-full discharge and bankfull discharge characteristics for the Olifants River.

Site Number	Bench (m)	Bench-full estimate criteria	Estimated bankfull (m)	Bankfull estimate criteria
1	-	-	1.57	Change in topography, start of reed growth
2	-	-	3.21	Change in topography, start of reed growth
3	-	-	2.58	Change in topography
4	-	-	2.77	Change in topography

Table 7.9: Morphological features for the Olifants River.

Site	Terrace 1 (m)	Vegetation	Sediment	Terrace 2 (m)	Vegetation	Sediment	Terrace 3 (m)	Vegetation	Sediment
1	4.47	grass, reeds and trees	gravel and finer	6.57	grass and trees	gravel and finer			
2	3.81	reeds and trees	boulders, cobble, gravel and sand	5.38	grass and trees	gravel and finer	7.61	grass and trees	sand and finer
3	5.08	reeds and trees	Gravel and finer	6.23	grass and trees	gravel and finer	7.62	grass and trees	sand and finer
4	6.17	reeds	Gravel and finer	7.89	grass and trees	gravel and finer	9.26	grass and trees	sand and finer

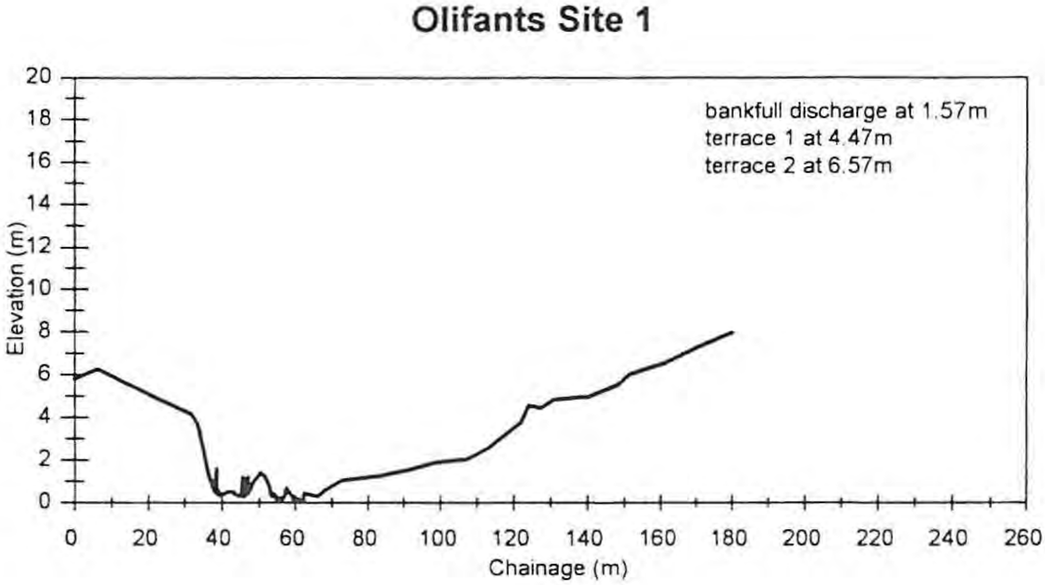

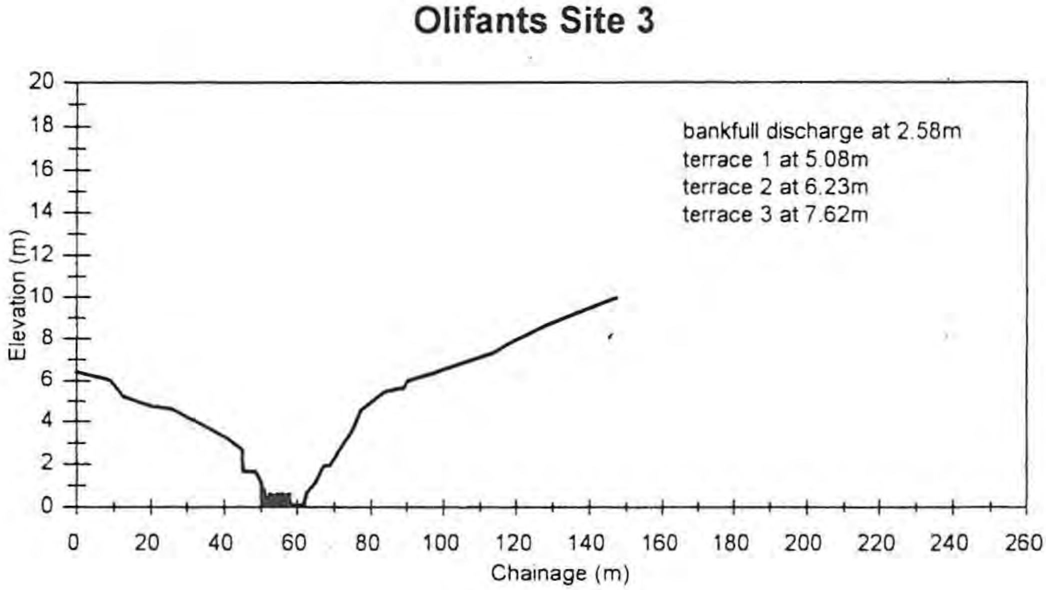

Figure 7.3: Cross-sections for sites 1 and 3 for the Olifants River.

Plate 7.5: Olifants Site 1 looking upstream.

Plate 7.6: Olifants Site 3 looking downstream.

7.2.4 Quality audit and summary

There are a number of issues that must be mentioned with respect to the cross-sectional surveys. First, 27 cross-sections were surveyed for the Mkomazi, 12 for the Mhlathuze and 26 for the Olifants River, a total of 65 cross-sections. Thirty-seven of these have been rated for stage discharge curves. These required repeated site visits. A minimum of four calibration visits were made, in some cases as many as seven calibration visits were achieved. Given time and financial constraints, it was not possible to survey any further cross-sections. The number of cross-sections may, therefore, be a limiting factor in terms of the representivity of the data.

Second, the number of cross-sections at each site varied. One of the reasons for this was the variable complexity of the sites. Where multiple channels occurred with different water levels, a greater number of cross-sections were necessary to adequately perform the hydraulic computations. For example, Site 1 on the Olifants River had four distributary channels, this required seven cross-sections to reflect the water levels at different discharges. Site 3 on the Mhlathuze on the other hand, was a simple sand-bed regime channel and therefore only one cross-section was used to represent the site. The number of cross-sections also depended on the reach type. For example where a pool-riffle reach type occurred, the cross-sections were situated to reflect both the pool and the riffle. It is argued that the cross-sections adequately represent the macro-reaches of the three rivers under investigation.

Third, the accuracy of the bed material transport computations is in part dependent on accurate surveying of the cross-sections. Any error in the cross-sectional surveys will be compounded in the hydraulic computations and in the bed material transport values. For this reason, the cross-sections were surveyed using a Electronic Total Station which results in a very accurate survey

7.3 Bed material data

Bed material was sampled to determine the calibre of bed material at each site so that it could be used in the bed material transport equations. The problem of obtaining an accurate, reliable and representative sample of bed material is well known (cf. Wolman, 1954; Church *et al.*, 1987). Authors have suggested different methods for bed material sampling. These include surface clast counts, surface and subsurface bulking and sieving (Ferguson & Ashworth, 1991), surface counts using a grid system (Wolman, 1954), pacing (Mosley & Tindale, 1985) and transect sampling (Kellerhals & Bray, 1971; Ibheken, 1974). Bed material sampling techniques differ and are adapted to the objectives of the survey as well as to financial and technological constraints.

Mosley & Tindale (1985) suggest that 70 samples per site are necessary to obtain a representative sample of the whole bed, while Wolman (1954) and Brusch (1961) suggest a sample of 60 is adequate. Based on the literature, as well as resource constraints, it was decided to use a combination of surface clast counts and bulk subsurface sampling and sieving, the details of which will be discussed with reference to each river. It was resolved to take a sample of the bed material at each site on one occasion only. This was done at low flow, which enabled the sampling of deeper pools, faster flowing riffles and rapids. While it is acknowledged that bed material characteristics can change over time, the logistics of bed material sampling, and the laboratory time necessary to process the samples made only one sample per site practical. Indeed, based on visual and photographic evidence there appeared to be little evidence to suggest any significant change in the composition of the bed material during the period of study.

7.3.1 Mkomazi River

A combination of surface clast counts and bulk subsurface sampling and sieving was used for the Mkomazi River. At least 500 samples were taken at each site. Where the samples were in the sand (>2 mm) to fine gravel (<10 mm) range, a bulk sample was taken and sieved. Where the size range was medium gravel (>10 mm) or larger, the size of the median axis was measured with either a pair of calipers or a measuring tape. Using this method, a curve was constructed to show the percentage finer bed material for each site. Figure 7.4 displays examples of the curves constructed for sites 1, 6, 9 and 13. From these curves, the D_{16}, D_{50} and D_{84} and so on were determined. Table 7.10 displays the results in tabular form.

The data indicate that the Mkomazi River is mainly a cobble-bed river. Most of the sites, with the exception of sites 4, 5 and 12, consist of over 70% gravel and cobble, with only small percentages of sand and virtually no silt or clay. The low values of silt and clay may reflect a sampling problem, in that the silt and clays could have been washed out of the sample before they could be placed in the sample bag. The data also show that the expected downstream fining of bed material in the Mkomazi River does not hold true. In fact, the general trend is an increase in the size of the bed material between sites 1 and 10. This holds true for the D_{16}, D_{50} and the D_{84}. Sites 11, 12 and 13 display variability in the downstream direction. Site 12 is predominantly a sand-bed channel but has a large D_{84}. Sites 8, 9 and 10 which are in the gorge section of the Mkomazi, reflect a very coarse bed with a large D_{84} and a high standard deviation and coefficient of variation. The characteristics of the bed material of the Mkomazi therefore reflect the channel type; flatter, wider sections are associated with relatively finer material, while the steeper gorge sections reflect coarser bed material with a high standard deviation and coefficient of variation. The notion of downstream fining does not appear to fit the bed material characteristics of the Mkomazi River, rather the bed material characteristics tend to reflect local hydraulic conditions. This issue has been discussed in Chapter 2.

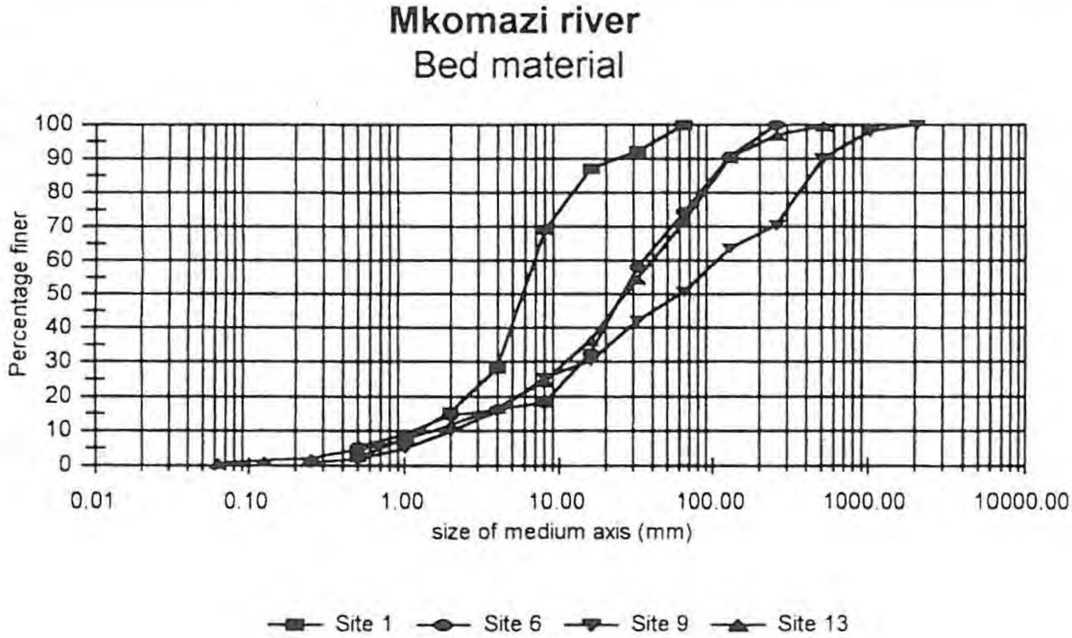

Figure 7.4 Bed material for sites 1, 6, 9 and 13 for the Mkomazi River.

Table 7.10 Bed material characteristics for the Mkomazi River.

Site	D_{16} (mm)	D_{50} (mm)	D_{84} (mm)	SD	Mean	CV	Silt + Clay %	Sand %	Gravel + Cobble + Boulder %
1	1.8	5.6	16	7.1	8.9	0.80	0	15.4	84.6
2	2.8	10	45	21.1	23.9	0.88	0	6.7	93.3
3	1.1	4.2	13.7	6.3	7.4	0.85	0	19.6	80.4
4	0.4	12	90	44.8	45.2	0.99	0	30.6	69.4
5	0.2	1.7	15	7.4	7.6	0.98	2.3	27.9	69.8
6	3.8	26	100	48.1	51.9	0.93	0	14.6	85.4
7	8.6	48	220	105.7	114.3	0.92	0	4	96
8	13	30	150	68.5	81.5	0.84	0	3.3	96.7
9	4.2	60	410	202.9	207.1	0.98	0	9.8	90.2
10	15	50	400	192.5	207.5	0.93	0	3.1	96.9
11	22	65	160	69	91	0.76	0	1.3	98.7
12	0.7	3.9	230	114.6	115.3	0.99	0	44.1	55.9
13	3.2	26	96	46.4	49.6	0.94	0.7	10.9	88.4

7.3.2 Mhlathuze River

For the Mhlathuze River, a combination of surface clast counts and bulk subsurface sampling and sieving was used for Site 1. However, for sites 2, 3 and 4 the bed material is in the sand-sized range (<2 mm). Here, thirty bulk samples were taken using a grid system at each site. These were analysed in the laboratory for grain-size analysis. Curves were constructed to show the percentage finer bed material for each site. Figure 7.5 displays the curves constructed for sites 1 to 4. From these curves, the D_{16}, D_{50} and D_{84} and so on were determined. Table 7.11 displays the results in tabular form.

The data show that the section of the Mhlathuze River under consideration is predominantly a sand-bed channel. Site 1 is a pool-riffle channel type and, therefore, the predominant bed material is gravel and cobble. However, sites 2, 3 and 4 are sand-bed channels, with sand constituting over 75% of the bed in all cases (Table 7.11). The depth of the sand is considerable. During the sampling of the bed, a 5 metre iron rod was inserted into the bed at sites 2, 3 and 4 and in all cases, the depth of the sand in the bed exceeded five metres. Although there was some gravel present at these sites, this did not exceed 32 mm in diameter. The mean grain size in the lower three sites was around 1 mm. Very little silt and clay was measured. The low standard deviation and coefficient of variation in the lower three sites confirm the homogeneity and well-sorted nature of the bed.

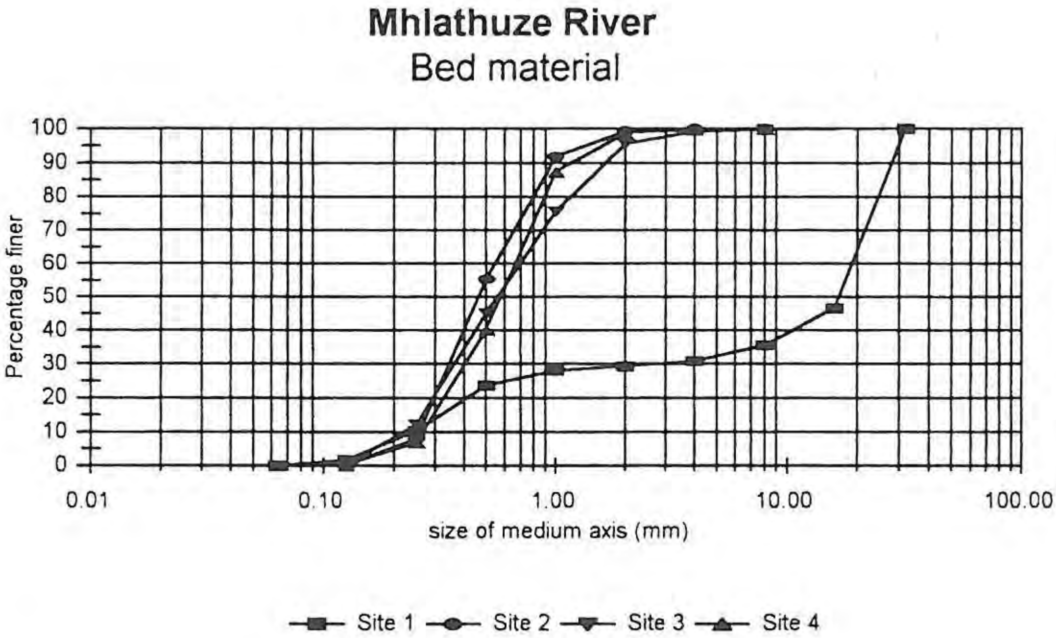

Figure 7.5: Bed material for sites 1 to 4 for the Mhlathuze River.

Table 7.11: Bed material characteristics for the Mhlathuze River.

Site	D_{16} (mm)	D_{50} (mm)	D_{84} (mm)	SD	Mean	CV	Silt + Clay %	Sand %	Gravel %
1	0.4	22	35	17.3	17.7	0.9	0.2	19.5	80.3
2	0.4	0.7	1.4	0.5	0.9	0.6	0.02	91.9	8.08
3	0.4	0.8	2.0	0.8	1.2	0.7	0.05	75.7	24.25
4	0.4	0.9	1.3	0.5	0.8	0.5	0.06	87.4	12.54

7.3.3 Olifants River system

A combination of surface clast counts and bulk subsurface sampling and sieving was used for the Olifants River system. A minimum of 500 samples were taken at each site. Curves were constructed to show the percentage finer bed material at each site. Figure 7.6 displays the curves constructed for sites 1 to 4. Table 7.12 displays the results in tabular form. The numbering of the sites on the Olifants River is confusing. It should be noted that sites 1 and 2 are on the Olifants proper, Site 3 is on the Klein Olifants and site 4 is on the Wilge River. The highest discharge occurs at Site 2, followed by sites 4, 1 and then 3. The data indicate that all the sites are dominated by coarse bed material. The material is often imbricated and armoured. There is very little silt, clay or sand on the bed. Site 1 consists mainly of gravel-sized material, while sites 2, 3 and 4 are dominated by boulder-sized bed material. There is very little sand sized material in the bed at any of the sites.

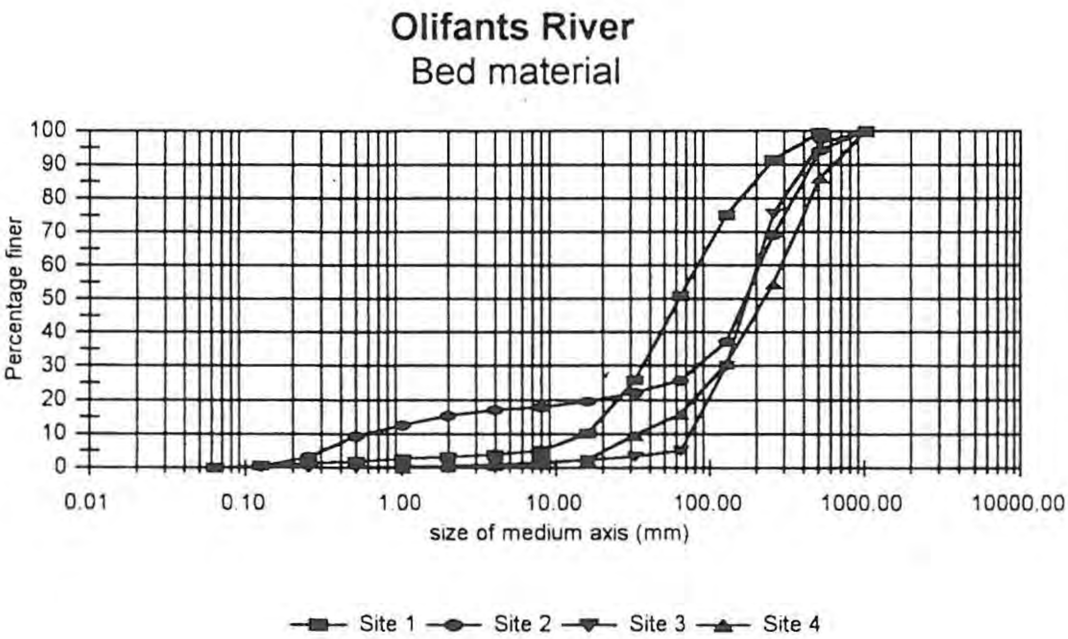

Figure 7.6: Bed material for sites 1 to 4 for the Olifants River.

Table 7.12: Bed material characteristics for the Olifants River and tributaries.

Site	D_{16} (mm)	D_{50} (mm)	D_{84} (mm)	SD	Mean	CV	Silt + Clay %	Sand %	Gravel + Cobble + Boulder %
1	22	96	277	128	149	0.85	0.6	2.6	96.8
2	5	220	520	258	263	0.98	0	12.6	87.4
3	140	250	480	170	310	0.55	0	0.4	99.6
4	90	320	500	205	295	0.69	0	0.2	99.8

7.3.4 Quality audit and summary

The accurate determination of the bed material for a site is difficult. This is especially so as bed material can change in the horizontal plane, with depth and over time. Due to logistical constraints, it was not possible to continuously sample the bed material, which is a limitation of the study. However, it is argued that the sampling programme resulted in a representative sample of the bed material, especially at sites containing a homogenous bed. The Mkomazi, Mhlathuze and Olifants Rivers display different bed material characteristics. The Mkomazi is mainly a cobble-bed river, the Mhlathuze is predominantly a flat, sand-bed channel, while the Olifants is a steep, cobble-bed river, with a very coarse armour layer in the boulder-size range.

7.4 Hydraulic computations

The aim of the hydraulic computations was to generate rated sections for each site. This was required for two reasons. First, the relationship between stage, discharge, wetted perimeter and water surface slope is necessary to determine bed material transport. Second, to relate stage to channel features. There are a number of means of calculating flow discharge from stage. Three common methods are the Chezy, Mannings and Darcy-Weisbach equations (Chang, 1988). It has been common practice in South Africa to use Manning's resistance equation (Broadhurst *et al.*, 1997). For the purpose of this study and for consistency, the most common flow resistance equation (Manning's) was used. A full description of this technique is available in most hydrological or hydraulic text books. Here, a short review will suffice. The derivation of the basic equations that govern open channel flow begins with the assumption that a fluid can be considered as a continuum (Lane, 1998). Manning's resistance equation is given by:

$$Q = \left(\frac{A^{1.667}}{P^{0.667}}\right)\left(\frac{\sqrt{S_f}}{n}\right) \qquad (7.1)$$

where

Q is the discharge (m^3s^{-1})

A is the cross-sectional flow area (m^2)

P is the wetted perimeter (m)

S_f is the friction slope (m/m)

n is the Manning resistance coefficient (s $m^{-1/3}$)

the 'resistance-friction slope' term in Equation 7.1 can be combined into a single term, given by

$$k = Q\left(\frac{P^{0.667}}{A^{1.667}}\right) \qquad (7.2)$$

Using Manning's, a table of observed and modelled discharge is generated. The modelled discharge is extrapolated beyond the range of field measurements by estimating the 'friction slope-resistance' (n). Estimating 'n' is problematic, but the use of photographs (Barnes, 1967) and previously modelled data (Chow, 1959) can help provide an adequate estimate. Indications are that the resistance coefficient reaches an asymptotic value with increasing discharge, but increases exponentially with reducing discharge as the flow depth becomes comparable to the height of the resistance elements (Broadhurst *et al.*, 1997). Applying Manning's to extreme low flows is difficult, when the flow depth is about the same depth as the resistance elements and, as a result, large coefficients are derived. In this case, the highest *n* value is applied.

Estimating the slope also proved problematic. The estimated slope was calculated as a function of the relationship between the regional slope (1:50 000 topographical map) and the lowest water surface slope measured in the field (Birkhead & James, 1998). The slope was estimated by:

$$Estimated\ slope = \frac{(RS+(LS-RS))}{(1+(0.01*Q))^{0.5}} \quad \ldots\ldots (7.3)$$

where

RS is the regional slope (m/m)

LS is the lowest water surface slope measured in the field (m/m)

The slope generally increases with increasing discharge, reaching an asymptotic level at approximately the regional slope (calculated off 1:50 000 topographical maps). However, this is not always the case. At some sites, the slope calculated in the field was greater than the regional slope. This situation occurs where the site is located on a steep section, often associated with strong bed rock control, or where the section traverses a riffle. In these instances, the slope decreases with increasing discharge as the riffle or rapid is drowned out. This has significant implications for sediment transport and will be discussed in greater detail in the following three chapters.

Once the observed and modelling stage discharge relations had been determined, a regression is fitted to the data. The general form of the regression is given in Equation 7.4:

$$y = a\,Q^{b} + c \quad \ldots\ldots (7.4)$$

where

y is the maximum flow depth (m)

a, b, c are coefficients

7.4.1 Mkomazi River

The aim of the hydraulic calculations was to develop stage-discharge curves for each of the cross-sections for the Mkomazi River. Manning's resistance equation was used in conjunction with the cross-sectional surveys and repeated site visits. Each re-survey involved the determination of water surface stage, water surface slope and discharge. Discharge measurements were made using an electro-magnetic Marsh-McBirney Flow Mate current metre. Flow readings were made at every metre or half metre at 0.6 depth from the surface. Using this technique, rating curves were calculated for each of the cross-sections for each site for the Mkomazi River. Figure 7.7 displays an example of a stage discharge curve generated for the Mkomazi River. Table 7.13 displays the coefficients from the regression analyses for the thirteen sites for the Mkomazi River. Using this technique, rating curves were developed for 27 cross-sections for the Mkomazi River.

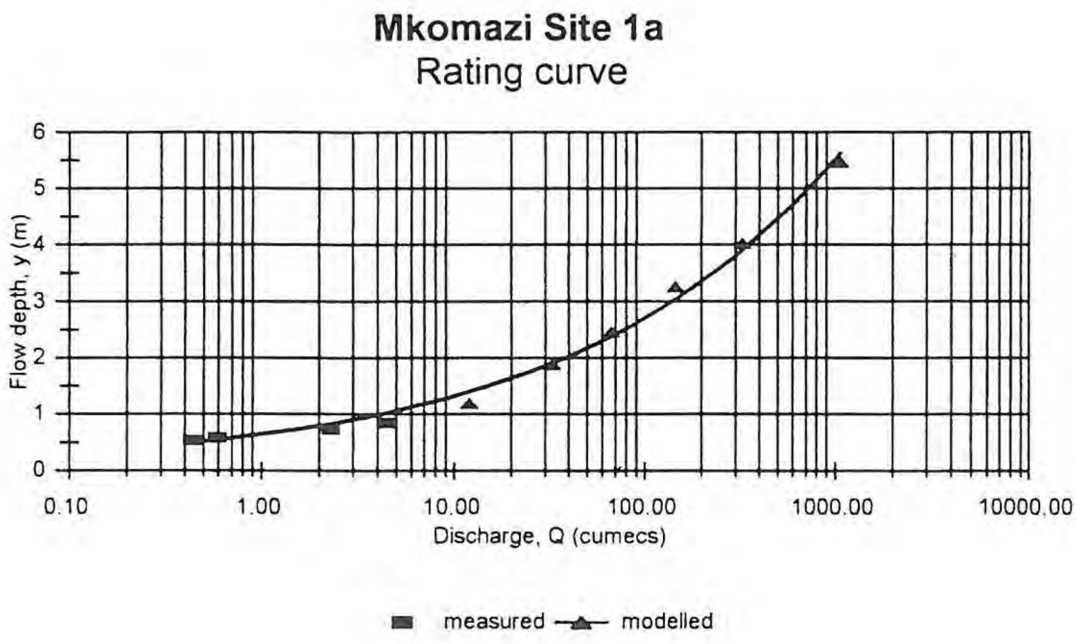

Figure 7.7: Hydraulic rating curve for Mkomazi Site 1, cross-section A.

Table 7.13: Coefficients to Equation 7.4 for thirteen sites for the Mkomazi River.

Site	Coefficient		
	a	b	c
1a	0.645	0.311	0
1b	0.665	0.302	0.326
1c (>10 m^3s^{-1})	0.297	0.402	0.512
1c (<10 m^3s^{-1})	0.732	0.264	0.617
2a	0.417	0.385	0.340
2b	0.388	0.383	0.297
2c	0.912	0.289	0
3a	0.600	0.356	0.229
3b	0.313	0.419	0.449
3c	0.847	0.293	0
4a	0.471	0.381	0.757
4b	0.485	0.373	0.500
5a	0.335	0.378	2.305
5b	0.563	0.331	1.357
6a	0.349	0.363	0.834
6b	0.255	0.390	0.599
6c	0.219	0.434	2.180
7a	0.232	0.443	0.546
7b	0.349	0.401	0.023
8a	0.122	0.486	0.630
8b	0.165	0.453	0.371
9a	0.234	0.394	0.656
9b	0.341	0.355	0.194
10a	0.158	0.450	0.725
10b	0.372	0.357	0

11	0.302	0.354	0
12	0.417	0.337	0.449
13	0.182	0.442	0.646

7.4.2 Mhlathuze River

The same technique for determining stage discharge curves for the Mkomazi River were applied to the four sites for the Mhlathuze River. These have been published (Jordanova, 1998 in Louw, 1998b). Where there were multiple channels at a site, the individual channels were modelled separately. When a critical discharge was reached such that the individual channels flowed as a discrete unit, a different rating was applied. In this manner it was possible to rate each of the distributary channels. Figure 7.8 displays an example of a stage discharge curve for Site 1b. Table 7.14 displays the coefficients from the regression analyses for the four sites. Using this technique, rating curves were developed for the four rated cross-sections for the Mhlathuze River.

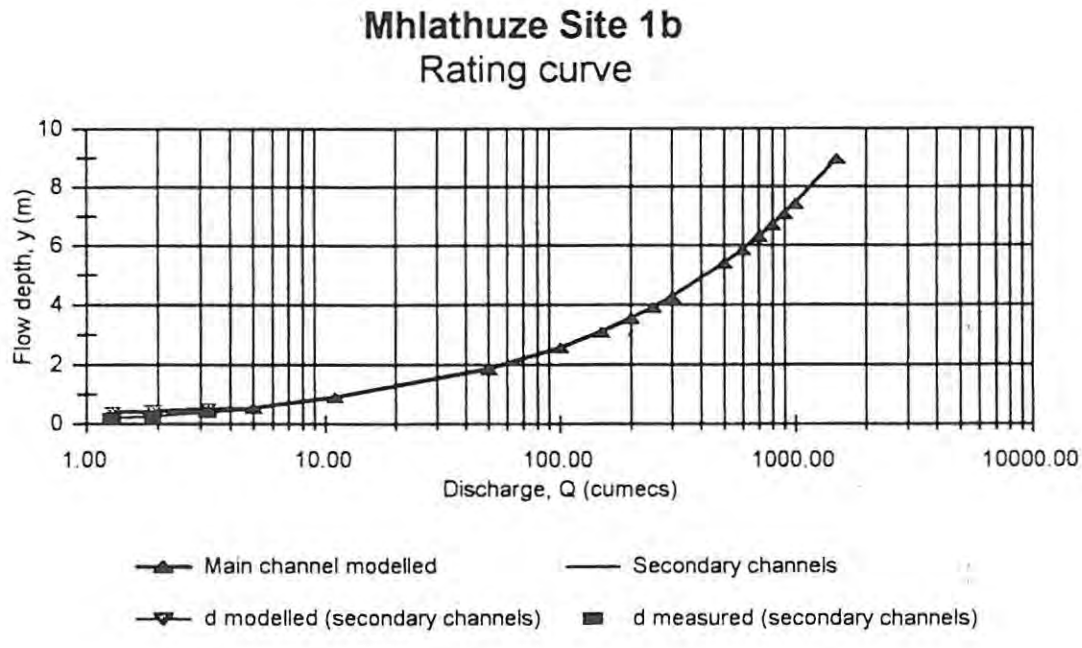

Figure 7.8: Hydraulic rating curve for Mhlathuze Site 1, cross-section B.

Table 7.14: Coefficients to Equation 7.4 for four sites for the Mhlathuze River.

Site	Coefficient		
	a	b	c
1a	0.370	0.443	0.60
1b (<11 m^3s^{-1})	0.377	0.248	0
1b (>11 m^3s^{-1})	0.165	0.722	0
2a	0.221	0.471	0
3a	0.337	0.415	0
4a	0.245	0.467	0.310

7.4.3 Olifants River

The same hydraulic technique was applied to the four sites for the Olifants River. These have been published (Jordanova, 1998 in Louw, 2000). Rating curves were calculated for each of the cross-sections for each site for the Olifants River. As in the Mkomazi and Mhlathuze Rivers, where there were multiple channels at a site, the individual channels were modelled separately. Figure 7.9 displays an example of a stage discharge curve calculated for the Olifants River Site 3. Table 7.15 displays the coefficients from the regression analyses for the four sites for the Olifants River. Using this technique, rating curves were developed for the four rated cross-sections for the Olifants River.

7.4.4 Quality audit and summary

The accuracy of the hydraulic computations depends on a number of factors: an adequate estimate of the boundary roughness 'n', the water surface slope, and the range of flows utilised to calibrate the rating curve. The modelled boundary roughness is subject to error. In an attempt to minimise possible error, values from photographs (Barnes, 1967), previously modelled data (Chow, 1959) and available roughness calculations from South Africa (Broadhurst *et al.*, 1997) were used. This increased the confidence in the boundary roughness estimates. The slope was calculated as a function of the relationship between the water surface slope measured in the field, and the regional slope as measured off a 1:50 000 topographical map. The resistance coefficient and energy gradient calculated for high flows probably achieves a higher degree of confidence, as local hydraulic controls become inundated and drowned-out, resulting in a tendency towards uniform water surface gradients and asymptotic resistance coefficient values.

The range of flows used to calibrate the rating curve for all three rivers were deemed acceptable. A minimum of four calibration site visits were undertaken for each of the sites. The range of flows varied, but were sufficient to provide a reasonable level of confidence in the rating procedure. During the period of study, the Mkomazi and Olifants Rivers experienced high flows, and thus the confidence in the hydraulic calculations for these two rivers is good. The Mhlathuze River proved to be problematic, as the flow was highly regulated, and therefore only low flows were used to calibrate the stage discharge curve. This means that the confidence in high flow hydraulic calculations is moderate to low.

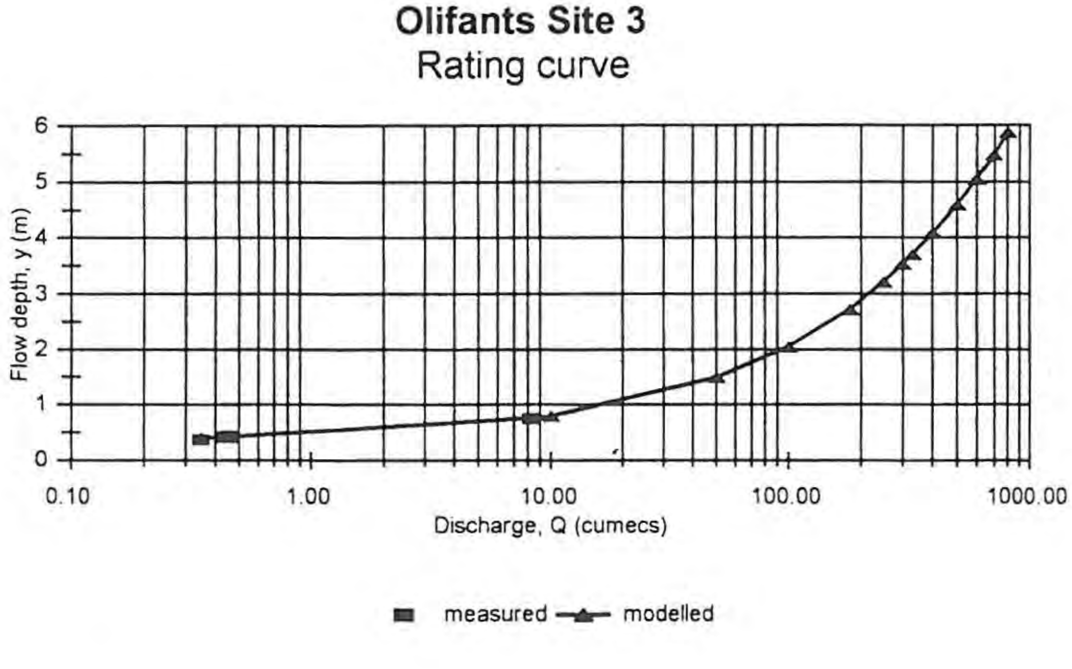

Figure 7.9: Hydraulic rating curve for Olifants Site 3.

Table 7.15: Coefficients to Equation 7.4 for four sites for the Olifants River.

Site	Coefficient		
	a	b	c
1 (<3.06 m^3s^{-1})	0.354	0.315	0
1 (<3.06 m^3s^{-1}<50 m^3s^{-1})	0.328	0.376	0
1 (>50 m^3s^{-1})	0.282	0.417	0
2 (<100 m^3s^{-1})	0.377	0.321	0
2 (>100 m^3s^{-1})	0.186	0.472	0
3	0.128	0.564	0.336
4 (<16.8 m^3s^{-1})	0.673	0.261	0
4 (>16.8 m^3s^{-1})	0.447	0.416	0

7.5 Summary and conclusions

The preceding discussion has presented the methods and results obtained from the cross-sectional data, the bed material analysis and the hydraulic computations. Of the three rivers selected for study, two, the Mkomazi and Olifants, contain a coarse heterogenous bed. The third river, the Mhlathuze, contains a homogenous, well-sorted sand-bed. All of the rivers are characterised by complex channels, with distinct in-channel benches and terraces.

Chapter 8: Bed Material Transport and Sediment-Maintenance Flushing Flow Methods

8.1 Introduction

This chapter is divided into two parts. The first part deals with the methods used for the bed material transport calculations, and the techniques employed in determining effective and dominant discharge. The second part of the chapter discusses the methods used in determining sediment-maintenance flushing flows.

8.2 Generating the effective discharge

The effective discharge was generated using the three bed material transport equations (see Section 8.2.1), together with the hydrology (Chapter 6), cross-sections, bed material data and hydraulic computations (Chapter 7). Section 8.2.5 presents the procedure that was used.

8.2.1 Bed material transport equations

Due to the large number of bed material transport formulae in existence, the selection of reliable equations suitable to the physical conditions of a particular river are of significance. For the purposes of this thesis, three bed material transport equations were selected. These are the Yang (1972), Ackers & White (1973), and Engelund & Hansen (1967) equations. The three equations chosen are all based on stream power, a factor considered to be more appropriate shear stress (Chang, 1988).

In a number of comparative tests, the Ackers & White (1973) formula has been shown to perform well (cf. Chang, 1988; Gomez & Church, 1989), it has also been widely used in South Africa (cf. Birkhead *et al.*, 2000). The formula accounts for bed load and suspended load and has been developed from best-fit curves from almost 1000 sets of laboratory data. The Ackers & White equation has been formulated for heterogenous gravel-bed rivers. As mentioned earlier the Mkomazi and Olifants Rivers consist of coarse cobble-beds, and it is argued that the Ackers & White formula is suitable to the physical conditions of these two rivers.

The Yang equation has also been shown to perform well in comparative tests (cf. Chang, 1988; Gomez & Church, 1989), and is a useful equation for a variety of bed-types. It has separate components for sand and for gravel and larger sized material. The Yang equations for sand and gravel are identical in general form, but have different numerical values for the coefficients relating to the variation in particle size. The equations can therefore be used with a reasonable amount of confidence for all three rivers under consideration. The final equation chosen was that of Engelund & Hansen (1967). This equation was developed specifically for regime-type sand-bed alluvial channels. The Mhlathuze is such a channel. Given the nature of the channels under consideration, it is argued that these formulae are suitable for predicting bed material transport.

In order to account (to some extent) for the heterogenous nature of the beds, the transport equations were applied to each grain size class separately, and later summed so that the relative proportions of each grain size class's contribution to the total transport rate could be accounted for. This does not imply that the equations account for the 'hiding factor' or the 'obstacle clasts' (cf. Figure 4.1). Rather, the data sets from which the Yang and Ackers & White equations were developed take into account the different types of bed material transport that occur in sand- and gravel-bed rivers through different coefficients

A number of assumptions were made in using these bed load equations. The first assumption made was that the bed material sampling programme for each site was representative of the supply of material to the channel (thus bed *material* transport as opposed to bed *load* transport). This assumption was made due to the lack of any viable alternative. Solving this problem would require an extensive modelling exercise linking sediment delivery from the catchment to the channel, which in itself would be based on a number of further assumptions. This solution fell outside the boundary of this research. A second assumption made was that the bed material size distribution could be averaged for the entire site and used to represent each cross-section. It is argued that although this may misrepresent certain cross-sections, the averaged effect will compensate for this and will provide a more representative result.

The third assumption made was that the supply of material to each site is constant, and that the relative proportion of sediment sizes (and volume) supplied to each site was the same as the relative proportions of the sizes (and volume) of the sampled bed material. This assumption was necessary, as the alternative would have necessitated a complete shift of research focus towards routing the sediment through the system, which again, would involve a further series of assumptions. [Birkhead *et al.* (2000), for example, in modelling sediment transport through the Sabie River, used one grain size (1.0 mm) to represent the entire bed load]. For this reason, an approach was adopted that uses channel cross-sections within a short reach. This allows the various hydraulic parameters to be measured accurately (see Chapter 7). The values that were generated were thus linked to individual cross-sections and represent bed material transport *potential* within the predictional limits of the equations.

The fourth assumption made was that where there is armouring, the armour needs to be mobilised before the sub-armour layer can be transported. This may mean that the transport values that were computed once the coarse armour layer is mobilised under-represents the actual transport rate.

The fifth assumption made was that average conditions could be used. Where depth or velocity was required, it was averaged over the cross-section. Although this may under-represent transport at certain points along the cross-section (for example, where local conditions create high velocities), it is argued that it will also over-represent transport at other points along the cross-section. In this way the averaged effect will provide the most consistent results.

Given the preceding assumptions, the following section provides an overview of the use of the three transport equations.

8.2.1.1 Yang's equation

Yang (1972; 1973; 1984) related the bed material load to the rate of energy dissipation of the flow. To solve Yang's (1972) formula, the settling velocity must be determined. The settling velocity partly determines the rate, mode and distance of transport by shearing forces in a fluid (Chang, 1988). The general method for calculating settling velocity is by the general drag equation. Stokes' law is applicable to particles of less than 60 microns which is clearly unsuitable for a general transport equation. The rate at which a particle settles in a stationary fluid depends on the viscosity and density of the fluid, and on the size, shape, density, roundness and surface texture of the particle. The difficulty is that no theory based on the physics of flow exists to predict the settling velocity of natural sediments. For this reason, workers in the field have produced empirical curves based on laboratory work. Due to limitations in the laboratory, most researchers have focussed on a limited range of particle and fluid properties, and several do not identify all the factors responsible for settling velocities. The result is that these curves are of limited use as this method is primarily applicable to spheres (James, 1998).

For natural sediments, the approach by Dietrich (1982) is deemed more appropriate. Dietrich's (1982) method accounts for size, density, shape and roundness. The method is as follows. First, the dimensionless particle size is determined:

$$D_* = \left(\frac{(\rho_s - \rho) g Dn^3}{\rho \nu^2} \right) \qquad (8.1)$$

where

D_* is the dimensionless particle size

ρ_s is the density of sediment (kg m^{-3})

ρ is the density of the water (kg m^{-3})

g is the gravitational acceleration (m s^{-2})

Dn is the nominal diameter (m)

ν is the kinematic viscosity of water (m^2 sec^{-1})

Second, the equation for predicting the settling velocity of spheres is calculated:

$$R_1 = -3.76715 + 1.92944(\log D_*) - 0.09815(\log D_*)^2 - 0.00575(\log D_*)^3 + 0.00056(\log D_*)^4 \qquad (8.2)$$

To account for the impact of shape on settling velocities, the Corey Shape Factor (CSF) is included (Corey, 1949). The shape factor which ranges from 0 to 1.0 is a ratio of the cross-sectional area of a sphere to the maximum cross-sectional area of an ellipsoid. The smaller the value, the flatter the particle.

$$CSF = \left(\frac{c}{\sqrt{ab}}\right) \qquad (8.3)$$

where

a is the longest axis (m)

b is the intermediate axis (m)

c is the shortest axis (m)

The CSF is used in the following form to account for natural particle shape, where the ratio of the settling velocity of a non-spherical, well rounded particle to the settling velocity of a sphere with the same D_* is calculated:

$$R_2 = \left[\log\left(1 - \left(\frac{1 - CSF}{0.85}\right)\right)\right] - (1 - CSF)^{2.3}\tanh\left(\log D_* - 4.6\right) + 0.3(0.5 - CSF)(1 - CSF)^2\left(\log D_* - 4.6\right) \qquad (8.4)$$

To account for the roundness of the particle, Dietrich (1982) developed the following equation which predicts the ratio of the settling velocity of an angular particle to that of a well rounded particle:

$$R_3 = \left[0.65 - \left(\frac{CSF}{2.83}\right)\tanh\left(\log D_* - 4.6\right)\right]^{1+\left(\frac{3.5-p}{2.5}\right)} \qquad (8.5)$$

where

p is the power roundness scale (0 is perfectly angular; 6 is perfectly round)

The estimation of p is highly subjective, and is usually estimated with the standard method to assign roundness based on diagrams, photographs, or verbal descriptions. The scale ranges from 0.0 for perfectly angular to 6.0 for perfectly round (Dietrich, 1982).

The dimensionless settling velocity is calculated:

$$W_* = R_3 10^{R_1+R_2} \qquad (8.6)$$

This can be converted into a value by:

$$w = \left[\frac{W_*(\rho_s-\rho)g\nu}{\rho}\right]^{1/3} \qquad (8.7)$$

Once the settling velocity has been calculated, it can be applied to Yang's equation.

Shear velocity is calculated:

$$U_* = (gRS)^{0.5} \qquad (8.8)$$

where

U_* is the shear velocity (m s^{-1})

R is the hydraulic radius (m)

S is the slope (m/m)

The Shear Reynolds number (SR) is determined:

$$SR = \left[\frac{U_* d}{\nu}\right] \qquad (8.9)$$

where

d is the geometric mean diameter of the sediment size class (m)

The critical velocity to settling velocity ratio is computed. The ratio of these two velocities is related to the Shear Reynolds number. In smooth and transitional regions where the Shear Reynold's number is between 1.2 and 70, the ratio is represented by Equation 8.10. In the rough region, where the Shear Reynolds number is greater than 70, the ratio is a constant - independent of the Shear Reynolds number (Equation 8.11).

$$If\ 1.2 \le \left(\frac{U_* d}{\nu}\right) \le 70, then$$

$$\left(\frac{U_c}{w_s}\right) = \left[\frac{2.5}{\log(U_* d / \nu) - 0.06}\right] + 0.66 \qquad (8.10)$$

$$If\ 70 \le \left(\frac{U_* d}{d}\right)$$

then .... (8.11)

$$\left(\frac{U_c}{w_s}\right) = 2.05$$

The sediment concentration for sand (<2 mm) is calculated (Equation 8.12). C_s is in parts per million by weight. The sediment concentration for gravel and larger (>2 mm) has the same form but has different numerical values for the coefficients (Equation 8.13).

$$\log C_s = 5.435 - 0.286\log\left(\frac{W_s d}{\nu}\right) - 0.457\log\left(\frac{U_*}{W_s}\right)$$
$$+\left[\left[1.799 - 0.409\log\left(\frac{W_s d}{\nu}\right) - 0.314\log\left(\frac{U_*}{W_s}\right)\right]\log\left(\left(\frac{US}{W_s}\right) - \left(\frac{U_c S}{W_s}\right)\right)\right] \quad \text{......... (8.12)}$$

$$\log C_s = 6.681 - 0.633\log\left(\frac{W_s d}{\nu}\right) - 4.816\log\left(\frac{U_*}{W_s}\right)$$
$$+\left[\left[2.784 - 0.305\log\left(\frac{W_s d}{\nu}\right) - 0.282\log\left(\frac{U_*}{W_s}\right)\right]\log\left(\left(\frac{US}{W_s}\right) - \left(\frac{U_c S}{W_s}\right)\right)\right] \quad \text{......... (8.13)}$$

8.2.1.2 Ackers & White equation

The Ackers & White formula (1973) is also based on the stream power concept (Ackers, 1993). Ackers & White (1973) related the concentration of bed material load as a function of sediment mobility. They relate the transport of coarse sediment to the stream power that generates the grain shear stress; this is reflected in the first part of the mobility number (Equation 8.18). Finer sediments which travel in suspension are assumed to be a function of the total bed shear; this is reflected in the second part of the mobility number (Equation 8.18). Ackers & White (1973) thus account for both modes of transport. Where only coarse sediments occur, the coefficient n is 0. Ackers & White (1973) have thus constructed an equation in which coarse sediment is considered to be transported mainly as a bed process. The fine sediment is considered to be transported within the body of the flow where it is suspended by stream turbulence.

The Ackers & White formula is thus written:

$$d_g = d\left[\frac{g(s-1)}{\nu^2}\right]^{1/3} \qquad (8.14)$$

where

d_g is the dimensionless grain diameter (m)

s is the specific gravity of the sediment

d is the geometric mean diameter of the sediment (m)

$$If, d_g 60 \geq d_g \geq 1$$

$$\log C = 2.86 \log d_g - (\log d_g)^2 - 3.53$$

$$n = 1 - 0.56 \log d_g$$

$$A = \left(\frac{0.23}{\sqrt{d_g}}\right) + 0.14 \qquad (8.15)$$

$$m = \left(\frac{9.66}{d_g}\right) + 1.34$$

$If, d_g \geq 60$

$$c = 0.025$$
$$n = 0$$
$$A = 0.17$$
$$m = 1.50 \qquad (8.16)$$

Shear velocity is calculated:

$$U_* = (gRS)^{0.5} \qquad (8.17)$$

The sediment mobility number (F_g) is determined from:

$$F_g = \left[\frac{U_*^n}{(gd(s-1))^{0.5}}\right]\left[\frac{U}{(32)^{1/2}\log(10R/d)}\right]^{1-n} \qquad (8.18)$$

where

R is the hydraulic radius (m)

Finally the sediment concentration is calculated (C_s):

$$C_s = cs\left(\frac{d}{R}\right)\left(\frac{U}{U_*}\right)^n\left(\left(\frac{F_g}{A}\right)-1\right)^m \qquad (8.19)$$

8.2.1.3 Engelund & Hansen equation

Engelund & Hansen (1967) used an adaptation of Bagnold's stream power concept to develop their model. The equation was developed specifically for regime-type alluvial sand-bed rivers. The equation relates the sediment concentration (ppm) to the rate of energy expenditure per unit weight of water (the U-S product) and the shear stress (the R-S product). Chang (1988) maintains that it can be applied to the upper flow regime to particle sizes greater than 0.15 mm without serious error. The Engelund & Hansen equation is thus written:

$$C_s = 0.05\left(\frac{s}{s-1}\right)\left[\frac{US}{\left((s-1)gd\right)^{0.5}}\right]\left[\frac{RS}{(s-1)d}\right] \qquad (8.20)$$

where

s is the specific gravity of the sediment

U is the average velocity (m s^{-1})

S is the energy gradient (m/m)

R is the hydraulic radius (m)

d is the geometric mean of the sediment class (m)

8.2.2 Hydrological data

In Chapter 6, the method of generating the daily times series was presented. The daily flow data was used to generate 1-day daily flow duration curves and flood frequency curves (annual and partial duration series). Using the 1-day daily flow duration curves, flow classes were calculated for each site. The breakdown of the individual flow classes was based on the assumption that flows equalled or exceeded 10% of the time or less would probably be those flows that would be the most significant in terms of bed material transport. In the light of this assumption, the flows from the 99.99% equalled or exceeded to the 10% equalled or exceeded are divided into 10% duration flow classes. The flow exceedences less than this are divided into smaller flow class durations, 5%, 4%, 0.9% and 0.09% respectively. The geometric mean of each flow class was then calculated.

8.2.3 Hydraulic data

Chapter 7 has presented the methods used to determine the stage-discharge relations for each of the cross-sections. These were applied to the flow classes calculated from the flow duration curves, and then related to the cross-sections at each site so that parameters such as width, mean depth, hydraulic radius, slope, perimeter and average velocity could be calculated for the geometric mean of each flow class.

8.2.4 Bed material data

Chapter 7 has presented the methods used and the data obtained for the bed material data. These data were used in determining the bed material transport for each of the rivers.

8.2.5 Bed material transport equations

Having obtained the above mentioned information, it was possible to apply the three bed material transport equations to each flow class for each site. It is important to note that the equations were utilised such that each grain-size class was calculated separately. This enabled the calculation of initiation of motion and settling velocity for each grain-size class, as well as the proportion that each size class contributed to the overall transport rate. The actual transport values for each flow class for each size class are presented in Appendix F. The procedure for applying the above methods to generate the bed material transport for each site is as follows:

For the Yang equation:

a) Compute the flow classes at each site from the hydrological information (Tables 9.1 to 9.4)

b) Compute the width, mean depth, hydraulic radius, slope, wetted perimeter and average velocity for each flow class from the cross-sectional data and hydraulic rating curves

c) Determine relative size classes for the bed material

d) For each bed material size class and for each flow class, compute the settling velocity using the Dietrich approach (Equations 8.1 to 8.8)

e) For each bed material size class and for each flow class, compute the Shear Reynolds number (Equation 8.9)

f) For each bed material size class and for each flow class, compute the velocity to settling velocity ratio for the sand class and the gravel and greater class (Equations 8.10 and 8.11)

g) For each bed material size class and for each flow class, compute the sediment concentration for the sand class and the gravel and greater class (Equations 8.12 and 8.13)

h) Compute the total annual load in tonnes for sand, for gravel and for cobbles and greater

i) Compute the total annual load in tonnes

j) Compute the sediment transported for each flow class in kg m^{-3} s^{-1}

k) Compute the percentage bed material moved as a proportion of the whole for each flow class

l) Compute the maximum competence for each flow class

For the Ackers & White equation:

a) Compute the flow classes at each site from the hydrological information (Tables 9.1 to 9.4)

b) Compute the width, mean depth, hydraulic radius, slope, wetted perimeter and average velocity for each flow class from the cross-sectional data and hydraulic rating curves

c) Determine relative size classes for the bed material

d) For each bed material size class and for each flow class, compute the dimensionless grain diameter (Equation 8.14)

e) For each bed material size class and for each flow class, compute the coefficients (Equations 8.15 and 8.16)

f) For each bed material size class and for each flow class, compute the shear velocity (Equation 8.17)

g) For each bed material size class and for each flow class, compute the sediment mobility for fine and coarse sediments (Equation 8.18)

h) For each bed material size class and for each flow class, compute the sediment concentration (Equation 8.19)

i) Compute the total annual load in tonnes for sand, for gravel and for cobbles and greater

j) Compute the total annual load in tonnes

k) Compute the sediment transported for each flow class in $kg.m^{-3}.s^{-1}$

l) Compute the percentage bed material moved as a proportion of the whole for each flow class

m) Compute the maximum competence for each flow class

For the Engelund & Hansen equation:

a) Compute the flow classes at each site from the hydrological information (Tables 9.1 to 9.4)

b) Compute the width, mean depth, hydraulic radius, slope, wetted perimeter and average velocity for each flow class from the cross-sectional data and hydraulic rating curves

c) Determine relative size classes for the bed material

d) For each bed material size class, for each flow class, compute the sediment concentration using the Engelund & Hansen model (Equation 8.20)

e) Compute the total annual load in tonnes for sand, for gravel and for cobbles and greater

f) Compute the total annual load in tonnes

g) Compute the sediment transported for each flow class in $kg\ m^{-3}\ s^{-1}$

h) Compute the percentage bed material moved as a proportion of the whole for each flow class

i) Compute the maximum competence for each flow class

8.2.6 Stream power and shear stress

Stream power was calculated for each flow class. Stream power (ω) has been shown to be an effective substitute for bed load transport potential. Williams (1983) has shown that a minimum power per unit area of 1000 Wm^{-2} or more will move boulders with an intermediate diameter of 1.5 m. The value is given in Watts per metre squared. Unit stream power is written:

$$\varpi = \frac{\gamma Q S}{w} \qquad (8.21)$$

where

γ is the specific weight of the fluid (9800 Nm^{-3})

Q is the discharge (m^3s^{-1})

w is the channel width (m)

Shear stress (τ) was also calculated. The conventional means of calculating boundary shear stress was utilised. The value is given in Newtons per metre squared. Average depth was used in calculating the boundary shear stress.

$$\tau = \rho g D S \qquad (8.22)$$

where

D is the average depth (area/width) (m)

8.2.7 Dominant discharge

Dominant discharge was calculated using the Marlette & Walker (1968) equation (see Equation 3.1). Dominant discharge was calculated separately from the data that were generated for the three transport equations.

8.3 Sediment-maintenance flushing flows

One of the consequences of impounded rivers is that reduced magnitude and frequency of flooding may lead to the accumulation of finer sediment on the channel bed. The channel may then narrow, resulting in increased flood risk and reducing the variety and areal extent of aquatic habitat. Furthermore, it was shown in Chapter 4 that unless the coarse bed is moved on a 'regular' basis, fine material may fill the interstices resulting in higher incipient motion values, which in turn may lead to further sedimentation. To avoid this situation, it is necessary to ensure that the sand- and gravel-sized material are moved through the river system. The determination of the magnitude and frequency of flows necessary to maintain the aquatic habitat in a natural condition is known as sediment-maintenance flushing flows (Reiser *et al.*, 1989). Two options for setting sediment-maintenance flushing flows were considered: the Milhous approach and the Relative Bed Stability (RBS) approach. These will be discussed in turn.

8.3.1 Milhous's approach

The Milhous approach uses a number of equations developed using the Oak Creek data to determine the maximum size of the wash load, suspended load and bed load for each flow class (Milhous, 1973). The hydraulic component of the model determines the conditions required to remove and transport sediment through the stream channel and to maintain the channel morphology (Milhous, 1998b). The maximum size of the sediment to be moved is the maximum size of the wash, suspended or bed load depending on the specified objective. The following equations were used to calculate the maximum size of the wash load ($d_{max\ w}$), suspended load ($d_{max\ s}$) and bed load ($d_{max\ bl}$).

$$d_{max\ w} = \frac{RS_e}{0.56(G_s - 1)} \qquad (8.23)$$

$$d_{max\ s} = \frac{RS_e}{0.28(G_s - 1)} \qquad (8.24)$$

$$d_{max\ bl} = d_{50_a}\left[\frac{RS_e}{0.018(G_s - 1)d_{50_a}}\right]^{2.85} \qquad (8.25)$$

where

R is the hydraulic radius (m)

S_e is the energy slope (m/m)

G_s is the specific gravity of the particles

d_{50a} is the median grain size of the stream bed armour and should only be used when the median size of the bed load is less than the median size of the armour (Milhous, 2000). The objective is to keep the bed material moving through the stream when the armour is relatively stable.

The equation used in the calculation of the median size of the bed load (d_{50bl}) is:

$$d_{50\ bl} = d_{50a}\left[\frac{RS_e}{0.046(G_s - 1)d_{50\ a}}\right]^{2.85} \qquad (8.26)$$

When the median size of the bed material is less than the median size of the armour, the bed load equations are for the calculation of the sizes of the bed load during flushing of the bed material, and not for general movement at higher stream flows. Earlier, Milhous & Bradley (1986) developed a stream substrate movement parameter, β, to determine the flushing flows needed in a stream. β is the critical dimensionless shear stress, calculated using the median size of the bed surface material. The equation for the substrate movement parameter beta (β) is:

$$\beta = \frac{RS_e}{d_{50a}(G_s - 1)} \qquad (8.27)$$

The selection of the values of the substrate movement parameters needed to define a flushing flow were developed from data obtained from bed load transport research in Oak Creek, Oregon (Milhous, 1973). The data indicated that the value of the β required for the removal of fines and sand from the surface of a gravel-bed river for surface flushing is 0.021, and for the removal of material within the substrate (depth flushing) is 0.035. An important inherent assumption is that the Oak Creek results can be extrapolated to other rivers.

The mode of sediment removal is important. Milhous (1998c) argues that the sediment should be moved as washload when the objective is to move sediment rapidly through the stream and where the presence of the target size is detrimental to the ecosystem. Sediment should be moved as suspended load when the objective is to move sediment at reasonable rates, but where some deposition is acceptable. Sediment should be moved as bed load when the larger sizes are to be scoured, for example the removal of gravel from a pool. The load size equations were developed using gravel-bed rivers, and hence it is probably unwise to use equations where the median size is less than 2.0 mm.

8.3.2 Relative Bed Stability (RBS)

The central assumption in the RBS approach is that a channel can become unstable when particle sizes equal to or greater than a critical percentile are moved at bankfull (or some other pre-determined stage) (Olsen *et al.*, 1997). For the purposes of this thesis, the critical particle size is taken as the D_{84} (i.e. the particle diameter for which 84% of the bed particles are finer). This is consistent with several studies (cf. Carling, 1988; Sidle, 1988; Leopold, 1997; Olsen *et al.*, 1997). The assumption in using the D_{84} is that a coarse grain size must be entrained before the bed becomes fully mobilised and unstable.

8.3.2.1 Calculating RBS for fine sediment

The first step in calculating RBS is to determine the threshold of motion. Mean shear stress over the bed was calculated using the DuBoys equation:

$$\tau_{bankfull} = \rho g R S \qquad (8.28)$$

Critical dimensionless shear stress (τ_{ci}*) is calculated. The value of τ_{ci}* varies as a function of absolute particle size (D_i) and the relative size of D_i/D_{50}. This dependence is explained in terms of particle hiding and exposure. Particles larger than the mean size are exposed to the flow due to their greater protrusion into the flow, and are thus more easily entrained than would be the case with more uniform sediment. The converse is true for particles smaller than the median grain size, which remain hidden in the armoured layer. Thus the Andrews (1983) equation is used:

$$\tau_{ci}^{*} = \theta\left(\frac{D_i}{D_{50}}\right)^{x} \qquad (8.29)$$

where

θ is dimensionless coefficient (usually 0.045) (after Komar, 1989; Petit, 1994; Olsen *et al.*, 1997)

x is the power slope relationship (usually 0.7) (after Komar, 1989; Petit, 1994; Olsen *et al.*, 1997)

D_i is the particle diameter (m)

D_r is the reference diameter (usually D_{84}) (m)

The Shields criterion was then used to predict the threshold of bed load initiation, where τ_{ci} is the critical dimensional stream bed shear stress:

$$\tau_{critical} = \tau_{ci} = \tau^*_{ci}(\rho_s - \rho)gD_i \quad (8.30)$$

To calculate RBS:

$$RBS_\tau = \frac{\tau_{critical}}{\tau_{bankfull}} \quad (8.31)$$

If $\tau_{critical}$ is greater than $\tau_{bankfull}$, then the stream channel can be considered to be stable. The higher the value of $\tau_{critical}$ over $\tau_{bankfull}$, the greater the stability of the channel. If $\tau_{critical}$ is less than $\tau_{bankfull}$, then the stream channel can be considered to be unstable. For example, if $\tau_{bankfull}$ is estimated to be 50 N/m^2 and $\tau_{critical}$ is 90 N/m^2, the RBS value would be 90/50 = 1.8, and thus the channel can be considered to be stable.

8.3.2.2 Calculating RBS for coarse sediment

The second RBS method used is for coarser material in a heterogenous bed. To achieve this the Bathurst *et al.* (1987) equation was used to calculate the bankfull unit discharge (D_{84}).

$$q_c = 0.15 g^{0.5} D^{1.5} S^{-1.12} \quad (8.32)$$

The hiding and exposure effects were modelled using the bankfull unit discharge:

$$q_{ci} = a \left(\frac{D_i}{D_r}\right)^b \qquad (8.33)$$

where

a is q_c

$$b = \frac{(5(1-x))}{3} \qquad (8.34)$$

The reference critical unit discharge is calculated:

$$q_c = 0.15 g^{0.5} D^{1.5} S^{1.12} \qquad (8.35)$$

and;

$$q_{critical} = 0.916 \left(\frac{D_i}{D'}\right)^{0.5} \qquad (8.36)$$

Finally:

$$RBS_q = \frac{q_{critical}}{q_{bankfull}} \qquad (8.37)$$

The RBS is used in a modified form for this thesis. The RBS value was calculated for a number of scenarios for each flow class, including the RBS for the D_{84}, D_{16}, D_{70}, D_{90}, gravel and sand classes. These are presented in Appendix H at the back of the thesis. The RBS index was only calculated using the shear stress values. The RBS using the unit stream power approach (Olsen *et al.*, 1997) was unclear (Equations 8.32 to 8.37), and could not be used with any degree of confidence.

8.4 Conclusion

The approach that has been outlined in this chapter was applied to all three rivers under consideration. The following two chapters present the results and discussion of the implementation of this approach to the Mkomazi (Chapter 9) and Mhlathuze and Olifants Rivers (Chapter 10).

Chapter 9: Results and Discussion - the Mkomazi River

9.1 Introduction

The aim of this chapter is to present the results obtained for the bed material transport analysis and the sediment-maintenance flushing flow computations for the unregulated Mkomazi River. The chapter is divided into two sections. The first section deals with the bed material transport analysis and the second section deals with the sediment-maintenance flushing flow computations. For the first section, the results are discussed in the context of a number of research questions:

1. *What are the channel morphology characteristics?*

2. *What is the dominant discharge?*

3. *What is the effective discharge?*

4. *Is there any relationship between estimated bankfull discharge, dominant discharge and effective discharge?*

It is important to note that the values that were obtained from the modelling exercise were compared as percentages, rather than assigning them absolute values. Appendix F displays the actual transport values. Summary tables of the bed material transport analysis for each of the sites are presented in Appendix G, while the summary tables for the sediment-maintenance flushing flows are available in Appendix H.

9.2 The Mkomazi River

9.2.1 Overview

The geographical setting of the Mkomazi River was described in Chapter 5. The Mkomazi River drains an area of around 4387 km^2 in KwaZulu-Natal, and is the last remaining large eastern sea-board perennial South African river that remains unimpounded. Thirteen sites were chosen for analysis along the Mkomazi. Tables 9.1 to 9.4 display the calculated flow classes for each of these sites from the 1-day daily flow duration curves. The geometric mean of each flow class was used in the bed material transport calculations to represent each flow class. For example, at Site 1 (Table 9.1) the range of flows experienced between 0.1% time equalled or exceeded and the 0.01% time equalled or exceeded is from 47.143 m^3s^{-1} to 102.772 m^3s^{-1}. The geometric mean of this class is 69.606 m^3s^{-1}. This was used in conjunction with the duration that each flow class represented as a proportion of one year (365.25 days). For example, a flow class that represents 0.09% of the time occurs for 0.3 days in one year.

Table 9.1: Flow classes calculated for the Mkomazi River sites 1 to 4. Values are in m^3s^{-1}.

% time equalled or exceeded	Q	Geometric mean flow class	Q	Geometric mean flow class	Q	Geometric mean flow class	Q	Geometric mean flow class
	Site 1		Site 2		Site 3		Site 4	
99.99	0.001		0.002		0.002		0.006	
90	0.198	0.015	0.342	0.025	1.008	0.044	1.062	0.079
80	0.305	0.246	0.526	0.424	1.551	1.250	1.634	1.317
70	0.414	0.355	0.714	0.613	2.106	1.807	2.218	1.904
60	0.558	0.480	0.963	0.830	2.839	2.445	2.991	2.576
50	0.770	0.655	1.330	1.132	3.920	3.336	4.130	3.515
40	1.113	0.926	1.923	1.599	5.667	4.713	5.971	4.966
30	1.737	1.391	3.000	2.402	8.842	7.079	9.316	7.458
20	2.863	2.230	4.946	3.852	14.577	11.353	15.358	11.961
10	5.563	3.991	9.608	6.893	28.319	20.318	29.836	21.406
5	9.271	7.181	16.013	12.404	47.197	36.559	49.725	38.518
1	19.561	13.467	34.909	23.643	99.585	68.557	104.920	72.230
0.1	47.143	30.367	84.130	54.193	216.100	146.698	227.677	154.557
0.01	102.772	69.606	183.404	124.217	436.522	307.136	459.907	323.589

Table 9.2: Flow classes calculated for the Mkomazi River sites 5 to 8. Values are in m^3s^{-1}.

% time equalled or exceeded	Q	Geometric mean flow class	Q	Geometric mean flow class	Q	Geometric mean flow class	Q	Geometric mean flow class
	Site 5		Site 6		Site 7		Site 8	
99.99	0.010		0.010		0.011		0.011	
90	1.782	0.133	1.818	0.136	1.926	0.144	1.980	0.148
80	2.742	2.211	2.798	2.255	2.964	2.389	3.047	2.456
70	3.722	3.195	3.798	3.260	4.023	3.453	4.136	3.550
60	5.019	4.322	5.121	4.410	5.425	4.672	5.577	4.803
50	6.930	5.898	7.070	6.017	7.490	6.374	7.700	6.553
40	10.019	8.332	10.221	8.501	10.828	9.006	11.132	9.258
30	15.632	12.515	15.948	12.767	16.895	13.526	17.369	13.905
20	25.770	20.071	26.290	20.476	27.852	21.693	28.633	22.301
10	50.064	35.919	51.076	36.644	54.110	38.821	55.627	39.909
5	83.437	64.631	85.123	65.937	90.180	69.854	92.708	71.813
1	208.593	131.926	212.807	134.591	225.449	142.586	231.770	146.584
0.1	406.756	291.284	414.974	297.169	439.626	314.822	451.952	323.649
0.01	622.337	503.130	634.910	513.294	672.627	543.787	691.486	559.033

Table 9.3: Flow classes calculated for the Mkomazi River sites 9 to 12. Values are in m^3s^{-1}.

% time equalled or exceeded	Q	Geometric mean flow class	Q	Geometric mean flow class	Q	Geometric mean flow class	Q	Geometric mean flow class
	Site 9		Site 10		Site 11		Site 12	
99.99	0.509		0.532		0.543		0.572	
90	3.272	1.290	3.421	1.349	3.495	1.378	3.681	1.451
80	4.445	3.814	4.647	3.987	4.748	4.074	5.000	4.290
70	5.889	5.116	6.157	5.349	6.290	5.465	6.625	5.756
60	8.140	6.924	8.510	7.238	8.695	7.396	9.158	7.789
50	11.273	9.579	11.785	10.015	12.041	10.232	12.682	10.777
40	16.040	13.447	16.769	14.058	17.133	14.363	18.045	15.128
30	25.008	20.028	26.145	20.938	26.713	21.394	28.134	22.531
20	40.921	31.990	42.781	33.444	43.711	34.171	46.036	35.988
10	74.805	55.327	78.206	57.842	79.906	59.099	84.156	62.243
5	114.842	92.686	120.062	96.899	122.672	99.006	129.197	104.272
1	301.740	186.151	314.740	194.392	323.410	199.182	340.400	209.711
0.1	588.380	421.352	613.740	439.509	630.640	451.614	663.770	475.339
0.01	900.230	727.789	939.010	759.150	964.890	780.063	1015.57	821.039

Table 9.4: Flow classes calculated for the Mkomazi River Site 13. Values are in m^3s^{-1}.

% time equalled or exceeded	Q	Geometric mean flow class
	Site 13	
99.99	0.578	
90	3.718	1.466
80	5.051	4.334
70	6.692	5.814
60	9.250	7.868
50	12.810	10.885
40	18.227	15.280
30	28.418	22.759
20	46.501	36.352
10	85.006	62.872
5	130.502	105.325
1	342.260	211.342
0.1	667.410	477.941
0.01	1021.130	825.538

9.3 Research questions

9.3.1 Research question 1: What are the channel morphology characteristics?

The results indicate that there is no consistent downstream trend (using MAR as a substitute for distance) in the estimated bankfull discharge (Figure 9.1). The R-squared value between estimated bankfull discharge and MAR is 0.04 (insignificant at the 95% level). The estimated bankfull discharge ranges from 117 m^3s^{-1} (Site 9) to 482 m^3s^{-1} (Site 3) (Table 9.5). The estimated return periods for the bankfull discharge range from 1.1 years to >39 years on the annual series with an average return period of 8.6 years, while the return periods for the partial series range from 0.1 years to >39 years with an average of 7.1 years (Table 9.6). Most of these values are higher than the average annual return period of 1.5 years suggested for bankfull discharge by Leopold (1997). Furthermore, the bankfull discharge as estimated in the field does not appear to be related to any particular flow return period (Table 9.7). The estimated bankfull discharge was compared to the 1.5 and 2.44 year return period for the annual series and the 0.9 and 2 year return period for the partial series - no relationship is evident (Table 9.7).

There are three possible explanations for this lack of trend. First, the field estimated bankfull discharges are incorrect. Second, there is no such thing as a bankfull stage/feature, and the variability of the hydrological regime coupled with strong bed rock control precludes such a stage/feature - the morphology of the channel is related more to the resistance of the channel perimeter to erosion than the shaping fluid (i.e. the flow). Third, the estimated bankfull condition may represent the active channel prior to the most recent flood, and in this sense, the equilibrium morphology has been disrupted by the flood. These issues will be discussed in a later in the chapter.

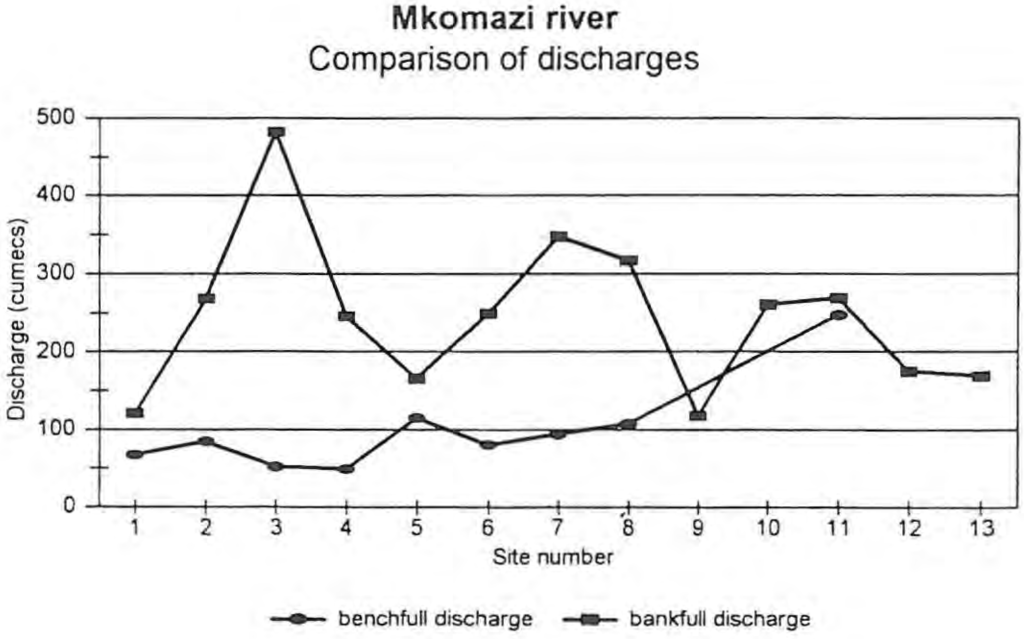

Figure 9.1: Inundation stage for the 'bench-full' discharge and the estimated bankfull discharge for the Mkomazi River.

There does not appear to be any consistent trend for the macro-reaches. Macro-reach 1 and 2 display evidence of some trend. Macro-reach 3 and 4, however, do not (Figure 9.1). The characteristics of the individual macro-reaches are given in Chapter 5 (sites 1, 2, 3 and 4 are in macro-reach 1, sites 5,6 and 7 are in macro-reach 2, sites 8 and 9 are in macro-reach 3, and sites 10, 11, 12 and 13 are in macro-reach 4). In macro-reach 1 the bankfull discharge estimate increases from site 1 to 3 (121 m^3s^{-1} to 482 m^3s^{-1}). Site 4 shows a reduced estimated bankfull discharge (246 m^3s^{-1}) (Table 9.5). In macro-reach 2, the estimated bankfull discharges are similar to those in macro-reach 1, but there is an overall increase within the reach. Macro-reach 3 consists of two sites, and it is thus hazardous to ascribe any trend to the results. In macro-reach 4 there is no real trend either. It is important to note that the validity of these comments are limited by the number of sites that represent each macro-reach.

There is a clear downstream trend in the 'bench-full' discharge (Figure 9.1). Although the calculated R-squared value between MAR and 'bench-full' discharge is 0.53 (insignificant at the 95% level), it is clear from Figure 9.1 that there is a consistent downstream increase in the 'bench-full' discharge. The 'bench-full' discharge ranges from 49 m^3s^{-1} at Site 4 to 247 m^3s^{-1} at Site 11 (Table 9.5). The return period of the bench ranges from 1.0 years to 10 years on the annual series with an average return period of 2.7 years, and 0.1 years to 8 years on the partial series with an average return period of 1.3 years (Table 9.6). It is clear that other than for sites 1 and 2, these values are in the range of the 1.50 year return period on the annual series that Leopold (1997) predicted for the bankfull discharge (Table 9.6). The only morphological feature that could be consistently related to a particular flow return period was the low bench.

Table 9.5: Summary data for the Mkomazi River. Data presented are the average data for each site. Values are in m^3s^{-1}.

Site	MAR	$Q_{1.5}$	$Q_{2.44}$	$Q_{p0.9}$	$Q_{p2.0}$	dominant discharge	effective discharge	bench	estimated Q_b	terrace 1	terrace 2	terrace 3
1	67	18	31	30	38	19	35	67	121	245	803	
2	122	31	55	53	68	28	74	84	268	602	1028	
3	356	89	148	146	180	69	138	52	482	1137	1527	
4	375	94	156	154	189	55	72	49	246	457	906	
5	634	182	293	286	347	136	291	115	165	537	1478	
6	640	186	299	294	354	119	225	80	249	899	2216	
7	681	197	317	310	375	242	276	94	347	1481		
8	698	203	326	320	385	62	147	107	316	1546	2722	3921
9	910	255	440	497	575	156	343		117	1457		
10	950	260	450	518	600	174	358		260	1113	4726	
11	976	268	470	532	617	208	367	247	268	855	3239	
12	1027	285	500	560	649	306	387		174	598	3183	
13	1032	290	501	563	653	154	300		169	675	4850	10164

where MAR is the Mean Annual Runoff in million cubic metres, $Q_{1.5}$ is the 1.5 year return period on the annual series, $Q_{2.44}$ is the 2.44 year return period on the annual series, $Q_{p0.9}$ is the 0.9 year return period on the partial series, $Q_{p2.0}$ is the 2.0 year return period on the partial series and estimated Q_b is estimated bankfull discharge.

Table 9.6: Discharges and return periods for morphological features for the Mkomazi River. Average values are displayed.

Site	1	2	3	4	5	6	7	8	9	10	11	12	13	Mean
bench	67	84.	52	49	115	80	94	107			247			
FFC	10	5.9	1.3	1.2	1.2	1	1	1.1			1.5			2.7
PDS	8	2.9	0.2	0.1	0.1	0.1	0.1	0.1			0.2			1.3
Estimated Qb	120	268	482	245	165	249	347	316	117	260	268	174	168	
FFC	>39	>39	10	7.2	1.4	2.1	3.4	2.7	1.1	1.5	1.5	1.3	1.2	8.6
PDS	>39	>39	6	4.6	0.2	0.5	1.5	0.9	0.1	0.2	0.2	0.9	0.1	7.1
terrace 1	245	602	1137	457	537	899	1481	1546	1457	1113	855	598	675	
FFC	>39	>39	>39	9.5	21.9	>39	>39	>39	>39	>39	>39	2.9	5	>39
PDS	>39	>39	>39	6.5	19.4	>39	>39	>39	>39	>39	>39	1.3	3.6	>39
terrace 2	803	1028	1527	906	1478	2216		2722		4726	3239	3183	4850	
FFC	>39	>39	>39	>39	>39	>39		>39		>39	>39	>39	>39	>39
PDS	>39	>39	>39	>39	>39	>39		>39		>39	>39	>39	>39	>39
terrace 3								3921					10164	
FFC								>39					>39	>39
PDS								>39					>39	>39

Values for bench, estimated Q_b, terrace 1, 2 and 3 are in m^3s^{-1}. FFC refers to the average annual return period on the annual series (years). PDS refers to the average return period for the partial duration series (years).

Table 9.7: R-squared values for the relationships between various parameters for the Mkomazi River (* represents statistical significance at the 95% level).

R^2	Q_b	DD (Y)	DD (AW)	DD (EH)	Q_e (Y)	Q_e (AW)	Q_e (EH)	$Q_{1.5}$	$Q_{2.44}$	$Q_{p0.9}$	$Q_{p2.0}$	B1	T1
Q_b	-												
DD (Y)	0.06	-											
DD (AW)	0.001	0.39	-										
DD (EH)	0.09	**0.88***	0.42	-									
Q_e (Y)	0.005	**0.72 ***			-								
Q_e (AW)	0.002		**0.77***		0.51	-							
Q_e (EH)	0.17			**0.88***	0.22	0.30	-						
$Q_{1.5}$	0.04	**0.79***	0.33	**0.82***	0.54	0.55	**0.71***	-					
$Q_{2.44}$	0.05	**0.83***	0.34	**0.82***	0.56	0.55	**0.71***		-				
$Q_{p0.9}$	0.06	**0.84***	0.31	**0.82***	0.57	0.54	**0.72***			-			
$Q_{p2.0}$	0.06	**0.84***	0.34	**0.83***	0.57	0.54	**0.72***				-		
B1		**0.73***	0.15	0.31	**0.82***	0.38	0.12	0.48	0.57	0.67	0.65	-	
T1		0.01	0.07	0.01	0.02	0.20	0.01	0.16	0.13	0.10	0.10		-

where

Q_b	is the estimated bankfull discharge
DD (Y)	is the dominant discharge using the Yang equation
DD (AW)	is the dominant discharge using the Ackers & White equation
DD (EH)	is the dominant discharge using the Engelund & Hansen equation
Q_e (Y)	is the effective discharge using the Yang equation
Q_e (AW)	is the effective discharge using the Ackers & White equation
Q_e (EH)	is the effective discharge using the Engelund & Hansen equation
$Q_{1.5}$	is the 1.5 year return period flow on the annual series
$Q_{2.44}$	is the 2.44 year return period flow on the annual series
$Q_{p0.9}$	is the 0.9 year return period on the partial duration series
$Q_{p2.0}$	is the 2.0 year return period on the partial duration series
B1	is the bench
T1	is the low terrace

The flow data as generated by the hydrological modelling indicates that many of the terraces are not inundated by the present flow regime (Table 9.6). One of the limitations of the hydrological modelling as carried out on the Mkomazi is that the upper end of the flow duration curve, especially the extreme events, is poorly represented. In Chapter 6, a table is provided of the known floods for the Mkomazi River, together with the closest monitoring site for this research (Table 6.4). In the middle parts of the catchment (catchment area 1744 km^2) for the period of record 1931 to 1990, four large floods have been identified. The site at which these floods were estimated is close to sites 5 and 6 (Table 9.6). Two terraces were identified at sites 5 and 6. At Site 5, the low terrace has an estimated inundation flow of 537 m^3s^{-1}, while the second terrace has an inundation flow of 1478 m^3s^{-1}. At Site 6, the low terrace is inundated at 899 m^3s^{-1}, while the second terrace is inundated at 2216 m^3s^{-1}. The largest flood on record close to this site is 2770 m^3s^{-1} in 1987. A flood of a similar magnitude (2010 m^3s^{-1}) occurred in 1975. These floods were sufficient to inundate these terraces. Van Bladeren (1992) has estimated the return period of these floods as being 50 to 100 years and 20 to 50 years respectively.

Using the hydraulics and cross-sectional data, it is clear that these floods achieve high velocities, shear stresses and stream power, and are capable of moving the coarsest bed material. At Site 5, the largest flood of 2770 m^3s^{-1} produced an estimated average velocity of c. 7 ms^{-1}, and a unit stream power of 1019 Wm^{-2}. It is possible that the terraces are features that have formed as a result of the bi-polar type flood frequency curve. Floods of this magnitude appear to have return periods of between 50 and 100 years, but are probably highly significant in terms of maintaining the channel form. (Whether or not these terraces are related to a different climate remains untested, and is beyond the scope of this research). At Site 6 the largest flood on record produces an estimated average velocity of c. 6 m^3s^{-1} and a unit stream power of around 1175 Wm^{-2}. This discharge also has the capacity to transport the coarsest bed material (cf. Williams, 1983). At sites 9 and 10, similar results were obtained (see Appendix G, Tables 21 to 24).

The best flood record of extreme floods available for the Mkomazi is close to the mouth. This is in close proximity to Site 12 and Site 13 (Table 9.6). Site 12 has two terraces, the upper terrace has an estimated inundation flow of 3183 m^3s^{-1}, while Site 13 has two terraces, one at 4850 m^3s^{-1} and a second, higher terrace with an estimated inundation flow of 10 164 m^3s^{-1}. Table 6.4 shows the historical flood record for a site just downstream of Site 13. The largest flood on record was estimated as 7250 m^3s^{-1} in 1856, with a similar sized flood in 1987 of 6830 m^3s^{-1}. There are a number of smaller floods on record, the smallest of which was 2880 m^3s^{-1} in 1976. During the period of record (1856 to 1990), there have been at least seven floods which have inundated the lower terraces at both sites. A simple calculation suggests that this inundation occurs approximately every 20 years. These flows produce high shear stresses and stream power, and are the only flows that are capable of transporting the coarsest bed material. This will be discussed in greater detail in Section 9.3.3.

9.3.2 Research question 2: What is the dominant discharge?

The dominant discharge was calculated from the transport equations using the Marlette & Walker (1968) equation. The dominant discharge reflects the discharge that transports over 50% of the bed material load. The results are presented in Table 9.8. The average dominant discharge increases downstream (Figure 9.2). The R-squared value calculated for the relationship between mean dominant discharge and MAR is 0.65 (significant at the 95% level).

The three transport equations used predict consistent values for dominant discharge (Table 9.8). The Ackers & White equation generally predicts the lowest transport rates for each site, and consequently predicts the highest dominant discharge. At Site 7a, the coarse bed material and high entrainment thresholds meant that the Ackers & White equation predicted that only the highest flow class could entrain any material, and consequently the calculated dominant discharge is high. At Site 7b the Ackers & White equation predicts that no bed material transport will occur. At Site 12, the wide channel results in very low stream power and consequently the dominant discharge is also high.

There is good agreement between the dominant discharge and the hydrological regime for the Yang and Engelund & Hansen equation, but not for the Ackers & White equation (Table 9.7). The R-squared value (significant at the 95% level) between the dominant discharge as estimated using the Yang equation and the 1.5 and 2.44 year return period on the annual series and the 0.9 year and 2.0 year return period on the partial series is 0.79, 0.83, 0.84 and 0.84 respectively (Table 9.7). There appears to be no relationship between the dominant discharge as estimated by the Ackers & White equation and the hydrological regime. However, there is good agreement for the Engelund & Hansen equation where the R-squared values (significant at the 95% level) are 0.82, 0.82, 0.82 and 0.83 for the 1.5 and 2.44 year return period on the annual series, and the 0.9 year and 2.0 year return period on the partial series respectively (Table 9.7). This is reflected in the relationship between the three transport equations for the estimated dominant discharge where there is agreement between the dominant discharge as estimated using the Yang and Engelund & Hansen equations (R-squared of 0.88), but no relationship between the dominant discharge estimated using the Ackers & White and Yang and Engelund & Hansen equations (R-squared values of 0.39 and 0.42 respectively) (Table 9.7).

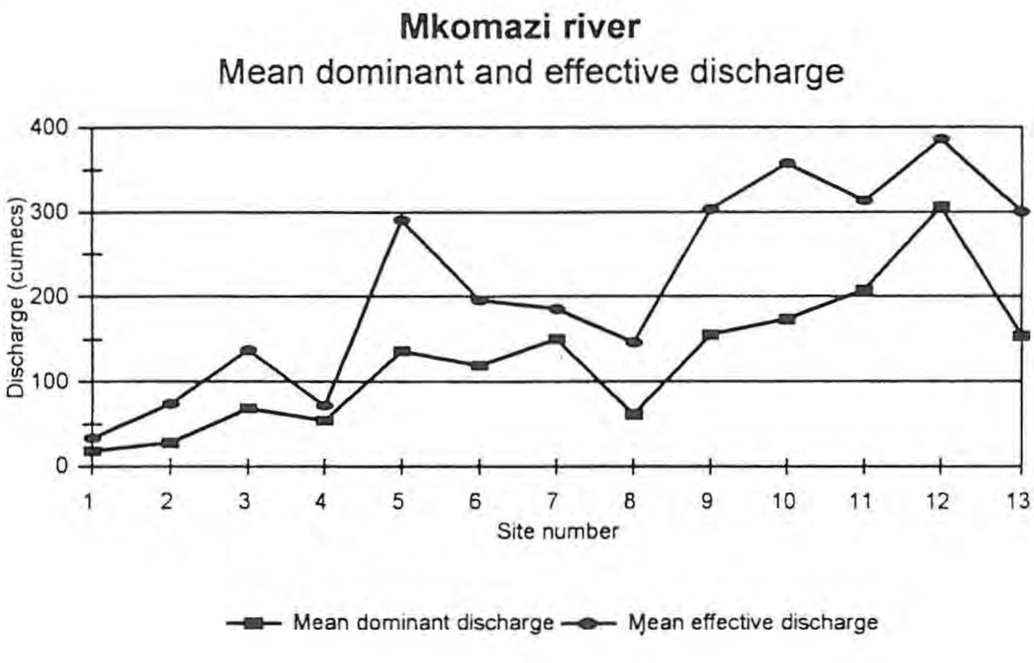

Figure 9.2: Mean dominant discharge and effective discharge for the Mkomazi River.

Table 9.8: Dominant discharge and effective discharge for the Mkomazi River. Values are in m^3s^{-1}. Note that the values are the geometric mean for a particular flow class.

Site	Dominant discharge (Yang)	Dominant discharge (Ackers & White)	Dominant discharge (Engelund & Hansen)	Effective discharge (Yang)	Effective discharge (Ackers & White)	Effective discharge (Engelund & Hansen)
1a	16.46	20.14	13.66	30.367	30.367	30.367
1b	19.30	21.22	13.60	30.367	30.367	30.367
1c	17.42	34.40	12.27	30.367	56.01	30.367
2a	24.19	41.04	18.96	54.193	124.21	54.193
2b	24.13	41.95	18.50	23.643	124.21	54.193
2c	31.17	31.17	18.31	54.193	124.21	54.193
3a	66.84	76.84	66.51	146.69	146.69	146.69
3b	58.00	62.90	66.13	68.557	146.69	146.69
3c	71.53	84.74	67.15	146.69	146.69	146.69
4a	53.14	57.22	51.68	72.23	72.23	72.23
4b	52.07	58.63	54.34	72.23	72.23	72.23
5a	127.19	149.96	132.50	291.28	291.28	291.28
5b	127.19	149.96	132.50	291.28	291.28	291.28
6a	119.89	136.95	119.29	134.59	297.16	39.27
6b	96.90	100.44	118.16	134.59	134.59	297.16
6c	117.48	144.86	117.10	134.59	297.16	297.16
7a	68.50	543.79	81.74	142.58	543.78	142.58
7b	125.25	0	86.12	142.58	0	142.58
8a	60.76	61.40	62.15	146.58	146.58	146.58
8b	61.51	62.30	62.69	146.58	146.58	146.58
9a	172.01	179.36	139.70	186.15	421.35	421.35
9b	130.10	176.24	139.04	186.15	186.15	421.35
10a	155.73	226.02	159.00	439.51	439.51	194.39
10b	142.48	204.96	155.34	194.39	439.51	439.51
11	217.82	280.81	124.63	451.61	451.61	199.18
12	206.73	502.47	209.41	209.71	475.33	475.33
13	146.73	150.74	165.74	211.34	211.34	477.94

9.3.3 Research question 3: What is the effective discharge?

For the purposes of this thesis, the effective discharge for the Mkomazi was taken to be the geometric mean of the flow class that transports the most bed material (Figure 9.3). In some senses this is misleading, as often one flow class (23.643 m^3s^{-1}) (as in Site 2a - Appendix G, Table 4) may represent say 36.82% of the bed material transported, while the flow class above it (54.193 m^3s^{-1}) represents 36.86% of the bed material transported (Yang equation). This results in a misleading representation of the effective discharge as the effective discharge flow class is taken as 54.193 m^3s^{-1} when in fact, this transports only 0.04% more material than the flow class below it. Furthermore, it should be noted that what appear to be large differences in effective discharge are simply a shift into the next flow class (Table 9.8). The effective discharge is thus sensitive to class definition.

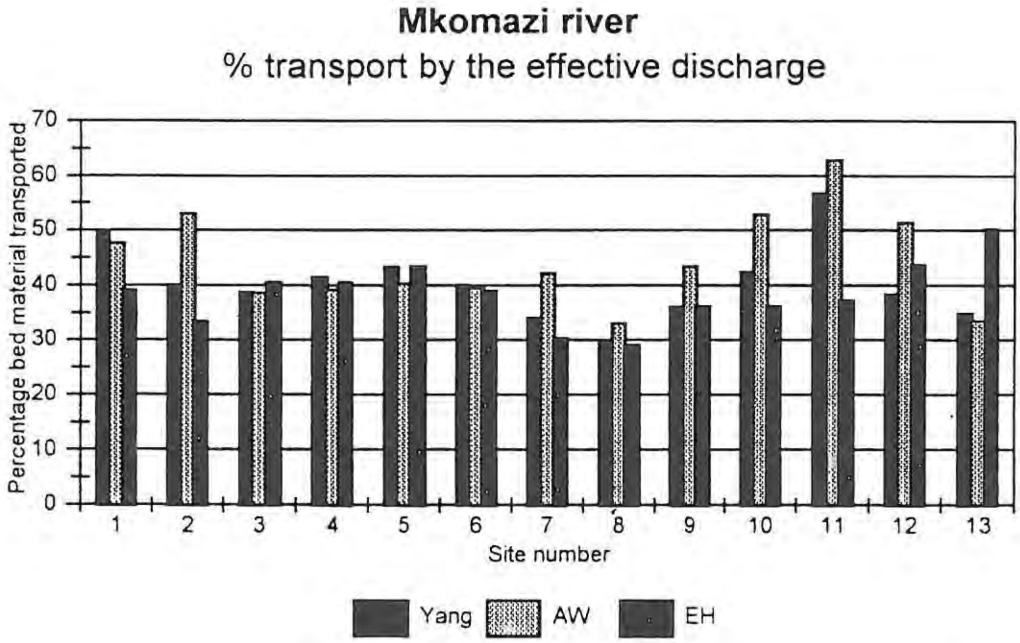

Figure 9.3: The percentage bed material transported by the effective discharge for the Mkomazi River.

For all sites, the most effective discharge was the discharge that was equalled or exceeded on average between 5% and 0.1% of the time, i.e. the upper two flow classes but one (5-1% and 1-0.1%) (Table 9.9). The value calculated for the effective discharge appears to be related to a combination of local conditions (channel geometry, slope, bed material calibre) and the manner in which the equations calculate the percentage transport. For example, in macro-reach 3, where there is high stream power and shear stress, flows become competent to transport bed material at lower flow classes. This results in the most effective discharge being predominantly in the 5-0.1% range. It also results in the upper three flow classes (5-1%; 1-0.1%; 0.01-0.01%) being less 'effective', and the bed material tends to be transported by a wider range of flow classes. A good example of this is Site 8 (Appendix G, Tables 19 to 20) which has a very steep, confined bed rock channel. Here, high shear stresses and stream power, even at lower flows, result in the upper three flow classes transporting just over 40% of the bed material. The flow classes lower than this thus account for 60% of the bed material transport.

Table 9.9: Effective discharge flow classes for the Mkomazi River.

Site	Yang (flow class)	Ackers & White (flow class)	Engelund & Hansen (flow class)
1a	1-0.1%	1-0.1%	1-0.1%
1b	1-0.1%	1-0.1%	1-0.1%
1c	1-0.1%	1-0.1%	1-0.1%
2a	1-0.1%	1-0.1%	1-0.1%
2b	5-1%	5-1%	1-0.1%
2c	1-0.1%	5-1%	1-0.1%
3a	1-0.1%	1-0.1%	1-0.1%
3b	5-1%	1-0.1%	1-0.1%
3c	1-0.1%	1-0.1%	1-0.1%
4a	5-1%	5-1%	5-1%
4b	5-1%	5-1%	5-1%
5a	1-0.1%	1-0.1%	1-0.1%
5b	1-0.1%	1-0.1%	1-0.1%
6a	5-1%	1-0.1%	1-0.1%
6b	5-1%	5-1%	1-0.1%
6c	5-1%	1-0.1%	1-0.1%
7a	5-1%	-	5-1%
7b	5-1%	-	5-1%
8a	5-1%	5-1%	5-1%
8b	5-1%	5-1%	5-1%
9a	5-1%	1-0.1%	1-0.1%
9b	5-1%	1-0.1%	1-0.1%
10a	1-0.1%	1-0.1%	5-1%
10b	5-1%	1-0.1%	1-0.1%
11	1-0.1%	1-0.1%	5-1%
12	5-1%	1-0.1%	1-0.1%
13	5-1%	5-1%	1-0.1%

As mentioned in Chapter 8, the flow classes greater than the 10% equalled or exceeded range were divided into 5%, 4%, 0.9% and 0.09% flow class durations respectively. The effective discharge is thus to some extent dependent on the division of the flow duration curve. To overcome this problem, cumulative sediment transport curves were constructed. These are presented in Figures 9.4 to 9.6. The results indicate that the bulk of the bed material transported (>80%) occurred (all three equations) between the 20% equalled or exceeded and 0.1% equalled or exceeded range. However, there are two outliers, these are sites 7 and 8. The steep slope and bed rock nature of Site 8 generates high unit stream power and velocities, which result in a greater proportion of the bed moving at lower flow classes than occurs at other sites, hence the different shaped curve. Site 7 has an extremely coarse bed so that for Site 7b, the Ackers & White equation predicts that no bed material transport occurs. For Site 7a, the Ackers & White equation predicts that transport will only occur at the highest flow class (i.e. 0.1-0.01%). This accounts for the two outliers.

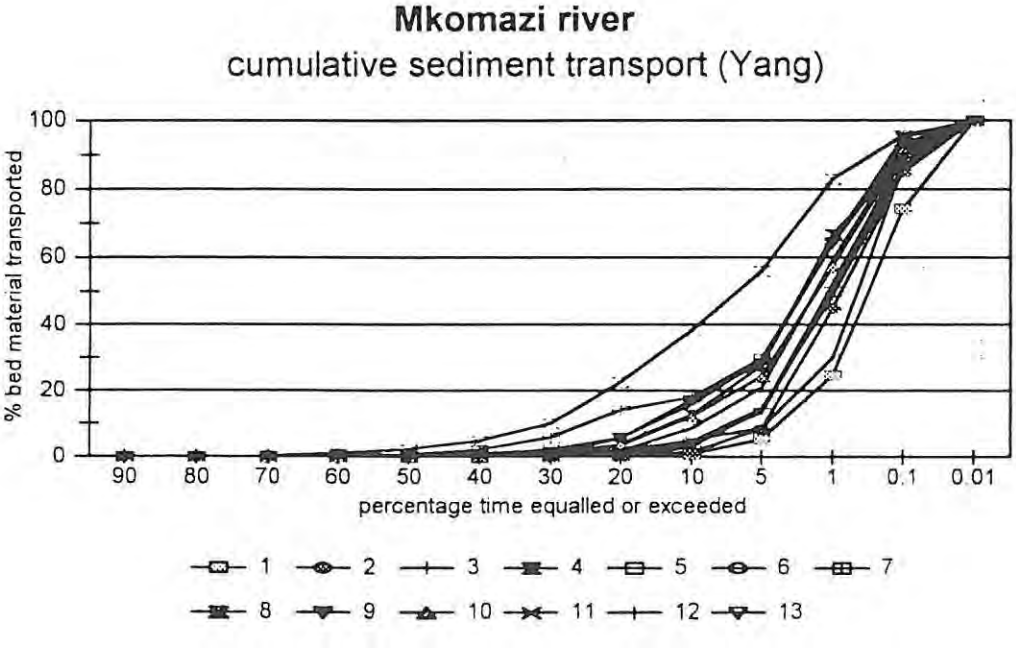

Figure 9.4: Cumulative sediment transport for the Yang equation for all sites for the Mkomazi River.

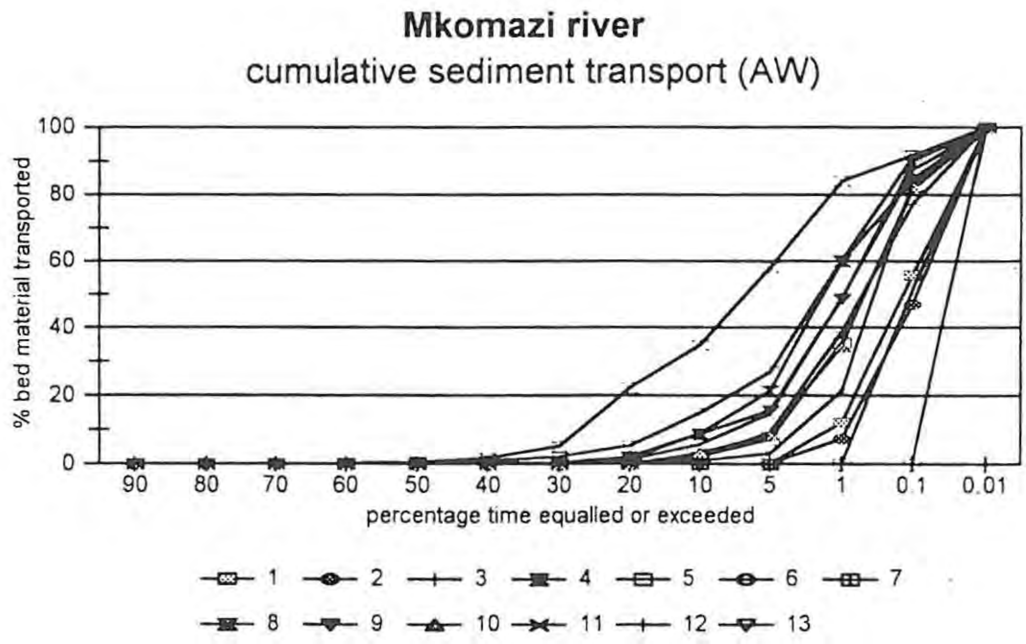

Figure 9.5: Cumulative sediment transport for the Ackers & White equation for all sites for the Mkomazi River.

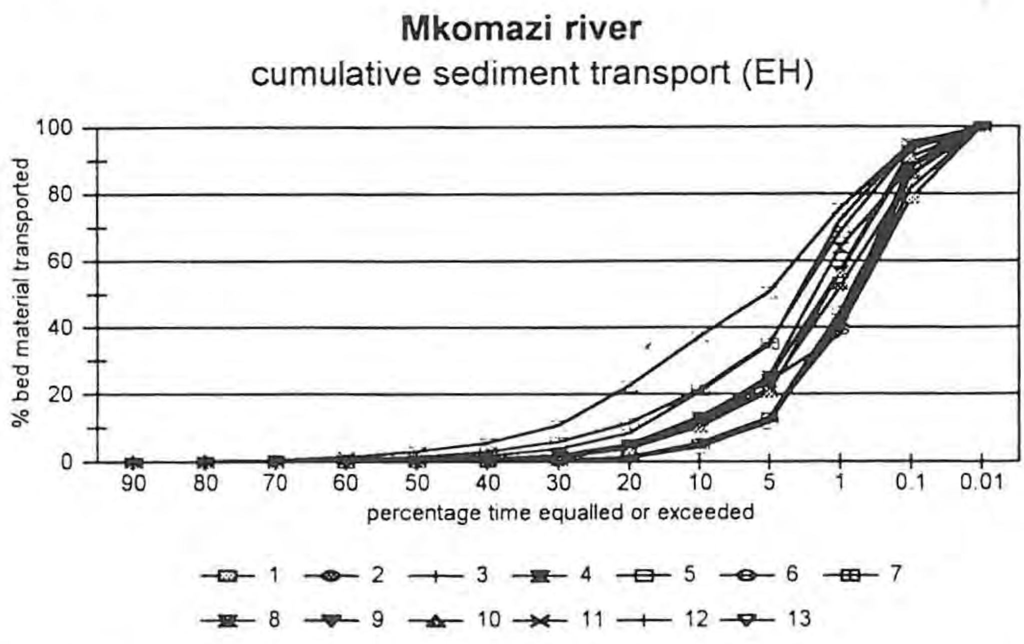

Figure 9.6: Cumulative sediment transport for the Engelund & Hansen equation for all sites for the Mkomazi River.

The effective discharge usually accounts for around 40% of the material transported (Figure 9.3). At the lower four sites (macro-reach 4) this value increases to around 50%. In effect, if the average calculated effective discharge for the Mkomazi River transports around 40% of the load, this means that a further 60% of the bed material is transported by flows other than the so-called effective discharge. This begs the question of how the remaining 60% is distributed around the effective discharge?

Data for the Yang equation indicate that very little transport occurs before the 50% equalled or exceeded on the flow duration curve (Figure 9.4). The remaining 60% of the bed material transported therefore occurs between the 50% equalled or exceeded and the 5% equalled or exceeded range. Data for the Ackers & White equation, shows a similar relationship, although in the case of the Ackers & White equation, very little transport (<10%) occurs before the 20% equalled or exceeded (Figure 9.5). The Engelund & Hansen equation also shows a similar distribution to the Yang and Ackers & White equation (Figure 9.6). There are two outliers for all these equations, sites 7 and 8 where, as was previously mentioned, local conditions result in a greater proportion of bed material moving at lower flow classes. The results demonstrate that the general trend is that most bed material is transported by flows with an exceedence of between 5% and 0.1% and that higher and lower flows transport proportionally less of the bed material.

Figure 9.7 shows the maximum competence of the highest flow class (0.1-0.01%) in relation to the D_{16}, D_{50} and D_{84} of the bed material (given the predictional limitations of the equations). The data indicate that at 10 of the 13 sites (1, 2, 4, 6, 7, 8, 9, 10, 12 and 13) both the Yang and Ackers & White equations predict that the highest flow class does not have the competence to transport the D_{84}. The Engelund & Hansen method, however computes that other than at sites 9, 10, 12 and 13, these flows have the competence to transport the D_{84}. The Engelund & Hansen equation was developed for alluvial sand-bed channels, and consequently the incipient motion values calculated by this equation for gravel- and cobble-bed rivers should be treated with circumspection. While this argument is not supported by field evidence and therefore remains untested, it does provide an indication of the relative stability of the coarse bed.

This finding begs the question, what discharge is competent to mobilise the coarse bed material? It was pointed out earlier in Section 9.3.1 that the stream power generated during high magnitude flood events is sufficient to transport even the coarsest material on the bed. Unit stream powers for these flood events are in the 1000 Wm^{-2} range - the stream power which according to Williams (1983) will move boulders of 1.5 m in diameter (Appendix G, Tables 1 to 29). It is argued that these floods perform two main tasks: first, they maintain the macro-channel and second, they generate sufficient stream power to mobilise the entire bed, thus 'resetting' the system. It may therefore be useful to begin to think in terms of two sets of effective discharge. For the majority of the time there are a set of discharges contained within the active channel banks (i.e. below the bankfull stage). These effective discharges (5-0.1% on the flow duration curve which occur on average 18 to 0.4 days a year) appear to account for the bulk of the bed material transported over a long period of time. It is likely that the 'bench-full' discharge and the bankfull discharge are the features related to these flows. A second category of high magnitude low frequency effective discharges termed 'reset discharges' are also significant as they 'reset' the system. The terraces in the macro-channel are probably related to these larger flood events which appear to occur on average once every 20 years or so. It is likely that the nested channel architecture is a response to these two categories of effective discharge.

These results compare well with results from other countries. Pickup & Warner (1976) for example working on the Cumberland basin in New South Wales, Australia, found that the effective discharge occurred on average between 1.15 years and 1.45 years on the annual series, while the estimated bankfull discharge stage had a return period between 4 to 7 years. Andrews (1980) has shown that for the Yampa River basin in the United States, the average effective discharge occurred between 1.5 and 11 days per year. Pitlick & Van Steeter (1998), also working in the United States on the upper Colorado River, found that the effective discharge was equalled or exceeded for 2% of the time, or approximately 7 days a year. The effective discharge transported approximately 30% of the annual load, while 80% of the total load was transported by the highest 10% of the flows. Similar results have been reported by Ashmore & Day (1988) and Nash (1994).

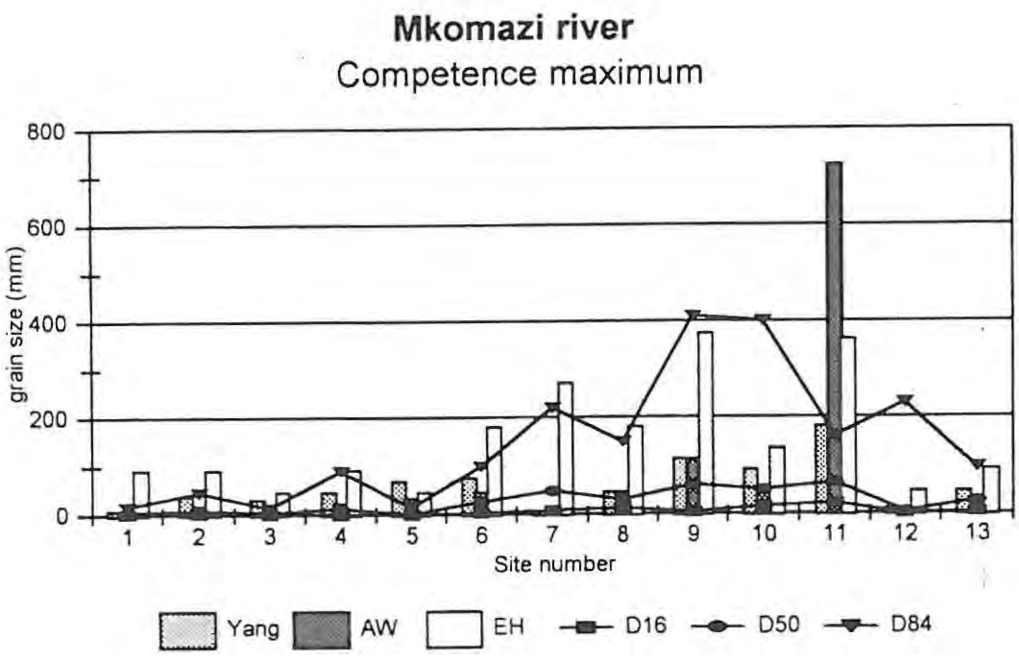

Figure 9.7: Maximum competence of the highest flow class for the Mkomazi River in relation to the particle size distribution at each site.

9.3.4 Research question 4: Is there any relationship between estimated bankfull discharge, dominant discharge and effective discharge?

There appears to be no agreement between the bankfull discharge and the dominant and effective discharge (Table 9.5). These findings were further checked by regressing the average estimated bankfull discharge and the average dominant and effective discharge. R-squared values of 0.01 and 0.10 respectively were computed. However, there is coarse agreement between the average 'bench-full discharge' and the average dominant and effective discharge (Figure 9.8). Statistically, however, there is no relationship between the bench-full discharge and the dominant and effective discharge for the Ackers & White and Engelund & Hansen equations (Table 9.7), but there is for the Yang equation (R-squared of 0.73 and 0.82 for the dominant discharge and effective discharge respectively). If the average 'bench-full' discharge is regressed against the average dominant discharge, an R-squared value of 0.58 is calculated. This is insignificant at the 95% level. Similarly, if the average 'bench-full' discharge is regressed against the average effective discharge an R-squared value of 0.54 is computed, this is also insignificant at the 95% level. Despite this statistical insignificance, Figure 9.8 demonstrates that there is coarse agreement between mean 'bench-full discharge', dominant discharge and effective discharge.

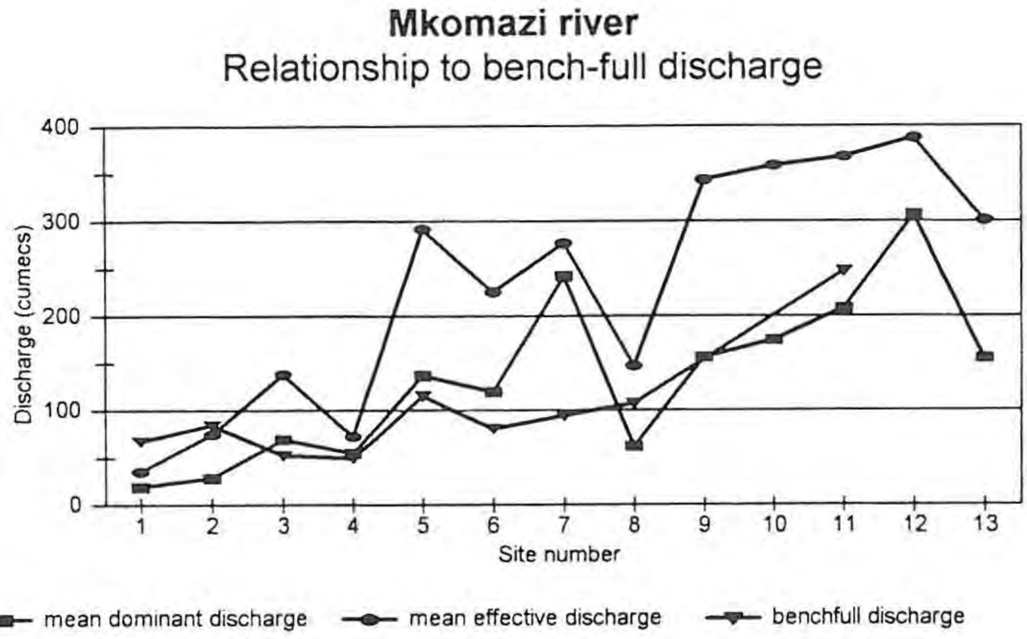

Figure 9.8: Relationship between 'bench-full' discharge and dominant and effective discharge for the Mkomazi River.

9.4 Synthesis

The results have been discussed in terms of the research qúestions set out at the beginning of the chapter. It has been argued that there is no significant downstream trend in estimated bankfull discharge. It was pointed out earlier that there are three possible explanations for this trend (see Section 9.3.1). It is argued that the strong bed rock control and variable hydrological regime suggests that it may be inappropriate to adopt the bankfull stage (defined as the boundary between the active channel and the macro-channel) as the effective discharge. It is likely that the morphology of the channel is related more to the resistance of the channel perimeter to erosion than to the shaping fluid. No relationship exists between the estimated bankfull discharge and the hydrological regime. However there does appear to be good agreement between the bench and the 0.9 and 2.0 year return period on the partial duration series.

The effective discharge as calculated by the three transport equations shows good internal consistency. The effective discharge is in the 5-0.1% range on the 1-day daily flow duration curve. It was also noted that the upper two but one flow classes account for the bulk (>80%) of the bed material transported in the Mkomazi. Although transport rates are high at the highest flow class (0.1-0.01%) this is more than offset by the limited duration, and consequently this flow class was never the effective discharge for any of the sites. It has also been demonstrated that the effective discharges do not have the energy to transport the entire bed. It is the larger floods, with average return periods of approximately 20 years that generate sufficient stream power and shear stress to mobilise the entire bed. It is argued that for the Mkomazi, it may be instructive to consider a range of effective discharges, first, the effective discharges that transport the most bed material over a long period of time and second, a 'reset discharge' that is able to mobilise the entire bed, thus serving as a channel forming discharge. These two sets of discharges are, in fact, the geomorphologically effective discharges for the Mkomazi River.

9.5 Sediment-maintenance flushing flows

This section of the chapter deals with the results obtained from the sediment-maintenance flushing flow computations. Milhous' approach for bed load and the β index were applied to the thirteen sites of the Mkomazi River. The results are provided in Appendix H at the back of the thesis. Table 9.10 presents a summary of the results. The table was constructed so that the β value and the d_{maxbl} and d_{max50} were compared to the equivalent result obtained for the three transport equations. For example, at Site 1a, the β index was calculated for the flow class 0.246 m^3s^{-1} as being 0.0513 (Appendix H, Table 1). This is more than sufficient to flush sands as a 'surface flush' and a 'depth flush'. (The β index predicts surface flushing for sands where β is equal to 0.021 and depth flushing for sand where β is equal to 0.035). This was compared to the equivalent initiation of motion for the sand-sized class predicted by the three transport equations. For Site 1a, Yang predicts sand motion at 3.991m^3s^{-1}, Ackers & White at 13.467 m^3s^{-1} and Engelund & Hansen at 0.355 m^3s^{-1} (Appendix G, Table 1). Thus the table (Table 9.10) is constructed in such a way as to compare the initiation of motion of the sand-sized material for the three transport equations to the 'surface' and 'depth' flushing as predicted by the β index. Where β predicts surface and depth flushing at lower flow classes than the equivalent for the transport equations, the letter 'L' (lower) is shown. Where β predicts surface and depth flushing at higher flow classes than the equivalent for the transport equations, the letter 'H' (higher) is shown.

It can be seen that at all sites (Table 9.10), other than sites 10b and 11, the Milhous β value predicts 'surface flushing' and 'depth flushing' at discharges lower than the equivalent Yang equation for sand. Similarly, the β value predicts surface and depth flushing at discharges (other than at Site 10b) well below the equivalent values predicted by the Ackers & White equation. The same general conclusion applies to the β value when compared to the equivalent Engelund & Hansen equation. In this case the β value predicts surface and depth flushing at higher flows than the equivalent value for the Engelund & Hansen equation at a number of sites (6a, 6b, 7a, 7b, 9a, 9b, 10b, 11 and 13).

Table 9.10 also shows the relationship between the maximum competence predicted from the Milhous equations (d_{maxbl} and d_{max50}) and the maximum competence calculated for the Yang, Ackers & White and Engelund & Hansen equations. The same approach was adopted for the β index. The letter 'L' is shown where the d_{maxbl} and d_{max50} predict lower maximum competence than the equivalent for the transport equations. 'H' is shown where the d_{maxbl} and d_{max50} predict higher maximum competence than the equivalent for the transport equations. It can be seen that for sites 1 to 5, 7, 10 and 12 the d_{maxbl} predicts considerably higher competence than the Yang and Ackers & White equation. However, at sites 6, 8, 9, 11 and 13, the Milhous equations predict lower competence maxima than the Yang and Ackers & White equations. The Engelund & Hansen equation on the other hand predicts higher competence than the Milhous equations at sites 2a, 2b, 2c, 4a, 4b, 6a, 6b, 6c, 7a, 7b, 8a, 8b, 9a, 9b, 11 and 12 and lower competence at sites 1a, 1b, 1c, 3a, 3b, 3c, 5a, 5b, 10a, 10b and 12.

The comparison of the competence of the d_{max50} and the maximum competence calculated from the three transport equations (Table 9.10) indicate that the d_{max50} predicts both higher and lower competence values, even at one site. At Site 1, for example (Table 9.10), d_{max50} predicts higher competence at cross-sections a and c and lower competence at cross-section b for the Yang equation. This trend is reflected at all of the sites for the d_{max50} for all the equations. There appears to be no consistency in the results obtained. This highlights one of the problems in determining sediment-maintenance flushing flows from equations that were developed for one river (Oak Creek in this case) and extrapolating them to other rivers. It is impossible to test which of the results are more accurate, as there is no actual bed material transport data for the Mkomazi against which to test these results. It is argued therefore that Milhous equations should be used with extreme caution.

Table 9.10: Comparison of the Milhous approach to the transport equations approach for the Mkomazi River.

Site	β			d_{maxhi}			d_{max50}		
	[1]Y	[1]AW	[1]EH	[2]Y	[2]AW	[2]EH	[2]Y	[2]AW	[2]EH
1a	L	L	L	H	H	H	H	H	L
1b	L	L	L	H	H	H	L	L	L
1c	L	L	L	H	H	H	H	L	H
2a	L	L	L	H	H	L	L	L	L
2b	L	L	L	H	H	L	L	L	L
2c	L	L	L	H	H	L	H	L	L
3a	L	L	L	H	H	H	H	H	L
3b	L	L	L	H	H	H	L	L	L
3c	L	L	L	H	H	H	H	H	L
4a	L	L	L	H	H	L	L	L	L
4b	L	L	L	H	H	L	L	L	L
5a	L	L	L	H	H	H	H	H	H
5b	L	L	L	H	H	H	H	H	H
6a	L	L	H	L	L	L	H	H	H
6b	L	L	H	L	L	L	L	L	L
6c	L	L	L	L	L	L	L	L	L
7a	L	L	H	H	H	L	L	H	L
7b	L	L	H	H	H	L	L	H	L
8a	L	L	L	L	L	L	L	L	L
8b	L	L	L	L	L	L	L	L	L
9a	L	L	H	L	L	L	L	L	L
9b	L	L	H	L	L	L	L	L	L
10a	L	L	L	H	H	H	L	H	L
10b	H	H	H	H	H	H	L	L	L
11	H	L	H	L	L	L	L	L	L
12	L	L	L	H	H	H	H	H	H
13	L	L	H	L	L	L	L	L	L

1 L = β predicts surface flushing and depth flushing at lower flows than the equivalent for the transport equations, where Y is Yang, AW is Ackers & White and EH is Engelund & Hansen equations.

H = β predicts surface flushing and depth flushing at higher flows than the equivalent for the transport equations.

2 L = d_{maxhi} and d_{max50} predict lower maximum competence than the equivalent for the transport equations.

H = d_{maxhi} and d_{max50} predict higher maximum competence than the equivalent for the transport equations.

Figure 9.9 shows the RBS values obtained for the Mkomazi River. The y-axis of the graph is the critical percentile on the 1-day daily flow duration curve where the D_{16} and D_{84} become mobile so that the bed can be considered to be unstable for that bed material size class (RBS). Similarly, the y-axis represents the critical percentage time equalled or exceeded on the 1-day daily flow duration curve where 'surface' (0.021 Milhous) and 'depth' (0.035 Milhous) flushing occurs. As can be seen, sites 1 to 5 of the Mkomazi are computed as becoming unstable at low flow classes, ranging from the 10th to 50th percentile with an average of around the 30th percentile. However, sites 6 to 13 show a different value. The RBS estimate is that the bed will become unstable at much higher flow classes, ranging from the 20th to the 99.99th percentile with an average of around the 85th percentile. These values are in excess of the β values calculated for Milhous. It is difficult to assess the accuracy of the RBS value without data against which to compare it. This again, stresses the need for caution in using methods that have not been thoroughly tested on a wide range of rivers, or have not been developed using a broad, comprehensive data set.

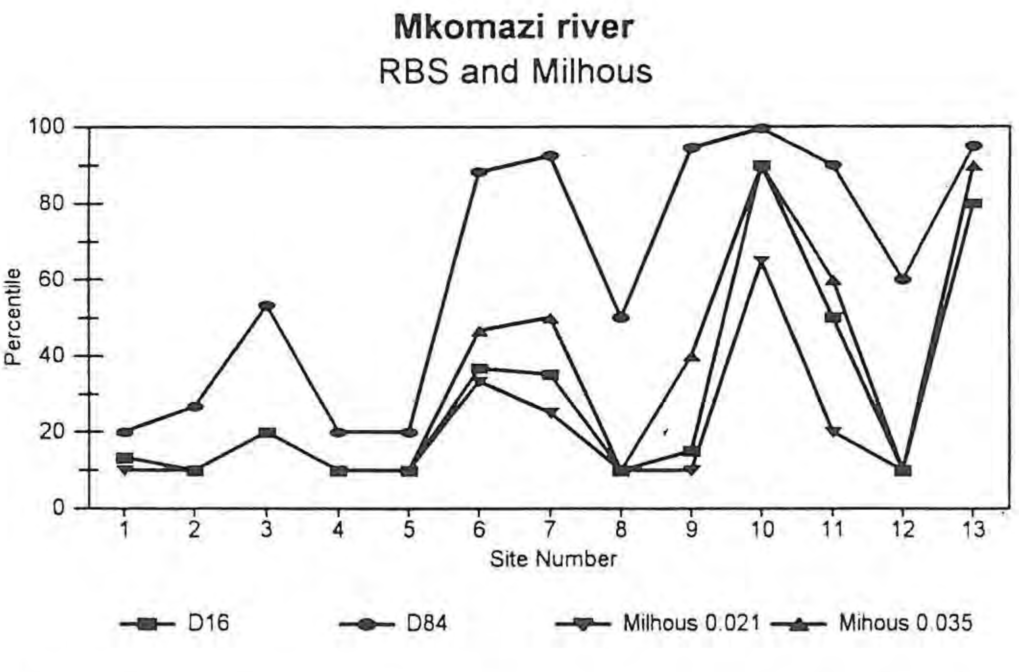

Figure 9.9: RBS values for the Mkomazi River. The β value is calculated for the 0.021 (surface) and 0.035 (depth) flushing flows. These values represent the flow class at which the β value is 0.021 and 0.035 respectively.

9.5.1 Effective discharge for sand, gravel and cobble

Using the method in outlined in Section 9.3.3., the effective discharge for sand, gravel and cobbles was calculated utilising the Yang equation, as this equation appeared to produce the most realistic results for the Mkomazi river. Figure 9.10 presents the summary data. It can been seen from this figure that although some variation exists, the effective discharge for the sand fraction generates a lower percentage of bed material transport than for the gravel- and cobble-fraction. This suggests that sand is being transported at a wider range of flow classes than gravel and cobble. This, however, is to be expected.

Table 9.11 displays the effective discharge flow classes for the sand, gravel and cobble fractions of the bed for the Yang equation. It can be seen that the effective discharge for the sand-sized fraction is mainly in the 5-1% class (18 out of 27 cross-sections), with the rest (9 out of 27 cross-sections) in the 1-0.1% flow class. The effective discharge for the gravel fraction is mainly in the 1-0.1% flow class (13 out of 27 cross-sections), followed by the 5-1% flow class (12 out of 27 cross-sections) and the 0.1-0.01% flow class (2 out of 27 cross-sections). For the cobble fraction, the effective discharge is mainly the 0.1-0.01% flow class (5 out of 8 cross-sections) followed by the 1-0.1% flow class (3 out of 8 cross-sections). As mentioned earlier, this demonstrates that a greater proportion of the sand-fraction of the bed is transported at low discharges than the gravel- and cobble-fraction of the bed. It is suggested that using this method may provide a more realistic estimate of the sediment-maintenance flushing flow requirement for the different grain-sized fractions, as the duration dimension is also incorporated.

Table 9.11: Effective discharge flow classes for the Mkomazi River for sand, gravel and cobble for the Yang equation.

Site	Sand (flow class)	Gravel (flow class)	Cobble (flow class)
1a	1-0.1%	1-0.1%	-
1b	1-0.1%	1-0.1%	-
1c	1-0.1%	0.1-0.01%	-
2a	5-1%	1-0.1%	-
2b	5-1%	1-0.1%	-
2c	1-0.1%	1-0.1%	-
3a	1-0.1%	1-0.1%	-
3b	5-1%	1-0.1%	-
3c	1-0.1%	1-0.1%	-
4a	5-1%	5-1%	-
4b	5-1%	5-1%	-
5a	1-0.1%	5-1%	-
5b	1-0.1%	1-0.1%	-
6a	5-1%	1-0.1%	-
6b	5-1%	5-1%	0.1-0.01%
6c	5-1%	5-1%	0.1-0.01%
7a	5-1%	5-1%	-
7b	5-1%	1-0.1%	0.1-0.01%
8a	5-1%	5-1%	-
8b	5-1%	5-1%	-
9a	5-1%	5-1%	1-0.1%
9b	5-1%	5-1%	1-0.1%
10a	5-1%	5-1%	0.1-0.01%
10b	5-1%	1-0.1%	0.1-0.01%
11	1-0.1%	1-0.1%	1-0.1%
12	5-1%	0.1-0.01%	-
13	5-1%	5-1%	-

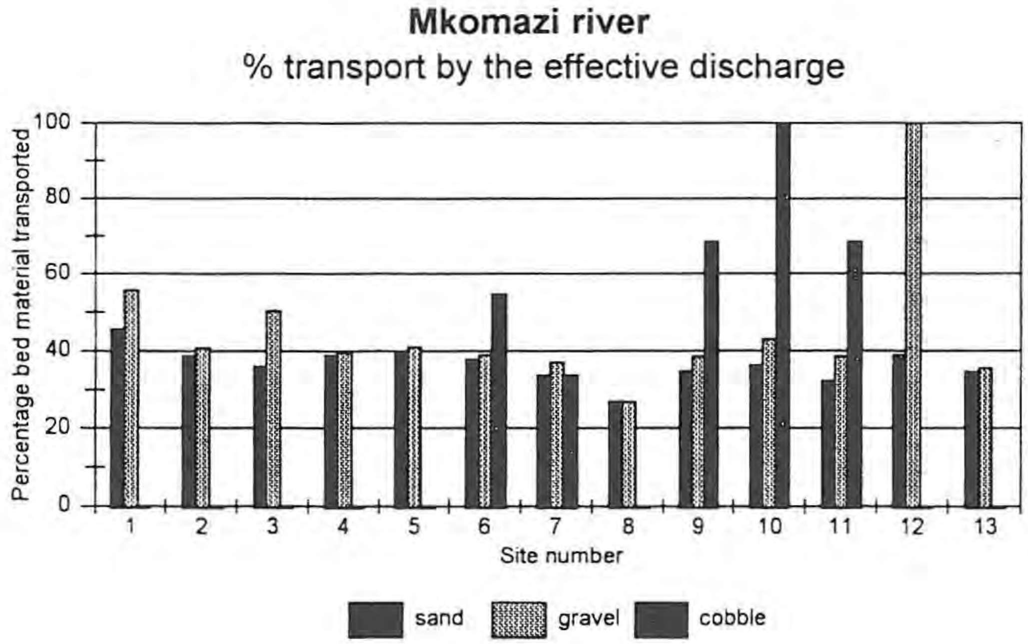

Figure 9.10: The effective discharge for sand, gravel and cobble using the Yang equation for the Mkomazi River.

9.6 Summary

The results from the sediment-maintenance flushing flow analysis indicate that the Milhous approach tends to predict incipient motion for sand at discharges well below the values predicted by the Yang and Ackers & White transport models. However, the values are similar to the levels predicted by the Engelund & Hansen model. This is probably because both the Engelund & Hansen model and the Milhous approach are based on a simple exponential stream power approach. The RBS method needs to be used with a degree of circumspection, as the approach is based on critical shear stress which has been shown to be inappropriate for coarse-bedded material (Yang, 1972). It is argued that both the Milhous and RBS methods should be used with caution. The methods were either developed from one data set (Oak Creek for Milhous) or are an amalgamation of existing equations (RBS approach). It is argued that using the effective discharge for different grain-sized classes may be a more appropriate way in which to define sediment-maintenance flushing flows. Although these models are imperfect, they are based on a broader data set, and can be chosen to satisfy the physical conditions of the channel.

9.7 Conclusions

The results suggest that the Mkomazi River does not conform to conventional wisdom developed for temperate alluvial rivers. It appears that the Mkomazi is strongly controlled by local conditions such as bed rock, a variable hydrological regime and a coarse heterogenous bed. There does not appear to be any relationship between the estimated bankfull discharge and the hydrological regime. However, there does appear to be some agreement between the 0.9 and 2.0 year return period on the partial duration series and the 'bench-full discharge'.

It has been argued that it is instructive to consider the magnitude-frequency debate in the Mkomazi River in terms of two sets of 'effective discharges'. First, an effective discharge that transports the most bed material over a long period of time - this has been shown to be in the 5-0.1% range on the 1-day daily flow duration curve, and second, a 'reset discharge' - a flood event with a return period in the range of 20 years that has the energy to mobilise the entire bed and therefore to maintain the channel.

It is suggested that the channel architecture of the Mkomazi is a response to these two sets of effective discharges. The active channel is controlled by the lower set of effective discharges, while the macro-channel and overall channel form is a response to the 'reset' discharge. It is argued that these two sets of effective discharges do not operate independently of each other, rather the effective discharge sets the template for the effectiveness of the 'reset' discharge.

Chapter 10: Results and Discussion - the Mhlathuze and Olifants Rivers

10.1 Introduction

This chapter will present the methods and results obtained for the bed material transport analysis and the sediment-maintenance flushing flow computations for the Mhlathuze and Olifants Rivers. Given the fact that these two rivers are both highly regulated and therefore disturbed, it is unlikely that any meaningful relationships can be developed between channel form, flow frequency and bed material transport. For this reason, the discussion will focus on answering a number of questions. These are:

1. *Do the results obtained from the two regulated systems add to the understanding gained from the Mkomazi River?*

2. *What is the impact of flow regulation on the relationships? Are the observed morphological conditions related to virgin flow conditions or to the regulated present-day conditions?*

3. *What lessons can be learnt for Instream Flow Requirement (IFR) assessments?*

4. *Given the results obtained, what flows should be recommended and why?*

In the context of these broad research questions, the chapter is divided into two sections, the first section considers the Mhlathuze River and the second section considers the Olifants River. The values calculated for the bed material transport analysis are available in Appendix F. Summary tables of all the results are presented in Appendix G. Summary tables for the sediment-maintenance flushing flows are available in Appendix H.

10.2 The Mhlathuze River

10.2.1 Overview

An overview of the Mhlathuze catchment has been presented in Chapter 5. A short summary is provided here. The Mhlathuze River drains an area of approximately 4209 km^2 in northern KwaZulu-Natal. Four sites were chosen for analysis for the Mhlathuze, all downstream of the Goedertrouw Dam. Site 1 is approximately 25 kilometres downstream of the Dam, while Site 2 is a further 35 kilometres downstream of Site 1. Between Site 1 and Site 2 a major tributary, the Mfule, joins the Mhlathuze. Site 2 is 35 kilometres downstream of Site 3. Site 4 (an artificial channel) is a further 15 kilometres downstream of Site 3. Between Site 3 and Site 4 a major tributary, the Nseleni joins the Mhlathuze. The lower three sites (i.e. sites 2, 3 and 4) are all single thread sand-bed regime channels, while Site 1 is a pool-riffle channel type with multiple distributaries.

The Mhlathuze is impounded by the Goedertrouw Dam which was completed in 1979. This has had a significant impact on the downstream hydrology of the river (Table 10.1). The MAR at Site 1 has been reduced from $185x10^6m^{-3}$ virgin flow to the present-day scenario of $64x10^6m^{-3}$. This represents only 34.8% of the virgin MAR at Site 1. Flow recovers downstream as tributary inputs mitigate the impact of the dam. At Site 4, for example, the virgin MAR was $362x10^6m^{-3}$ while the present day MAR is $217x10^6m^{-3}$, this represents 60.9% of the virgin MAR. It can also be seen from Table 10.1 that under virgin flow conditions, the ratio of increase of MAR between the sites was considerably less than it is for the present-day. The virgin MAR nearly doubled between Site 1 and Site 4 (1.96), while for the present-day, the rate of increase is by a factor of 3.39. This has significant implications for the channel morphology and bed material transport and will be discussed in greater detail later in the chapter.

As mentioned previously, characteristic of the Mhlathuze catchment and northern KwaZulu-Natal generally, is the passage of tropical cyclones and cut-off low pressure systems through the region. Table 6.5 in Chapter 6 displays the highest flood peaks on record for the Mhlathuze River. The values calculated for the 1984 and 1987 floods (below Goedertrouw Dam) are 2420 m^3s^{-1} and 3590 m^3s^{-1} respectively. Van Bladeren (1992) estimated that were it not for the Goedertrouw Dam, these floods would have been 4790 m^3s^{-1} and 6000 m^3s^{-1} respectively. The Goedertrouw has therefore not only reduced the MAR downstream, but it has also attenuated the flood peaks.

Table 10.1: MAR for four sites for the Mhlathuze River (million cubic metres).

Site number	Virgin MAR	Increase ratio	Present-day MAR	Increase ratio	% of Virgin MAR
1	185		64		34.8
2	255	1.38	127	1.98	49.8
3	313	1.69	176	2.75	56.2
4	362	1.96	217	3.39	60.9

The methods that were used to obtain the daily flow time series for the virgin and present-day data for the Mhlathuze were presented in Chapters 6 and 8. Tables 10.2 and 10.3 present the flow classes calculated for the Mhlathuze River for the virgin and present-day data.

Table 10.2: Flow classes calculated for the Mhlathuze River for the virgin data. Values are in m^3s^{-1}.

% time equalled or exceeded	Q	Geometric mean flow class	Q	Geometric mean flow class	Q	Geometric mean flow class	Q	Geometric mean flow class
	Site 1		Site 2		Site 3		Site 4	
99.99	0		0		0		0	
90	0.371	0	0.488	0	0.716	0	1.190	0
80	0.690	0.506	0.883	0.656	1.212	0.932	1.917	1.510
70	1.061	0.856	1.401	1.112	1.833	1.491	2.700	2.275
60	1.543	1.280	2.115	1.721	2.666	2.211	3.684	3.154
50	2.070	1.787	2.882	2.469	3.592	3.095	4.790	4.201
40	2.781	2.399	3.876	3.342	4.708	4.112	6.028	5.373
30	3.817	3.258	5.273	4.521	6.250	5.424	7.715	6.820
20	5.575	4.613	7.657	6.354	8.950	7.479	10.758	9.110
10	10.371	7.604	14.067	10.378	16.729	12.236	18.665	14.170
5	17.354	13.416	22.795	17.907	27.311	21.375	29.973	23.653
1	51.662	29.942	64.646	38.388	86.701	48.661	93.994	53.078
0.1	408.492	145.270	594.222	195.995	695.125	245.495	737.033	263.205
0.01	2472.70	1020.30	3466.99	1435.327	4337.55	1736.416	4642.44	1849.76

Table 10.3: Flow classes calculated for the Mhlathuze River for the present-day data. Values are in m^3s^{-1}.

% time equalled or exceeded	Q	Geometric mean flow class	Q	Geometric mean flow class	Q	Geometric mean flow class	Q	Geometric mean flow class
	Site 1		Site 2		Site 3		Site 4	
99.99	0		0		0		0	
90	0.279	0	0.306	0	0.369	0	0.537	0
80	0.346	0.311	0.407	0.353	0.498	0.429	0.803	0.657
70	0.405	0.374	0.508	0.455	0.640	0.565	1.178	0.973
60	0.477	0.440	0.720	0.605	0.934	0.773	1.644	1.392
50	0.556	0.515	0.960	0.831	1.268	1.088	2.126	1.870
40	0.641	0.597	1.294	1.115	1.718	1.476	2.750	2.418
30	0.756	0.696	1.772	1.514	2.350	2.009	3.580	3.138
20	0.927	0.837	2.573	2.135	3.424	2.837	4.954	4.211
10	1.593	1.215	4.821	3.522	6.963	4.883	9.055	6.698
5	4.214	2.591	9.521	6.775	15.325	10.330	17.973	12.757
1	23.950	10.046	42.711	20.166	61.555	30.714	68.765	35.156
0.1	200.832	69.354	438.769	136.895	552.808	184.467	596.202	202.479
0.01	1763.52	595.123	2729.08	1094.27	3598.66	1410.45	3929.17	1530.55

10.2.2 Analysis of channel morphology

The field methods that were used to classify the morphological features for the Mkomazi River were applied to the Mhlathuze River. It is argued that it is likely that the channel morphology will have adjusted to the imposed change in flow regime. For this reason, the field classification was subject to further analysis. This was achieved through the following method. The inundation frequencies for the different morphological features were tabulated. Inundation frequencies were then used to correlate features between sites. It is important to note that this was done for the terraces only. The adjusted discharge values were then used to explore other relationships. Tables 10.4 to 10.8 display these data.

Table 10.4: Discharge data for the Mhlathuze River. Values are in m^3s^{-1}.

Site	1 pool	1 riffle	2	3	4	Average
Virgin MAR	185	185	255	313	362	
Present-day MAR	64	64	127	176	217	
Virgin flow						
$Q_{1.5}$	40	40	47	88	90	66
$Q_{2.33}$	105	105	118	168	178	142
$Q_{p\ 0.9}$	130	130	190	244	257	205
$Q_{p\ 2.0}$	244	244	417	542	593	449
Present-day flow						
$Q_{1.5}$	13	13	20	50	68	38
$Q_{2.33}$	32	32	52	105	142	83
$Q_{p\ 0.9}$	68	68	139	181	210	149
$Q_{p\ 0.9}$	153	153	269	377	464	316
Morphological flows						
bench	27		36		77	47
Estimated Q_b	116	64	196	149	234	152
terrace 1		332	568	531	1380	
terrace 2		1061	1007	1768		
Dominant discharge						
Virgin flow						
Yang	39	16	108	130	52	
Ackers & White	62	18	105	153	100	
Engelund & Hansen	47	29	246	185	106	
Present-day flow						
Yang	52	8	146	154	104	
Ackers & White	70	7	137	124	122	
Engelund & Hansen	45	28	305	229	131	

Effective discharge					
Virgin flow					
Yang	1020	145	1435	1736	1850
Ackers & White	1020	145	1435	245	1850
Engelund & Hansen	1020	145	1435	1736	1850
Present-day flow					
Yang	595	10	1094	1410	1531
Ackers & White	595	10	1094	184	1531
Engelund & Hansen	595	69	1094	1410	1531

Table 10.5: Inundation frequencies and discharges for different morphological features for the virgin annual series data for the Mhlathuze River.

Site	Bench return period	Discharge m^3s^{-1}	Estimated Q_b return period	Discharge m^3s^{-1}	Terrace 1 return period	Discharge m^3s^{-1}	Terrace 2 return period	Discharge m^3s^{-1}
1 pool	1.3	27	2.5	116				
1 riffle			1.8	64	6.8	332	16	1061
2	1.3	36	3.4	196	7.5	568	12	1006
3			2.3	149	4.9	531	16	1768
4	1.4	77	3	234			13	1380
Average	1.3		2.6		6.4		14	

Table 10.6: Inundation frequencies for different morphological features for the present-day annual series data for the Mhlathuze River.

Site	Bench return period	Discharge m^3s^{-1}	Estimated Q_b return period	Discharge m^3s^{-1}	Terrace 1 return period	Discharge m^3s^{-1}	Terrace 2 return period	Discharge m^3s^{-1}
1 pool	2.2	27	4.3	116				
1 riffle			3.5	64	10	332	26	1061
2	2.3	36	4.2	196	9	568	21	1007
3			2.6	149	9.5	531	30	1768
4	1.8	77	3.8	234			19	1380
Average	2.1		3.7		9.5		24	

Table 10.7: Inundation frequencies for different morphological features for the virgin partial series data for the Mhlathuze River.

Site	Bench return period	Discharge m^3s^{-1}	Estimated Q_b return period	Discharge m^3s^{-1}	Terrace 1 return period	Discharge m^3s^{-1}	Terrace 2 return period	Discharge m^3s^{-1}
1 pool	0.1	27	0.8	116				
1 riffle			0.4	64	2.6	332	11	1061
2	0.1	36	0.9	196	2.6	568	7.5	1007
3			0.6	149	1.9	531	11	1768
4	0.3	77	0.8	234			6.7	1380
Average	0.2		0.7		2.4		9.1	

Table 10.8: Inundation frequencies for different morphological features for the present-day partial series data for the Mhlathuze River.

Site	Bench return period	Discharge m^3s^{-1}	Estimated Q_b return period	Discharge m^3s^{-1}	Terrace 1 return period	Discharge m^3s^{-1}	Terrace 2 return period	Discharge m^3s^{-1}
1 pool	0.3	27	1.5	116				
1 riffle			0.9	64	7.5	332	17	1061
2	0.3	36	1.2	196	4.9	568	15	1007
3			0.8	149	2.6	531	16	1768
4	0.4	77	1	234			15	1380
Average	0.3		1.1		5		16	

10.2.2.1 Virgin conditions

Given the fact that there were only four sites selected for analysis for the Mhlathuze River, no statistical analyses (R-squared values) could be reliably applied to the data. The data is thus discussed in relation to general trends displayed.

The estimated bankfull discharges for four sites on the Mhlathuze, range from 64 m^3s^{-1} (Site 1) to 234 m^3s^{-1} (Site 4) (Table 10.4). The flood frequency analysis indicates that the bankfull stage ranges from a 1.8 year to a 3.4 year return period on the annual series, with an average of 2.6 years (Table 10.5). The partial series ranges from 0.4 years to 0.9 years with an average return period of 0.7 years (Table 10.7). These values are outside the range estimated for alluvial channels in temperate climes (Leopold, 1997), but they are close.

The bench has an average annual return period of 1.3 years on the annual series and 0.2 years on the partial series (Table 10.5 and Table 10.7). This is in good agreement with the 1.5 year return period predicted for the bankfull event by Leopold (1997). It is possible that the bench is in fact what Leopold refers to as the bankfull stage. This will be discussed later in the chapter.

Terrace 1 has an average return period on the annual series of 6.4 years and 2.4 years on the partial series, while Terrace 2 has an average return period of 14 years on the annual series and 9.1 years on the partial series (Table 10.5 and Table 10.7). It is evident that under virgin flow conditions, these terraces were regularly inundated.

The value of the 1.5 year return flood on the annual series ranges from 40 m^3s^{-1} at Site 1 to 90 m^3s^{-1} at Site 4, with an average value for the four sites of 66 m^3s^{-1} (Table 10.4). This is considerably less than the average estimated bankfull discharge of 152 m^3s^{-1}, but is in the same range as the average estimated 'bench-full' discharge of 47 m^3s^{-1}(Table 10.4). The 2.44 year return period on the annual series ranges from 105 m^3s^{-1} at Site 1 to 178 m^3s^{-1} at Site 4, with an average value of 142 m^3s^{-1}, this is similar to the average estimated bankfull discharge of 152 m^3s^{-1} (Table 10.4). The average 0.9 year and 2.0 year return period on the partial series (205 m^3s^{-1} and 449 m^3s^{-1} respectively) is greater than the average estimated bankfull discharge (152 m^3s^{-1}) (Table 10.4).

Figure 10.1 displays the plot of the relationship between the inundation discharge and the Mean Annual Runoff (MAR) for the different morphological features for the virgin flow. The data shows that there is a clear increase in inundation discharge for each of the morphological features in the downstream direction. This would suggest that the Mhlathuze River is functioning as an alluvial system in the sense that it has the capacity to change its boundary in response to the observed discharge of water and sediment.

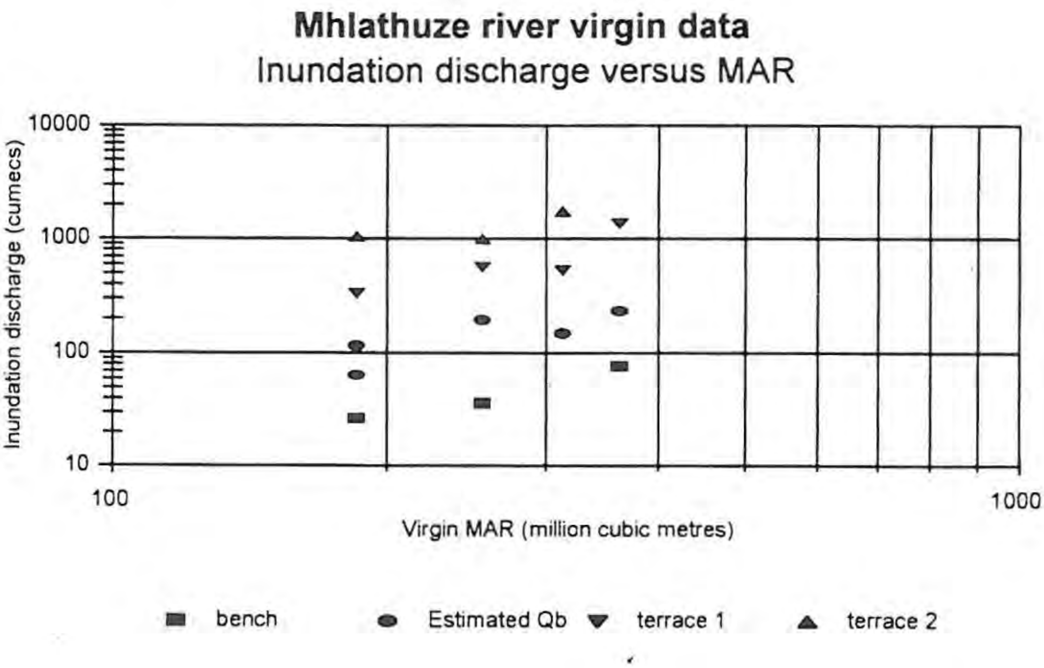

Figure 10.1: Inundation discharge versus Mean Annual Runoff for different morphological features for the virgin data for the Mhlathuze River.

10.2.2.2 Present-day conditions

The morphological features were identified in the field, and hence the stage at which each morphological feature (estimated bankfull discharge for example) becomes inundated will remain the same for virgin and present-day conditions (this assumes that the channel morphology has remained constant). What does change is the inundation return period. This can be seen from the data presented in Tables 10.4 to 10.8. For the annual series data, the average return periods have increased. The average 'bench-full' discharge return period changes from 1.3 years to 2.1 years, the average estimated bankfull discharge from 2.6 years to 3.7 years, Terrace 1 from 6.4 years to 9.5 years and terrace 2 from 14 years to 24 years (Tables 10.5 and 10.6). A similar trend is evident for the partial series.

It is instructive to note that under the present-day flow conditions, good agreement exists between the 1.5 year return period on the annual series and the average 'bench-full' return period. The average 1.5 year return period discharge for the four sites is 38 m^3s^{-1}, while the average 'bench-full' discharge for return period 1.5 years is 47 m^3s^{-1} (Table 10.4). The average estimated bankfull discharge for the four sites is 152 m^3s^{-1}, while the average 0.9 year return period on the partial series is 205 m^3s^{-1} (Table 10.4 and 10.6). This is also reflected in the average estimated bankfull discharge return period of the partial series which is 1.1 years (Table 10.8). Thus it would appear that general agreement exists between the present-day flow regime and the 'bench-full' discharge. Given the limitations of the data, this would suggest that the Mhlathuze below the Goedertrouw Dam has, to some extent, adjusted to the present-day regulated flow regime. However, it is important to point out that this adjustment is only possible because the Mhlathuze below the Goedertrouw Dam is an alluvial sand-bed channel and is free to alter its boundary. In a controlled or semi-controlled channel such as the Mkomazi, it is unlikely that such an adjustment could occur as rapidly as it has in the Mhlathuze River.

It has been demonstrated that considerable change has occurred in the hydrological regime since the construction of the Goedertrouw Dam. It was also noted earlier that under virgin flow conditions, the increase in MAR between sites 1 and 4 is by a factor of 1.96 (Table 10.1). Under present-day conditions, this increase is considerably greater (3.39). This situation reflects the impact of the Dam and the flow recovery due to two major tributary inputs downstream of Goedertrouw Dam, the Mfule and Nseleni. It is argued that the dam has trapped a significant portion of the bed load. Evidence at Site 1 from aerial photography analysis has confirmed that this, together with the flow reduction, has resulted in significant downstream narrowing and deepening of the channel with a concomitant encroachment of riparian vegetation (Dollar, 1998b). It is only when the Mfule joins the Mhlathuze between Site 1 and Site 2 that the channel recovers, not only in terms of flow, but also in terms of sediment load. Thus, there is considerable evidence to suggest that the regulated flow regime has had a noticeable impact on the channel morphology of the Mhlathuze River, particularly at Site 1. On the basis of conventional wisdom, it is possible to argue that this adjustment is an attempt by the river to alter its morphology in sympathy with the imposed regulated flow regime.

10.2.3 Dominant discharge

10.2.3.1 Virgin flow

The dominant discharge was computed using the Marlette & Walker (1968) equation. The dominant discharge as predicted by the different transport equations shows good consistency (Table 10.4). Figure 10.2 shows the plot of the relationship between dominant discharge and estimated bankfull discharge. The limited data set shows a reasonable relationship. However, due to the limited data set, this cannot be tested statistically.

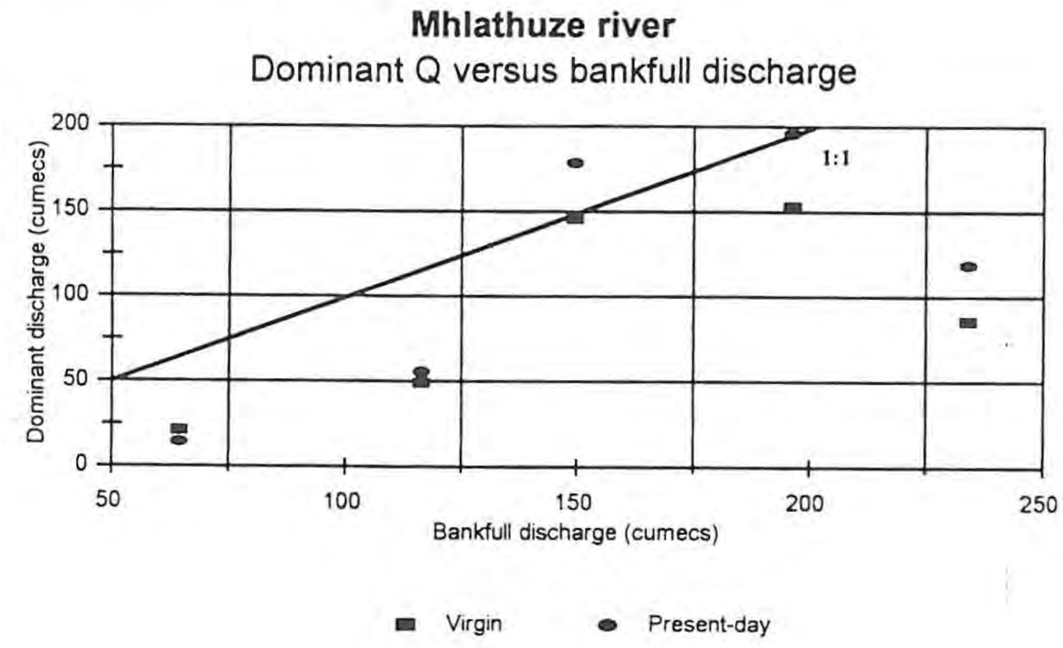

Figure 10.2: Dominant discharge versus bankfull discharge for virgin and present-day flow for the Mhlathuze River.

10.2.3.2 Present-day flow

The dominant discharge for the Mhlathuze increases (other than Site 1 riffle) under present-day flow conditions (Table 10.4). This does not imply that the load increases under present-day flow conditions, rather, it points to the fact that higher flows (classes) are necessary to transport the dominant discharge (i.e. the discharge that transports over 50% of the bed material load). The three transport equations predict a reduction in transport capacity (see Table 10.9) with the magnitude of reduction decreasing with distance from the impoundment. This is due to flow recovery from the input of discharge from downstream tributaries. This is also reflected in the MAR (Table 10.1).

Table 10.9: Bed material transport capacity for the Mhlathuze River for virgin and present-day flow conditions. Values are in tonnes per annum.

Site	Yang equation	Ackers & White equation	Engelund & Hansen equation
1 virgin pool	358 413.98	69 022.46	2 508 133.52
1 present-day pool	108 274.69	15 304.99	838 594.89
Reduction factor	*3.31*	*4.51*	*2.99*
1 virgin riffle	1 633 893.07	560 810.19	78 763 611.41
1 present-day riffle	395 246.16	102 732.94	20 145 380.49
Reduction factor	*4.13*	*5.45*	*3.91*
2 virgin	226 158.36	31 364.30	1 765 064.19
2 present-day	130 082.20	17 631.78	985 260.14
Reduction factor	*1.73*	*1.78*	*1.79*
3 virgin	131 497.28	44 935.26	242 999.47
3 present-day	85 222.71	28 725.44	158 773.38
Reduction factor	*1.54*	*1.56*	*1.53*
4 virgin	142 855.25	54 707.55	180 059.54
4 present-day	86 362.39	29 982.55	111 659.97
Reduction factor	*1.65*	*1.82*	*1.63*

The data in Table 10.9 shows that Site 1 riffle has a greater transport capacity than Site 1 pool. The reason is that the riffle has a greater energy gradient than the pool (although this equalises at higher flows), and thus the riffle generates greater unit stream power than the pool section (Appendix G, Tables 28 to 31). The three transport equations are based on stream power and, consequently, the predicted transport capacity at the riffle is greater than for the pool section. The transport equations predict that it is only at high discharge flow classes that the pools generate sufficient stream power to transport significant quantities of sediment.

Figures 10.3 and 10.4 display the relationship between mean dominant discharge and MAR for the virgin and present-day flow respectively. Also presented is the plotted relationship between mean stream power and mean dominant discharge for the virgin and present-day time series (Figures 10.5 and 10.6). These plots indicate no clear trend.

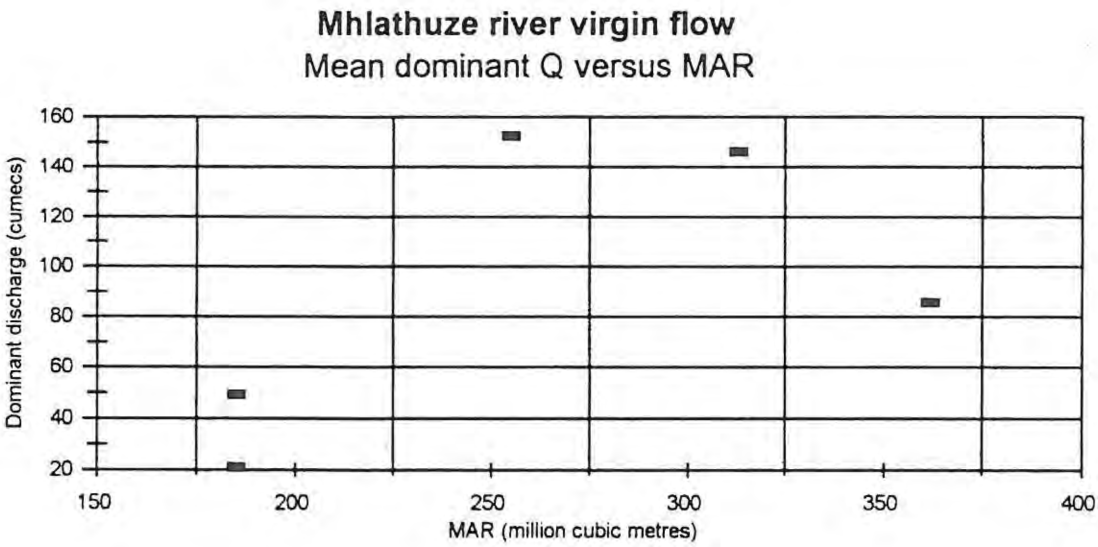

Figure 10.3: Mean dominant discharge versus MAR for the Mhlathuze River virgin flow.

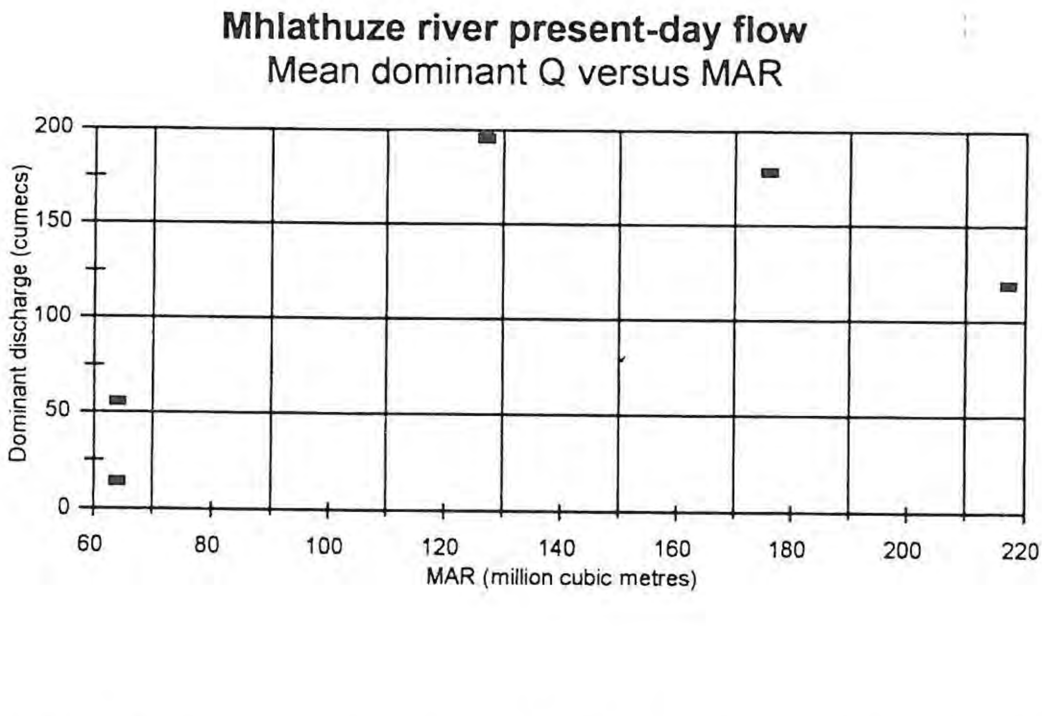

Figure 10.4: Mean dominant discharge versus MAR for the Mhlathuze River present-day flow.

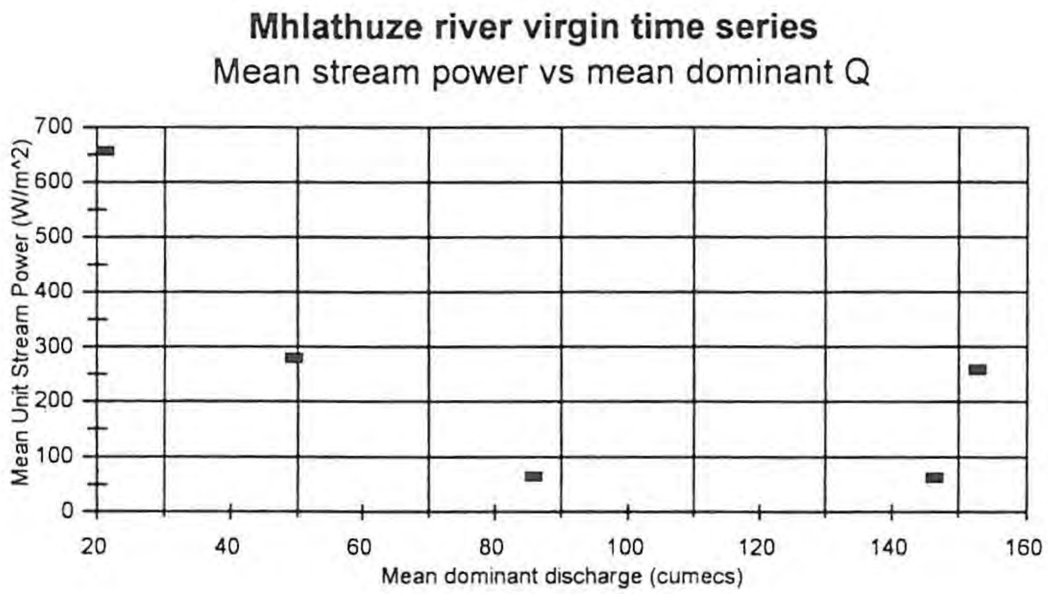

Figure 10.5: Mean stream power versus mean dominant discharge for the Mhlathuze River virgin flow.

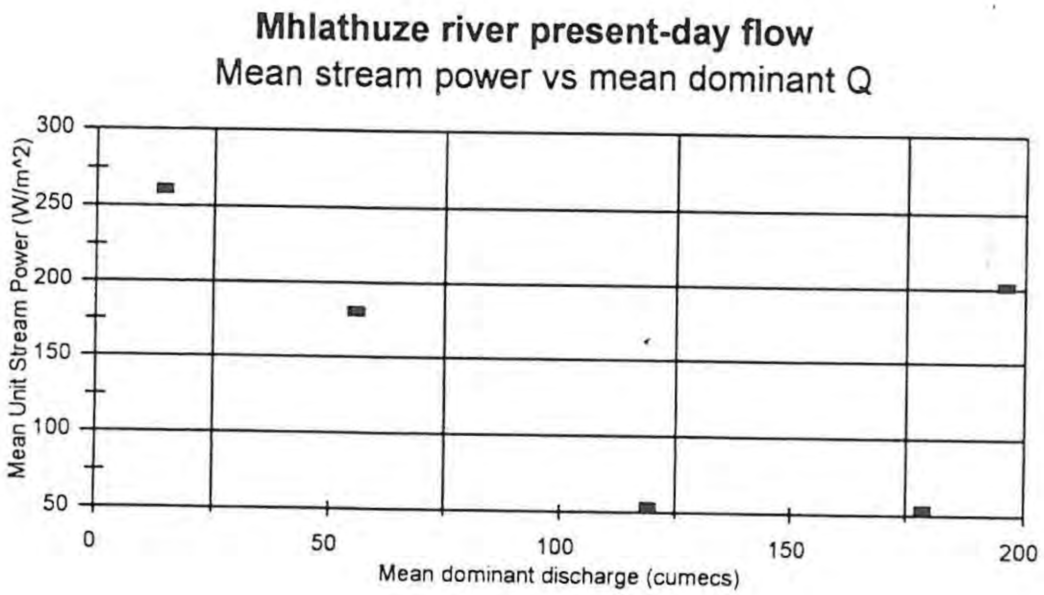

Figure 10.6: Mean stream power versus mean dominant discharge for the Mhlathuze River present-day flow.

10.2.4 Effective discharge

10.2.4.1 Virgin flow

The effective discharge is defined as the geometric mean of the flow class that transports the most bed material over a long period of time. It therefore represents a flow class between two exceedences. For the Mhlathuze River the time frame is 33 years of daily flow data. For the virgin flow record, all sites along the Mhlathuze were represented by an effective discharge that was equalled or exceeded between 1-0.01% (Table 10.10).

The effective discharge for all sites other than Site 1 riffle are in excess of the dominant discharge, the estimated bankfull discharge, or the $Q_{1.5}$, $Q_{2.44}$, $Q_{p0.9}$ and $Q_{p2.0}$ (Table 10.4). It should be noted that the two cyclones that impacted on the Mhlathuze in 1984 and 1987 (see Chapter 5) have skewed the flow duration curves and flood frequency curves, such that the highest flow class (0.01% equalled or exceeded) is almost seven times larger than the second highest flow class (0.1% equalled or exceeded)(Tables 10.2 and 10.3). The bi-polar flood frequency curve has resulted in the generation of extremely high values for the effective discharge.

Table 10.10: Effective discharge flow classes for the Mhlathuze River.

Site	Yang (flow class)	Ackers & White (flow class)	Engelund & Hansen (flow class)	Yang (flow class)	Ackers & White (flow class)	Engelund & Hansen (flow class)
	Virgin flow			Present-day flow		
1 pool	0.1-0.01%	0.1-0.01%	0.1-0.01%	0.1-0.01%	0.1-0.01%	0.1-0.01%
1 riffle	1-0.1%	1-0.1%	1-0.1%	5-1%	5-1%	1-0.1%
2	0.1-0.01%	0.1-0.01%	0.1-0.01%	0.1-0.01%	0.1-0.01%	0.1-0.01%
3	0.1-0.01%	1-0.1%	0.1-0.01%	0.1-0.01%	1-0.1%	0.1-0.01%
4	0.1-0.01%	0.1-0.01%	0.1-0.01%	0.1-0.01%	0.1-0.01%	0.1-0.01%

The upper three flow classes (5-1%; 1-0.1%; 0.1-0.01%) are the most significant in terms of effectiveness (Figure 10.7). It is only at Site 1 riffle, that the upper three flow classes do not account for more than 80% of the bed material transported (Figure 10.7). At Site 1 pool, and sites 2, 3 and 4, the effective discharge accounts for over 40% of the bed material moved (Figure 10.8). The effective discharge calculated for the Engelund & Hansen model is in excess of 58% for three sites (2, 3 and 4). This begs the question, how is the remaining bed material transported around the effective discharge?

Figures 10.9, 10.10 and 10.11 display the distribution of the cumulative sediment transport for the three transport equations. The Yang equation indicates that other than Site 1 riffle, the four sites along the Mhlathuze show similar shaped curves. It was noted in the previous paragraph that the bulk of the bed is transported by the upper three flow classes. For the Yang equation, less than 10% of the total bed material load is transported by flows less than the 20th percentile (Figure 10.9). However, the curve for Site 1 riffle displays a different shape, as the steeper slope and higher unit stream power at the riffle results in higher predicted transport capacities at lower discharges - hence the different shaped curve. A similar trend is displayed for the Ackers & White equation (Figure 10.10). The Engelund & Hansen equation predicts higher transport values at lower discharges, consequently the shape of the curves are slightly different (Figure 10.11). However, the Engelund & Hansen equation also predicts that over 90% of the bed material is carried by flows greater than the 20th percentile. It is evident that although the transport equations predict different transport volumes (Table 10.9), they all predict similar trends.

The data for the virgin flow indicates that for the Mhlathuze sand-bed sites, virgin flow conditions are more than sufficient to mobilise the entire bed (Figure 10.12). It should be noted that relative to the Mkomazi, the Mhlathuze sand-bed sites generate low unit stream power and shear stresses. This is a function of the low slope and the wide channel. For example, the unit stream power at the 0.1-0.01% flow class for sites 2, 3 and 4 is 260 Wm^{-2}, 86 Wm^{-2} and 65 Wm^{-2} respectively (Appendix G, Tables 32 to 37). At Site 1, the unit stream power is 280 Wm^{-2} at the pool section and 1073 Wm^{-2} at the riffle section (Appendix G, Tables 30 and 31). The higher values are the result of a narrower, deeper channel and a steeper slope. These low stream power values at sites 2, 3 and 4 preclude the transport of coarse material, even at high flows. However, as it is, there is no coarse material to transport.

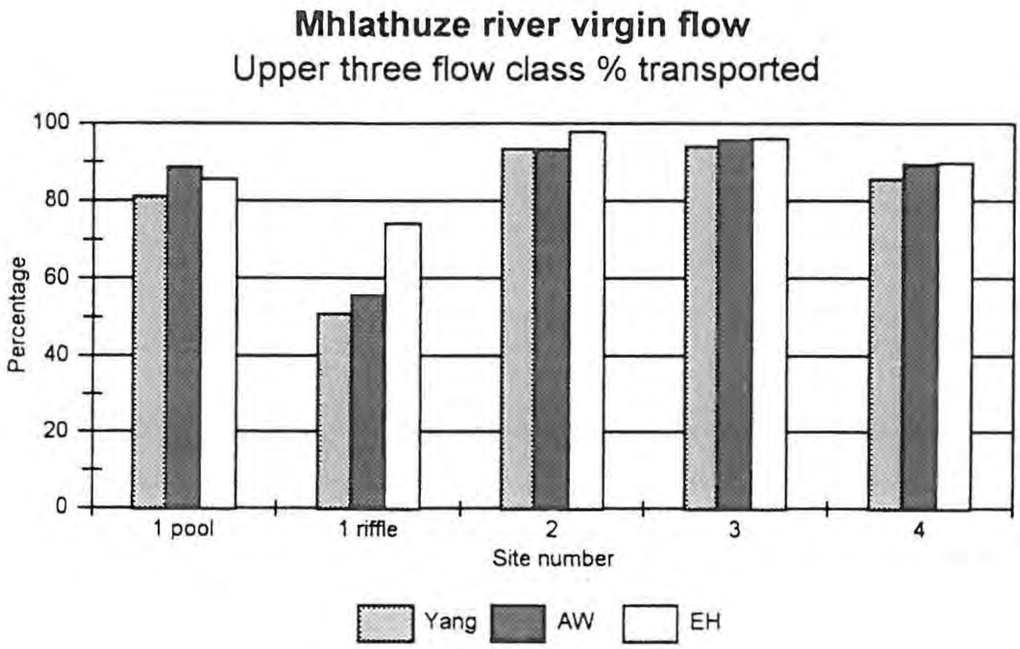

Figure 10.7: Effective discharge for the upper three flow classes (5-1%; 1-0.1% and 0.1-0.01%) for virgin flow for the Mhlathuze River.

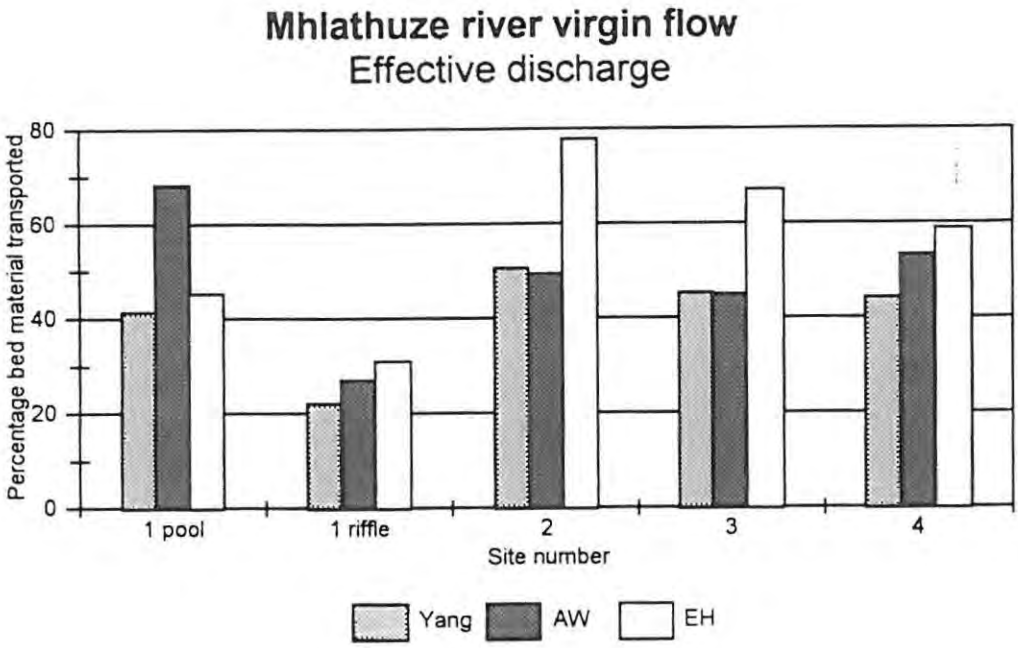

Figure 10.8: Effective discharge for virgin flow for the Mhlathuze River.

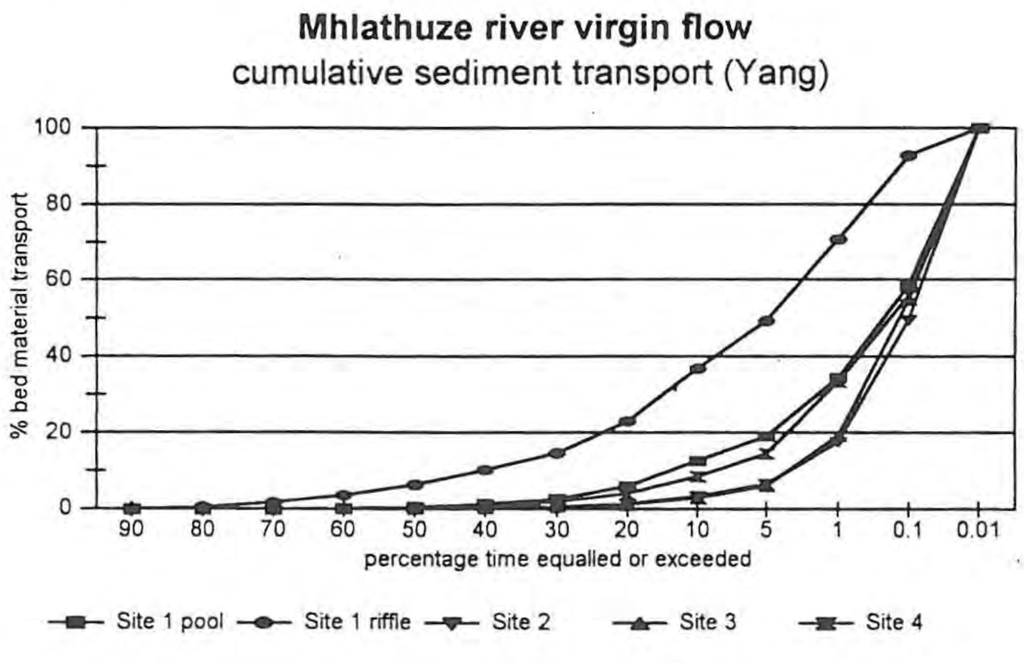

Figure 10.9: Cumulative sediment transport for the Yang equation for all sites for the virgin flow for the Mhlathuze River.

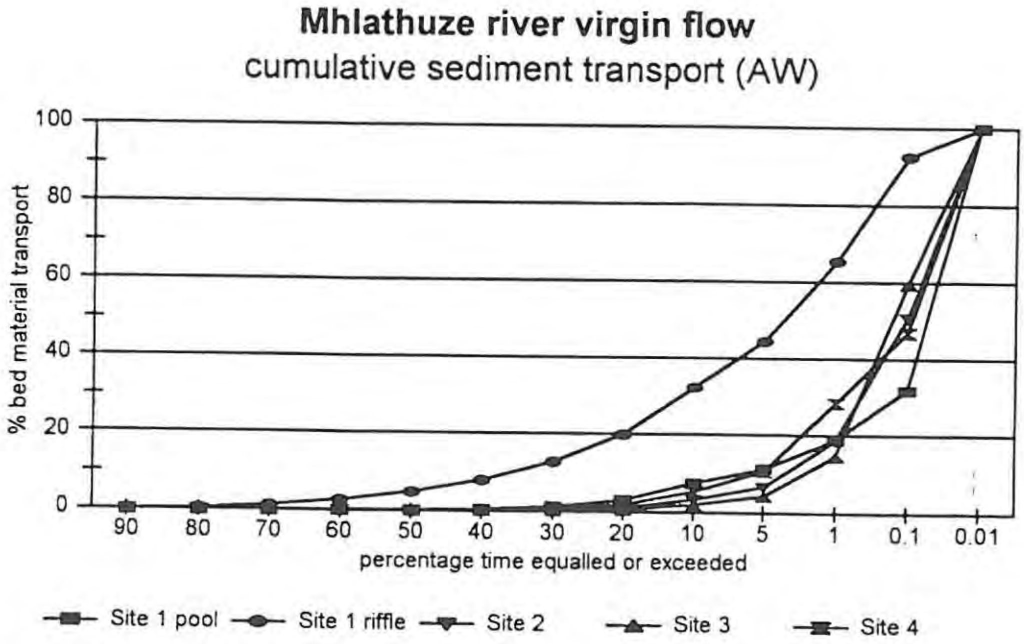

Figure 10.10: Cumulative sediment transport for the Ackers & White equation for all sites for the virgin flow for the Mhlathuze River.

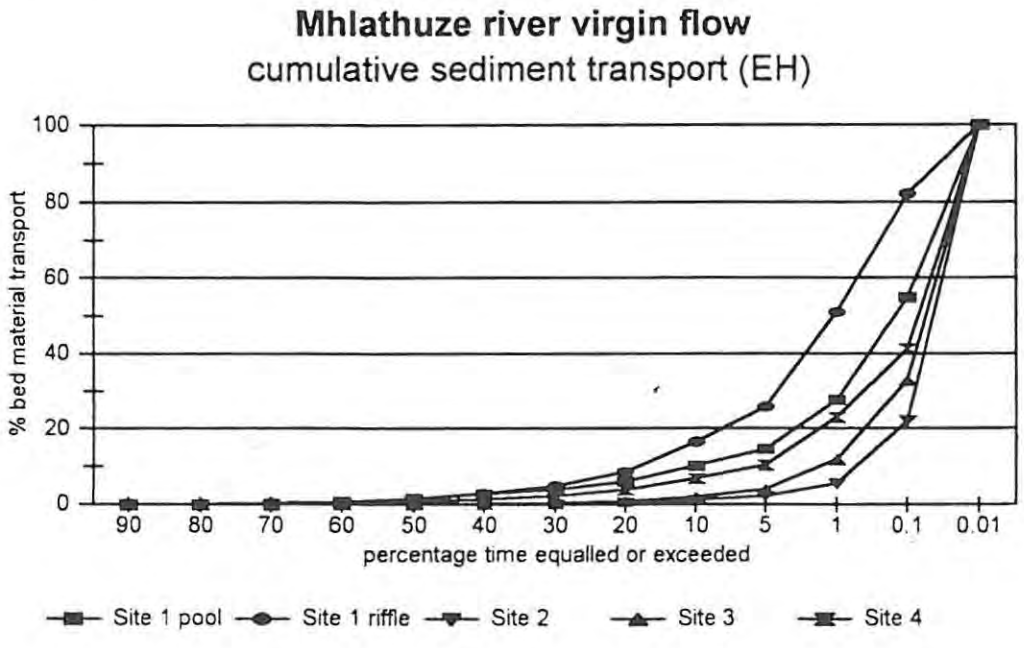

Figure 10.11: Cumulative sediment transport for the Engelund & Hansen equation for all sites for the virgin flow for the Mhlathuze River.

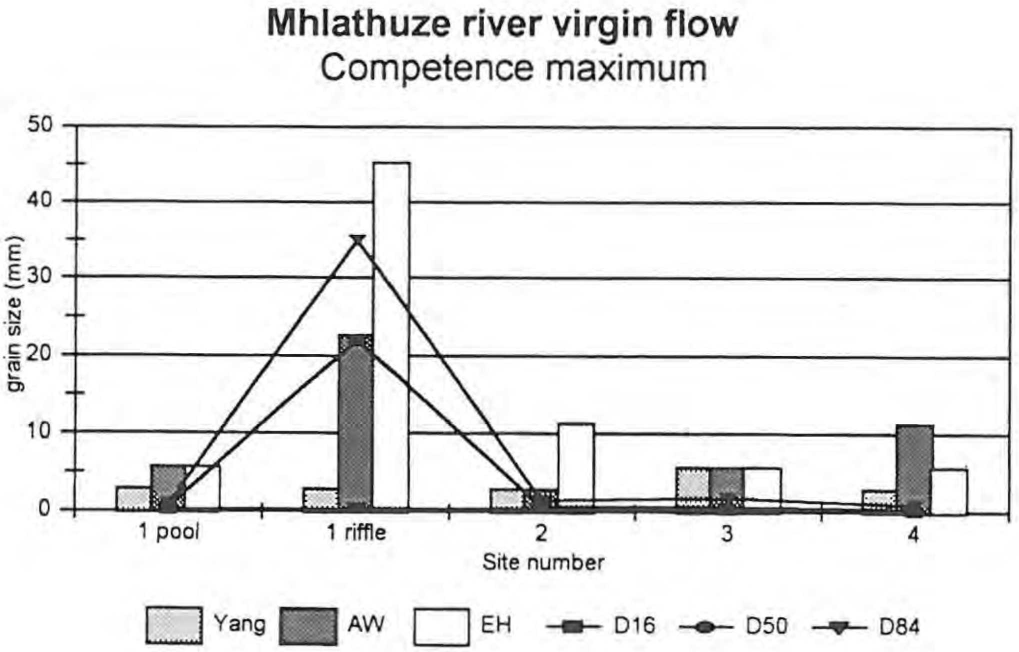

Figure 10.12: Maximum competence for the Mhlathuze River for virgin flow.

Figures 10.13 and 10.14 present the relationship between MAR and the mean effective discharge for the Mhlathuze for the virgin and present-day flow. Although it is not possible to test this relationship statistically, the results suggest that effective discharge increases with MAR. This would indicate that bed material transport is, in part, a function of discharge for the Mhlathuze. This is so because of the mobility of the sand-bed. This relationship is not as clear for the Mkomazi or Olifants Rivers.

The plot of the relationship between mean unit stream power and mean effective discharge for the virgin and present-day data is presented in Figures 10.15 and 10.16. Again, although it is not possible to test this relationship statistically, it is evident that an inverse relationship exists between effective discharge and stream power. Higher effective discharges appear to be associated with lower unit stream powers. Although this seems to be counter-intuitive, this is to be expected for the Mhlathuze, as high stream powers initiate transport at lower discharges, and hence the effective discharges are lower.

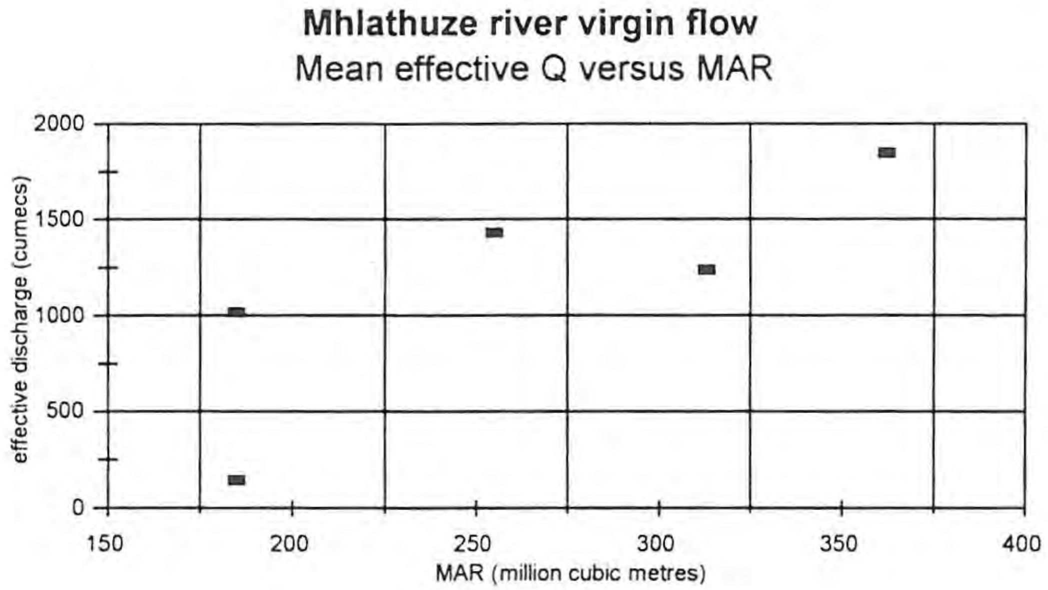

Figure 10.13: Mean effective discharge versus MAR for the Mhlathuze River virgin flow.

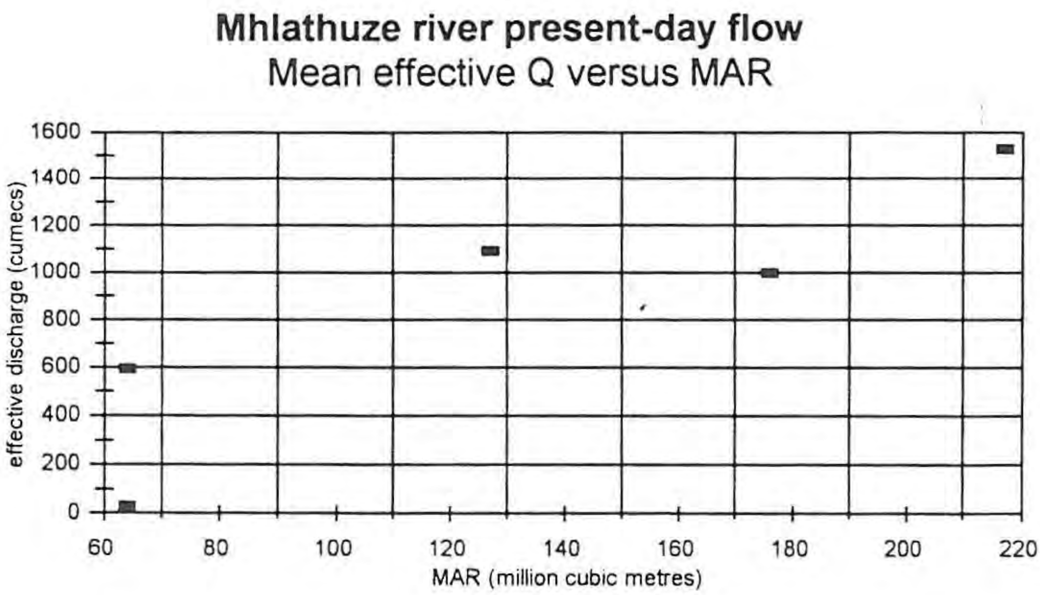

Figure 10.14: Mean effective discharge versus MAR for the Mhlathuze River present-day flow.

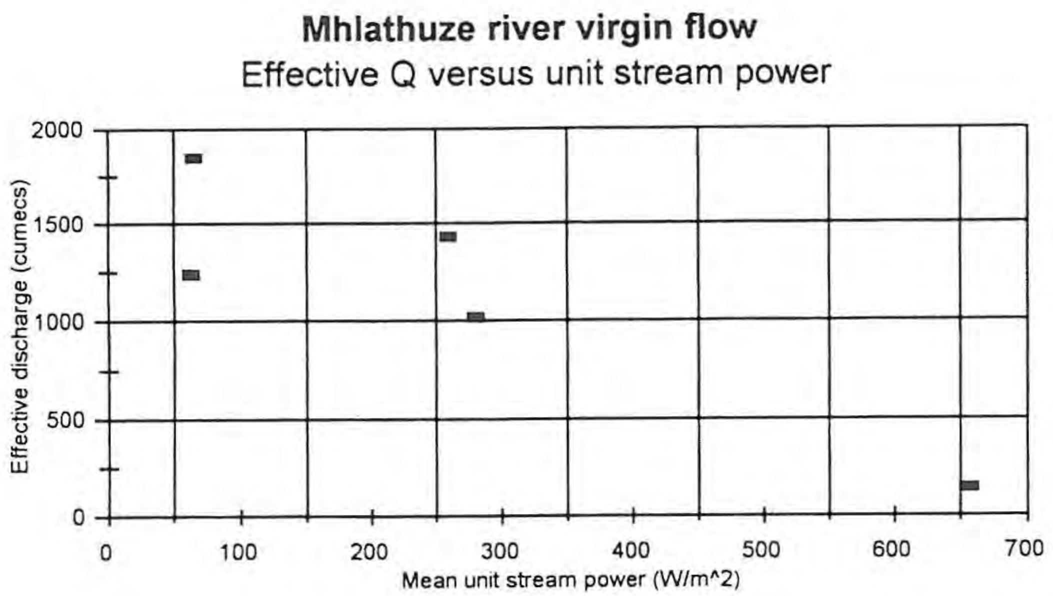

Figure 10.15: Effective discharge versus unit stream power for the Mhlathuze River virgin flow.

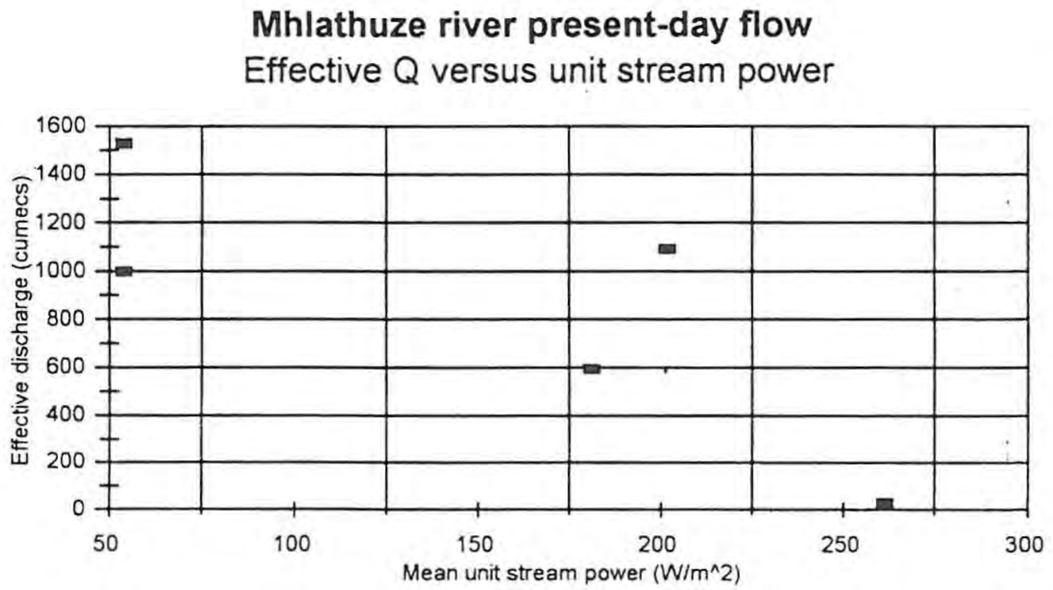

Figure 10.16: Effective discharge versus unit stream power for the Mhlathuze River present-day flow.

10.2.4.2 Present-day flow

The effective discharge is greater for the virgin flow than for the present-day flow. For example, the effective discharge calculated using the Yang equation is 1020 m^3s^{-1} at Site 1 pool under virgin conditions, this declines to 595 m^3s^{-1} under present-day conditions. Similar results are obtained at all sites for the different equations (Table 10.4). This is to be expected, as the effective discharge is the geometric mean of the flow class that transports the most bed material.

Of significance is the impact of the regulated flow environment on the shear stress and unit stream power. The boundary shear stress and unit stream power has been reduced for the effective discharges. Figure 10.17 shows the data for the unit stream power for the effective discharge for the Yang equation. The effective discharge for Site 1 pool (1020 m^3s^{-1}) under virgin conditions produced a unit stream power value of 280 Wm^{-2} (Figure 10.17), while the effective discharge for the present-day conditions (595 m^3s^{-1}) produces a unit stream power of 181 Wm^{-2}. Thus, while the discharge under present-day conditions represents 58% of the virgin flow, the present-day unit stream power represents 65% of the virgin unit stream power. At Site 1 riffle this is even more marked with the unit stream power declining from over 650 Wm^{-2} under virgin flow conditions to just over 200 Wm^{-2} under present-day conditions. At Site 2, the difference in unit stream power is small (260 Wm^{-2} for the virgin conditions and 202 Wm^{-2} for the present-day conditions). At sites 3 and 4 the difference is insignificant (86 Wm^{-2} for Site 3 virgin as opposed to 72 Wm^{-2} for Site 3 present-day, and 65 Wm^{-2} for Site 4 virgin and 54 Wm^{-2} for Site 4 present-day). As is the case with the total load, this disparity reduces with distance from the dam, and for the same reasons. It is important to note that although at these low stream powers the river is competent to transport the bed material, the overall volume of sediment moved is considerably less (Table 10.9). The transport of bed material for the Mhlathuze appears to be mainly a function of flow volume and duration, as the bulk of the bed is sand-sized and is thus mobile even under low flow conditions. It should be re-emphasised that these relationships may not hold true for gravel- or cobble-bed rivers.

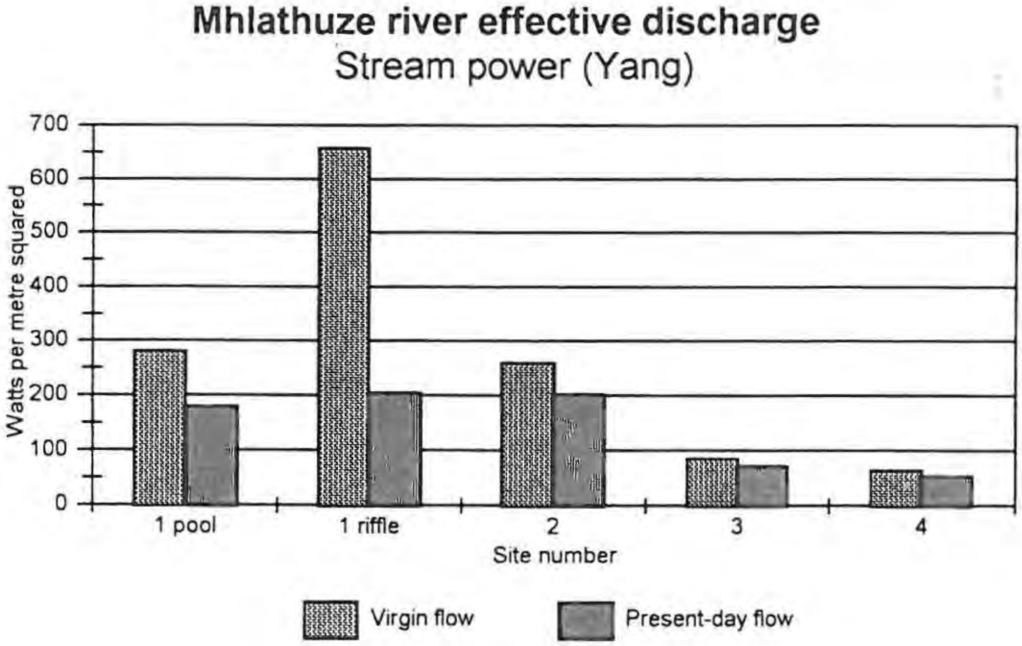

Figure 10.17: Unit stream power for the Mhlathuze River using the Yang equation.

Figures 10.18, 10.19 and 10.20 display the distribution of the cumulative bed material transport for the three transport equations for the present-day flow. It has been mentioned earlier that the total bed material load for the present-day discharge is considerably less than the total load for the virgin discharge (Table 10.9). It was also mentioned earlier that for the virgin flow, all three transport equations predict that over 90% of the total bed load was transported by flows that were equalled or exceeded 20% of the time or greater on the flow duration curve. For the present-day flow, the curves have all shifted to the right. This means that other than for Site 1 riffle, 90% of the total bed load is transported by the top 5% of the flows (Figures 10.18 to 10.20). This represents a significant change in the effectiveness of the flow regime. Under the virgin flow conditions it appears that there was a more even distribution of the load between the flow classes. Under present-day flow environment, not only has the total load been reduced by a factor between 3.5 (the average for the three equations for Site 1 pool) and 1.54 (the average for the three equations for Site 4) (Table 10.9) but there has also been a clear change in the way in which the load is distributed around the duration curve. This is of significance in recommending flows for the Instream Flow Requirement (IFRs) and will be discussed further in Section 10.2.8.

It could, however, be argued that reduced transport capacity may be of limited significance, as long as a balance exists between the amount of material transported to the river system and the amount of material transported out of the system. However, where there are significant inputs of sediment from downstream tributaries (such as the Mfule and Nseleni for the Mhlathuze), it is likely that sediment accumulation will occur downstream of these tributary junctions which will lead to channel aggradation. Under present-day conditions, the Mhlathuze is still competent to transport bed material at reduced (regulated) flows, but this is only due to the high mobility of the sand-bed. The reduced flow means that a reduced volume of material is being transported (i.e. the capacity of the Mhlathuze is reduced) despite the present-day regulated system's competence to transport the bed material. There is also no danger of fine material filling the interstices of coarser material. Were the Mhlathuze River a heterogenous gravel- or cobble-bed river (such as the Mkomazi or Olifants), then a greatly reduced flow regime would be expected to have a different impact. This will be expanded on later in the chapter.

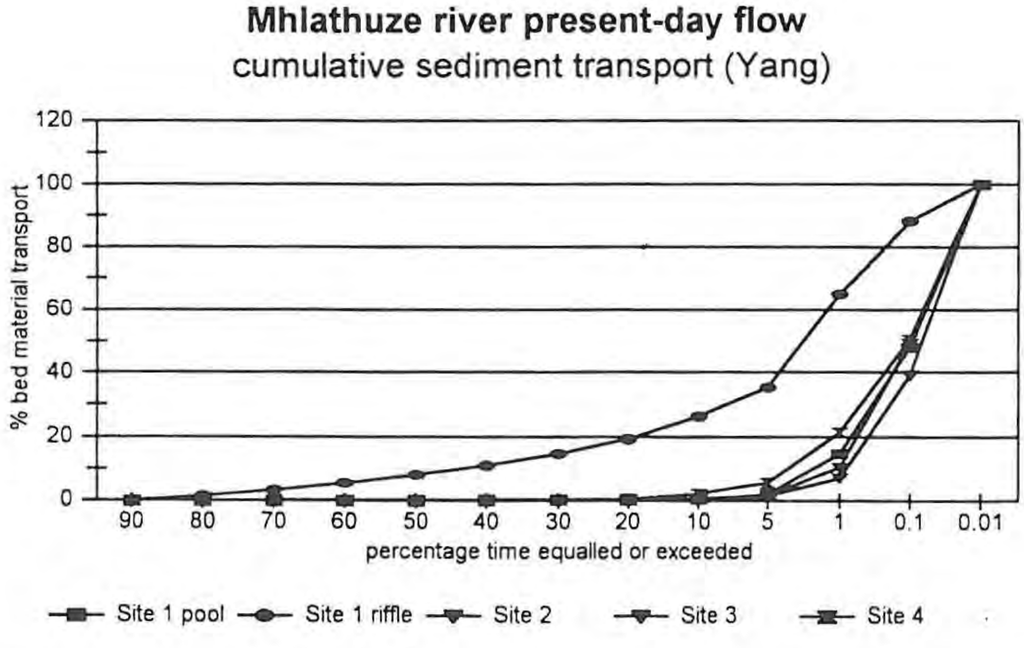

Figure 10.18: Cumulative sediment transport for the Yang equation for all sites for the present-day flow for the Mhlathuze River.

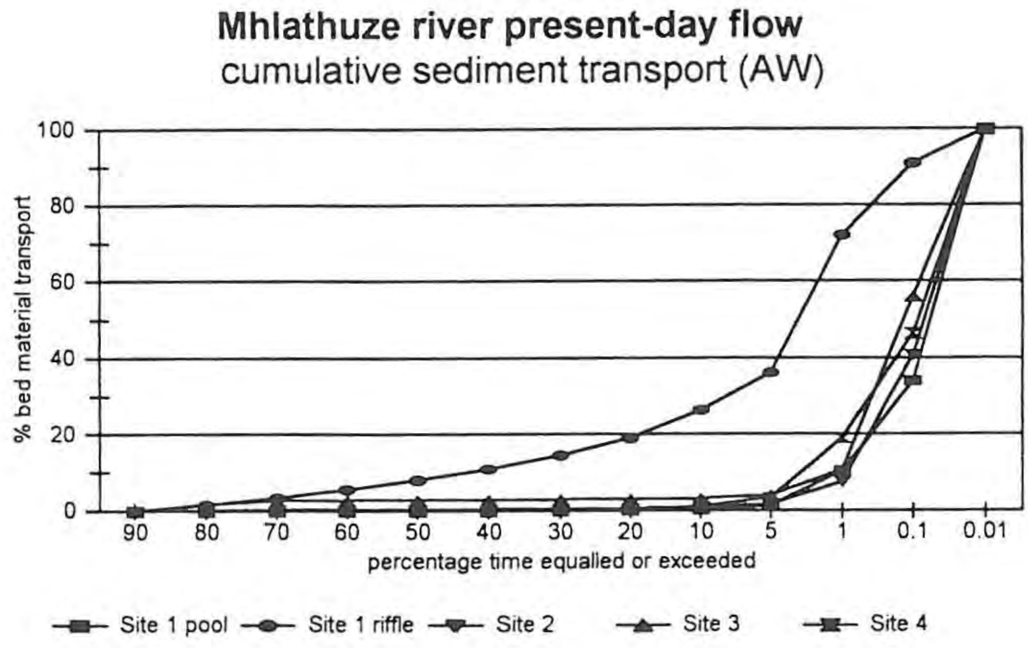

Figure 10.19: Cumulative sediment transport for the Ackers & White equation for all sites for the present-day flow for the Mhlathuze River.

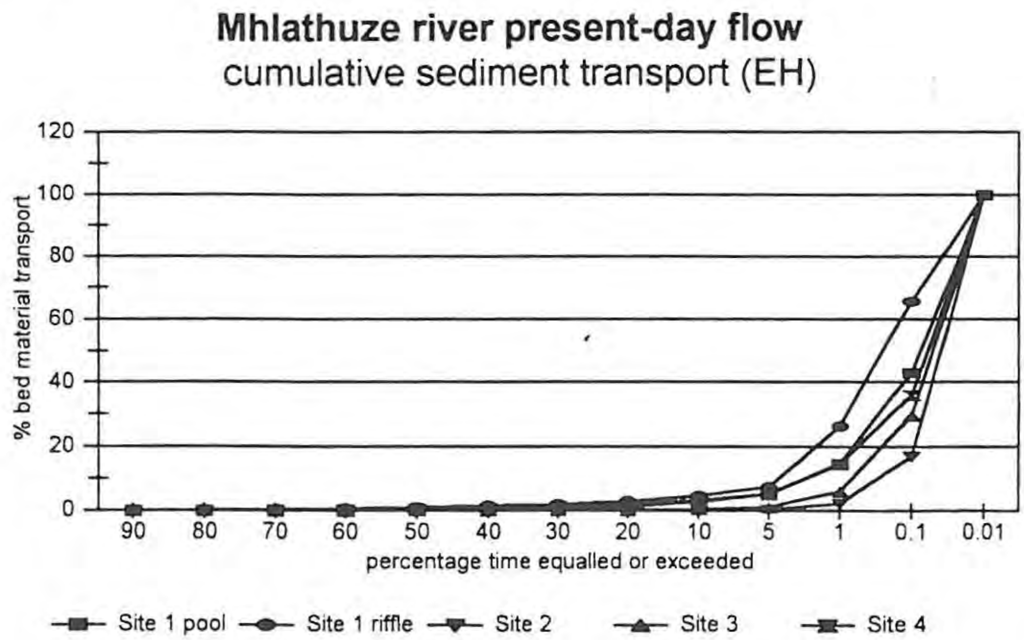

Figure 10.20: Cumulative sediment transport for the Engelund & Hansen equation for all sites for the present-day flow for the Mhlathuze River.

10.2.5 Synthesis

The Mhlathuze River is a sand-bed river and, as such, these findings demonstrate that bed material transport occurs at even the lowest flow classes. It was also mentioned that the construction of the Goedertrouw Dam has had a significant impact on the flow regime, with a reduction of up to 60% of the MAR immediately downstream of the dam. The effective discharge has been reduced by almost 50% at all sites. While these reduced flows remain competent to mobilise the bed material, the volume of the transported material has been reduced due to a reduction in the transport capacity associated with a reduction in unit stream power. The cumulative sediment transport curves have shifted to the right under the present-day flow environment, which would suggest a higher percentage of the bed material is being transported by less frequent flows. This, however, points to the fact that under present-day conditions, the higher flows are of greater significance, as these are the flows that are more 'effective'.

It is argued that the Mhlathuze River has adjusted its channel morphology in sympathy with the regulated flow regime. There is evidence to suggest that a new set of in-channel features are developing, and that the present-day in-channel bench is in fact the new bankfull discharge. This is supported by the hydrological data. These findings suggest that methods used for setting a regulated Instream Flow Requirement (IFR) on the basis of morphological features in the channel (e.g. the bankfull stage) may be inappropriate. This issue will be discussed in greater detail in Section 10.2.8.

It should be noted that the effective discharges calculated for the Mhlathuze River are far higher than for the Mkomazi or Olifants Rivers. This is significant, as it illustrates the importance of the the flow regime. The upper part of the flow duration curve displays a marked steepening due to the occurrence of tropical cyclones and cut-off lows which appear to occur on average every twenty years or so in northern KwaZulu-Natal. The high variability of the Mhlathuze increases the importance of the higher flows. It is also clear that, under present-day flow conditions, the morphological features are inundated less frequently (approximately half the time) than would be the case under the virgin flow regime. It is argued that due to the sand-bed nature of the Mhlathuze River, the channel can accommodate significant reductions in flow without crossing the threshold of instability, provided that the amount of sediment transported into the system is balanced by the amount of sediment that the channel can transport out of the system.

10.2.6 Sediment-maintenance flushing flows

In Chapter 8, the methods used for determining sediment-maintenance flushing flows were presented. This section will report on the results for the regulated Mhlathuze River. Refer to the relevant sections on sediment-maintenance flushing flows in Chapter 8 and Chapter 9.

The Milhous approach was found to be inappropriate for sand-bed rivers. This is not surprising given that the equations generated by Milhous were developed for a gravel-bed river. In fact, Milhous (1998a) himself cautions that the equations should not be used when the D_{50} is less than 2.0 mm. The values that were calculated were clearly inappropriate. However, for the purposes of consistency, the calculations are available at the back of the report in Appendix H.

Figure 10.21 shows RBS values obtained for the Mhlathuze virgin flow data. Also shown is the β value calculated for the 0.021 (surface) and 0.035 (depth) flushing flows. These values represent the flow class at which the β value is 0.021 and 0.035 respectively. The tables displaying these results are available in Appendix H at the back of the report. The data indicate that the Mhlathuze has the potential to become unstable at very low flows (as low as the 10^{th} percentile). This is to be expected as the Mhlathuze is a sand-bed channel and transport occurs at very low flows. The calculated effective and dominant discharges are far in excess of the discharge at which the RBS value estimates the bed will become unstable.

The data for the present-day flow indicates that the flow class at which the bed becomes unstable is the same for all sites, other than Site 1 riffle. Here the RBS estimates that the bed will become unstable at the 99^{th} percentile flow class as opposed to the 95^{th} percentile under virgin conditions (Figure 10.22). Similarly, the β value for the 0.021 and 0.035 changes from the 40^{th} and 80^{th}

percentile under virgin flow conditions respectively, to the 90th and 99th percentile for present-day conditions. This confirms the results generated by the transport equations where the cumulative transport curve has shifted to the right. It is suggested that these two methods are inappropriate for sand-bed channels.

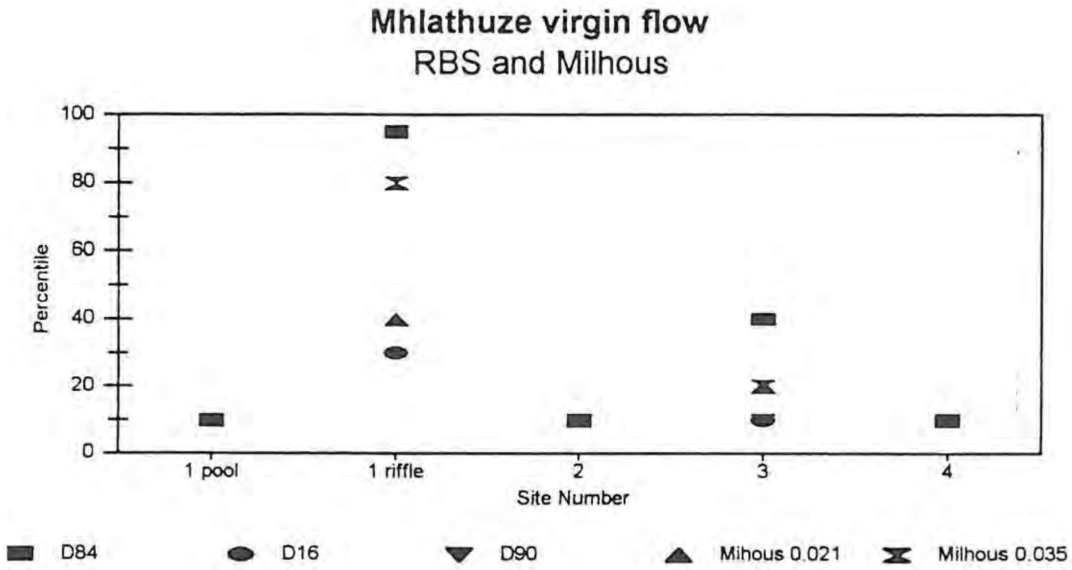

Figure 10.21: RBS values calculated for the Mhlathuze River virgin flow. The β value calculated for the 0.021 (surface) and 0.035 (depth) flushing flows. These values represent the flow class at which the β value is 0.021 and 0.035 respectively.

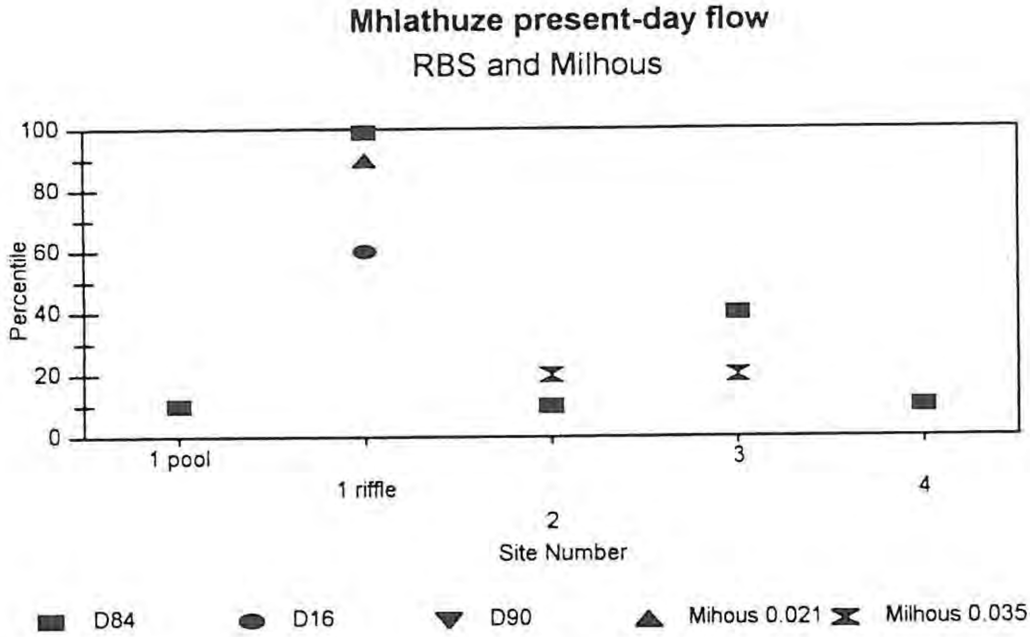

Figure 10.22: RBS values calculated for the Mhlathuze River present-day flow. The β value calculated for the 0.021 (surface) and 0.035 (depth) flushing flows. These values represent the flow class at which the β value is 0.021 and 0.035 respectively.

10.2.6.1 Effective discharge for sand and gravel

The effective discharge for sand and gravel was calculated using the same technique as outlined for the Mkomazi River. This was done for virgin and present-day conditions for the Mhlathuze River. Results from the virgin flow (Figure 10.23) indicate that the percentage bed material transported by the effective discharge for sand is generally less than that for gravel. This would suggest that the sand is being transported by a wider range of flow classes than the gravel, which is to be expected. Results from the present-day flow indicate that the percentage transported by the effective discharge for sand and gravel has changed (Figure 10.24). A number of points are evident. First, the percentage bed material transported by the most effective discharge has increased for both sand and gravel (Figures 10.23 and 10.24). It is clear that not only has the volume of sediment being transported by the present-day flow changed, but so too has the proportion of sand and gravel being transported by the different flow classes. This result indicates that under present-day conditions less bed material is being transported and that the material that is being transported is being transported by a smaller range of flow classes. This finding is in agreement with the results presented in Section 10.2.4.1.

This has not, however, changed the effective discharge flow classes (Table 10.11). This would suggest that although the capacity of the flow has changed, the competence has not.

Table 10.11: Effective discharge flow classes for the Mhlathuze River for sand and gravel for the Yang equation.

Site	Sand (flow class)	Gravel (flow class)	Sand (flow class)	Gravel (flow class)
	Virgin flow		Present-day flow	
1 pool	0.1-0.01%	0.1-0.01%	0.1-0.01%	0.1-0.01%
1 riffle	1-0.1%	1-0.1%	1-0.1%	1-0.1%
2	0.1-0.01%	0.1-0.01%	0.1-0.01%	0.1-0.01%
3	0.1-0.01%	0.1-0.01%	0.1-0.01%	0.1-0.01%
4	0.1-0.01%	0.1-0.01%	0.1-0.01%	0.1-0.01%

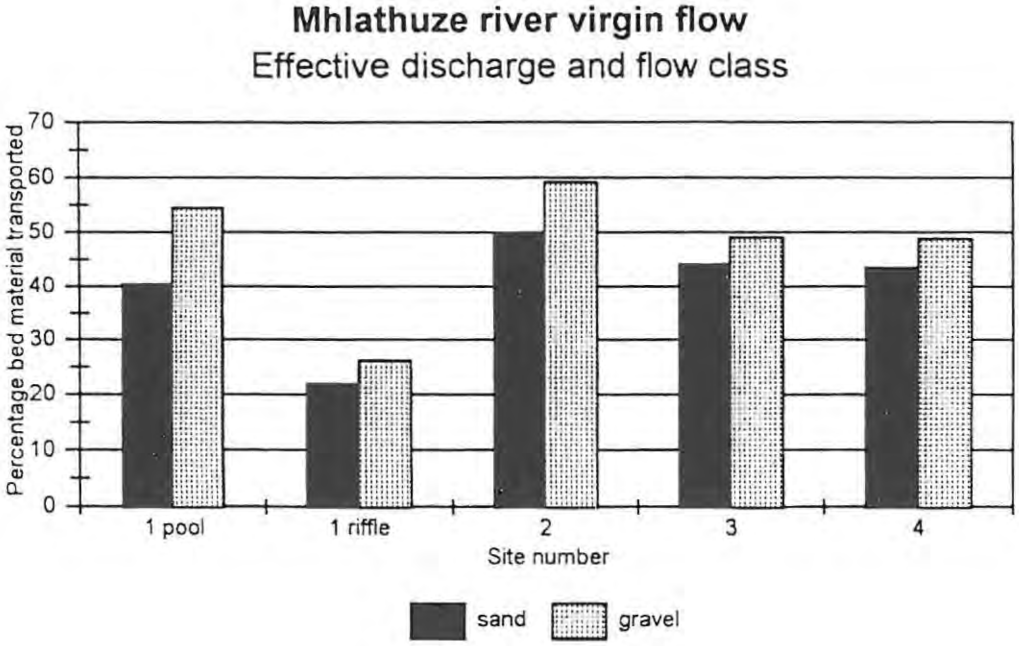

Figure 10.23: The percentage bed material transported by the effective discharge for the Mhlathuze River virgin flow for sand and gravel.

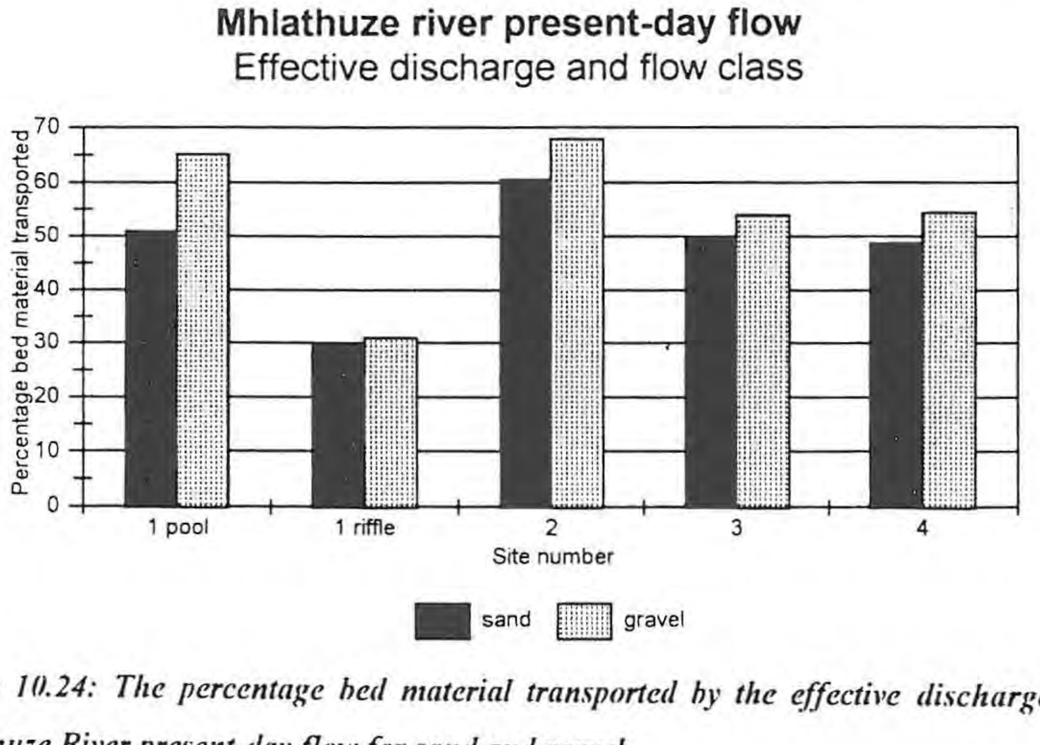

Figure 10.24: The percentage bed material transported by the effective discharge for the Mhlathuze River present-day flow for sand and gravel.

10.2.7 Synthesis

The results highlight a number of issues. First, the regulated flow regime has reduced the bed material transport capacity of the Mhlathuze River by nearly four times immediately below Goedertrouw Dam, and by approximately 1.5 times near the mouth. [This may have a number of indirect impacts, such as increased coastal erosion and degradation of beaches (cf. Cooper, 1991)]. Second, it could be argued that due to the high mobility of the sand bed this may be of limited significance, provided that the amount of bed material supplied to the channel equals the amount of material transported out of the channel. However, this is not the case for the Mhlathuze River. The channel immediately downstream of the dam has narrowed and deepened in response to the regulated flow. It has effectively been stripped of its sediment and consequently a new channel form has developed. This impact is compensated for in the downstream direction by the input of sediment and discharge from the Mfule and Nseleni tributaries. It is suggested that the input of sediment and discharge from downstream tributaries is likely to have resulted in channel aggradation. This would suggest that the impact of the regulation changes in the downstream direction. Immediately below the Dam, channel narrowing and deepening occurs in response to a markedly reduced discharge and bed material load. Further downstream, below major tributary inputs, this impact is compensated for by inputs of water and sediment to the main stem. The alluvial sand-bed system has therefore adjusted its channel geometry in sympathy with the regulated flow regime.

If the above hypothesis is correct, then the following should also be true: under virgin flow conditions, the bench should have been absent and the estimated bankfull discharge should have been the equilibrium condition. If the bench is indeed a modern feature and related to modern flows, then the recurrence interval of the inundation should be approximately the same as the recurrence interval of the bankfull level under virgin flows. Furthermore, if the upper sites are incising then the recurrence intervals should be relatively high. If the lower sites are aggrading, then the recurrence intervals should be relatively low. The lack of a bench at Site 3 suggests that the present bankfull level may be the closer to the true bankfull level than at the other sites. The data therefore support this hypothesis.

10.2.8. Implications for Instream Flow Requirements (IFRs)

In setting a regulated flow regime that would attempt to mimic the significant pre-impoundment discharges, it is necessary that the geomorphological objectives be clearly stated. In the case of the Mhlathuze River, where clear evidence exists that the regulated flow regime has had a significant impact on channel morphology and bed load transport capacity, it may be useful to set flow objectives that maintain certain aspects of the existing channel, rather than attempting to set flows to return the channel to a pre-impoundment state. It may be necessary, therefore, to set different flow requirements for Site 1 which is immediately below the Dam and which is incising and narrowing, as opposed to sites 2, 3 and 4 which are below the confluence of the Mfule and Nseleni tributaries, and are therefore probably aggrading.

Given the fact that the Goedertrouw Dam has a near 100% trap efficiency and that there are no major tributary inputs of sediment between the dam and Site 1, it is unlikely that channel aggradation will occur. It is more likely that the channel will maintain its downward trajectory and continue to narrow and deepen. To avoid this scenario, it may be useful to set an IFR that will ensure that the channel maintains its present width and topographic diversity. For this reason, the channel maintenance flows should not be pinned to present-day morphological features. Flows should be recommended that seek to maintain the status quo of the channel, as it is clear that it is not possible to return the channel to the pre-impoundment condition. Channel maintenance flows need to be set close to the effective discharge. It is important to note that the effective discharge also implies flow duration. It may be possible to manipulate the hydrograph of the dam releases (especially in mobile sand-bed channels) to optimise sediment transport and achieve a desired channel condition.

Furthermore, it has been demonstrated that due to flow regulation, the high magnitude low frequency flows assume greater significance in transporting the bed material. It is argued that these flows need to be allowed through the channel reach.

For Site 1, the following objectives might be set:

- to remove fine sediment from the pool;
- to remove fine sediment from the gravel and cobble substrate in the riffle;
- to entrain the coarse material on the riffle, thereby exposing subsurface material to transport and maintaining a loose structure;
- to maintain the active channel width and topographic diversity; and
- to allow large floods to move through the reach.

The sand-bed channels (sites 2, 3 and 4) are highly mobile. However, if the regulated flow regime does not have the capacity to transport the sediment input, then aggradation will occur. It is argued that the development of inset channel benches are probably a response by the Mhlathuze River to the regulated flow environment. Unless a balance between the input and output of sediment is achieved, the long-term trajectory for the Mhlathuze at these lower three sites is one of aggradation. This effect can be mitigated to some extent by flooding. However, given that the Goedertrouw Dam has had the effect of attenuating the flood peaks, present-day floods do not have the same capacity as they had in the past. However, they are of greater significance as they are relatively more 'effective' under present-day conditions.

For sites 2, 3 and 4 the following flow objectives might be set:

- to maintain the equilibrium of the channel by setting flows that transport the same amount of material entering the channel as that leaving the channel; and
- to allow large floods to move through the channel reach.

It is clear from the channel geometry of the Mhlathuze River that the river has adjusted to a highly variable flow regime. Flooding forms an important part of the operation of the system. As long as the system remains regulated, geomorphological responses are inevitable.

10.3 The Olifants River

10.3.1 Overview

The Olifants River is a highveld river in the Gauteng and Mpumalanga provinces of South Africa. An overview of the Olifants River has been presented in Chapter 5. A short summary is provided here. The upper Olifants drains an area of approximately 10 841 km^2. The upper Olifants system consists of three main stems, the Wilge to the west, the Klein Olifants to the east and the Olifants proper. The channel is strongly controlled by bed rock and by numerous lineaments and faults that traverse the river. The bed material is predominantly cobble-sized. The three main stems have been impounded by a number of dams. The Wilge River is impounded by two major dams, the Bronkhorstspruit Dam and the Premier Dam. The Bronkhorstspruit Dam is nearly 80 kilometres upstream of Site 4. Downstream of the Bronkhorstspruit Dam is Premier Dam, Site 4 is approximately 40 kilometres downstream of Premier Dam. The main Olifants stem is regulated by two dams, the Witbank Dam and the Doornpoort Dam. Site 1 is 15 kilometres downstream of Doornpoort Dam. The Klein Olifants River is impounded by Middelburg Dam, Site 3 is approximately 45 kilometres downstream of Middelburg Dam. Site 2, which is the lowest site on the Olifants system is thus regulated by five impoundments. These impoundments have been in place for some time (over 50 years) and have had a major impact on the flow regime of the Olifants system.

The flow classes calculated for the Olifants River are presented in Table 10.12. The methods for determining the bed material transport, effective discharge and dominant discharge were the same as those used for the Mkomazi and Mhlathuze Rivers. It should be pointed out that the sites on the Olifants River could not be related to any longitudinal downstream changes, as two of the sites are on tributaries of the Olifants [Sites 3 (Wilge River) and 4 (Klein Olifants River)]. They were, however, related to the Mean Annual Runoff (MAR).

It is important to re-emphasize that the hydrological data that were generated for the Olifants River relate to the virgin flow conditions. As explained earlier, this was due to the fact that no present-day daily data could be generated, as information on the operational procedures of the controlling dams was unobtainable or not available. The field methods that were applied to the classification of the morphological features of the Mkomazi and Mhlathuze Rivers were also applied to the Olifants River.

Table 10.12: Flow classes calculated for the Olifants River. Values are in m^3s^{-1}. MAR is in million cubic metres.

% time equalled or exceeded	Q	Geometric mean flow class	Q	Geometric mean flow class	Q	Geometric mean flow class	Q	Geometric mean flow class
	Site 1		Site 2		Site 3		Site 4	
	147 MAR		449.3 MAR		81.6 MAR		166.9 MAR	
99.99	0.010		0.206		0.025		0.120	
90	0.225	0.047	1.304	0.518	0.187	0.068	0.708	0.291
80	0.297	0.259	1.835	1.547	0.258	0.220	0.982	0.834
70	0.381	0.336	2.414	2.105	0.330	0.292	1.258	1.111
60	0.527	0.448	3.234	2.794	0.411	0.368	1.604	1.421
50	0.833	0.663	4.649	3.877	0.530	0.467	2.048	1.812
40	1.420	1.086	7.164	5.771	0.771	0.639	2.744	2.371
30	2.534	1.897	11.581	9.109	1.280	0.993	3.934	3.286
20	4.846	3.504	19.241	14.927	2.281	1.709	6.487	5.052
10	11.189	7.364	37.182	26.747	5.010	3.381	13.316	9.294
5	20.143	15.013	59.991	47.229	9.250	6.808	22.712	13.391
1	53.385	32.792	149.093	94.574	25.635	15.399	62.252	37.601
0.1	229.474	110.682	520.063	278.456	107.155	52.411	237.66	121.635
0.01	568.686	361.246	1001.28	721.615	324.499	186.472	605.96	379.494

10.3.2 Analysis of channel morphology

The estimated bankfull discharge for the Olifants River ranges from 62 m^3s^{-1} (Site 1) to 418 m^3s^{-1} (Site 2) (Table 10.13). On the annual series, these stages are inundated by flows ranging from a 1.6 to 9.5 year return period, with an average of 5.8 years (Table 10.14). The partial series ranges from 0.3 years to 4.2 years with an average of 1.7 years (Table 10.15). The results for the annual series other than for Site 1 are considerably higher than the conventional wisdom suggested by Leopold (1997).

The results indicate good general agreement exists between the estimated bankfull discharge and the 1.5 and 2.44 year return period flows at Site 1 (Table 10.13). At Site 2, the estimated bankfull discharge is similar to the 2.0 year return period on the partial series. At Site 3, the estimated bankfull discharge is greater than any of the calculated return periods, while at Site 4 the estimated bankfull discharge is close to the 2.44 year return period on the annual series. It appears that no consistent agreement exists between the estimated bankfull discharge and any hydrological statistic for the Olifants system. Furthermore, this does not appear to be related to channel type. Sites 1 and 2 are both multiple-channel types with partial bed rock control and a number of distributary channels. Yet Site 1 shows good agreement between the estimated bankfull discharge and the 1.5 and 2.44 year return period on the annual series, but Site 2 does not. Site 3 is strongly bed rock controlled, and the estimated bankfull discharge (160 m^3s^{-1}) is well in excess of any calculated hydrological statistic (Table 10.13). Site 4 is a cobble-bed channel, with the estimated bankfull discharge (80 m^3s^{-1}) almost twice that of the 1.5 year return period on the annual series (49 m^3s^{-1}), but considerably less than the 0.9 and 2.0 year return period on the partial series (126 m^3s^{-1} and 192 m^3s^{-1} respectively) (Table 10.12). The estimated bankfull discharge for the four sites for the Olifants system therefore display no consistent relationship with any calculated hydrological statistic.

This finding is also reflected in the relationship between the MAR and the inundation bankfull discharge. Figure 10.25 displays the relationship between the inundation discharge and MAR for the Olifants River. The estimated bankfull discharge does not appear to increase with increasing MAR. Only terrace 3 displays a definite increase in the downstream direction (using MAR as a surrogate for downstream changes). Terraces 1 and 2 display no clear trend. This may reflect local conditions in that there is strong bed rock control at these sites and the channel boundary is not free to adjust to the flow regime, or the terraces may reflect the imprint of a relict flow regime.

Table 10.13: Morphological data for the Olifants River. Values are in m^3s^{-1}.

Site	3	1	4	2	Average
Virgin MAR	185	255	313	362	
$Q_{1.5}$	31	54	49	127	65
$Q_{2.33}$	41	75	73	190	95
$Q_{p\,0.9}$	46	97	126	274	136
$Q_{p\,20}$	81	178	192	440	223
Morphological flows					
Estimated Q_b	160	62	80	418	
terrace 1	605	756	551	621	
terrace 2	889		993	1245	
terrace 3	1295	1899	1462	2598	
Dominant discharge					
Yang	39	27	28	19	
Ackers & White	64	32		29	
Engelund & Hansen	63	32	43	27	
Average	55	30	36	25	
Effective discharge					
Yang	52	33	38	95	
Ackers & White	52	111		95	
Engelund & Hansen	186	111	379	278	
Average	97	85	209	156	

Table 10.14: Inundation frequencies for different morphological features for the annual data for the Olifants River.

Site	Estimated Q_b return period	Discharge m^3s^{-1}	Terrace 1 return period	Discharge m^3s^{-1}	Terrace 2 return period	Discharge m^3s^{-1}	Terrace 3 return period	Discharge m^3s^{-1}
3	9.5	160	>64	605	>64	889	>64	1295
1	1.6	62	>64	756			>64	1899
4	2.8	80	30	551	>64	993	>64	1462
2	9.2	418	15.8	621	>64	1245	>64	2598
Average	5.8							

Table 10.15: Inundation frequencies for different morphological features for the partial series data for the Olifants River.

Site	Estimated Q_b return period	Discharge m^3s^{-1}	Terrace 1 return period	Discharge m^3s^{-1}	Terrace 2 return period	Discharge m^3s^{-1}	Terrace 3 return period	Discharge m^3s^{-1}
3	4.2	160	>64	605	>64	889	>64	1295
1	0.3	62	>64	756			>64	1899
4	0.4	80	15	551	>64	993	>64	1462
2	1.9	418	3.8	621	>64	1245	>64	2598
Average	1.7							

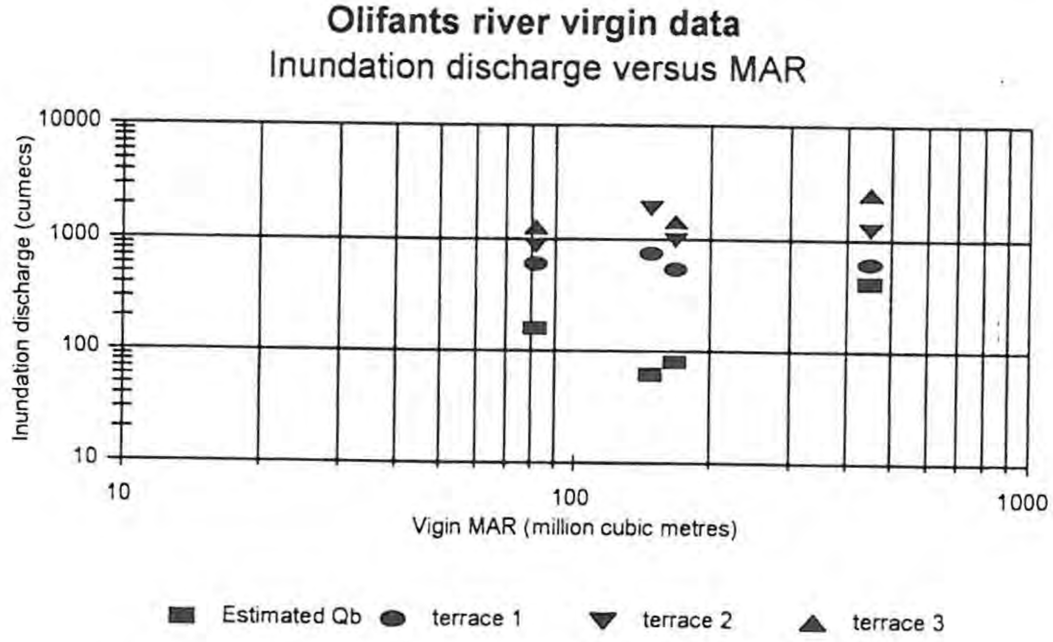

Figure 10.25: Relationship between inundation discharge and virgin MAR for the Olifants River.

10.3.3 Dominant discharge

The dominant discharge as calculated by the Marlette & Walker (1968) equation shows different values for each of the three bed material equations (Table 10.13). The dominant discharge values for the Yang equation range from 19 m^3s^{-1} (Site 2) to 39 m^3s^{-1} (Site 3). The values for the Ackers & White and Engelund & Hansen equations range from 29 m^3s^{-1} (Site 2) to 64 m^3s^{-1} (Site 3) and 27m^3s^{-1} (Site 2) to 63 m^3s^{-1} (Site 3) respectively (Table 10.13). No dominant discharge was calculated for the Ackers & White equation for Site 4, as the equation predicted that even under the highest flow class conditions no bed material transport would occur. The dominant discharge is generally lower than the 1.5 and 2.44 year return period on the annual series and the 0.9 and 2.0 year return period on the partial duration series (Table 10.13).

Figure 10.26 displays the plot of the relationship between MAR and dominant discharge. Although not tested statistically, the result indicates that an inverse relationship exists between MAR and dominant discharge. The higher the MAR, the lower the dominant discharge. Also presented is the relationship between mean stream power per unit area and the mean dominant discharge (Figure 10.27), no clear trend is evident.

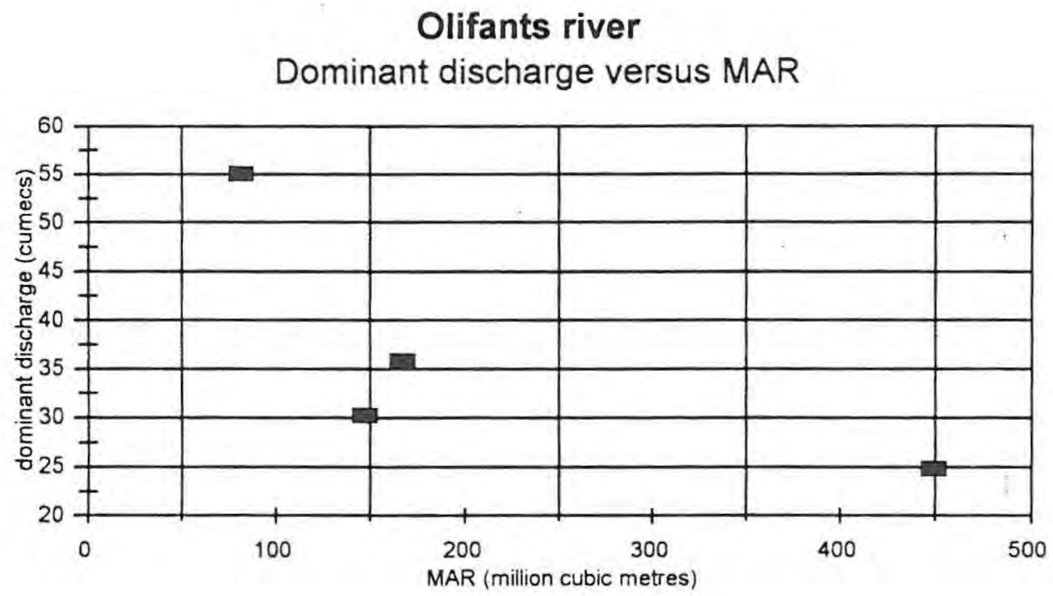

Figure 10.26: Plot of average dominant discharge versus MAR for the Olifants River.

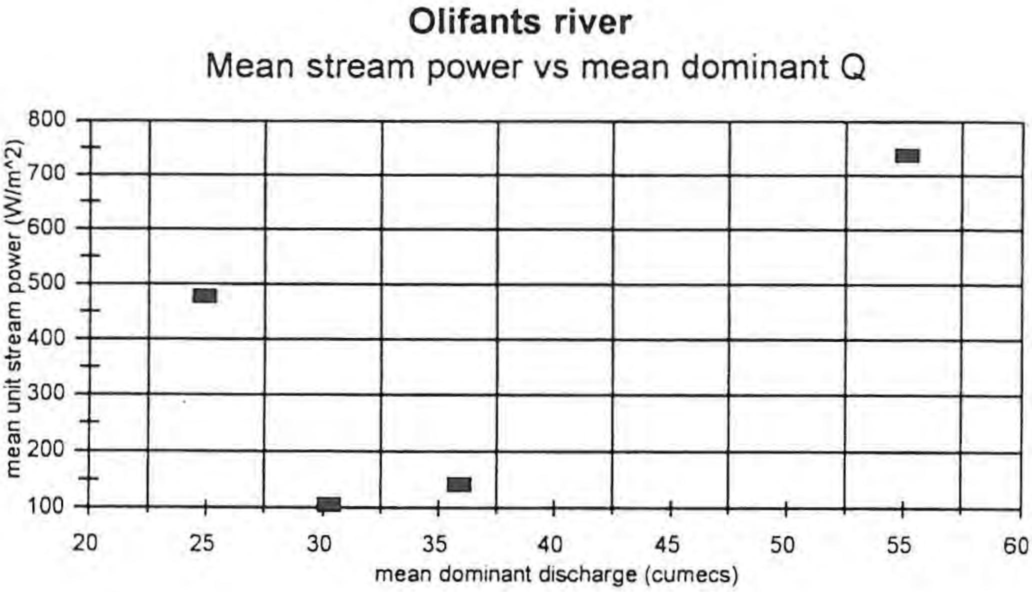

Figure 10.27: Mean stream power per unit area versus mean dominant discharge for the Olifants River.

10.3.4 Effective discharge

The effective discharges as calculated by the Yang and Ackers & White equations range from 33 m^3s^{-1} (Site 1) to 95 m^3s^{-1} (Site 2) for the Yang equation, and 52 m^3s^{-1} (Site 3) to 111 m^3s^{-1} (Site 1) for the Ackers & White equation. The Engelund & Hansen equation predicts values ranging from 111 m^3s^{-1} (Site 1) to 379 m^3s^{-1} (Site 3)(Table 10.13). The Engelund & Hansen equation predicts a significantly higher effective discharge than the Yang and Ackers & White equations. This is likely a function of the inappropriate application of the model to coarse-bedded channels.

Table 10.16 presents the effective discharge flow classes for the Olifants River. The effective discharges range from the 5-0.01% range. The Yang equation predicts effective discharge in the 5-1% range for sites 1, 2 and 4 and 1-0.1% range at Site 3. The Ackers & White equation predicts from the 5-1% class for Site 2, and 1-0.1% for sites 1 and 3. No transport is predicted for Site 4. Engelund & Hansen predicts higher transport values, with effective discharges in the 1-0.1% and 0.1-0.01% flow classes.

Table 10.16: Effective discharge flow classes for the Olifants River.

Site	Yang (flow class)	Ackers & White (flow class)	Engelund & Hansen (flow class)
1	5-1%	1-0.1%	1-0.1%
2	5-1%	5-1%	1-0.1%
3	1-0.1%	1-0.1%	0.1-0.01%
4	5-1%		0.1-0.01%

It is evident that the upper three flow classes are responsible for over 60% of the bed material transported at each of the sites (Figure 10.28). The effective discharge transports between 32% and 51% of the bed material at the four sites (Figure 10.29). As with the Mkomazi and Mhlathuze, this begs the question of how is the remaining 60% or so of the bed material load distributed around the effective discharge. Figures 10.30 to 10.32 display the cumulative sediment transport curves for the three transport equations. The results indicate that very little bed material transport occurs before the 20% equalled or exceeded flow for the Ackers & White and Engelund & Hansen equation (Figures 10.31 and 10.32). The Yang equation computes a slightly higher proportion of bed material transported at lower flows (Figure 10.30). This is reflected in the effective discharge flow classes (Table 10.16). It is clear that over 90% of the bed material for the sites is transported by flows that are equalled or exceeded by the 20^{th} percentile and greater. Flows lower than this are simply not competent to transport significant quantities of bed material.

However, what is evident is that the flow does not appear to be competent to move the entire bed (Figure 10.33). At sites 1, 2 and 3, the transport models predict that the D_{50} and below are moved at the highest flows. However, at sites 1, 3 and 4 the Yang and Ackers & White equations predict that the highest flow class does not have the competence to transport the D_{84}. In contrast, the Engelund & Hansen model predicts that the D_{84} is moved at the highest flow class. Field observation suggests that the Engelund & Hansen model over-predicts incipient motion. The Engelund & Hansen model is also designed for alluvial sand-bed rivers and, consequently, this model cannot be reliably applied to a coarse cobble-bed channel. It would appear that given the coarse nature of the bed, not all of the bed becomes mobile, even at the highest predicted discharges.

The highest modelled flows generated for the Olifants River are not sufficient to inundate the upper two terraces (Appendix G, Tables 38 to 41). If flows of sufficient magnitude were able to inundate these terraces, however, the shear stresses and unit stream power generated would be sufficient to mobilise the entire bed. For example, the unit stream power generated at the terrace 3 inundation stage at Site 3 is 2683 Wm^{-2} (Appendix G, Table 40). Similar, large values are generated at terrace 2 and 3 (2260 Wm^{-2} and 2018 Wm^{-2} respectively). Unfortunately, no historical flood data are available for the Olifants system, and hence it remains untested whether these terraces are inundated by high magnitude low frequency events.

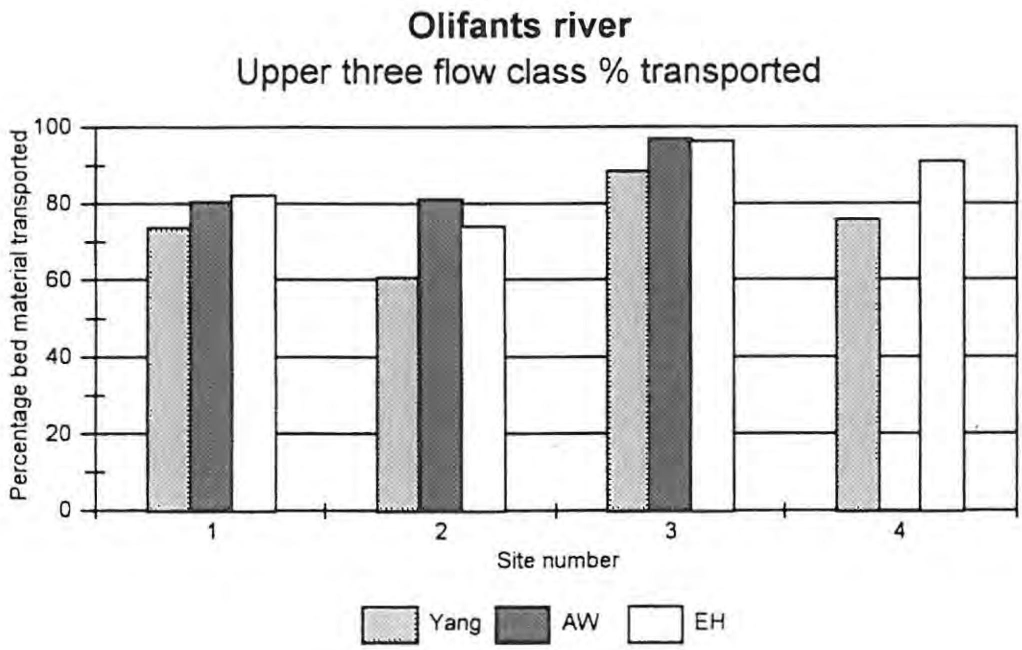

Figure 10.28: Percentage bed material transported by the upper three flow classes (5-1%; 1-0.1% and 0.1-0.01%) for the Olifants River.

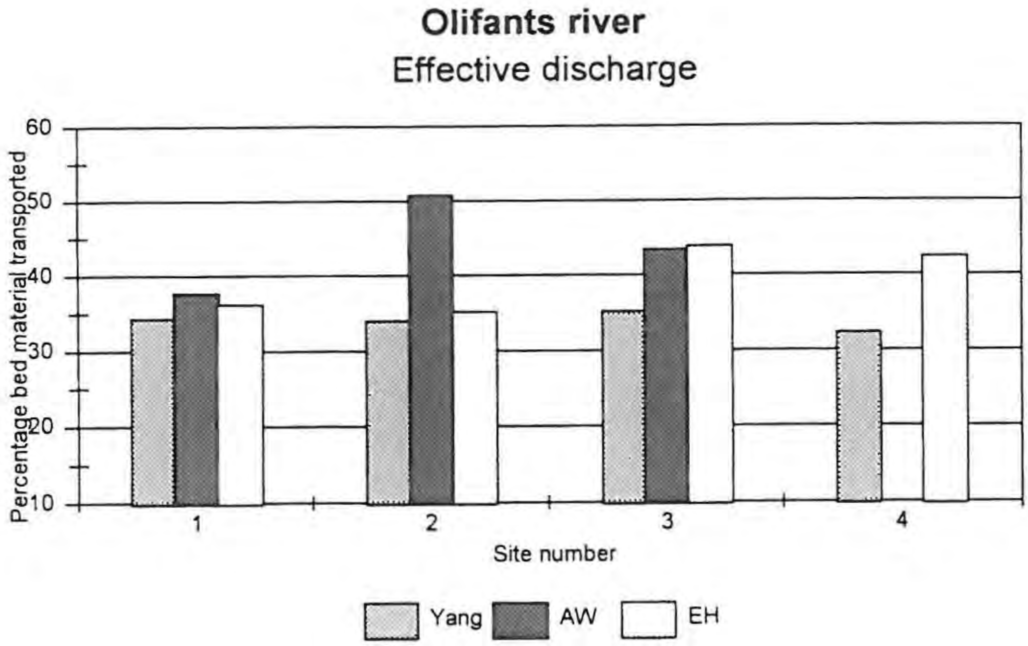

Figure 10.29: Percentage bed material transported by the effective discharge for the Olifants River.

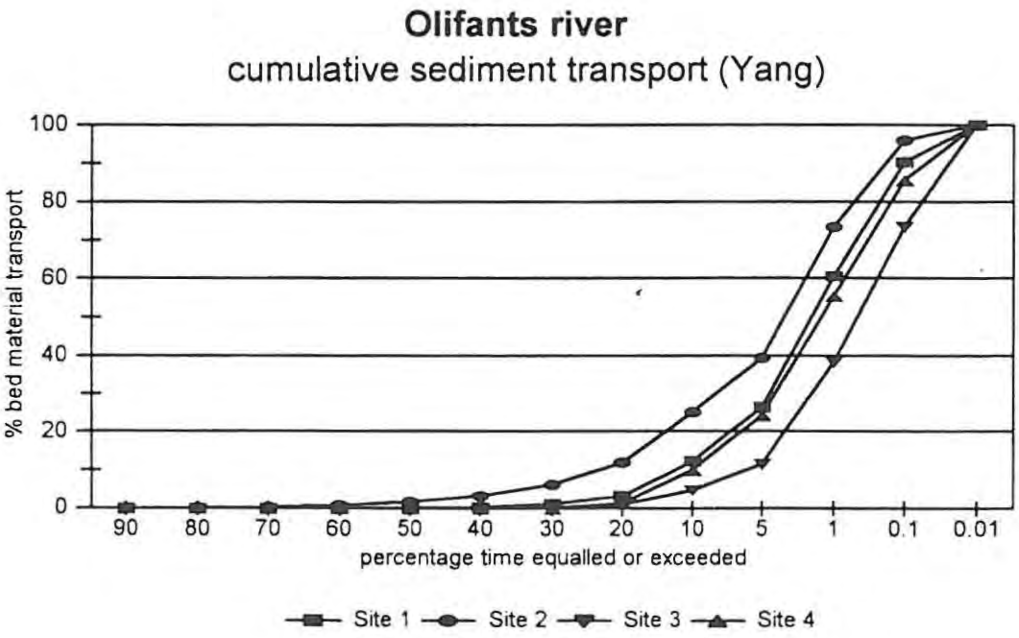

Figure 10.30: Cumulative sediment transport for the Yang equation for the Olifants River.

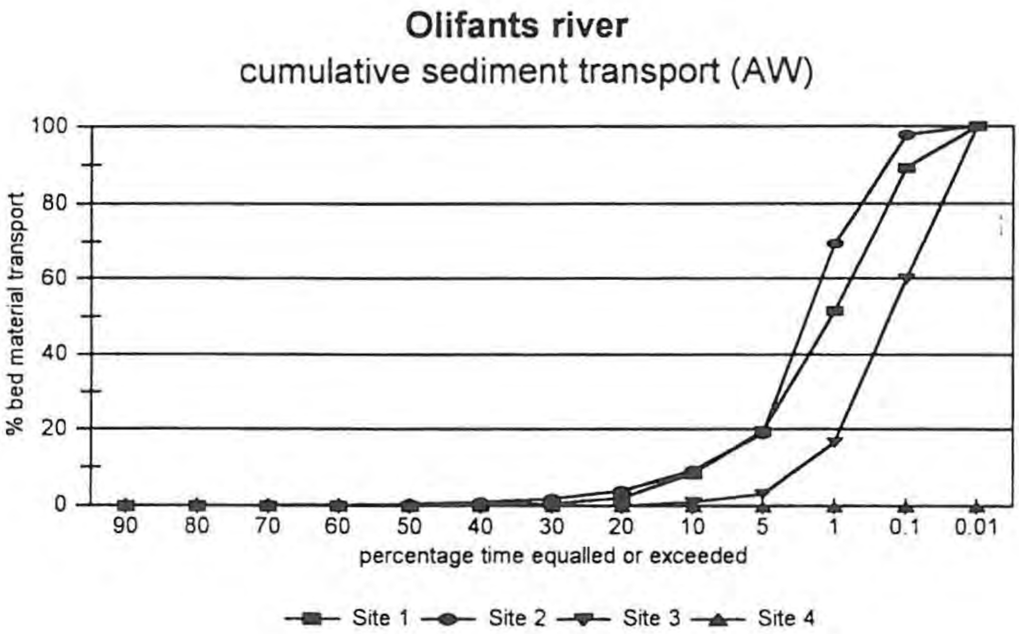

Figure 10.31: Cumulative sediment transport for the Ackers & White equation for the Olifants River.

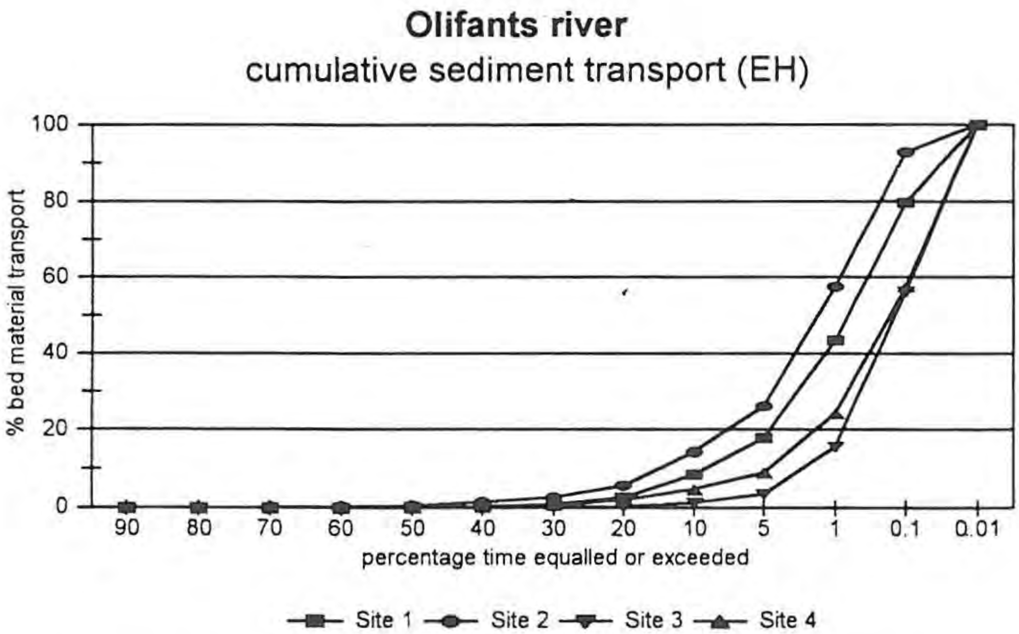

Figure 10.32: Cumulative sediment transport for the Engelund & Hansen equation for the Olifants River.

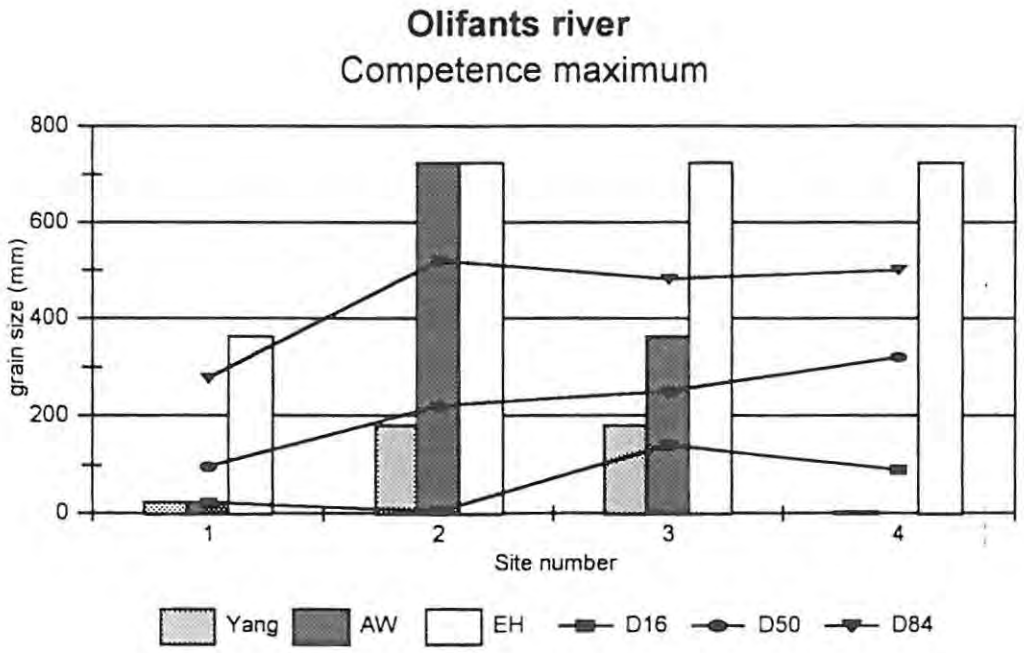

Figure 10.33: Maximum competence for the Olifants River.

10.3.5 Synthesis

The Olifants River is strongly controlled by bed rock, local hydraulic conditions and coarse bed material. The effective discharges are in the 5-0.01% range on the 1-day daily flow duration curve. It has been shown that the coarse fraction of the bed material (i.e. D_{84} and greater) remains immobile, even under the highest flow class, despite the high shear stress and unit stream power generated at a number of the sites. The material that is transported is mainly fine gravel. This results in the calculation of low effective discharges, as the flow in the lower flow classes is competent to transport significant quantities of the fine bed material, but is unable to mobilise the entire bed. It has also been demonstrated that should the flow reach the stage of the upper two terraces, sufficient stream power would be generated to transport the entire bed. Thus it could be argued that like the Mkomazi, the Olifants has developed a channel architecture that is related to a highly variable, bi-polar type flood regime. It may therefore be erroneous to think of one 'effective discharge' for the Olifants. Instead a set of effective discharges may be of significance.

10.3.6 Sediment-maintenance flushing flows

The same methods that were used to determine the sediment-maintenance flushing flows for the Mkomazi and Mhlathuze Rivers were applied to the Olifants River. Table 10.17 presents a summary of the results. It can be seen that at all sites, except Site 4 (Ackers & White equation), the Milhous β value predicts surface flushing and depth flushing at higher discharges than the equivalent transport equations for sand. The internal consistency of Mihous' approach was also tested. It was assumed that the β value of 0.021 (surface flushing of fines and sand) and 0.035 (depth flushing) would be equivalent to the discharge at which the d_{maxbl} and d_{50bl} (see Equations 8.25 and 8.26) would be 1.0 mm (sand) and 2.0 mm (gravel). Table 10.17 illustrates this relationship. It can be seen that in all cases, the β value predicts surface flushing and depth flushing at lower flow values than the equivalent flow at which motion begins for the 1.0 mm and 2.0 mm grain sizes.

Table 10.17 also shows the relationship between the maximum competence predicted from the Milhous equations (d_{maxbl} and d_{max50}) and the maximum competence calculated from the Yang, Ackers & White and Engelund & Hansen equations. It can be seen that for sites 1, 2 and 3, the d_{maxbl} predicts considerably lower competence than the three transport equations. However, at Site 4 the Milhous equations predict a higher competence maximum than the three transport equations. The comparison of the competence of the D_{50} and the maximum competence calculated from the three transport equations (Table 10.17) indicate the d_{max50} in most cases predicts a lower competence than the three transport equations. It appears that the d_{max50} is closer in value to the maximum competence predicted by the transport equations.

Table 10.17: Comparison of the Milhous approach to the transport equations approach for the Olifants River.

Site	β			β		d_{maxbl}			d_{max50}		
	¹Y	¹AW	¹EH	¹d_{maxbl}	¹d_{50bl}	²Y	²AW	²EH	²Y	²AW	²EH
1	H	H	H	L	L	L	L	L	L	L	L
2	H	H	H	L	L	L	L	L	L	L	L
3	H	H	H	L	L	L	L	L	L	L	L
4	H	L	H	L	L	H	H	L	L	H	L

1 L = β predicts surface flushing and depth flushing at lower flows than the equivalent for the transport equations, where Y is Yang, AW is Ackers & White and EH is Engelund & Hansen

H = β predicts surface flushing and depth flushing at higher flows than the equivalent for the transport equations, where Y is Yang, AW is Ackers & White and EH is Engelund & Hansen

2 L = d_{mxbl} and d_{max50} predict lower maximum competence than the equivalent for the transport equations

H = d_{mxbl} and d_{max50} predict higher maximum competence than the equivalent for the transport equations

Figure 10.34 provides the RBS values obtained for the Olifants River. Also shown is the β value calculated for the 0.021 (surface) and 0.035 (depth) flushing flows. These values represent the flow class at which the β value is 0.021 and 0.035 respectively. The tables displaying these results are available in Appendix H at the back of the thesis. The RBS values indicate that the Olifants River has an extremely stable bed. The RBS value predicts that sites 1 and 4 become unstable at the 99.99th percentile flow (i.e. the flow that is equalled or exceeded 0.01% of the time). At sites 2 and 3, however, the flow regime does not have the capacity to create the conditions necessary for channel instability, i.e. the RBS values predict that even under the highest flow conditions the D_{84} will not be mobilised.

If the values for the RBS are compared with the effective and dominant discharges, the values show a distinct difference. The effective and dominant discharges are well below the RBS values. It has already been mentioned that the transport equations generally estimated a poor relationship between the β value and the sand and gravel competent flows.

These results confirm the results from the three transport equations, these being that the Olifants River has an immobile bed and that there is unlikely to be any channel instability (based on the RBS calculations). However, the β index predicts that higher discharges are necessary to transport sand and gravel than the three transport equations and, in sympathy, predict lower competence for the given flow classes than the three transport equations. It has been noted earlier, however, that these two sediment-maintenance flushing flow methods should be used with caution.

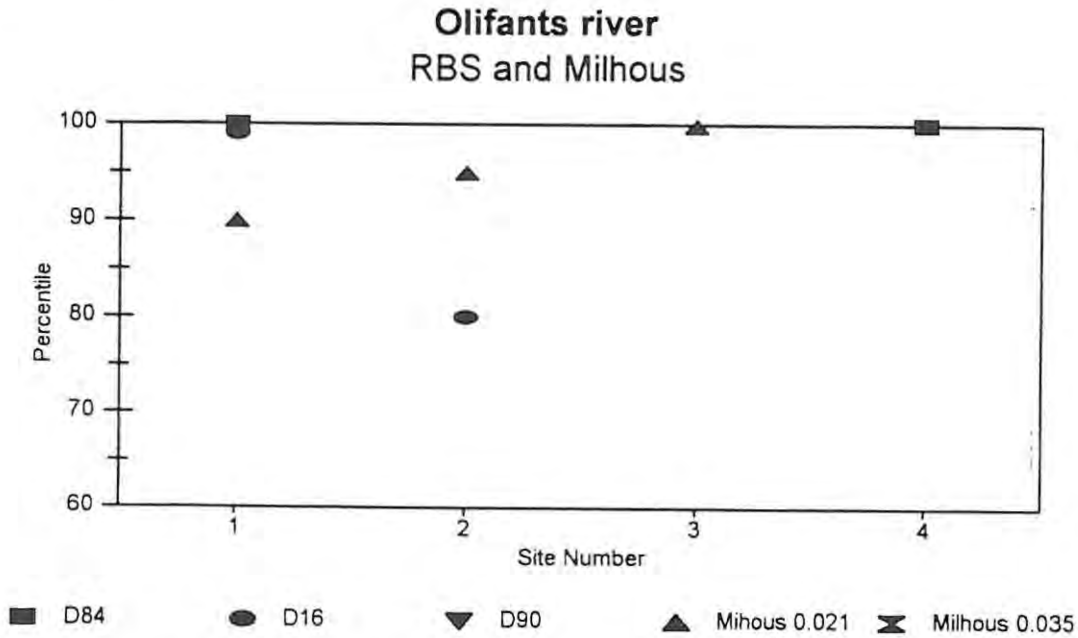

***Figure 10.34:** RBS values calculated for the Olifants River. The β value calculated for the 0.021 (surface) and 0.035 (depth) flushing flows. These values represent the flow class at which the β value is 0.021 and 0.035 respectively.*

10.3.6.1 Effective discharge for sand, gravel and cobble

The effective discharge for sand, gravel and cobble was calculated in the same manner as for the Mkomazi and Mhlathuze Rivers. Figure 10.35 demonstrates that the percentage bed material transport for the effective discharge flow class is lower for sand, followed by gravel and cobble. Furthermore, it is only at Site 2 and 3 that the effective discharge transports cobble. The results indicate different effective discharges and different effective discharge flow classes for sand, gravel and cobble (Table 10.18). The effective discharge for the sand class is generally lower than that for gravel and cobble. This is to be expected as sand transport occurs over a wider range of flow classes than does gravel and cobble. This technique provides a useful means of setting sediment-maintenance flows, as it does not rely solely on incipient motion, but includes the duration dimension. It is suggested that this technique is more appropriate than the Milhous or RBS approach.

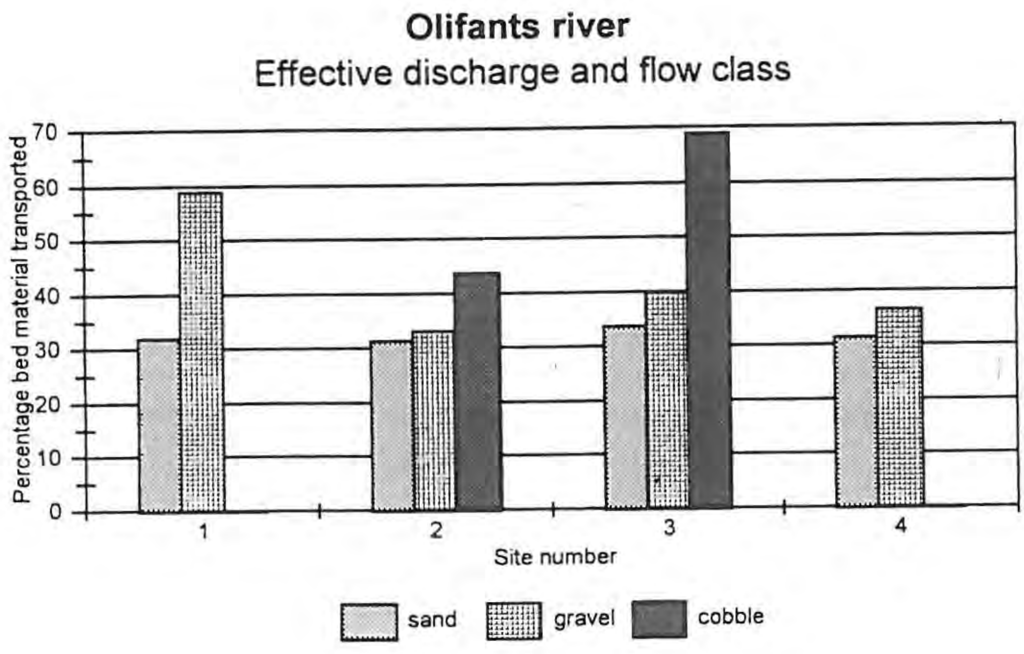

Figure 10.35: The percentage bed material transported by the effective discharge for the Olifants River for sand, gravel and cobble for the Yang equation.

Table 10.18: Effective discharge flow classes for the Olifants River for sand, gravel and cobble for the Yang equation.

Site	Sand (flow class)	Gravel (flow class)	Cobble (flow class)
1	5-1%	5-1%	-
2	5-1%	5-1%	5-1%
3	1-0.1%	1-0.1%	0.1-0.01%
4	1-0.1%	1-0.1%	-

10.3.7 Implications for Instream Flow Requirements (IFRs)

The results generated from the analysis of the Olifants River can be used to make recommendations for IFRs for the Olifants system. It is argued that the Olifants system is strongly controlled by bed rock and that little channel change is likely to occur. It has also been pointed out that the coarse bed material is mobile only under the highest flow conditions. At some sites, the armour-layer remains immobile even under the highest flows generated by the predicted virgin flow conditions. This situation is almost certainly likely to exist under the present-day regulated flow environment. This is despite the fact that all of the sites on the Olifants generate high unit stream power. The high unit stream power allows for transport of the finer portion of the bed material at lower flow classes, and hence the effective discharges are lower than those calculated for the Mhlathuze River. It can be argued that the regulated flow environment has had little impact on the channel morphology, and the channel maintenance flow is probably the 1 in 20 year flood which is able to mobilise the entire bed. The objectives of the IFR are therefore different to those stated for the Mhlathuze. The following flow objectives might be set:

- to periodically remove fine sediment from the gravel and cobble substrate;
- to periodically move gravel through the coarse cobble-bed; and
- to ensure that large flood events (1 in 20 years) are allowed to move through the system to ensure that the subsurface material is turned over and thereby maintain a loose bed structure.

It is important to point out that in a system such as the Olifants, where boundary resistance to flow deformation is strong, morphological features such as the estimated bankfull discharge should be used with caution in setting IFRs. In these systems the estimated bankfull discharge is not necessarily the same as the effective discharge or the dominant discharge. Given this scenario, it is probably wise to recommend two sets of effective discharge: first, an effective discharge that achieves the first two objectives outlined above; and second, a 'reset' discharge, a large flood event that serves as the channel forming discharge.

10.4 Summary and conclusions

The results presented have indicated that the approach that has been adopted in determining the magnitude and frequency of channel forming discharge and sediment-maintenance flushing flows can be applied in a meaningful way to regulated rivers. This section will consider the results in the light of the research questions posed at the beginning of the chapter. The first research question posed was *Do the results obtained from the two regulated systems add to the understanding gained from the Mkomazi?* It is argued that the channel morphology and bed material transport in the Mhlathuze River have been considerably altered by the regulated flow environment imposed by the Goedertrouw Dam. This has resulted in channel narrowing and deepening immediately below the dam, and channel aggradation downstream of major sediment inputs from tributaries. The Olifants River on the other hand shows a high degree of resilience to change, probably due to the strong bed rock control of the channel boundary and the coarse heterogenous bed. Indeed little change is likely to occur other than possible further channel armouring or aggradation. Aggradation is unlikely given the high unit stream power generated in the Olifants system even under low flow conditions. It is probable that the Olifants system is supply-limited and that the coarse bed material is a reflection of this state.

The second research question that was posed was, *What is the impact of flow regulation on the relationships, and are the observed morphological conditions related to virgin flow conditions or to the regulated present-day conditions?* It has been demonstrated that for the Mhlathuze, the present observed morphological relations are related to present-day flow conditions. It has also been suggested that the Olifants system is a more resilient system, and that the observed morphological conditions are likely to be more permanent given the strong bed rock control in the channel perimeter.

The third research question posed was, *What lessons can be learnt for Instream Flow Requirements (IFRs)?* It is important to realise that fluvial systems may respond very differently to a regulated flow environment. Both the Mhlathuze and Olifants systems display highly variable hydrological regimes under virgin flow conditions (CV of 0.93 and 0.70 for the Mhlathuze and Olifants Rivers respectively), and yet they respond very differently to the imposed change. The Mhlathuze shows major geometry and bed material transport capacity changes, while the Olifants indicates very little adjustment. It would appear that channel boundary conditions are of great significance in determining the impact of flow regulation. This must be taken into account when setting IFRs.

The final research question was, *Given the results obtained, what flows should be recommended and why?* It has been suggested that for the Mhlathuze, different flows should be recommended for the site immediately below the Dam, and for those sites downstream of the major tributaries. Where tributary inputs of discharge and sediment occur, bed mobility conditions and degree of human impact need to be taken into consideration. It is argued that flows should be set close to the effective discharge to ensure that the amount of sediment entering a channel reach is equivalent to the amount of sediment exiting a reach (i.e. an equilibrium state). Two sets of effective discharges were recommended for the Olifants system: first, the effective discharge that would ensure that fine material, sand and gravel would be flushed through the system thereby preventing fine material entering the interstitial zone. Second, that high magnitude low frequency 'reset' flood events should be allowed to move through the system to ensure that bed is overturned occasionally, thereby maintaining the channel form.

Chapter 11: Discussion, Synthesis and Conclusions

11.1 Introduction

The title of this thesis is 'the determination of geomorphologically effective flows for selected eastern sea-board rivers in South Africa'. This thesis has attempted to achieve this by adding value to the theoretical and applied understanding of the magnitude and frequency of channel forming discharge for selected southern African rivers. The methods developed and results achieved using the magnitude-frequency approach have been presented in the previous five chapters (Chapters 6 to 10). These were developed in the context of conventional fluvial wisdom (Chapters 2, 3 and 4). This chapter will aim to synthesise the results within the framework of the research objectives outlined in Chapter 1, and to discuss their implications for river management in southern Africa, with particular reference to Instream Flow Requirements (IFRs). The research products and recommendations for future research are also discussed.

The objectives as outlined in Chapter 1 were:

Objective 1: *To review the literature to assess the limitations of fluvial geomorphological knowledge in southern Africa.*

Objective 2: *To use cross-sectional data, bed material class, hydrology, hydraulics and relevant bed material transport equations to assess the relationship between channel form and bed material transport to flow discharge for selected rivers.*

Objective 3: *To determine the magnitude and frequency of channel forming discharge by determining the natural bankfull discharge with respect to channel form for selected rivers.*

Objective 4: *To develop a model of channel forming discharge for selected rivers.*

11.2 Objective 1 - To review the literature to assess the limitations of fluvial geomorphological knowledge in southern Africa.

In Chapter 2, a discussion on the state of knowledge of southern African fluvial systems was presented. The review highlighted the fragmentary state of knowledge of modern channel processes and process-form relationships for southern African rivers. However, it revealed that there is generally good information at a macro-scale on the origins of many of southern Africa's fluvial systems. Many southern African fluvial systems have undergone major changes in form, geographical position, flow and sediment load during the Gondwana and post-Gondwana era in the last 180 million years. This has been in response to both climate change and tectonic activity. It is evident that the past has left an imprint on modern channels, and this needs to be accounted for in seeking to understand how modern southern African fluvial systems function. This is particularly significant as regards two factors: the nature of river long profiles, and the importance of the palaeoflood regime and climatic variability.

First, it was noted that many of southern Africa's fluvial systems display irregular long profiles. For management purposes, this irregularity has made it necessary to divide fluvial systems into macro-reaches, with each macro-reach displaying a distinct reach type and channel pattern (Rowntree & Wadeson, 1999). These macro-reaches are usually separated by means of major breaks in slope and/or geology. It is argued that these irregular profiles probably result from variable rock-type and, for the eastern sea-board rivers, tectonic activity during the Miocene and the Pliocene. The lack of a smooth profile suggests that local controls are significant, as rivers may adjust over short distances where the banks are easily erodible, but the whole channel will not be adjusted to its water and sediment discharge. Furthermore, many of southern Africa's fluvial systems are strongly or partly controlled by bed rock. It is therefore advanced that conventional fluvial wisdom developed from research on alluvial systems in temperate climates should not be directly applied to the southern African environment.

Second, research on South African palaeoflood hydrology has shown that periods of above and below average flooding have occurred, with concomitant changes in sedimentation patterns in the recent past. Long-term cycles have been shown to be related to Quaternary glacial and interglacial cycles, but shorter term cycles occur within stadia and inter-stadia periods (Dollar & Goudie, 2000). Furthermore, it has recently been argued that discharge records from the Zambezi River reflect an 80-year oscillation in response to the Gleissberg sun-spot cycle (McCarthy *et al.*, 2000). These cyclical climate changes have significant implications for sediment storage and channel geometry.

Zawada *et al.* (1996) have submitted that the current flood regime for most South African rivers is a recent one, having only come into existence around 1850. The significance of this is evident. If indeed the flow environment in South Africa is a recent one, one would expect that fluvial systems are still adjusting to the new flow regime. If there are smaller, more frequent cycles within this record (for example Gleissberg cycles of 80 years or the 18-year rainfall cycle which is reflected in the flow record) this further complicates an already complex and dynamic situation. Many South African fluvial systems are highly regulated systems and are therefore also adjusting to an imposed regulated flow regime. The implications thereof are immense, specifically in terms of channel morphology, sediment transport and aquatic habitat. It is within this historical template that modern southern African fluvial systems should be assessed.

The review also highlighted the fragmentary nature of current knowledge of modern fluvial system processes. This has begun to be addressed with the advent of channel process studies which were initiated in southern Africa in the late 1980s and early 1990s. The paucity of information relating to the magnitude and frequency of the channel forming discharge has proved a severe limitation of modern channel studies in southern Africa. Newson (1996) notes that South African rivers cannot be 'made-to-fit' the models of alluvial channels of humid regions, particularly given the predominant combination of unpredictable droughts and a steep flood curve. This is particularly relevant to this discussion, as southern African fluvial systems display a highly variable hydrology.

It is clear from the preceding discussion that an indigenous understanding of how southern African fluvial systems function is of importance, as the approach taken to understanding fluvial systems has major implications for management. A classic example of this is the previously stated legal case in the United States (Gordon, 1995), where Luna B. Leopold and Stanley M. Schumm presented conflicting evidence regarding the water requirements of the Platte River in Colorado. Their approaches to assessing the river's water requirements differed fundamentally and therefore the methods that each applied and the answers that were subsequently generated were inconsistent (see Table 11.1). There is a danger that unless fluvial systems are understood in their proper context, within appropriate spatial and temporal time-scales, that an inadequate understanding of their physical functioning will be developed, resulting in the systems being poorly managed. This is of course a question of perspective. It is the opinion of the author that all these factors must be considered when attempting to understand the magnitude and frequency of channel forming discharges for southern African rivers, particularly when selecting or recommending a flow regime that will best 'mimic' the 'natural' flow regime (IFRs for example).

Table 11.1: Summary of points made by the United States and Opposition on sediment movement in mountain streams (modified after Gordon, 1995).

United States (Leopold position)	Opposition (Schumm position)
Sediment supplied were of sufficient quantity to fill in the channels if maintenance flows were not provided.	The amount of sediment supplied by the mountain streams was very small and mostly wash load. Only small flows, if any, were needed to move this sediment.
Materials forming the stream boundaries were able to be moved at bankfull flows or less.	The stream boundaries were composed of coarse materials which would not move at bankfull flow.
The streams were hydraulically controlled, meaning that a unique relationship exists between discharge and the amount of sediment transported. If flows were reduced, but sediment supply remained the same, then aggradation would occur.	The streams were supply-limited, meaning there was less sediment available than the streams could carry. Flows could be reduced and the streams would still be able to carry the sediment load.

11.3 Objective 2 - To use cross-sectional data, bed material class, hydrology, hydraulics and relevant bed material transport equations to assess the relationship between channel form and bed material transport to flow discharge for selected rivers.

The concept of a relationship between channel form, bed material transport and flow discharge has been discussed at length in Chapter 3. It is appropriate here to highlight the most salient points before discussing this relationship with regard to the Mkomazi, Mhlathuze and Olifants Rivers. Theories of channel formation and maintenance fall within two basic models. The first arises from the hydraulic geometry approach as applied to sand and gravel-bed alluvial rivers and has been developed by the 'Leopold' school of thought. It argues that 'rivers are the authors of their own geometry', and that over time rivers will adjust their dimensions to convey the intermediate flows and associated sediments within their banks i.e. those which occurred a few times a year on average. Very large flows occur too infrequently and very small flows carry too little sediment to shape the active channel. This model considers the bankfull flow, that flow that just reaches the level of the floodplain, to be the channel forming discharge. This is closely coincident with the effective discharge, the flow that carries the most sediment over a long period of time. Bankfull flow is thought to occur approximately 1 to 2 years on average. This first model rests on the assumption that an alluvial river can be considered to be in quasi-equilibrium. Over a reasonable period of time, a river in quasi-equilibrium will deliver the same amount of sediment downstream as is supplied to it from the upstream catchment. If this balance is upset, then the river would be in disequilibrium, and hence instability and channel adjustment will occur.

The second model, the 'Structural' model, is one which has been applied to bed rock or partially bed rock controlled rivers, to steep mountain rivers, or to dryland type rivers with a highly variable climate and hydrological regime. These types of rivers are not fully adjustable and are unlikely to be in equilibrium with the imposed flow. Their dimensions and form are often influenced by non-fluvial factors including bed rock, large boulders, or structural features such as faulting. The structural model postulates that these rivers are formed by floods much larger than the bankfull event (as suggested by the Leopold model). In the Platte River in the United States, Harvey (cited in Gordon, 1995) has referred to 'courses of convenience' and 'relic channel' to describe a channel with bed material that is immobile under frequently occurring flows. Smaller material that is washed into streams during storm events can easily be transported by relatively low flows. It is argued that these streams do not carry a high bed material load relative to their transport capacity and are therefore supply-limited. In these channels no relationship exists between the dimensions of the channel perimeter and the frequently occurring flows, this may be because the rivers were shaped by some past event, such as a mega-flood or glacial action.

River managers should be aware of these contrasting process-response models as applied to alluvial and non-alluvial channels. The response to flow regulation or to a change in sediment load is likely to differ in each channel type. In alluvial channels, any change to the flow regime is likely to result in channel adjustment as the system adjusts to a modified discharge. Where the flow regime is regulated such that the magnitude and frequency of flows are reduced, and yet sediment continues to enter the channel from upstream areas and tributaries, it is likely that sediment will accumulate and vegetation will encroach into the channel, thus creating a reduced channel capacity adjusted to the less frequent flood flows. This will in turn exacerbate the impact of flooding by high magnitude events. When high flows do pass through the impacted sites, accelerated stream channel erosion, deposition, lateral migration and/or avulsion may result.

Non-alluvial channels are less likely to adjust their channel form in response to flow regulation. A regulated flow environment which reduces the magnitude of the annual and more frequent floods will not have a major impact, as these smaller flows are simply not 'effective'. Channel maintenance is performed by large floods which are less likely to be affected by flow regulation. In this sense, these channels can be regarded as being resilient, as within threshold limits, the river is able to accommodate changes in the flow and sediment regime without experiencing major alterations.

An awareness of these two contrasting models is of critical importance to understanding and managing southern African fluvial systems. The above discussion begs the question, which model best applies to southern African fluvial systems? Results from the Mkomazi River have shown that no relationship exists between the bankfull discharge and the hydrological regime, the effective discharge and the dominant discharge. However, there does appear to be good agreement between the inundation stage of the bench and the 0.9 year and 2.0 year return period on the partial duration series, and the bench and the dominant discharge and effective discharge as calculated by the Yang equation. The effective discharge as calculated by the three transport equations for each of the sites for the Mkomazi is shown to be in the 5-0.1% range on the 1-day daily flow duration curve. The upper two but one flow classes account for the bulk of the bed material transported (>80%). It has therefore been argued that no single effective discharge exists for the Mkomazi River, but rather that there are a range of effective discharges that are responsible for bed material transport.

It has also been pointed out that only large floods with average return periods of around 20 years generate sufficient stream power and shear stress to mobilise the entire bed. These large floods inundate the terraces. It has therefore been suggested that, for the Mkomazi River, it may be instructive to think in terms of two sets of effective discharges. First, a range of discharges that transport the most bed material over a long period of time and approximate a 'bench-full' discharge, and second, a 'reset' discharge, i.e. large floods with return periods in the 20 year range that are able to mobilise the entire bed and serve as channel maintenance discharges for the entire bed as well as the macro-channel.

The author has cautioned that it is hazardous to use morphological features such as the bankfull stage against which to pin the channel maintenance flood. In the case of the Mkomazi, the estimated bankfull discharge is not the same as the dominant discharge or the effective discharge. Discharges relating to the lower bench may be more significant. Thus for the Mkomazi it appears that the 'Leopold' model is inappropriate. The Mkomazi does not 'fit' the second model either, in that the results show that although large floods are important in the Mkomazi (as it is these floods that are able to mobilise the entire bed and reset the whole channel), there are also a range of discharges in the 5-0.1% range on the 1-day daily flow duration curve that are responsible for the bulk of the bed material transport. It is argued that this bi-polar type flood frequency curve may be responsible for the gross channel architecture. The macro-channel is maintained by the large flood events, and the active channel is maintained both by the range of effective discharges and the 'reset' discharges. These are the geomorphologically 'effective' flows.

The techniques and methods that were developed for the unregulated Mkomazi River were then applied to two highly regulated systems, the Mhlathuze and Olifants Rivers. Results from the Mhlathuze River have indicated that the Goedertrouw Dam has had a considerable impact on the downstream channel morphology and bed material transport capacity and consequently the effective and dominant discharges. It has been suggested that the Mhlathuze River is now adjusting its channel geometry in sympathy with the regulated flow environment. Utilising the present-day flow regime, it was noted that there appears to be a good relationship between estimated bankfull discharge and dominant discharge. This is a function of the hydrological regime of the Mhlathuze which has a markedly skewed flood frequency curve, due to the occurrence of cut-off low pressure systems which cause regular flooding in northern KwaZulu-Natal. Under the present-day regulated flow environment, the discharge volumes and peaks have been reduced. This has resulted in an increase in return period inundation levels (for example, the estimated bankfull discharge average return flow is 3.7 years under present-day conditions as opposed to 2.6 years for virgin flow conditions), but a reduction in the effective discharge with concomitant reductions in unit stream power and boundary shear stress. Under present-day conditions it has been demonstrated that the total bed material load has been reduced by up to three times, but there has also been a clear change in the way in which the load has been distributed around the duration curve. Under present-day conditions, over 90% of the total bed material load is transported by the top 5% of the flows, whereas under virgin flow conditions 90% of the total bed material load was transported by the top 20% of the flows.

It appears that the Mhlathuze River fits neither the 'Leopold' nor the 'Structural' model. There appears to be no relationship between the estimated bankfull discharge, the dominant discharge and the effective discharge. The effective discharge is in excess of estimated bankfull discharge and dominant discharge. The Mhlathuze does not fit the second model either, in that the river is not controlled or semi-controlled by bed rock, all flows are competent to transport the bed, and the channel perimeter is capable of freely changing its form in response to the imposed discharge and sediment regime. It is the author's opinion that this disequilibrium is probably a function of the regulated flow regime, but this remains untested.

The Olifants River is steep bed rock controlled system with coarse bed material. The estimated bankfull discharge has an average return period of 5.8 years on the annual series, which is considerably higher than the conventional wisdom suggested by Leopold (1997). Furthermore, there appears to be no relationship between the estimated bankfull discharge and any hydrological statistic. The effective discharge flow class is in the 5-0.01% range on the 1-day daily flow duration curve. The upper three flow classes account for over 60% of the bed material transported at each of the sites, while over 90% of the bed material is transported by flows that are equalled or exceeded by the 20th percentile flow or greater. It has also been pointed out that even the highest flows simulated for the Olifants River do not generate sufficient energy to mobilise the entire bed. It is useful to consider the Olifants River as being adapted to a highly variable bi-polar type flood regime. It is erroneous to think of one 'effective' discharge, but rather a range of effective discharges are of significance.

The importance of thresholds and initiation of motion in assessing the impact of flow regulation should not be underrated. Where coarse gravel- or cobble-bed rivers occur, even minor reductions in flow may be sufficient to retard bed material transport if shear stress or stream power fall below a critical level. Critical shear stress and stream power may not be as significant in mobile sand-bed channels such as the Mhlathuze, but they are highly significant in coarse-bedded channels. It is thus instructive to consider the significance of flow reduction not only in terms of volume and duration, but also in terms of magnitude.

11.4 Objective 3 - To determine the magnitude and frequency of channel forming discharge by determining the natural bankfull discharge with respect to channel form for selected rivers.

It has been demonstrated that it is erroneous to simply apply a morphological criterion such as the bankfull discharge as the channel forming discharge in regulated systems, or systems controlled or partly controlled by bed rock. It has been argued that where possible (for example in true alluvial systems), fluvial systems will adjust their geometry in sympathy with an imposed regulated flow regime. To set an IFR based on morphological criteria in these regulated systems may well have the effect of entrenching and accelerating morphological change. In controlled or semi-controlled systems, it is likely that the resistance of the boundary to erosion overrides the significance of a bankfull equilibrium stage. The inset bench in the active channel is probably related to reconstruction following the last flood event and is therefore unlikely to be an equilibrium form. It is therefore argued that using morphological features on which to pin a channel maintenance flow should be avoided.

11.5 Objective 4 - To develop a model of channel forming discharge for selected rivers

It would appear from the results of research on the Mkomazi, Mhlathuze and Olifants Rivers that neither model of channel adjustment adequately reflects the southern African situation. There are a number of reasons why this may be so. Many of southern Africa's fluvial systems are bed rock or partially bed rock controlled and flow within confined macro-channels with an inset active channel. Inset within the active channel is often a channel bench (Figure 2.3). It is argued that this channel form is a response to climatic history, tectonic history and a highly variable flow regime. It is possible that some highveld rivers, such as the Olifants, have an immobile coarse armour or pavement that may have been a response to a previously wetter climate with larger, more frequent floods. If this is the case then cognisance must be taken of this when setting a regulated flow regime.

It may be more useful to develop a third model for southern African rivers, one placed somewhere between the 'Leopold' alluvial model and the 'Structural' model. This model would argue that two sets of effective discharges are of significance. First, a range of effective discharges in the 5-0.01% flow duration class that are responsible for the bulk of the bed material transport and largely determine the morphological adjustment of the active channel; and second, a 'reset' discharge, composed of the large floods that occur on average every 20 years or so which maintain the macro-channel and mobilise the entire bed, thus 'resetting' the system. These two categories of effective discharge will have different outcomes in bed rock controlled or semi-controlled systems and alluvial systems. It is suggested that because of the 'resetting' it is unlikely that the active channel will achieve a true equilibrium form, but that rather it is constantly being reconstructed after major events, hence the ubiquitous inset channel benches.

11.6 Implications for science of fluvial geomorphology

The results indicate that the three rivers under consideration fall into the category of two-stage channels (macro-active channel) that have been discussed earlier in the thesis (see Chapter 3). Although these channels are more confined, their architecture suggests that they are similar to the rivers draining the lowveld of southern Africa (cf. van Niekerk & Heritage, 1993; Rowntree & Wadeson, 1999), the seasonal tropics in India (cf. Gupta, 1995) and those in eastern Australia (cf. Erskine & Warner, 1998) in that there is a nested channel pattern with a clear distinction between the active and macro channel.

The atmospheric conditions of these regions generates a highly varied flow pattern (seasonally and decadal) (cf. the discussion on FDR/DDR's in Chapter 3) and consequently the channel architecture is characterised by a nested two-stage channel. There is need for further research which aims to link form to process in these systems, and to determine the extent to which boundary resistance affects channel form.

11.7 Implications for river management

These results have a number of implications for river management in southern Africa. Currently, protection of the river resource is sought through application of the Resource Directed Measures of the Department of Water Affairs and Forestry, operationalised through the Ecological Reserve determination process. For large developments this has been achieved through defining the Instream Flow Requirement (IFR) of a river using the Building Block Methodology (BBM). The BBM seeks to determine the flow regime required to maintain the river at some pre-determined conservation status (King & Louw, 1998). The BBM method is based on the concept that the stream ecosystem is adapted to a range of flows that are categorised into three groups: low flows, freshes, and floods (King & Louw, 1998). As mentioned earlier, Rowntree & Wadeson (1999) have suggested that three basic problems require information for IFRs: flows that maintain the spatial and temporal availability of habitats, the maintenance of substratum characteristics, and the maintenance of channel form. Rowntree & Wadeson (1999) have developed the hydraulic biotope concept to account for the information needs of the first problem. The latter two information requirements can be achieved by utilising the magnitude-frequency approach. These two information needs are related to the freshes and flood flow groups for the BBM.

It has been suggested that the geomorphologist's first task in the IFR assessment is to estimate the range of flows necessary to maintain channel form and to predict the morphological changes that are likely to occur (cf. Rowntree & Wadeson, 1997). This 'channel maintenance' flow has been difficult to predict, as no information has been forthcoming in southern African. In the past, common practice has been to apply the alluvial model, defining the channel forming discharge as that which equates to the bankfull level, often taken as the bench where this is clearly the most active feature. It is argued that data can be generated to satisfy this information requirement by applying the technique whereby the relationship between effective discharge, dominant discharge and channel morphology is determined. For the Mkomazi River, for example morphological adjustment will occur unless flows are recommended that are able to transport the same amount of material exiting a reach as that entering the reach. The most effective range of flows are in the 5-0.1% range. This implies a magnitude as well as a duration. It is also argued that it is necessary for large floods to be allowed to move through the system as a 'reset' discharge, for the reasons mentioned above.

The second way in which this research contributes to southern African river management is through identifying the range of flows that are necessary for the maintenance of substratum characteristics. This information requirement is closely linked to the maintenance of channel form, and the two are difficult to separate. However, in this thesis the maintenance of substratum characteristics refers to the seasonal flushing of finer sediments from the bed. A number of methods have been tested for the Mkomazi, Mhlathuze and Olifants Rivers. It was been shown that the use of these methods in isolation can generate meaningless results, as they have often been developed for one channel type (alluvial for example) and thus cannot be applied to other channel types (gravel or cobble-bed for example). It is important that these methods are used circumspectly, and that each method is used in rivers similar to those from whence they are derived.

11.7.1 Methodological issues

A number of considerations arise from the methods used for this research. These relate to the nature of the bed material transport equations used, to the determination of sediment-maintenance flushing flows, to the relevance of using the dominant discharge and effective discharge approach, and to the significance of morphological features. Each of these will be addressed in turn.

For the purposes of this research, three bed material transport equations were used. The rationale behind choosing them has been discussed in Chapter 8. It must be re-emphasised that these equations should be only be used in the physical environment (i.e. channel type) for which they were developed. The Engelund & Hansen model, for example, is unsuitable for anything other than sand-bed rivers. The data requirements to run these models are fairly intensive and costly to procure, and the computation procedures are long. The equations all generate different absolute values, but often show similar trends. It is recommended that attention is paid to these trends rather than assigning precision to the results. It was pointed out in Chapters 4 and 8 that a number of assumptions need to be made when using these equations. The scientist must be aware of the limitations of the models. It is recommended that either the Yang or the Ackers & White model be applied for rivers which have a coarse gravel-bed. For alluvial sand-bed rivers, it is possible to apply either the Yang or the Engelund & Hansen model. It may be possible at some further stage to calibrate these equations for selected southern African rivers, but this requires measured bed load data which does not exist at present.

The second important consideration is that the methods used for determining sediment-maintenance flushing flows should be used with extreme caution. The Milhous and RBS approaches were developed for individual rivers, thus limiting their extrapolation potential. It is recommended that the sediment-maintenance flushing flows are calculated using the effective discharges for different grain-sized classes using the bed material transport equations. This is recommended for two reasons. First, they were developed from a broader data set, and second, the flushing flows for different grain-sized classes account for incipient motion as well as duration.

The third point of discussion is the relevance of the dominant discharge and effective discharge approach. It is argued that the effective discharge provides a very useful approach to identifying those flows which are significant for particular channel types. The dominant discharge of Marlette & Walker (1968) is computed from the flow classes, and although it provides a useful average discharge that transports 50% of the bed material, it does not account for the fact that there are a range of flows that can be considered to be effective. Therefore it can be argued that the effective discharge approach which considers the effect of each flow class separately is perhaps more appropriate. The use of the cumulative curves for displaying the flow range over which most bed material is moved is particularly effective in this regard.

The fourth consideration is the significance of morphological features. One of the limitations of the thesis was correctly identifying the in-channel morphological features. Of particular significance is the refinement of the definition of in-channel features in an objective way and then to associate them with flow and process. Of great importance is the correct identification of the bankfull discharge and the 'bench-full' discharge. With more data it may be possible to relate particular features to salient channel characteristics (degree of bed rock influence, channel gradient etc) both within a river and between rivers. In regulated systems, or in systems recovering from a major reset event, the bench is probably the new bankfull stage. Active channel incision or widening may result in an exaggerated estimate of the bankfull event. It is thus evident that the discharge related significance of morphological features identified in the field is often unclear. It is recommended that, in setting IFRs, a combination of an interpretation of the morphological features present and calculation of the effective discharge is used. This provides a useful means of identifying whether the river under consideration has in fact adjusted its geometry in sympathy with the regulated flow. Flow objectives can then be set depending on whether restoration to the 'natural state' is required, or whether maintaining the status quo is acceptable.

11.8 Research products and recommendations for future research

Two major products have been developed during this research. The first is a set of methods and techniques that have been developed and tested to identify the range of flows necessary to maintain channel form and equilibrium for selected southern African rivers. The second product is that geomorphologists now have a better understanding of the range of flows that maintain channel form for southern African rivers. It was argued earlier that a major problem in river management is an inadequate understanding of the role of bed material transport in rivers. This research has gone some way to answering a number of questions. It has, however, also highlighted others.

There are a number of ways in which this research can be carried forward. First, the method has been applied successfully to three rivers that are reasonably representative of the eastern-sea board rivers, however, application of the method to other rivers (such as rivers in the Western Cape or more arid systems in the Karoo) would generate further useful information. Second, it would be helpful to install bed load monitoring devices, such as bed load traps, to generate base-line data. These data will be invaluable in the future. It may also serve to provide input data so that bed load transport models can be developed and/or calibrated for southern African rivers. Third, it would be useful to streamline the method that was developed in this thesis. While the method provides useful information, it is time consuming. Developing a computer-based program to improve the efficiency and accessibility of the method is recommended.

11.9 Conclusion

In conclusion, the objectives of this thesis and the extent to which they have been achieved are presented in Table 11.2.

Table 11.2: Objectives and achievements of the thesis.

Objective	**Achievement**
To review the literature to assess the limitations of fluvial geomorphological knowledge in southern Africa.	Review of present state of knowledge has been achieved.
To use cross-sectional data, bed material class, hydrology, hydraulics and relevant bed material transport equations to assess the relationship between channel form and bed material transport to flow discharge for selected rivers.	Relationship between channel form and bed material transport is not always clear. Effective discharge, dominant discharge and bankfull discharge are not necessarily the same flows. Channel forming discharge is related to a set of flows: a range of effective flows between 5-0.01% on the 1-day daily flow duration curve; and 'reset' flows, floods with an average return period of around 20 years.
To determine the magnitude and frequency of channel forming discharge by determining the natural bankfull discharge with respect to channel form for selected rivers.	Morphological features should be used with caution in attempting to define channel forming or sediment-maintenance flushing flows, as southern African rivers have been highly regulated and bed rock control is strong.
To develop a model of channel forming discharge for selected rivers.	Southern African fluvial systems do not fit traditional paradigms of fluvial knowledge. Indigenous knowledge needs to be developed to cater for distinctive southern African fluvial systems.

Reference list

Ackers, P. 1972. River regime: research and application, *Journal of the Institute of Water Engineers*, 26, 257-281.

Ackers, P. 1993. Sediment transport in open channels: Ackers & White update, *Proceedings of the Institution of Civil Engineers Water Maritime and Energy*, Water Board Technical Note 619, 101, 247-249.

Ackers, P. & Charlton, F.G. 1970. Meander geometry arising from varying flows, *Journal of Hydrology* 11, 230-252.

Ackers, P. & White, W.R. 1973. Sediment transport: A new approach and analysis, *Journal of the Hydraulics Division*, American Society of Civil Engineers 99 (HY11), 2041-2060.

Arnell, N.W. 1992. Impacts of climatic change on river flow regimes in the UK, *Journal of the Institute of Water and Environmental Management* 6, 432-442.

Alexander, W.J.R. 1976. *Flood frequency estimation methods*, Technical Note 65, Department of Water Affairs, Government Printer, Pretoria.

Alexander, W.J.R. 1979. *Some unsolved problems in river flow*, Department of Water Affairs Technical Report TR 89, Department of Water Affairs, Government Printer, Pretoria.

Allen, J.R.L. 1974. Reaction, relaxation and lag in natural sedimentary systems: general principles, examples and lessons, *Earth Science Reviews* 10, 263-342.

Alonso, C.V. 1980. Selecting a formula to estimate sediment transport capacity in non-vegetated channels, In; Knisel, W.G. (Ed), *CREAMS: A field scale model for Chemicals, Runoff and Erosion from Agricultural Management System*, U.S. Department of Agriculture, Conservation Research Report 26, 426-439.

Anderson, M.G. & Calver, A. 1977. On the persistence of landscape features formed by a large flood, *Transactions of the Institute of British Geographers* N52, 2, 243-254.

Andrews, E.D. 1980. Effective and bankfull discharges of streams in the Yampa River basin, Colorado and Wyoming, *Journal of Hydrology* 46, 311-330.

Andrews, E.D. 1983. Entrainment of gravel from naturally sorted river bed material, *Geological Society of America Bulletin* 94, 1225-1231.

Andrews, E.D. 1994. Marginal bed load transport in a gravel bed stream, Sageten Creek, California, *Water Resources Research* 30, 2241-2250.

Andrews, E.D. & Nankervis, J.M. 1995. Effective discharge and the design of channel maintenance flows for gravel-bed rivers, In Costa, J.E.; Miller, A.J.; Potter, K.P. & Wilcock, P.R. (Eds.), *Natural and anthropogenic influences in fluvial geomorphology*, American Geophysical Union Monograph 89, 151-164.

ASCE, Task Committee. 1992. Sediment and aquatic habitat in river systems, *Journal of Hydraulic Engineering* 118, 5, 669-687.

Ashmore, P. 1991. Channel morphology and bed load pulses in braided gravel-bed streams, *Geografiska Annaler* 73A, 37-52.

Ashmore, P.E. & Day, T.J. 1988. Effective discharge for suspended sediment transport in streams of the Seskatchewan river basin, *Water Resources Research* 24, 864-870.

Ashworth, P.J. & Ferguson, R.I. 1989. Size selective entrainment of bed load in gravel bed streams, *Water Resources Research* 25, 627-634.

Ashworth, P.J.; Ferguson, R.I.; Ashmore, P.E.; Paola, C.; Powell, D.M. & Prestegaard, K.L. 1992. Measurements in a braided river chute and lobe. 2. Sorting of bed load during entrainment, transport and deposition, *Water Resources Research* 28, 1887-1896.

Bagnold, R.A. 1966. An approach to the sediment transport problem from general physics, *United States Geological Survey Professional Paper 422-J*.

Bagnold, R.A. 1973. The nature of saltation and of bedload transport in water, *Proceedings of the Royal Society of London* A332, 473-504.

Bagnold, R.A. 1980. An empirical correlation of bedload transport rates in flumes and natural rivers, *Proceedings of the Royal Society of London Series* A 372, 453-473.

Baker, V.R. 1973. Paleohydrology and sedimentology of Lake Missoula flooding in eastern Washington, *Geological Society of America Special Paper 144*.

Baker, V.R. 1977. Stream-channel response to floods, with examples from central Texas, *Geological Society of America Bulletin* 88, 1057-1071.

Baker, V.R. 1988. Flood erosion, In Baker, V.R.; Kochel, R.C. & Patton, P.C. (Eds.), *Flood geomorphology*, Wiley, New York, 81-95.

Baker, V.R. & Costa, J.E. 1987. Flood power, In Mayer, L. & Nash, D (Eds.), *Catastrophic flooding*, Allen and Unwin, London, 1-22.

Baker, V.R. & Pickup, G. 1987. Flood geomorphology of Katherine Gorge, Northern Territory, Australia, *Geological Society of America Bulletin* 88, 1057-1071.

Baker, V.R. & Kali, V.S. 1998. The role of extreme floods in shaping bedrock channels, In Tinkler, K.J. & Wohl, E.E. (Eds.), *Rivers over rock: fluvial processes in bedrock channels*, American Geophysical Monograph 107, American Geophysical Union, 153-165.

Barnes, H.H. 1967. Roughness characteristics of natural channels, *Geological Survey Professional Water-Supply Paper 1849*, United States Government Printing Office, Washington.

Bathurst, J.D. 1987a. Measuring and modelling bedload transport in channels with coarse bed materials, In Richards, K. (Ed.), *River channels, environment and process*, Basil Blackwell, Oxford, 272-294.

Bathurst, J.C. 1987b. Critical conditions for bed material movement in steep, boulder-bed streams, In Erosion and sedimentation in Pacific Rim, *International Association of Hydrological Sciences Publication* No. 165, Institute of Hydrology, Wallingford, 309-318.

Bathurst, J.C.; Graf, W.H. & Cao, H.H. 1987. Bed load discharge equations for steep mountain rivers, In Thorne, C.R.; Bathurst, J.C. & Hey, R.D. (Eds.), *Sediment transport in gravel-bed rivers*, Wiley, Chichester, 453-477.

Beaumont, R.D. 1981. The effect of land use changes on the stability of the Hout Bay River, *Municipal Engineer* 12, 2, 79-87.

Beaumont, P. & Oberlander, T.M. 1971. Observations on stream discharge and competence at Mosaic Canyon, Death Valley, California, *Geological Society of America Bulletin*, 82, 1695-1698.

Beckedahl, H.R. & Moon, B.P. 1980. The identification of superimposed drainage systems through morphometric analysis, *South African Geographer* 8, 25-29.

Begg, G. 1988. The 1987 Natal floods, *Natal Town and Regional Planning Commission*, Newsletter No 11, Pietermartizburg.

Bendix, J. 1999. Stream power influence on southern Californian riparian vegetation, *Journal of Vegetation Science* 10, 243-252.

Beschta, R.L. 1981. Patterns of sediment and organic matter transport in Oregon Coast Ranges stream, *International Association of Scientists and Hydrologists Publication* 132, 179-188.

Birkhead, A.L; Heritage, G.L.; White, H. & van Niekerk, A.W. 1996. Ground-penetrating radar as a tool for mapping the phreatic surface, bedrock profile and alluvial stratigraphy in the Sabie River, Kruger National Park, *Journal of Soil and Water Conservation* 51, 3, 234-241.

Birkhead, A.L. & James, C.S. 1998. Modelling geomorphic change in the Sabie River, South Africa, *Proceedings Hydra Storm*, International conference on Hydraulics in Civil Engineering, 27 to 30 September 1998, Adelaide, Australia.

Birkhead, A.L.; Heritage, G.L.; James, C.S.; Rogers, K.H. & van Niekerk, A.W. 2000. *Geomorphological change models for the Sabie River in the Kruger National Park*, Water Research Commission Report No. 782/1/00, Water Research Commission, Pretoria.

Blench, T. 1957. *Regime behaviour of canals and rivers*, Butterworths, London.

Blum, M.D.; Toomey, R.S. & Valastro, S. 1994. Fluvial response to Late Quaternary climatic and environmental change, Edwards Plateau, Texas. *Palaeogeography, Palaeoclimatology, Palaeoecology* 108, 1-21.

Boon, P.J.; Calow, P. & Petts, G.E. (Eds.), 1992. *River conservation and management*, Chichester, Wiley.

Boshof, P.; Kovacs, Z.; van Bladeren, D. & Zawada, P.K. 1993. Potential benefits from palaeoflood investigations in South Africa, *Journal of the South African Institute of Civil Engineers* 35, 25-26.

Bradley, W.C.; Fahnestock, R.K. & Rownekamp, E.T. 1972. Coarse sediment transport by flood flows on Knik river, Alaska, *Geological Society of America Bulletin* 83, 1261-1284.

Bray, D.I. 1975. Representative discharges for gravel-bed rivers in Alberta, Canada, *Journal of Hydrology* 27, 143-153.

Brayshaw, A.C. 1985. Bed microtopography and entrainment thresholds in gravel-bed rivers, *Geological Society of America Bulletin* 96, 218-223.

Brayshaw, A.C.; Frostick, L.E. & Reid, I. 1983. The hydrodynamics of particle clusters and sediment entrainment in coarse alluvial channels, *Sedimentology* 30, 137-143.

Bremner, J.M.; Rogers, J. & Willis, J.P. 1991. Sedimentological aspects of the 1988 Orange River Floods, *Transactions of the Royal Society of South Africa* 47, 3, 247-293.

Brizga, S. & Finlayson, B. 2000. The management of unstable rivers: The Avon River, Victoria, Australia, In Brizga, S. & Finlayson, B. (Eds.), *River management: the Australasian experience*, Chichester, Wiley, 247-263.

Broadhurst, L.J.; Heritage, G.L.; van Niekerk, A.W.; James, C.S. & Rogers, K.H. 1997. *Translating discharge into local hydraulic conditions on the Sabie River: an assessment of channel flow resistance*, Water Research Commission Report No. 474/2/97, Water Research Commission, Pretoria.

Brooks, A.P. 1995. River channel restoration: theory and practise, In Gurnell, A.M. & Petts, G.E (Eds.), *Changing river channels*, Wiley, Chichester, 369-388.

Brooks, A.P. & Brierley, G.J. 1998. Geomorphic reponses of lower Bega River to catchment disturbance, 1851-1926, *Geomorphology* 18, 3-4, 291-304.

Brooks, A.P. & Brierley, G.J. 2000. The role of European disturbance in the metamorphosis of the Lower Bega River, In Brizga, S. & Finlayson, B. (Eds.), *River management: the Australasian Experience*, Wiley, Chichester, 221-246.

Brusch, L.M. 1961. Drainage basins, channels and flow characteristics of selected streams in central Pennysylvania, *United States Geological Survey Professional Paper* 282F.

Bruwer, C.A. & Ashton, P.J. 1989. Flow-modifying structures and their impacts on lotic systems, In Ferrar, A.A. (Ed.), *Ecological flow requirements for South African rivers*, South African National Scientific Programmes Report No. 162, 3-16.

Brykowicz, K.; Rotter, A. & Waksmundzki, K. 1973. Hydrographical and morphological effects of the catastrophic rainfall in July 1970 in the source area of the Vistula, *Folia Geographica, Series Geographica-Physical* 7, 115-129.

Burkham, D.E. 1972. Channel changes on the Gila river in Safford Valley, Arizona, 1846-1970, *United States Geological Survey Professional Paper* 655-G.

Carey, W.P. 1985. Variability in measured bedload transport rates, *American Water Research Association Bulletin* 21, 39-48.

Carling, P.A. 1983. Threshold of coarse sediment transport in broad and narrow rivers, *Earth Surface Processes and Landforms* 8, 1-18.

Carling, P.A. 1988. The concept of dominant discharge as applied to two gravel-bed streams in relation to channel stability thresholds, *Earth Surface Processes and Landforms* 13, 355-367.

Carling, P.A. & Beven, K. 1989. The hydrology, sedimentology, and geomorphological implications of floods: An overview, In Beven, K. & Carling, P.A. (Eds.), *Floods: hydrological, sedimentological and geomorphological implications*, Wiley, Chichester, 1-9.

Carling, P.A.; Williams, J.J.; Kelsey, A.; Glasiter, M.S. & Orr, H.G. 1998. Coarse bedload transport in a mountain river, *Earth Surface Processes and Landforms* 23, 141-157.

Carling, P.A. & Tinkler, K. 1998. Conditions for the entrainment of cuboid boulders in bedrock streams: an historical review of literature with respect to recent investigations, In Tinkler, K.J. & Wohl, E.E. (Eds.), *Rivers over rock: fluvial processes in bedrock channels*, American Geophysical

Monograph 107, American Geophysical Union, Washington, 19-34.

Carson, M.A. & Griffiths, G.A. 1989. Gravel transport in the braided Waimakariri River: mechanisms, measurements and predictions, *Journal of Hydrology* 109, 210-220.

Chang, H.H. 1988. *Fluvial processes in river engineering*, Wiley, New York.

Cheshire, P. 1994. *Geology and geomorphology of the Sabie River, Kruger National Park and its catchment area*, Centre for Water in the Environment, Unpublished Report No. 1/94, University of the Witwatersrand, Johannesburg.

Chow, V.T. 1959. *Open channel hydraulics*, McGraw-Hill, New York.

Chunnet, I.E. 1994. The Ventersdorp Contact Reef - a historical Perspective, *South African Journal of Geology* 97, 3, 239-246.

Chunnet, Fourie & Partners. 1990. *Water for nature, hydrology, Sabie River catchment, Kruger National Park rivers research programme*, Department of Water Affairs and Forestry Report No. P.X.300/00/0490, Volumes 1-10, Pretoria.

Church, M. 1983. Patterns of instability in a wandering gravel-bed channel, *International Association of Sedimentologists Special Publication 6*, 169-180.

Church, M. & Jones, D. 1982. Channel bars in gravel-bed rivers, In Hey, R.D.; Bathurst, J.C. & Thornes, C.R. (Eds.), *Gravel-bed rivers*, Chichester, Wiley, 291-338.

Church, M.A.; McLean, D.G. & Wolcott, J.F. 1987. River bed gravels: sampling and analysis, In Thorne, C.R.; Bathurst, J.C. and Hey, R.D. (Eds.), *Sediment transport in gravel-bed rivers*, Chichester, Wiley, 43-88.

Church, M.; Kellerhals, R. & Day, T.J. 1989. Regional clastic sediment yield in British Columbia, *Canadian Journal of Earth Sciences* 26, 31-45.

Clarke, F.E. 1973. The great Tunisian flood, *Journal of Research*, U.S. Geological Survey 1, 121-124.

Cleaves, E.T.; Godfrey, A.E. & Bricker, O.P. 1970. Geochemical balance of a small watershed and its geomorphic implications, *Geological Society of America Bulletin* 81, 3015-3022.

Cooke, H.B.S. 1976. The palaegeography of the Middle Kalahari of Northern Botswana and adjacent areas, In *Symosium on the Okavango Delta*, Gaberone, Botswana Society, 21-29.

Cooper, J.A.G. 1991. *Shore-line changes on the Natal coast, Tugela river mouth to Cape St Lucia*, Natal Town and Regional Planning Report No. 76, Pietermaritzburg.

Corey, A.T. 1949. *Influence of shape on the fall velocity of sand grains*, Unpublished MSc thesis, Colorado A&M College, Fort Collins, Colorado.

Costa, J.E. 1974. Response and recovery of a Piedmont watershed from tropical storm Agnes, June 1972, *Water Resources Research* 10, 106-112.

Costa, J.E. & O'Connor, J.E. 1995. Geomorphically effective floods, In Costa, J.E.; Miller, A.J.; Potter, K.P. & Wilcock, P.R. (Eds.), *Natural and anthropogenic influences in fluvial geomorphology*, American Geophysical Union Monograph 89, 45-56.

Dardis, G.F.; Beckedahl, H.R. & Stone, A.W. 1988. Fluvial systems, In Moon, B.P. & Dardis, G.F. (Eds.), *The geomorphology of southern Africa*. Johannesburg: Southern Books, 30-56.

Davies, B.R. 1989. Where rivers once flowed, *Conserva* 4, 2, 12-15.

Davies, B. & Day, J. 1996. *Vanishing Waters*, University of Cape Town Press, Cape Town.

Davies, T.A.; Hay, W.W.; Southam, J.R. & Worsley, T.R. 1977. Estimates of Cainozoic oceanic sedimentation rates, *Science* 197, 53-55.

Davis, J.A.; Rutherfurd, I.D. & Finlayson, B.L. 1999. The Eppalock soil conservation project: Victoria, Australia: the prevention of reservoir sedimentation and the politics of catchment management, *Australian Geographical Studies* 37, 1, 37-49.

de Kock, W.P. 1941. The Ventersdorp Contact Reef: its nature, mode of occurrence and economic significance with special reference to the far West Rand, *Transactions of the Geological Society of South Africa* XLIII, 85-108.

De Ploey, J. 1989. *Soil erosion map of western Europe*. Cremlingen-Destedt, Catena Verlag

De Wit, M.C.J. 1993. *Cainozoic evolution of drainage systems of the North-West Cape*, Unpublished PhD Thesis, University of Cape Town, Cape Town.

Dietrich, W.E. 1982. Settling velocity of natural particles, *Water Resources Research* 18, 6, 1615-1626.

Dietrich, W.E. & Dunne, T. 1978. Sediment budget for a small catchment in mountainous terrain, *Zeitschrift für Geomorphologie* NF 29, 191-206.

Dietrich, W.E.; Smith, J.D. & Dunne, T. 1979. Flow and sediment transport in a sand bedded meander, *Journal of Geology* 87, 305-315.

Dingle, R.V. & Hendey, Q.B. 1984. Mesozoic and Tertiary sediment supply to the Western Cape basin and palaeodrainage systems in south-western Africa, *Marine Geology* 56, 13-26.

Diplas, P. 1987. Bedload transport in gravel-bed streams, *Journal of Hydraulic Engineering*, American Society of Civil Engineers 113, 277-292

Dix, O.R. 1984. Braided-stream deposition in the Mpembeni River, Zululand, *South African Journal of Science* 80, 41-42.

Dollar, E.S.J. 1990. *The effect of reservoir construction on flow regime and channel morphology on the Keiskamma river*, Paper Presented to the South African Geographical Society Student Conference, University of Port Elizabeth, Port Elizabeth.

Dollar, E.S.J. 1992. *An historical study of channel change in the Bell River, North Eastern Cape*, Unpublished MSc Thesis, Rhodes University, Grahamstown.

Dollar, E.S.J. 1998a. Palaeofluvial geomorphology in southern Africa: a review, *Progress in Physical Geography* 22, 3, 325-349.

Dollar, E.S.J. 1998b. Geomorphology, In Louw, D. *Starter Document for IFR specialist meeting*, Mhlathuze ecological (quantity) reserve study, 26-30 October 1998, Mtunzini, IWR Environmental, Pretoria.

Dollar, E.S.J. 2000. Fluvial geomorphology, *Progress in Physical Geography* 24, 3, 431-452.

Dollar, E.S.J. & Rowntree, K.M. 1995. Hydroclimatic trends, sediment sources and geomorphic response in the Bell River Catchment, Eastern Cape Drakensberg, South Africa, *South African Geographical Journal* 77, 1, 21-32.

Dollar, E.S.J. & Goudie, A.S. 2000. Environmental Change, In Fox, R.C. & Rowntree, K.M. (Eds.), *The geography of South Africa in a changing world*, Oxford University Press, Cape Town, 31-59.

du Plessis, A.J.E. 2000. *The response of two interrelated river components, geomorphology and riparian vegetation to interbasin water transfers in the Orange-Fish-Sundays river interbasin transfer scheme*, Unpublished MSc thesis, Rhodes University, Grahamstown.

DuBoys, P. 1879. Le Rhone et les Rivieres a Lit Affouillable, *Annales des Ponts et Chaussees* 18, 141-195.

Du Toit, A.L. 1910. The evolution of the river system of Griqualand West, *Transactions of the Royal Society of South Africa* 1, 347-362.

Dunkerley, D.L. 1990. The development of armour in the Tambo river, Victoria, Australia, *Earth Surface Processes and Landforms* 15, 405-412.

Dunkerley, D.L. 1992. Channel geometry, bed material, and inferred flow conditions in ephemeral stream systems, Barrier Range, Western NSW, Australia, *Hydrological Processes* 6, 417-433.

Dunne, T. & Leopold, L.B. 1978. *Water in environmental planning*, W.H. Freeman and Company, San Fransisco.

Dury, G.H. 1959. Analysis of regional flood frequency on the Nene and the Great Ouse, *Geographical Journal* 125, 223-229.

Dury, G.H. 1961. Bankfull discharge: an example of it statistical relationships, *International Association of Scientific Hydrologists* 3, 48-55.

Dury, G.H. 1969. Hydraulic geometry, In Chorley, R.J (Ed.), *Water, earth and man*, London, Methuen, 319-330.

Dury, G.H. 1976. Discharge prediction, present and former, from channel dimensions, *Journal of Hydrology* 30, 219-245.

Dury, G.H.; Hails, J.R. & Robbie, H.B. 1963. Bankfull discharge and the magnitude- frequency series, *Australian Journal of Science* 26, 123-124.

Einstein, H.A. 1950. The bed-load function for sediment transportation in open channel flows, *United States Department of Agriculture Technical Bulletin* 1026.

Ellery, W.N. 1988. *Channel blockage and abandonment in northeastern Okavango Delta: the role of Cyperus Papyrus*, Unpublished MSc Thesis, University of the Witwatersrand, Johannesburg.

Ellery, W.N.; Ellery, K.; Rogers, K.H.; McCarthy, T.S. & Walker, B.H. 1990. Vegetation of channels of the northeastern Okavango Delta, Botswana, *African Journal of Ecology* 28, 276-290.

Ellery, W.N.; Ellery, K.; Rogers, K.H.; McCarthy, T.S. & Walker, B.H. 1993. Vegetation, hydrology and sedimentation processes as determinants of channel form and dynamics in the northeastern Okavango delta, Botswana, *African Journal of Ecology* 31, 10-25.

Engelund, F. & Hansen, E. 1967. *A monograph on sediment transport in alluvial streams*, Teknisk Vorlag, Copenhagen, Denmark.

Environmental Agency, 1998. *National centre for risk analysis and options appraisal: river geomorphology: a practical guide*, Guidance Note 18, Environmental Agency, Bristol.

Eriksson, P.G. 1986. Aeolian dune and alluvial fan deposits in the Clarens Formation of the Natal Drakensberg, *Transactions of the Geological Society of South Africa* 89, 389-394.

Erskine, W.D. & Warner, R.F. 1998. Further assessment of flood- and drought- dominated regimes in south-eastern Australia, *Australia Geographer* 29, 2, 257-261.

Fair, T.J.D. 1978. The geomorphology of central and southern Africa, In Werger, M.J.A. (Ed.), *Biogeography and ecology of southern Africa*, The Hague, Dr. W. Junk, 3-17.

Ferguson, R. 1987. Hydraulic and sedimentary controls of channel pattern, In Richards, K (Ed.), *River channels, environment and process*, Basil Blackwell, Oxford, 129-158.

Ferguson, R.I.; Prestegaard, K.L. & Ashworth, P.J. 1989. Influence of sand on hydraulics and gravel transport in a braided gravel-bed river, *Water Resources Research* 25, 643-653.

Ferguson, R. & Ashworth, P. 1991. Slope-induced changes in channel character along a gravel-bed stream: The Allt Dubhaig, Scotland, *Earth Surface Processes and Landforms* 16, 65-82.

Finlayson, B.L.; Gippel, C.J. & Brizga, S.O. 1994. Effects of reservoirs on downstream habitat, *Water* 21, 4, 15-20.

Frissel, C.A.; Liss, W.J.; Warren, C.E. & Hurley, M.D. 1986. A hierarchical framework for stream classification: viewing streams in a watershed context, *Environmental Management* 10, 2, 199-214.

Garbharran, H.P. 1983. Factor analysis and the study of drainage basin characteristics and lithology in the Umlazi area, *South African Geographical Journal* 65, 135-140.

Gevers, T.W. 1948. Drying rivers in the northeastern Transvaal, *South African Geographical Journal* 30, 17-44.

Gill, M.A. 1965. Reply to paper on dominant discharges at Platte-Missouri confluence, *Journal of the Hydraulics Division*, Proceedings of the American Society of Civil Engineers WW4, 527-529.

Gilvear, D.J. 1994. Fluvial geomorphology at work: a U.K. perspective, *Scottish Association of Geography Teachers* 23, 30-42.

Gippel, C.J. & Stewardson, M.J. 1995. Development of an environmental flow management strategy for the Thomson river, Victoria, Australia, *Regulated Rivers: Research and Management*, 10, 121-135.

Goff, J.R. & Ashmore, P. 1994. Gravel transport and morphological change in braided Sunwapta river, Alberta, Canada, *Earth Surface Processes and Landforms* 19, 195-212.

Gomez, B. 1983. Temporal variations in bedload transport rates: the effect of progressive bed armouring, *Earth Surface Processes and Landforms* 8, 41-54.

Gomez, B. 1995. Bedload transport and changing grain size distributions, In Gurnell, A. & Petts, G.E. (Eds.), *Changing river channels*, Wiley, New York, 177-199.

Gomez, B. & Church, M. 1989. An assessment of bed load sediment transport formulae for gravel bed rivers, *Water Resources Research* 25, 6, 1161-1186.

Gordon, N. 1995. *Summary of technical testimony in the Colorado Water Division 1 trial*, USDA Forest Service General Technical Report RM-GTR-270, USDA, Fort Collins, Colorado.

Gordon, N.D.; McMahon, T.A. & Finlayson, B.L. 1992. *Stream hydrology: An introduction for ecologists*, Wiley, Chichester.

Görgens, A. & Hughes, D.A. 1982. Synthesis of streamflow information relating to the semi-arid Karoo biome of South Africa, *South African Journal of Science* 78, 58-68.

Graf, W.H. 1971. *Hydraulics of sediment transport*, McGraw-Hill, New York.

Graf, W.L. 1988. *Fluvial processes in dryland rivers*, Springer-Verlag, Berlin.

Grayson, R.B.; Kenyon, C.; Finlayson, B.L. & Gippel, C.J. 1998. Bathymetric and core analysis of the Latrobe river delta to assist in catchment management, *Journal of Environmental Management* 52, 361-372.

Gregory, K.J. 1976. Lichens and determination of river channel capacity, *Earth Surface Processes* 1, 273-285.

Gupta, A. 1995. Magnitude, frequency and special factors affecting channel form and process in the seasonal tropics, In Costa, J.E.; Miller, A.J.; Potter, K.W. & Wilcock, P.R. (Eds.), *Natural and anthropogenic influences in fluvial geomorphology*, American Geophysical Monograph 89, American Geophysical Union, Washington, 45-56.

Gupta, A. & Fox, H. 1974. Effects of high magnitude floods on channel form: a case study in the Maryland Piedmont, *Water Resources Research* 10, 499-509.
Gregory, D.I. & Schumm, S.A. 1987. The effect of active tectonics on alluvial river morphology, In Richards, K. (Ed.), *River channels, environment and process*, Basil Blackwell, Oxford, 41-68.

Hack, J.T. & Goodlett, J.C. 1960. Geomorphology and forest ecology of a mountain region in the Central Appalachians, *United States Geological Survey Professional Paper* 347.

Hall, R.C.B. 1994. Supporting evidence for the placement of the inter-reef lavas and associated sediments within the Venterspost Conglomerate Formation: Kloof Gold Mine, *South African Journal of Geology* 97, 3, 297-307.

Harvey, A.M. 1969. Channel capacity and the adjustment of streams to hydrologic regime, *Journal of Hydrology* 8, 82-98.

Harvey, A.M. 1984. Geomorphological response to an extreme flood: a case from southeast Spain, *Earth Surface Processes and Landforms* 9, 267-279.

Harvey, A.M.; Hitchcock, D.H. & Hughes, D.J. 1979. Event frequency and morphological adjustment of fluvial systems in upland Britain, In Rhodes, D.D. & Williams, G.P. (Eds.), *Adjustments to the fluvial system*, Kendall/Hunt, Dubuque, Iowa, 139-167.

Haschenburger, J.K. & Church, M. 1998. Bed material transport estimated from the virtual velocity of sediment, *Earth Surface Processes and Landforms* 23, 791-808.

Hassan, M.A. & Reid, I. 1990. The influence of microform bed roughness elements on flow and sediment transport in gravel bed rivers, *Earth Surface Processes and Landforms* 15, 739-750.

Hattingh, J. 1996. *Late Cenozoic drainage evolution in the Algoa Basin with special reference to the Sundays River valley*, Unpublished PhD Thesis, University of Port Elizabeth, Port Elizabeth.

Helgren, D.M. 1979. *River of diamonds: an alluvial history of the lower Vaal basin*. Chicago: Department of Geography, University of Chicago Research Series No. 186.

Helley, E.J. 1969. Field measurements of the initiation of large bed particle motion in Blue Creek near Klamath, California, *United States Geological Survey Professional Paper* 562-G.

Henning, L.T.; Els, B.G. & Mayer, J.J. 1994. The Ventersdorp Contact Placer at Western Deep Levels Gold Mine - an ancient terraced fluvial system, *South African Journal of Geology* 97, 308-318.

Heritage, G.L. & van Niekerk, A.W. 1994. Morphological response of the Sabie River to changing flow and sediment regimes, *Proceedings of the South African Institute of Civil Engineers Conference*, Johannesburg, 389-403.

Heritage, G.L.; van Niekerk, A.W.; Moon, B.P.; Broadhurst, L.J.; Rogers, K.H. & James, C.S. 1995. *The geomorphological response to the changing flow regimes of the Sabie and Letaba River systems*, Report to the Water Research Commission K5/376, Water Research Commission, Pretoria.

Heritage, G.L.; van Niekerk, A.W.; Moon, B.P.; Broadhurst, L.J.; Rogers, K.H. & James, C.S. 1997. *The geomorphological response to changes in flow regime of the Sabie and Letaba River systems*, Water Research Commission Report No. 376/1/96, Volume 1, Water Research Commission, Pretoria.

Hey, R.D. & Thorne, C.R. 1983. Accuracy of surface samples from gravel-bed material, *Journal of Hydraulic Engineering* 109, 18047, 842-851.

Hickin, E.J. 1967. Channel morphology, bankfull stage and bankfull discharge of streams near Sydney, *Australian Journal of Science* 30, 274-275.

Hickin, E.J. 1983. River channel changes: retrospect and prospect, In Collinson, J.D. & Lewin, J. (Eds.), *Modern and ancient fluvial systems*, Blackwell Scientific, London, 61-83.

Hoey, T. 1992. Temporal variations in bedload transport rates and sediment storage in gravel-bed rivers, *Progress in Physical Geography* 16, 319-338.

Hoey, T.B. & Sutherland, A.J. 1991. Channel morphology and bedload pulses in braided rivers, a laboratory study, *Earth Surface Processes and Landforms* 14, 16, 447-462.

Huggett, R.J. 1994. Fluvialism or diluvialism? Changing views on superfloods and landscape change, *Progress in Physical Geography* 18, 3, 335-342.

Hughes, D.A. (Ed.). 1994. *Nahoon River release: environmental monitoring of the release of Kubusi River water from the Wriggleswade Dam and canal system into the Nahoon River catchment with specific reference to water flow, chemistry, invertebrate biology and geomorphological characteristics*, Report to Subdirectorate Environmental Studies, Department of Water Affairs and Forestry, Institute for Water Research and Department of Geography, Rhodes University, Grahamstown, Department of Water Affairs and Forestry Report No. VS/600/08/E001.

Hughes, D.A. & Smakthin, V. 1996. Daily flow time series patching or extension: a spatial interpolation approach based on flow duration curves, *Hydrological Sciences Journal* 41, 6, 851-871

Hughes, D.A. & Smakthin, V. 1998. Mhlathuze river IFR - Hydrology starter document, In Louw, D., *Starter Document for IFR Specialist Meeting*, Mhlathuze Ecological (Quantity) Reserve Study, IWR Environmental, Pretoria.

Hughes, D.A. 2000. Hydrology, In Louw, D. *Olifants river ecological water requirements assessment*, Starter document: Upper Olifants specialist meeting, IWR Environmental, Pretoria.

Ibheken, H. 1974. A simple sieving and splitting device for the field analysis of coarse grained sediments, *Journal of Sedimentary Petrology* 44, 3, 939-946.

Illenberger, W.K. 1992. *Sediment dynamics of the Sundays River mouth area, Algoa Bay*, Unpublished PhD thesis, University of Port Elizabeth, Port Elizabeth.

Illenberger, W.K. 1993. Variations of sediment dynamics in Algoa Bay during the Holocene, *South African Journal of Science* 89, 187-195.

Inglis, C.C. 1941. Meandering of rivers, *Central Board Of Irrigation (India) Publication* 24, 98-114.

Inglis, C.C. 1947. *Meanders and their bearing on river training*, Maritime Paper 7, Institute of Civil Engineers.

Jackson, W.L. & Beschta, R.L. 1982. A model of two-phase bed load transport in an Oregon Coast Range stream, *Earth Surface Processes and Landforms* 7, 517-527.

James, C.S 1998: Personal communication.

Johnson, R.A. 1983. *Stream channel response to extreme rainfall events: the Hurricane Camille storm in central Nelson county*, Unpublished Masters Thesis, University of Virginia, Charlotteville.

Johnston, C.E.; Andrews, E.D. & Pitlick, J. 1998. In situ determination of particle friction angles of fluvial gravels, *Water Resources Research* 34, 8, 2017-2030.

Karin, F. 1998. Bed material discharge prediction for non-uniform bed sediments, *Journal of Hydraulic Engineering* 124, 6, 597-604.

Keller, E.A. 1971. Areal sorting of bed load material: the hypothesis of velocity reversal, *Bulletin of the Geological Society of America* 83, 753-756.

Kellerhals, R. & Bray, D.I. 1971. Sampling procedures for coarse fluvial sediments, *Journal of Hydraulic Engineering* 97, 1165-1180.

Kennedy, R.C. 1895. Prevention of silting in irrigation canals, *Institute of Civil Engineers Proceedings* 119, 281-290.

Kennedy, B.A. 1972. Bankfull discharge and meander forms, *Area* 4, 209-212.

Kilpatrick, F.A. & Barnes, H.H. 1964. Channel geometry of Piedmont streams as related to frequency of floods, *United States Geological Survey Professional Paper* 422-E.

King, J.M.; Tharme, R.; Bruwer, C. & Louw, D. 1993. Explanation of the Building Block Methodology, *Olifants River (Rosendal Dam) IFR Work session*, 24-26 August 1993, Department of Water Affairs and Forestry, Pretoria.

King, J.M. & Tharme, R.E. 1994. *Assessment of the instream flow incremental methodology and initial development of alternative instream flow methodologies for South Africa*, Water Research Commission Report No. 295/1/94, Water Research Commission, Pretoria.

King, J.M. & Louw, D. 1998. Instream flow assessments for regulated rivers in South Africa using the Building Block Methodology, *Aquatic Ecosystem Health and Management* 1, 2, 109-124.

King, L.C. 1963. *South African scenery: a textbook of geomorphology*, Edinburgh, Oliver and Boyd.

Kirkup, H.; Brierley, G.; Brooks, A. & Pitman, A. 1998. Temporal variability of climate in south-eastern Australia: a reassessment of flood- and drought-dominated regimes, *Australian Geographer* 29, 2, 241-255.

Klingeman, P.C. & Emmett, W.W. 1982. Gravel-bed transport processes, In Hey, R.D.; Bathurst, J.C. & Thorne, C.R. (Eds.), *Gravel-bed rivers*, Wiley, Chichester, 141-169.

Knighton, A.D. 1987. River channel adjustment, the downstream dimension, In Richards, K. (Ed.), *River channel changes, environment and process*, Basil Blackwell, Oxford, 95-128.

Knighton, A.D. 1998. *Fluvial forms and processes: a new perspective*, Arnold, London.

Kochel, R.C. 1988. Geomorphic impact of large floods: review and new perspectives on magnitude and frequency, In Baker, V.R.; Kochel, R.C. & Patton, P.C. (Eds.), *Flood geomorphology*, Wiley, New York, 169-187.

Komar, P.D. 1987. Selective grain entrainment by a current from a bed of mixed sizes: a re-analysis, *Journal of Sedimentary Petrology* 57, 203-211.

Komar, P.D. 1989. Flow-competence evaluations of the hydraulic parameters of floods: an assessment of the technique, In Beven, K. & Carling, P. (Eds.), *Floods: hydrological, sedimentological and geomorphological implications*, Wiley, Chichester, 107-134.

Komura, S. 1968. Discussion of 'Dominant discharges at Platte-Missouri Confluence', *Journal of the Hydraulics Division*, American Society of Civil Engineers 94, 525-527.

Komura, S. & Gill, M.A. 1968. Comment, *Journal of the Hydraulics Division*, American Society of Civil Engineers WW4, 525-529.

Kondolf, G.M. 1995. Managing bedload sediment in regulated rivers: examples from California, U.S.A., In Costa, J.E.; Miller, A.J.; Potter, K.W. & Wilcock, P.R. (Eds.) *Natural and anthropogenic influences in fluvial geomorphology*, American Geophysical Union, Geophysical Monograph 89, 165-176.

Kondolf, G.M. & Wolman, M.G. 1993. The sizes of Salmonid spawning gravels, *Water Resources Research* 29, 7, 2275-2285.

Kondolf, G.M. & Wilcock, P.R. 1996. The flushing flow problem: defining and evaluating objectives, *Water Resources Research* 32, 8, 2589-2599.

Kovacs, Z.P. 1980. *Maximum flood-peak discharges in South Africa: an empirical approach*, Department of Water Affairs and Forestry Technical Report TR 105, Pretoria.

Kovacs, Z.P. 1985. Hydrology of the Mfolozi River, In Looser, U. (Ed.), *Sediment problems in the Mfolozi catchment, assessment of research requirements*, Hydrological Research Institute, Department of Water Affairs, Government Printer, Pretoria.

Kovacs, Z.P. 1988: *Regional maximum floods in southern Africa*, Technical Report TR137, Directorate of Hydrology, Department of Water Affairs and Forestry, Government Printer, Pretoria.

Kovacs, Z.P.; du Plessis, D.B.; Bracher, P.R.; Dunn, P. & Mallory, G.C.L. 1985. *Documentation of the 1984 Domoina floods*, Technical Report No. 122, Department of Water Affairs, Government Printer, Pretoria.

Krapez, B. 1985. The Ventersdorp Contact Placer: a gold/pyrite placer of stream and debris flow origin from the Archaean Witwatersrand Basin of South Africa, *Journal of Sedimentology* 32, 223-234.

Kuhnle, R.A. 1992. Bed load transport during rising and falling stages on two small streams, *Earth Surface Processes and Landforms* 17, 191-197.

Kuhnle, R.A. & Southard, J.B. 1988. Bed load transport fluctuations in a gravel bed laboratory channel, *Water Resources Research* 24, 247-260.

Lacey, G. 1930. Stable channels in alluvium, *Institute of Civil Engineers Proceedings* 229, 259-384.

Lane, E.W. 1957. A study of the shape of channels formed by natural streams flowing in erodible materials, *MRD Sediment Series No 9*.

Lane, S.N. 1998. Hydraulic modelling in hydrology and geomorphology: a review of high resolution approaches, *Hydrological Processes* 11, 1131-1150.

Lane, S.N.; Richards, K.S. & Chandler, J.H. 1996. Discharge and sediment supply controls on erosion and deposition in a dynamic alluvial channel, *Geomorphology* 15, 1-15.

Laronne. J.B. & Reid, I. 1993. Very high rates of bedload sediment transport in desert ephemeral rivers, *Nature* 366, 148-150.

Lekach, J & Schick, A.P. 1983. Evidence for transport of bedload in waves: analysis of fluvial sediment samples in a small upland stream channel, *Catena* 10, 267-279.

Le Blanc-Smith, G. & Eriksson, K.A. 1979. A fluvioglacial and glaciolacustrine deltaic depositional model for Permo-Carboniferous coals of the north-eastern Karoo basin, South Africa, *Palaeogeography, Palaeoclimatology, Palaeoecology* 27, 67-84.

Le Roux, J.S. 1990. Spatial variations in the rate of fluvial erosion (sediment production) over South Africa, *Water SA* 16, 3, 185-194.

Leopold, L.B. 1994. *A view of a river*, Harvard University Press, Cambridge.

Leopold, L.B. 1997. *Water, rivers and creeks*, University Science Books, California.

Leopold, L.B. & Maddock, T.C. 1953. The hydraulic geometry of stream channels and some physiographic implications, *United States Geological Survey Professional Paper* 252.

Leopold, L.B. & Wolman, M.G. 1957. River channel patterns, braided, meandering and straight, *United States Geological Survey Professional Paper* 282B.

Leopold, L.B. & Emmett, W.W. 1976. Bedload measurements, East Fork river, Wyoming, *Geology* 73, 4, 1000-1004.

Leopold, L.B.; Wolman, M.G. & Miller, J.P. 1964. *Fluvial processes in geomorphology*, W.H. Freeman, San Fransisco.

Lewin, J. 1989. Floods in fuvial gomorphology, In Beven, K. & Carling, P. (Eds.), *Floods: hydrological, sedimentological and geomorphological implications*, Wiley, Chichester, 265-284.

Lewis, A.D. 1936. *Silting of four large reservoirs in South Africa*, Communication No. 5, 2nd Congress on Large Dams, Washington.

Looser, J.U. 1989. Methods to determine the origin and delivery of sediment in the Mfolozi catchment, In Kienzle, S. & Maaren, H. (Eds.), *Proceedings of the 4th South African National Hydrological Symposium*, University of Pretoria, 20-22 November 1989, 347-354.

Louw, D. 1998a. *Mkomazi IFR study*, Starter document for IFR workshop, IWR Environmental, Pretoria.

Louw, D. 1998b. *Mhlathuze ecological (Quantity) reserve study*, Starter document for IFR specialist meeting, IWR Environmental, Pretoria.

Louw, D. 2000. *Olifants river ecological water requirements assessment*, Starter document, Upper Olifants specialist meeting, IWR Environmental, Pretoria.

Macklin, M.G. & Lewin, J. 1992. Channel changes since 1783 on the regulated river Tay, Scotland: Implications for flood hazard management, *Regulated Rivers: Research and Management* 23, 113-126.

MacWha, M. 1994. The influence of landscape on the Ventersdorp Contact Reef at Western Deep Levels South Mine, *South African Journal of Geology* 97, 319-331.

Magilligan, F.J. 1992. Thresholds and spatial variability of flood power during extreme floods, *Geomorphology* 5, 373-390.

Magilligan, F.J.; Phillips, J.D; James, L.A. & Gomez, B. 1998. Geomorphic and sedimentological controls on the effectiveness of an extreme flood, *Journal of Geology* 106, 87-95.

Marlette, R.R. & Walker, R.H. 1968. Dominant discharge at the Platte-Missouri confluence, Proceedings of the American Society of Civil Engineers, *Journal of the Waterways and Harbours Division* 94, 23-32.

Martin, A.K. 1987. Comparison of sediment rates in Natal valley, south-west Indian Ocean with modern sediment yields in east coast rivers of southern Africa, *South African Journal of Science* 83, 716-724.

Mason, C.E. 1924. Silt in the Vaal river, *Rand Water Board Annual Report*, 40-42.

Maud, R.R. 1996. The macro-geomorphology of the Eastern Cape, In Lewis, C.A. (Ed.), *The geomorphology of the Eastern Cape*, Grahamstown, Grocott and Sherry, 1-18.

Maud, R.R. & Partridge, T.C. 1988. Regional geomorphic evidence for climatic change in southern Africa since the Mesozoic, *Palaeoecology of Africa* 18, 337-348.

McCabe, G.J. & Hay, L.E. 1995. Hydrological effects of hypothetical climate change in the East River basin, Colorado, USA, *Hydrological Sciences Journal* 40, 3, 303-318.

McCarthy, T.S. 1992. Physical and biological processes controlling the Okavango Delta - A review of recent research, *Botswana Notes and Records* 24, 57-86.

McCarthy, T.S.; Ellery, W.N.; Rogers, K.H.; Cairncross, B. & Ellery, K. 1986. The roles of changing sedimentation and plant growth in changing flow patterns in the Okavango Delta, Botswana, *South African Journal of Science* 82, 579-584.

McCarthy, T.S.; Ellery, W.N.; Ellery, K. & Rogers, K.H. 1987. Observations on the abandoned Ndoqa channel of the Okavango Delta, *Botswana Notes and Records* 19, 83-89.

McCarthy, T.S.; Stanistreet, I.G.; Cairncross, B.; Ellery, W.N.; Ellery, K; Alephs, R. & Grobicki, T.S.A. 1988. Incremental aggradation on the Okavango Delta fan, Botswana, *Geomorphology* 1, 267-278.

McCarthy, T.S.; Stanistreet, I.G. & Cairncross, B. 1991. The sedimentary dynamics of active fluvial channels on the Okavango Fan, Botswana, *Sedimentology* 38, 471-487.

McCarthy, T.S.; Ellery, W.N. & Stanistreet, I.G. 1992. Avulsion mechanisms on the Okavango Fan, Botswana: the control of a fluvial system by vegetation, *Sedimentology* 389, 779-795.

McCarthy, T.S.; Cooper, G.R.J.; Tyson, P.D. & Ellery, W.N. 2000. Seasonal flooding in the Okavango Delta, Botswana - recent history and future prospects, *South African Journal of Science* 96, 25-33.

McEwan, L.J. 1989. River channel changes in response to flooding in the Upper Dee catchment, Aberdeenshire, over the last 200 years, In Beven, K. & Carling, P. (Eds.), *Floods: hydrological, sedimentological and geomorphological implications*, Wiley, Chichester, 219-238.

McGregor, G.K. 1999. *The geomorphological impacts of impoundments with particular reference to tributary bar development on the Keiskamma river, Eastern Cape*, Unpublished MSc thesis, Rhodes University, Grahamstown.

McLean, D.G. 1985. Sensitivity analysis of bed load equations, *Proceedings of the Canadian Society of Civil Engineers*, Saskatoon Conference 18, 1-15.

McMahon, T.A.; Finlayson, B.L.; Haines, A.T. & Srikanthan, R. 1992. *Global hydrology*, Catena Paperback, Cremlingen.

McMahon, T.A. & Finlayson, B.L. 1995. Reservoir system management and environmental flows, *Lakes and Reservoirs: Research and Management* 1, 65-76.

McPherson, H.J. & Rannie, W.F. 1969. Geomorphic effects of the May 1967 flood in Graburn Watershed, Cyprus Hills, Alberta, Canada, *Journal of Hydrology* 9, 307-321.

Meade, R.H. 1983. Sources, sinks and storage of river sediment in the Atlantic drainage of the United States, *Journal of Geology* 90, 3, 139-157.

Meyer-Peter, E. & Müller, R. 1948. *Formula of bed-load transport*, International Association for Hydraulic Structures Research, Report of Second Meeting, Stockholm, 39-64.

Midgley, D.C.; Pitman, W.V. & Middleton, B.J. 1994. *Surface Water Resources of South Africa, 1990*, Water Research Commission Report No. 298/1/94, Water Research Commission, Pretoria.

Milhous, R.T. 1973. *Sediment transport in a gravel-bottomed stream*, Unpublished PhD thesis, Oregon State University, Corvallis.

Milhous, R.T. 1998a. Modelling instream flow needs: the link between sediment and aquatic habitat, *Regulated Rivers: Research and Management* 14, 79-94.

Milhous, R.T. 1998b. Impact of major storms on subsequent sediment transport: South Fork Trinity River, California, *Hydrology Days*, Proceedings of the American Geophysical Union, March 30-April 2, 1998, Colorado State University, Fort Collins, Colorado, 189-200.

Milhous, R.T. 1998c. On sediment and habitat in the Upper Animas River watershed, Colorado, *Water Resources Engineering 98*, Proceedings of the International Water Resources Engineering Conference, American Society of Civil Engineers, Virgina, 678-683.

Milhous, R.T. 2000. Personal communication.

Milhous, R.T. & Bradley, J.B. 1986. Physical habitat simulation and the movable bed, In Karamouz, M.; Baumli. G.R. & Brick, W.J. (Eds.), *Water Forum '86: World Water Issues in Evolution*, American Society of Civil Engineers, New York, 1976-1983.

Milhous, R.T.; Updike, M.A. & Schneider, D.M. 1989. *Physical habitat simulation system reference manual version II*, Instream Flow Information Paper No. 26, United States Fish and Wildlife Service Biological Report 89(16), Washington D.C..

Milhous, R.T.; Dodge, R.A. & Johnson, P.L. 1994. Bed material and numerical modelling in a gravel/cobble bed stream, *Hydraulic Engineering '94*, Proceedings of the 1994 Conference, American Society of Civil Engineers, Buffalo, New York, 1055-1059.

Miller, T.K. 1984. A system model of stream-channel shape and size, *Bulletin of the Geological Society of America* 95, 237-241.

Miller, A.J. 1990. Flood hydrology and geomorphic effectiveness in the central Appalachians, *Earth Surface Processes and Landforms* 15, 119-134.

Miller, M.C.; McCave, I.N. & Komar, P.D. 1977. Threshold of sediment motion under unidirectonal currents, *Sedimentology* 24, 801-829.

Milliman, J.D. & Meade, R.H. 1983. World-wide delivery of river sediment to the oceans, *Journal of Geology* 91, 1, 1-21.

Misri, R.L.; Garde, R.J. & Ranga Raju, K.G. 1984. Bed load transport of coarse nonuniform sediment, *Journal of Hydraulic Engineering*, American Society of Civil Engineers 110, 3, 312-328.

Moog, D.B. & Whiting, P.J. 1998. Annual hysteresis in bed load rating curves, *Water Resources Research* 34, 9, 2393-2399.

Moon, B.P.; van Niekerk, A.W.; Heritage, G.L.; Rogers, K.H. & James, C.S. 1997. A geomorphological approach to the management of rivers in the Kruger National Park: the case of the Sabie River, *Transactions of the Institute of British Geographers* NS22, 31-48.

Morisawa, M. 1985. *Rivers*, Longman, London.

Mosley, M.P. & Tindale, D.S. 1985. Sediment variability and bed material sampling in gravel-bed rivers, *Earth Surface Processes and Landforms* 10, 465-480.

Mosley, P. & Jowett, I. 1999. River morphology and management in New Zealand, *Progress in Physical Geography* 23, 4, 541-565.

Moss, J.H. & Kochel, R.C. 1978. Unexpected geomorphic effects of the Hurricane Agnes storm and flood, Conestoga drainage basin, south eastern Pennsylvania, *Journal of Geology* 86, 1, 1-11.

Murgatroyd, A.L. 1979. Geologically normal and accelerated rates of erosion in Natal, *South African Journal of Science* 75, 395-396.

Nanson, C.G. 1974. Bedload and suspended load transport in a small steep mountain stream, *American Journal of Science* 274, 471-486.

Nanson, G.C. 1986. Episodes of vertical accretion and catastrophic stripping: A model of disequilibrium flood-plain development, *Geological Society of America Bulletin* 97, 1467-1475.

Nash, D.B. 1994. Effective sediment-transporting discharge from magnitude-frequency analysis, *Journal of Geology* 102, 79-95.

Neill, C.R. 1968. Note on the initial movement of coarse uniform bed-material, *Journal of Hydraulics Research* 6, 2, 173-176.

Newson, M.D. 1995. Fluvial geomorphology and environmental design, In Gurnell, A.M. & Petts, G.E. (Eds.), *Changing river channels*, Wiley, Chichester, 413-432.

Newson, M.D. 1996. *An assessment of the current and potential role of fluvial geomorphology in support of sustainable river management practices in South Africa*, Water Research Commission Report KV83/96, Water Research Commission, Pretoria.

Newson, M.D. & Sear, D. 1998. The role of geomorphology in monitoring and managing river sediment systems, *Journal of the Chartered Institution of Water and Environmental Management* 12, 1, 18-24.

Newson, M.D.; Clark, M.J.; Sear, D.A. & Brookes, A. 1998. The geomorphological basis for classifying rivers, *Aquatic Conservation: Marine and Freshwater Ecosystems* 8, 415-430.

Nicholas, A.P.; Ashworth, P.J.; Kirkby, M.J.; Macklin, M.G. & Murray, J. 1995. Sediment slugs: large-scale fluctuations in flume sediment transport rates and storage volumes, *Progress in Physical Geography* 19, 4, 500-519.

Nixon, M. 1959. A study of bankfull discharge of Rivers in England and Wales, *Proceedings of the Institute of Civil Engineers* 12, 157-174.

Nordin, C.F. 1963. A preliminary study of sediment transport parameters, Rio Puerco near Bernado, New Mexico, *United States Geological Survey Professional Paper* 462-F.

Olsen, D.S.; Whitaker, A.C. & Potts, D.F. 1997. Assessing stream channel stability thresholds using flow competence estimates at the bankfull stage, *Journal of the American Water Resources Association* 33, 6, 1197-1207.

Orndorff, R.L. & Whiting, P.J. 1999. Computing effective discharge with S-PLUS, *Computers and Geosciences* 25, 5, 559-565.

Osterkamp, W.R. & Hedman, E.R. 1977. Variation of width and discharge for natural high-gradient stream channels, *Water Resources Research* 13, 2, 256-258.

Osterkamp, W.R.; Lane, L.J. & Foster, G.R. 1983. An analytical treatment of channel-morphology relations, *United States Geological Survey Professional Paper* 1288.

Padmore, C.L. 1997. Biotopes and their hydraulics: a method for defining the physical component of freshwater quality, In Boon, P.J. & Howell, D.L. (Eds.), *Freshwater quality: defining the indefinable*, Scottish Natural Heritage, Edinburgh, 251-257.

Palmer, R. & O'Keeffe, J. 1985. *Downstream effects of the impoundments on the Buffalo River eastern Cape Province*, In Lesolivet, C. & Maison, E. (Eds.), Rhodes University Institute for Freshwater Studies Report No. 18, 1-8.

Palmer, R.W. & O'Keeffe, J.H. 1990. Transported material in a small river with multiple impoundments, *Freshwater Biology* 24, 563-575.

Park, C.C. 1981. Man, river systems and environmental impacts, *Progress in Physical Geography* 5, 1, 1-31.

Parker, G.; Klingeman, P.C. & McLean, D.G. 1982. Bed load and size distribution in paved gravel-bed streams, *Journal of the Hydraulics Division*, American Society of Civil Engineers 108 (HY4), 544-571.

Partridge, T.C. 1988. Geomorphological perspectives on recent environmental change in southern Africa, In MacDonald, I.A.W. & Crawford, R.J.M. (Eds.), *Long term data series relating to southern Africa's renewable resources*, South African Natural Scientific Programmes Report 157, Pretoria, 367-378.

Partridge, T.C. 1990. Cainozoic environmental changes in southern Africa, *South African Journal of Science* 86, 315-317.

Partridge, T.C. & Maud, R.R. 1987. Geomorphic evolution of southern Africa since the Mesozoic, *South African Journal of Geology* 90, 179-208.

Partridge, T.C.; Avery, D.M; Botha, G.A.; Brink, J.S.; Deacon, J.; Herbert, R.S.; Maud, R.R.; Scholtz, A.; Scott, L.; Talma, A.S. & Vogel, J.S. 1990. Late Pleistocene and Holocene climate change in southern Africa, *South African Journal of Science* 86, 302-305.

Patton, P.C.; Baker, V.R. & Kochel, R.C. 1979. Slack-water deposits: A geomorphic technique for the interpretation of fluvial palaeohydrology, In Rhodes, D.D. & Williams, G.P. (Eds), *Adjustments to the fluvial system*, Kendall/Hunt, Dubuque, Iowa, 225-253.

Perry, J.E. 1985. Lateral stability of the lower reachs of the Mzumbe River, Natal, In Schulze, R.E. (Ed.), *Proceedings of the Second South African National Hydrology Symposium*, Pietermaritzburg, 219-228.

Petit, F. 1994. Dimensionless critical shear stress evaluations from flume experiments using different gravel beds, *Earth Surface Processes and Landforms* 19, 565-576.

Petts, G.E. 1985. *Impounded rivers: perspectives for ecological management*, Wiley, New York.

Petts, G.E. 1996. Water allocation to protect river ecosystems, *Regulated Rivers: Research and Management* 12, 353-365.

Phillips, B.C. & Sutherland, A.J. 1989. Spatial lag effects in bed load sediment transport, *Journal of Hydraulic Research* 27, 115-133.

Pickup, G. 1976. Geomorphic effects of changes in runoff, Cumberland basin, NSW, *Australian Geographer* 13, 188-193.

Pickup, G. 1991. Event frequency and landscape stability on the floodplain systems of arid Central Australia, *Quaternary Science Review* 10, 463-473.

Pickup, G. & Warner, R.F. 1976. Effects of hydrologic regime on magnitude and frequency of dominant discharge, *Journal of Hydrology* 29, 51-75.

Pickup, G. & Rieger, W.A. 1979. A conceptual model of the relationship between channel characteristics and discharge, *Earth Surface Processes* 4, 37-42.

Pickup, G.; Higgins, R.J. & Grant, I. 1983. Modelling sediment transport as a moving wave - the transfer and deposition of mining waste, *Journal of Hydrology* 60, 281-301.

Pitlick, J. & Van Steeter, M.M. 1998. Geomorphology and endangered fish habitats of the upper Colorado river. 2. Linking sediment transport to habitat maintenance, *Water Resources Research* 34, 2, 303-316.

Pitman, W.V. & Pullen, R.A. 1989. The impact of minor dams on the water resources of the upper Olifants basin, In Kienzle, S. & Maaren, H. (Eds.), *Proceedings of the 4th South African National Hydrological Symposium*, University of Pretoria, 20-22 November 1989, 45-54.

Poesen, J.W.A. & Hooke, J.M. 1997. Erosion, flooding and channel management in Mediterranean environments of southern Europe, *Progress in Physical Geography* 21, 2, 157-199.

Prins, A. & De Vries, M. 1971. On dominant discharge concepts for rivers, *Proceedings of the XIV Congress of the International Association for Hydraulic Research* XIV, 161-170.

Proffitt, G.T. & Sutherland, A.J. 1983. Transport of non-uniform sediments, *Journal of Hydraulics Research* 21, 33-43.

Reid, I.; Frostick, L.E. & Layman, J.T. 1985. The incidence and nature of bedload transport during flood-flows in coarse-grained alluvial channels, *Earth Surface Processes and Landforms* 10, 33-44.

Reid, I. & Frostick, L.E. 1987. Toward a better understanding of bedload transport, In Ethridge, F.G.; Flores, R.M. & Harvey, M.A. (Eds.), *Recent developments in fluvial sedimentology*, Society of Economic Palaeontologists and Mineralogists, Special Publication 39, Tulsa, Oklahoma, 13-19.

Reid, I. & Laronne, J.B. 1995. Bedload sediment transport in an ephemeral stream and a comparison with seasonal and perennial counterparts, *Water Resources Research* 31, 773-781.

Reid, I.; Powell, D.M. & Church, M. 1996. Prediction of bedload transport by desert flash-floods, *Journal of Hydraulic Engineering*, American Society of Civil Engineers 122, 170-173.

Reid, I.; Bathurst, J.C.; Carling, P.A.; Walling, D.E. & Webb, B.W. 1997. Sediment erosion, transport and deposition, In Thorne, C.R.; Hey, R.D. & Newson, M.D. (Eds.), *Applied fluvial geomorphology for river engineering and management*, Wiley, Chichester, 95-135.

Reid, I. & Frostick, L.E. 1997. Channel form, flows and sediments in deserts, In Thomas, D.S.G. (Ed.) *Arid zone geomorphology*, Wiley, Chichester, 205-229.

Reid, I.; Laronne, J.B. & Powell, D.M. 1998. Flash-flood and bedload dynamics of desert gravel-bed streams, *Hydrological Processes* 12, 543-557.

Reiser, D.W.; Ramey, M.P. & Wesche, T.A. 1989. Flushing flows, In Gore, J.A. & Petts, G.E. (Eds.), *Alternatives in regulated river management*, CRC Press, Boca Raton, 91-135.

Rhoads, B.L. 1994a. Fluvial geomorphology, *Progress in Physical Geography* 18, 1, 103-123.

Rhoads, B.L. 1994b. Fluvial geomorphology, *Progress in Physical Geography* 18, 4, 588-608.

Richards, K. 1982. *Rivers: form and process in alluvial channels*, Methuen, London.

Riley, S.J. 1972. A comparison of morphometric measures of bankfull, *Journal of Hydrology* 17, 23-31.

Roberts, D.F. 1952. An analysis of the amount of silt carried by South African rivers, *Transactions of the South African Society of Civil Engineers* 2, 5, 147-159.

Rooseboom, A. 1978. Sediment loads in South African rivers, *Water SA* 4, 1, 14-17. (in Afrikaans)

Rooseboom, A. 1992. *Sediment transport in rivers and reservoirs, a southern African perspective*, Water Research Commission Report No. 297/1/92, Water Research Commission, Pretoria.

Rooseboom, A. & Harmse, H.J. Von M. 1979. Changes in the sediment load of the Orange River during the period 1929-1969, *Scientific Publications of the International Association of Hydrologists* 128, 459-470.

Rooseboom, A. & le Grange, A. 1992. Equilibrium scour in rivers with sandbeds, *Water SA* 18, 4, 287-292.

Rooseboom, A.; Verster, E.; Zietsman, H.L. & Lotriet, H.H. 1992. *The development of a new sediment yield map of southern Africa*, Water Research Commission Report No. 297/2/92, Water Research Commission, Pretoria.

Rosgen, D. 1996. *Applied river morphology*, Printed Media Companies, Minnesota.

Rowntree, K.M. 1991. An assessment of the potential impact of alien invasive vegetation on the geomorphology of river channels in South Africa, *South African Journal of Aquatic Science* 17, 1/2, 28-43.

Rowntree, K.M. 2000. Fluvial geomorphology, In King, J.M.; de Villiers, M. & Tharme, R.E. (Eds.), *Environmental flow assessments for rivers: manual for the Building Block Methodology*, Water Research Commission Report, Pretoria (in press).

Rowntree, K.M. & Dollar, E.S.J. 1996a. Contemporary channel processes, In Lewis, C.A. (Ed.), *The geomorphology of the Eastern Cape, South Africa*, Grocott and Sherry, Grahamstown, 33-51.

Rowntree, K.M. & Dollar, E.S.J. 1996b. Controls on channel form and channel change in the Bell river, Eastern Cape, South Africa, *South African Geographical Journal* 78, 1, 20-28.

Rowntree, K.M. & Dollar, E.S.J. 1999. Vegetation controls on channel stability in the Bell river, Eastern Cape, South Africa, *Earth Surface Processes and Landforms* 24, 127-134.

Rowntree K.M. & Wadeson, R.A. 1996. Translating channel morphology into hydraulic habitat: application of the hydraulic biotope concept to an assessment of discharge related habitat changes, *Proceedings 2nd IAHR International Symposium on Hydraulics and Habitats, Quebec City*, June 11-14, 1996, Paper No. A283, 12.

Rowntree, K.M. & Wadeson, R.A. 1997. A hierarchical model for the assessment of instream flow requirements, *Geoöko plus 4*, 4, 85-100.

Rowntree, K.M. & Wadeson, R.A. 1999. *A hierarchical geomorphological model for the classification of selected South African rivers*, Water Research Commission Report No. 497/1/99, Water Research Commission, Pretoria.

Rutherfurd, I. 2000. Some human impacts on Australian stream channel morphology, In Brizga, S. & Finlayson, B. (Eds.) *River management: the Australasian experience*, Wiley, Chichester, 11-49.

Schmidt, K-H. & Ergenzinger, P. 1992. Bedload entrainment, travel lengths, step lengths, rest periods - studies with passive (iron, magnetic) and active (radio) tracer techniques, *Earth Surface Processes and Landforms* 17, 147-165.

Schoklitsch, A. 1934. Der geschiebetrieb und die geschiebefracht, *Wasskraft Wasserwirtschaft* 4, 1-7.

Schoklitsch, R. 1950. *Handbuch des wasserbaues*, Springer-Verlag, New York.

Schumm, S.A. 1971. Fluvial geomorphology, channel adjustments and river metamorphosis, In Shen, H.W. (Ed.), *River mechanics*, 1, Fort Collins, Colorado, 5.1-5.22.

Schumm, S.A. 1977. *The fluvial system*, Wiley, New York.

Schumm, S.A. & Lichty, R.W. 1963. Channel widening and flood plain construction along Cimarron river in southwestern Kansas, *United States Geological Survey Professional Paper* 352-D.

Schumm, S.A. & Lichty, R.W. 1965. Time, space and causality in geomorphology, *American Journal of Science* 263, 110-119.

Schumm, S.A. & Khan, H.R. 1972. Experimental study of channel patterns, *Geological Society of America Bulletin* 83, 1755-1770.

Schumm, S.A.; Mosley, M.P. & Weaver, W.E. 1987. *Experimental fluvial geomorphology*, Wiley, New York.

Schwartz, R.K.; Hughes, L.A.; Hansen, E.M.; Peterson, M.A. & Kelly, D.B. 1975. The Black Hills-Rapid city flood of June 9-10 1972, a description of the storm and the flood, *United States Geological Survey Professional Paper* 877.

Shaw, P.A. 1984. A historical note on the outflows of the Okavango Delta system, *Botswana Notes and Records* 16, 127-130.

Shields, A. 1936. *Application of similarity principles and turbulence research to bed-load movement*, Soil conservation service laboratory, California Institute of Technology, Pasadena, California.

Shih, S-M. & Komar, P.D. 1990. Differential bedload transport rates in a gravel-bed stream: a grain-size distribution approach, *Earth Surface Processes and Landforms* 15, 539-552.

Sidle, R.C. 1988. Bedload transport regime of a small forest stream, *Water Resources Research* 24, 207-218.

Siesser, W.G. 1978. Aridification of the Namib desert: evidence from the Ocean cores, In Van Zinderen Bakker, E.M. (Ed.), *Antarctic glacial history and world palaeoenvironments*, A.A. Balkema, Rotterdam, 105-113.

Simons, D.B. & Şentürk, F. 1977. *Sediment transport technology*, Water Resources Publications, Fort Collins, Colorado.

Simons, D.B. & Simons, R.K. 1987. Differences between gravel- and sand-bed rivers, In Thorne, C.R.; Bathurst, J.C. & Hey, R.D. (Eds.), *Sediment transport in gravel-bed rivers*, Wiley, Chichester, 3-15.

Smart, G.M. 1984. Sediment transport formula for steep channels, *Journal of Hydraulic Engineering*, American Society of Civil Engineers 110, 267-276.

Smith, A.M. 1991. Extreme palaeofloods: their climatic significance and the chances of floods of similar magnitude occurring, *South African Journal of Science* 87, 219-220.

Smith, A.M. 1992a. Palaeoflood hydrology of the Lower Umgeni River from a reach south of the Inanda dam, *South African Geographical Journal* 2, 63-68.

Smith, A.M. 1992b. Holocene palaeoclimate trends from palaeoflood analysis, *Palaeogeography, Palaeoclimatology, Palaeoecology* 97, 235-240.

Smith, R.M.H. 1995. Changing fluvial environments across the Permian-Triassic boundary in the Karoo Basin, South Africa and possible causes of tetrapod extinctions, *Palaeogeography, Palaeoclimatology, Palaeoecology* 117, 81-104.

Smith, R.M.H.; Turner, B.R.; Hancox, J. & Groenewald, G. 1997. Evolving fluvial landscapes in the main Karoo basin, *Guidebook 6th International Conference of Fluvial Sedimentology*. University of Cape Town, South Africa, 1-162.

Smith, A.M. & Zawada, P.K. 1990. Palaeoflood hydrology: a tool for South Africa? - an example from the Crocodile river near Brits, Transvaal, South Africa, *Water SA* 16, 3, 195-200.

Stevens, M.A.; Simons, D.B. & Richardson, E.V. 1975. Nonequilibrium river basins, *Journal of the Hydraulics Division*, American Society of Civil Engineers 101, HY53, 557-566.

Straub, L.G. 1935. *Missouri river report*, House Document 238, Appendix XV, Corps of Engineers, United States Department of the Army to the 73rd United States Congress, 2nd session.

Stuckmann, G. 1969. *The floods of Sept-Oct 1969 in Tunisia, Part II, Morphological Effects*, UNESCO, Paris, June 1970.

Swart, D.H.; Crowley, J.B.; Möller, J.P. & De Wet, A. 1990. Nature and behaviour of the flood at the river mouth, *Transactions of the Royal Society of South Africa* 47, 3, 217-245.

Tacconi, P. & Billi, P. 1987. Bed load transport measurement by vortex-tube trap on Vorginio Creek, Italy, In Thorne, C.R.; Bathurst, J.C. & Hey, R.D. (Eds.), *Sediment transport in gravel-bed rivers*, Wiley, Chichester, 583-616.

Thomas, M.F. & Thorp, M.P. 1995. Geomorphic response to rapid climatic and hydrologic change during the Late Pleistocene and Early Holocene in the Humid and Sub-Humid tropics, *Quaternary Science Review* 14, 193-207.

Thorne, C.R. 1991. Analysis of channel instability due to catchment land-use change, In Peters, N.E. & Walling, D.E. (Eds.), *Sediment and stream water quality in a changing environment*, International Association of Hydrological Sciences Publication 203, 111-122.

Thornes, J.B. 1976. Semi-arid erosion systems: case studies from Spain, *London School of Economics Geographical Papers*, 7, 79pp.

Thornes, J.B. 1977. Channel changes in ephemeral streams: observations, problems and models, In Gregory, K.J. (Ed.), *River channel changes*, Wiley, Chichester, 317-335.

Tinkler, K.J. & Wohl, E.E. (Eds.) 1998. *Rivers over rock: Fluvial processes in bedrock channels*, American Geophysical Union, Geophysical Monograph 107, Washington.

Tricart, J. 1961. Mechanismes normeaux et phenonmenes catastrohiqes dans l'evolution des versants du Basin de Guil, Hautes Alps, France, *Zeitschrift für Geomorphologie* 5, 277-301.

Trimble, S.W. 1997. Streambank fish-shelter structures help stabilize tributary streams in Wisconsin, *Environmental Geology* 32, 3, 230-234.

Turner, B.R. 1980. Palaeohydraulics of an Upper Triassic braided river system in the main Karoo Basin, South Africa, *Transactions of the Geological Society of South Africa* 83, 425-431.

Tyson, P.D. 1986. *Climate change and variability in South Africa*, Oxford University Press, Cape Town.

Tyson, P.D. & Lindesay, J.A. 1992. The climate of the last 2000 years in southern Africa, *The Holocene* 2, 3, 271-278.

van Bladeren, D. 1992. *Historical flood documentation series No. 1: Natal and Transkei, 1848-1989*, Department of Water Affairs and Forestry Technical Report TR 147, Pretoria.

van Bladeren, D. & Burger, C.E. 1989. *Documentation of the September 1987 Natal floods*, Technical Report No.139, Department of Water Affairs, Pretoria, South Africa.

van Coller, A.L. 1993. *Riparian vegetation of the Sabie River: relating spatial distribution patterns to the physical environment*, MSc thesis, University of the Witwatersrand, Johannesburg.

Van Coller, A.L.; Heritage, G.L. & Rogers, K.H. 1995. Linking riparian vegetation distribution and flow regime of the Sabie River through fluvial geomorphology, In *Proceedings of the Seventh South African National Hydrological Symposium*, Grahamstown, South Africa.

van Coller, A.L.; Rogers, K.H. & Heritage, G.L. 1997. Linking riparian vegetation types and fluvial geomorphology along the Sabie River within the Kruger National Park, South Africa, *African Journal of Ecology* 35, 194-212.

van Heerden, I. L. & Swart, D.H. 1986. Fluvial processes in the Mfolozi Flats and the consequences for St Lucia estuary, In Schulze, R.E. (Ed.), *Proceedings of the Second South African National Hydrology Symposium*, 1985, ACRU Report 22, University of Natal, Pietermaritzburg, 202-219.

van Niekerk, A.W. & Heritage, G.L. 1993. *Geomorphology of the Sabie River: overview and classification*. Centre for Water in the Environment Report No. 2/93, University of the Witwatersrand, Johannesburg.

van Niekerk, A.W.; Heritage, G.L. & Moon, B.P. 1995. River classification for management: the geomorphology of the Sabie River in the Eastern Transvaal, *South African Geographical Journal* 77, 2, 68-76.

Van Steeter, M.M. & Pitlick, J. 1998. Geomorphology and endangered fish habitats of the upper Colorado river, 1. Historic changes in streamflow, sediment load, and channel morphology, *Water Resources Research* 34, 2, 287-307.

van Wyk, N.J. 1989. River flow information during floods in the Vaal and Orange River systems, In Kienzle, S. & Maaren, H. (Eds.), *Proceedings of the 4th South African National Hydrological Symposium*, University of Pretoria, 20-22 November 1989, 180-185.

van Warmelo, W. 1922a. Hydrography of the Vaal River, *South African Irrigation Magazine* 1, 3, 111-116.

van Warmelo, W. 1922b. Hydrography of the Orange River, *South African Irrigation Magazine* 1, 4, 172-174.

van Warmelo, W. 1922c. Hydrography of the Orange River between junction Vaal River and the sea, *South African Irrigation Magazine* 1, 5, 244-246.

Vanoni, V.A. 1964. *Measurements of critical shear stress for entraining fine sediments in a boundary layer*, California Institute Technology Report, KH-R-7.

Venter, F.J. 1991. *Fisiese kenmerke van bereike van standhoudende riviere in die Nasionale Kruger Wildtuin*, Paper Presented at the First Research Meeting of the Kruger National Park Rivers Research Program.

Venter, F.J. & Bristow, J.W. 1986. An account of the geomorphology and drainage of the Kruger National Park, *Koedoe* 29, 117-124.

Viljoen, M.J. and Reimold, W.U. 1994. The Ventersdorp Contact Reef revisited - an introduction, *South African Journal of Geology* 97, 234-237.

Visser, J.N.J. 1989. The Permo-Carboniferous Dwyka Formation of southern Africa: deposition by a predominantly subpolar marine ice sheet, *Palaeogeography, Palaeoclimatology, Palaeoecology* 70, 377-391.

Vogt, I. 1992. *Short term geomorphological changes in the Sabie and Letaba Rivers in the Kruger National Park*, Unpublished MSc thesis, University of Witwatersrand, Johannesburg.

Vogt, I. & Moon, B.P. 1989. Short term geomorphological change in Kruger National Park rivers, In De Vos, V.; Randall, R.M.; Novellie, P.; Gertenbach, W.P.D. & Bryden, H.B.T. (Eds.), *Progress Report of Research Projects Undertaken in South African National Parks*, No. 7, Division of Research and Scientific Liaison, National Parks Board, Skukuza, South Africa, 193-194.

Wadeson, R.A. 1989. *A geomorphological evaluation of river zonation concepts: a case study from the Buffalo river catchment*, Unpublished B.A. (Hons) thesis, Rhodes University, Grahamstown.

Wadeson, R.A. 1994. A geomorphological approach to the identification and classification of instream flow requirements, *Southern African Journal of Aquatic Sciences* 20, 1/2, 38-61.

Wadeson, R.A. 1995. *The development of the hydraulic biotope concept within a catchment based hierarchical geomorphological model*, Unpublished PhD thesis, Rhodes University, Grahamstown.

Wadeson, R.A. & Rowntree, K.M. 1994. A hierarchical geomorphological model for the classification of South African River Systems, In Uys, M.C. (Ed.), Classification of rivers and environmental health indicators, *Proceedings of a Joint South African Australian Workshop*, Cape Town, 49-67.

Walling, D.E. 1996. Hydrology and rivers, In Adams, W.M.; Goudie, A.S. & Orme, A.R. (Eds.), *The physical geography of Africa*, Oxford University Press, Oxford, 103-121.

Walsh, R.P.D.; Davies, H.R.J. & Musa, S.B. 1994. Flood frequency and impacts at Khartoum since the early nineteenth century, *Geographical Journal* 160, 3, 266-279.

Warner, R.F. 1987. Spatial adjustment to temporal variations in flood regime in some Australian rivers, In Richards, K.S. (Ed.), *River channel changes, environment and process*, Basil Blackwell, Oxford, 14-40.

Warren, C.H. 1922. Determination of silt in flood water of the Great Fish River, *South African Irrigation Magazine* 1, 2, 40-42.

Weiss, H.W. & Midgley, D.C. 1976. *The influence on St Lucia estuary of changes in the Mfolozi*, In St Lucia Scientific Advisory Workshop Meeting, Charters Creek, 15-17 February 1976, Natal Parks Board, Paper 5.

Wharburton, J. 1992. Observations of bedload transport and channel bed changes in a proglacial mountain stream, *Arctic and Alpine Research* 24, 195-203.

White, W.R.; Milli, H. & Crabtree, A.D. 1975. Sediment transport theories: a review, *Proceedings of the Institute of Civil Engineers* 2, 59, 265-292.

White, W.R. & Day, T.J. 1982. Transport of graded gravel bed material, In Hey, R.D.; Bathurst, J.C. & Thorne, C.R. (Eds.), *Gravel-bed rivers*, Wiley, Chichester, 181-223.

Wiberg, P.L. & Smith, J.D. 1987. Calculations of the critical shear stress for motion of uniform and heterogeneous sediments, *Water Resources Research* 23, 8, 1471-1480.

Wilcock, P.R. 1992. Flow competence: a criticism of a classic concept, *Earth Surface Processes and Landforms* 17, 289-298.

Wilcock, P.R. 1998. Two-fraction model of initial sediment motion in gravel-bed rivers, *Science* 280, 410-412.

Wilcock, P.R. & Southard, J.B. 1989. Bed load transport of mixed-size sediment: fractional transport rates, bed forms and the development of a coarse bed-surface layer, *Water Resources Research* 25, 1629-1641.

Wilcock, P.R.; Barta, A.F.; Shea, C.C.; Kondolf, G.M.; Matthews, W.V.G. & Pitlick, J. 1996a. Observations of flow and sediment entrainment on a large gravel-bed river, *Water Resources Research* 32, 9, 2897-2909

Wilcock, P.R.; Kondolf, G.H.; Matthews, W.V.G. & Barta, A.F. 1996b. Specification of sediment maintenance flows for a large gravel-bed river, *Water Resources Research* 32, 9, 2911-2921.

Williams, G.P. 1978. Bankfull discharge of rivers, *Water Resources Research* 14, 6, 164-168.

Williams, G.P. 1983. Palaeohydrological methods and some examples from Swedish fluvial environments, 1. Cobble and boulder deposits, *Geografiska Annaler* 65A, 227-243.

Williams, G.P. & Guy, H.P. 1973. Erosional and depositional aspects of Hurricane Camille, in Virginia, 1969, *United States Geological Survey Professional Paper 804*.

Wilson, B.H. & Dincer, T. 1976. An introduction to the hydrology and hydrography of the Okavango Delta, *Proceedings of Symposium on the Okavango Delta and its utilisation*, Botswana Society, Gaborone, L. Barker Press, New York, 33-48.

Wohl, E.E. 1992. Gradient irregularity in the Herbert Gorge of northeastern Australia, *Earth Surface Processes and Landforms* 17, 69-84.

Wolman, M.G. 1954. A method of sampling coarse river bed material, *Transactions of the American Geophysical Union* 35, 6, 951-956.

Wolman, M.G. & Gerson, R. 1978. Relative scales of time and effectiveness of climate in watershed geomorphlogy, *Earth Surface Processes* 3, 189-208.

Wolman, M.G. & Miller, J.P. 1960. Magnitude and frequency of forces in geomorphic processes, *Journal of Geology* 68, 1, 54-74.

Woodyer, K.D. 1968. Bankfull frequency in rivers, *Journal of Hydrology* 6, 114-142.

Yalin, M.S. 1963. *Mechanics of sediment transport*, Pergamon, Oxford.

Yang, C.T. 1972. Unit stream power and sediment transport, *Journal of the Hydraulics Division*, American Society of Civil Engineers 98 (HY10), 1805-1826.

Yang, C.T. 1973. Incipient motion and sediment transport, *Journal of the Hydraulics Division*, American Society of Civil Engineers 99 (HY10), 1679-1704.

Yang, C.T. 1984. Unit stream power equation for gravel, *Journal of the Hydraulics Division*, American Society of Civil Engineers 110 (HY12), 1783-1798.

Zawada, P.K. 1991. Palaeofloods and their climatic record, *South African Journal of Science* 87, 362.

Zawada, P.K. 1994. Palaeoflood hydrology of the Buffels River, Laingsburg, South Africa: was the 1981 flood the largest? *South African Journal of Geology* 97, 21-32.

Zawada, P.K. 1996. *Palaeoflood hydrology of selected South African rivers*, Unpublished PhD thesis, University of Port Elizabeth, Port Elizabeth.

Zawada, P.K. 1997. Palaeoflood hydrology: method and application in flood-prone southern Africa, *South African Journal of Science* 93, 111-132.

Zawada, P.K.; Hattingh, J. & van Bladeren, D. 1996. *Palaeoflood hydrological analysis of selected South African rivers*. Water Research Commission Report No. 509/1/96, Water Research Commission, Pretoria.

Zhang, D.D. 1998. Geomorphological problems of the middle reaches of the Tsangpo river, Tibet, *Earth Surface Processes and Landforms* 23, 889-903.

APPENDIX A

SKETCH MAP, PHOTOS AND CROSS-SECTIONS FOR ALL RIVERS

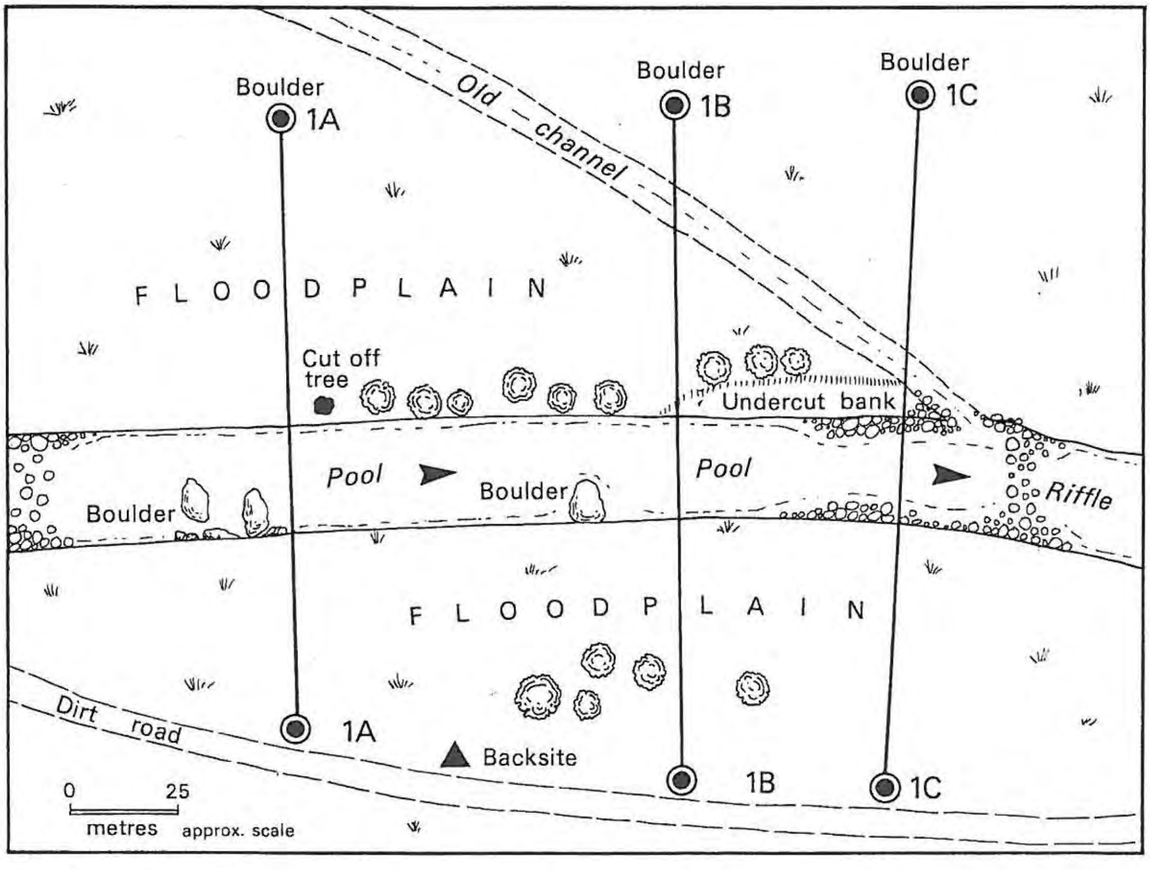

Mkomazi River Site 1

Mkomazi Site 1
Section A

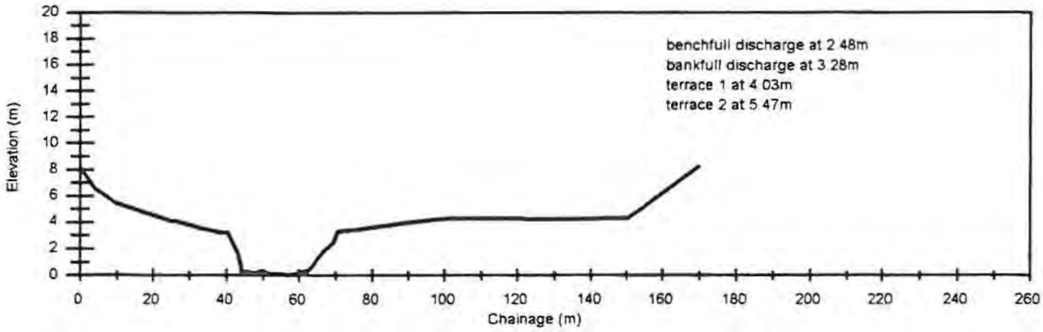

Mkomazi Site 1
Section B

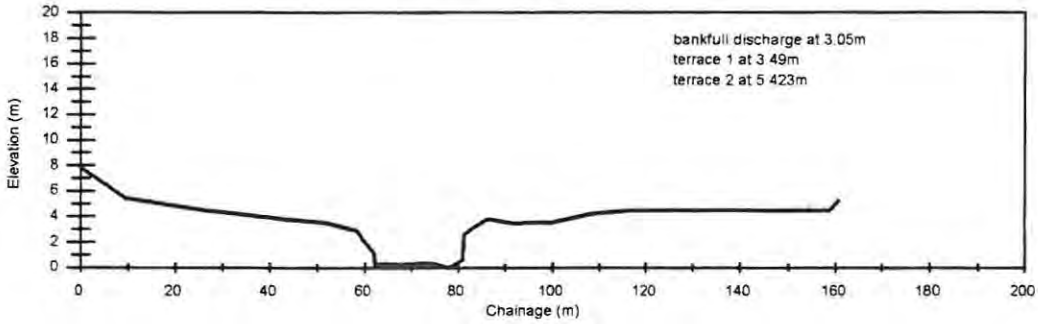

Mkomazi Site 1
Section C

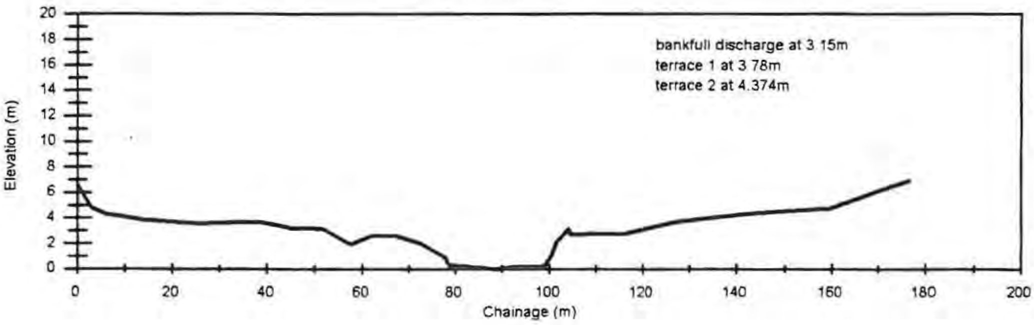

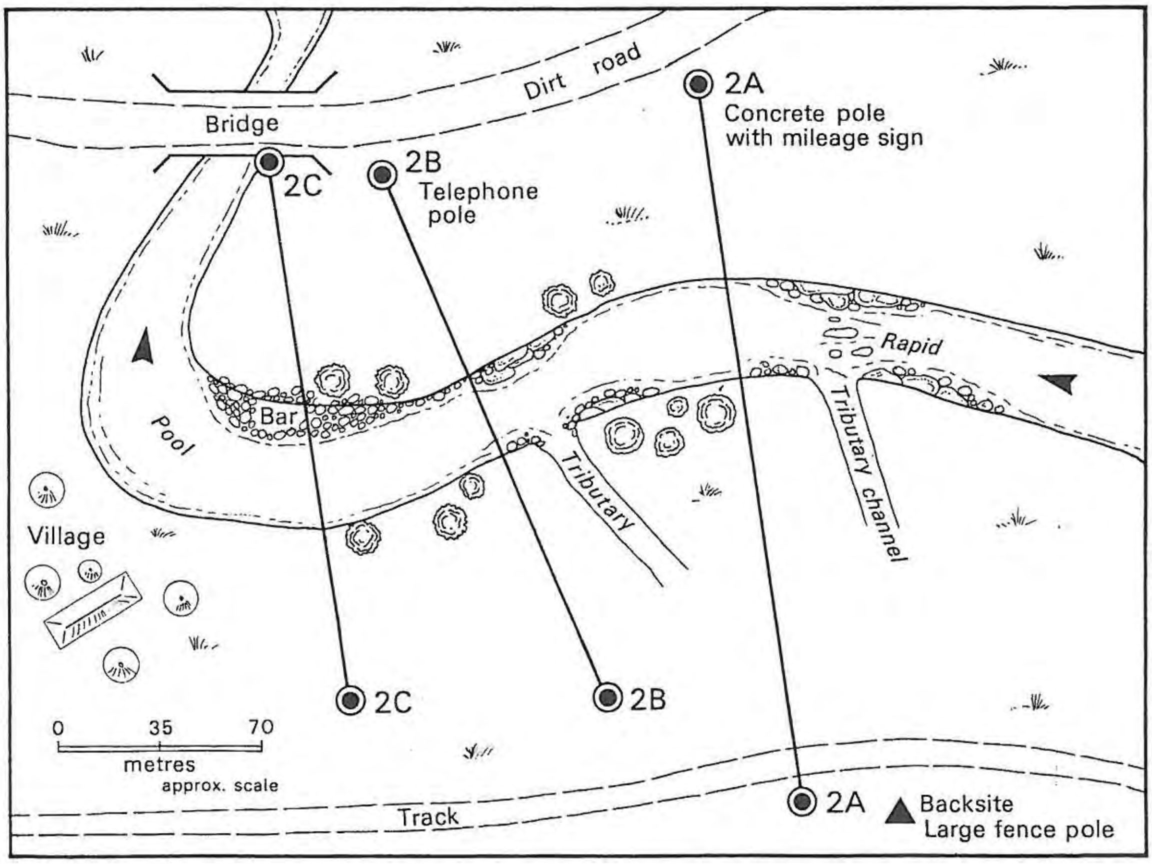

Mkomazi River Site 2

Mkomazi Site 2
Section A

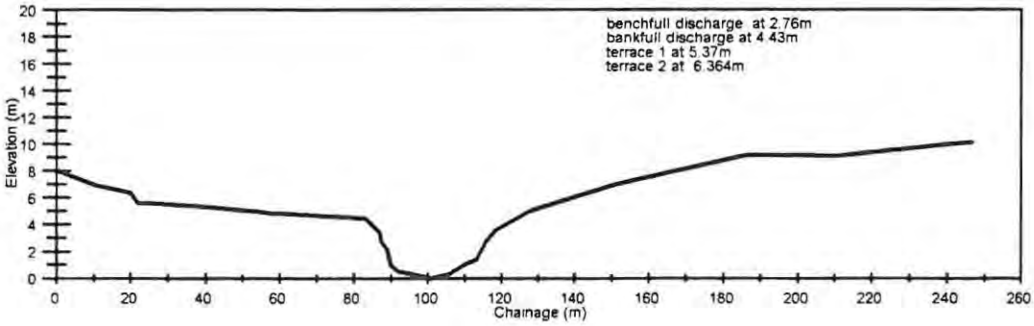

Mkomazi Site 2
Section B

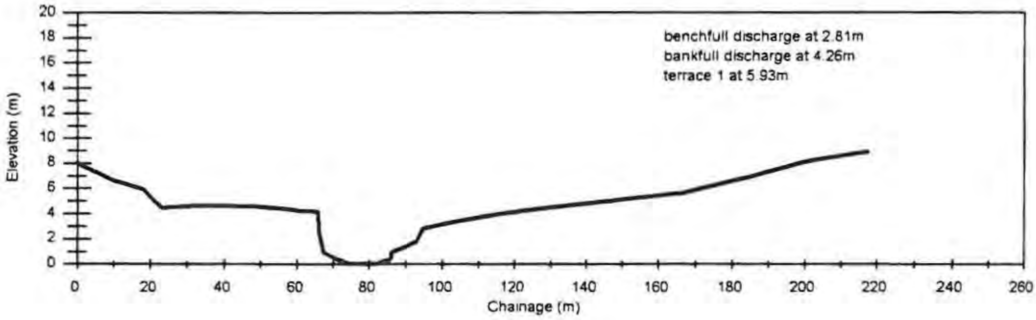

Mkomazi Site 2
Section C

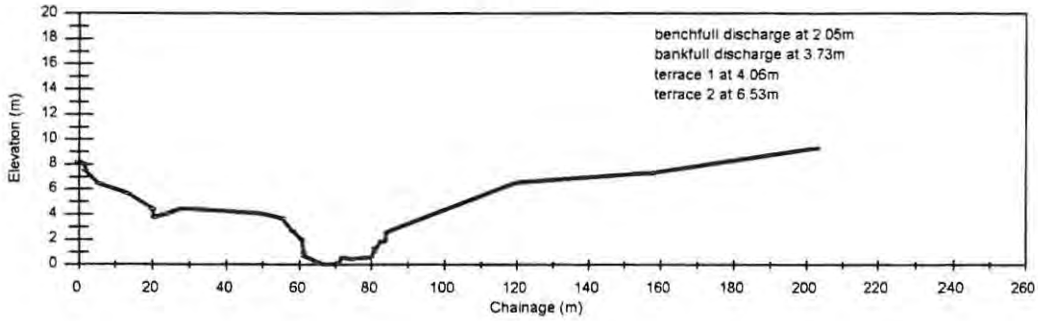

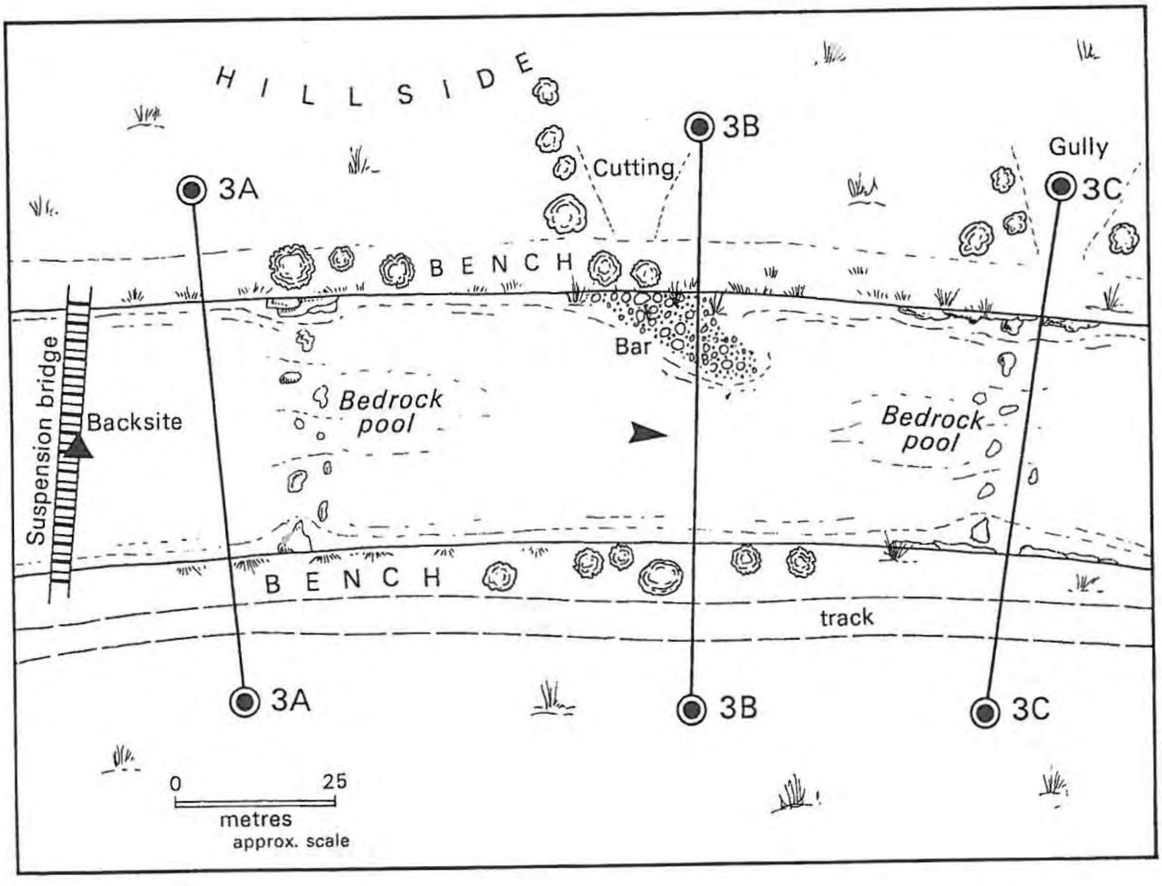

Mkomazi River Site 3

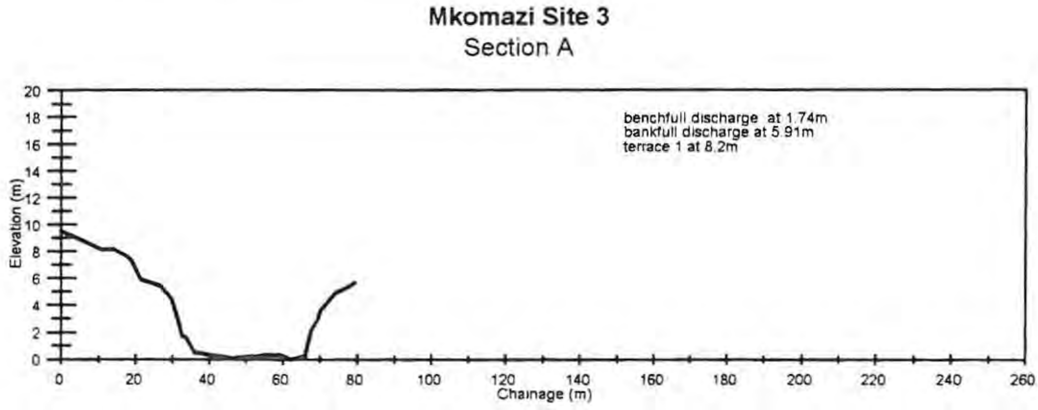
Mkomazi Site 3
Section A
benchfull discharge at 1.74m
bankfull discharge at 5.91m
terrace 1 at 8.2m
Elevation (m)
Chainage (m)

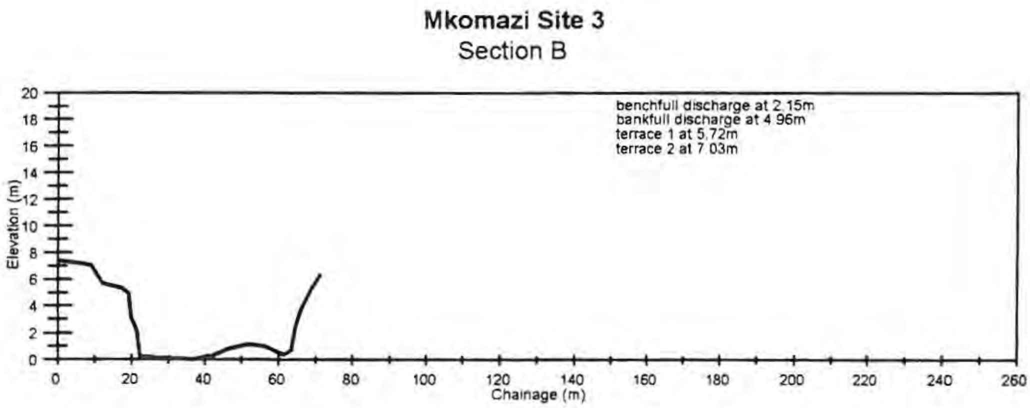
Mkomazi Site 3
Section B
benchfull discharge at 2.15m
bankfull discharge at 4.96m
terrace 1 at 5.72m
terrace 2 at 7.03m
Elevation (m)
Chainage (m)

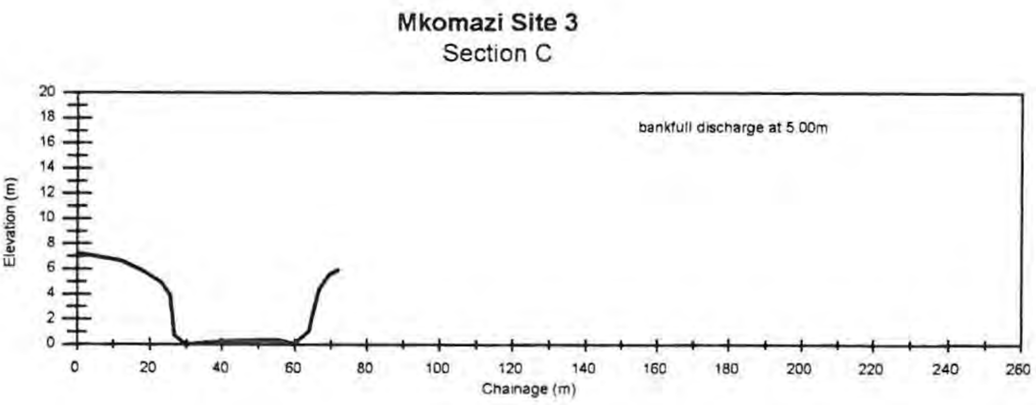
Mkomazi Site 3
Section C
bankfull discharge at 5.00m
Elevation (m)
Chainage (m)

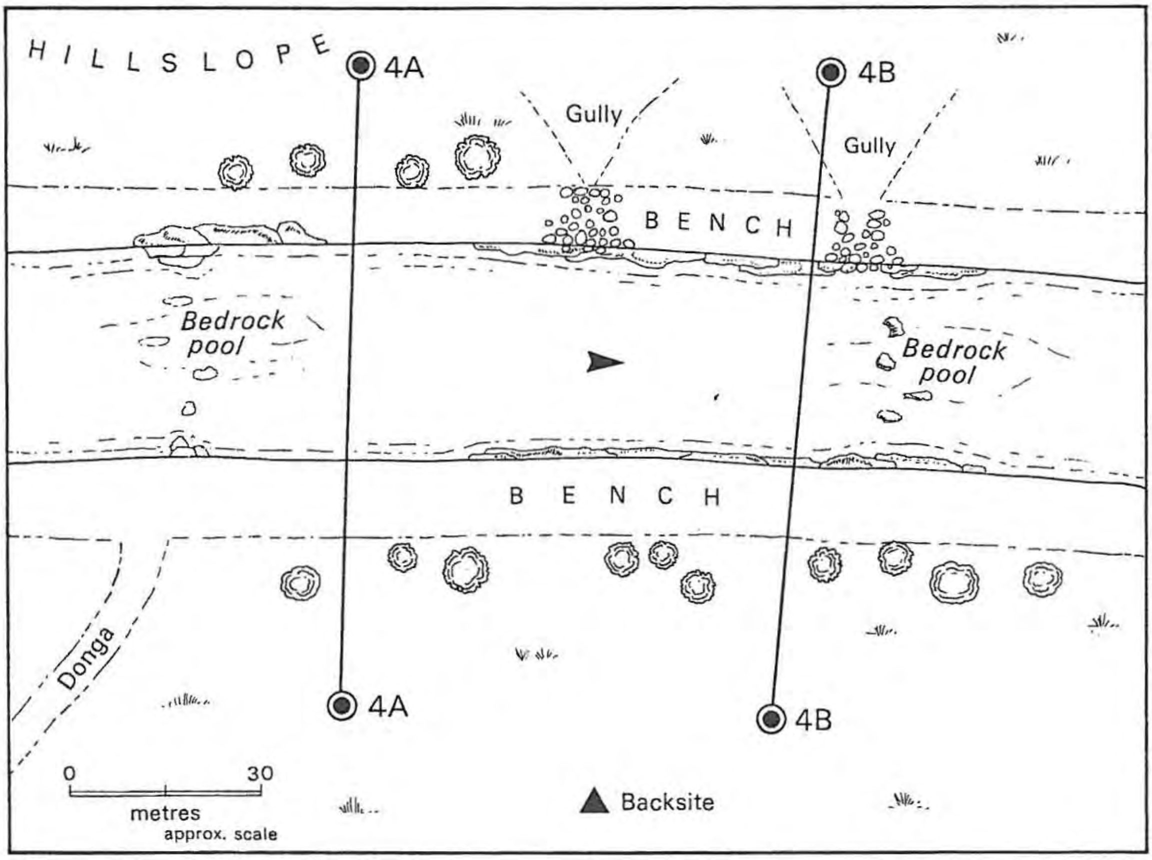

Mkomazi River Site 4

Mkomazi Site 4
Section A

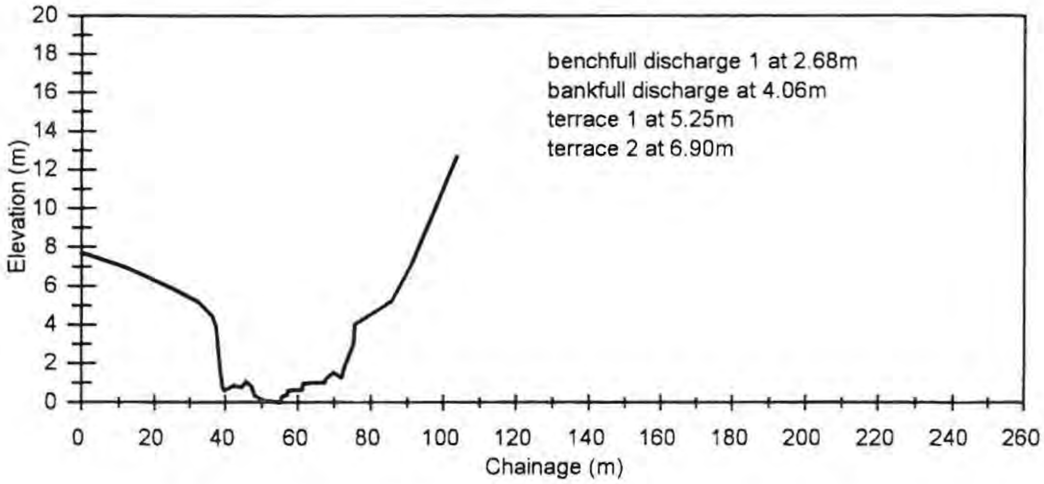

Mkomazi Site 4
Section B

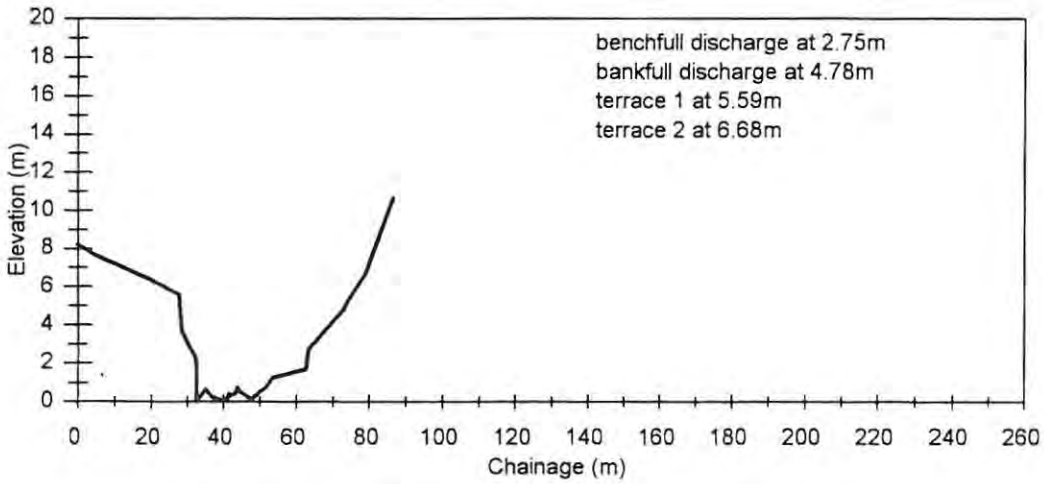

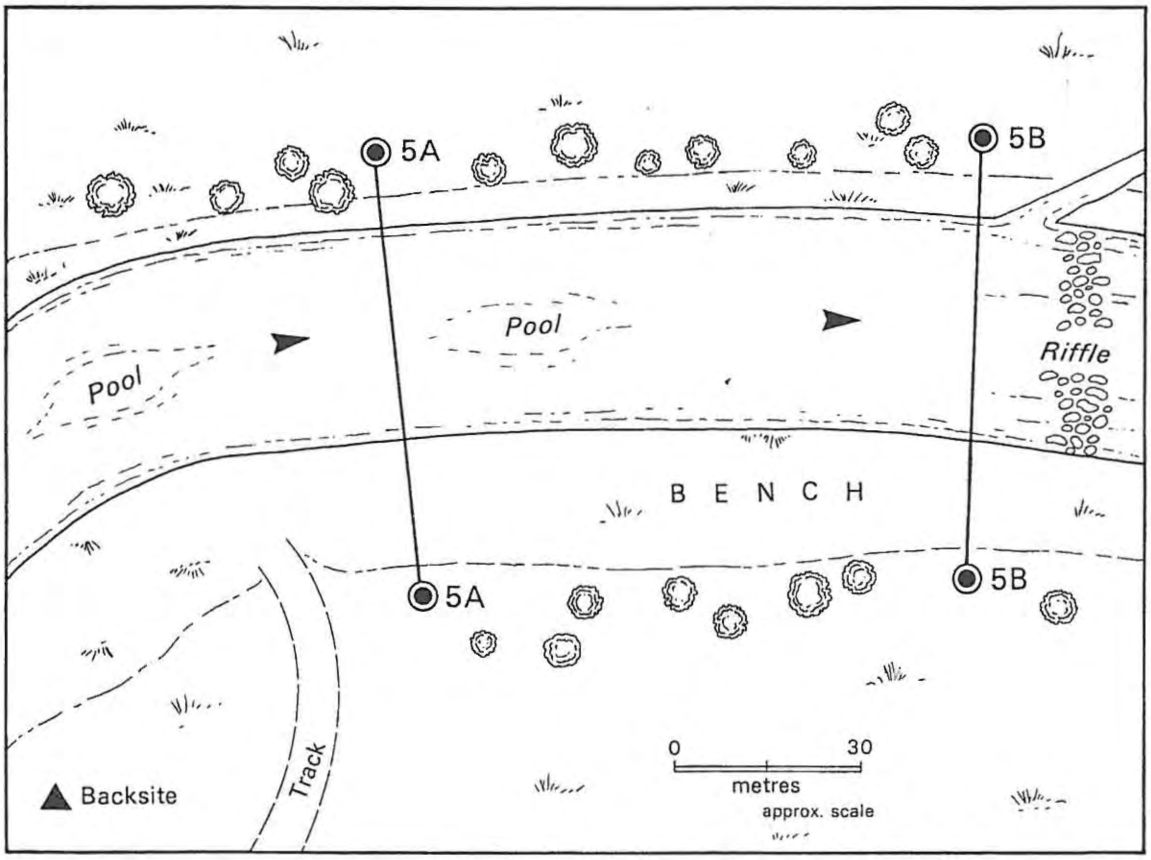

Mkomazi River Site 5

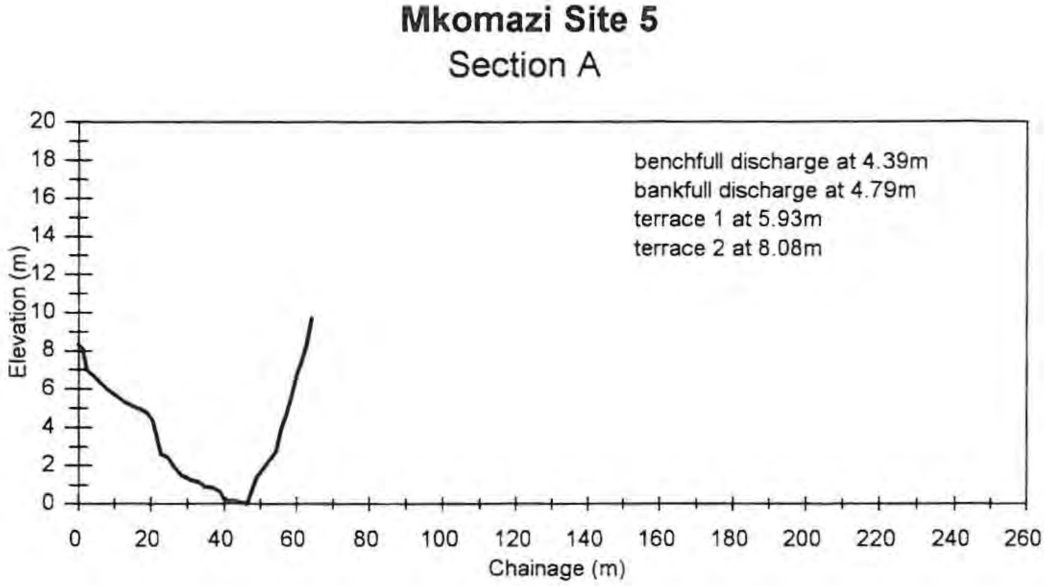
Mkomazi Site 5
Section A
benchfull discharge at 4.39m
bankfull discharge at 4.79m
terrace 1 at 5.93m
terrace 2 at 8.08m
Elevation (m)
Chainage (m)
0
2
4
6
8
10
12
14
16
18
20
0
20
40
60
80
100
120
140
160
180
200
220
240
260

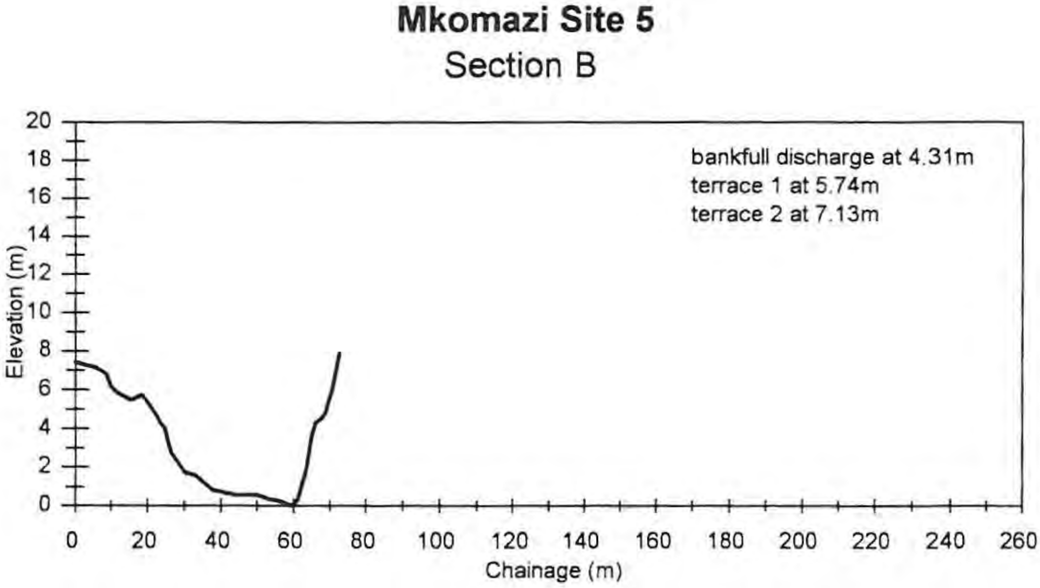
Mkomazi Site 5
Section B
bankfull discharge at 4.31m
terrace 1 at 5.74m
terrace 2 at 7.13m
Elevation (m)
Chainage (m)
0
2
4
6
8
10
12
14
16
18
20
0
20
40
60
80
100
120
140
160
180
200
220
240
260

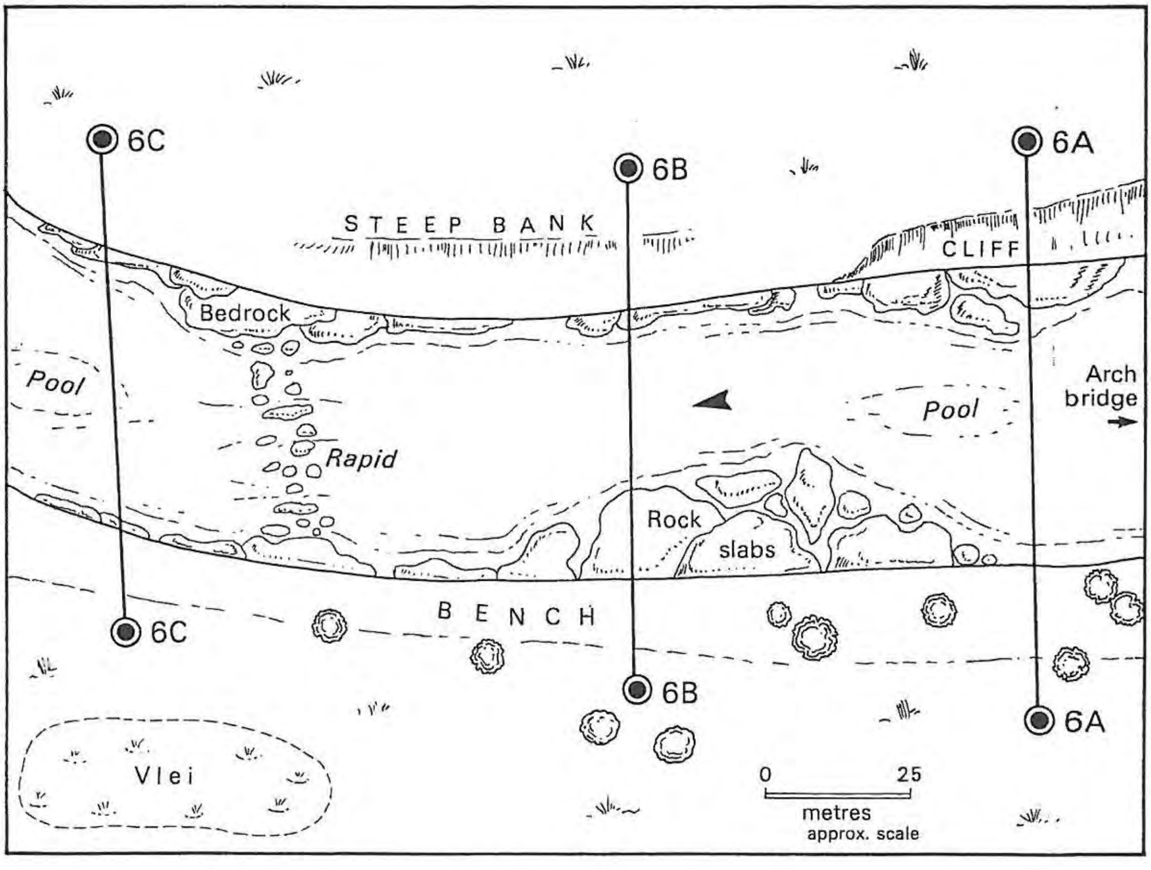

Mkomazi River Site 6

Mkomazi Site 6
Section A

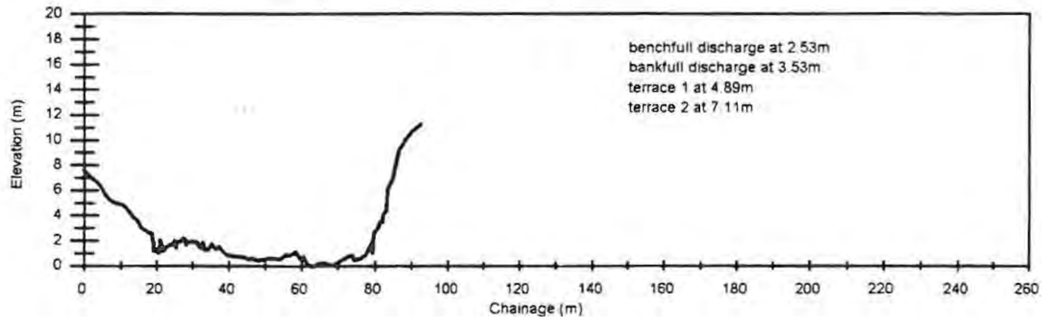

Mkomazi Site 6
Section B

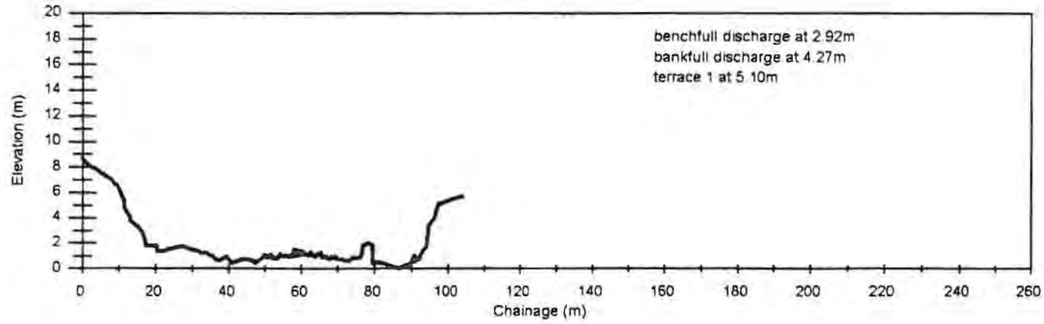

Mkomazi Site 6
Section C

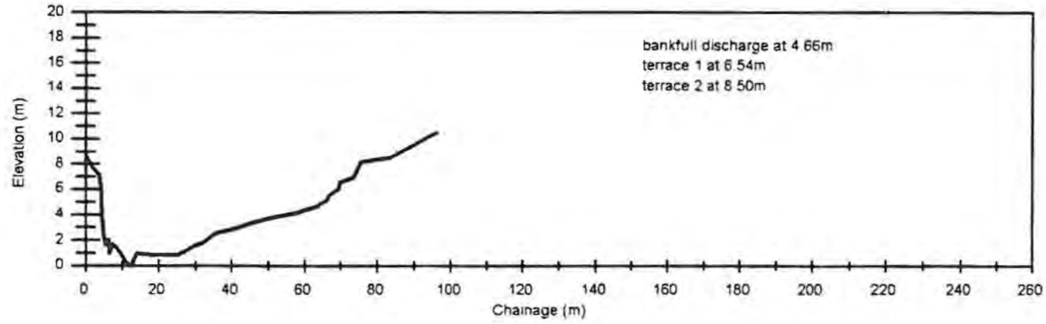

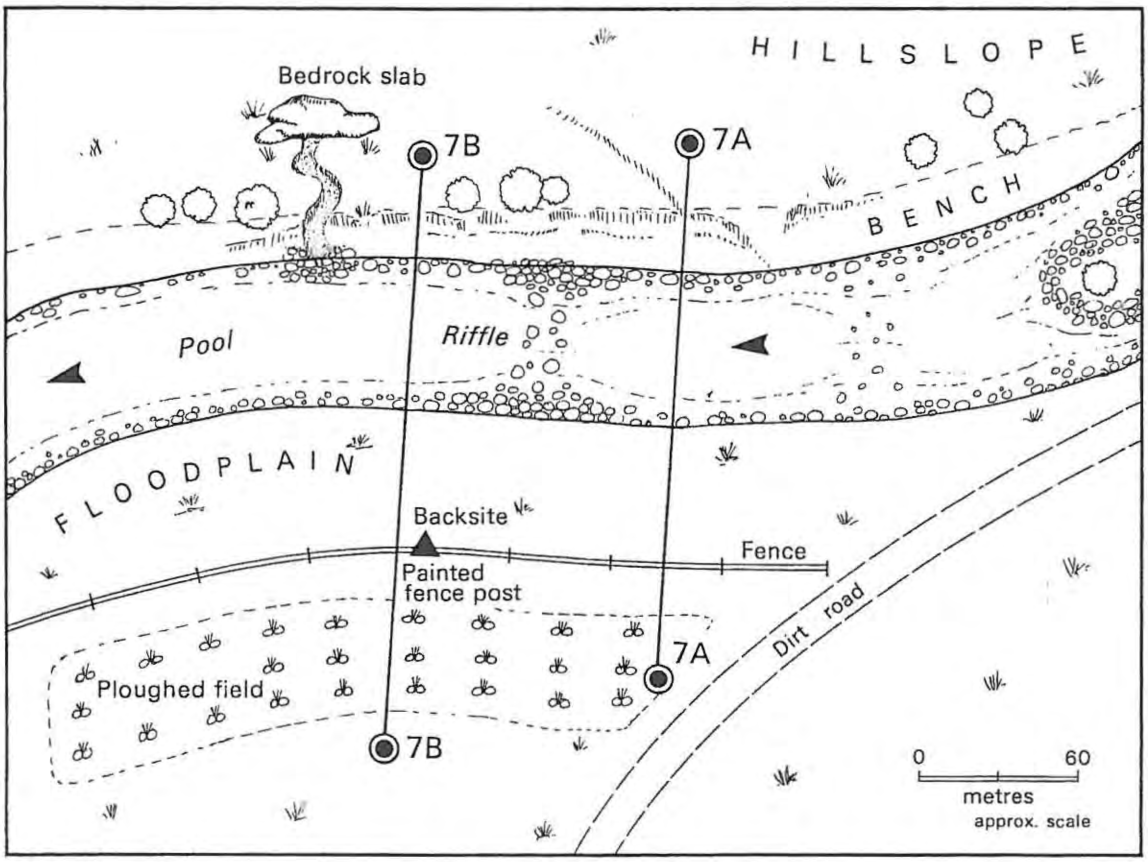

Mkomazi River Site 7

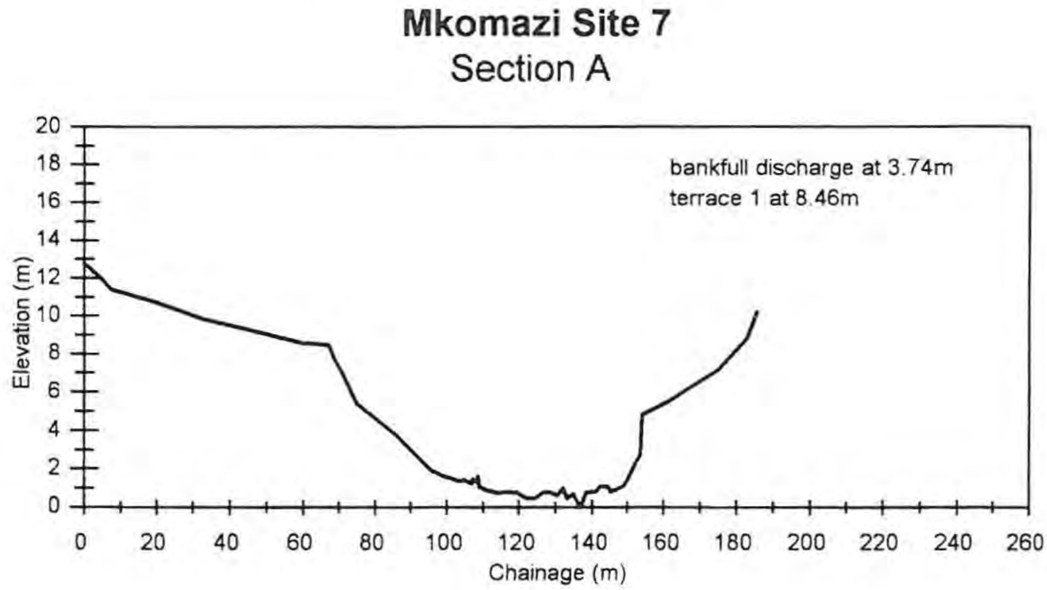
Mkomazi Site 7
Section A
bankfull discharge at 3.74m
terrace 1 at 8.46m
Elevation (m)
Chainage (m)
0
2
4
6
8
10
12
14
16
18
20
0 20 40 60 80 100 120 140 160 180 200 220 240 260

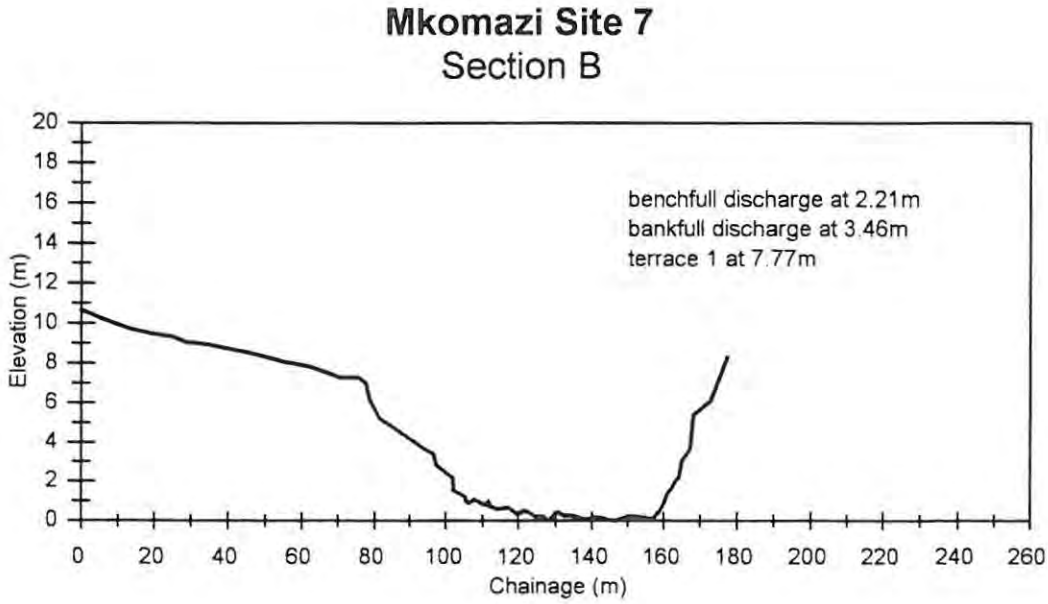
Mkomazi Site 7
Section B
benchfull discharge at 2.21m
bankfull discharge at 3.46m
terrace 1 at 7.77m
Elevation (m)
Chainage (m)
0
2
4
6
8
10
12
14
16
18
20
0 20 40 60 80 100 120 140 160 180 200 220 240 260

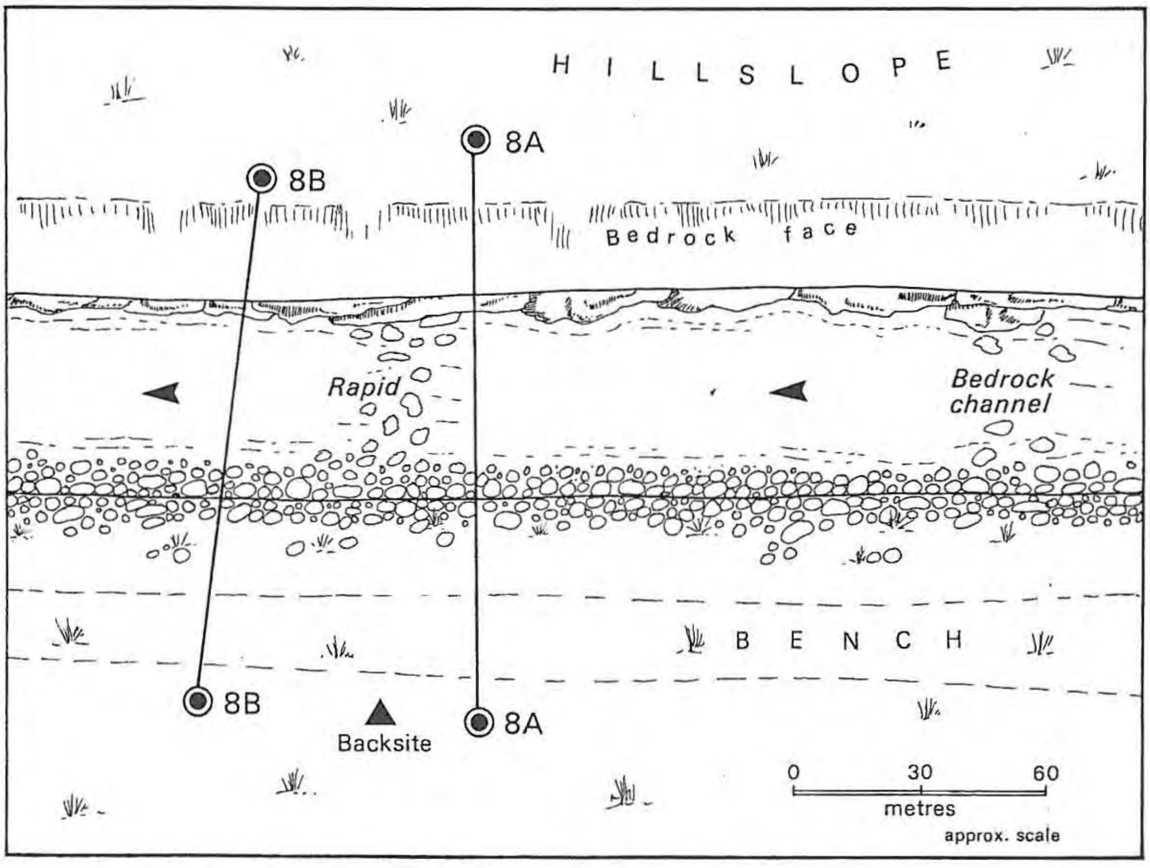

Mkomazi River Site 8

Mkomazi Site 8
Section A

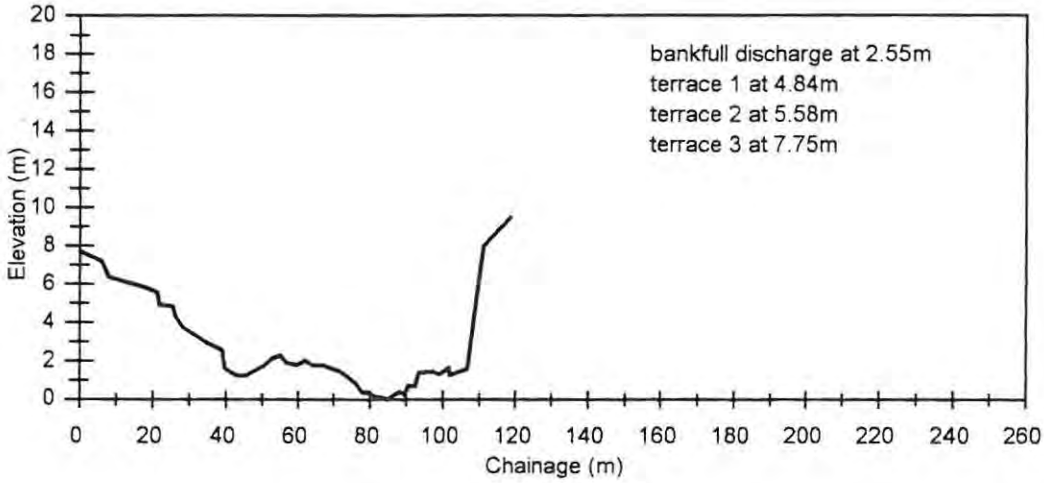

Mkomazi Site 8
Section B

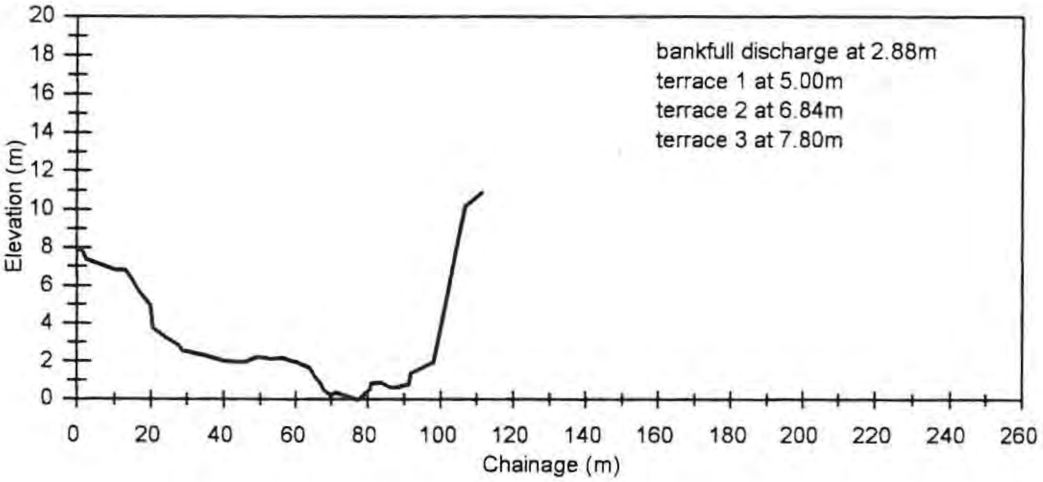

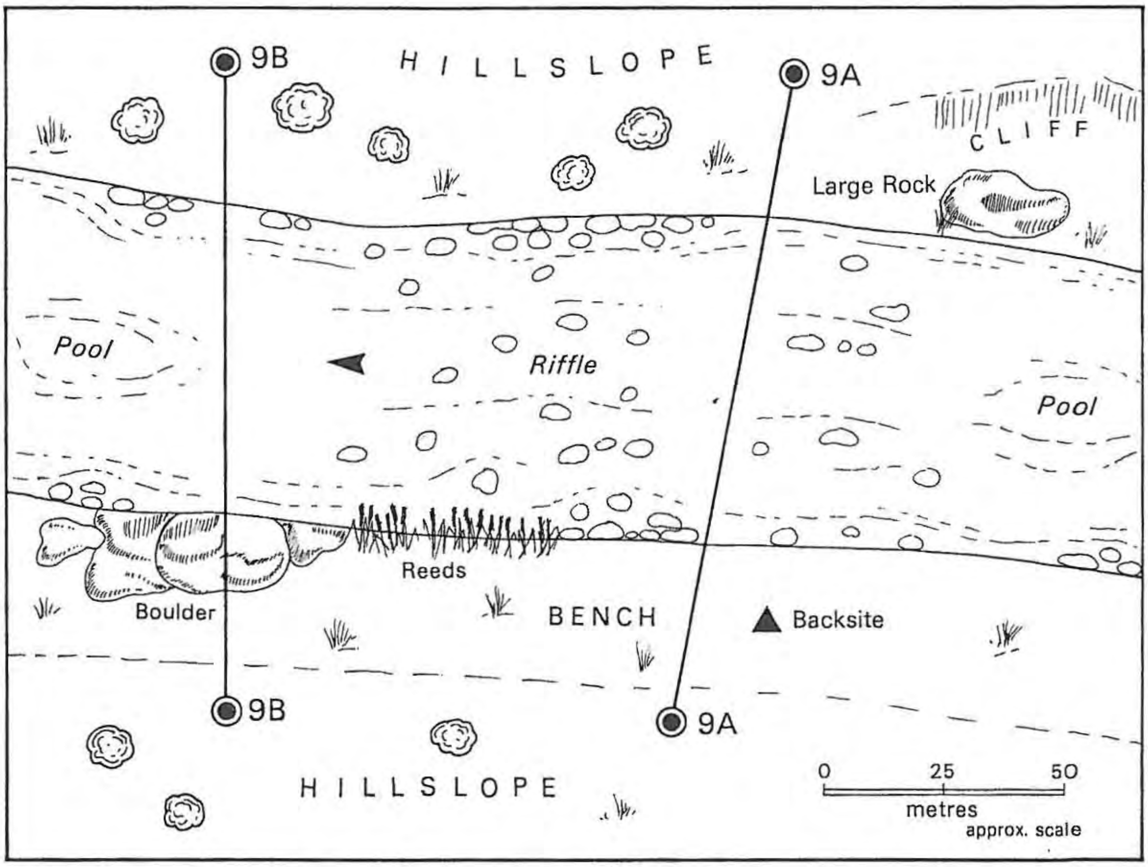

Mkomazi River Site 9

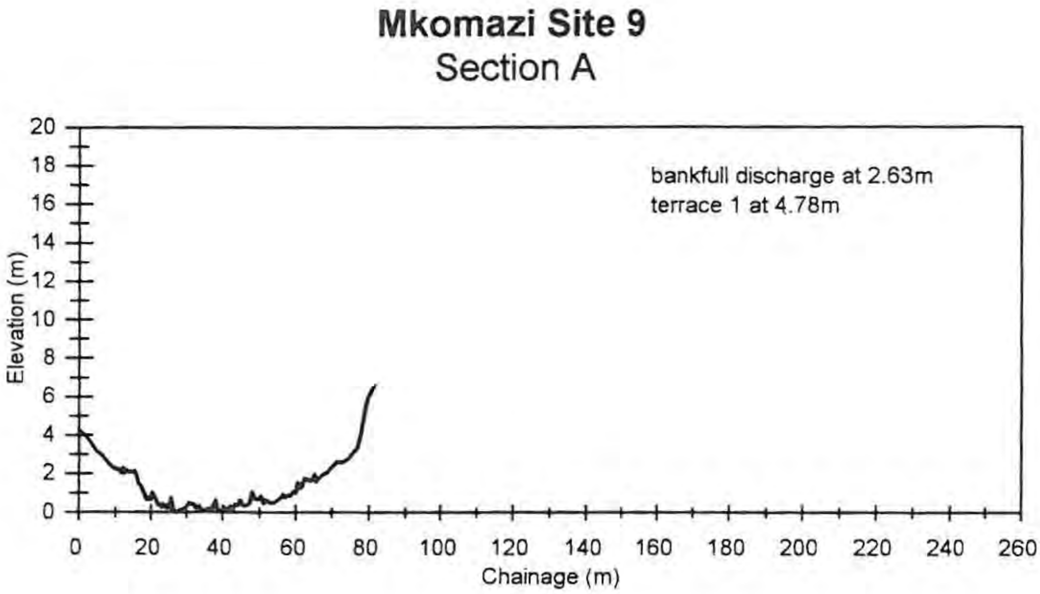
Mkomazi Site 9
Section A
bankfull discharge at 2.63m
terrace 1 at 4.78m
Elevation (m)
Chainage (m)
0
2
4
6
8
10
12
14
16
18
20
0 20 40 60 80 100 120 140 160 180 200 220 240 260

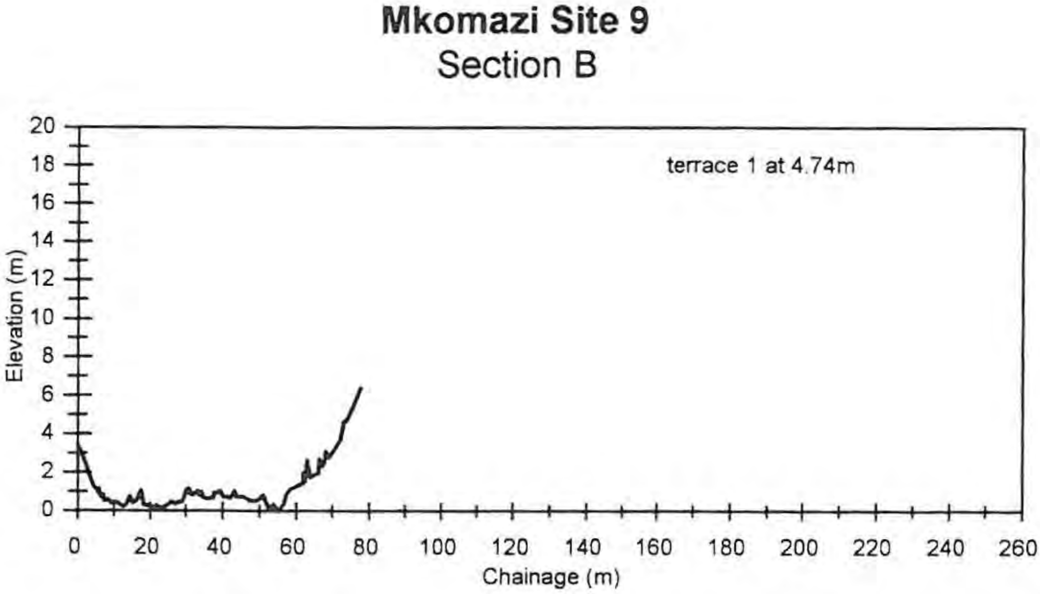
Mkomazi Site 9
Section B
terrace 1 at 4.74m
Elevation (m)
Chainage (m)
0
2
4
6
8
10
12
14
16
18
20
0 20 40 60 80 100 120 140 160 180 200 220 240 260

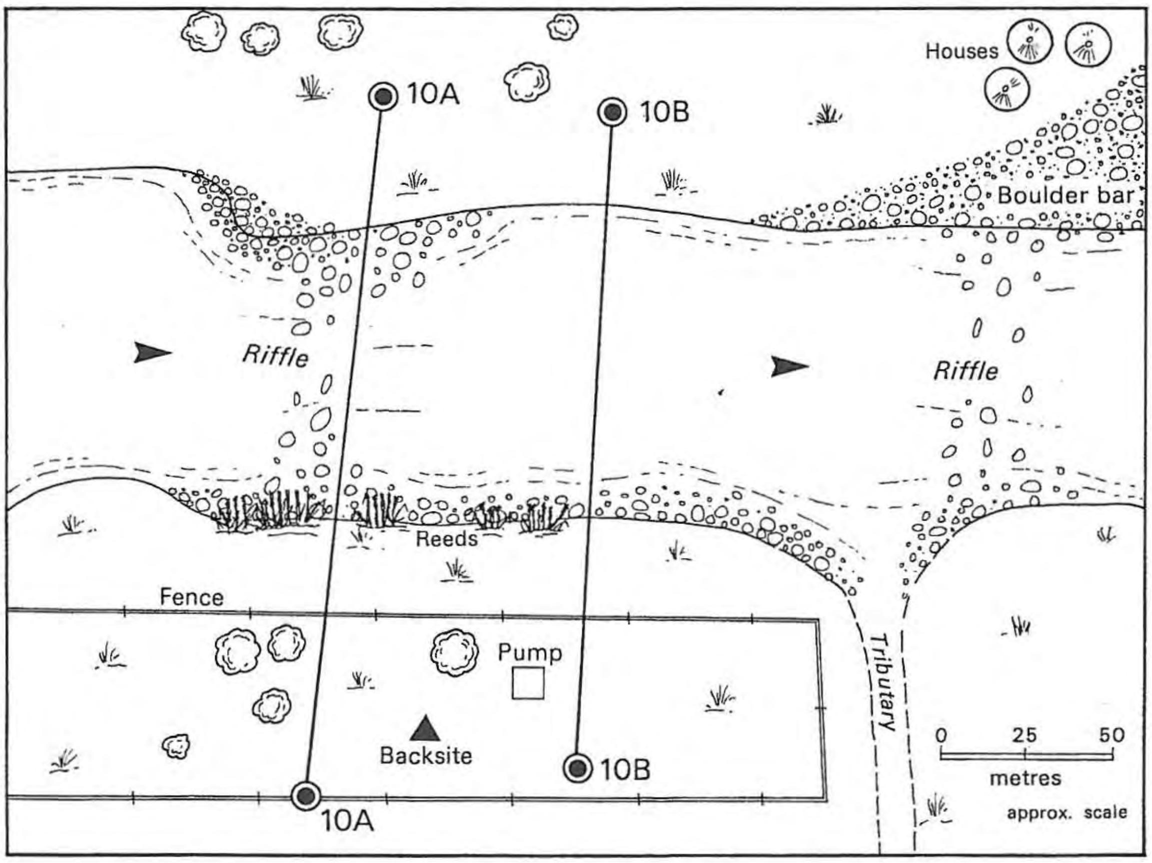

Mkomazi River Site 10

Mkomazi Site 10
Section A

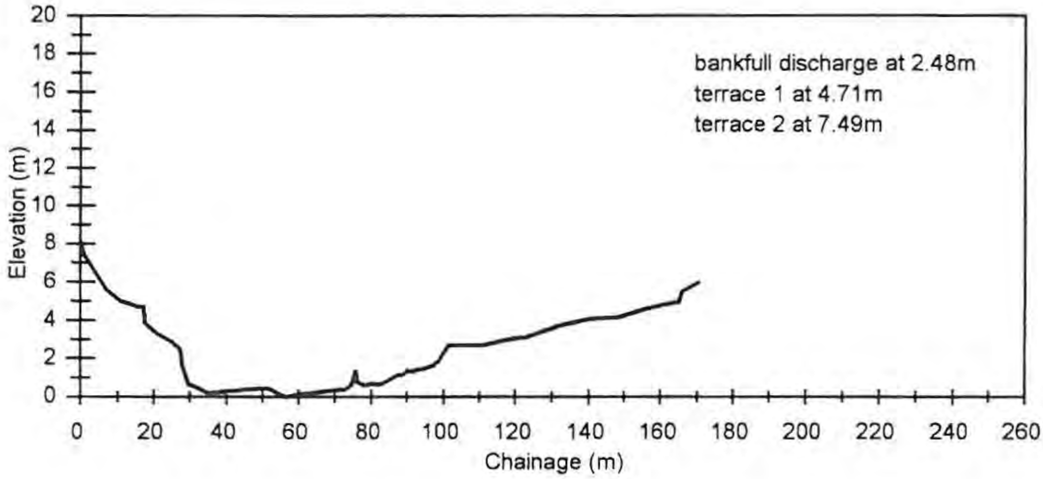

Mkomazi Site 10
Section B

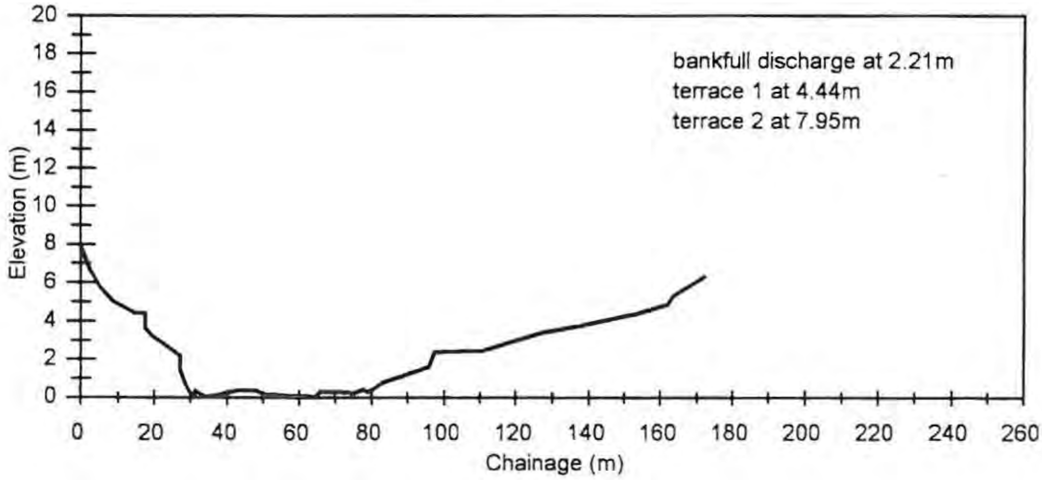

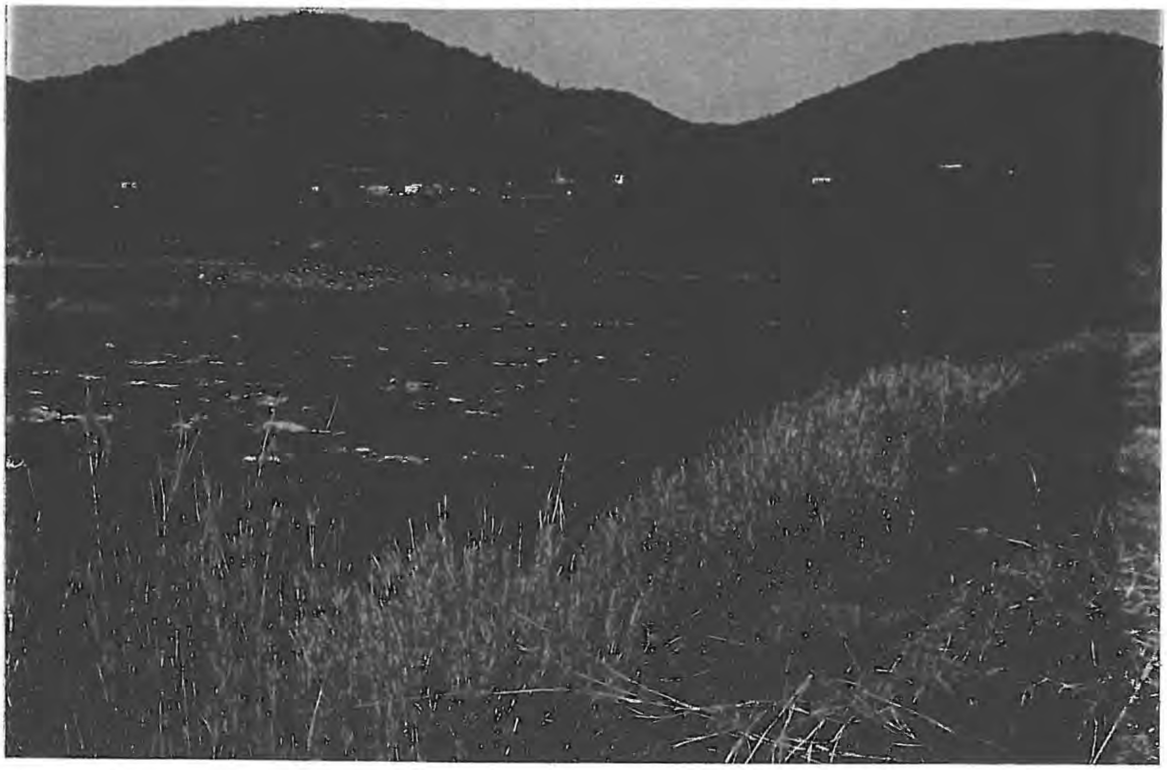

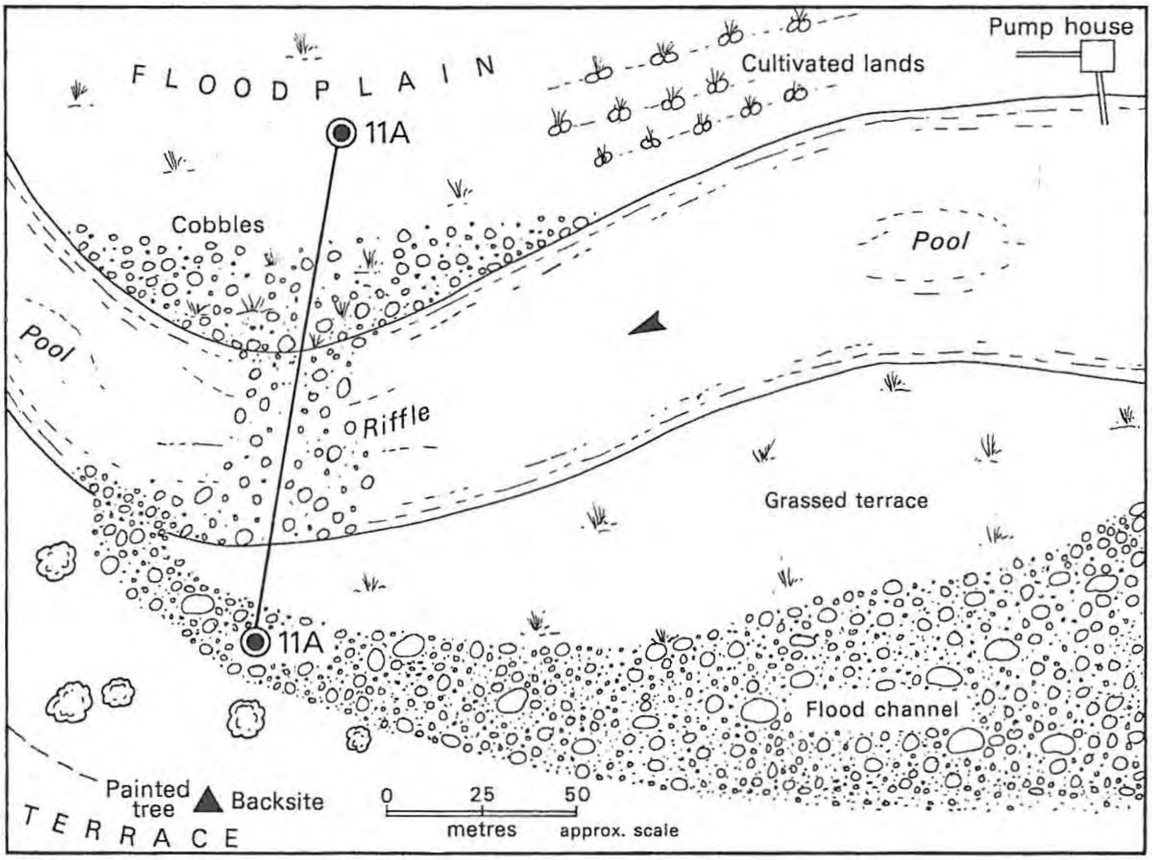

Mkomazi River Site 11

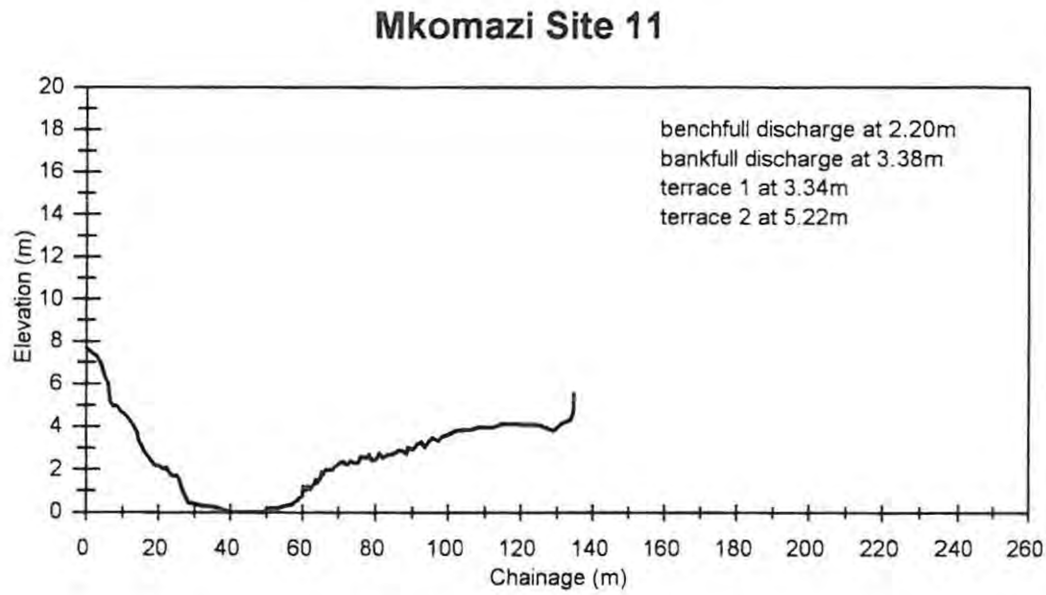
Mkomazi Site 11
benchfull discharge at 2.20m
bankfull discharge at 3.38m
terrace 1 at 3.34m
terrace 2 at 5.22m
Elevation (m)
Chainage (m)
0
2
4
6
8
10
12
14
16
18
20
0
20
40
60
80
100
120
140
160
180
200
220
240
260

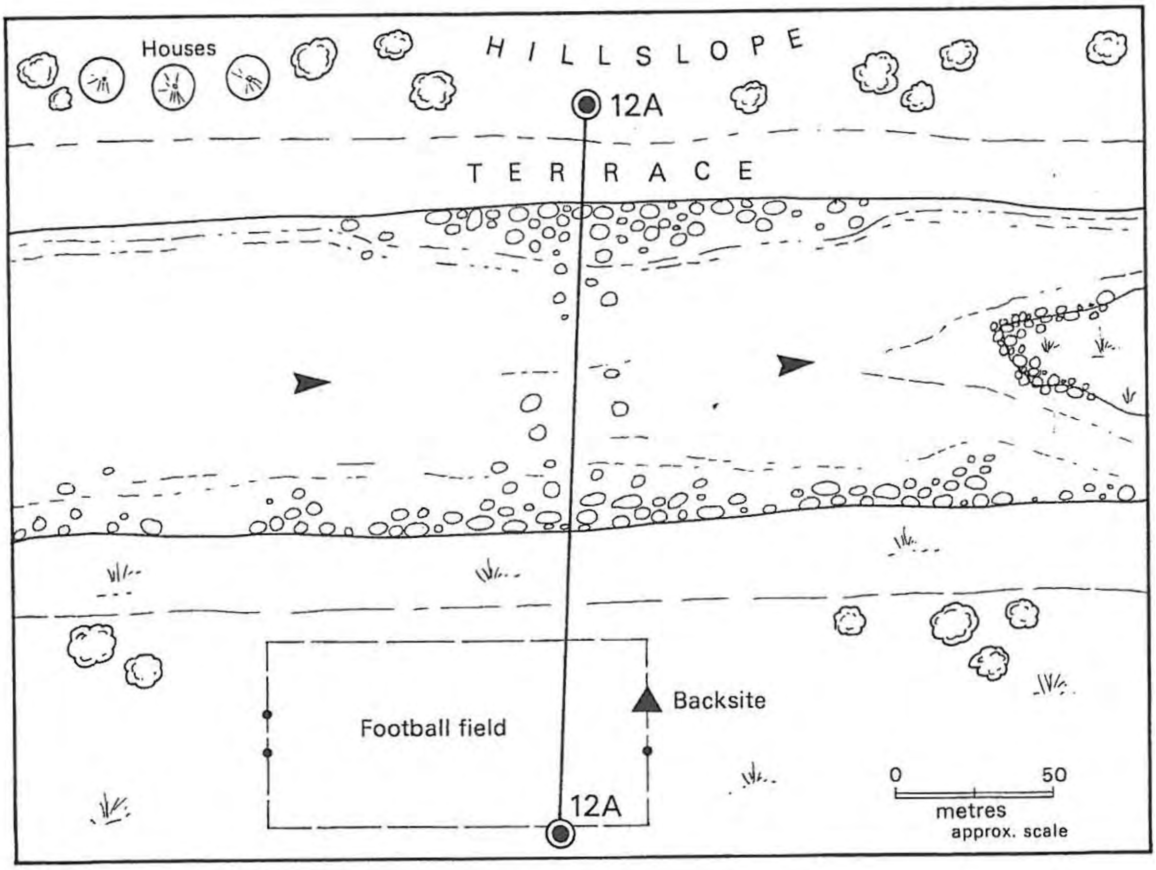

Mkomazi River Site 12

Mkomazi Site 12

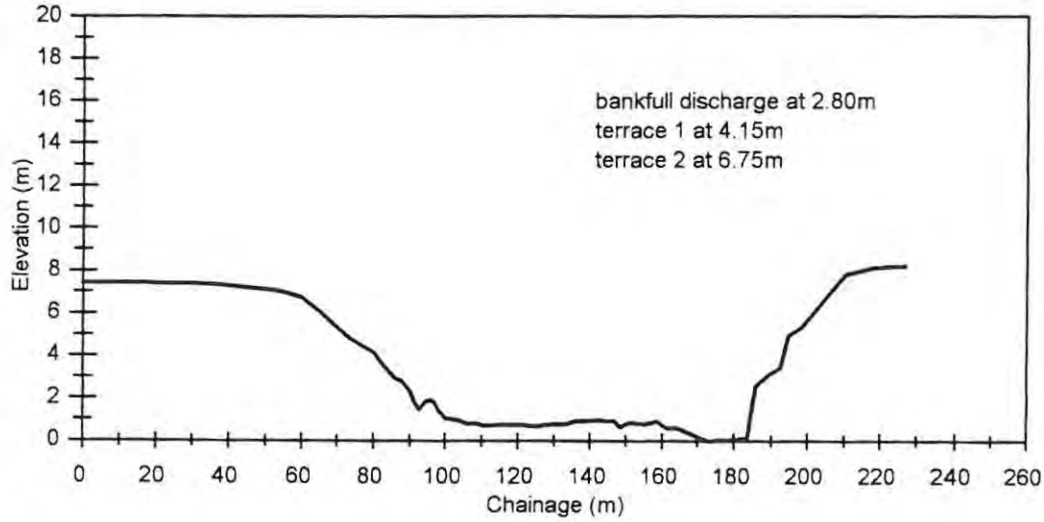

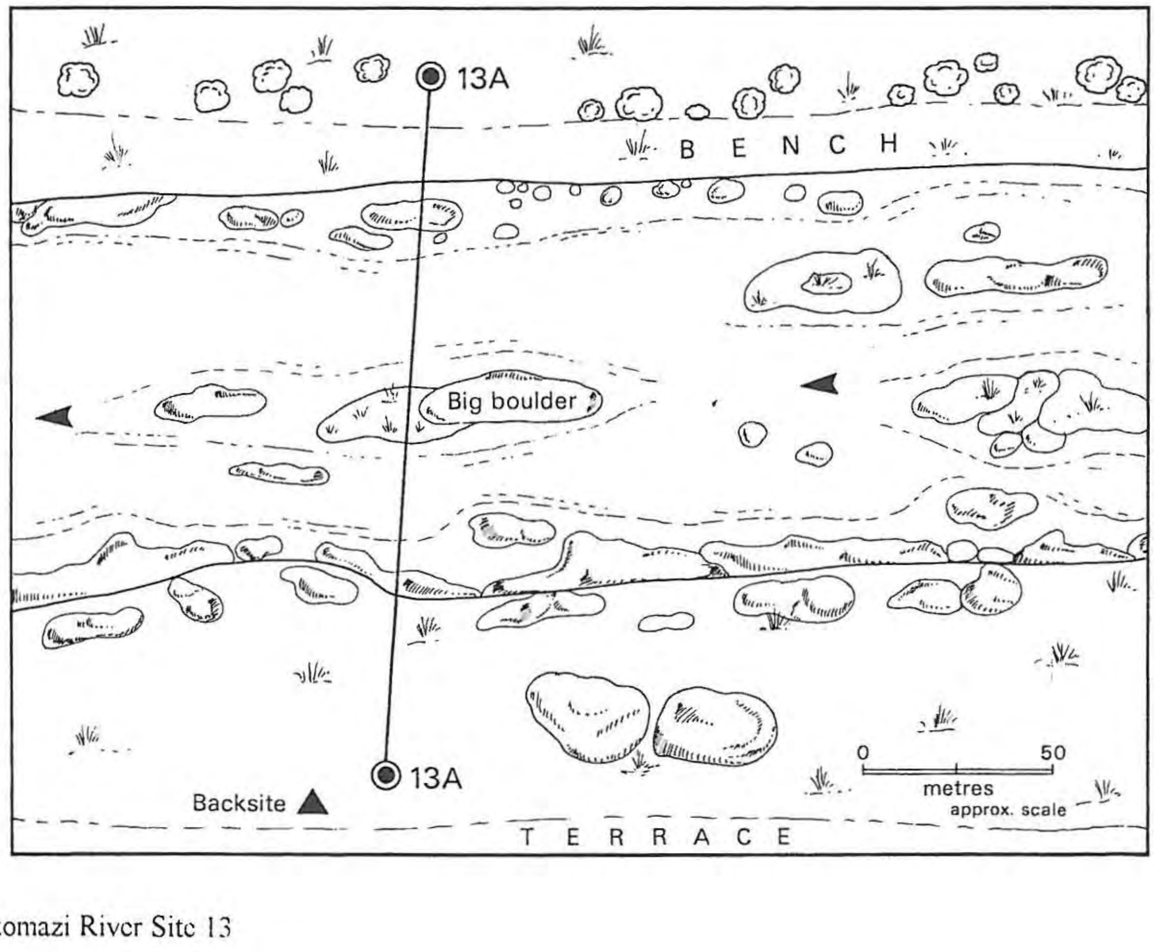

Mkomazi River Site 13

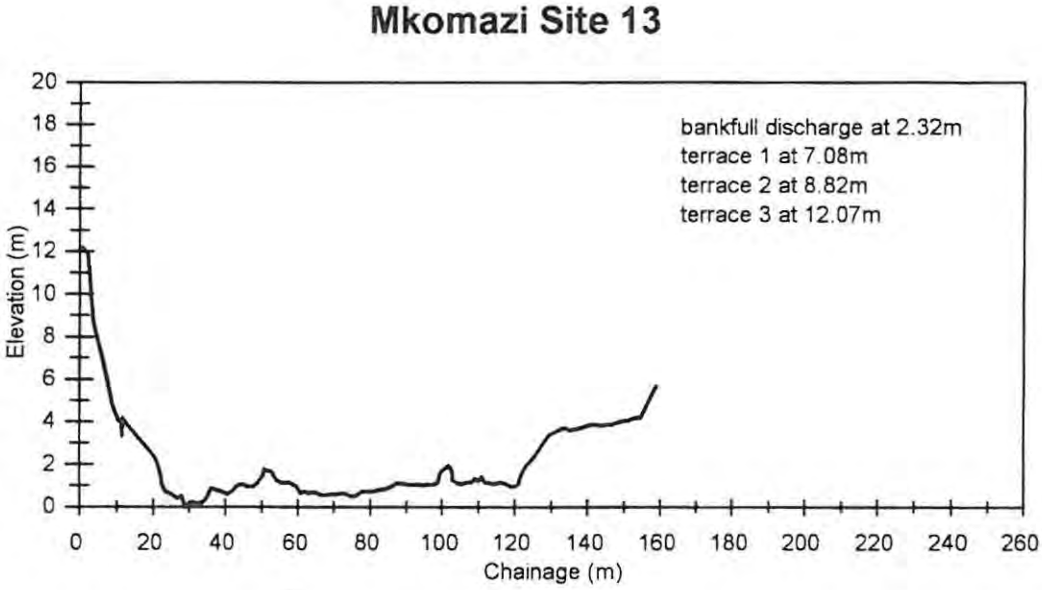
Mkomazi Site 13
bankfull discharge at 2.32m
terrace 1 at 7.08m
terrace 2 at 8.82m
terrace 3 at 12.07m
Elevation (m)
Chainage (m)
0
2
4
6
8
10
12
14
16
18
20
0
20
40
60
80
100
120
140
160
180
200
220
240
260

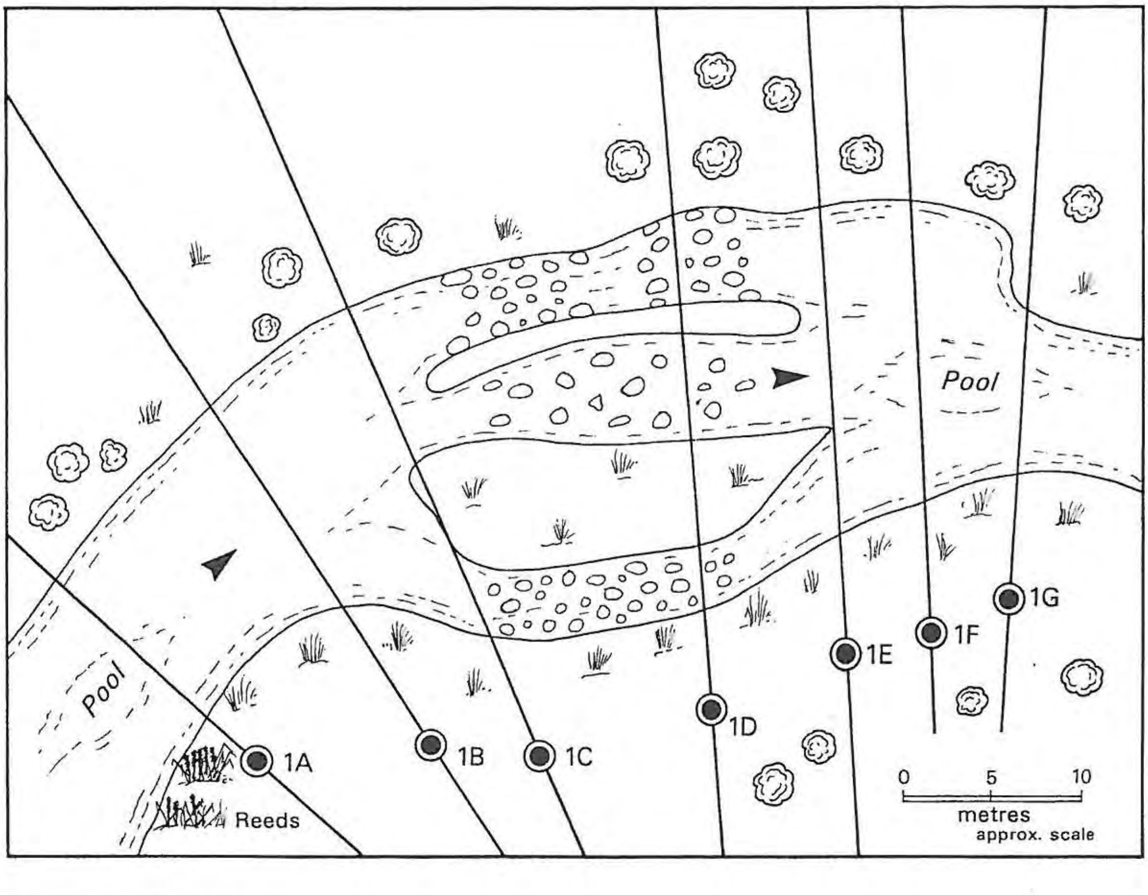

Mhlathuze River Site 1

Mhlathuze Site 1
Pool section

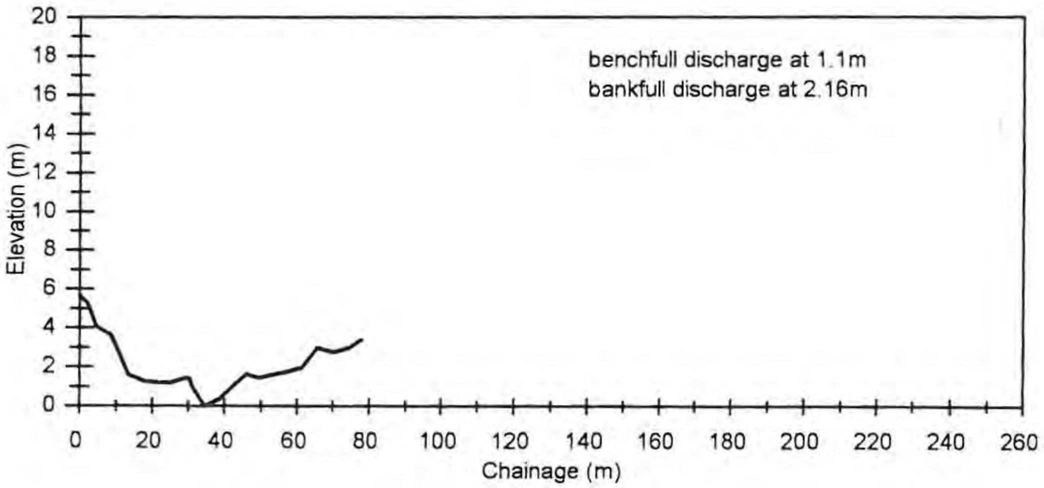

Mhlathuze Site 1
Riffle section

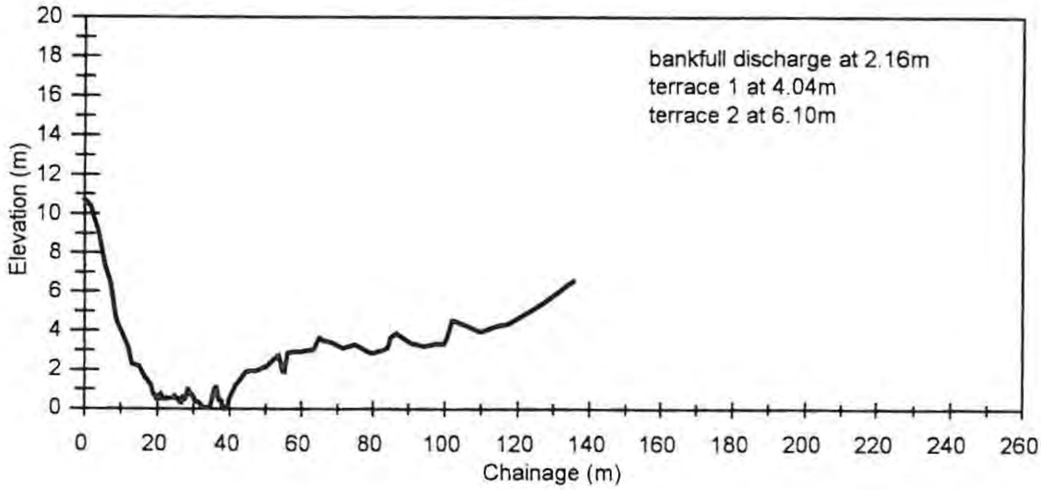

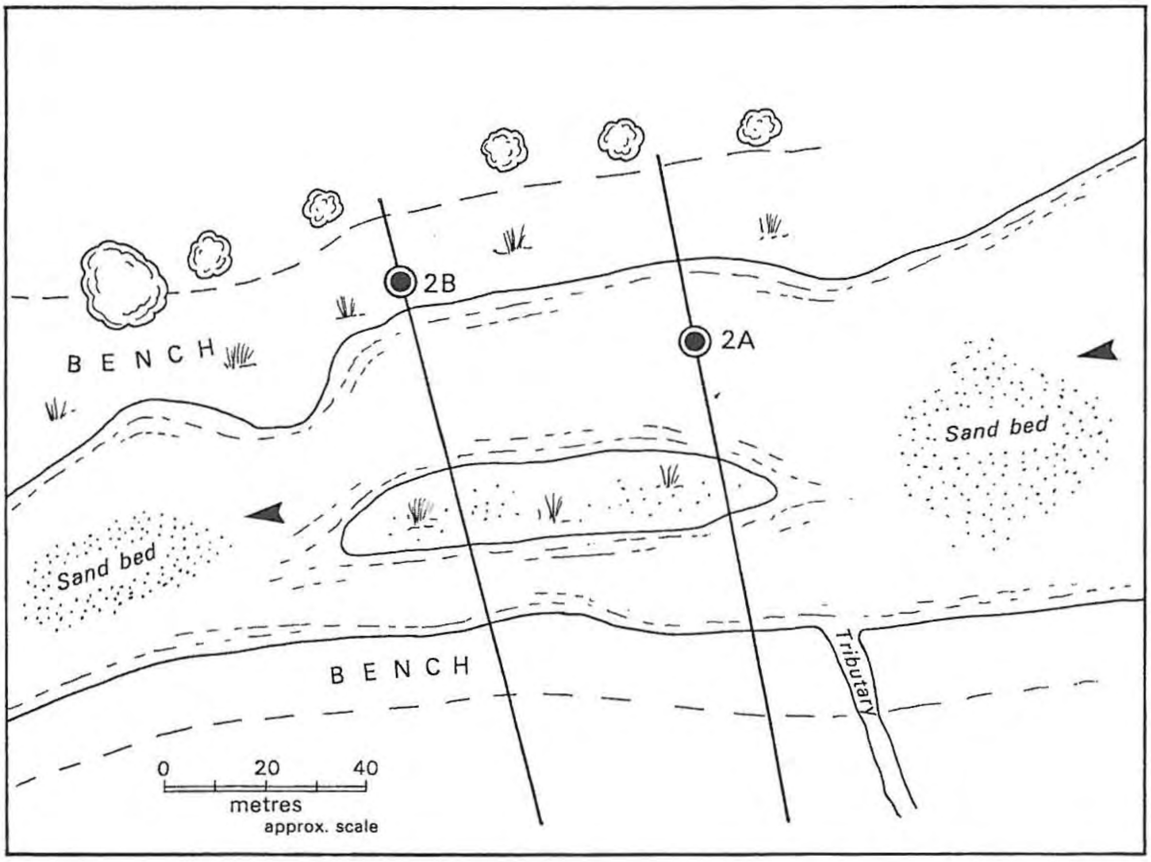

Mhlathuze River Site 2

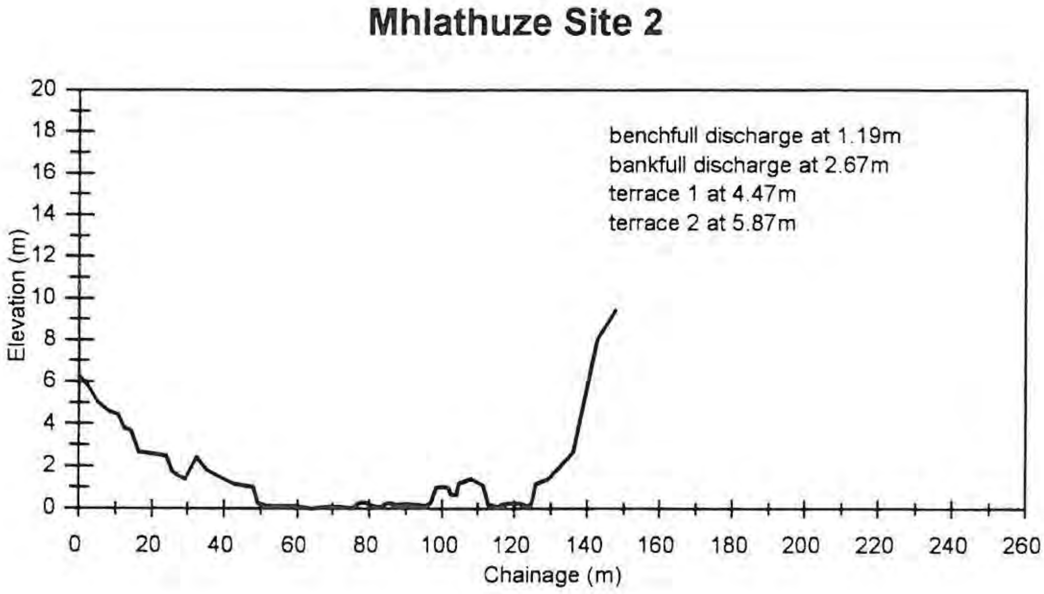
Mhlathuze Site 2
benchfull discharge at 1.19m
bankfull discharge at 2.67m
terrace 1 at 4.47m
terrace 2 at 5.87m
Elevation (m)
Chainage (m)
0
2
4
6
8
10
12
14
16
18
20
0
20
40
60
80
100
120
140
160
180
200
220
240
260

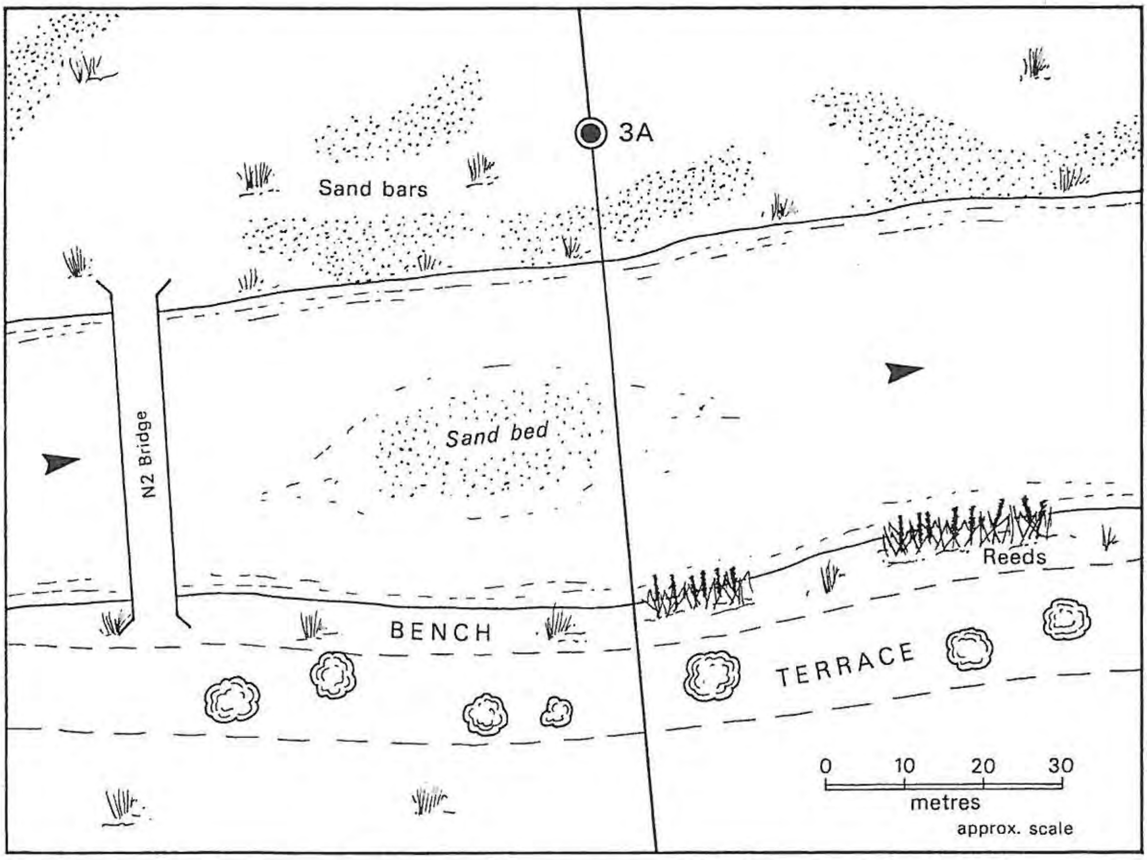

Mhlathuze River Site 3

Mhlathuze Site 3

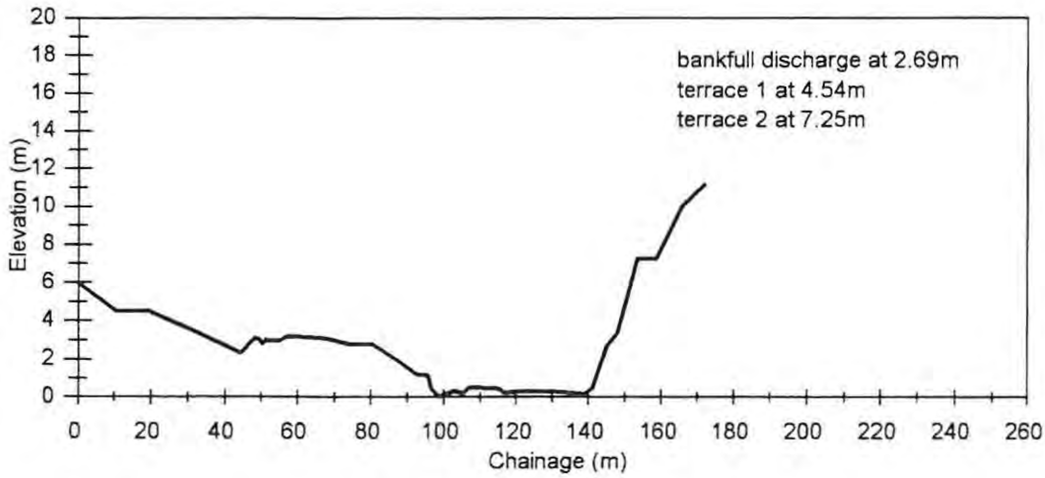

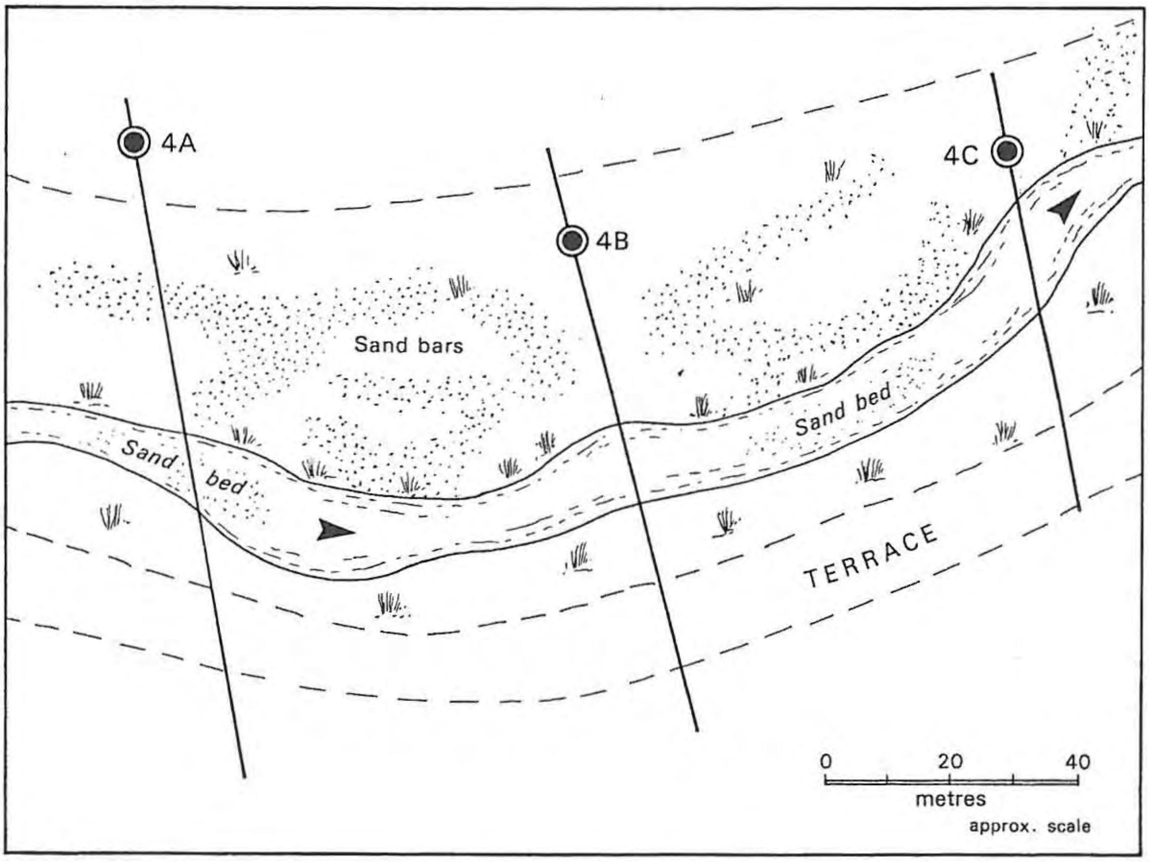

Mhlathuze River Site 4

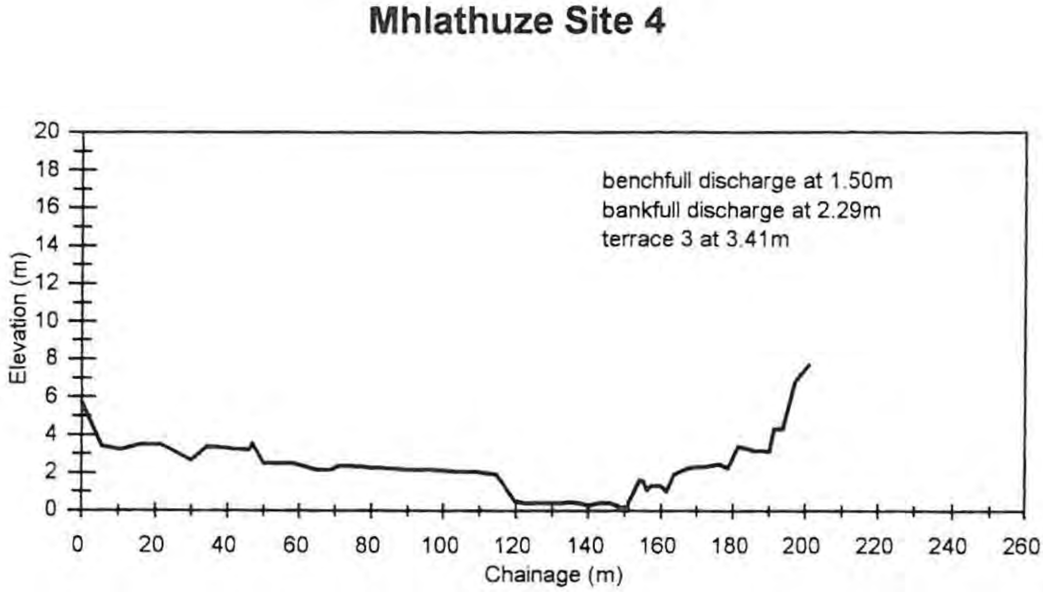
Mhlathuze Site 4
benchfull discharge at 1.50m
bankfull discharge at 2.29m
terrace 3 at 3.41m
Elevation (m)
Chainage (m)
0
2
4
6
8
10
12
14
16
18
20
0
20
40
60
80
100
120
140
160
180
200
220
240
260

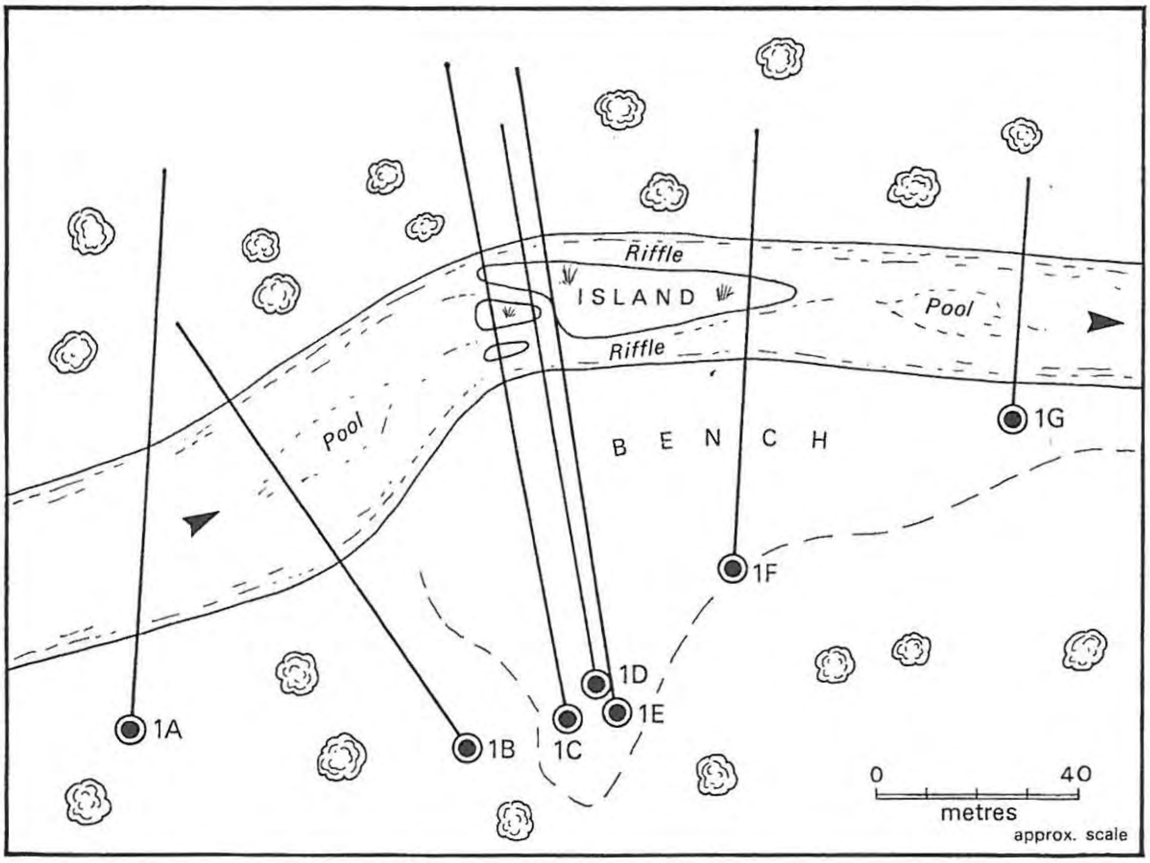

Olifants River Site 1

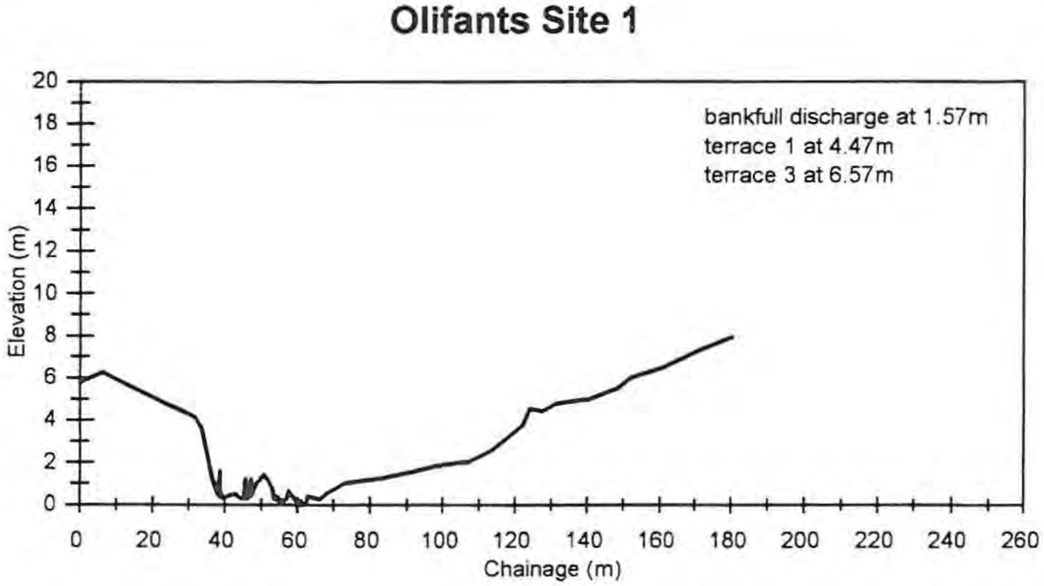
Olifants Site 1
bankfull discharge at 1.57m
terrace 1 at 4.47m
terrace 3 at 6.57m
Elevation (m)
Chainage (m)
20
18
16
14
12
10
8
6
4
2
0
0
20
40
60
80
100
120
140
160
180
200
220
240
260

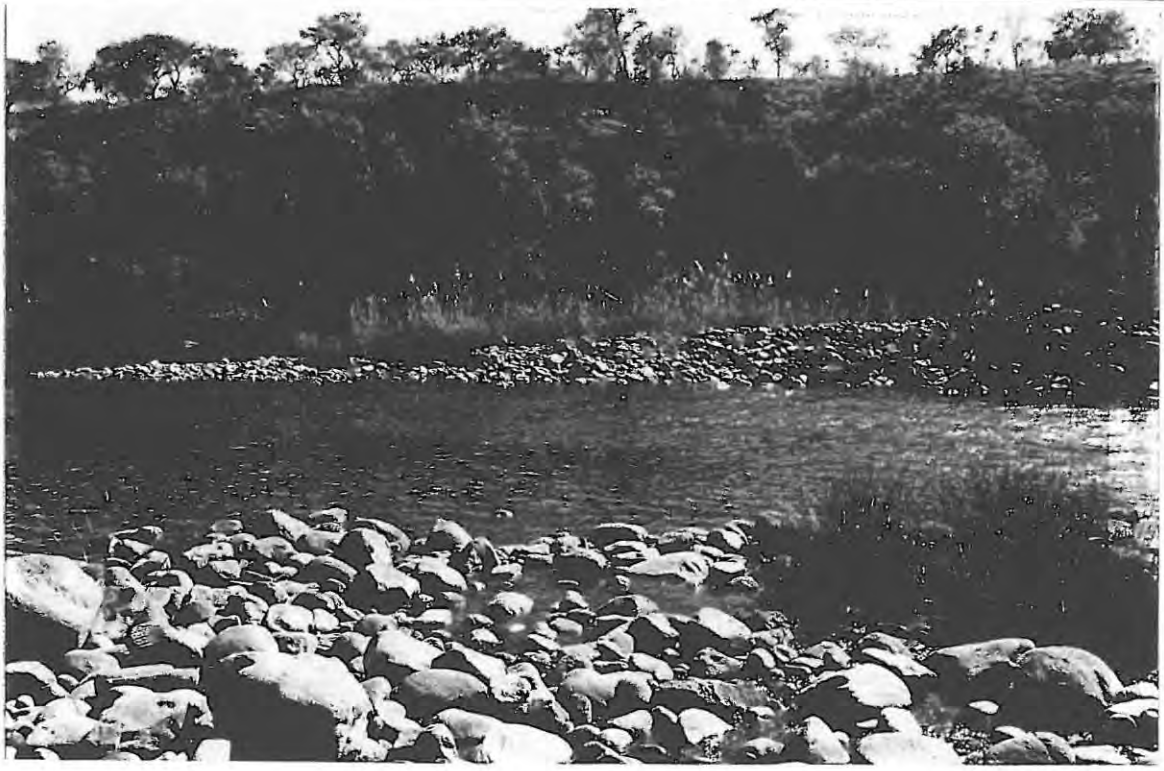

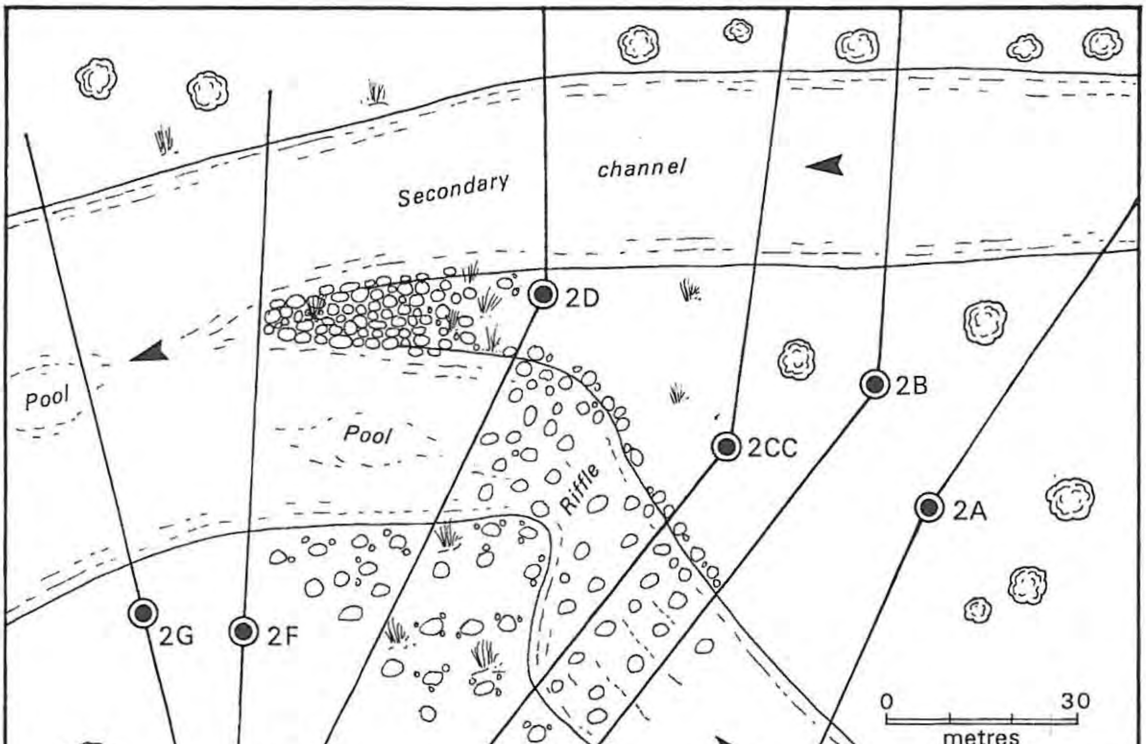

Olifants River Site 2

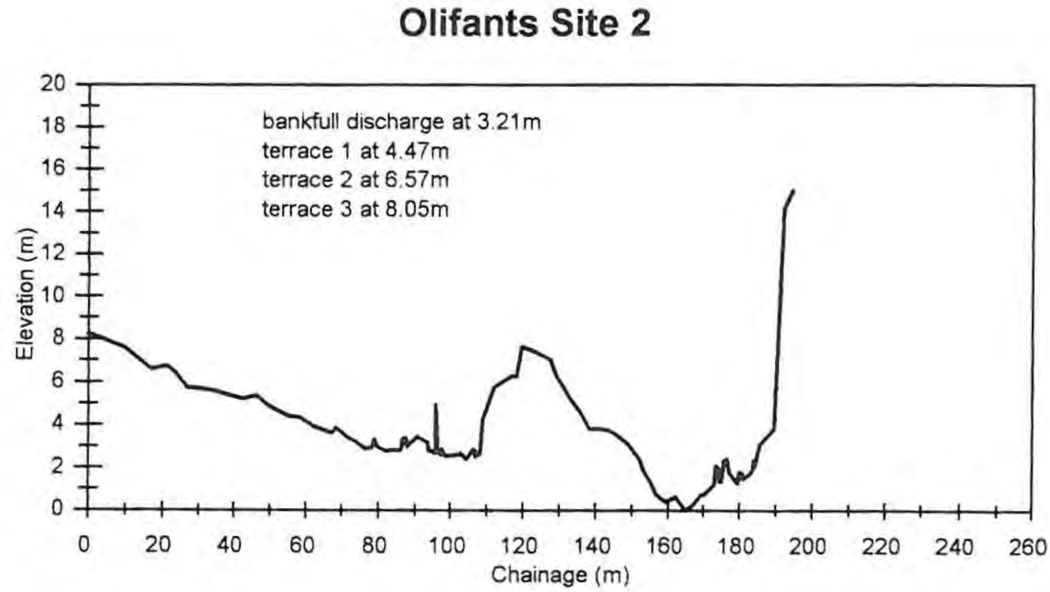
Olifants Site 2
bankfull discharge at 3.21m
terrace 1 at 4.47m
terrace 2 at 6.57m
terrace 3 at 8.05m
Elevation (m)
Chainage (m)
0
2
4
6
8
10
12
14
16
18
20
0
20
40
60
80
100
120
140
160
180
200
220
240
260

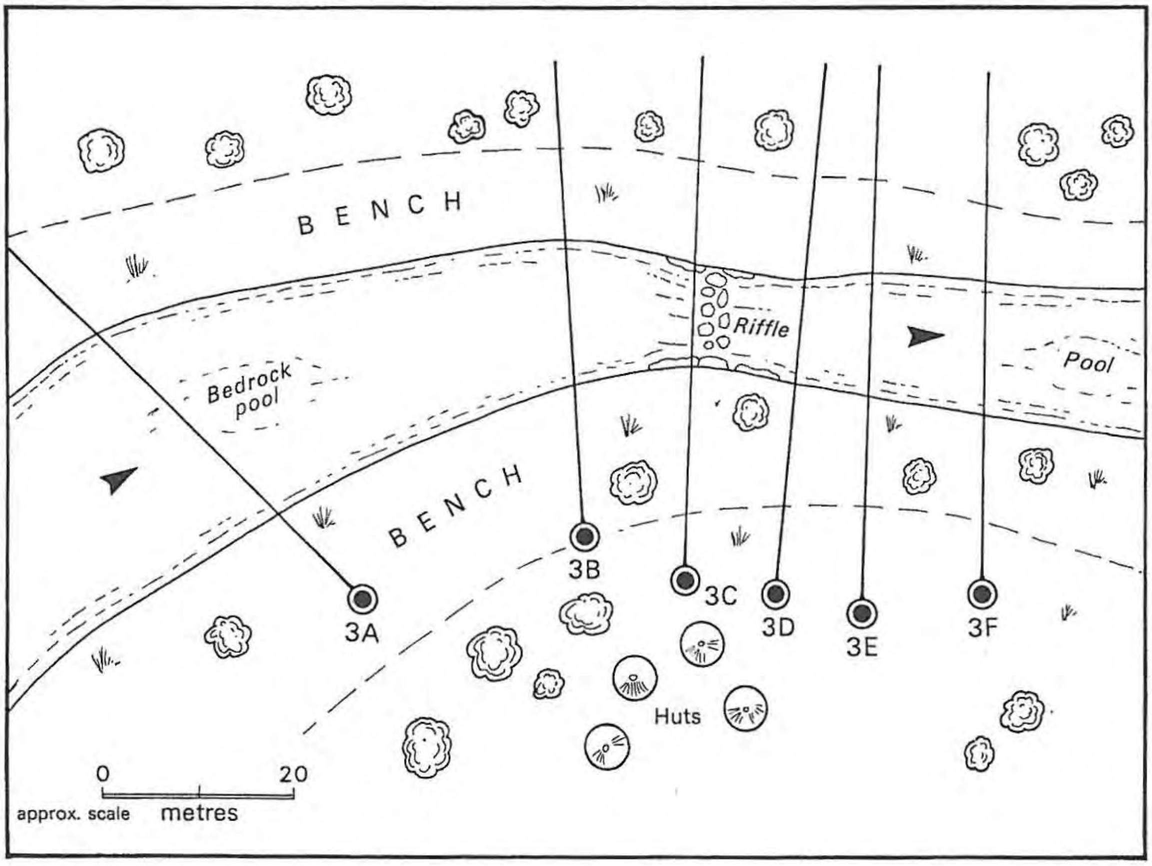

Olifants River Site 3

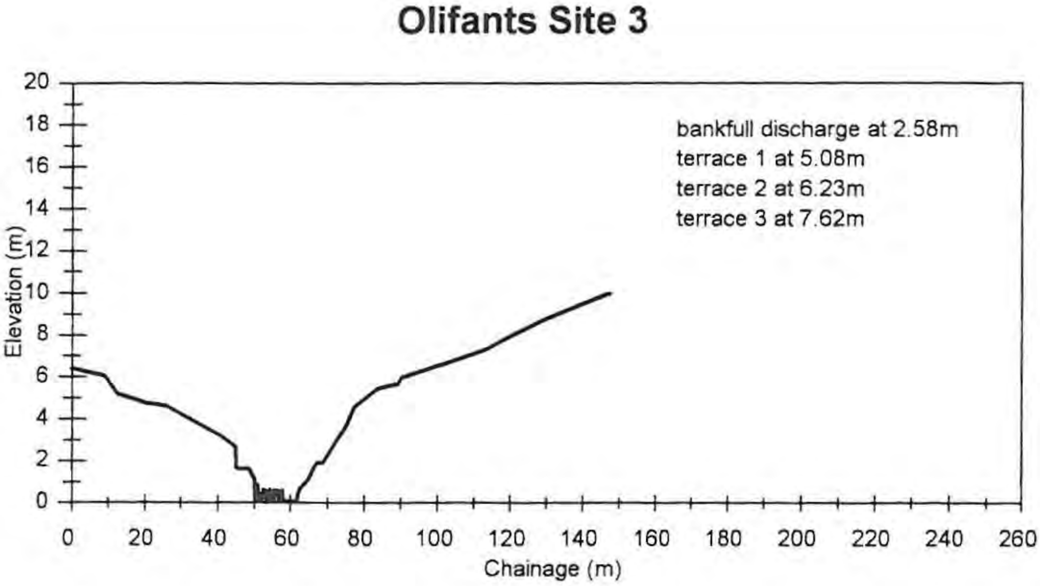

Olifants Site 3
bankfull discharge at 2.58m
terrace 1 at 5.08m
terrace 2 at 6.23m
terrace 3 at 7.62m
Elevation (m)
0
2
4
6
8
10
12
14
16
18
20
Chainage (m)
0
20
40
60
80
100
120
140
160
180
200
220
240
260

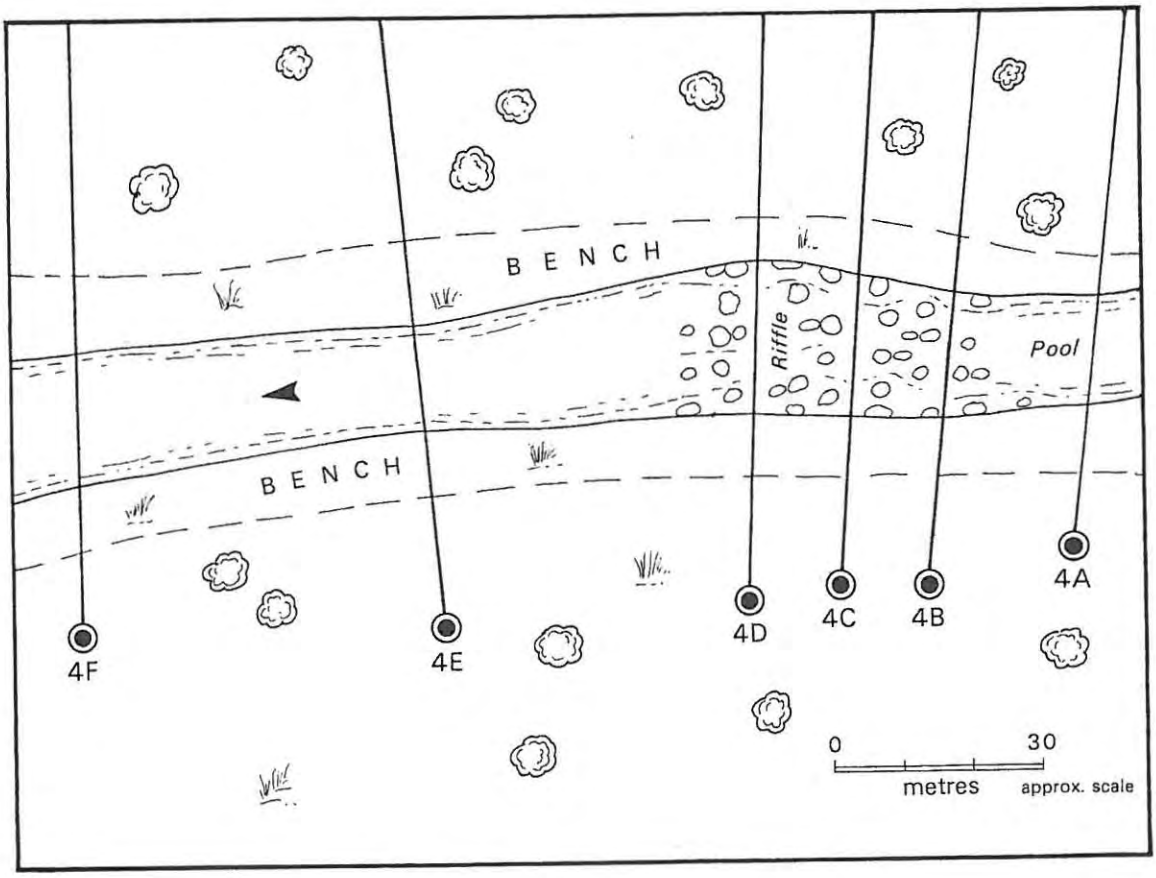

Olifants River Site 4

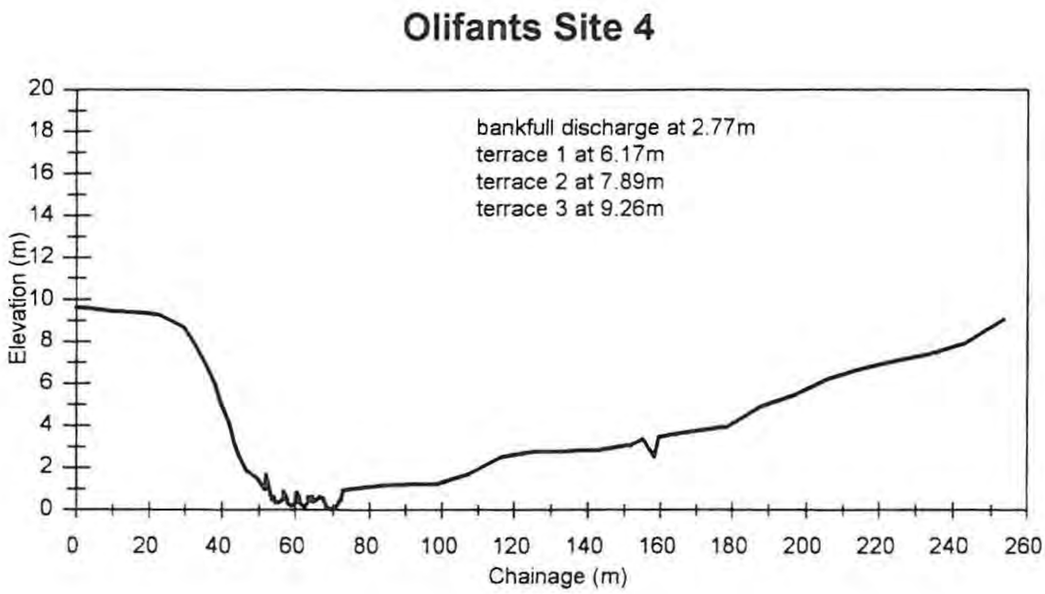
Olifants Site 4
bankfull discharge at 2.77m
terrace 1 at 6.17m
terrace 2 at 7.89m
terrace 3 at 9.26m
Elevation (m)
Chainage (m)
0
2
4
6
8
10
12
14
16
18
20
0
20
40
60
80
100
120
140
160
180
200
220
240
260

APPENDIX B

DAILY TIME SERIES FOR ALL RIVERS

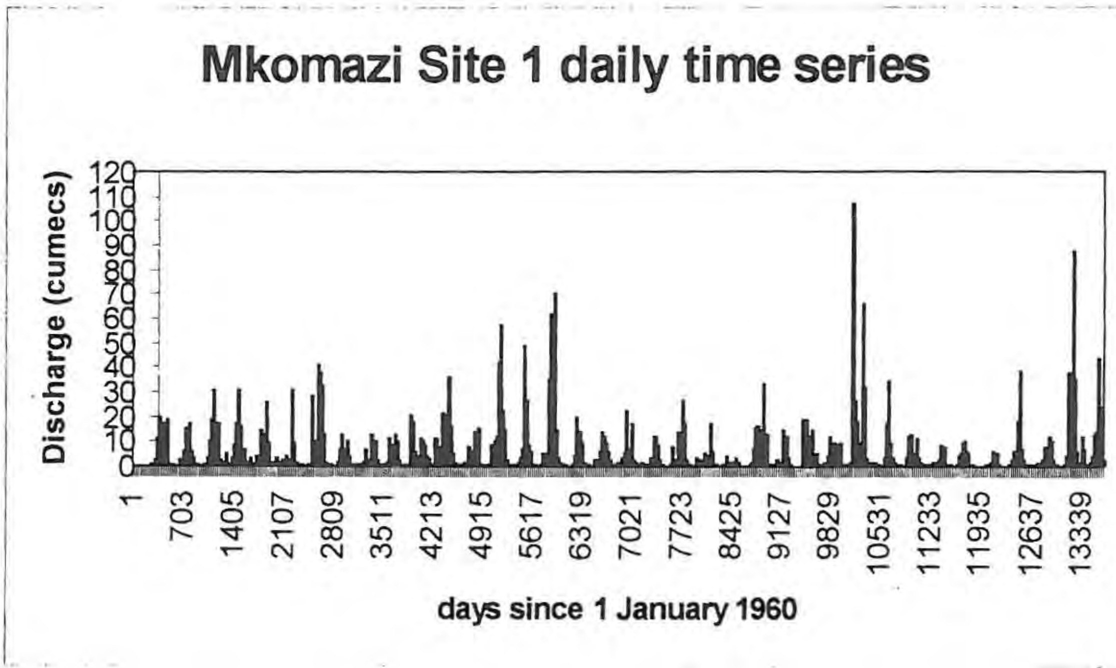
Mkomazi Site 1 daily time series
Discharge (cumecs)
0
10
20
30
40
50
60
70
80
90
100
110
120
1
703
1405
2107
2809
3511
4213
4915
5617
6319
7021
7723
8425
9127
9829
10531
11233
11935
12637
13339
days since 1 January 1960

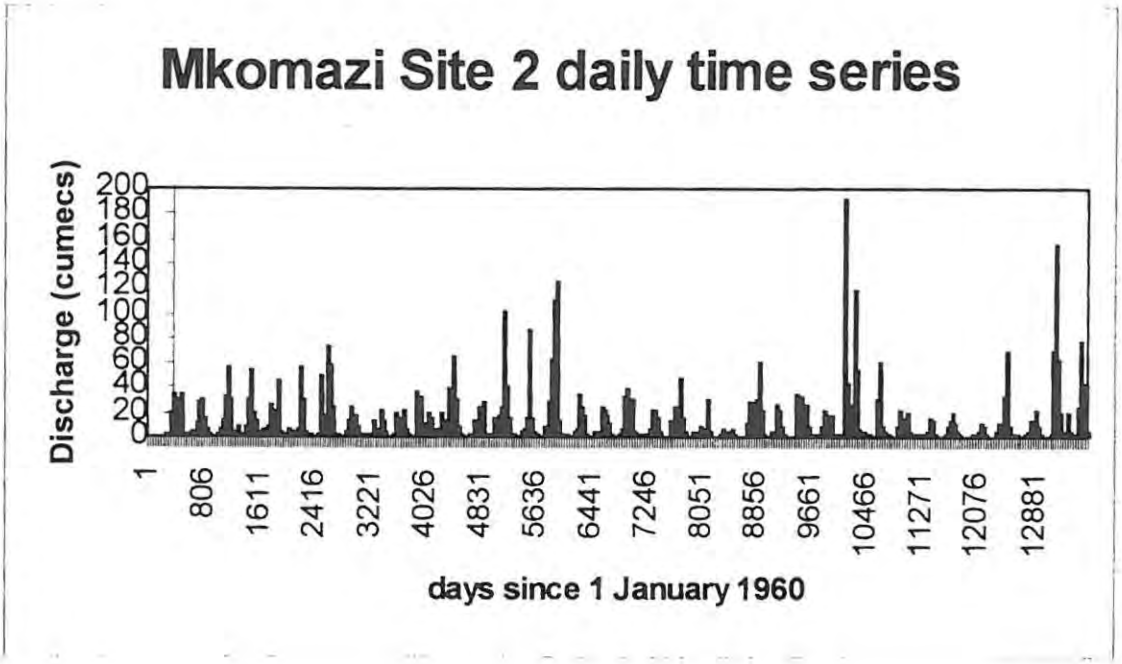
Mkomazi Site 2 daily time series
Discharge (cumecs)
0
20
40
60
80
100
120
140
160
180
200
1
806
1611
2416
3221
4026
4831
5636
6441
7246
8051
8856
9661
10466
11271
12076
12881
days since 1 January 1960

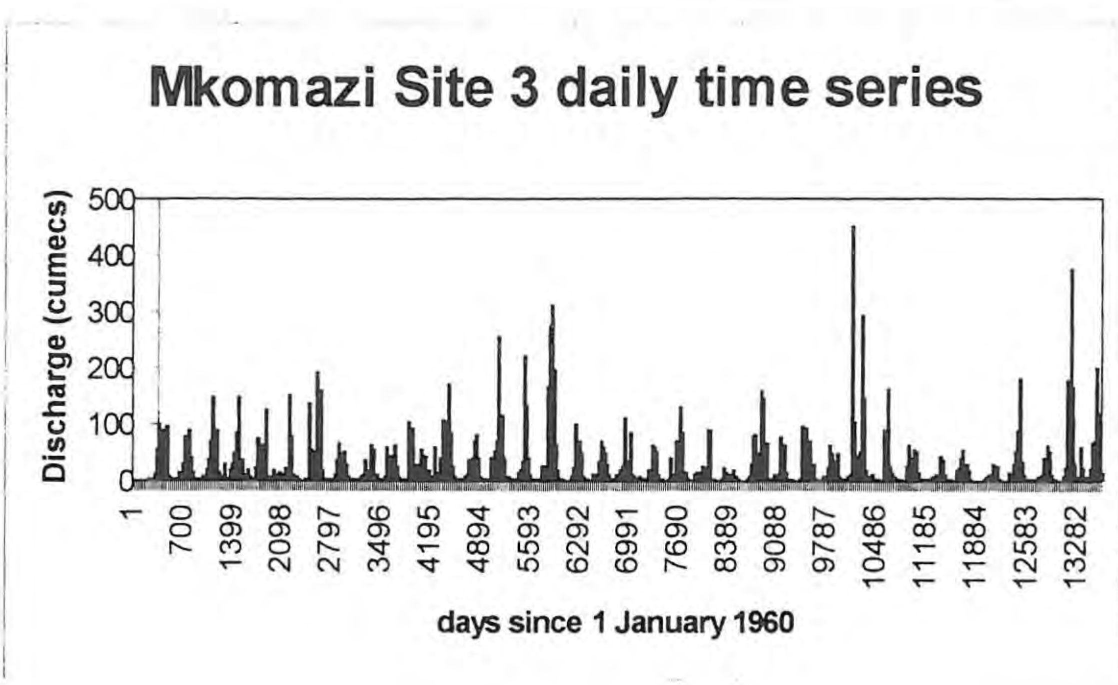
Mkomazi Site 3 daily time series
Discharge (cumecs)
0
100
200
300
400
500
1
700
1399
2098
2797
3496
4195
4894
5593
6292
6991
7690
8389
9088
9787
10486
11185
11884
12583
13282
days since 1 January 1960

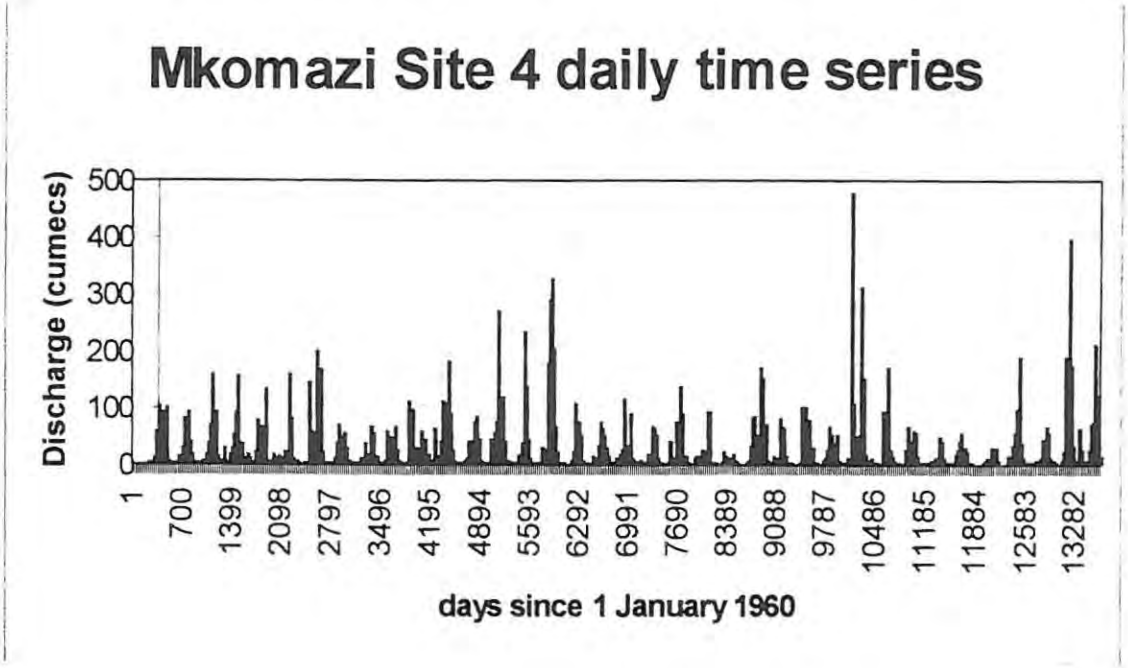
Mkomazi Site 4 daily time series
Discharge (cumecs)
0
100
200
300
400
500
1
700
1399
2098
2797
3496
4195
4894
5593
6292
6991
7690
8389
9088
9787
10486
11185
11884
12583
13282
days since 1 January 1960

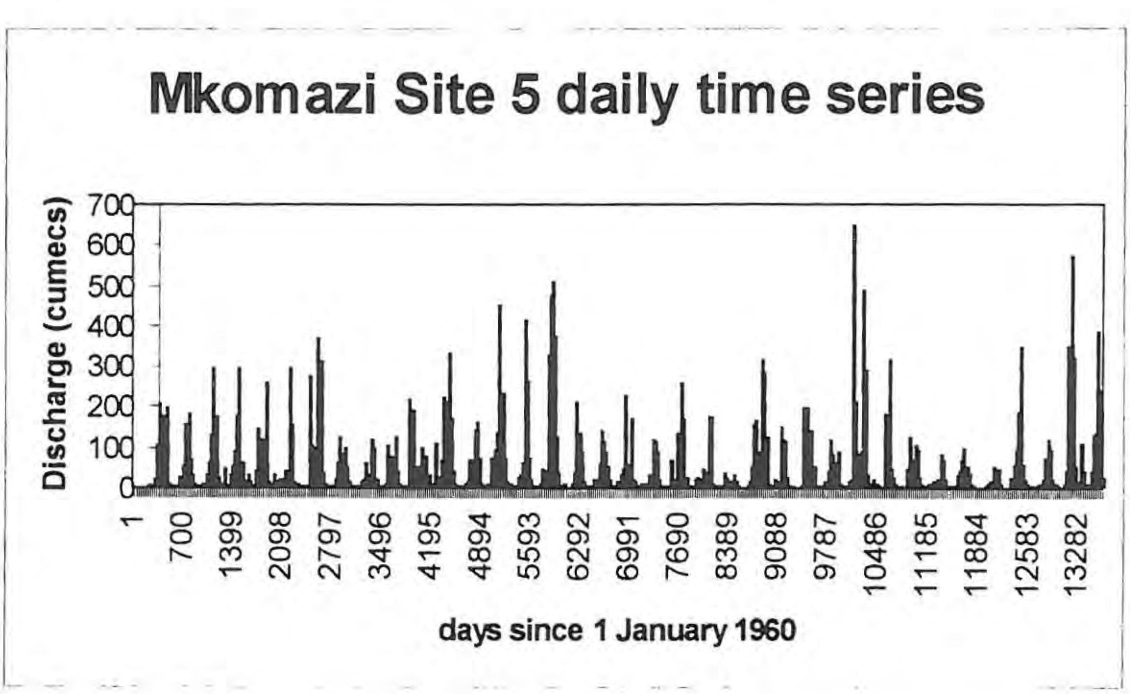
Mkomazi Site 5 daily time series
Discharge (cumecs)
0
100
200
300
400
500
600
700
1
700
1399
2098
2797
3496
4195
4894
5593
6292
6991
7690
8389
9088
9787
10486
11185
11884
12583
13282
days since 1 January 1960

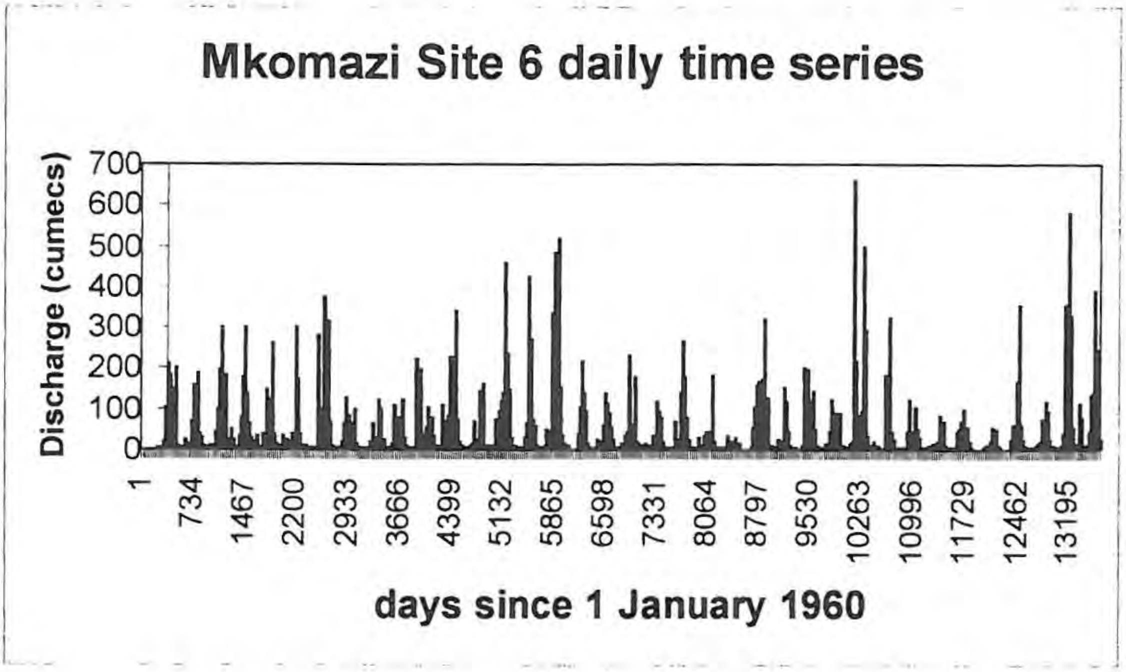
Mkomazi Site 6 daily time series
Discharge (cumecs)
0
100
200
300
400
500
600
700
1
734
1467
2200
2933
3666
4399
5132
5865
6598
7331
8064
8797
9530
10263
10996
11729
12462
13195
days since 1 January 1960

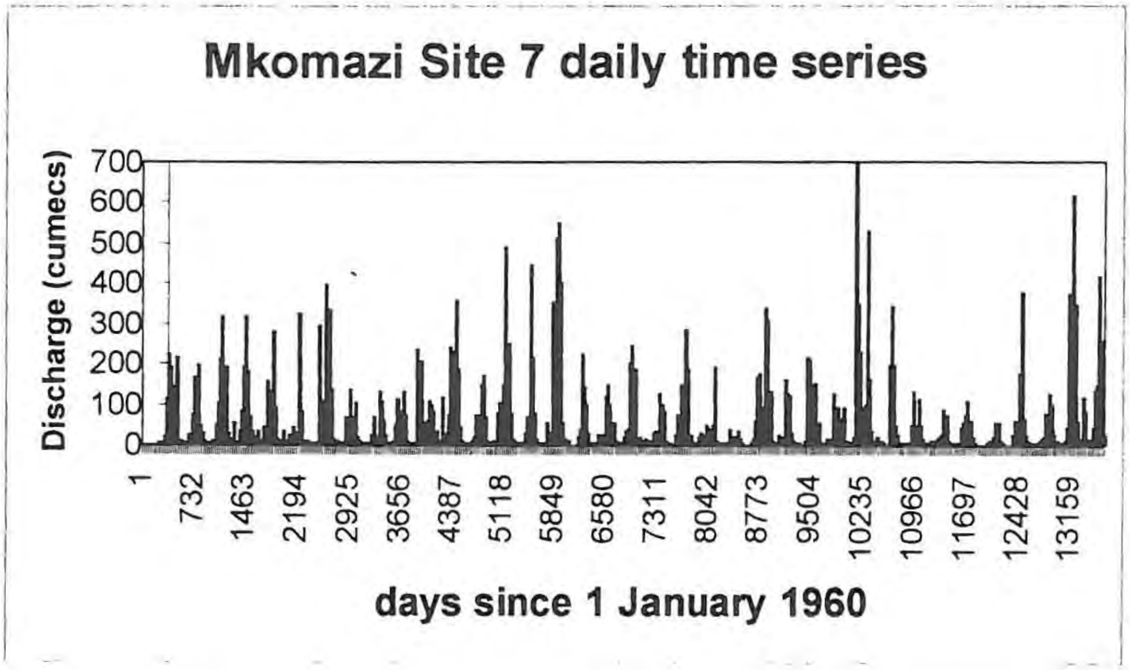
Mkomazi Site 7 daily time series
Discharge (cumecs)
700
600
500
400
300
200
100
0
1
732
1463
2194
2925
3656
4387
5118
5849
6580
7311
8042
8773
9504
10235
10966
11697
12428
13159
days since 1 January 1960

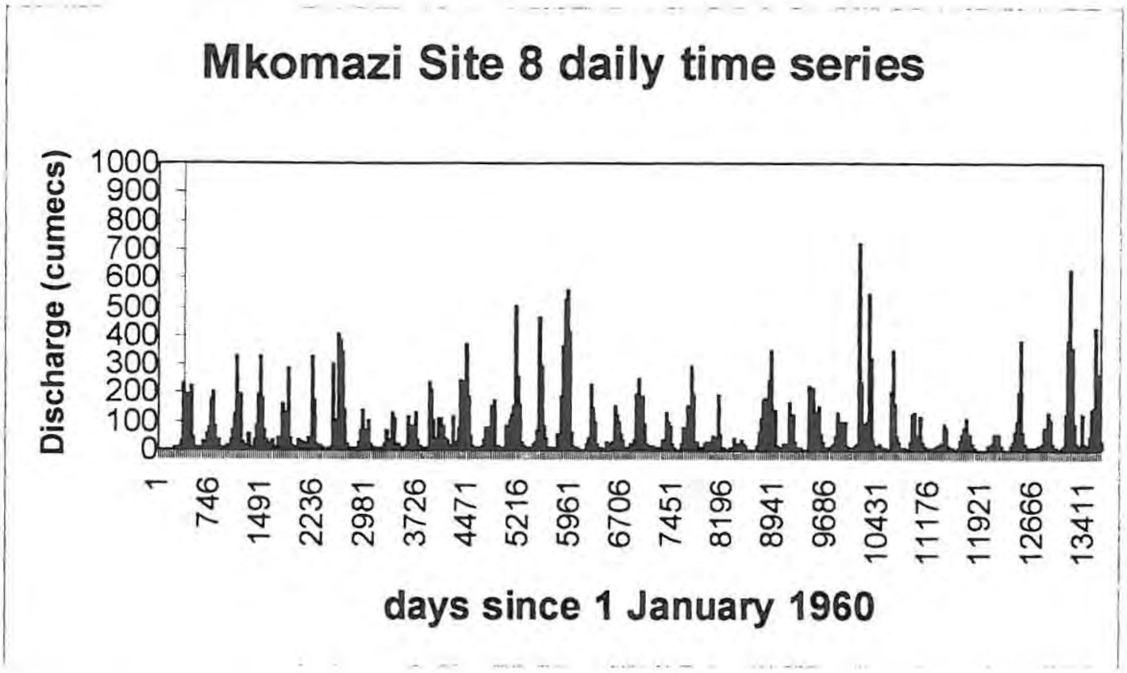
Mkomazi Site 8 daily time series
Discharge (cumecs)
1000
900
800
700
600
500
400
300
200
100
0
1
746
1491
2236
2981
3726
4471
5216
5961
6706
7451
8196
8941
9686
10431
11176
11921
12666
13411
days since 1 January 1960

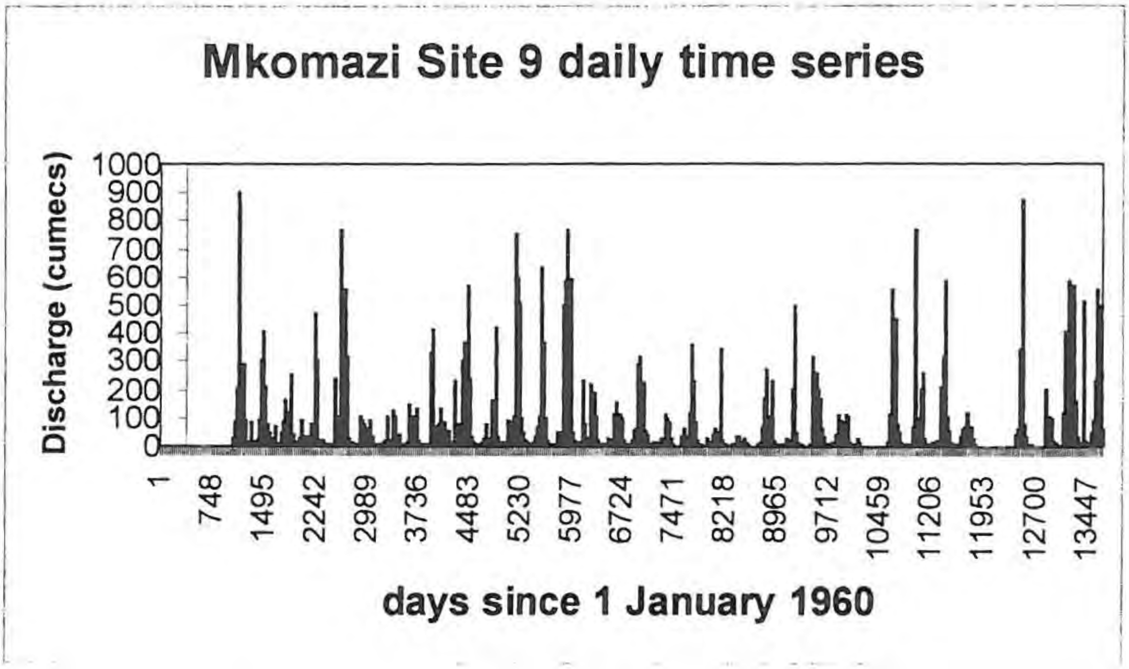
Mkomazi Site 9 daily time series
Discharge (cumecs)
1000
900
800
700
600
500
400
300
200
100
0
1
748
1495
2242
2989
3736
4483
5230
5977
6724
7471
8218
8965
9712
10459
11206
11953
12700
13447
days since 1 January 1960

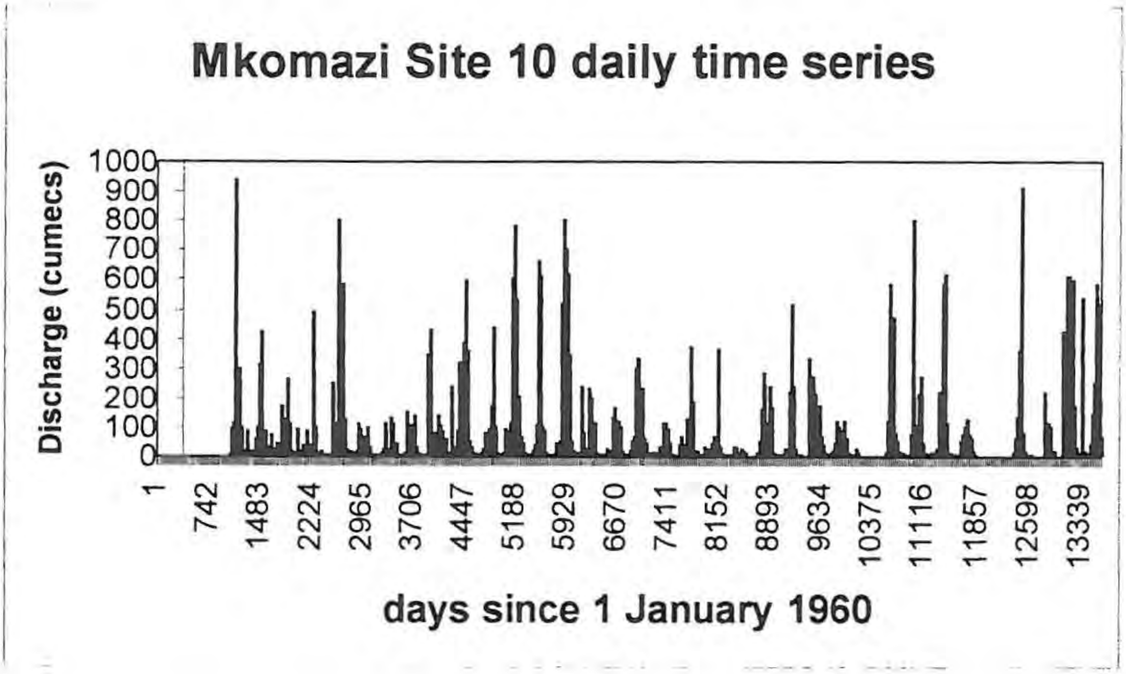
Mkomazi Site 10 daily time series
Discharge (cumecs)
1000
900
800
700
600
500
400
300
200
100
0
1
742
1483
2224
2965
3706
4447
5188
5929
6670
7411
8152
8893
9634
10375
11116
11857
12598
13339
days since 1 January 1960

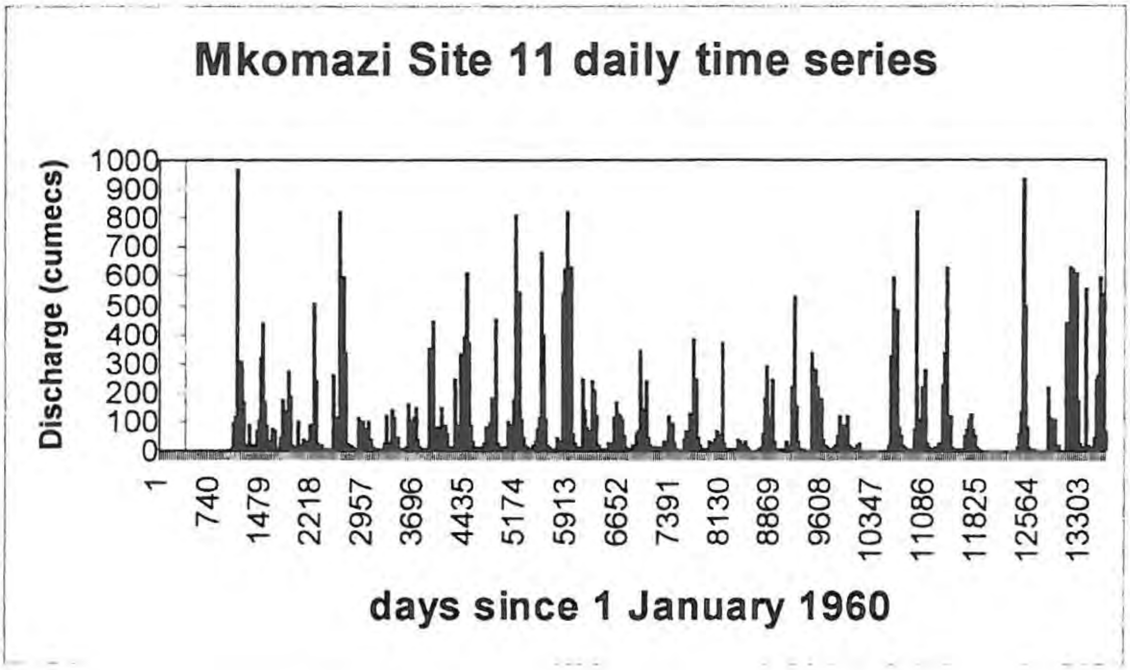
Mkomazi Site 11 daily time series
Discharge (cumecs)
1000
900
800
700
600
500
400
300
200
100
0
1
740
1479
2218
2957
3696
4435
5174
5913
6652
7391
8130
8869
9608
10347
11086
11825
12564
13303
days since 1 January 1960

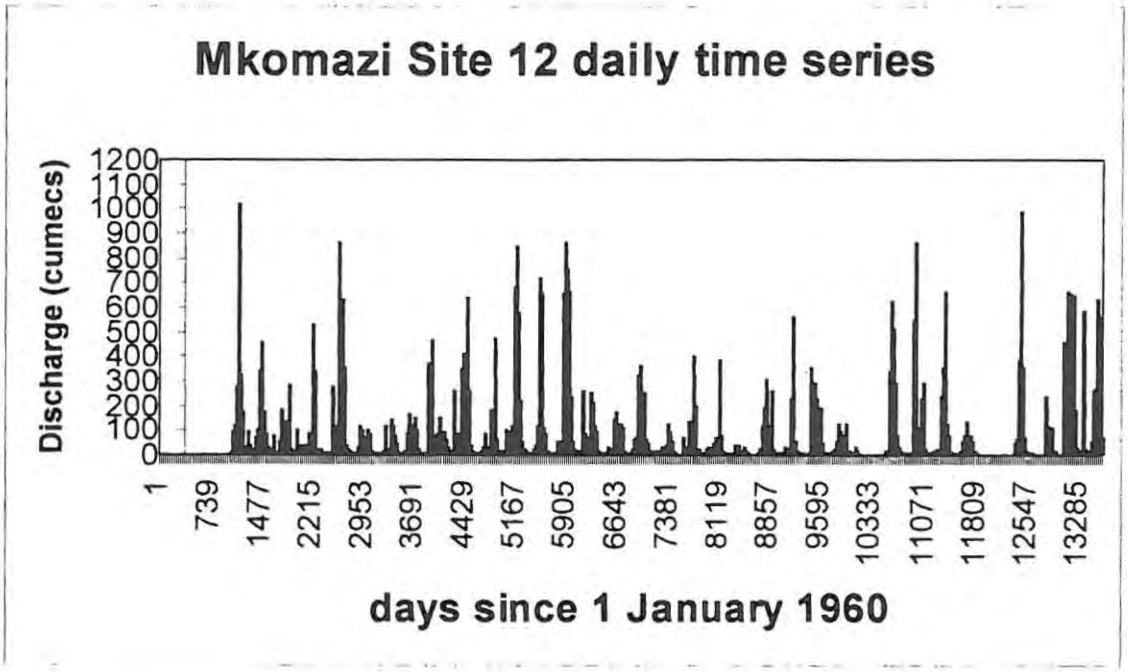
Mkomazi Site 12 daily time series
Discharge (cumecs)
1200
1100
1000
900
800
700
600
500
400
300
200
100
0
1
739
1477
2215
2953
3691
4429
5167
5905
6643
7381
8119
8857
9595
10333
11071
11809
12547
13285
days since 1 January 1960

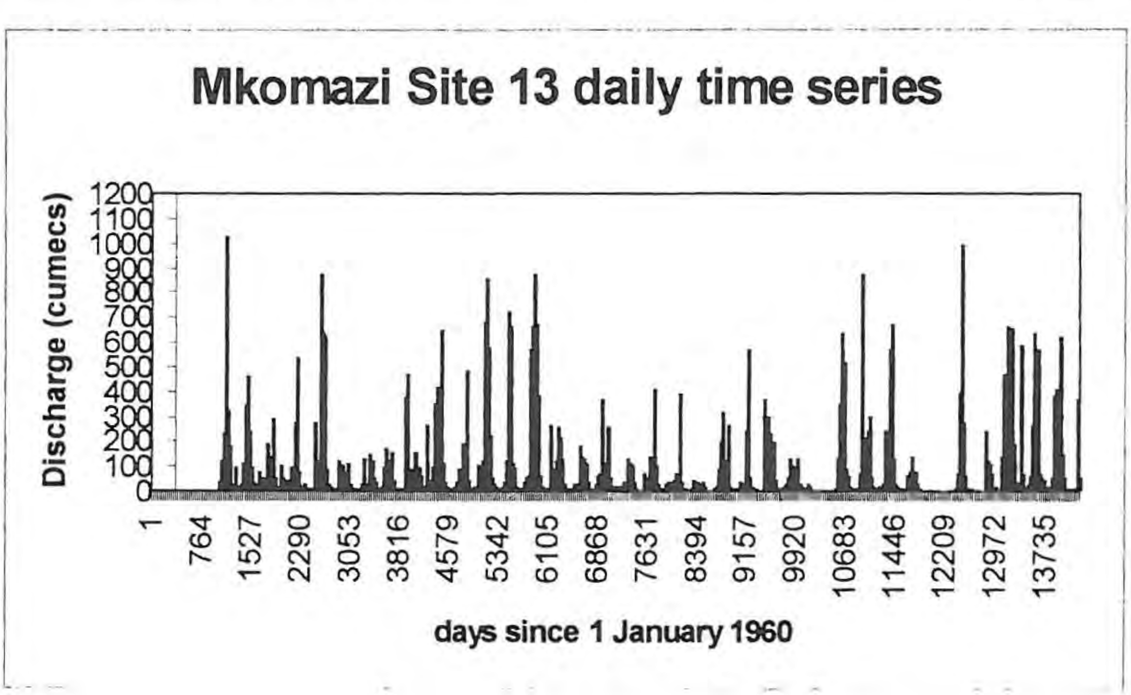
Mkomazi Site 13 daily time series
Discharge (cumecs)
1200
1100
1000
900
800
700
600
500
400
300
200
100
0
1
764
1527
2290
3053
3816
4579
5342
6105
6868
7631
8394
9157
9920
10683
11446
12209
12972
13735
days since 1 January 1960

Mhlathuze Site 1 daily time series (Virgin)

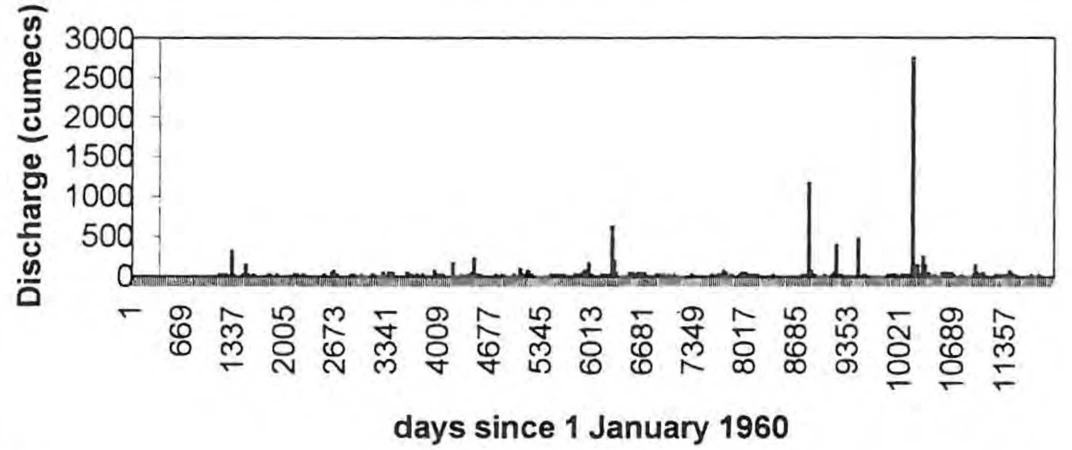

Mhlathuze Site 1 daily time series (Present-day)

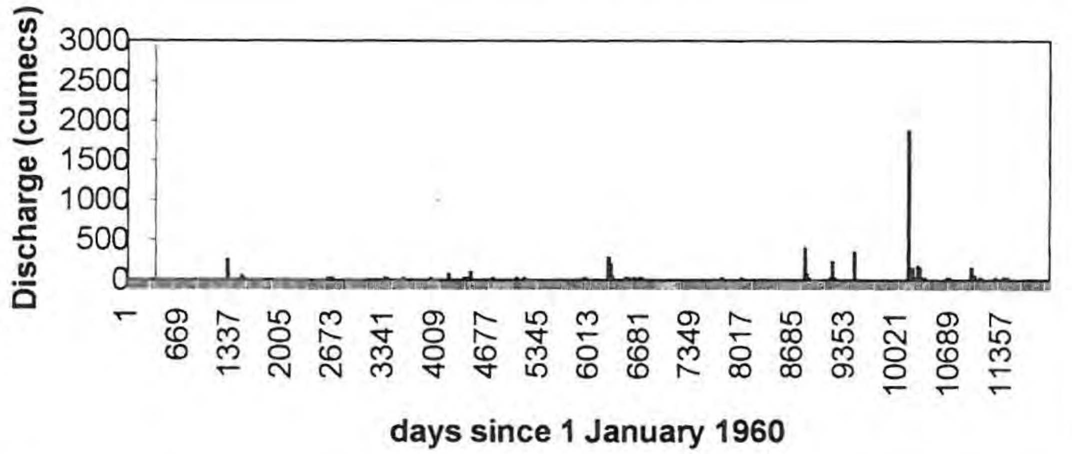

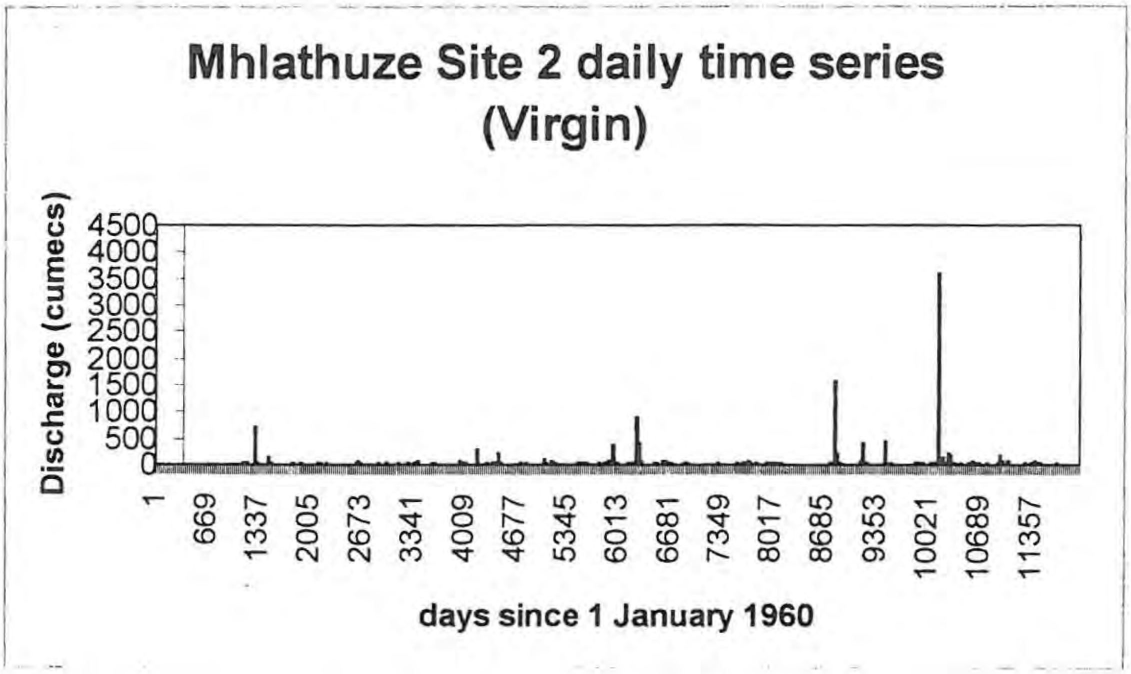
Mhlathuze Site 2 daily time series
(Virgin)
Discharge (cumecs)
4500
4000
3500
3000
2500
2000
1500
1000
500
0
1
669
1337
2005
2673
3341
4009
4677
5345
6013
6681
7349
8017
8685
9353
10021
10689
11357
days since 1 January 1960

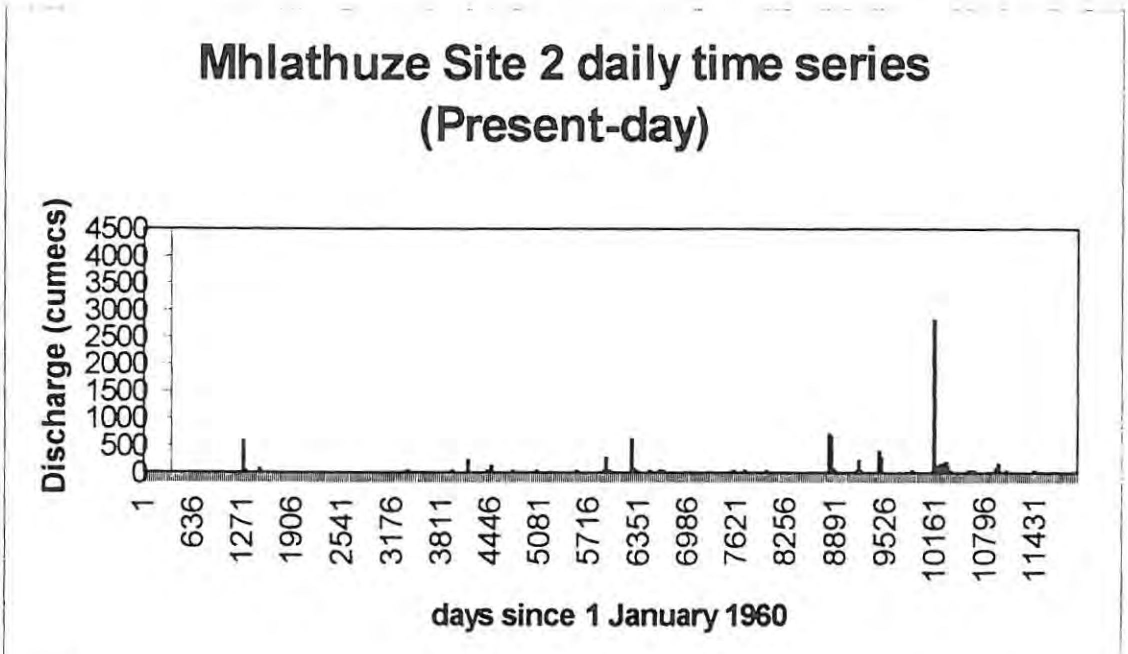
Mhlathuze Site 2 daily time series
(Present-day)
Discharge (cumecs)
4500
4000
3500
3000
2500
2000
1500
1000
500
0
1
636
1271
1906
2541
3176
3811
4446
5081
5716
6351
6986
7621
8256
8891
9526
10161
10796
11431
days since 1 January 1960

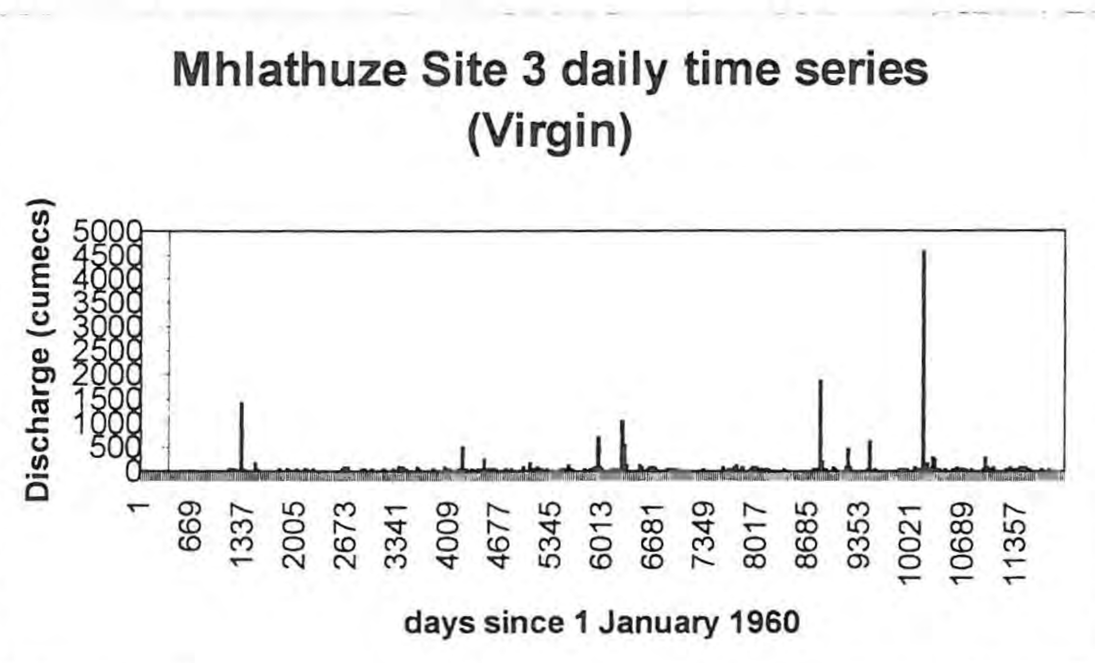
Mhlathuze Site 3 daily time series
(Virgin)
Discharge (cumecs)
5000
4500
4000
3500
3000
2500
2000
1500
1000
500
0
1
669
1337
2005
2673
3341
4009
4677
5345
6013
6681
7349
8017
8685
9353
10021
10689
11357
days since 1 January 1960

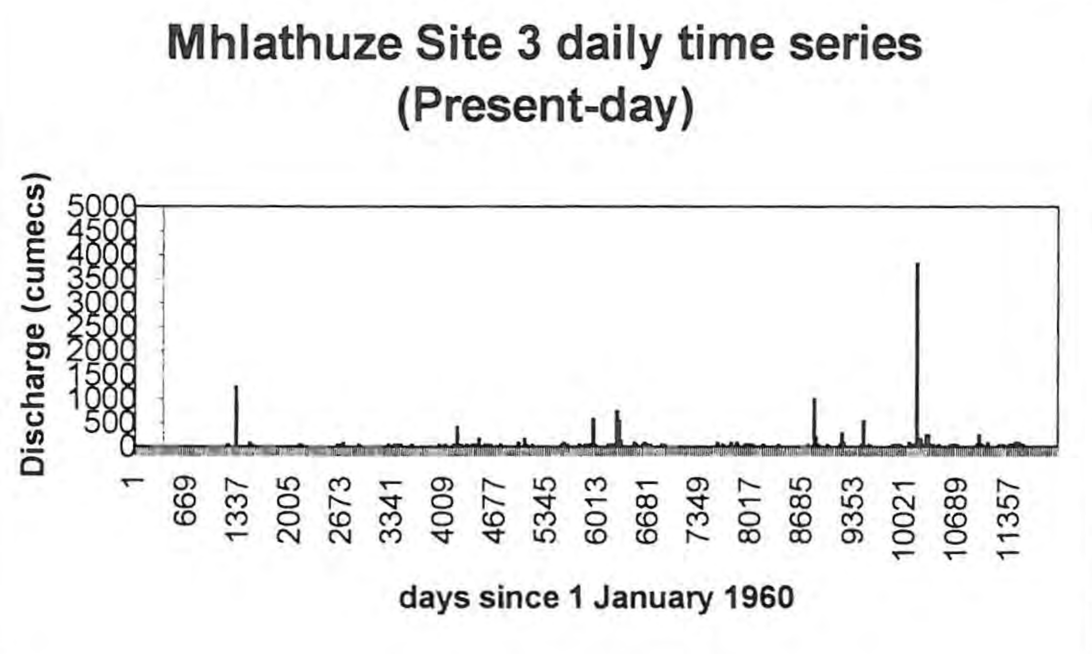
Mhlathuze Site 3 daily time series
(Present-day)
Discharge (cumecs)
5000
4500
4000
3500
3000
2500
2000
1500
1000
500
0
1
669
1337
2005
2673
3341
4009
4677
5345
6013
6681
7349
8017
8685
9353
10021
10689
11357
days since 1 January 1960

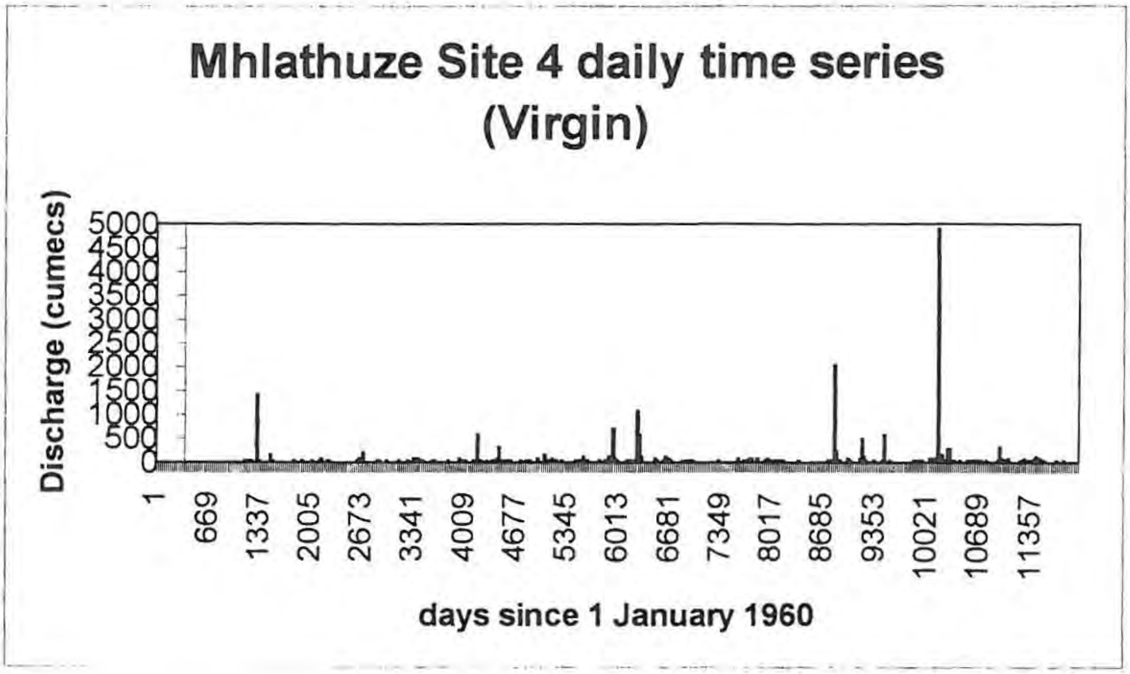
Mhlathuze Site 4 daily time series
(Virgin)
Discharge (cumecs)
5000
4500
4000
3500
3000
2500
2000
1500
1000
500
0
1
669
1337
2005
2673
3341
4009
4677
5345
6013
6681
7349
8017
8685
9353
10021
10689
11357
days since 1 January 1960

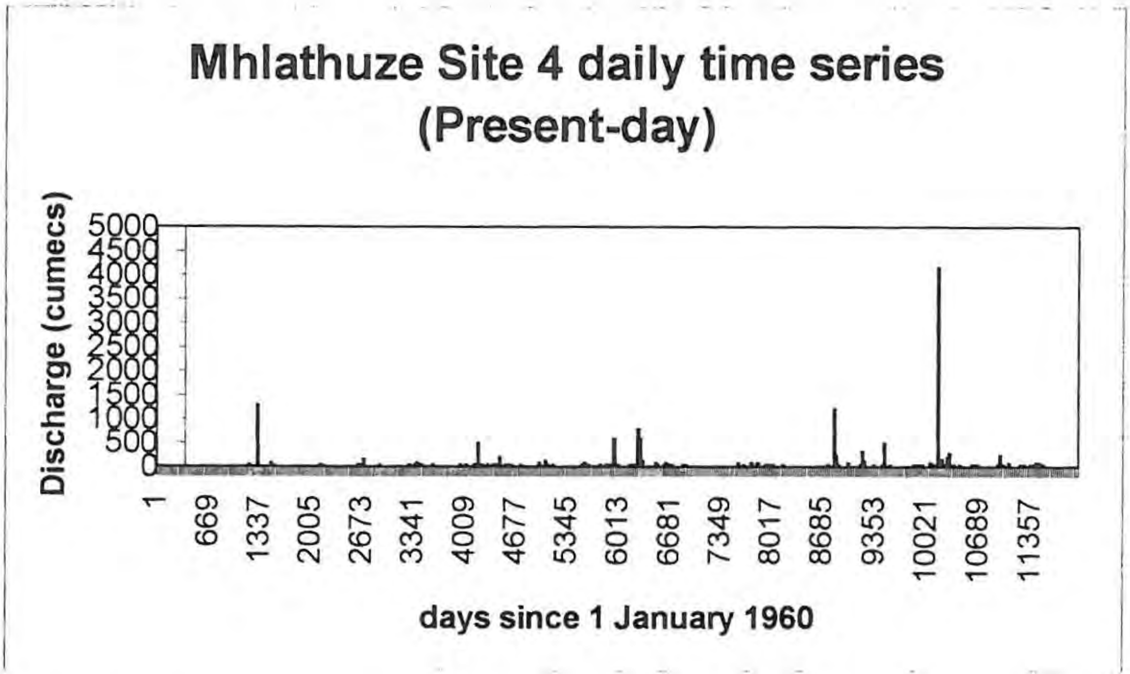
Mhlathuze Site 4 daily time series
(Present-day)
Discharge (cumecs)
5000
4500
4000
3500
3000
2500
2000
1500
1000
500
0
1
669
1337
2005
2673
3341
4009
4677
5345
6013
6681
7349
8017
8685
9353
10021
10689
11357
days since 1 January 1960

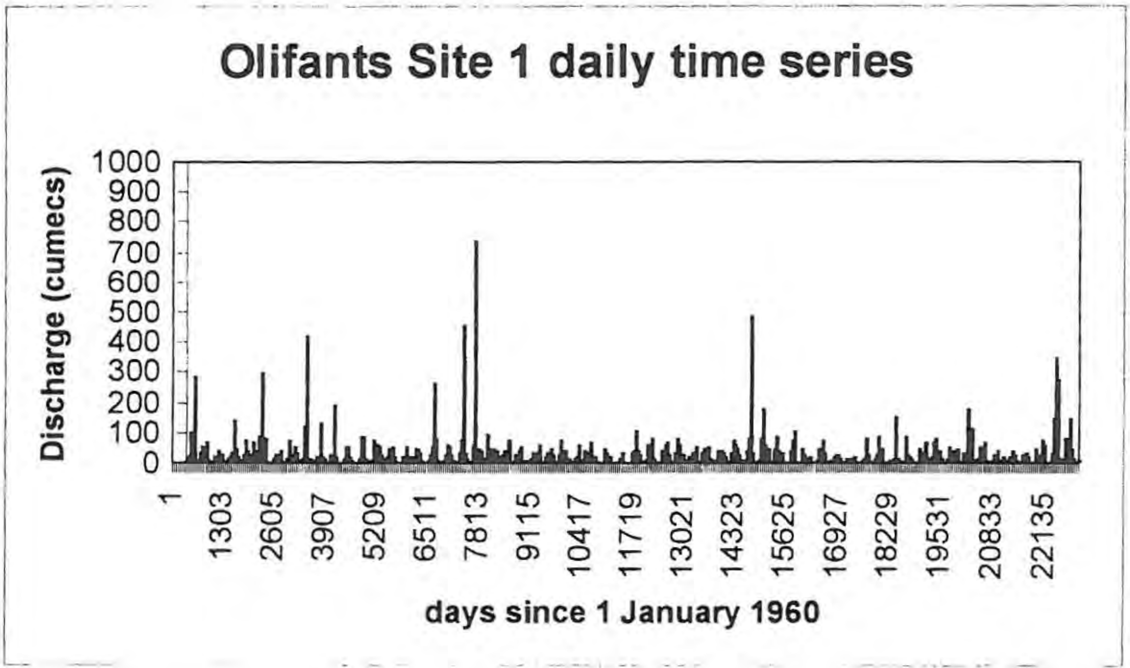
Olifants Site 1 daily time series
Discharge (cumecs)
1000
900
800
700
600
500
400
300
200
100
0
1
1303
2605
3907
5209
6511
7813
9115
10417
11719
13021
14323
15625
16927
18229
19531
20833
22135
days since 1 January 1960

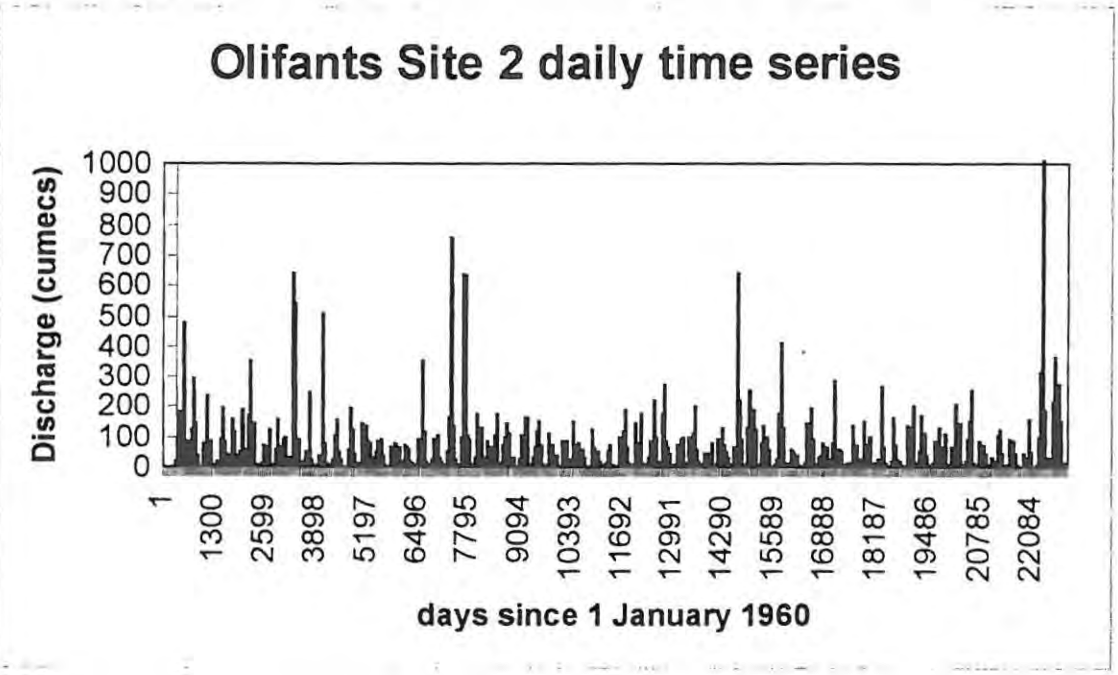
Olifants Site 2 daily time series
Discharge (cumecs)
1000
900
800
700
600
500
400
300
200
100
0
1
1300
2599
3898
5197
6496
7795
9094
10393
11692
12991
14290
15589
16888
18187
19486
20785
22084
days since 1 January 1960

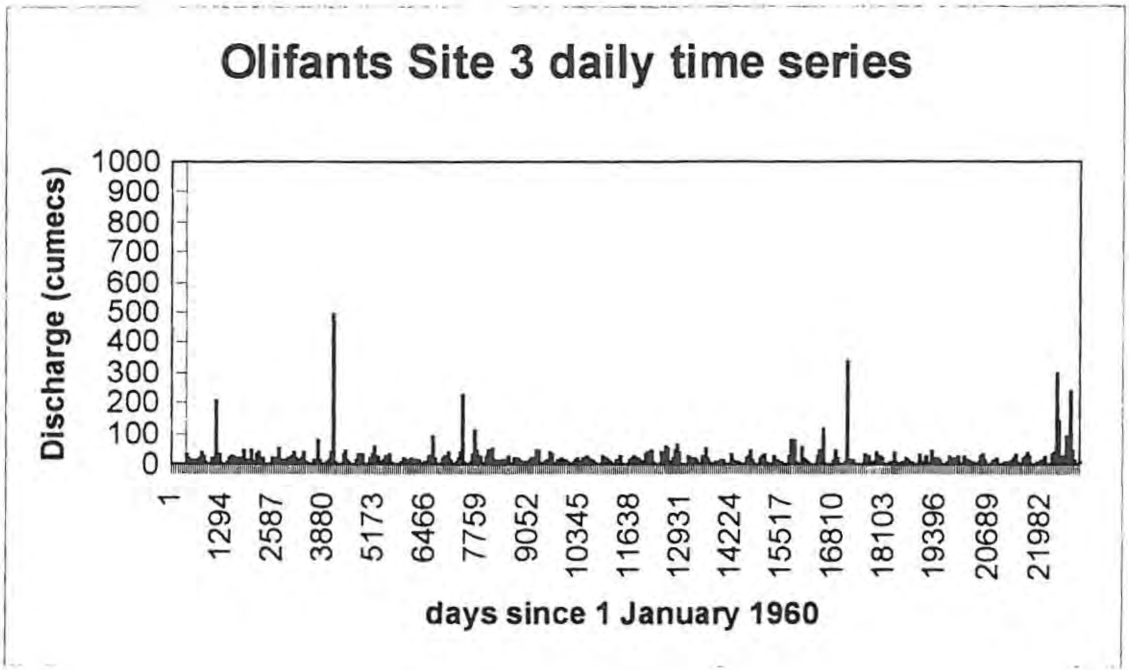
Olifants Site 3 daily time series
Discharge (cumecs)
0
100
200
300
400
500
600
700
800
900
1000
1
1294
2587
3880
5173
6466
7759
9052
10345
11638
12931
14224
15517
16810
18103
19396
20689
21982
days since 1 January 1960

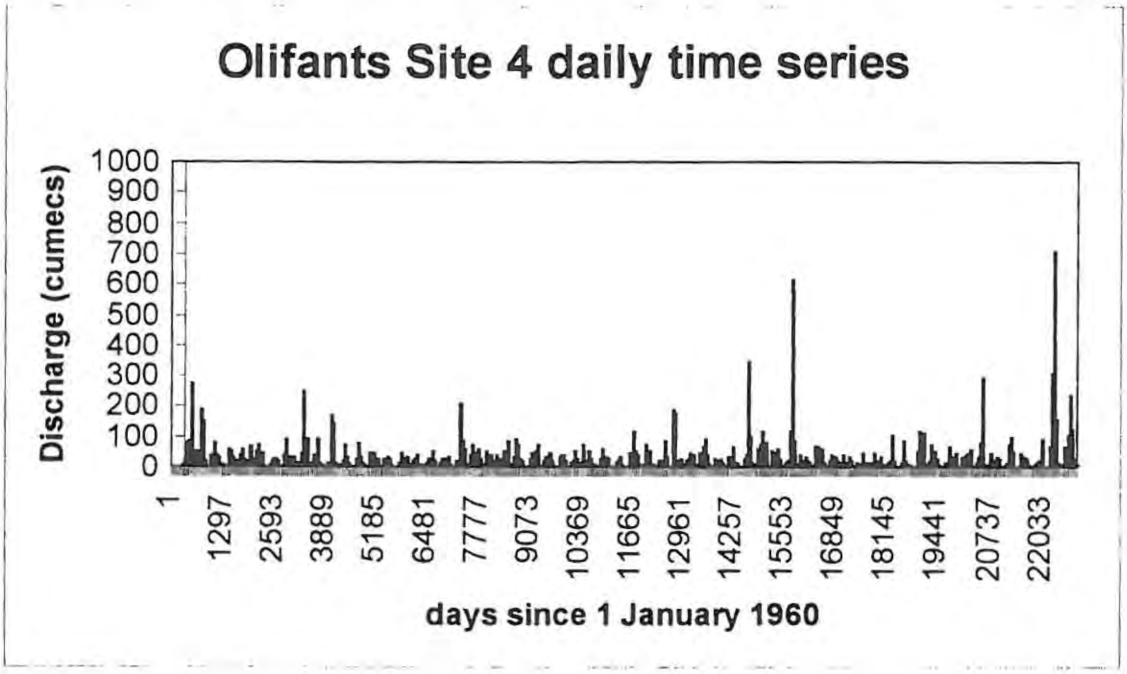
Olifants Site 4 daily time series
Discharge (cumecs)
0
100
200
300
400
500
600
700
800
900
1000
1
1297
2593
3889
5185
6481
7777
9073
10369
11665
12961
14257
15553
16849
18145
19441
20737
22033
days since 1 January 1960

APPENDIX C

ANNUAL SERIES FLOOD FREQUENCY CURVES

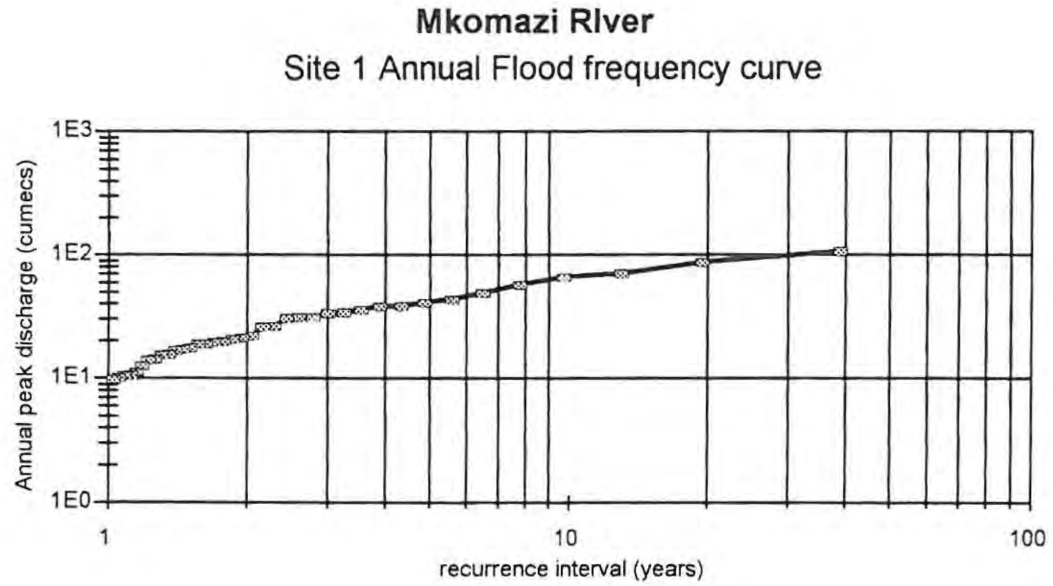
Mkomazi RIver
Site 1 Annual Flood frequency curve
Annual peak discharge (cumecs)
1E3
1E2
1E1
1E0
1
10
100
recurrence interval (years)

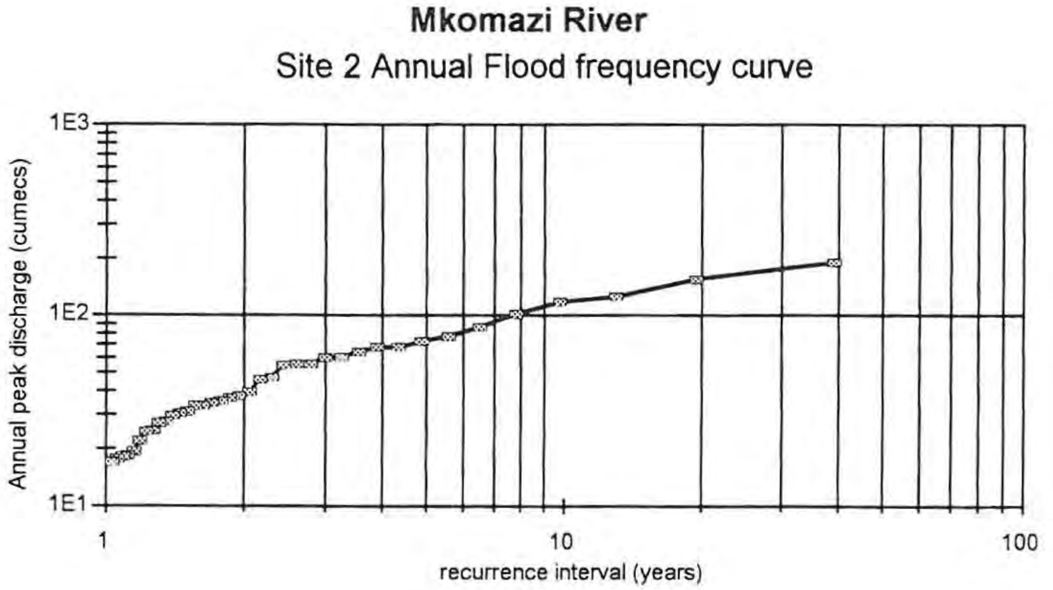
Mkomazi River
Site 2 Annual Flood frequency curve
Annual peak discharge (cumecs)
1E3
1E2
1E1
1
10
100
recurrence interval (years)

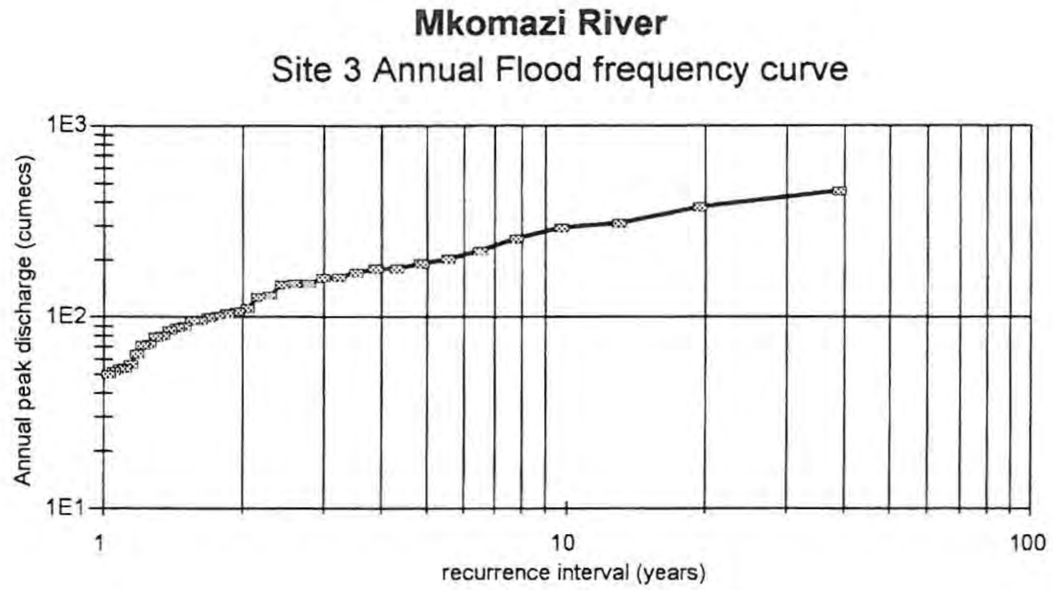
Mkomazi River
Site 3 Annual Flood frequency curve
1E3
1E2
1E1
Annual peak discharge (cumecs)
1
10
100
recurrence interval (years)

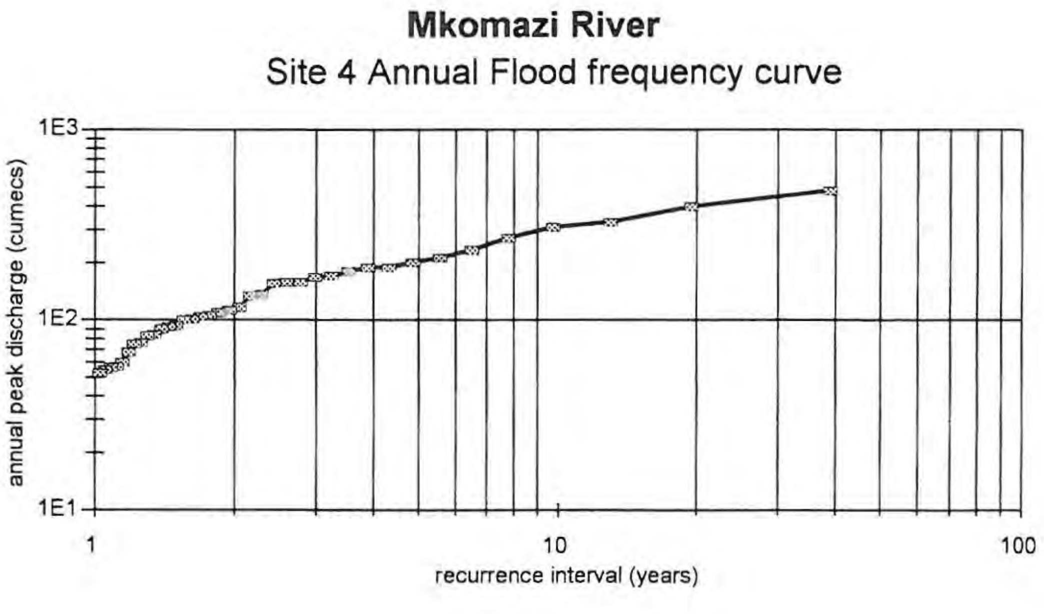
Mkomazi River
Site 4 Annual Flood frequency curve
1E3
1E2
1E1
annual peak discharge (cumecs)
1
10
100
recurrence interval (years)

Mkomazi River
Site 5 Annual Flood frequency curve

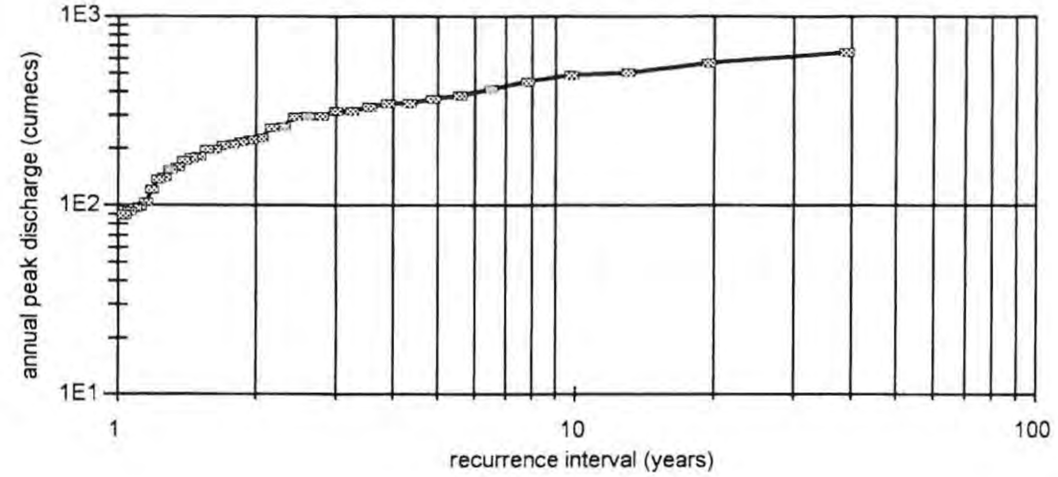

Mkomazi River
Site 6 Annual Flood frequency curve

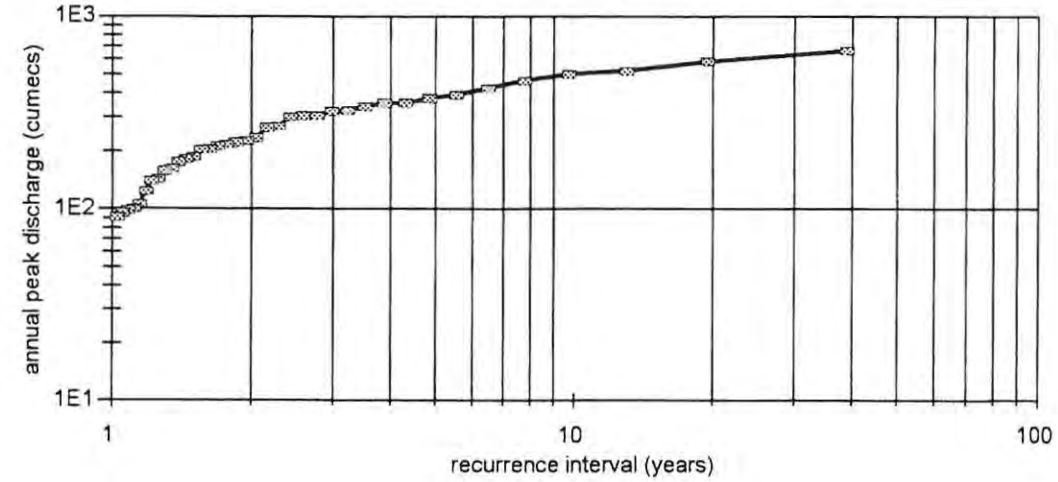

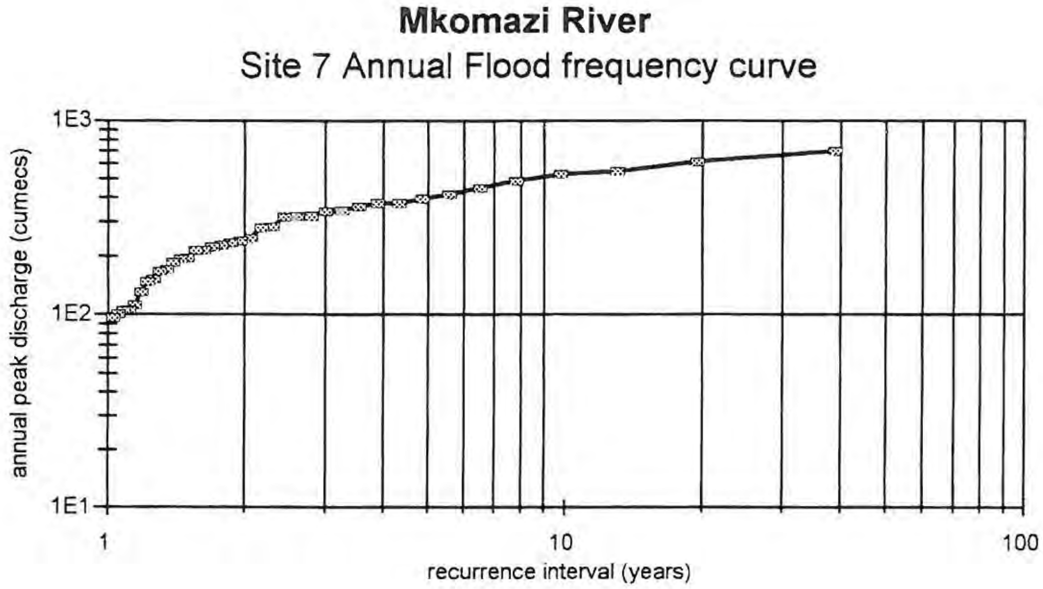
Mkomazi River
Site 7 Annual Flood frequency curve
1E3
1E2
1E1
annual peak discharge (cumecs)
1
10
100
recurrence interval (years)

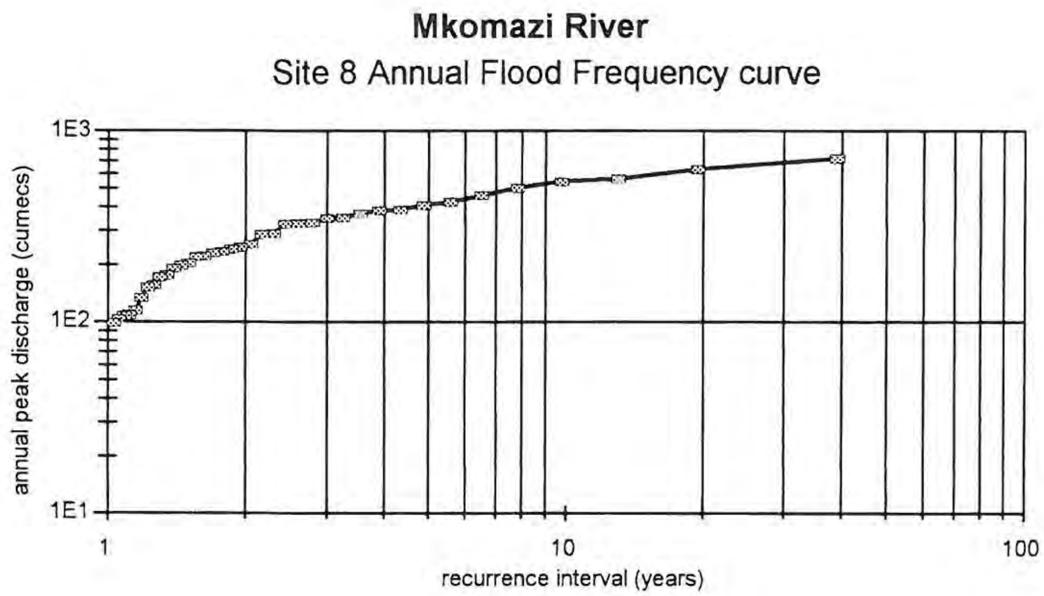
Mkomazi River
Site 8 Annual Flood Frequency curve
1E3
1E2
1E1
annual peak discharge (cumecs)
1
10
100
recurrence interval (years)

Mkomazi River
Site 9 Annual Flood frequency curve

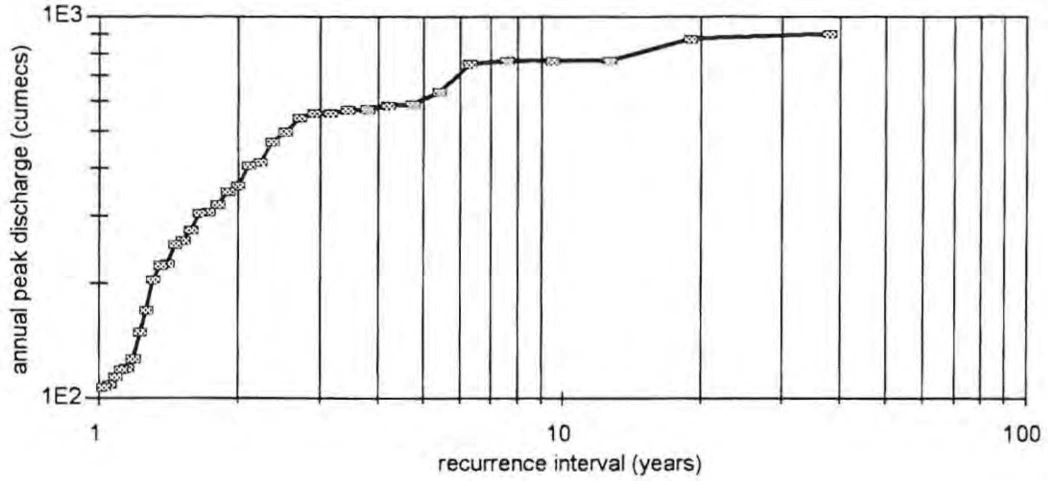

Mkomazi River
Site 10 Annual Flood frequency curve

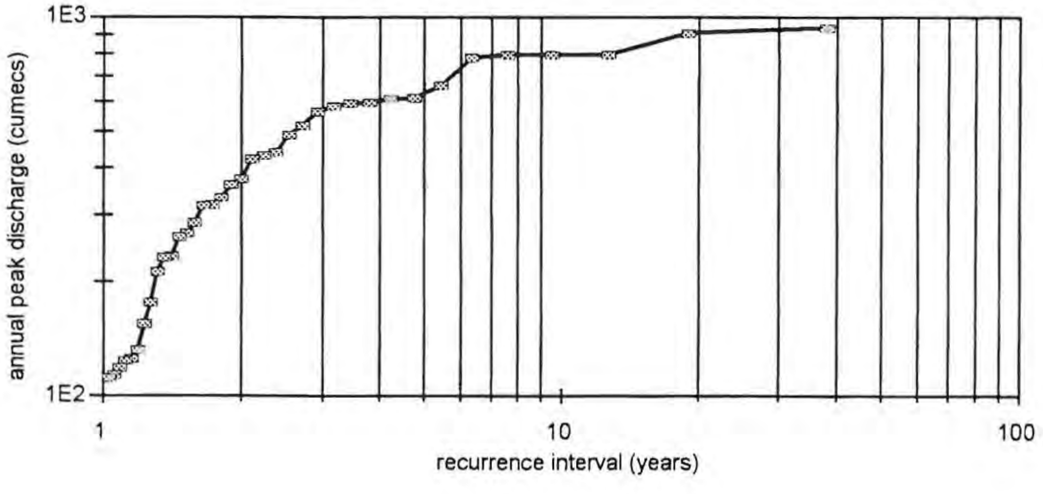

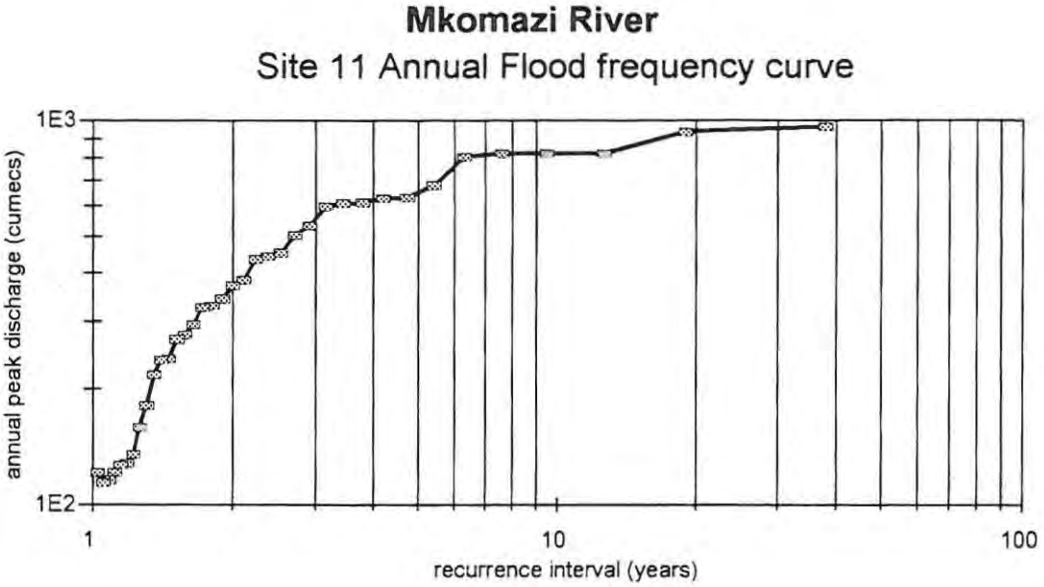
Mkomazi River
Site 11 Annual Flood frequency curve
1E3
1E2
annual peak discharge (cumecs)
1
10
100
recurrence interval (years)

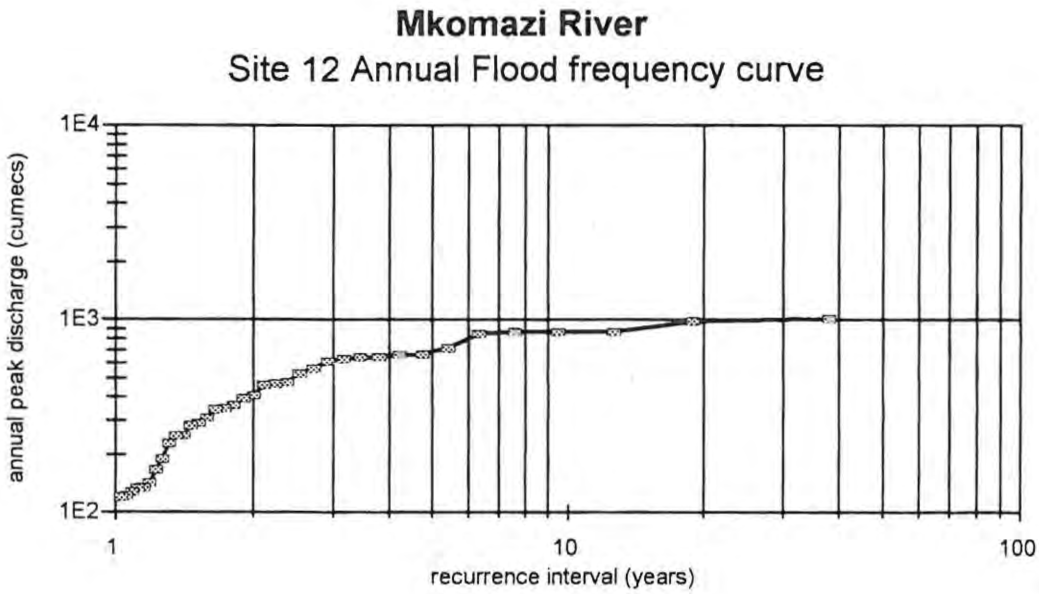
Mkomazi River
Site 12 Annual Flood frequency curve
1E4
1E3
1E2
annual peak discharge (cumecs)
1
10
100
recurrence interval (years)

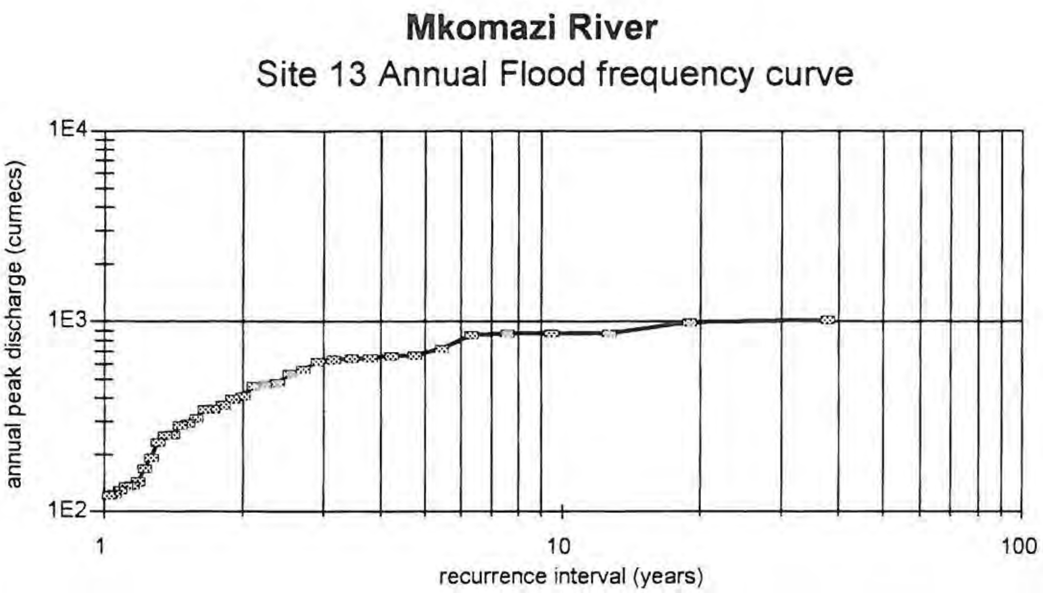
Mkomazi River
Site 13 Annual Flood frequency curve
1E4
1E3
1E2
annual peak discharge (cumecs)
1
10
100
recurrence interval (years)

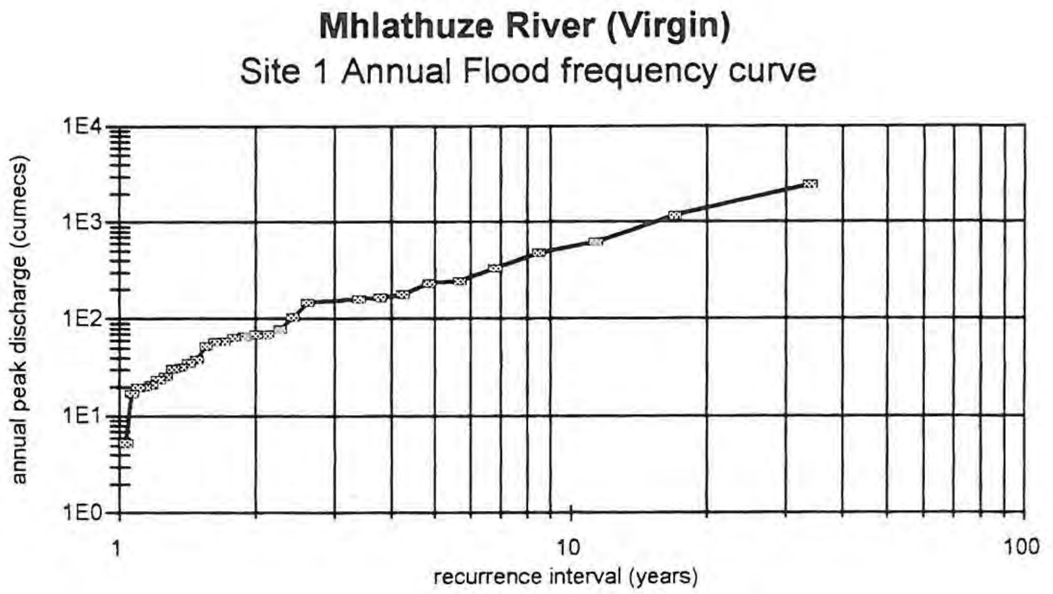
Mhlathuze River (Virgin)
Site 1 Annual Flood frequency curve
annual peak discharge (cumecs)
1E4
1E3
1E2
1E1
1E0
1
10
100
recurrence interval (years)

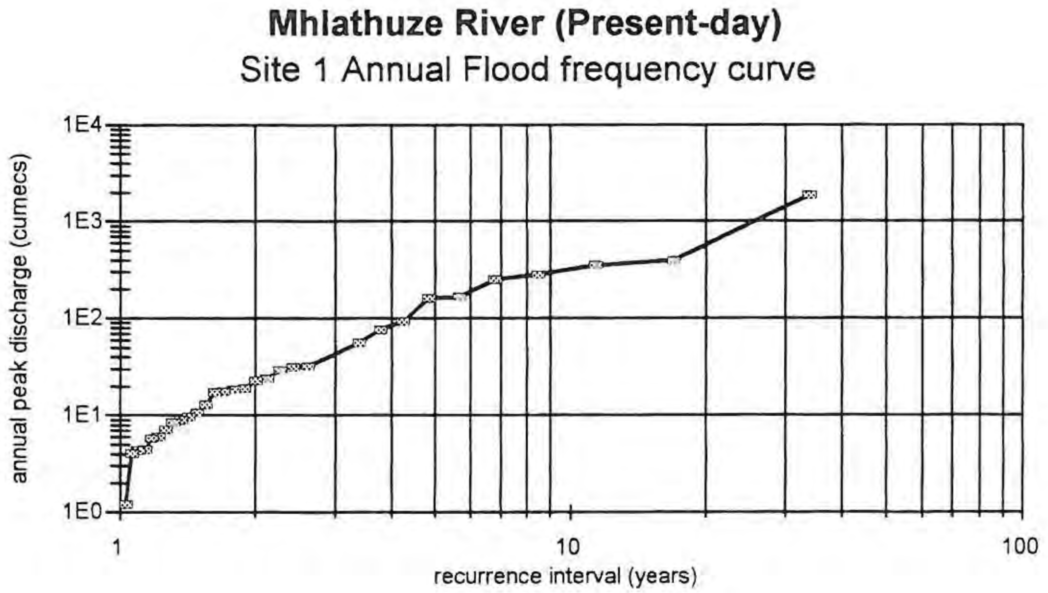
Mhlathuze River (Present-day)
Site 1 Annual Flood frequency curve
annual peak discharge (cumecs)
1E4
1E3
1E2
1E1
1E0
1
10
100
recurrence interval (years)

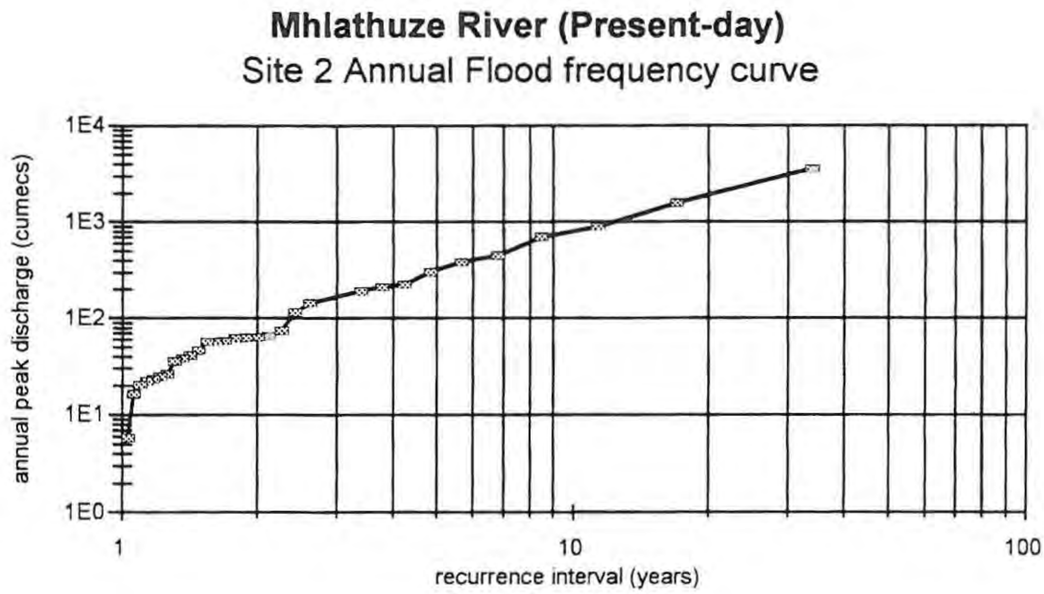
Mhlathuze River (Present-day)
Site 2 Annual Flood frequency curve
annual peak discharge (cumecs)
1E4
1E3
1E2
1E1
1E0
1
10
100
recurrence interval (years)

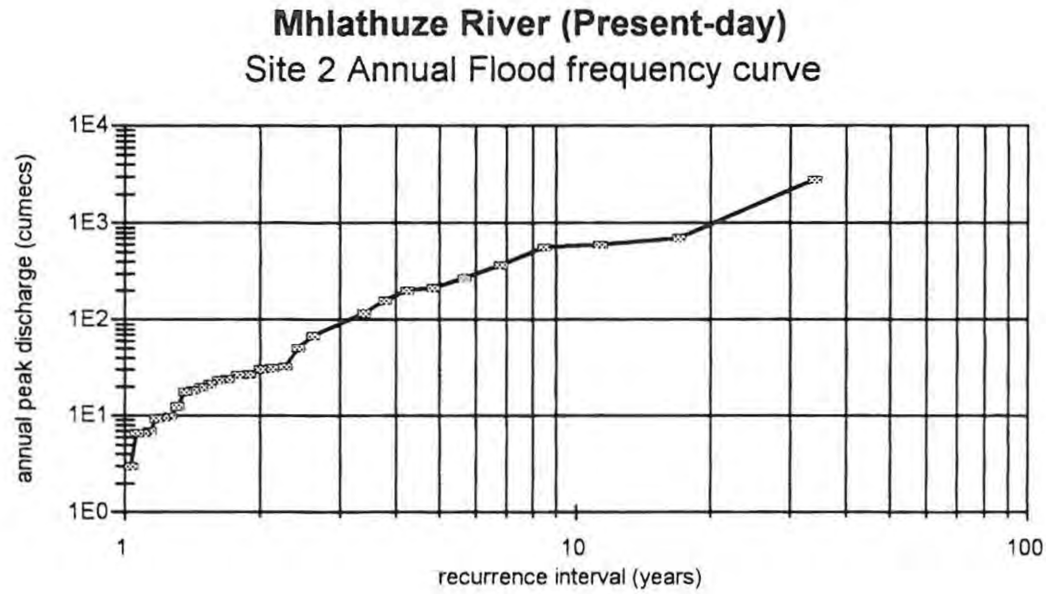
Mhlathuze River (Present-day)
Site 2 Annual Flood frequency curve
annual peak discharge (cumecs)
1E4
1E3
1E2
1E1
1E0
1
10
100
recurrence interval (years)

Mhlathuze River (Virgin)

Site 3 Annual Flood frequency curve

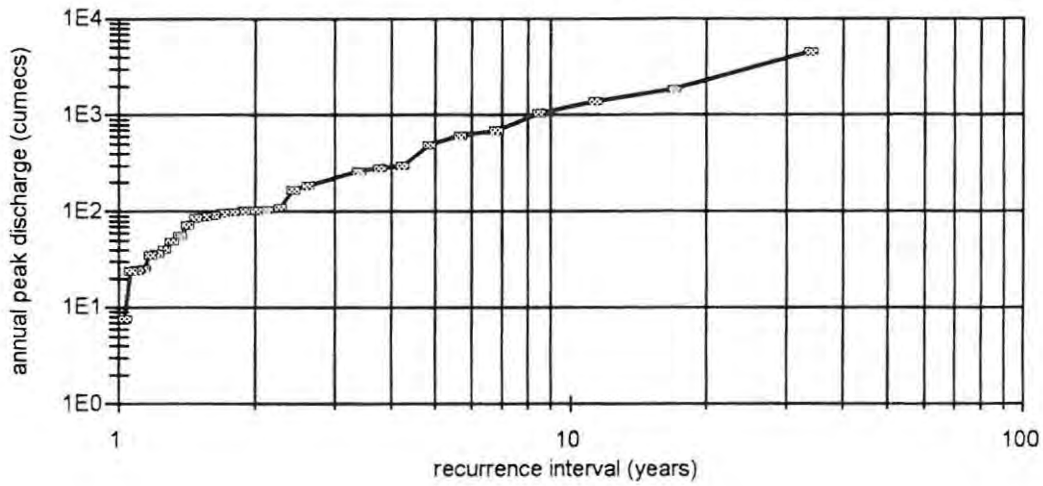

Mhlathuze River (Present-day)

Site 2 Annual Flood frequency curve

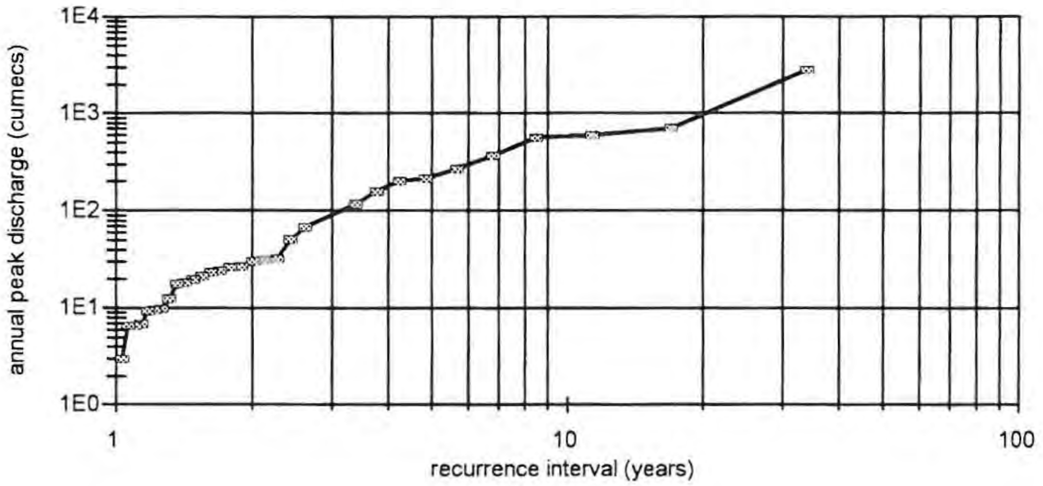

Mhlathuze River (Virgin)
Site 4 Annual Flood frequency curve

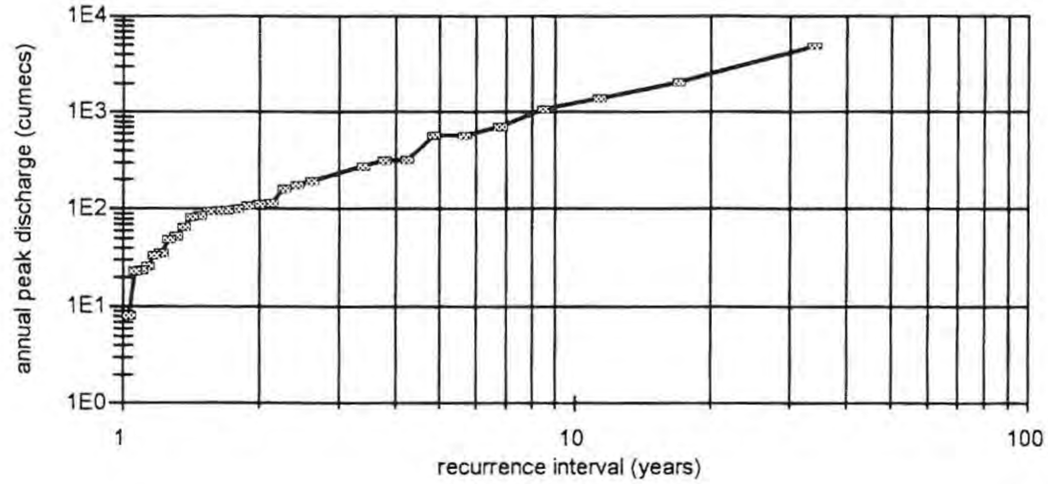

Mhlathuze River (Present-day)
Site 4 Annual Flood frequency curve

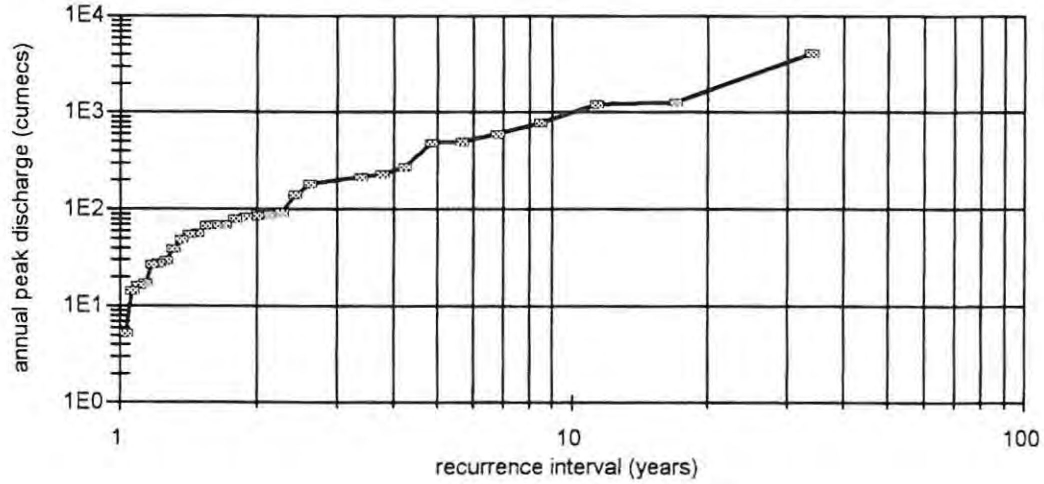

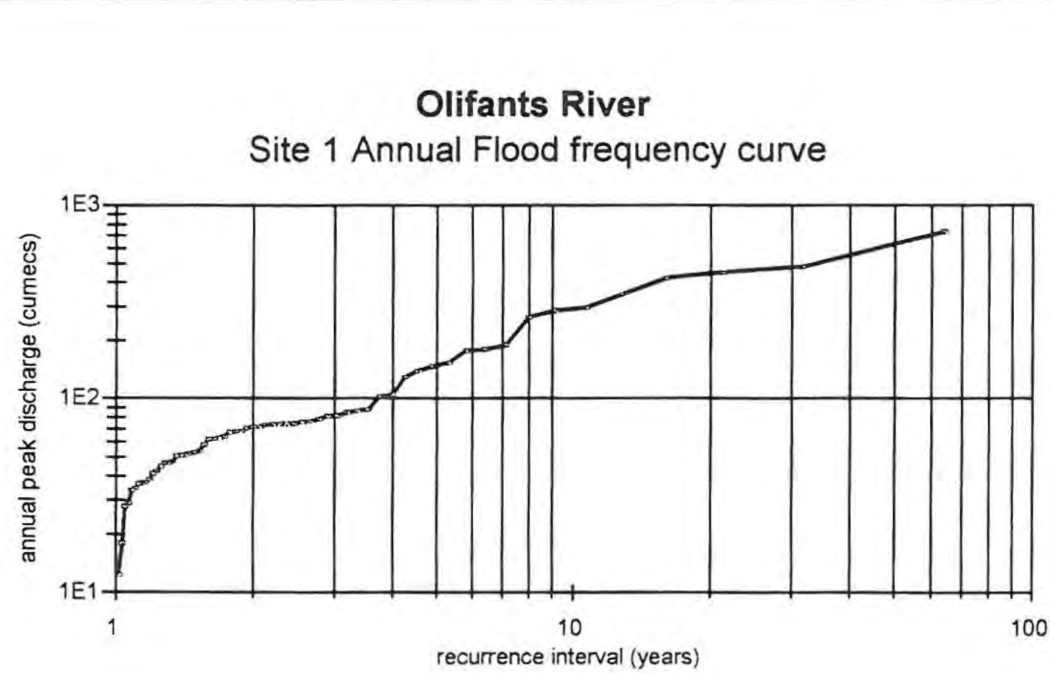

Olifants River
Site 1 Annual Flood frequency curve
annual peak discharge (cumecs)
1E3
1E2
1E1
1
10
100
recurrence interval (years)

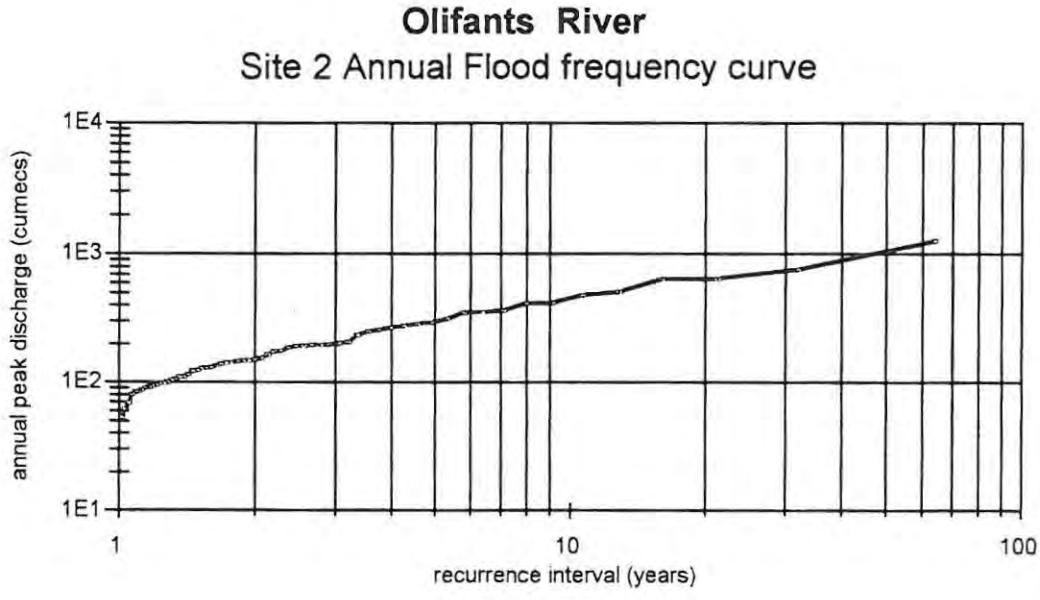

Olifants River
Site 2 Annual Flood frequency curve
annual peak discharge (cumecs)
1E4
1E3
1E2
1E1
1
10
100
recurrence interval (years)

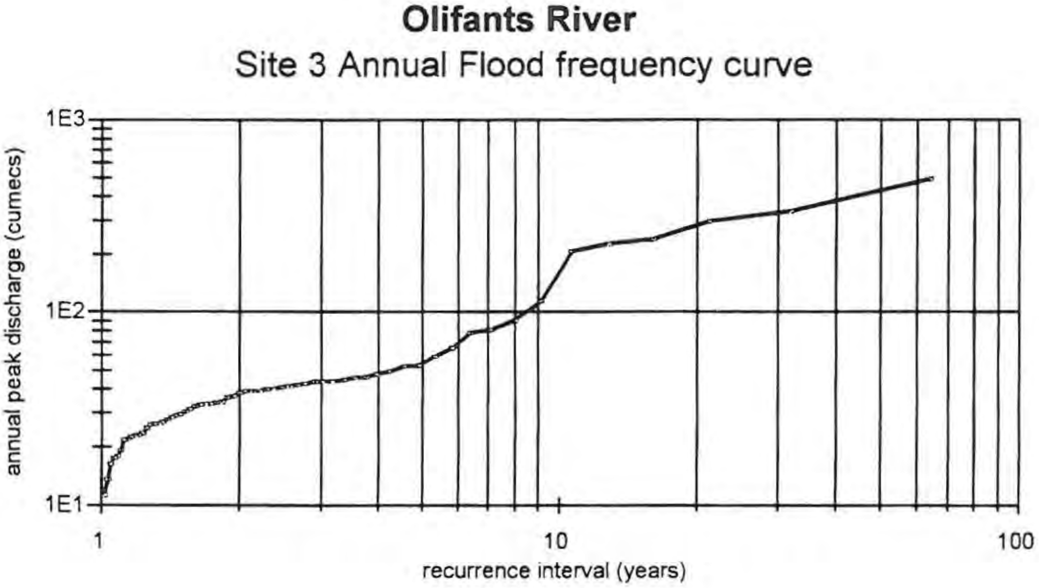
Olifants River
Site 3 Annual Flood frequency curve
1E3
1E2
1E1
annual peak discharge (cumecs)
1
10
100
recurrence interval (years)

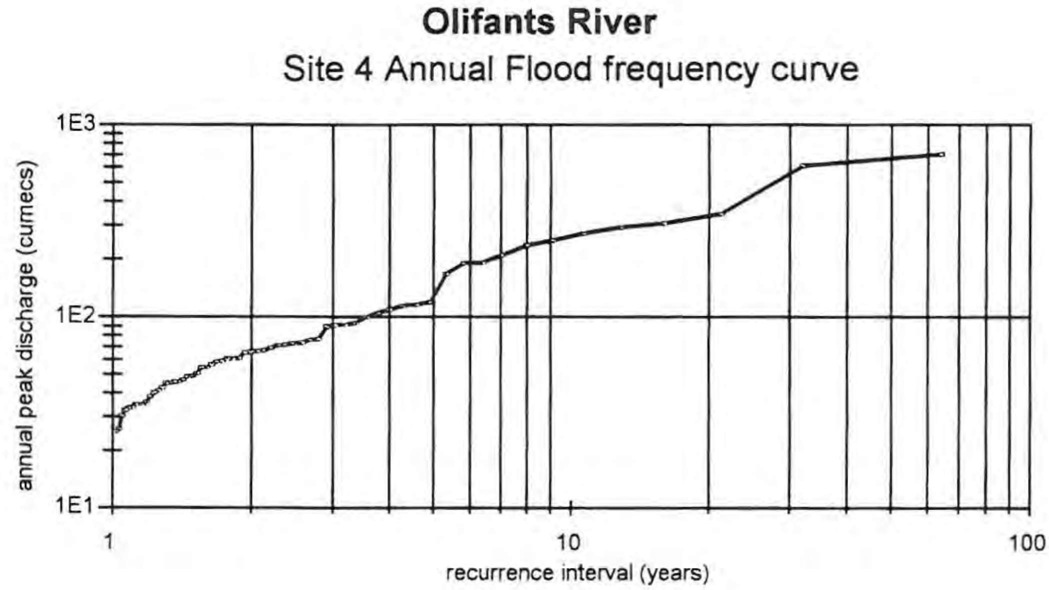
Olifants River
Site 4 Annual Flood frequency curve
1E3
1E2
1E1
annual peak discharge (cumecs)
1
10
100
recurrence interval (years)

APPENDIX D

FLOOD FREQUENCY CURVES FOR ALL RIVERS

(PARTIAL SERIES)

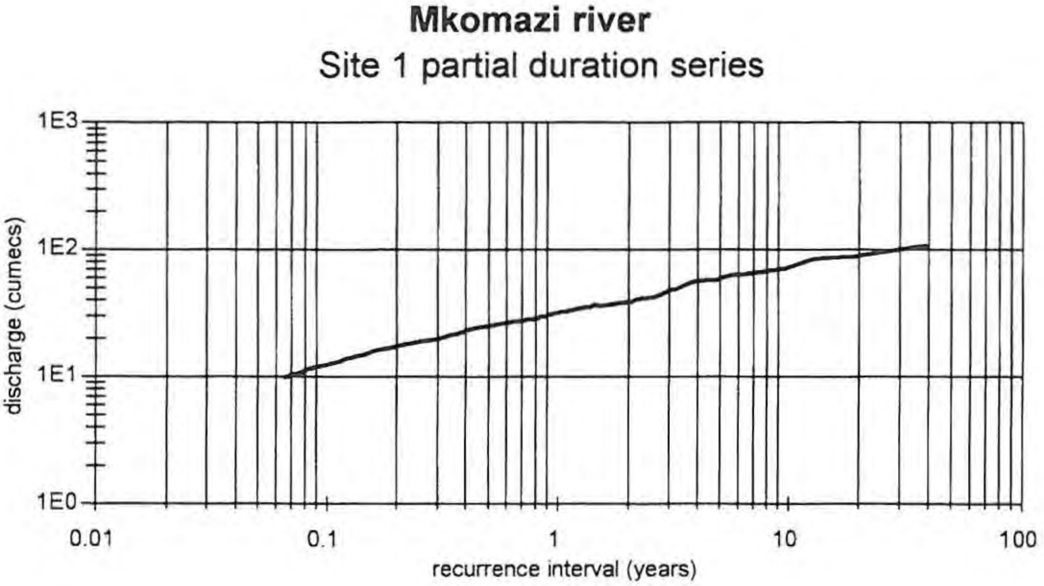
Mkomazi river
Site 1 partial duration series
1E3
1E2
1E1
1E0
discharge (cumecs)
0.01
0.1
1
10
100
recurrence interval (years)

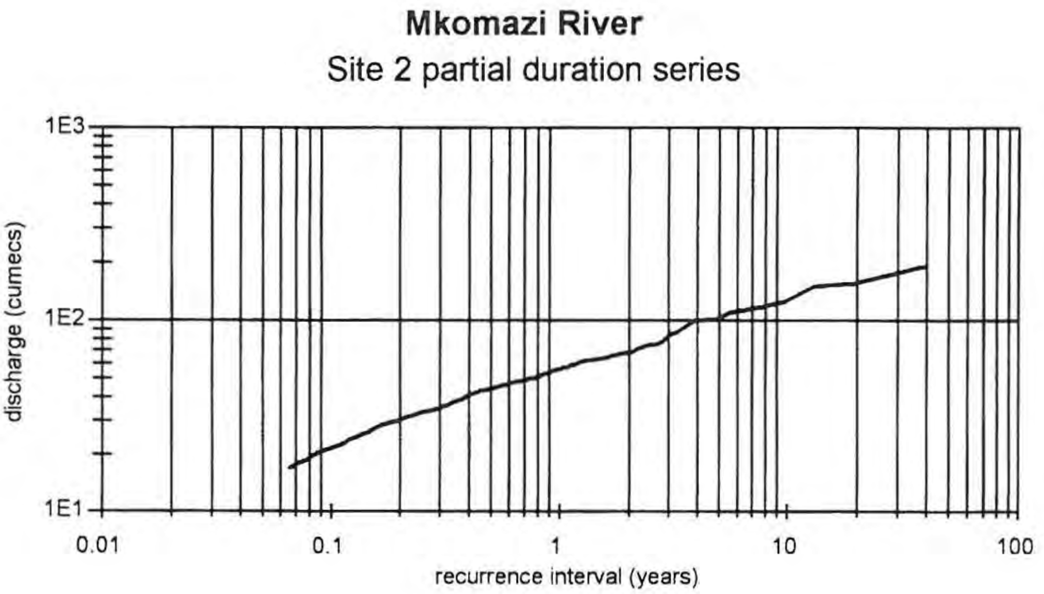
Mkomazi River
Site 2 partial duration series
1E3
1E2
1E1
discharge (cumecs)
0.01
0.1
1
10
100
recurrence interval (years)

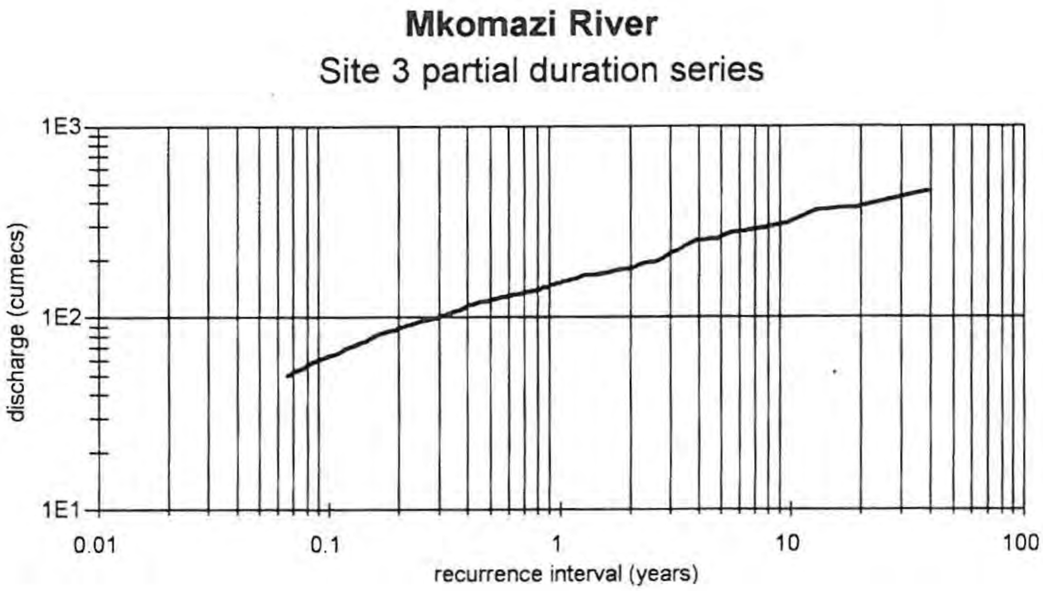
Mkomazi River
Site 3 partial duration series
1E3
1E2
1E1
discharge (cumecs)
0.01
0.1
1
10
100
recurrence interval (years)

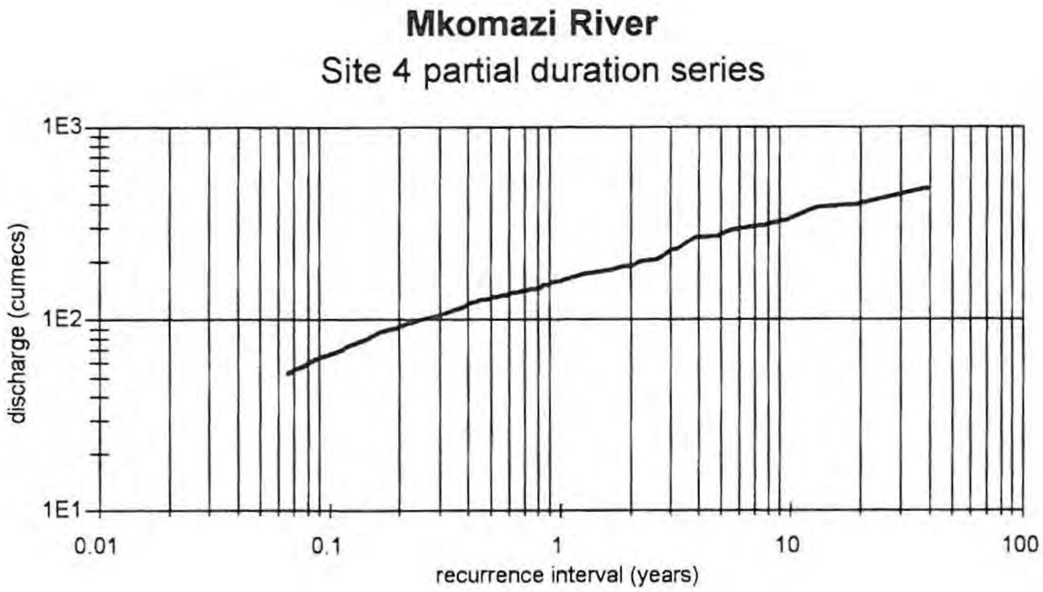
Mkomazi River
Site 4 partial duration series
1E3
1E2
1E1
discharge (cumecs)
0.01
0.1
1
10
100
recurrence interval (years)

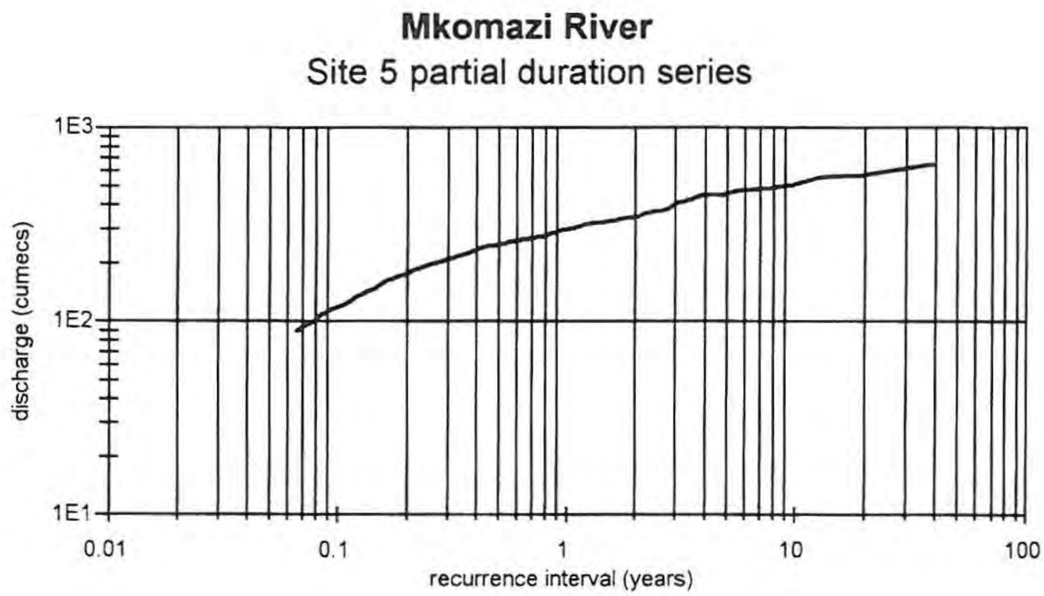
Mkomazi River
Site 5 partial duration series
1E3
1E2
1E1
discharge (cumecs)
0.01
0.1
1
10
100
recurrence interval (years)

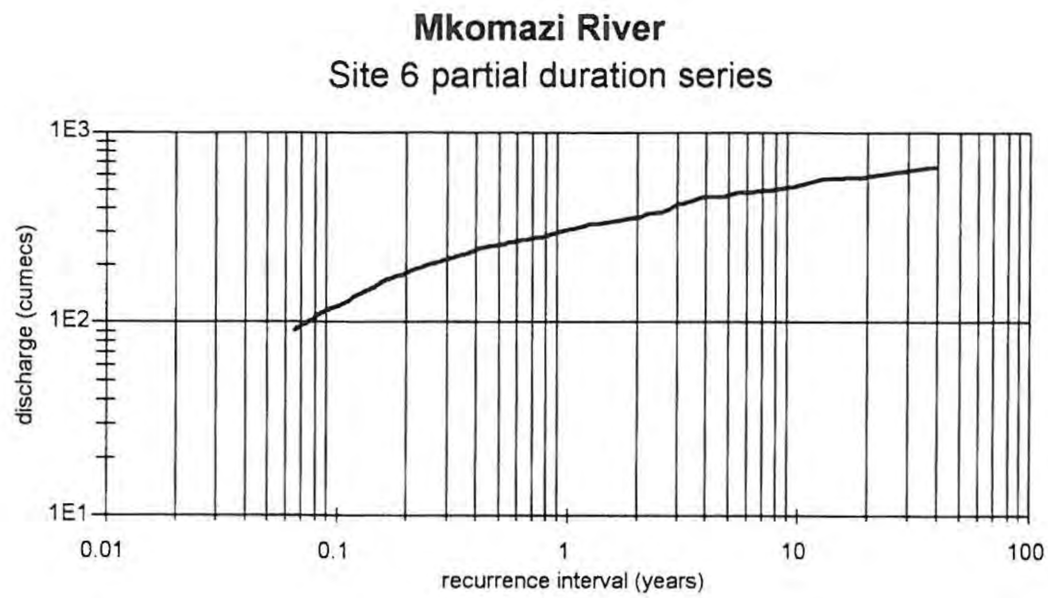
Mkomazi River
Site 6 partial duration series
1E3
1E2
1E1
discharge (cumecs)
0.01
0.1
1
10
100
recurrence interval (years)

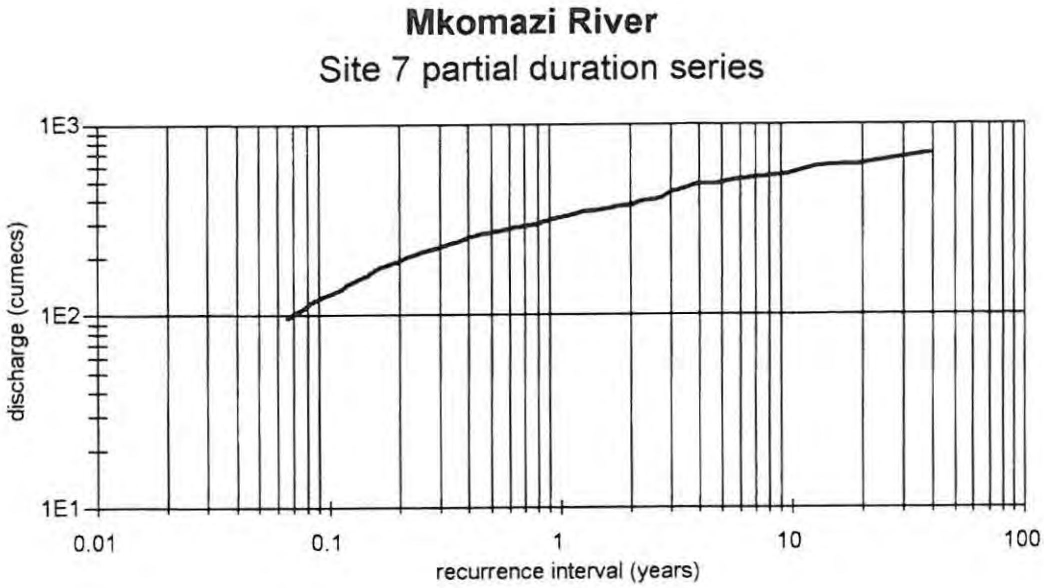

Mkomazi River
Site 7 partial duration series
1E3
1E2
1E1
discharge (cumecs)
0.01
0.1
1
10
100
recurrence interval (years)

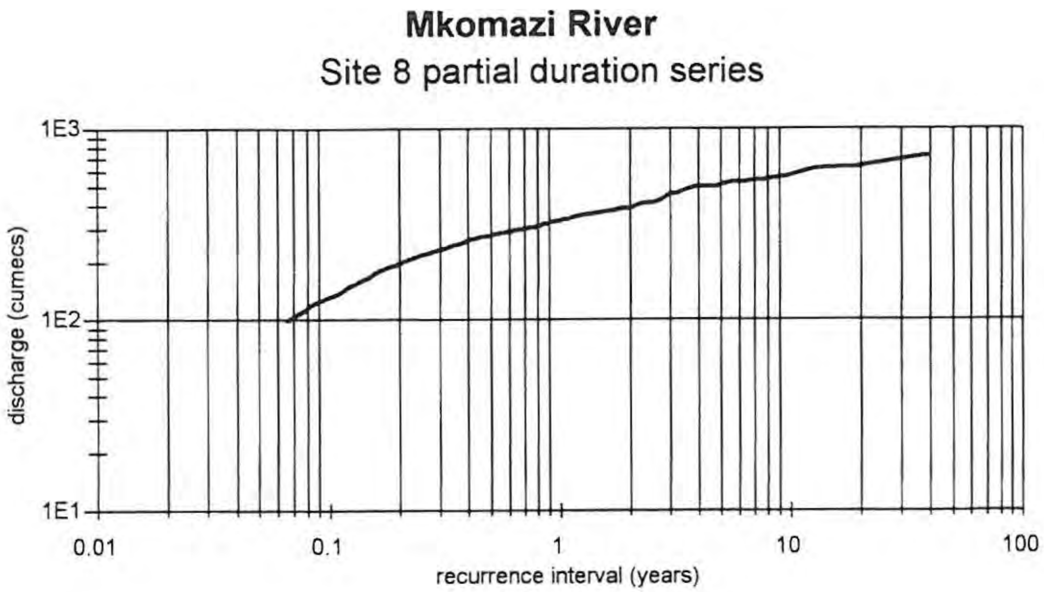

Mkomazi River
Site 8 partial duration series
1E3
1E2
1E1
discharge (cumecs)
0.01
0.1
1
10
100
recurrence interval (years)

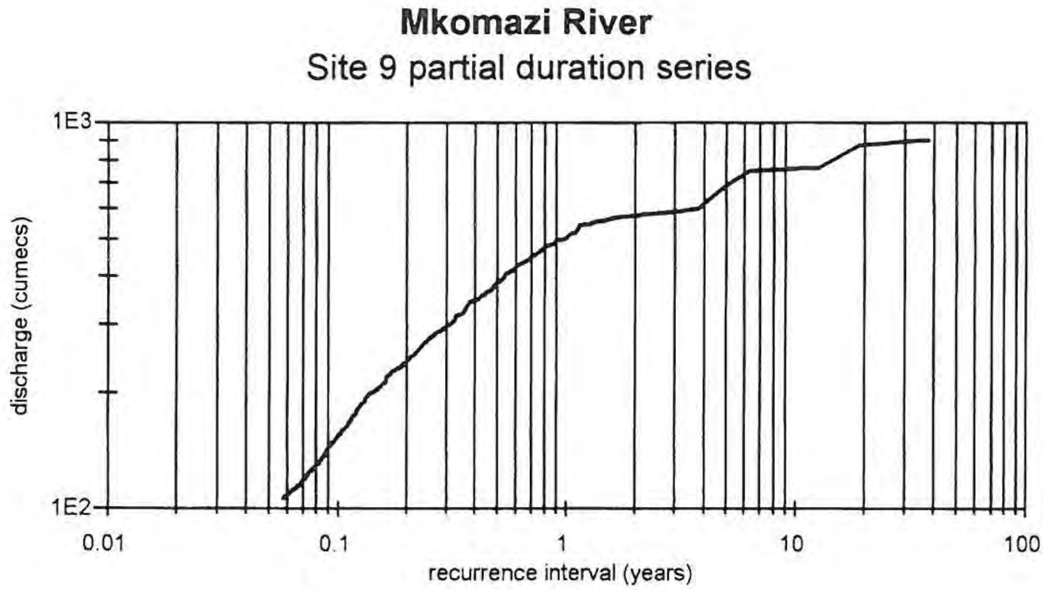
Mkomazi River
Site 9 partial duration series
1E3
1E2
discharge (cumecs)
0.01
0.1
1
10
100
recurrence interval (years)

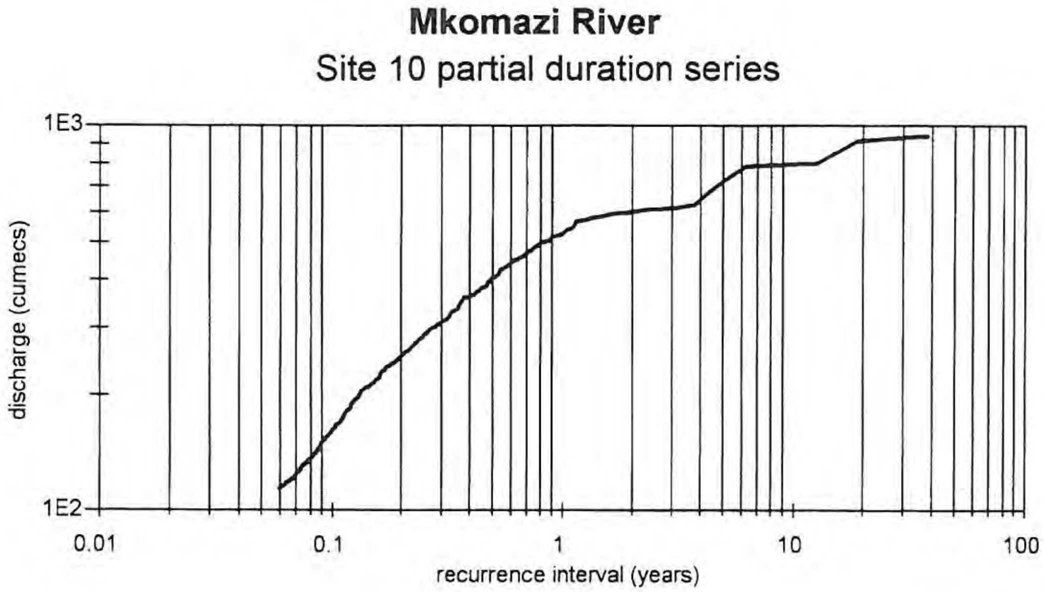
Mkomazi River
Site 10 partial duration series
1E3
1E2
discharge (cumecs)
0.01
0.1
1
10
100
recurrence interval (years)

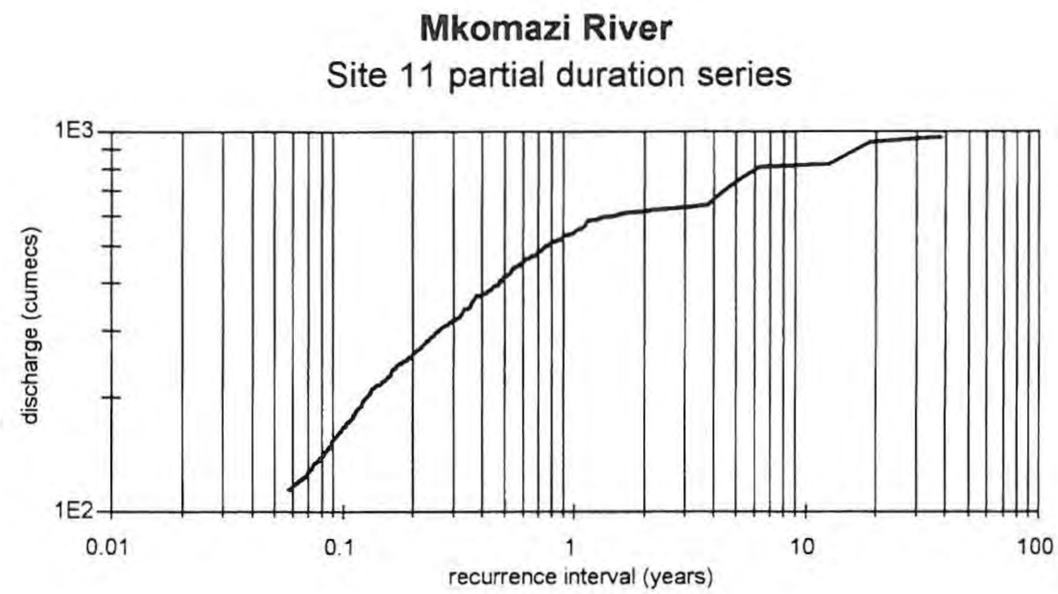

Mkomazi River
Site 11 partial duration series
1E3
1E2
discharge (cumecs)
0.01
0.1
1
10
100
recurrence interval (years)

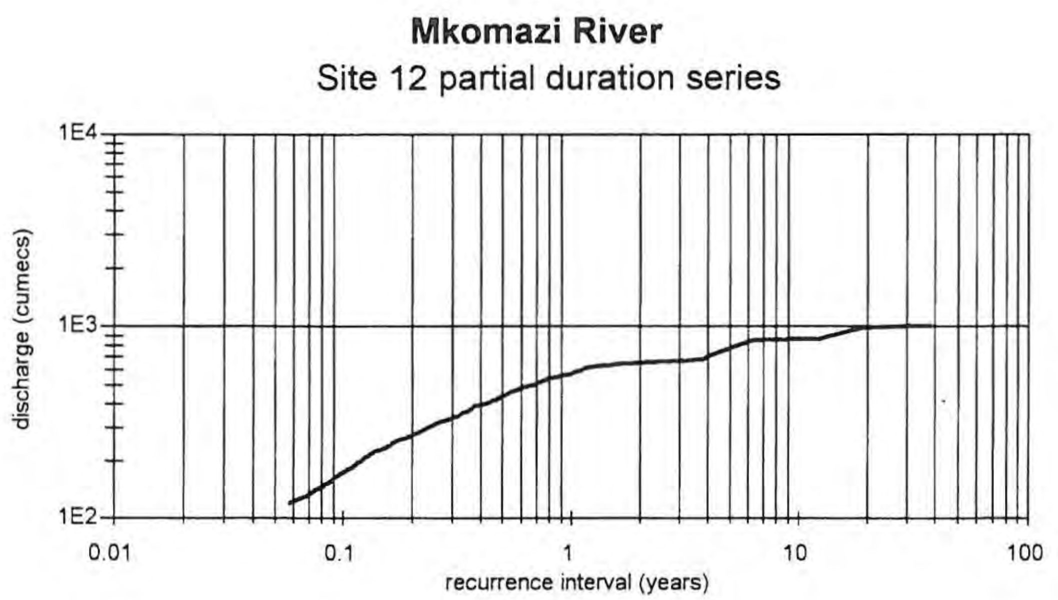

Mkomazi River
Site 12 partial duration series
1E4
1E3
1E2
discharge (cumecs)
0.01
0.1
1
10
100
recurrence interval (years)

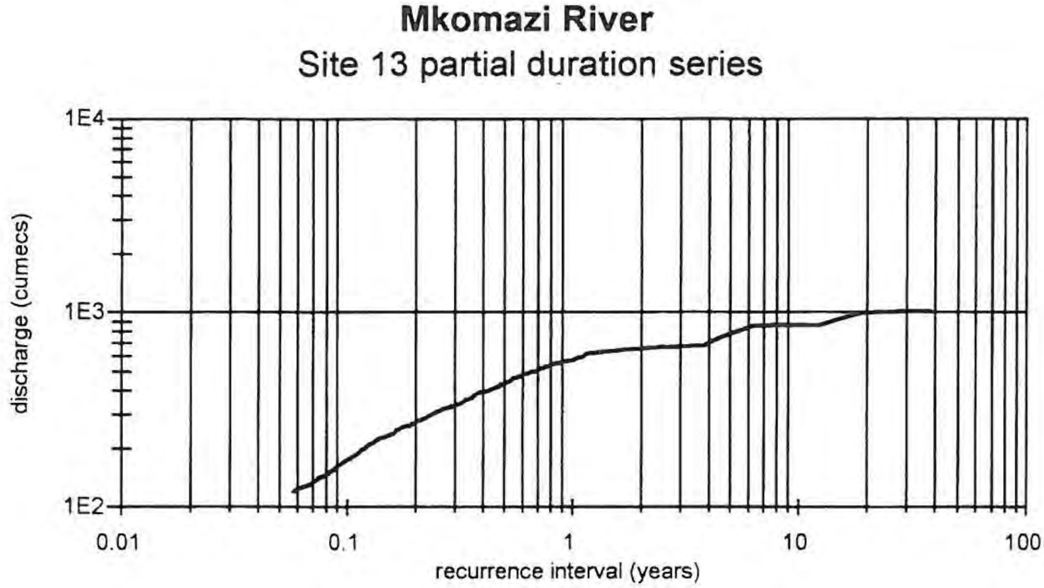
Mkomazi River
Site 13 partial duration series
1E4
1E3
1E2
discharge (cumecs)
0.01
0.1
1
10
100
recurrence interval (years)

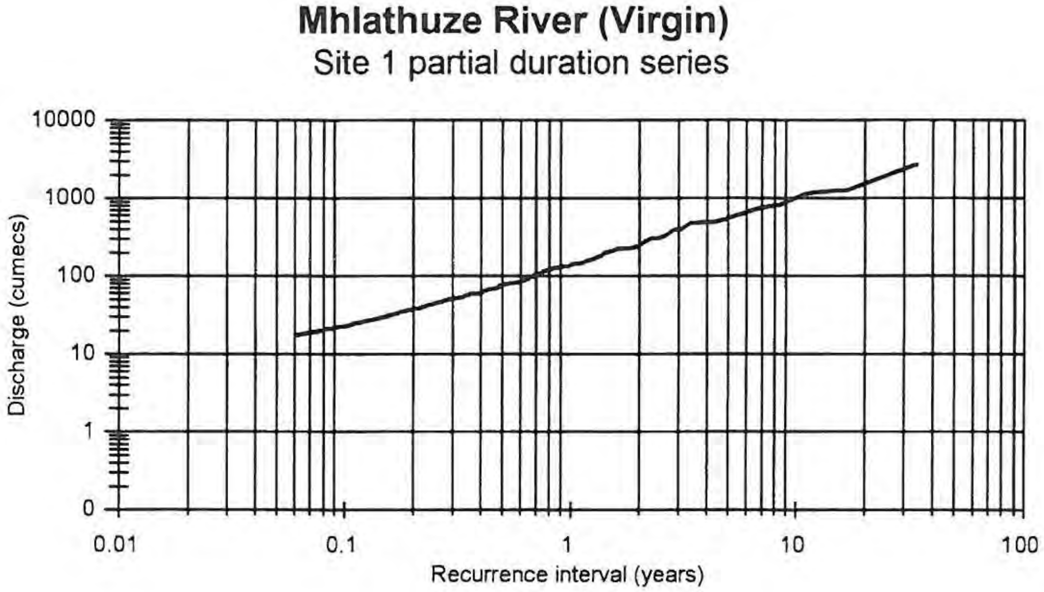
Mhlathuze River (Virgin)
Site 1 partial duration series
10000
1000
100
10
1
0
Discharge (cumecs)
0.01
0.1
1
10
100
Recurrence interval (years)

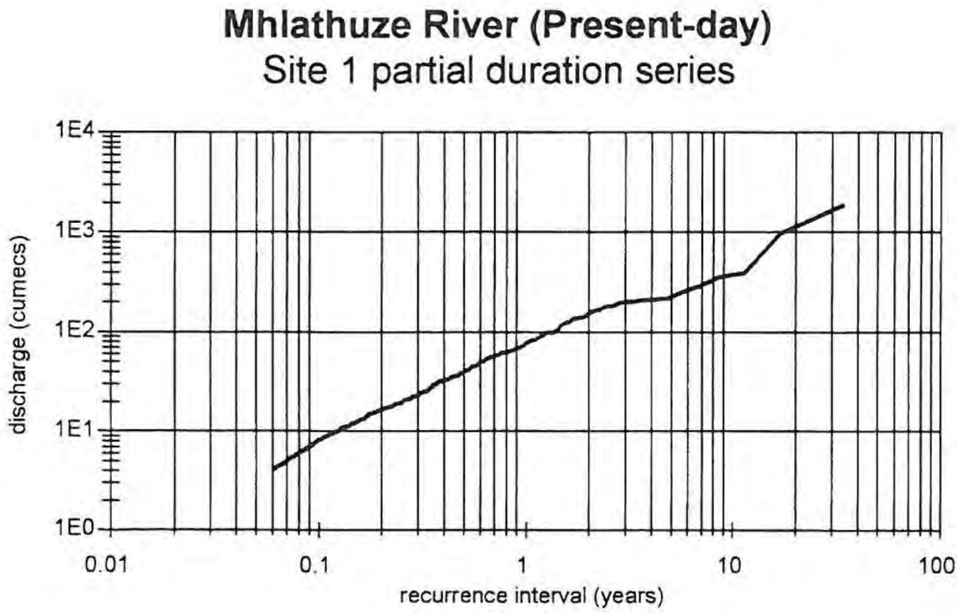
Mhlathuze River (Present-day)
Site 1 partial duration series
1E4
1E3
1E2
1E1
1E0
discharge (cumecs)
0.01
0.1
1
10
100
recurrence interval (years)

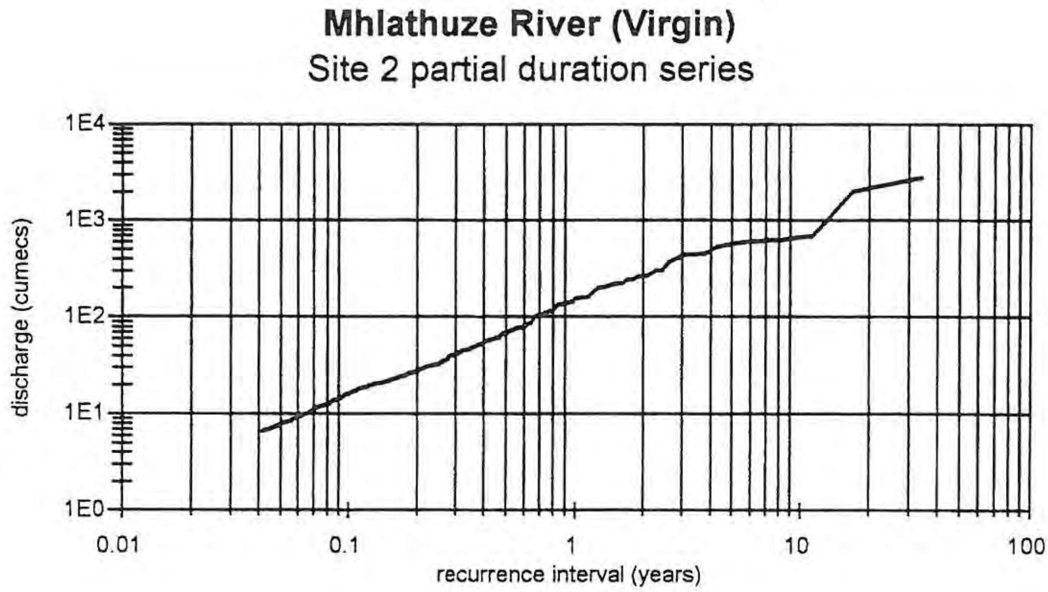
Mhlathuze River (Virgin)
Site 2 partial duration series
discharge (cumecs)
1E4
1E3
1E2
1E1
1E0
0.01
0.1
1
10
100
recurrence interval (years)

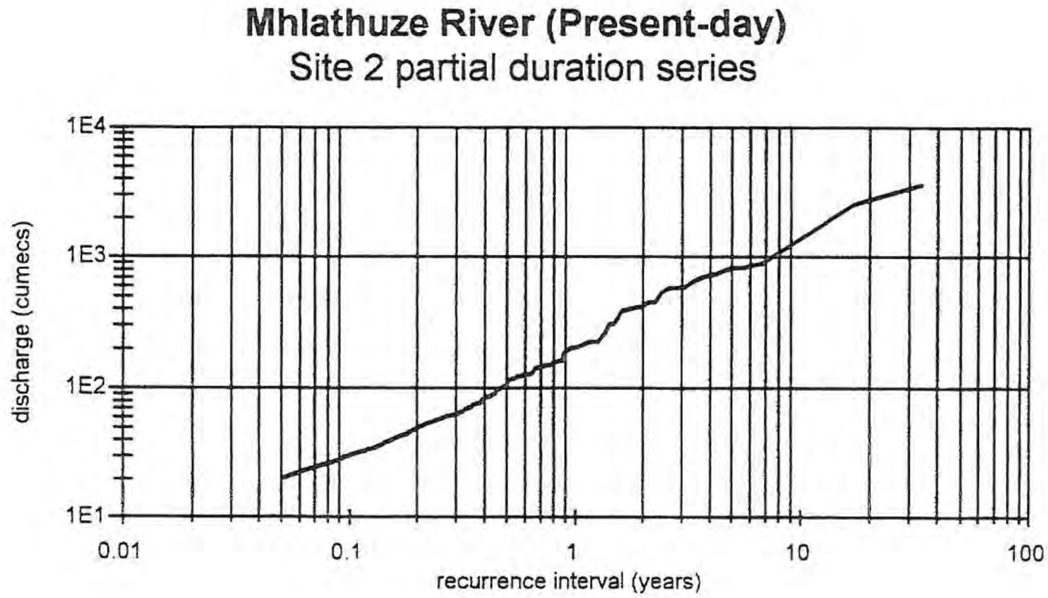
Mhlathuze River (Present-day)
Site 2 partial duration series
discharge (cumecs)
1E4
1E3
1E2
1E1
0.01
0.1
1
10
100
recurrence interval (years)

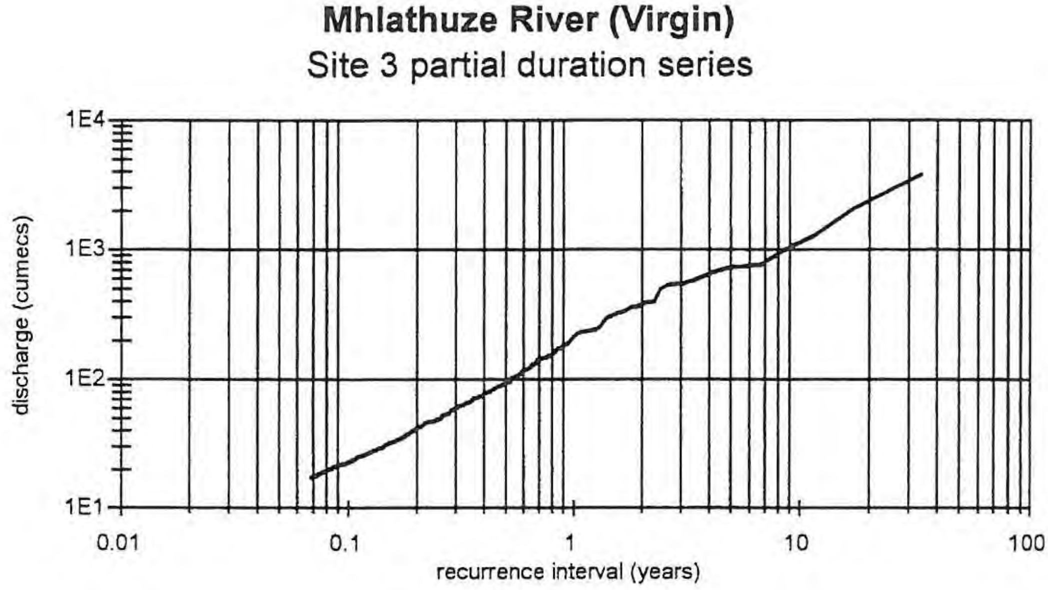
Mhlathuze River (Virgin)
Site 3 partial duration series
discharge (cumecs)
1E4
1E3
1E2
1E1
0.01
0.1
1
10
100
recurrence interval (years)

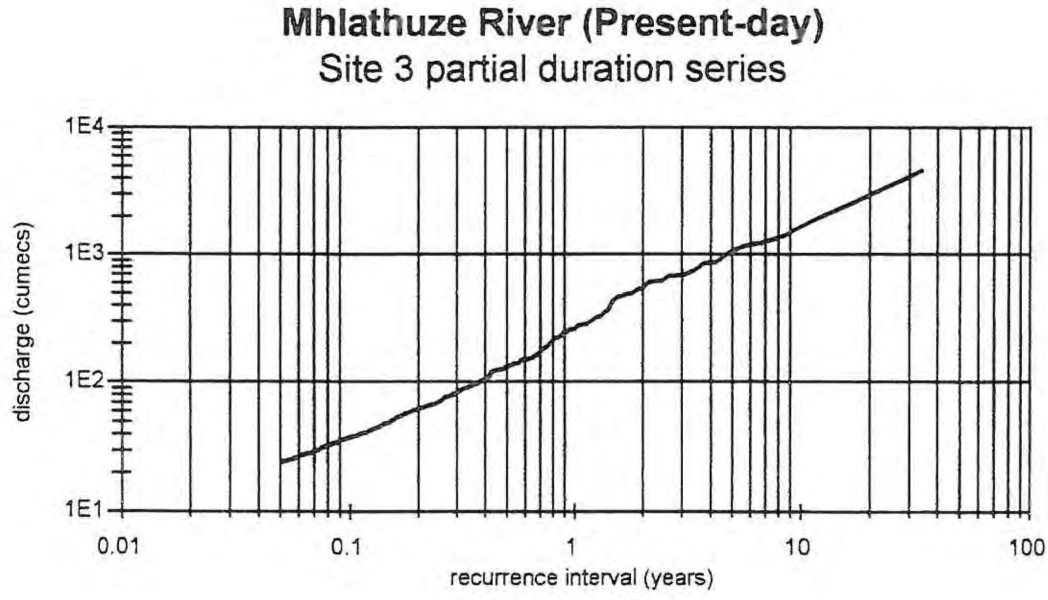
Mhlathuze River (Present-day)
Site 3 partial duration series
discharge (cumecs)
1E4
1E3
1E2
1E1
0.01
0.1
1
10
100
recurrence interval (years)

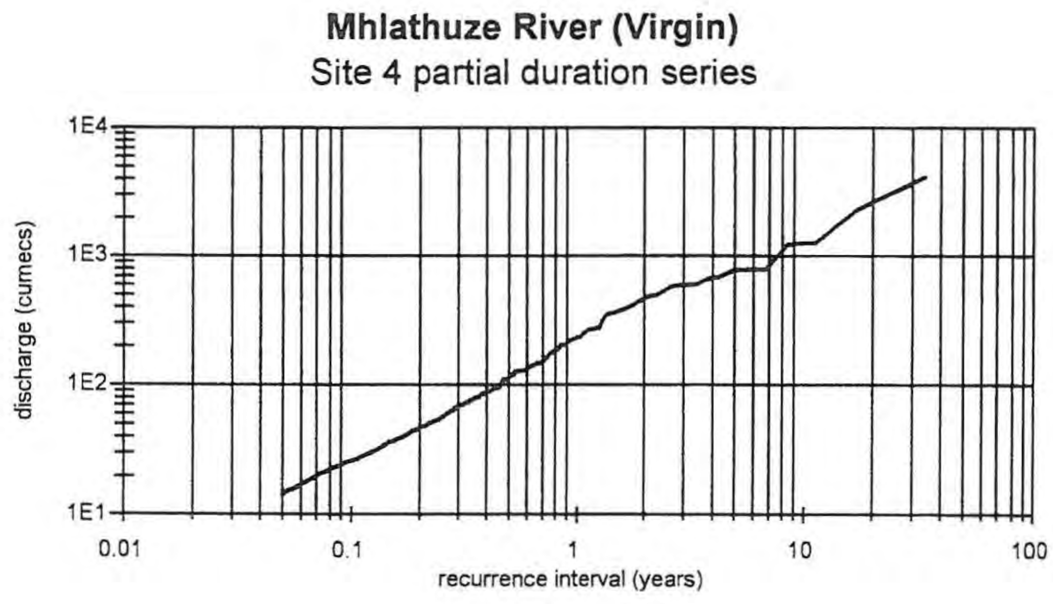
Mhlathuze River (Virgin)
Site 4 partial duration series
1E4
1E3
1E2
1E1
discharge (cumecs)
0.01
0.1
1
10
100
recurrence interval (years)

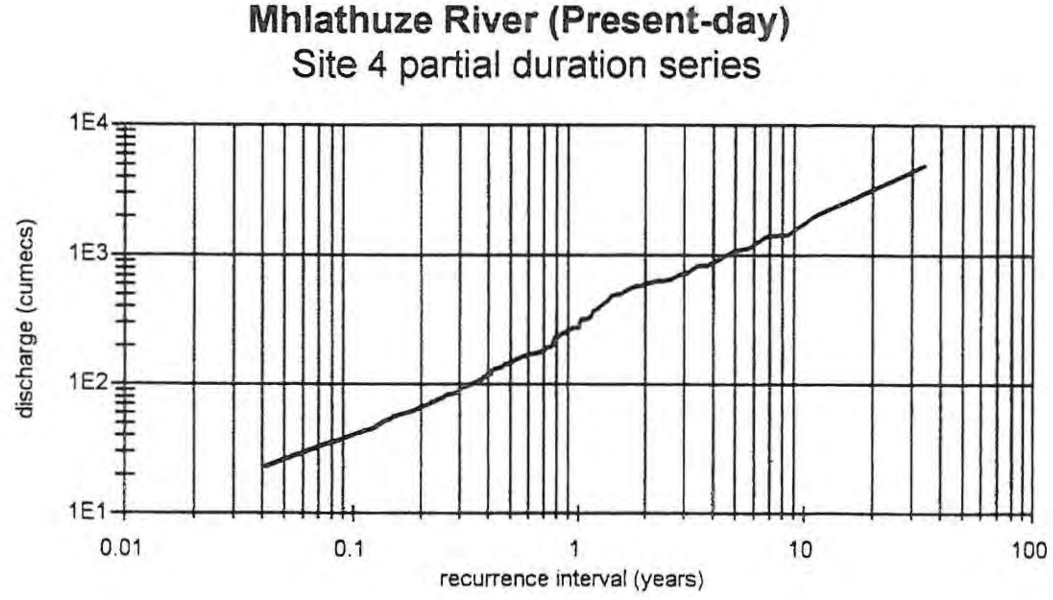
Mhlathuze River (Present-day)
Site 4 partial duration series
1E4
1E3
1E2
1E1
discharge (cumecs)
0.01
0.1
1
10
100
recurrence interval (years)

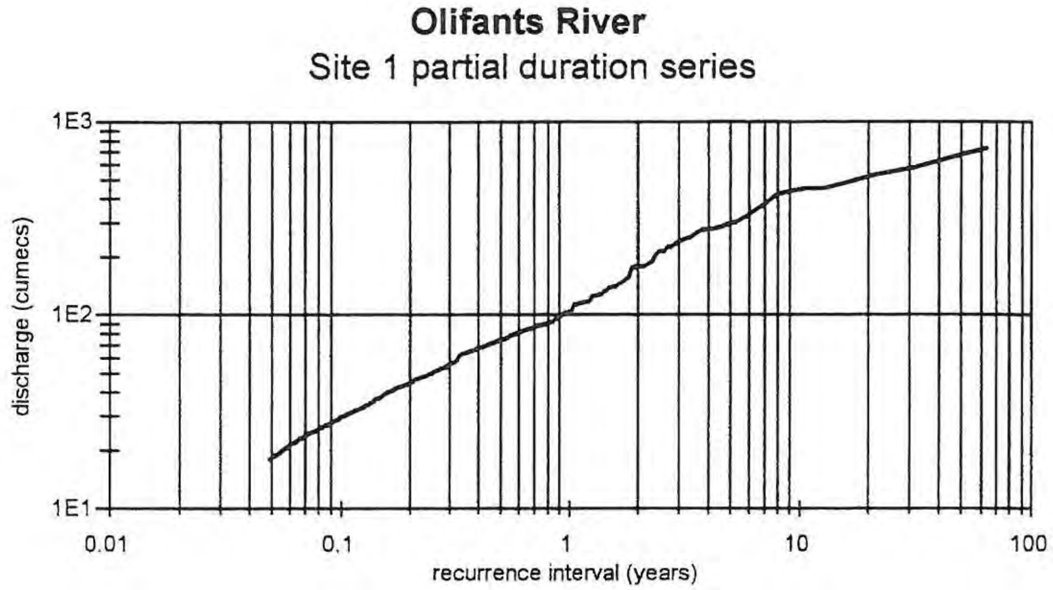
Olifants River
Site 1 partial duration series
1E3
1E2
1E1
discharge (cumecs)
0.01
0.1
1
10
100
recurrence interval (years)

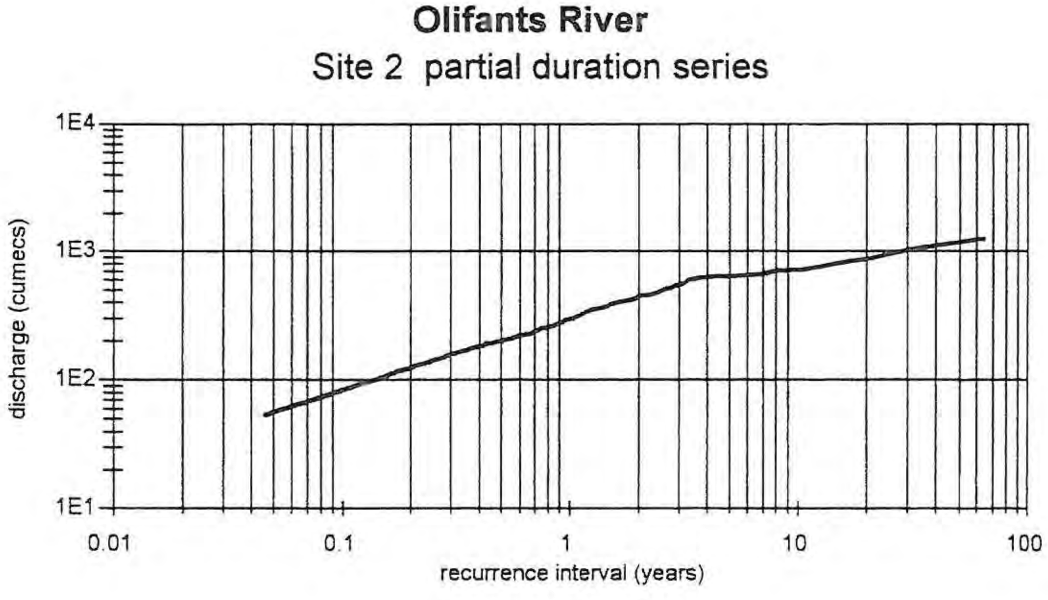
Olifants River
Site 2 partial duration series
1E4
1E3
1E2
1E1
discharge (cumecs)
0.01
0.1
1
10
100
recurrence interval (years)

Olifants River
Site 3 partial duration series`

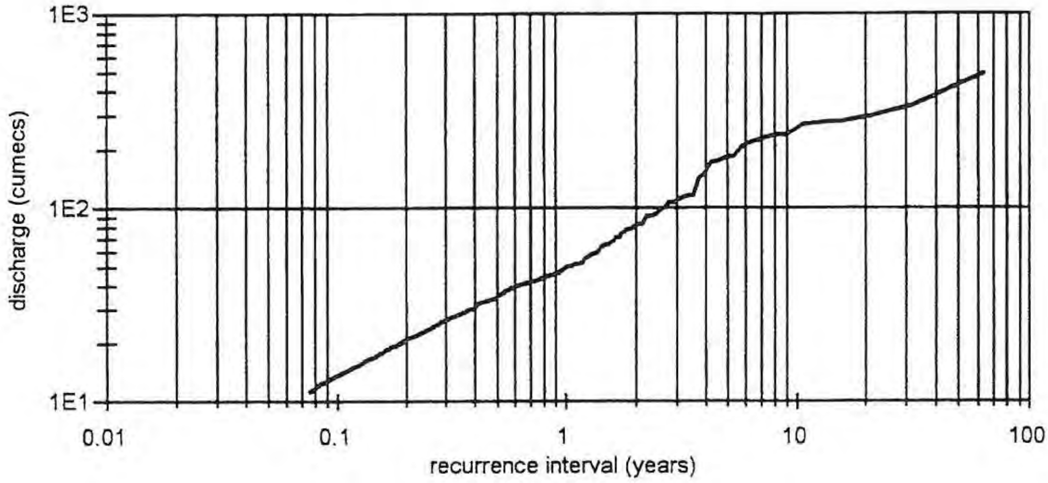

Olifants River
Site 4 partial duration series

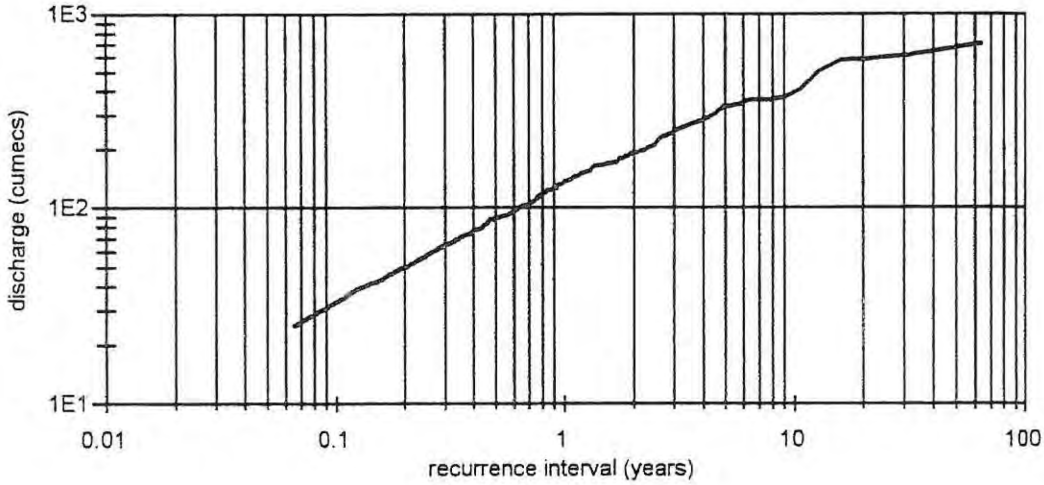

APPENDIX E

HYDRAULIC DATA FOR ALL RIVERS

Mkomazi Site 1a
Rating curve

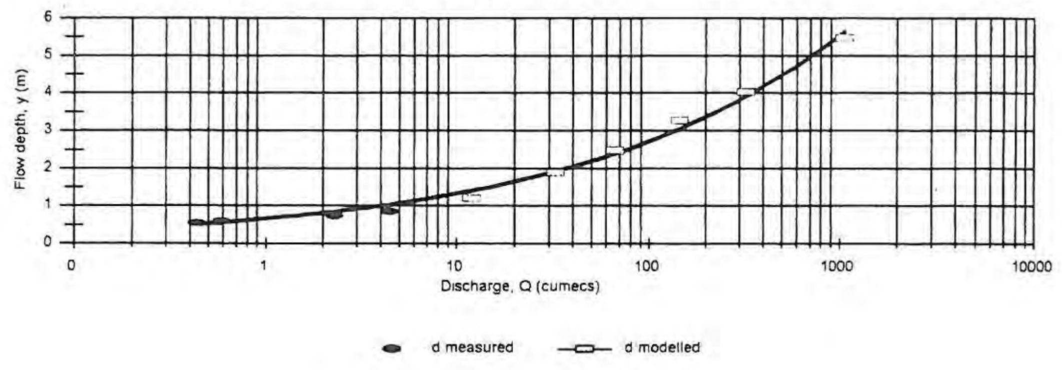

Mkomazi Site 1b
Rating curve

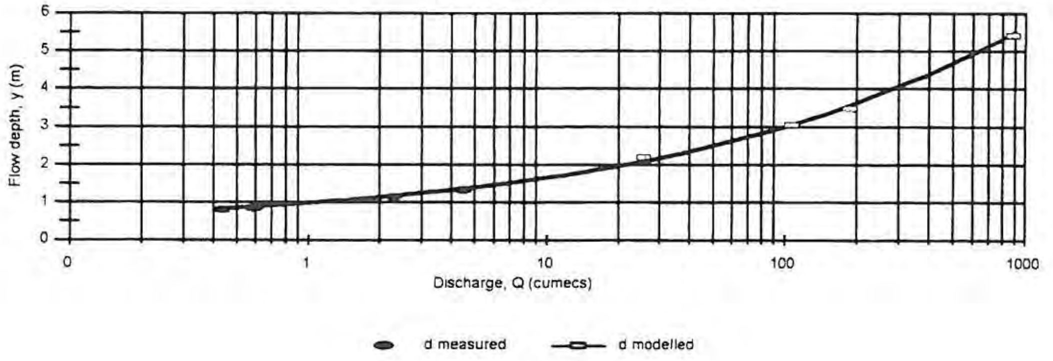

Mkomazi Site 1c
Rating curve

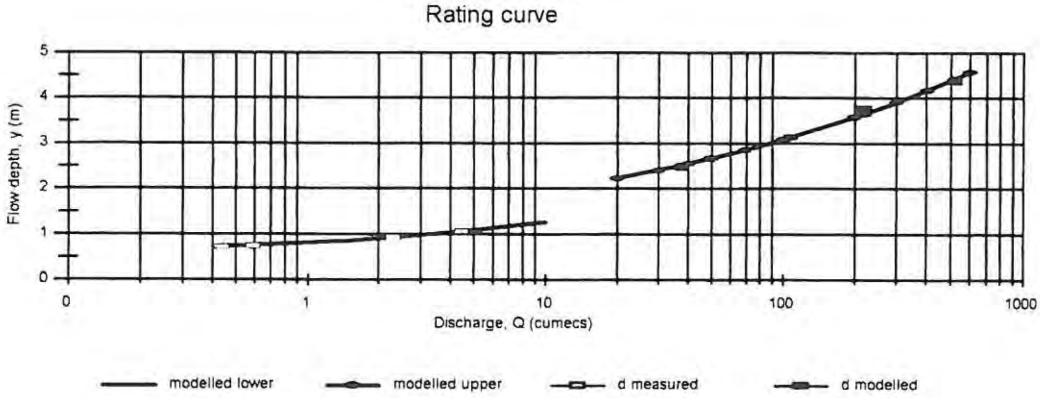

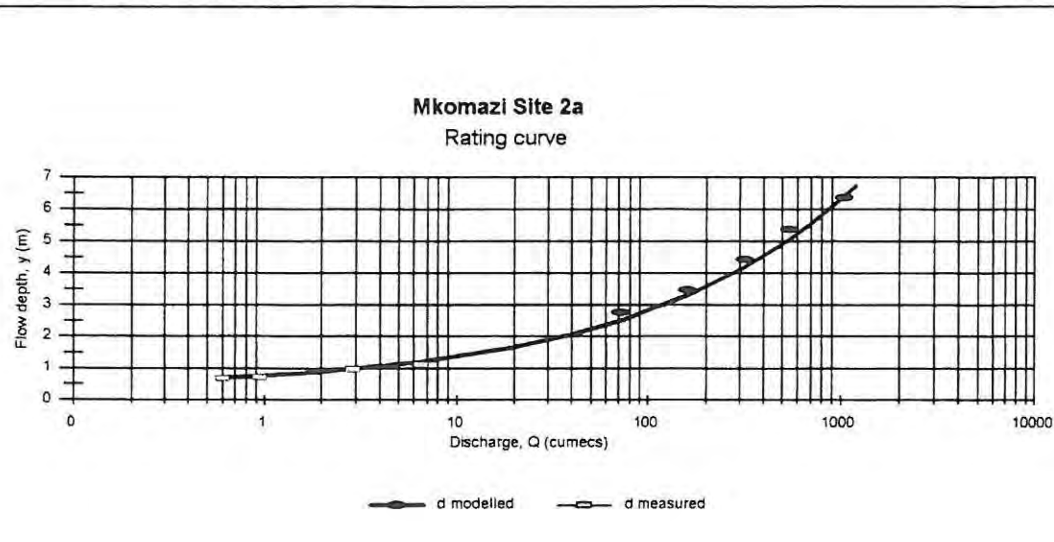
Mkomazi Site 2a
Rating curve
Flow depth, y (m)
7
6
5
4
3
2
1
0
0
1
10
100
1000
10000
Discharge, Q (cumecs)
d modelled
d measured

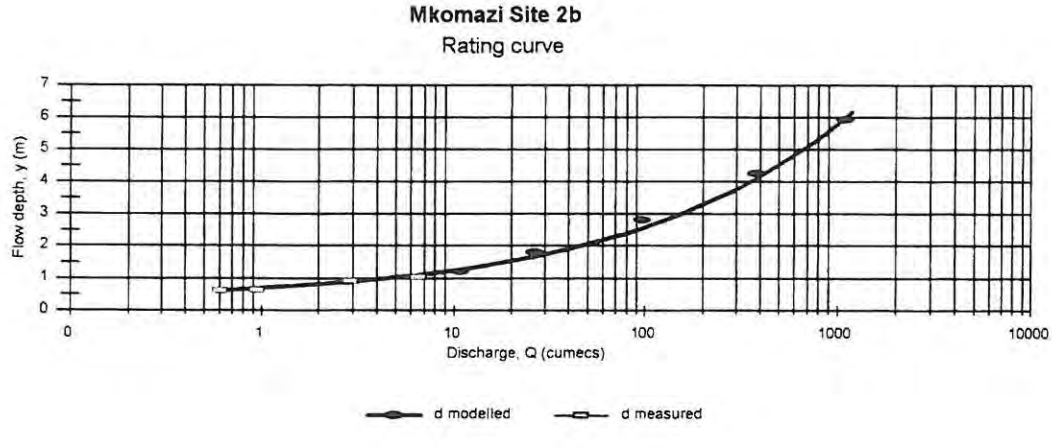
Mkomazi Site 2b
Rating curve
Flow depth, y (m)
7
6
5
4
3
2
1
0
0
1
10
100
1000
10000
Discharge, Q (cumecs)
d modelled
d measured

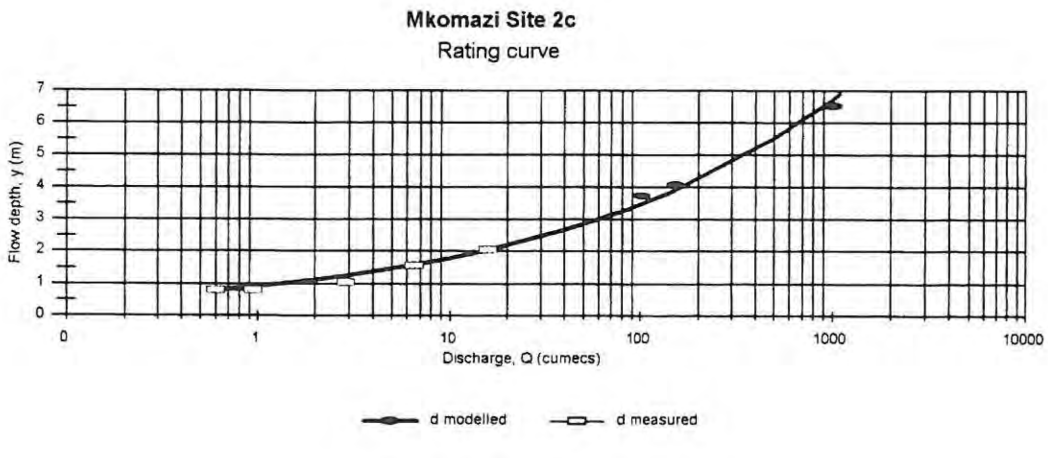
Mkomazi Site 2c
Rating curve
Flow depth, y (m)
7
6
5
4
3
2
1
0
0
1
10
100
1000
10000
Discharge, Q (cumecs)
d modelled
d measured

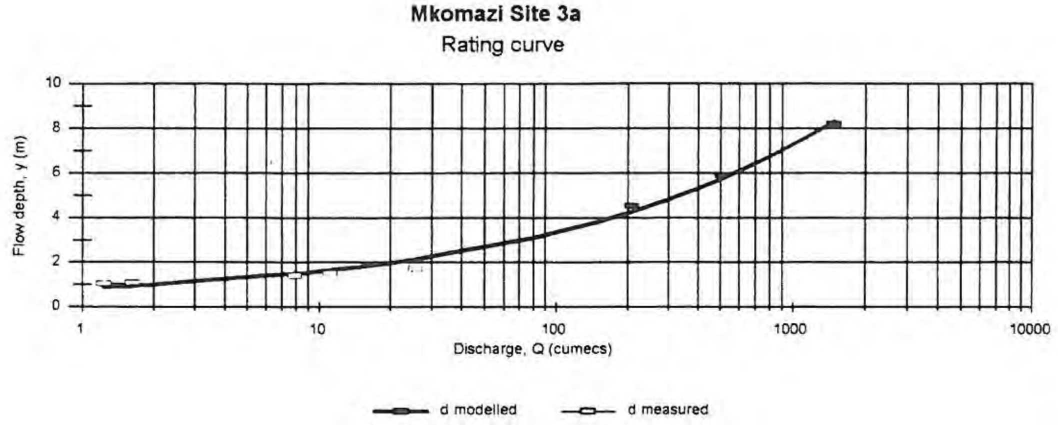
Mkomazi Site 3a
Rating curve
Flow depth, y (m)
0
2
4
6
8
10
1
10
100
1000
10000
Discharge, Q (cumecs)
d modelled
d measured

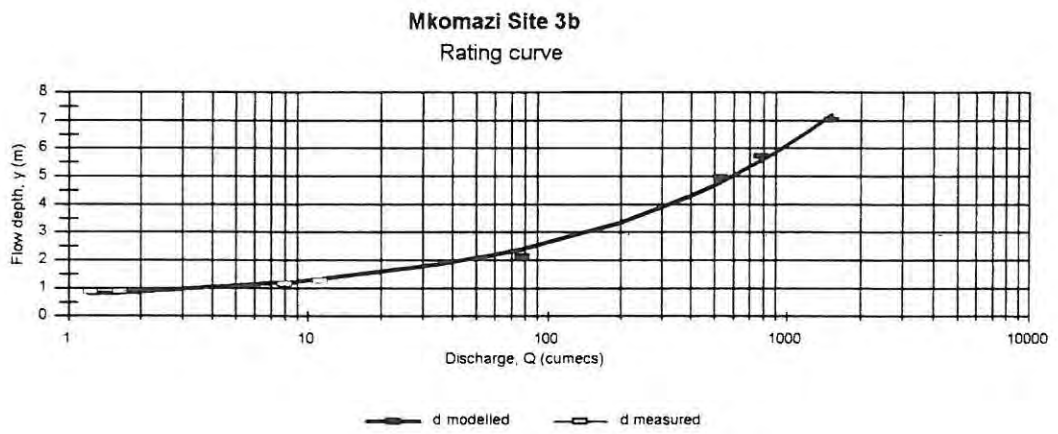
Mkomazi Site 3b
Rating curve
Flow depth, y (m)
0
1
2
3
4
5
6
7
8
1
10
100
1000
10000
Discharge, Q (cumecs)
d modelled
d measured

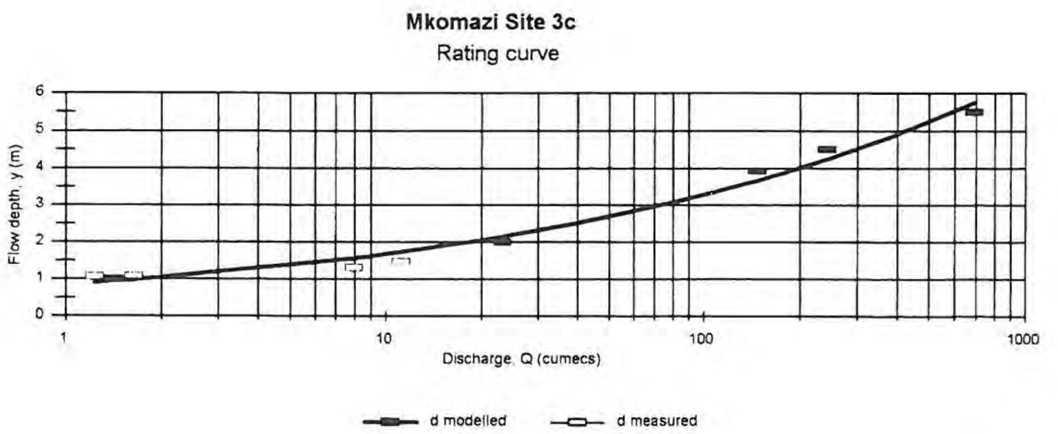
Mkomazi Site 3c
Rating curve
Flow depth, y (m)
0
1
2
3
4
5
6
1
10
100
1000
Discharge, Q (cumecs)
d modelled
d measured

Mkomazi Site 4a
Rating curve

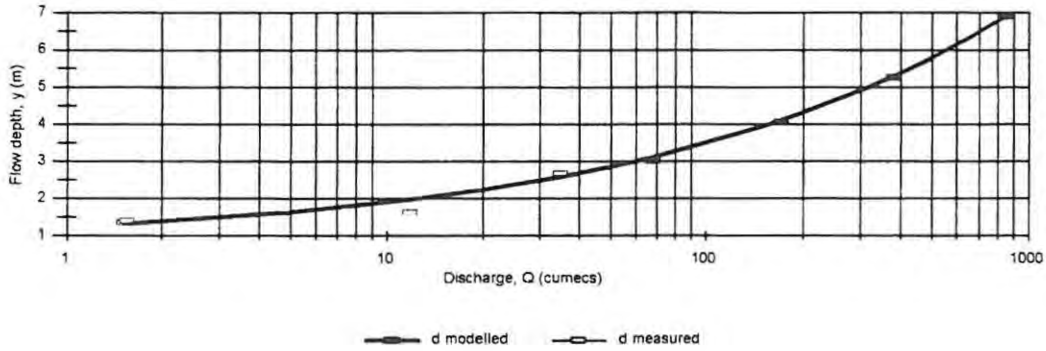

Mkomazi Site 4b
Rating curve

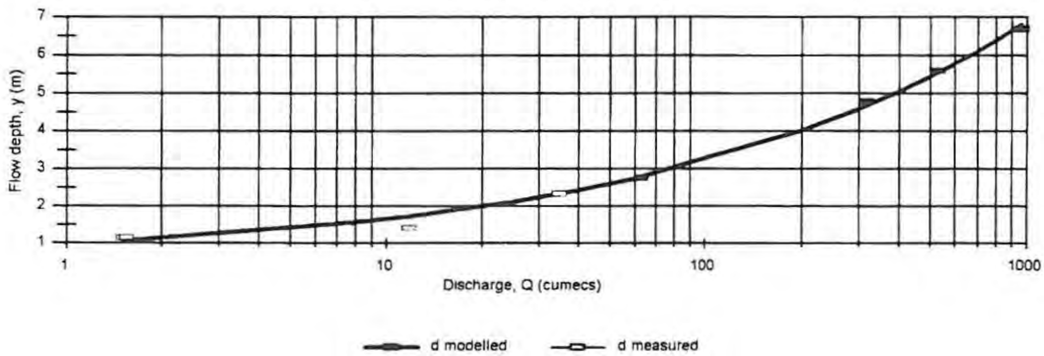

Mkomazi Site 5a
Rating curve

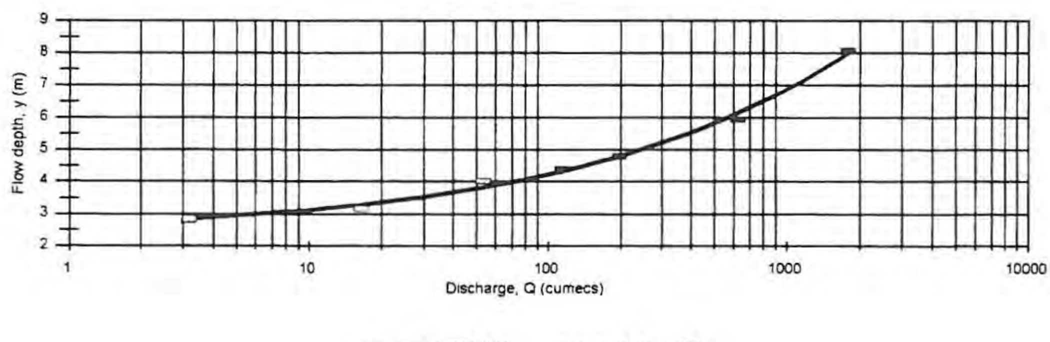

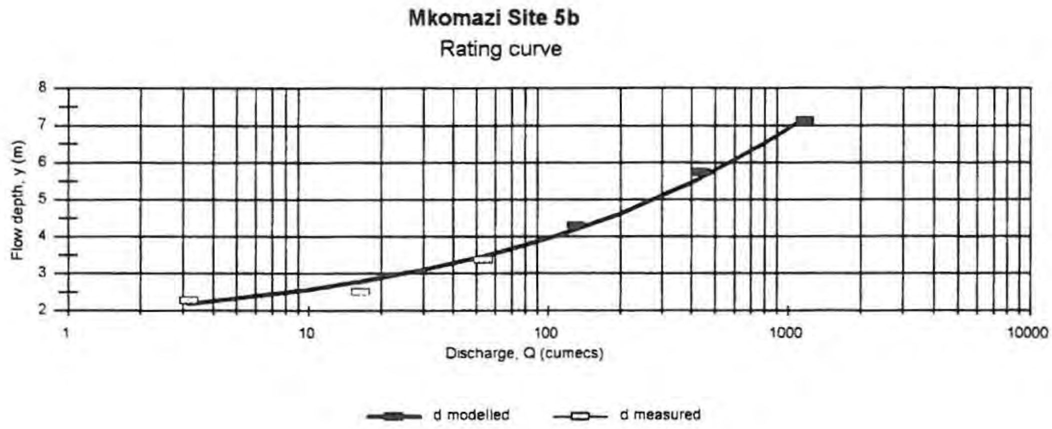
Mkomazi Site 5b
Rating curve
Flow depth, y (m)
8
7
6
5
4
3
2
1
10
100
1000
10000
Discharge, Q (cumecs)
d modelled
d measured

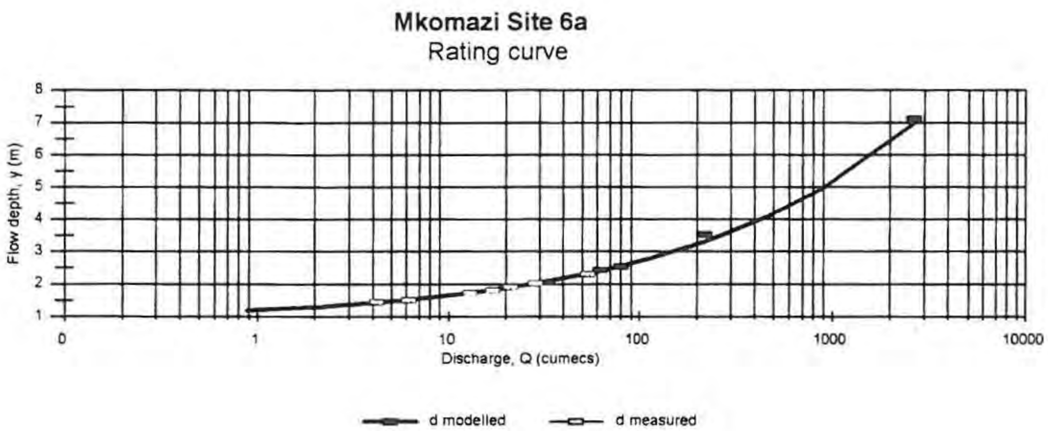
Mkomazi Site 6a
Rating curve
Flow depth, y (m)
8
7
6
5
4
3
2
1
0
1
10
100
1000
10000
Discharge, Q (cumecs)
d modelled
d measured

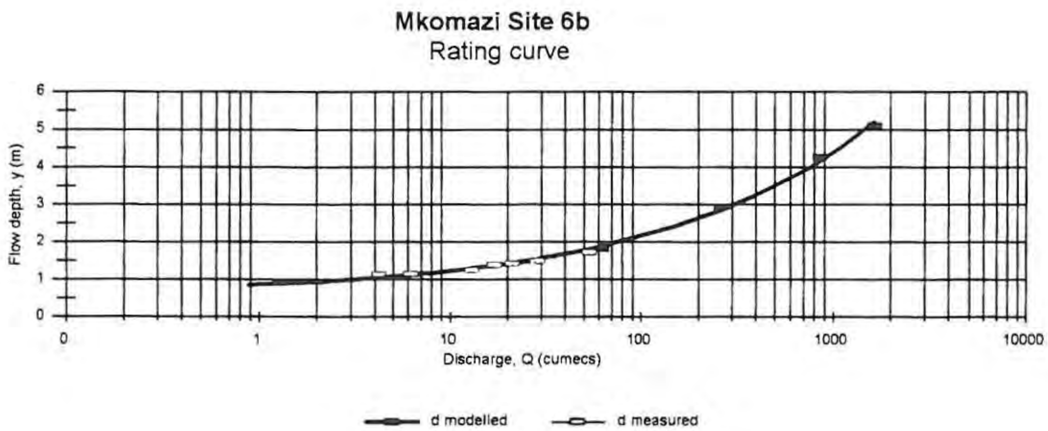
Mkomazi Site 6b
Rating curve
Flow depth, y (m)
6
5
4
3
2
1
0
0
1
10
100
1000
10000
Discharge, Q (cumecs)
d modelled
d measured

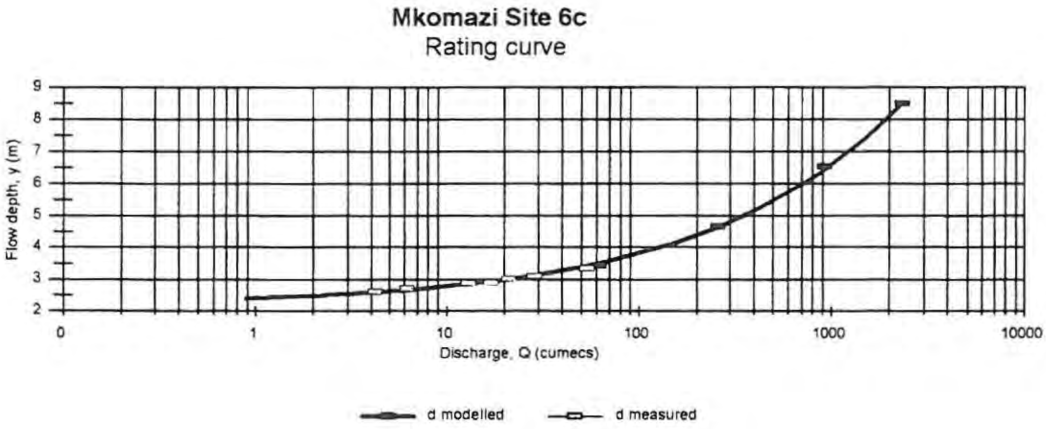
Mkomazi Site 6c
Rating curve
Flow depth, y (m)
9
8
7
6
5
4
3
2
0
1
10
100
1000
10000
Discharge, Q (cumecs)
d modelled
d measured

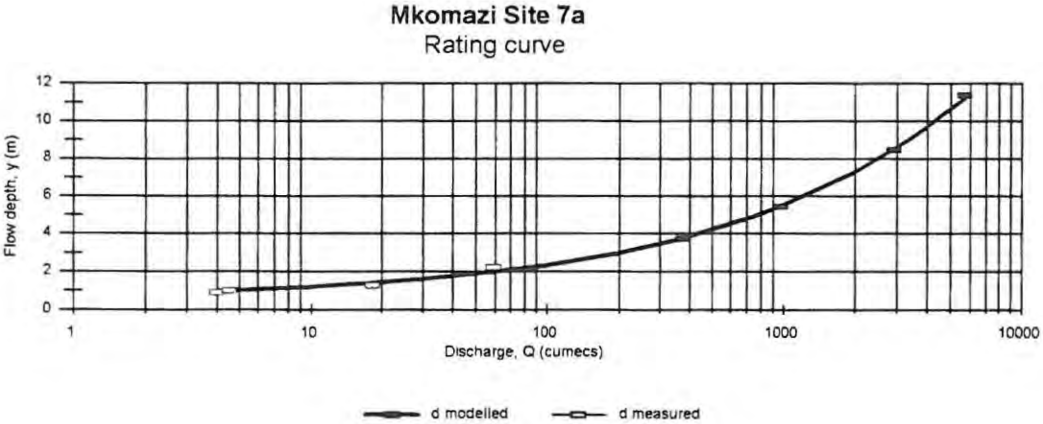
Mkomazi Site 7a
Rating curve
Flow depth, y (m)
12
10
8
6
4
2
0
1
10
100
1000
10000
Discharge, Q (cumecs)
d modelled
d measured

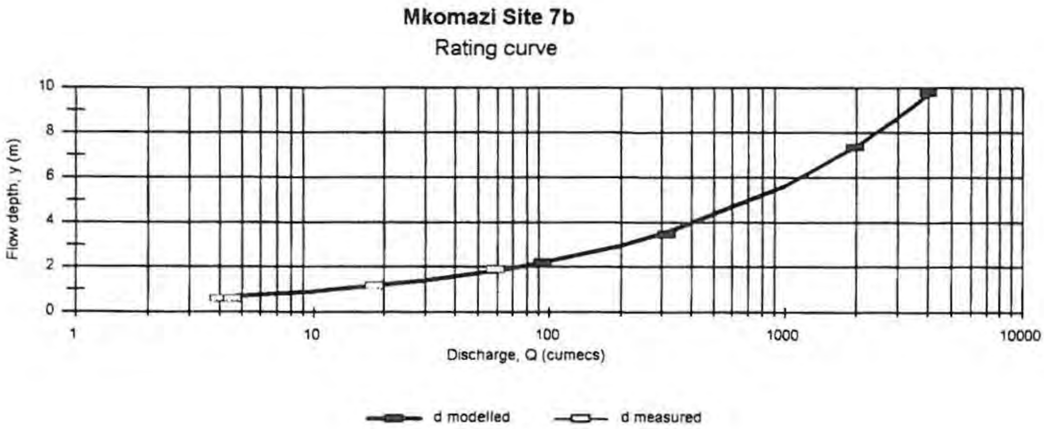
Mkomazi Site 7b
Rating curve
Flow depth, y (m)
10
8
6
4
2
0
1
10
100
1000
10000
Discharge, Q (cumecs)
d modelled
d measured

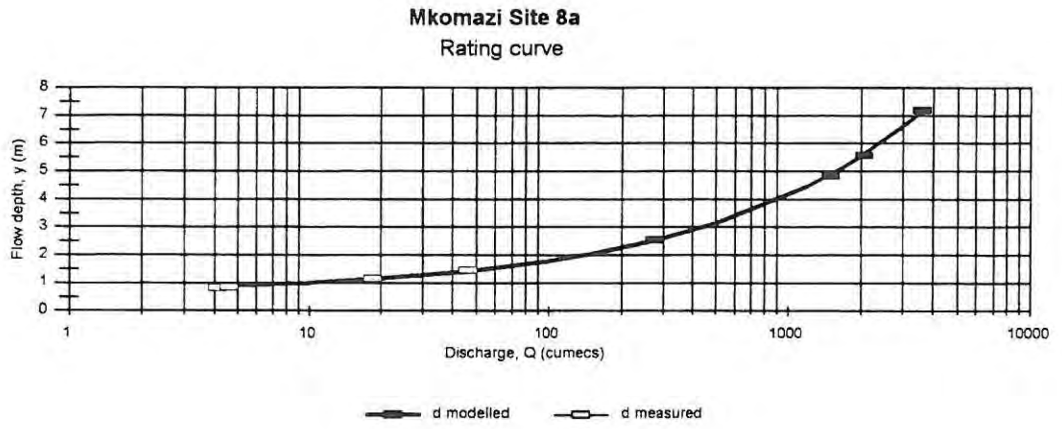
Mkomazi Site 8a
Rating curve
Flow depth, y (m)
0
1
2
3
4
5
6
7
8
1
10
100
1000
10000
Discharge, Q (cumecs)
d modelled
d measured

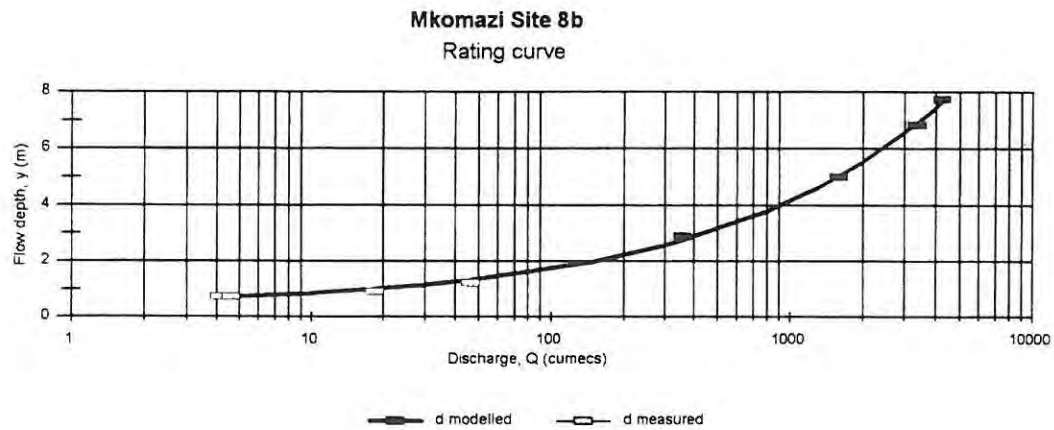
Mkomazi Site 8b
Rating curve
Flow depth, y (m)
0
2
4
6
8
1
10
100
1000
10000
Discharge, Q (cumecs)
d modelled
d measured

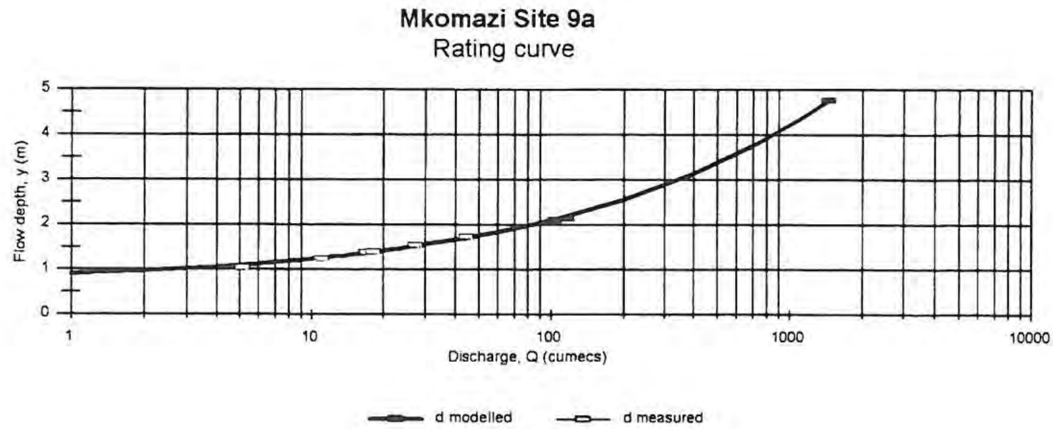
Mkomazi Site 9a
Rating curve
Flow depth, y (m)
0
1
2
3
4
5
1
10
100
1000
10000
Discharge, Q (cumecs)
d modelled
d measured

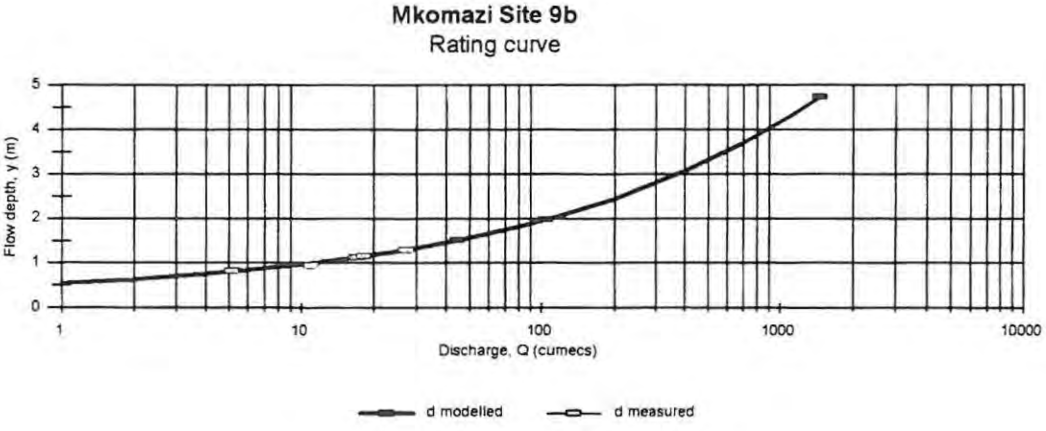
Mkomazi Site 9b
Rating curve
Flow depth, y (m)
Discharge, Q (cumecs)
d modelled
d measured

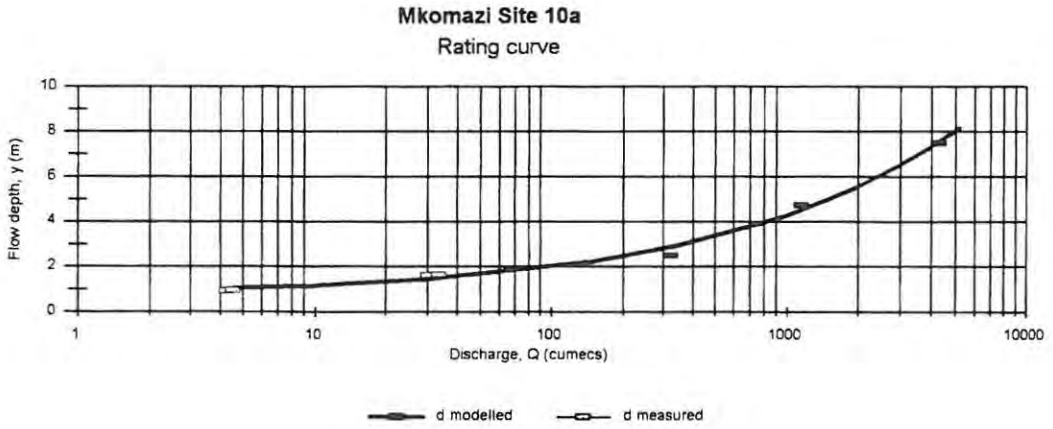
Mkomazi Site 10a
Rating curve
Flow depth, y (m)
Discharge, Q (cumecs)
d modelled
d measured

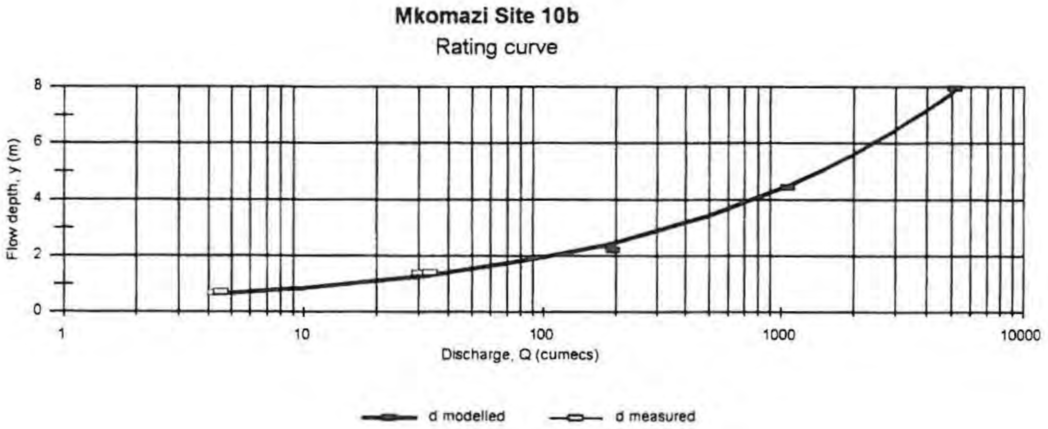
Mkomazi Site 10b
Rating curve
Flow depth, y (m)
Discharge, Q (cumecs)
d modelled
d measured

Mkomazi Site 11
Rating curve

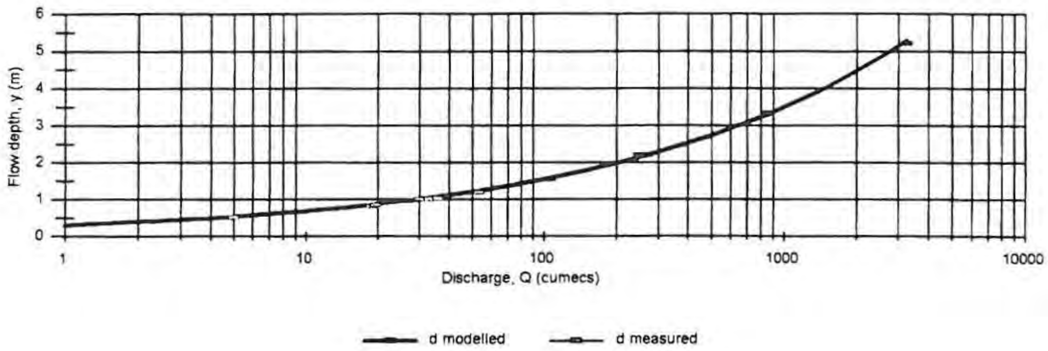

Mkomazi Site 12
Rating curve

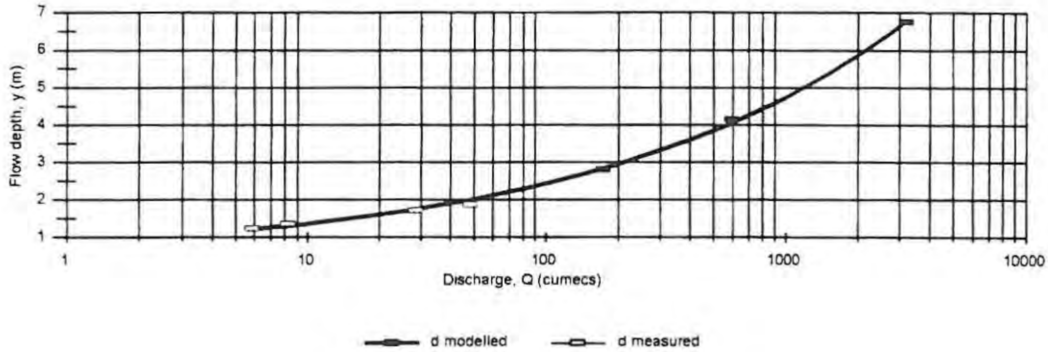

Mkomazi Site 13
Rating curve

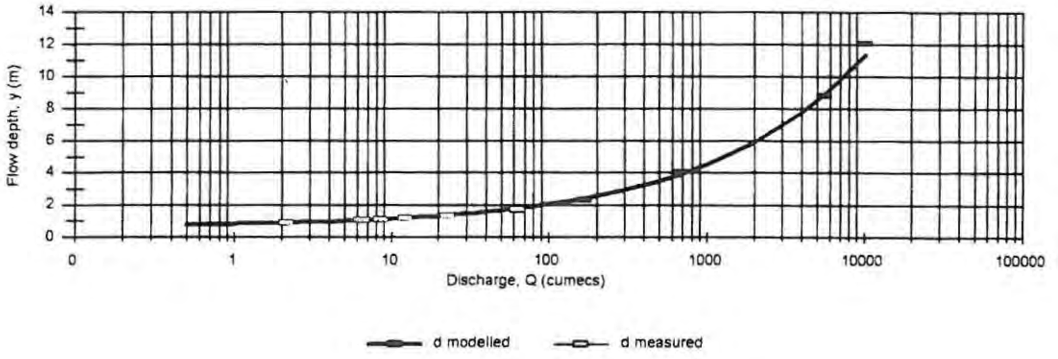

Mhlathuze Site 1 pool
Rating curve

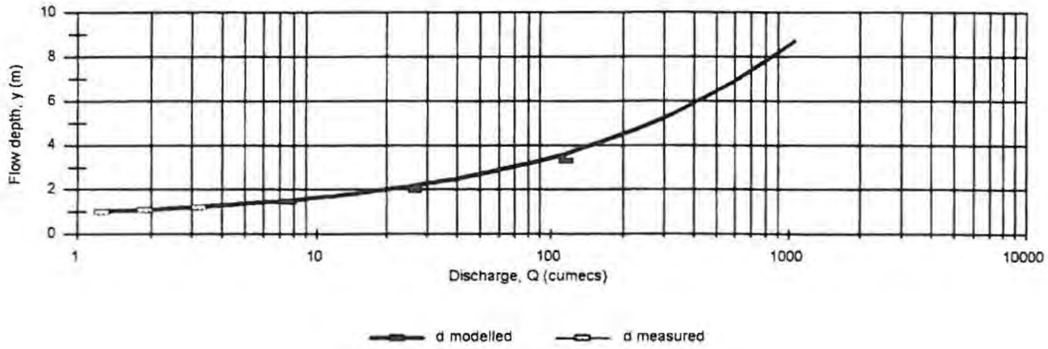

Mhlathuze Site 1 riffle
Rating curve

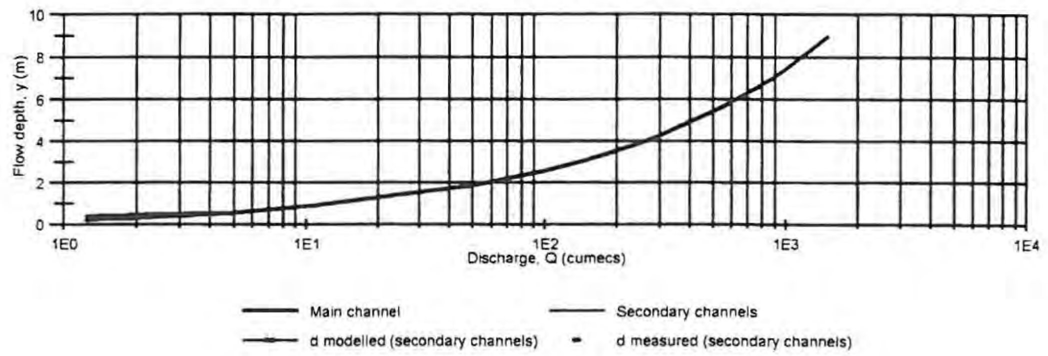

Mhlathuze Site 2
Rating curve

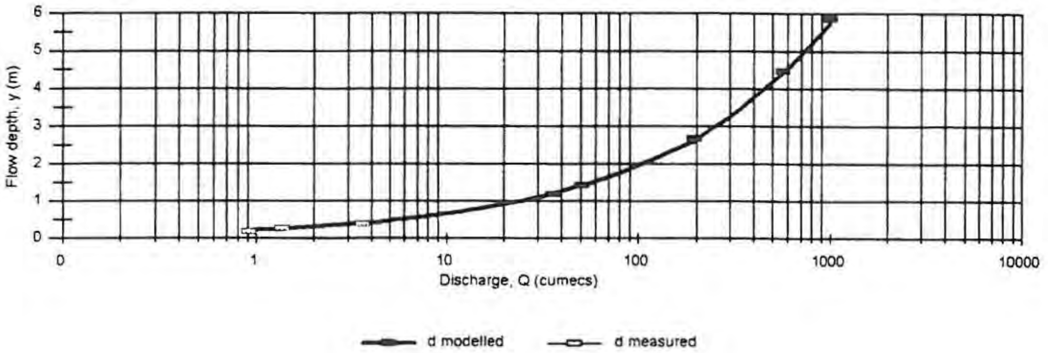

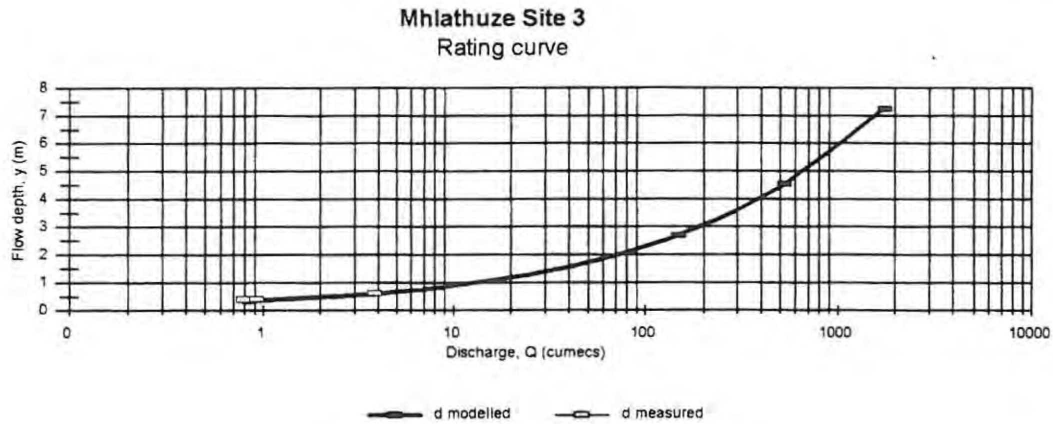
Mhlathuze Site 3
Rating curve
Flow depth, y (m)
0
1
2
3
4
5
6
7
8
0
1
10
100
1000
10000
Discharge, Q (cumecs)
d modelled
d measured

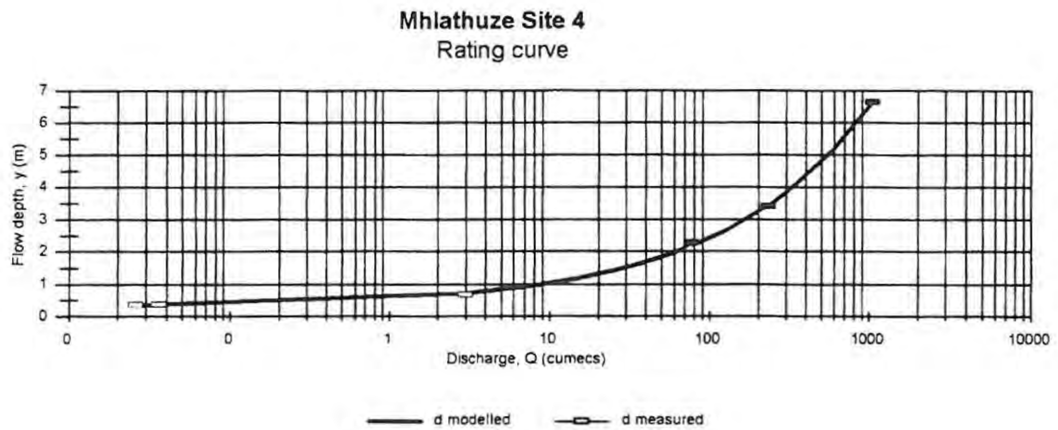
Mhlathuze Site 4
Rating curve
Flow depth, y (m)
0
1
2
3
4
5
6
7
0
0
1
10
100
1000
10000
Discharge, Q (cumecs)
d modelled
d measured

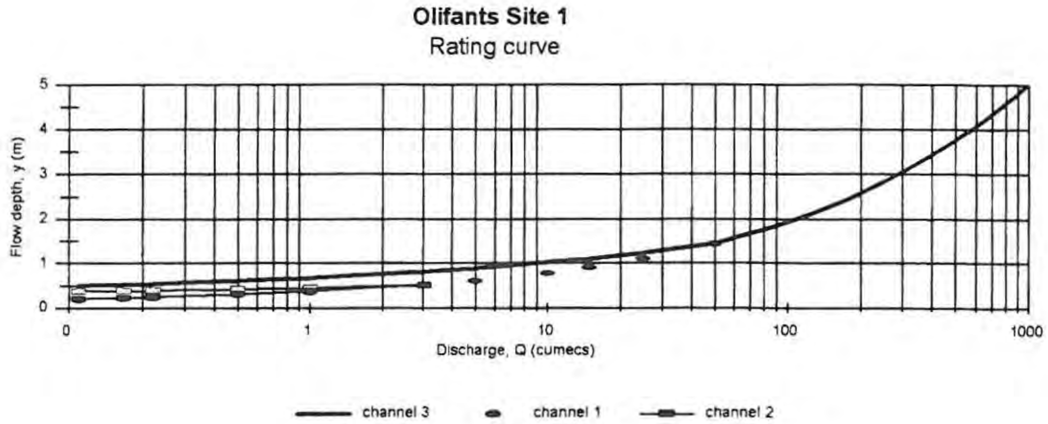
Olifants Site 1
Rating curve
Flow depth, y (m)
5
4
3
2
1
0
0
1
10
100
1000
Discharge, Q (cumecs)
channel 3
channel 1
channel 2

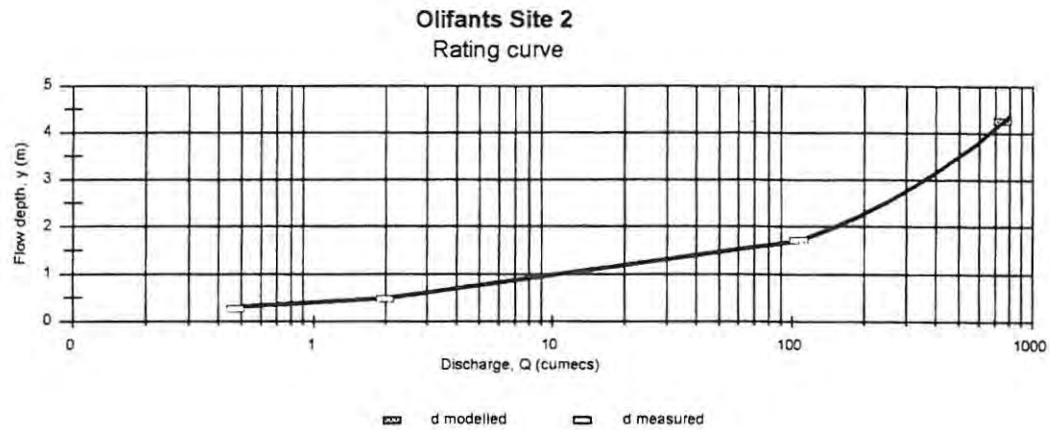
Olifants Site 2
Rating curve
Flow depth, y (m)
5
4
3
2
1
0
0
1
10
100
1000
Discharge, Q (cumecs)
d modelled
d measured

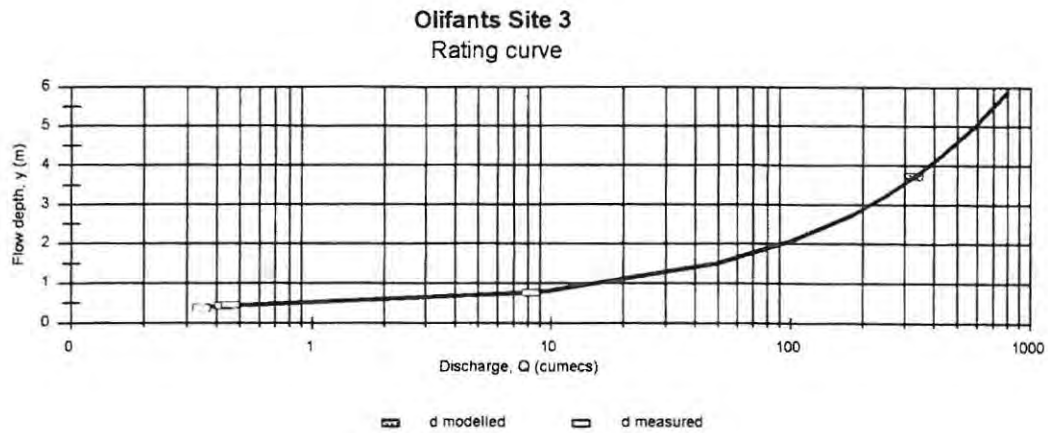
Olifants Site 3
Rating curve
Flow depth, y (m)
6
5
4
3
2
1
0
0
1
10
100
1000
Discharge, Q (cumecs)
d modelled
d measured

Olifants Site 4
Rating curve

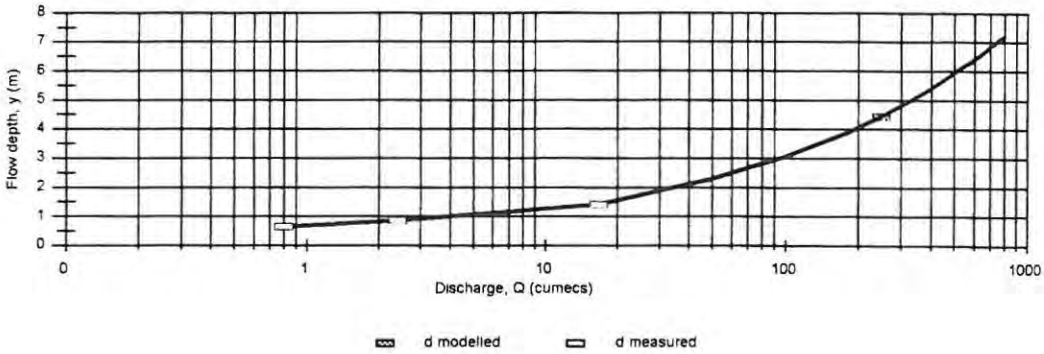

APPENDIX F

TRANSPORT VALUES FOR ALL RIVERS

Q	is discharge in m^3s^{-1}
Yang	is the load calculated in tonnes per annum for the Yang equation
% time	is the percentage of total load calculated by the flow discharge
cum %	is the cumulative percentage
AW	is the load calculated in tonnes per annum for the Ackers and White equation
EH	is the load calculated in tonnes per annum for the Engelund and Hansen equation

Table 1 Bed material load for Mkomazi Site 1a

Q	Yang	% time	cum %	AW	% time	cum %	EH	% time	cum %
0.015	0.00	0.00	0.00	0.00	0.00	0.00	0.00	0.00	0.00
0.246	0.00	0.00	0.00	0.00	0.00	0.00	0.00	0.00	0.00
0.355	0.00	0.00	0.00	0.00	0.00	0.00	3.09	0.01	0.01
0.480	0.00	0.00	0.00	0.00	0.00	0.00	6.05	0.02	0.02
0.655	0.00	0.00	0.00	0.00	0.00	0.00	15.90	0.04	0.06
0.926	0.00	0.00	0.00	0.00	0.00	0.00	41.49	0.10	0.17
1.391	0.00	0.00	0.00	0.00	0.00	0.00	111.93	0.28	0.45
2.230	0.00	0.00	0.00	0.00	0.00	0.00	308.78	0.77	1.22
3.991	70.86	1.08	1.08	0.00	0.00	0.00	1324.21	3.31	4.52
7.181	282.59	4.31	5.39	0.00	0.00	0.00	2694.39	6.73	11.25
13.467	1826.96	27.86	33.25	48.23	20.13	20.13	9989.27	24.94	36.19
30.367	3092.50	47.15	80.40	102.21	42.67	62.80	15972.51	39.88	76.07
69.606	1285.47	19.60	100.00	89.11	37.20	100.00	9584.86	23.93	100.00
Sum	6558.37	100.00		239.56	100.00		40052.49	100.00	

Table 2 Bed material load for Mkomazi Site 1b

Q	Yang	% time	cum %	AW	% time	cum %	EH	% time	cum %
0.01	0.00	0.00	0.00	0.00	0.00	0.00	0.00	0.00	0.00
0.25	0.00	0.00	0.00	0.00	0.00	0.00	0.00	0.00	0.00
0.35	0.00	0.00	0.00	0.00	0.00	0.00	3.34	0.01	0.01
0.48	0.00	0.00	0.00	0.00	0.00	0.00	6.52	0.02	0.02
0.66	0.00	0.00	0.00	0.00	0.00	0.00	15.81	0.04	0.06
0.93	0.00	0.00	0.00	0.00	0.00	0.00	41.43	0.10	0.16
1.39	0.00	0.00	0.00	0.00	0.00	0.00	115.41	0.27	0.43
2.23	0.00	0.00	0.00	0.00	0.00	0.00	334.76	0.78	1.21
3.99	0.00	0.00	0.00	0.00	0.00	0.00	1427.62	3.33	4.54
7.18	128.41	2.44	2.44	0.00	0.00	0.00	2916.78	6.81	11.35
13.47	1074.91	20.44	22.88	27.87	16.54	16.54	10782.44	25.18	36.53
30.37	2818.71	53.59	76.46	74.55	44.24	60.78	16774.01	39.16	75.69
69.61	1237.93	23.54	100.00	66.09	39.22	100.00	10411.84	24.31	100.00
Sum	5259.96	100.00		168.51	100.00		42829.95	100.00	

Table 3 Bed material load for Mkomazi Site 1c

Q	Yang	% time	cum %	AW	% time	cum %	EH	% time	cum %
0.015	0.00	0.00	0.00	0.00	0.00	0.00	0.00	0.00	0.00
0.246	0.00	0.00	0.00	0.00	0.00	0.00	0.00	0.00	0.00
0.355	0.00	0.00	0.00	0.00	0.00	0.00	1.87	0.01	0.01
0.480	0.00	0.00	0.00	0.00	0.00	0.00	5.85	0.02	0.03
0.655	0.00	0.00	0.00	0.00	0.00	0.00	14.22	0.05	0.08
0.926	0.00	0.00	0.00	0.00	0.00	0.00	36.81	0.14	0.22
1.391	0.00	0.00	0.00	0.00	0.00	0.00	102.57	0.39	0.62
2.230	0.00	0.00	0.00	0.00	0.00	0.00	295.01	1.13	1.74
3.991	28.91	1.31	1.31	0.00	0.00	0.00	1261.87	4.82	6.56
7.181	154.12	7.01	8.32	0.00	0.00	0.00	2557.65	9.77	16.33
13.467	220.28	10.02	18.34	0.00	0.00	0.00	7617.27	29.09	45.42
30.367	1053.91	47.93	66.28	18.91	43.99	43.99	10019.06	38.26	83.68
69.606	741.49	33.72	100.00	24.08	56.01	100.00	4273.93	16.32	100.00
sum	2198.70	100.00		42.99	100.00		26186.11	100.00	

Table 4 Bed material load for Mkomazi Site 2a

Q	Yang	% time	cum %	AW	% time	cum %	EH	% time	cum %
0.025	0.00	0.00	0.00	0.00	0.00	0.00	0.00	0.00	0.00
0.424	0.00	0.00	0.00	0.00	0.00	0.00	2.31	0.01	0.01
0.613	0.00	0.00	0.00	0.00	0.00	0.00	10.79	0.06	0.07
0.830	0.00	0.00	0.00	0.00	0.00	0.00	19.27	0.10	0.17
1.132	0.00	0.00	0.00	0.00	0.00	0.00	34.61	0.18	0.36
1.599	0.00	0.00	0.00	0.00	0.00	0.00	72.07	0.38	0.74
2.402	0.00	0.00	0.00	0.00	0.00	0.00	164.82	0.88	1.62
3.852	0.00	0.00	0.00	0.00	0.00	0.00	425.16	2.27	3.89
6.893	165.34	2.46	2.46	0.00	0.00	0.00	1261.27	6.74	10.63
12.404	672.39	10.01	12.47	0.00	0.00	0.00	1879.27	10.04	20.67
23.643	2473.03	36.82	49.29	61.54	11.56	11.56	5558.05	29.68	50.35
54.193	2475.66	36.86	86.15	225.69	42.41	53.98	6446.16	34.43	84.78
124.217	930.02	13.85	100.00	244.92	46.02	100.00	2850.43	15.22	100.00
sum	6716.44	100.00		532.16	100.00		18724.22	100.00	

Table 5 Bed material load for Mkomazi Site 2b

Q	Yang	% time	cum %	AW	% time	cum %	EH	% time	cum %
0.025	0.00	0.00	0.00	0.00	0.00	0.00	0.00	0.00	0.00
0.424	0.00	0.00	0.00	0.00	0.00	0.00	2.28	0.01	0.01
0.613	0.00	0.00	0.00	0.00	0.00	0.00	10.75	0.06	0.07
0.830	0.00	0.00	0.00	0.00	0.00	0.00	19.34	0.10	0.17
1.132	0.00	0.00	0.00	0.00	0.00	0.00	35.24	0.19	0.36
1.599	0.00	0.00	0.00	0.00	0.00	0.00	74.15	0.40	0.76
2.402	0.00	0.00	0.00	0.00	0.00	0.00	171.81	0.92	1.68
3.852	0.00	0.00	0.00	0.00	0.00	0.00	447.80	2.40	4.09
6.893	170.75	2.34	2.34	0.00	0.00	0.00	1337.59	7.18	11.27
12.404	764.53	10.46	12.80	0.00	0.00	0.00	1976.28	10.61	21.88
23.643	2675.76	36.62	49.42	80.15	10.65	10.65	5510.68	29.59	51.48
54.193	2653.75	36.32	85.74	329.76	43.80	54.45	6159.52	33.08	84.55
124.217	1042.11	14.26	100.00	342.94	45.55	100.00	2876.88	15.45	100.00
sum	7306.91	100.00		752.85	100.00		18622.32	100.00	

Table 6 Bed material load for Mkomazi Site 2c

Q	Yang	% time	cum %	AW	% time	cum %	EH	% time	cum %
0.025	0.00	0.00	0.00	0.00	0.00	0.00	0.00	0.00	0.00
0.424	0.00	0.00	0.00	0.00	0.00	0.00	1.97	0.01	0.01
0.613	0.00	0.00	0.00	0.00	0.00	0.00	4.09	0.02	0.04
0.830	0.00	0.00	0.00	0.00	0.00	0.00	17.51	0.10	0.14
1.132	0.00	0.00	0.00	0.00	0.00	0.00	31.14	0.18	0.32
1.599	0.00	0.00	0.00	0.00	0.00	0.00	66.19	0.39	0.71
2.402	0.00	0.00	0.00	0.00	0.00	0.00	155.62	0.91	1.62
3.852	0.00	0.00	0.00	0.00	0.00	0.00	470.19	2.76	4.39
6.893	0.00	0.00	0.00	0.00	0.00	0.00	1258.23	7.39	11.78
12.404	0.00	0.00	0.00	0.00	0.00	0.00	1866.17	10.97	22.75
23.643	1355.44	36.19	36.19	0.00	0.00	0.00	5398.83	31.73	54.47
54.193	1754.01	46.83	83.02	34.42	32.52	32.52	5596.43	32.89	87.36
124.217	636.11	16.98	100.00	71.41	67.48	100.00	2150.76	12.64	100.00
sum	3745.57	100.00		105.83	100.00		17017.13	100.00	

Table 7 Bed material load for Mkomazi Site 3a

Q	Yang	% time	cum %	AW	% time	cum %	EH	% time	cum %
0.044	0.00	0.00	0.00	0.00	0.00	0.00	0.00	0.00	0.00
1.250	0.00	0.00	0.00	0.00	0.00	0.00	0.00	0.00	0.00
1.807	0.00	0.00	0.00	0.00	0.00	0.00	0.00	0.00	0.00
2.445	0.00	0.00	0.00	0.00	0.00	0.00	13.42	0.01	0.01
3.336	0.00	0.00	0.00	0.00	0.00	0.00	24.75	0.03	0.04
4.713	0.00	0.00	0.00	0.00	0.00	0.00	66.61	0.07	0.11
7.079	0.00	0.00	0.00	0.00	0.00	0.00	232.91	0.25	0.36
11.353	127.70	0.49	0.49	0.00	0.00	0.00	738.14	0.80	1.16
20.318	882.99	3.42	3.92	0.00	0.00	0.00	3256.53	3.52	4.68
36.559	2543.88	9.86	13.77	167.37	6.97	6.97	7357.93	7.95	12.63
68.557	8277.66	32.08	45.85	763.95	31.81	38.77	26978.21	29.15	41.79
146.698	10465.64	40.56	86.41	902.49	37.57	76.35	37595.00	40.63	82.41
307.136	3506.68	13.59	100.00	568.12	23.65	100.00	16277.06	17.59	100.00
sum	25804.54	100.00		2401.94	100.00		92540.58	100.00	

Table 8 Bed material load for Mkomazi Site 3b

Q	Yang	% time	cum %	AW	% time	cum %	EH	% time	cum %
0.044	0.00	0.00	0.00	0.00	0.00	0.00	0.00	0.00	0.00
1.250	0.00	0.00	0.00	0.00	0.00	0.00	0.00	0.00	0.00
1.807	0.00	0.00	0.00	0.00	0.00	0.00	6.84	0.01	0.01
2.445	0.00	0.00	0.00	0.00	0.00	0.00	16.88	0.02	0.03
3.336	0.00	0.00	0.00	0.00	0.00	0.00	29.25	0.04	0.06
4.713	26.57	0.06	0.06	0.00	0.00	0.00	88.01	0.11	0.17
7.079	115.14	0.28	0.34	0.00	0.00	0.00	217.66	0.27	0.44
11.353	545.12	1.32	1.66	76.36	0.86	0.86	666.19	0.82	1.26
20.318	2486.56	6.02	7.68	406.77	4.58	5.44	2929.91	3.59	4.84
36.559	5076.52	12.29	19.97	934.37	10.53	15.97	6447.59	7.90	12.74
68.557	14632.31	35.41	55.38	2817.44	31.74	47.71	22997.90	28.17	40.92
146.698	13949.56	33.76	89.14	3289.50	37.06	84.76	32858.62	40.25	81.17
307.136	4487.15	10.86	100.00	1352.53	15.24	100.00	15371.79	18.83	100.00
sum	41318.92	100.00		8876.97	100.00		81630.65	100.00	

Table 9 Bed material load for Mkomazi Site 3c

Q	Yang	% time	cum %	AW	% time	cum %	EH	% time	cum %
0.044	0.00	0.00	0.00	0.00	0.00	0.00	0.00	0.00	0.00
1.250	0.00	0.00	0.00	0.00	0.00	0.00	0.00	0.00	0.00
1.807	0.00	0.00	0.00	0.00	0.00	0.00	0.00	0.00	0.00
2.445	0.00	0.00	0.00	0.00	0.00	0.00	11.65	0.01	0.01
3.336	0.00	0.00	0.00	0.00	0.00	0.00	21.51	0.02	0.04
4.713	0.00	0.00	0.00	0.00	0.00	0.00	57.83	0.06	0.10
7.079	0.00	0.00	0.00	0.00	0.00	0.00	204.07	0.23	0.33
11.353	48.26	0.20	0.20	0.00	0.00	0.00	793.99	0.89	1.21
20.318	530.87	2.16	2.35	0.00	0.00	0.00	2983.92	3.33	4.54
36.559	1902.18	7.73	10.08	102.99	5.02	5.02	6793.92	7.58	12.12
68.557	8578.97	34.86	44.94	505.53	24.63	29.64	25404.66	28.33	40.45
146.698	9965.87	40.49	85.44	848.18	41.32	70.97	36630.51	40.85	81.29
307.136	3584.04	14.56	100.00	595.99	29.03	100.00	16778.42	18.71	100.00
sum	24610.19	100.00		2052.69	100.00		89680.47	100.00	

Table 10 Bed material load for Mkomazi Site 4a

Q	Yang	% time	cum %	AW	% time	cum %	EH	% time	cum %
0.079	0.00	0.00	0.00	0.00	0.00	0.00	0.93	0.00	0.00
1.317	0.00	0.00	0.00	0.00	0.00	0.00	201.62	0.03	0.03
1.904	0.00	0.00	0.00	0.00	0.00	0.00	402.18	0.07	0.10
2.576	11.48	0.01	0.01	0.00	0.00	0.00	703.38	0.12	0.22
3.515	48.23	0.05	0.07	0.00	0.00	0.00	1252.40	0.21	0.43
4.966	137.85	0.15	0.22	0.00	0.00	0.00	2503.92	0.42	0.86
7.458	552.87	0.61	0.83	39.93	0.35	0.35	6094.55	1.03	1.89
11.961	2027.79	2.25	3.09	138.65	1.23	1.58	15514.96	2.63	4.52
21.406	7961.87	8.84	11.93	763.35	6.75	8.33	49012.93	8.30	12.82
38.518	14054.23	15.61	27.54	1516.01	13.41	21.74	84219.75	14.26	27.08
72.230	37245.30	41.37	68.92	4834.57	42.76	64.50	249348.49	42.23	69.31
154.557	18846.13	20.94	89.85	1875.69	16.59	81.10	104019.06	17.62	86.93
323.589	9134.05	10.15	100.00	2137.17	18.90	100.00	77181.26	13.07	100.00
sum	90019.78	100.00		11305.36	100.00		590455.45	100.00	

Table 11 Bed material load for Mkomazi Site 4b

Q	Yang	% time	cum %	AW	% time	cum %	EH	% time	cum %
0.079	0.00	0.00	0.00	0.00	0.00	0.00	0.94	0.00	0.00
1.317	0.00	0.00	0.00	0.00	0.00	0.00	279.12	0.04	0.04
1.904	19.24	0.01	0.01	0.00	0.00	0.00	574.14	0.08	0.11
2.576	56.41	0.04	0.06	0.00	0.00	0.00	1030.34	0.14	0.25
3.515	148.38	0.11	0.16	13.56	0.05	0.05	1858.64	0.25	0.49
4.966	475.93	0.35	0.51	38.51	0.14	0.19	3373.21	0.44	0.94
7.458	1378.06	1.01	1.52	147.24	0.53	0.72	7444.89	0.98	1.92
11.961	3989.00	2.92	4.44	512.04	1.84	2.56	17084.83	2.25	4.17
21.406	12295.99	9.00	13.45	1909.82	6.87	9.43	58613.95	7.73	11.90
38.518	19908.59	14.58	28.02	3189.60	11.47	20.89	92180.73	12.15	24.05
72.230	49763.12	36.44	64.46	9626.04	34.61	55.51	260893.28	34.40	58.45
154.557	37572.18	27.51	91.97	9176.26	33.00	88.50	229211.56	30.22	88.67
323.589	10963.82	8.03	100.00	3197.09	11.50	100.00	85943.87	11.33	100.00
sum	136570.72	100.00		27810.16	100.00		758489.49	100.00	

Table 12 Bed material load for Mkomazi Site 5a

Q	Yang	% time	cum %	AW	% time	cum %	EH	% time	cum %
0.133	0.00	0.00	0.00	0.00	0.00	0.00	0.00	0.00	0.00
2.211	0.00	0.00	0.00	0.00	0.00	0.00	0.00	0.00	0.00
3.195	0.00	0.00	0.00	0.00	0.00	0.00	0.00	0.00	0.00
4.322	0.00	0.00	0.00	0.00	0.00	0.00	312.92	0.01	0.01
5.898	34.24	0.01	0.01	0.00	0.00	0.00	825.57	0.03	0.04
8.332	150.44	0.03	0.04	38.39	0.01	0.01	2289.73	0.07	0.11
12.515	576.28	0.13	0.17	170.17	0.05	0.06	6758.18	0.22	0.33
20.071	2528.74	0.57	0.74	900.93	0.26	0.32	21734.21	0.69	1.02
35.919	15105.41	3.39	4.13	6022.18	1.73	2.05	102442.49	3.27	4.29
64.631	41686.27	9.37	13.50	17345.00	4.98	7.03	226153.43	7.23	11.52
131.926	162008.28	36.40	49.90	97513.79	28.00	35.03	974021.57	31.12	42.64
291.284	177850.45	39.96	89.85	167476.42	48.10	83.13	1444988.40	46.16	88.80
503.130	45165.32	10.15	100.00	58738.08	16.87	100.00	350597.73	11.20	100.00
sum	445105.42	100.00		348204.96	100.00		3130124.23	100.00	

Table 13 Bed material load for Mkomazi Site 5b

Q	Yang	% time	cum %	AW	% time	cum %	EH	% time	cum %
0.133	0.00	0.00	0.00	0.00	0.00	0.00	0.00	0.00	0.00
2.211	0.00	0.00	0.00	0.00	0.00	0.00	0.00	0.00	0.00
3.195	0.00	0.00	0.00	0.00	0.00	0.00	0.00	0.00	0.00
4.322	0.00	0.00	0.00	0.00	0.00	0.00	271.37	0.01	0.01
5.898	33.85	0.01	0.01	0.00	0.00	0.00	751.81	0.03	0.04
8.332	139.59	0.04	0.05	35.34	0.02	0.02	2070.46	0.08	0.11
12.515	516.73	0.14	0.19	148.15	0.06	0.08	6018.00	0.22	0.33
20.071	2166.53	0.60	0.80	739.22	0.32	0.40	19324.84	0.70	1.03
35.919	12191.27	3.40	4.20	4482.94	1.92	2.32	90178.17	3.27	4.31
64.631	32797.81	9.15	13.34	12417.00	5.32	7.64	199204.71	7.23	11.54
131.926	131316.40	36.63	49.97	66857.51	28.64	36.28	858990.63	31.18	42.72
291.284	143270.38	39.96	89.93	109780.34	47.03	83.31	1277291.98	46.37	89.09
503.130	36107.09	10.07	100.00	38955.45	16.69	100.00	300647.58	10.91	100.00
sum	358539.65	100.00		233415.95	100.00		2754749.55	100.00	

Table 14 Bed material load for Mkomazi Site 6a

Q	Yang	% time	cum %	AW	% time	cum %	EH	% time	cum %
0.136	0.00	0.00	0.00	0.00	0.00	0.00	0.00	0.00	0.00
2.255	0.00	0.00	0.00	0.00	0.00	0.00	39.57	0.01	0.01
3.260	0.00	0.00	0.00	0.00	0.00	0.00	91.81	0.02	0.03
4.410	0.00	0.00	0.00	0.00	0.00	0.00	181.81	0.05	0.08
6.017	0.00	0.00	0.00	0.00	0.00	0.00	371.67	0.10	0.18
8.501	0.00	0.00	0.00	0.00	0.00	0.00	800.13	0.21	0.39
12.767	177.34	0.17	0.17	0.00	0.00	0.00	1904.85	0.50	0.89
20.476	779.38	0.76	0.94	0.00	0.00	0.00	5244.10	1.37	2.26
36.644	4725.49	4.63	5.56	275.93	3.11	3.11	18134.37	4.75	7.02
65.937	12285.59	12.03	17.60	705.60	7.94	11.05	33799.22	8.86	15.88
134.591	40502.41	39.66	57.26	3048.29	34.31	45.36	127232.94	33.35	49.23
297.169	35295.56	34.57	91.83	3638.19	40.95	86.32	149807.41	39.27	88.50
513.294	8347.75	8.17	100.00	1215.40	13.68	100.00	43856.55	11.50	100.00
sum	102113.52	100.00		8883.42	100.00		381464.43	100.00	

Table 15 Bed material load for Mkomazi Site 6b

Q	Yang	% time	cum %	AW	% time	cum %	EH	% time	cum %
0.136	0.00	0.00	0.00	0.00	0.00	0.00	0.00	0.00	0.00
2.255	0.00	0.00	0.00	0.00	0.00	0.00	52.67	0.02	0.02
3.260	25.66	0.02	0.02	0.00	0.00	0.00	122.79	0.04	0.05
4.410	66.61	0.05	0.07	0.00	0.00	0.00	202.11	0.06	0.12
6.017	154.86	0.11	0.17	18.97	0.08	0.08	384.93	0.12	0.24
8.501	458.20	0.32	0.50	60.98	0.26	0.34	788.53	0.24	0.48
12.767	1160.84	0.82	1.32	199.36	0.85	1.19	1566.12	0.48	0.96
20.476	3972.08	2.81	4.12	582.46	2.47	3.66	4736.22	1.46	2.43
36.644	13228.74	9.34	13.47	1973.23	8.38	12.04	15881.51	4.91	7.33
65.937	19144.12	13.52	26.99	2942.27	12.50	24.54	28653.45	8.85	16.18
134.591	50872.09	35.93	62.92	7975.73	33.87	58.41	106955.42	33.04	49.22
297.169	42588.88	30.08	93.00	7533.20	31.99	90.40	126953.68	39.21	88.43
513.294	9912.44	7.00	100.00	2260.28	9.60	100.00	37457.82	11.57	100.00
sum	141584.52	100.00		23546.47	100.00		323755.25	100.00	

Table 16 Bed material load for Mkomazi Site 6c

Q	Yang	% time	cum %	AW	% time	cum %	EH	% time	cum %
0.136	0.00	0.00	0.00	0.00	0.00	0.00	0.00	0.00	0.00
2.255	0.00	0.00	0.00	0.00	0.00	0.00	34.29	0.01	0.01
3.260	0.00	0.00	0.00	0.00	0.00	0.00	82.11	0.02	0.03
4.410	0.00	0.00	0.00	0.00	0.00	0.00	160.10	0.04	0.07
6.017	0.00	0.00	0.00	0.00	0.00	0.00	333.32	0.08	0.15
8.501	0.00	0.00	0.00	0.00	0.00	0.00	733.95	0.19	0.34
12.767	148.55	0.12	0.12	0.00	0.00	0.00	1788.46	0.45	0.79
20.476	952.29	0.78	0.90	0.00	0.00	0.00	5495.72	1.39	2.18
36.644	6785.15	5.52	6.42	315.10	2.14	2.14	20591.75	5.19	7.37
65.937	14822.25	12.07	18.49	986.37	6.71	8.85	36491.18	9.20	16.57
134.591	47663.23	38.81	57.30	4930.15	33.54	42.39	133249.23	33.61	50.18
297.169	42587.38	34.68	91.98	6425.06	43.70	86.09	153003.55	38.59	88.77
513.294	9851.84	8.02	100.00	2044.81	13.91	100.00	44516.44	11.23	100.00
sum	122810.70	100.00		14701.49	100.00		396480.11	100.00	

Table 17 Bed material load for Mkomazi Site 7a

Q	Yang	% time	cum %	AW	% time	cum %	EH	% time	cum %
0.144	0.00	0.00	0.00	0.00	0.00	0.00	0.92	0.00	0.00
2.389	23.56	0.12	0.12	0.00	0.00	0.00	164.33	0.16	0.16
3.453	57.91	0.30	0.42	0.00	0.00	0.00	298.51	0.29	0.44
4.672	105.39	0.54	0.96	0.00	0.00	0.00	473.27	0.45	0.90
6.374	183.28	0.94	1.90	0.00	0.00	0.00	813.29	0.78	1.68
9.006	481.78	2.48	4.38	0.00	0.00	0.00	1543.60	1.48	3.16
13.526	1093.92	5.63	10.01	0.00	0.00	0.00	3201.71	3.07	6.23
21.693	2393.74	12.32	22.33	0.00	0.00	0.00	6483.49	6.22	12.45
38.821	1469.09	7.56	29.89	0.00	0.00	0.00	10425.97	10.00	22.44
69.854	2754.31	14.17	44.07	0.00	0.00	0.00	14293.84	13.71	36.15
142.586	5936.54	30.55	74.62	0.00	0.00	0.00	33951.57	32.56	68.71
314.822	3964.06	20.40	95.02	0.00	0.00	0.00	25923.50	24.86	93.56
543.787	967.99	4.98	100.00	20.81	100.00	100.00	6712.24	6.44	100.00
sum	19431.57	100.00		20.81	100.00		104286.24	100.00	

Table 18 Bed material load for Mkomazi Site 7b

Q	Yang	% time	cum %	AW	% time	cum %	EH	% time	cum %
0.144	0.00	0.00	0.00	0.00	0.00	0.00	0.00	0.00	0.00
2.389	0.00	0.00	0.00	0.00	0.00	0.00	124.16	0.13	0.13
3.453	0.00	0.00	0.00	0.00	0.00	0.00	243.36	0.26	0.39
4.672	0.00	0.00	0.00	0.00	0.00	0.00	378.84	0.40	0.79
6.374	0.00	0.00	0.00	0.00	0.00	0.00	659.29	0.70	1.49
9.006	0.00	0.00	0.00	0.00	0.00	0.00	1280.86	1.36	2.84
13.526	159.90	2.07	2.07	0.00	0.00	0.00	2520.99	2.67	5.51
21.693	315.48	4.08	6.14	0.00	0.00	0.00	4472.95	4.73	10.24
38.821	0.00	0.00	6.14	0.00	0.00	0.00	9428.67	9.98	20.22
69.854	733.64	9.48	15.62	0.00	0.00	0.00	13429.37	14.21	34.44
142.586	2911.44	37.61	53.22	0.00	0.00	0.00	32025.17	33.89	68.33
314.822	2851.15	36.83	90.05	0.00	0.00	0.00	24432.32	25.86	94.18
543.787	770.09	9.95	100.00	0.00	0.00	0.00	5494.73	5.82	100.00
sum	7741.71	100.00		0.00	0.00		94490.71	100.00	

Table 19 Bed material load for Mkomazi Site 8a

Q	Yang	% time	cum %	AW	% time	cum %	EH	% time	cum %
0.148	0.00	0.00	0.00	0.00	0.00	0.00	1.88	0.00	0.00
2.456	0.00	0.00	0.00	0.00	0.00	0.00	524.13	0.21	0.21
3.55	153.17	0.17	0.17	0.00	0.00	0.00	1052.77	0.43	0.64
4.803	1256.05	1.37	1.54	86.02	0.66	0.66	3108.83	1.27	1.91
6.553	1107.46	1.21	2.75	43.72	0.34	1.00	3337.61	1.36	3.28
9.258	2313.17	2.53	5.29	131.40	1.01	2.01	6189.20	2.53	5.80
13.905	4791.93	5.24	10.53	449.82	3.47	5.48	12840.78	5.24	11.04
22.301	11437.28	12.52	23.05	2261.75	17.44	22.92	28864.33	11.78	22.82
39.909	14195.38	15.54	38.59	1646.55	12.70	35.62	36054.31	14.72	37.54
71.813	16116.76	17.64	56.22	2851.81	21.99	57.61	32535.23	13.28	50.82
146.584	24545.99	26.87	83.09	3433.05	26.47	84.08	61026.95	24.91	75.73
323.649	11721.10	12.83	95.92	1011.22	7.80	91.87	47016.02	19.19	94.92
559.033	3729.44	4.08	100.00	1053.76	8.13	100.00	12451.23	5.08	100.00
sum	91367.73	100.00		12969.10	100.00		245003.25	100.00	

Table 20 Bed material load for Mkomazi Site 8b

Q	Yang	% time	cum %	AW	% time	cum %	EH	% time	cum %
0.15	0.00	0.00	0.00	0.00	0.00	0.00	1.88	0.00	0.00
2.46	0.00	0.00	0.00	0.00	0.00	0.00	524.13	0.22	0.22
3.55	153.17	0.17	0.17	0.00	0.00	0.00	1052.77	0.43	0.65
4.80	458.75	0.51	0.67	0.00	0.00	0.00	1756.73	0.72	1.37
6.55	1107.46	1.22	1.90	43.72	0.33	0.33	3337.65	1.37	2.74
9.26	2283.98	2.52	4.41	131.40	0.99	1.32	6189.20	2.54	5.28
13.91	4791.93	5.28	9.70	449.82	3.39	4.71	12840.78	5.27	10.55
22.30	11583.27	12.77	22.47	2261.75	17.05	21.76	28864.33	11.85	22.41
39.91	14195.38	15.65	38.12	1646.55	12.41	34.17	36054.43	14.80	37.21
71.81	16116.76	17.77	55.90	3236.28	24.39	58.56	32535.23	13.36	50.57
146.58	24545.99	27.07	82.96	3433.05	25.88	84.44	60907.35	25.01	75.58
323.65	11721.10	12.92	95.89	1011.22	7.62	92.06	47015.47	19.31	94.89
559.03	3729.44	4.11	100.00	1053.76	7.94	100.00	12451.11	5.11	100.00
sum	90687.22	100.00		13267.54	100.00		243531.05	100.00	

Table 21 Bed material load for Mkomazi Site 9a

Q	Yang	% time	cum %	AW	% time	cum %	EH	% time	cum %
1.290	0.00	0.00	0.00	0.00	0.00	10.00	72.71	0.00	0.00
3.814	31.53	0.01	0.01	0.00	0.00	20.00	855.08	0.04	0.04
5.116	72.08	0.02	0.03	0.00	0.00	30.00	1566.60	0.07	0.12
6.924	195.39	0.05	0.08	0.00	0.00	40.00	2858.95	0.13	0.25
9.579	458.09	0.12	0.20	36.10	0.04	50.00	5435.81	0.25	0.51
13.447	1306.50	0.34	0.54	86.08	0.10	59.99	11143.47	0.52	1.03
20.028	3823.85	1.00	1.54	290.07	0.35	69.99	25177.16	1.18	2.21
31.990	15111.06	3.94	5.48	1019.93	1.23	79.99	64337.37	3.02	5.23
55.327	43726.23	11.40	16.88	3913.18	4.72	89.99	176960.77	8.30	13.53
92.686	53999.68	14.08	30.96	5391.61	6.51	94.99	244747.74	11.48	25.01
186.151	134118.40	34.97	65.93	28223.74	34.08	98.99	696223.53	32.66	57.67
421.352	118732.61	30.96	96.89	38858.85	46.92	99.94	800506.74	37.55	95.22
727.789	11923.40	3.11	100.00	5007.01	6.07	100.00	101962.83	4.78	100.00
sum	383498.82	100.00		82826.56	100.00		2131848.75	100.00	

Table 22 Bed material load for Mkomazi Site 9b

Q	Yang	% time	cum %	AW	% time	cum %	EH	% time	cum %
1.290	0.00	0.00	0.00	0.00	0.00	0.00	72.71	0.00	0.00
3.814	31.53	0.01	0.01	0.00	0.00	0.00	855.08	0.04	0.04
5.116	72.08	0.02	0.03	0.00	0.00	0.00	1566.60	0.07	0.11
6.924	195.39	0.05	0.08	0.00	0.00	0.00	2858.95	0.13	0.25
9.579	430.64	0.12	0.20	37.91	0.04	0.04	5099.05	0.23	0.48
13.447	1306.50	0.36	0.56	86.08	0.10	0.14	11151.11	0.51	0.99
20.028	3823.85	1.05	1.60	290.07	0.33	0.47	25177.16	1.15	2.14
31.990	15111.16	4.14	5.74	1019.93	1.15	1.61	62319.29	2.85	5.00
55.327	43726.23	11.97	17.71	3913.18	4.40	6.02	176961.64	8.11	13.10
92.686	31318.21	8.57	26.28	6591.53	7.42	13.43	244747.74	11.21	24.31
186.151	134118.40	36.71	62.99	28223.74	31.75	45.18	696198.18	31.89	56.20
421.352	111304.45	30.47	93.46	36442.97	41.00	86.18	750738.79	34.39	90.59
727.789	23906.56	6.54	100.00	12284.72	13.82	100.00	205354.81	9.41	100.00
sum	365344.99	100.00		88890.12	100.00		2183101.10	100.00	

Table 23 Bed material load for Mkomazi Site 10a

Q	Yang	% time	cum %	AW	% time	cum %	EH	% time	cum %
1.349	0.00	0.00	0.00	0.00	0.00	0.00	0.00	0.00	0.00
3.987	0.00	0.00	0.00	0.00	0.00	0.00	25.01	0.01	0.01
5.349	0.00	0.00	0.00	0.00	0.00	0.00	44.60	0.03	0.04
7.238	0.00	0.00	0.00	0.00	0.00	0.00	118.84	0.07	0.11
10.015	0.00	0.00	0.00	0.00	0.00	0.00	240.96	0.14	0.25
14.058	71.86	0.12	0.12	0.00	0.00	0.00	469.58	0.27	0.52
20.938	314.80	0.53	0.65	0.00	0.00	0.00	1359.56	0.79	1.31
33.444	1125.45	1.90	2.55	0.00	0.00	0.00	3751.16	2.17	3.48
57.842	4816.25	8.13	10.68	297.48	2.60	2.60	11047.87	6.39	9.86
96.899	6855.55	11.57	22.25	616.84	5.39	7.99	17579.60	10.17	20.03
194.392	18707.10	31.57	53.82	2506.19	21.91	29.90	63537.41	36.74	56.77
439.509	21648.32	36.53	90.35	5916.09	51.71	81.61	59389.57	34.34	91.12
759.150	5715.40	9.65	100.00	2104.05	18.39	100.00	15363.55	8.88	100.00
sum	59254.73	100.00		11440.66	100.00		172927.68	100.00	

Table 24 Bed material load for Mkomazi Site 10b

Q	Yang	% time	cum %	AW	% time	cum %	EH	% time	cum %
1.349	0.00	0.00	0.00	0.00	0.00	0.00	0.00	0.00	0.00
3.987	0.00	0.00	0.00	0.00	0.00	0.00	26.73	0.02	0.02
5.349	0.00	0.00	0.00	0.00	0.00	0.00	47.45	0.03	0.04
7.238	0.00	0.00	0.00	0.00	0.00	0.00	110.58	0.07	0.11
10.015	57.89	0.11	0.11	0.00	0.00	0.00	258.17	0.16	0.27
14.058	123.06	0.24	0.35	0.00	0.00	0.00	537.80	0.32	0.59
20.938	424.86	0.83	1.18	0.00	0.00	0.00	1208.56	0.73	1.32
33.444	1559.84	3.04	4.22	0.00	0.00	0.00	3968.40	2.39	3.72
57.842	4889.75	9.52	13.74	299.67	4.04	4.04	11311.06	6.83	10.54
96.899	6599.83	12.85	26.58	384.34	5.19	9.23	18108.14	10.93	21.47
194.392	17494.09	34.06	60.64	2217.90	29.92	39.15	57134.52	34.48	55.95
439.509	16141.66	31.43	92.07	3294.01	44.44	83.59	57453.11	34.67	90.62
759.150	4073.57	7.93	100.00	1215.93	16.41	100.00	15547.74	9.38	100.00
sum	51364.54	100.00		7411.85	100.00		165712.25	100.00	

Table 25 Bed material load for Mkomazi Site 11

Q	Yang	% time	cum %	AW	% time	cum %	EH	% time	cum %
1.378	0.00	0.00	0.00	0.00	0.00	0.00	56.42	0.01	0.01
4.074	47.92	0.01	0.01	0.00	0.00	0.00	425.58	0.09	0.10
5.465	172.52	0.02	0.03	0.00	0.00	0.00	754.81	0.16	0.27
7.396	482.97	0.07	0.10	0.00	0.00	0.00	1285.98	0.28	0.55
10.232	1001.97	0.14	0.23	38.72	0.01	0.01	2334.52	0.50	1.05
14.363	1883.73	0.26	0.49	82.97	0.02	0.03	4277.02	0.92	1.97
21.394	3714.36	0.51	1.00	184.91	0.04	0.06	8819.97	1.91	3.88
34.171	8052.87	1.11	2.11	712.45	0.15	0.21	20856.48	4.51	8.39
59.099	20559.35	2.83	4.94	3903.97	0.82	1.04	56570.40	12.22	20.61
99.006	28058.14	3.86	8.80	9640.53	2.03	3.07	65475.70	14.15	34.76
199.182	153921.73	21.18	29.98	87109.07	18.35	21.42	172656.98	37.31	72.06
451.614	412639.85	56.78	86.76	298281.78	62.85	84.27	107568.84	23.24	95.31
780.063	96254.04	13.24	100.00	74633.53	15.73	100.00	21716.05	4.69	100.00
sum	726789.43	100.00		474587.93	100.00		462798.75	100.00	

Table 26 Bed material load for Mkomazi Site 12

Q	Yang	% time	cum %	AW	% time	cum %	EH	% time	cum %
1.451	0.00	0.00	0.00	0.00	0.00	0.00	0.00	0.00	0.00
4.290	0.00	0.00	0.00	0.00	0.00	0.00	0.00	0.00	0.00
5.756	0.00	0.00	0.00	0.00	0.00	0.00	0.00	0.00	0.00
7.789	0.00	0.00	0.00	0.00	0.00	0.00	0.00	0.00	0.00
10.777	0.00	0.00	0.00	0.00	0.00	0.00	0.00	0.00	0.00
15.128	0.00	0.00	0.00	0.00	0.00	0.00	0.00	0.00	0.00
22.531	0.00	0.00	0.00	0.00	0.00	0.00	103.94	0.27	0.27
35.988	0.00	0.00	0.00	0.00	0.00	0.00	440.08	1.13	1.40
62.243	527.77	3.08	3.08	0.00	0.00	0.00	1270.46	3.26	4.66
104.272	1852.43	10.81	13.89	0.00	0.00	0.00	2842.51	7.30	11.96
209.711	6584.29	38.43	52.32	0.00	0.00	0.00	11565.61	29.70	41.66
475.339	6475.50	37.79	90.12	227.34	51.35	51.35	17004.63	43.67	85.34
821.039	1693.58	9.88	100.00	215.36	48.65	100.00	5708.71	14.66	100.00
sum	17133.57	100.00		442.70	100.00		38935.94	100.00	

Table 27 Bed material load for Mkomazi Site 13

Q	Yang	% time	cum %	AW	% time	cum %	EH	% time	cum %
1.466	0.00	0.00	0.00	0.00	0.00	0.00	8.23	0.00	0.00
4.334	28.48	0.03	0.03	0.00	0.00	0.00	70.86	0.03	0.03
5.814	54.47	0.05	0.08	0.00	0.00	0.00	160.36	0.07	0.10
7.868	155.24	0.14	0.22	44.76	0.17	0.17	332.36	0.14	0.24
10.885	279.36	0.25	0.47	74.45	0.29	0.46	438.86	0.19	0.43
15.280	608.11	0.55	1.03	148.16	0.57	1.04	936.57	0.40	0.82
22.759	1387.88	1.26	2.29	310.10	1.20	2.24	2354.41	1.00	1.82
36.352	3873.52	3.53	5.82	817.64	3.17	5.41	5967.32	2.53	4.35
62.872	10906.11	9.94	15.76	2453.38	9.51	14.91	16856.29	7.14	11.49
105.325	14850.24	13.53	29.29	3076.28	11.92	26.83	29138.43	12.34	23.83
211.342	38356.40	34.95	64.25	8660.58	33.55	60.38	33153.49	14.04	37.88
477.941	32188.36	29.33	93.58	8091.56	31.35	91.73	118535.04	50.21	88.09
825.538	7047.68	6.42	100.00	2133.97	8.27	100.00	28102.84	11.91	100.00
sum	109735.84	100.00		25810.88	100.00		236055.06	100.00	

Table 28 Bed material load for Mhlathuze Site 1 pool virgin flow

Q	Yang	% time	cum %	AW	% time	cum %	EH	% time	cum %
0.000	0.00	0.00	0.00	0.00	0.00	0.00	0.00	0.00	0.00
0.506	17.76	0.00	0.00	1.79	0.00	0.00	1950.05	0.08	0.08
0.856	110.02	0.03	0.04	12.36	0.02	0.02	5092.17	0.20	0.28
1.280	391.96	0.11	0.15	37.17	0.05	0.07	10450.26	0.42	0.70
1.787	1367.43	0.38	0.53	109.15	0.16	0.23	19352.68	0.77	1.47
2.399	2911.51	0.81	1.34	252.66	0.37	0.60	32435.75	1.29	2.76
3.258	5001.40	1.40	2.73	559.69	0.81	1.41	27050.07	1.08	3.84
4.613	11451.27	3.19	5.93	1279.91	1.85	3.26	56339.53	2.25	6.09
7.604	23990.04	6.69	12.62	2922.63	4.23	7.50	103998.42	4.15	10.23
13.416	23294.32	6.50	19.12	2724.77	3.95	11.45	109045.36	4.35	14.58
29.942	54012.15	15.07	34.19	5176.98	7.50	18.95	326491.31	13.02	27.60
145.270	87904.12	24.53	58.72	8867.31	12.85	31.79	684249.86	27.28	54.88
1020.298	147962.01	41.28	100.00	47078.04	68.21	100.00	1131678.08	45.12	100.00
sum	358413.98	100.00		69022.46	100.00		2508133.52	100.00	

Table 29 Bed material load for Mhlathuze Site 1 pool present-day flow

Q	Yang	% time	cum %	AW	% time	cum %	EH	% time	cum %
0.000	0.00	0.00	0.00	0.00	0.00	0.00	0.00	0.00	0.00
0.311	2.44	0.00	0.00	0.00	0.00	0.00	803.10	0.10	0.10
0.374	4.33	0.00	0.01	0.00	0.00	0.00	1138.21	0.14	0.23
0.440	8.38	0.01	0.01	0.00	0.00	0.00	1549.64	0.18	0.42
0.515	19.86	0.02	0.03	1.88	0.01	0.01	2027.13	0.24	0.66
0.597	36.28	0.03	0.07	2.85	0.02	0.03	2670.66	0.32	0.98
0.696	61.28	0.06	0.12	6.80	0.04	0.08	3561.47	0.42	1.40
0.837	104.12	0.10	0.22	11.64	0.08	0.15	4894.98	0.58	1.98
1.215	296.54	0.27	0.49	32.80	0.21	0.37	9769.86	1.17	3.15
2.591	1713.23	1.58	2.07	154.28	1.01	1.37	18082.88	2.16	5.31
10.046	13719.03	12.67	14.75	1373.22	8.97	10.35	79078.60	9.43	14.74
69.354	35992.90	33.24	47.99	3617.68	23.64	33.98	236924.76	28.25	42.99
595.123	56316.31	52.01	100.00	10103.83	66.02	100.00	478093.61	57.01	100.00
sum	108274.69	100.00		15304.99	100.00		838594.89	100.00	

Table 30 Bed material load for Mhlathuze Site 1 riffle virgin flow

Q	Yang	% time	cum %	AW	% time	cum %	EH	% time	cum %
0.000	0.00	0.00	0.00	0.00	0.00	0.00	0.00	0.00	0.00
0.506	10010.78	0.61	0.61	2517.57	0.45	0.45	73056.27	0.09	0.09
0.856	18513.08	1.13	1.75	4682.38	0.83	1.28	177756.93	0.23	0.32
1.280	30068.79	1.84	3.59	7811.75	1.39	2.68	354106.30	0.45	0.77
1.787	45156.84	2.76	6.35	12175.48	2.17	4.85	619828.20	0.79	1.55
2.399	64460.65	3.95	10.30	18050.88	3.22	8.07	1008273.49	1.28	2.84
3.258	71588.66	4.38	14.68	26766.53	4.77	12.84	1642917.38	2.09	4.92
4.613	134369.62	8.22	22.90	40111.89	7.15	19.99	2856622.58	3.63	8.55
7.604	224677.08	13.75	36.65	69088.75	12.32	32.31	6249390.83	7.93	16.48
13.416	205731.22	12.59	49.24	67738.75	12.08	44.39	7325646.85	9.30	25.78
29.942	350426.62	21.45	70.69	120829.37	21.55	65.94	19876611.01	25.24	51.02
145.270	360163.71	22.04	92.73	151117.34	26.95	92.88	24420290.66	31.00	82.02
1020.298	118726.01	7.27	100.00	39919.49	7.12	100.00	14159110.90	17.98	100.00
sum	1633893.07	100.00		560810.19	100.00		78763611.41	100.00	

Table 31 Bed material load for Mhlathuze Site 1 riffle present-day flow

Q	Yang	% time	cum %	AW	% time	cum %	EH	% time	cum %
0.000	0.00	0.00	0.00	0.00	0.00	0.00	0.00	0.00	0.00
0.311	5914.14	1.50	1.50	1562.28	1.52	1.52	33551.82	0.17	0.17
0.374	7240.96	1.83	3.33	1903.39	1.85	3.37	43890.48	0.22	0.38
0.440	8516.69	2.15	5.48	2188.42	2.13	5.50	57420.18	0.29	0.67
0.515	10168.51	2.57	8.06	2604.32	2.54	8.04	75182.05	0.37	1.04
0.597	11960.04	3.03	11.08	3030.35	2.95	10.99	98240.43	0.49	1.53
0.696	14350.92	3.63	14.71	3645.83	3.55	14.54	127758.82	0.63	2.16
0.837	17960.14	4.54	19.26	4623.71	4.50	19.04	171162.22	0.85	3.01
1.215	28111.50	7.11	26.37	7422.03	7.22	26.26	323252.56	1.60	4.62
2.591	35313.78	8.93	35.30	10183.82	9.91	36.18	568649.20	2.82	7.44
10.046	117307.07	29.68	64.98	36872.99	35.89	72.07	3779259.09	18.76	26.20
69.354	91554.38	23.16	88.15	19317.68	18.80	90.87	7931878.16	39.37	65.57
595.123	46848.03	11.85	100.00	9378.12	9.13	100.00	6935135.47	34.43	100.00
sum	395246.16	100.00		102732.94	100.00		20145380.49	100.00	

Table 32 Bed material load for Mhlathuze Site 2 virgin flow

Q	Yang	% time	cum %	AW	% time	cum %	EH	% time	cum %
0.000	0.00	0.00	0.00	0.00	0.00	10.00	0.00	0.00	0.00
0.656	67.28	0.03	0.03	12.89	0.04	20.00	69.98	0.00	0.00
1.112	73.71	0.03	0.06	13.15	0.04	30.00	150.99	0.01	0.01
1.721	125.85	0.06	0.12	18.51	0.06	40.00	305.31	0.02	0.03
2.469	205.54	0.09	0.21	30.44	0.10	50.00	646.89	0.04	0.07
3.342	384.12	0.17	0.38	48.48	0.15	59.99	1193.99	0.07	0.13
4.521	725.63	0.32	0.70	79.69	0.25	69.99	2163.06	0.12	0.26
6.354	1507.31	0.67	1.37	199.16	0.63	79.99	4240.41	0.24	0.50
10.378	4606.01	2.04	3.40	665.95	2.12	89.99	12260.67	0.69	1.19
17.907	7296.21	3.23	6.63	1027.29	3.28	94.99	17320.87	0.98	2.17
38.388	24731.30	10.94	17.56	3749.03	11.95	98.99	57965.20	3.28	5.46
195.995	72310.64	31.97	49.54	10078.38	32.13	99.94	294315.03	16.67	22.13
1435.327	114124.77	50.46	100.00	15441.34	49.25	100.00	1374431.80	77.87	100.00
sum	226158.37	100.00		31364.30	100.00		1765064.20	100.00	

Table 33 Bed material load for Mhlathuze Site 2 present-day flow

Q	Yang	% time	cum %	AW	% time	cum %	EH	% time	cum %
0.000	0.00	0.00	0.00	0.00	0.00	0.00	0.00	0.00	0.00
0.353	58.47	0.04	0.04	48.13	0.27	0.27	27.94	0.00	0.00
0.455	46.87	0.04	0.08	12.75	0.07	0.35	36.16	0.00	0.01
0.605	52.65	0.04	0.12	9.52	0.05	0.40	57.94	0.01	0.01
0.831	72.09	0.06	0.18	12.32	0.07	0.47	96.04	0.01	0.02
1.115	66.80	0.05	0.23	11.29	0.06	0.53	135.40	0.01	0.04
1.514	88.26	0.07	0.30	14.61	0.08	0.62	223.47	0.02	0.06
2.135	149.95	0.12	0.41	22.96	0.13	0.75	437.04	0.04	0.10
3.522	403.70	0.31	0.72	48.87	0.28	1.02	1184.89	0.12	0.22
6.775	869.94	0.67	1.39	115.03	0.65	1.68	2397.07	0.24	0.47
20.166	7407.02	5.69	7.08	1031.52	5.85	7.53	17400.97	1.77	2.23
136.895	41638.71	32.01	39.09	5864.02	33.26	40.78	144490.80	14.67	16.90
1094.274	79227.75	60.91	100.00	10440.77	59.22	100.00	818772.44	83.10	100.00
sum	130082.22	100.00		17631.78	100.00		985260.14	100.00	

Table 34 Bed material load for Mhlathuze Site 3 virgin flow

Q	Yang	% time	cum %	AW	% time	cum %	EH	% time	cum %
0.000	0.00	0.00	0.00	0.00	0.00	0.00	0.00	0.00	0.00
0.932	41.56	0.03	0.03	16.05	0.04	0.04	18.57	0.01	0.01
1.491	0.00	0.00	0.03	0.00	0.00	0.04	0.00	0.00	0.01
2.211	80.25	0.06	0.09	16.80	0.04	0.07	105.62	0.04	0.05
3.095	122.87	0.09	0.19	25.47	0.06	0.13	173.03	0.07	0.12
4.112	203.96	0.16	0.34	41.75	0.09	0.22	304.32	0.13	0.25
5.424	344.12	0.26	0.60	69.95	0.16	0.38	526.61	0.22	0.46
7.479	712.76	0.54	1.14	169.56	0.38	0.76	1024.35	0.42	0.89
12.236	2212.00	1.68	2.83	565.64	1.26	2.01	2708.18	1.11	2.00
21.375	4265.07	3.24	6.07	1086.40	2.42	4.43	5018.55	2.07	4.07
48.661	17377.46	13.22	19.29	4657.19	10.36	14.80	18967.49	7.81	11.87
245.495	46692.52	35.51	54.79	20174.16	44.90	59.69	51135.12	21.04	32.91
1736.416	59444.72	45.21	100.00	18112.29	40.31	100.00	163017.62	67.09	100.00
sum	131497.28	100.00		44935.27	100.00		242999.47	100.00	

Table 35 Bed material load for Mhlathuze Site 3 present-day flow

Q	Yang	% time	cum %	AW	% time	cum %	EH	% time	cum %
0.000	0.00	0.00	0.00	0.00	0.00	0.00	0.00	0.00	0.00
0.429	95.23	0.11	0.11	517.36	1.80	1.80	13.58	0.01	0.01
0.565	77.19	0.09	0.20	239.91	0.84	2.64	15.82	0.01	0.02
0.773	56.11	0.07	0.27	61.72	0.21	2.85	18.71	0.01	0.03
1.088	40.76	0.05	0.32	10.57	0.04	2.89	28.85	0.02	0.05
1.476	48.92	0.06	0.37	10.75	0.04	2.93	50.82	0.03	0.08
2.009	71.90	0.08	0.46	15.58	0.05	2.98	89.96	0.06	0.14
2.837	112.72	0.13	0.59	24.60	0.09	3.07	146.71	0.09	0.23
4.883	194.01	0.23	0.82	61.74	0.21	3.28	428.67	0.27	0.50
10.330	770.97	0.90	1.72	198.52	0.69	3.97	968.96	0.61	1.11
30.714	7368.79	8.65	10.37	1951.82	6.79	10.77	7950.97	5.01	6.12
184.467	33108.56	38.85	49.22	13017.64	45.32	56.08	37113.98	23.37	29.49
1410.450	43277.57	50.78	100.00	12615.23	43.92	100.00	111950.34	70.51	100.00
sum	85222.71	100.00		28725.44	100.00		158777.38	100.00	

Table 36 Bed material load for Mhlathuze Site 4 virgin flow

Q	Yang	% time	cum %	AW	% time	cum %	EH	% time	cum %
0.000	0.00	0.00	0.00	0.00	0.00	0.00	0.00	0.00	0.00
1.510	16.09	0.01	0.01	0.00	0.00	0.00	88.23	0.05	0.05
2.275	63.56	0.04	0.06	0.00	0.00	0.00	197.71	0.11	0.16
3.154	169.27	0.12	0.17	25.86	0.05	0.05	376.34	0.21	0.36
4.201	347.86	0.24	0.42	65.84	0.12	0.17	660.49	0.36	0.72
5.373	732.77	0.51	0.93	148.42	0.27	0.44	1085.00	0.59	1.32
6.820	1431.18	1.00	1.93	296.99	0.54	0.98	1729.46	0.94	2.26
9.110	2895.05	2.03	3.96	638.88	1.17	2.15	3040.12	1.66	3.92
14.170	6559.32	4.59	8.55	1781.92	3.26	5.41	5452.55	2.98	6.90
23.653	8585.33	6.01	14.56	2933.87	5.36	10.77	6408.04	3.50	10.40
53.078	26706.24	18.69	33.26	9689.94	17.71	28.48	23068.23	12.60	23.00
263.205	32410.68	22.69	55.94	10035.76	18.34	46.83	33444.91	18.27	41.27
1849.764	62937.89	44.06	100.00	29090.08	53.17	100.00	107508.45	58.73	100.00
sum	142855.25	100.00		54707.55	100.00		183059.54	100.00	

Table 37 Bed material load for Mhlathuze Site 4 present-day

Q	Yang	% time	cum %	AW	% time	cum %	EH	% time	cum %
0.000	0.00	0.00	0.00	0.00	0.00	0.00	0.00	0.00	0.00
0.657	0.00	0.00	0.00	0.00	0.00	0.00	16.64	0.01	0.01
0.973	0.00	0.00	0.00	0.00	0.00	0.00	35.68	0.03	0.05
1.392	12.10	0.01	0.01	0.00	0.00	0.00	72.66	0.07	0.11
1.870	23.22	0.03	0.04	0.00	0.00	0.00	130.08	0.12	0.23
2.418	74.11	0.09	0.13	0.00	0.00	0.00	215.93	0.19	0.42
3.138	158.32	0.18	0.31	23.06	0.08	0.08	360.08	0.32	0.74
4.211	337.14	0.39	0.70	49.13	0.16	0.24	642.88	0.58	1.32
6.698	1341.73	1.55	2.25	267.81	0.89	1.13	1615.94	1.45	2.77
12.757	2990.14	3.46	5.72	707.11	2.36	3.49	2766.30	2.48	5.24
35.156	13489.26	15.62	21.34	4669.03	15.57	19.06	10410.12	9.32	14.57
202.479	25169.95	29.14	50.48	8202.25	27.36	46.42	24068.01	21.55	36.12
1530.548	42766.43	49.52	100.00	16064.15	53.58	100.00	71325.65	63.88	100.00
sum	86362.40	100.00		29982.55	100.00		111659.97	100.00	

Table 38 Bed material load for Olifants Site 1

Q	Yang	% time	cum %	AW	% time	cum %	EH	% time	cum %
0.047	0.00	0.00	0.00	0.00	0.00	0.00	3.22	0.00	0.00
0.259	3.11	0.01	0.01	0.00	0.00	0.00	48.02	0.02	0.02
0.336	6.03	0.02	0.03	0.00	0.00	0.00	73.39	0.03	0.05
0.448	11.65	0.04	0.07	1.36	0.02	0.02	121.90	0.05	0.10
0.663	25.47	0.09	0.16	3.14	0.05	0.08	236.92	0.10	0.20
1.088	78.86	0.27	0.43	8.61	0.15	0.22	554.56	0.23	0.43
1.897	225.21	0.77	1.20	30.99	0.53	0.76	1401.54	0.58	1.01
3.504	610.65	2.09	3.29	75.69	1.30	2.05	4147.73	1.72	2.73
7.364	2623.88	8.98	12.27	366.68	6.29	8.34	14106.79	5.84	8.57
15.013	4111.63	14.07	26.34	652.12	11.18	19.52	22593.70	9.35	17.92
32.792	10018.20	34.29	60.63	1865.39	31.98	51.49	61887.87	25.62	43.53
110.682	8667.30	29.67	90.30	2198.08	37.68	89.17	87353.68	36.16	79.69
361.246	2834.94	9.70	100.00	631.76	10.83	100.00	49068.26	20.31	100.00
sum	29216.94	100.00		5833.81	100.00		241597.59	100.00	

Table 39 Bed material load for Olifants Site 2

Q	Yang	% time	cum %	AW	% time	cum %	EH	% time	cum %
0.518	1071.59	0.04	0.04	232.08	0.01	0.01	3714.57	0.01	0.01
1.547	5562.06	0.23	0.27	1302.26	0.06	0.07	23603.19	0.05	0.06
2.105	2066.09	0.09	0.36	2066.09	0.09	0.16	41074.30	0.09	0.16
2.794	13157.19	0.54	0.90	3205.21	0.14	0.31	68719.26	0.16	0.31
3.877	21027.34	0.87	1.76	5321.48	0.24	0.55	122995.34	0.28	0.60
5.771	36882.56	1.52	3.28	9862.68	0.45	0.99	247536.02	0.57	1.16
9.109	70333.52	2.89	6.18	20428.82	0.92	1.91	548025.34	1.26	2.42
14.927	139894.72	5.76	11.93	44456.42	2.01	3.92	1309708.58	3.01	5.43
26.747	317107.12	13.05	24.98	117879.23	5.32	9.24	3704141.94	8.50	13.93
47.229	349833.60	14.39	39.38	211840.95	9.56	18.80	5139749.07	11.79	25.72
94.574	825695.58	33.98	73.35	1123710.12	50.71	69.50	13672379.55	31.37	57.09
278.456	549683.59	22.62	95.97	626482.90	28.27	97.77	15329879.41	35.18	92.27
721.615	97964.66	4.03	100.00	49333.81	2.23	100.00	3368383.07	7.73	100.00
sum	2430279.61	100.00		2216122.07	100.00		43579909.65	100.00	

Table 40 Bed material load for Olifants Site 3

Q	Yang	% time	cum %	AW	% time	cum %	EH	% time	cum %
0.068	0.00	0.00	0.00	0.00	0.00	0.00	0.00	0.00	0.00
0.220	0.00	0.00	0.00	0.00	0.00	0.00	0.96	0.00	0.00
0.292	0.00	0.00	0.00	0.00	0.00	0.00	1.77	0.00	0.00
0.368	0.00	0.00	0.00	0.00	0.00	0.00	4.03	0.01	0.01
0.467	0.00	0.00	0.00	0.00	0.00	0.00	6.49	0.01	0.02
0.639	7.38	0.13	0.13	0.00	0.00	0.00	12.60	0.02	0.05
0.993	6.29	0.11	0.24	0.00	0.00	0.00	35.75	0.06	0.11
1.709	43.70	0.77	1.01	4.01	0.11	0.11	116.35	0.21	0.32
3.381	215.50	3.79	4.79	34.57	0.97	1.09	570.91	1.02	1.33
6.808	381.85	6.71	11.50	72.73	2.05	3.13	1271.64	2.26	3.60
15.399	1518.31	26.67	38.17	478.95	13.47	16.61	6749.61	12.01	15.61
52.411	2003.30	35.19	73.36	1544.33	43.45	60.05	22810.94	40.59	56.20
186.472	1516.60	26.64	100.00	1419.82	39.95	100.00	24611.11	43.80	100.00
sum	5692.94	100.00		3554.42	100.00		56192.15	100.00	

Table 41 Bed material load for Olifants Site 4

Q	Yang	% time	cum %	AW	% time	cum %	EH	% time	cum %
0.291	0.00	0.00	0.00	0.00			0.00	0.00	0.00
0.834	0.00	0.00	0.00	0.00			0.00	0.00	0.00
1.111	0.00	0.00	0.00	0.00			0.00	0.00	0.00
1.421	0.00	0.00	0.00	0.00			0.00	0.00	0.00
1.812	0.00	0.00	0.00	0.00			5.07	0.08	0.08
2.371	0.00	0.00	0.00	0.00			15.39	0.24	0.31
3.286	0.00	0.00	0.00	0.00			31.38	0.48	0.79
5.052	12.15	1.40	1.40	0.00			77.46	1.19	1.98
9.294	74.78	8.61	10.01	0.00			190.05	2.91	4.89
17.391	123.19	14.19	24.20	0.00			273.60	4.19	9.07
37.601	271.30	31.25	55.45	0.00			993.16	15.20	24.27
121.635	261.56	30.13	85.58	0.00			2179.69	33.35	57.62
379.494	125.16	14.42	100.00	0.00			2769.72	42.38	100.00
sum	868.14	100.00		0.00			6535.51	100.00	

APPENDIX G

SUMMARY TABLES FOR ALL RIVERS

The following tables contain a number of symbols. The list below explains their meaning.

%	percentage duration on the 1-day daily flow duration curve
Q	discharge (m^3s^{-1})
R	hydraulic radius (m)
V	mean cross-sectional velocity (ms^{-1})
S	slope (m/m)
D_{16}	the sediment size in millimetres at which 16% of the sediment is finer
D_{50}	the sediment size in millimetres at which 50% of the sediment is finer
D_{84}	the sediment size in millimetres at which 84% of the sediment is finer
FFC	the flood frequency curve on the annual series. The values are return periods in years
PDS	the flood frequency curve on the partial duration series. The values are return periods in years
Max Y	the maximum competence in millimetres predicted using the Yang equation
Max AW	the maximum competence in millimetres predicted using the Ackers and White equation
Max EH	the maximum competence in millimetres predicted using the Engelund and Hansen equation
% tran Y	the percentage of bed material transported using the Yang equation
% tran AW	the percentage of bed material transported using the Ackers and White equation
% tran EH	the percentage of bed material transported using the Engelund and Hansen equation
τ	boundary shear stress calculated using average depth (area/width) in Newton metres squared
$\acute{\omega}$	unit stream power in Watts per metre squared
$Q_{1.5}$	The 1.5 year return period on the annual flood frequency curve
$Q_{2.44}$	The 2.44 year return period on the annual flood frequency curve
$Q_{0.9}$	The 0.9 year return period on the partial duration series flood frequency curve
$Q_{2.0}$	The 2.0 year return period on the partial duration series flood frequency curve

Table 1 Summary table for Mkomazi Site 1a

%	Q	R	V	S	D_{16}	D_{50}	D_{84}	FFC	PDS	Max Y	Max AW	Max EH	% tran Y	%tran AW	% tran EH	τ	ώ
9.999	0.015	0.141	0.006	0.0017	1.8	5.8	16			0	0	0	0	0	0	17.85	0.11
9.999	0.246	0.219	0.059	0.0021	1.8	5.8	16			0	0	0	0	0	0	28.29	1.63
9.999	0.355	0.266	0.070	0.0022	1.8	5.8	16			0	0	1.414	0	0	0.01	33.02	2.33
9.999	0.480	0.308	0.081	0.0023	1.8	5.8	16			0	0	1.414	0	0	0.02	38.13	3.10
9.999	0.655	0.356	0.094	0.0024	1.8	5.8	16			0	0	2.828	0	0	0.04	43.78	4.15
9.999	0.926	0.414	0.113	0.0026	1.8	5.8	16			0	0	11.314	0	0	0.10	50.22	5.72
9.999	1.391	0.489	0.142	0.0028	1.8	5.8	16			0	0	11.314	0	0	0.28	58.32	8.29
9.999	2.230	0.587	0.185	0.0031	1.8	5.8	16			0	0	11.314	0	0	0.77	68.22	12.67
9.999	3.991	0.726	0.260	0.0035	1.8	5.8	16			0.707	0	22.627	1.08	0	3.31	80.81	21.05
4.999	7.181	0.887	0.368	0.0041	1.8	5.8	16			1.414	0	22.627	4.31	0	6.73	93.79	34.60
3.999	13.467	1.086	0.538	0.0047	1.8	5.8	16	1.2	0.12	2.828	0.707	22.627	27.86	20.13	24.94	106.67	57.42
0.949	30.367	1.382	0.878	0.0058	1.8	5.8	16	2.4	0.93	2.828	1.414	90.510	47.15	42.67	39.88	116.81	102.59
0.08	69.606	1.702	1.434	0.0070	1.8	5.8	16	10.1	8.10	11.314	11.314	90.510	19.60	37.20	23.93	120.83	173.02

Feature	Q	R	V	S	D_{16}	D_{50}	D_{84}	FFC	PDS	τ	ώ
bench	67.07	1.737	1.333	0.0060	1.8	5.8	16	10	8	107.46	143.26
Estimated Q	145.97	2.118	1.987	0.0100	1.8	5.8	16	39	39	219.76	436.88
terrace 1	327.64	1.669	2.973	0.0135	1.8	5.8	16	39	39	227.74	677.11
terrace 2	1059.83	1.959	3.639	0.0135	1.8	5.8	16	39	39	263.21	957.90

Annual series flood frequency curve		Dominant discharge			Partial series flood frequency curve	
$Q_{1.5}$	$Q_{2.44}$	Yang	AW	EH	$Q_{0.9}$	$Q_{2.0}$
17.53	30.617	16.46	20.14	13.66	29.9	38.2

Table 2 Summary table for Mkomazi Site 1b

%	Q	R	V	S	D_{16}	D_{50}	D_{84}	FFC	PDS	Max Y	Max AW	Max EH	% tran Y	%tran AW	% tran EH	τ	ω
9.999	0.015	0.240	0.003	0.0017	1.8	5.6	16			0	0	0	0	0	0	4.12	0.01
9.999	0.246	0.460	0.027	0.0022	1.8	5.6	16			0	0	0	0	0	0	10.13	0.28
9.999	0.355	0.510	0.036	0.0023	1.8	5.6	16			0	0	1.414	0	0	0.01	11.76	0.42
9.999	0.480	0.550	0.044	0.0024	1.8	5.6	16			0	0	1.414	0	0	0.02	13.37	0.59
9.999	0.655	0.60	0.055	0.0025	1.8	5.6	16			0	0	2.828	0	0	0.04	15.31	0.85
9.999	0.926	0.66	0.071	0.0026	1.8	5.6	16			0	0	11.314	0	0	0.10	17.92	1.27
9.999	1.391	0.73	0.095	0.0029	1.8	5.6	16			0	0	11.314	0	0	0.27	21.71	2.06
9.999	2.230	0.83	0.133	0.0031	1.8	5.6	16			0	0	11.314	0	0	0.78	27.31	3.63
9.999	3.991	0.98	0.195	0.0036	1.8	5.6	16			0	0	22.627	0	0	3.33	37.28	7.27
4.999	7.181	1.11	0.303	0.0041	1.8	5.6	16			0.707	0	22.627	2.44	0	6.81	48.59	14.72
3.999	13.467	1.29	0.468	0.0048	1.8	5.6	16	1.2	0.12	1.414	0.707	22.627	20.44	16.54	25.18	66.53	31.16
0.949	30.367	1.57	0.816	0.0058	1.8	5.6	16	2.4	0.93	2.828	1.414	90.51	53.59	44.24	39.16	99.67	81.34
0.08	69.606	1.91	1.425	0.0070	1.8	5.6	16	10.1	8.1	11.314	11.314	90.51	23.54	39.22	24.31	147.94	210.85

Feature	Q	R	V	S	D_{16}	D_{50}	D_{84}	FFC	PDS	τ	ω
Estimated Q	107.53	1.53	1.88	0.010	1.8	5.6	16	39	39	214.62	405.52
terrace 1	187.55	1.79	2.69	0.012	1.8	5.6	16	39	39	228.61	615.39
terrace 2	829.69	1.93	3.09	0.0135	1.8	5.6	16	39	39	233.82	724.43

Annual series flood frequency curve		Dominant discharge			Partial series flood frequency curve	
$Q_{1.5}$	$Q_{2.44}$	Yang	AW	EH	$Q_{0.9}$	$Q_{2.0}$
17.53	30.617	19.3	21.22	13.6	29.9	38.2

Table 3 Summary table for Mkomazi Site 1c

%	Q	R	V	S	D_{16}	D_{50}	D_{84}	FFC	PDS	Max Y	Max AW	Max EH	% tran Y	%tran AW	% tran EH	τ	ω
9.999	0.015	0.385	0.002	0.0017	1.8	5.6	16			0	0	0	0	0	0	6.64	0.01
9.999	0.246	0.487	0.023	0.0022	1.8	5.6	16			0	0	0	0	0	0	10.44	0.24
9.999	0.355	0.512	0.032	0.0023	1.8	5.6	16			0	0	0.707	0	0	0.01	11.53	0.36
9.999	0.480	0.534	0.041	0.0024	1.8	5.6	16			0	0	1.414	0	0	0.02	12.58	0.51
9.999	0.655	0.560	0.053	0.0025	1.8	5.6	16			0	0	2.828	0	0	0.05	13.87	0.73
9.999	0.926	0.593	0.070	0.0026	1.8	5.6	16			0	0	11.314	0	0	0.14	15.59	1.09
9.999	1.391	0.638	0.097	0.0029	1.8	5.6	16			0	0	11.314	0	0	0.39	18.12	1.75
9.999	2.230	0.699	0.139	0.0031	1.8	5.6	16			0	0	11.314	0	0	1.13	21.90	3.05
9.999	3.991	0.786	0.216	0.0036	1.8	5.6	16			0.707	0	22.627	1.31	0	4.82	28.10	6.08
4.999	7.181	0.891	0.295	0.0041	1.8	5.6	16			0.707	0	22.627	7.01	0	9.77	36.70	12.15
3.999	13.467	1.229	0.331	0.0048	1.8	5.6	16	1.2	0.12	0.707	0	22.627	10.02	0	29.09	70.31	20.75
0.949	30.367	1.448	0.527	0.0058	1.8	5.6	16	2.4	0.93	2.828	0.707	45.255	47.93	43.99	38.26	85.54	45.07
0.08	69.606	1.453	0.885	0.0070	1.8	5.6	16	10.1	8.1	2.828	1.414	90.510	33.72	56.01	16.32	86.38	76.47

Feature	Q	R	V	S	D_{16}	D_{50}	D_{84}	FFC	PDS	τ	ω
Estimated Q	108.01	1.35	1.11	0.0080	1.8	5.6	16	39	39	111.09	123.38
terrace 1	219.370	1.38	1.45	0.0090	1.8	5.6	16	39	39	120.70	174.62
terrace 2	518.150	1.63	2.29	0.0135	1.8	5.6	16	39	39	217.85	499.96

Annual series flood frequency curve		Dominant discharge			Partial series flood frequency curve	
$Q_{1.5}$	$Q_{2.44}$	Yang	AW	EH	$Q_{0.9}$	$Q_{2.0}$
17.53	30.617	17.42	34.4	12.27	29.9	38.2

Table 4 Summary table for Mkomazi Site 2a

%	Q	R	V	S	D_{16}	D_{50}	D_{84}	FFC	PDS	Max Y	Max AW	Max EH	% tran Y	%tran AW	% tran EH	τ	ώ
9.999	0.025	0.221	0.009	0.0030	2.8	10	45			0	0	0	0	0	0	6.58	0.06
9.999	0.424	0.356	0.074	0.0031	2.8	10	45			0	0	1.414	0	0	0.01	10.73	0.80
9.999	0.613	0.389	0.095	0.0031	2.8	10	45			0	0	5.651	0	0	0.06	11.78	1.12
9.999	0.830	0.420	0.116	0.0031	2.8	10	45			0	0	5.651	0	0	0.10	12.77	1.48
9.999	1.132	0.455	0.141	0.0031	2.8	10	45			0	0	5.651	0	0	0.18	13.89	1.96
9.999	1.599	0.499	0.175	0.0031	2.8	10	45			0	0	11.314	0	0	0.38	15.31	2.68
9.999	2.402	0.556	0.225	0.0031	2.8	10	45			0	0	22.627	0	0	0.88	17.17	3.86
9.999	3.852	0.638	0.296	0.0032	2.8	10	45			0	0	22.627	0	0	2.27	19.93	5.90
9.999	6.893	0.758	0.413	0.0032	2.8	10	45			1.414	0	22.627	2.46	0	6.74	24.06	9.94
4.999	12.404	0.908	0.571	0.0032	2.8	10	45			2.828	0	22.627	10.01	0	10.04	29.37	16.76
3.999	23.643	1.166	0.811	0.0033	2.8	10	45	1.2	0.12	2.828	1.414	22.627	36.82	11.56	29.68	38.76	31.43
0.049	54.193	1.573	1.276	0.0034	2.8	10	45	2.44	0.93	11.314	5.651	90.51	36.86	42.41	34.43	54.20	69.14
0.08	124.21	2.051	1.982	0.0035	2.8	10	45	12.5	9.7	45.255	22.629	90.51	13.85	46.02	15.22	73.26	145.17

Feature	Q	R	V	S	D_{16}	D_{50}	D_{84}	FFC	PDS	τ	ώ
bench	71.77	1.884	1.289	0.0035	2.8	10	45	4.8	2.17	260.17	335.52
Estimated Q	320.05	2.610	2.884	0.0037	2.8	10	45	39	39	267.73	772.16
terrace 1	542.84	1.848	3.095	0.0038	2.8	10	45	39	39	111.05	343.78
terrace 2	1046.21	2.297	3.625	0.0039	2.8	10	45	39	39	137.55	498.74

Annual series flood frequency curve		Dominant discharge			Partial series flood frequency curve	
$Q_{1.5}$	$Q_{2.44}$	Yang	AW	EH	$Q_{0.9}$	$Q_{2.0}$
31.13	54.64	24.19	41.04	18.96	53	68.25

Table 5 Summary table for Mkomazi Site 2b

%	Q	R	V	S	D_{16}	D_{50}	D_{84}	FFC	PDS	Max Y	Max AW	Max EH	% tran Y	%tran AW	% tran EH	τ	ώ
9.999	0.025	0.286	0.006	0.0030	2.8	10	45			0	0	0	0	0	0	8.5	0.05
9.999	0.424	0.427	0.061	0.0031	2.8	10	45			0	0	1.414	0	0	0.01	12.93	0.79
9.999	0.613	0.460	0.080	0.0031	2.8	10	45			0	0	5.651	0	0	0.06	14.00	1.13
9.999	0.830	0.489	0.100	0.0031	2.8	10	45			0	0	5.651	0	0	0.10	14.97	1.50
9.999	1.132	0.523	0.125	0.0031	2.8	10	45			0	0	5.651	0	0	0.17	16.10	2.01
9.999	1.599	0.565	0.159	0.0031	2.8	10	45			0	0	11.314	0	0	0.40	17.50	2.79
9.999	2.402	0.621	0.210	0.0031	2.8	10	45			0	0	22.627	0	0	0.92	19.42	4.08
9.999	3.852	0.693	0.287	0.0032	2.8	10	45			0	0	22.627	0	0	2.40	21.92	6.29
9.999	6.893	0.800	0.415	0.0032	2.8	10	45			1.414	0	22.627	2.34	0	7.18	25.67	10.645
4.999	12.404	0.921	0.592	0.0032	2.8	10	45			2.828	0	22.627	10.46	0	10.61	30.11	17.82
3.999	23.643	1.094	0.857	0.0033	2.8	10	45	1.2	0.12	2.828	1.414	22.627	36.62	10.65	29.59	36.61	31.37
0.949	54.193	1.427	1.344	0.0034	2.8	10	45	2.44	0.93	11.314	5.651	90.51	36.32	43.8	33.08	49.31	66.28
0.08	124.21	1.950	2.104	0.0035	2.8	10	45	12.5	9.7	45.255	22.627	90.51	14.26	45.55	15.45	70.38	148.07

Feature	Q	R	V	S	D_{16}	D_{50}	D_{84}	FFC	PDS	τ	ώ
bench	96.95	1.99	1.60	0.0037	2.8	10	45	7	3.6	76.46	122.58
Estimated Q	381.50	1.89	3.14	0.0038	2.8	10	45	39	39	73.97	232.58
terrace 1	1110.75	2.09	3.40	0.0039	2.8	10	45	39	39	81.62	277.74

Annual series flood frequency curve		Dominant discharge			Partial series flood frequency curve	
$Q_{1.5}$	$Q_{2.44}$	Yang	AW	EH	$Q_{0.9}$	$Q_{2.0}$
31.13	54.64	24.13	41.95	18.50	53	68.25

Table 6 Summary table for Mkomazi Site 2c

%	Q	R	V	S	D_{16}	D_{50}	D_{84}	FFC	PDS	Max Y	Max AW	Max EH	% tran Y	%tran AW	% tran EH	τ	ω
9.999	0.025	0.222	0.016	0.0030	2.8	10	45			0	0	0	0	0	0	6.63	0.11
9.999	0.424	0.357	0.063	0.0031	2.8	10	45			0	0	1.414	0	0	0.01	10.85	0.69
9.999	0.613	0.430	0.075	0.0031	2.8	10	45			0	0	1.414	0	0	0.02	13.18	0.98
9.999	0.830	0.495	0.087	0.0031	2.8	10	45			0	0	5.651	0	0	0.10	15.26	1.32
9.999	1.132	0.566	0.102	0.0031	2.8	10	45			0	0	5.651	0	0	0.18	17.61	1.79
9.999	1.599	0.652	0.123	0.0031	2.8	10	45			0	0	11.314	0	0	0.39	20.46	2.51
9.999	2.402	0.767	0.154	0.0031	2.8	10	45			0	0	22.627	0	0	0.91	24.25	3.74
9.999	3.852	0.908	0.203	0.0032	2.8	10	45			0	0	22.627	0	0	2.76	29.23	5.92
9.999	6.893	1.092	0.286	0.0032	2.8	10	45			0	0	22.627	0	0	7.39	35.83	10.25
4.999	12.404	1.265	0.407	0.0032	2.8	10	45			0	0	22.627	0	0	10.97	42.33	17.23
3.999	23.643	1.536	0.598	0.0033	2.8	10	45	1.2	0.12	2.828	0	22.627	36.19	0	31.73	52.78	31.54
0.949	54.193	1.793	0.972	0.0034	2.8	10	45	2.44	0.93	2.828	1.414	90.51	46.83	30.52	32.89	63.10	61.35
0.08	124.21	2.034	1.508	0.0035	2.8	10	45	12.5	9.7	22.627	11.314	90.51	16.98	67.48	12.64	72.83	109.81

Feature	Q	R	V	S	D_{16}	D_{50}	D_{84}	FFC	PDS	τ	ω
bench	15.833	1.40	0.46	0.0035	1.8	5.6	45			50.70	23.41
Estimated Q.	102.184	2.05	1.21	0.0036	1.8	5.6	45	7.8	5	75.99	92.04
terrace 1	152.965	1.86	1.53	0.0037	1.8	5.6	45	19	13.5	70.28	107.78
terrace 2	1010.589	2.79	3.10	0.0039	1.8	5.6	45	39	39	109.27	338.38

Annual series flood frequency curve		Dominant discharge			Partial series flood frequency curve	
$Q_{1.5}$	$Q_{2.44}$	Yang	AW	EH	$Q_{0.9}$	$Q_{2.0}$
31.13	54.64	31.17	31.17	18.31	53	68.25

Table 7 Summary table for Mkomazi Site 3a

%	Q	R	V	S	D_{16}	D_{50}	D_{84}	FFC	PDS	Max Y	Max AW	Max EH	% tran Y	%tran AW	% tran EH	τ	ώ
9.999	0.044	0.198	0.008	0.0003	1.1	4.2	13.7			0	0	0	0	0	0	0.52	0.00
9.999	1.250	0.616	0.064	0.0005	1.1	4.2	13.7			0	0	0	0	0	0	2.91	0.19
9.999	1.807	0.699	0.080	0.0005	1.1	4.2	13.7			0	0	0	0	0	0	3.64	0.29
9.999	2.445	0.775	0.097	0.0006	1.1	4.2	13.7			0	0	0.707	0	0	0.01	4.38	0.43
9.999	3.336	0.861	0.118	0.0006	1.1	4.2	13.7			0	0	0.707	0	0	0.03	5.32	0.63
9.999	4.713	0.967	0.147	0.0007	1.1	4.2	13.7			0	0	0.707	0	0	0.07	6.60	0.97
9.999	7.079	1.106	0.189	0.0008	1.1	4.2	13.7			0	0	1.414	0	0	0.25	8.50	1.61
9.999	11.353	1.290	0.253	0.0009	1.1	4.2	13.7			0.707	0	1.414	0.49	0	0.80	11.39	2.88
9.999	20.318	1.547	0.361	0.0010	1.1	4.2	13.7			1.414	0	11.314	3.42	0	3.52	16.18	5.84
4.999	36.559	1.884	0.517	0.0012	1.1	4.2	13.7			2.828	0.707	11.314	9.86	6.97	7.95	23.25	12.02
3.999	68.557	2.301	0.756	0.0014	1.1	4.2	13.7	1.2	0.12	2.828	1.414	22.627	32.08	31.81	29.15	33.40	25.26
0.949	146.69	2.893	1.192	0.0017	1.1	4.2	13.7	2.4	0.92	5.651	1.414	45.255	40.56	37.57	40.63	49.91	59.50
0.08	307.13	3.482	1.824	0.0019	1.1	4.2	13.7	12.5	9.5	22.627	11.314	45.255	13.59	23.65	17.59	68.82	125.56

Feature	Q	R	V	S	D_{16}	D_{50}	D_{84}	FFC	PDS	τ	ώ
bench	25.641	1.33	0.54	0.0012	1.1	4.2	13.7			16.15	8.69
Estimated Q.	509.403	3.43	2.27	0.0025	1.1	4.2	13.7	39	39	88.35	200.88
terrace 1	1491.261	3.54	3.54	0.0029	1.1	4.2	13.7	39	39	102.14	361.95

Annual series flood frequency curve		Dominant discharge			Partial series flood frequency curve	
$Q_{1.5}$	$Q_{2.44}$	Yang	AW	EH	$Q_{0.9}$	$Q_{2.0}$
89.45	147.960	66.84	76.84	66.51	146	179.5

Table 8 Summary table for Mkomazi Site 3b

%	Q	R	V	S	D_{16}	D_{50}	D_{84}	FFC	PDS	Max Y	Max AW	Max EH	% tran Y	%tran AW	% tran EH	τ	ω
9.999	0.044	0.349	0.007	0.0003	1.1	4.2	13.7			0	0	0	0	0	0	0.92	0.01
9.999	1.250	0.505	0.110	0.0005	1.1	4.2	13.7			0	0	0	0	0	0	2.42	0.27
9.999	1.807	0.522	0.143	0.0005	1.1	4.2	13.7			0	0	0.707	0	0	0.01	2.76	0.39
9.999	2.445	0.540	0.175	0.0006	1.1	4.2	13.7			0	0	0.707	0	0	0.02	3.10	0.54
9.999	3.336	0.561	0.214	0.0006	1.1	4.2	13.7			0	0	0.707	0	0	0.04	3.52	0.75
9.999	4.713	0.587	0.264	0.0007	1.1	4.2	13.7			0.707	0	1.414	0.06	0	0.11	4.06	1.07
9.999	7.079	0.592	0.330	0.0008	1.1	4.2	13.7			0.707	0	1.414	0.28	0	0.27	4.60	1.52
9.999	11.353	0.703	0.419	0.0009	1.1	4.2	13.7			1.414	0.707	1.414	1.32	0.86	0.82	6.29	2.63
9.999	20.318	0.804	0.562	0.0010	1.1	4.2	13.7			2.828	0.707	11.314	6.02	4.58	3.59	9.48	5.33
4.999	36.559	1.129	0.756	0.0012	1.1	4.2	13.7			2.828	1.414	11.314	12.29	10.53	7.9	14.12	10.68
3.999	68.557	1.430	1.037	0.0014	1.1	4.2	13.7	1.2	0.12	5.651	2.828	22.627	35.41	31.74	28.17	21.07	21.84
0.949	146.69	1.989	1.517	0.0017	1.1	4.2	13.7	2.4	0.92	22.627	11.314	22.627	33.76	37.06	40.25	34.79	52.78
0.08	307.13	2.714	2.210	0.0019	1.1	4.2	13.7	12.5	9.5	45.255	22.627	45.555	10.86	15.24	18.83	55.06	121.65

Feature	Q	R	V	S	D_{16}	D_{50}	D_{84}	FFC	PDS	τ	ω
bench	78.15	1.53	1.13	0.0018	1.1	4.2	13.7	1.3	0.15	28.43	32.08
Estimated Q_c	530.73	3.71	2.66	0.0025	1.1	4.2	13.7	-39	-39	99.59	265.15
terrace 1	783.19	3.83	3.27	0.0029	1.1	4.2	13.7	-39	-39	116.33	380.40
terrace 2	1526.88	4.37	4.76	0.0029	1.1	4.2	13.7	-39	-39	131.63	626.06

Annual series flood frequency curve		Dominant discharge			Partial series flood frequency curve	
$Q_{1.5}$	$Q_{2.44}$	Yang	AW	EH	$Q_{0.9}$	$Q_{2.8}$
89.45	147.960	58	62.9	66.13	146	179.5

Table 9 Summary table for Mkomazi Site 3c

%	Q	R	V	S	D_{16}	D_{50}	D_{84}	FFC	PDS	Max Y	Max AW	Max EH	% tran Y	%tran AW	% tran EH	τ	ώ
9.999	0.044	0.122	0.012	0.0003	1.1	4.2	13.7			0	0	0	0	0	0	0.32	0.00
9.999	1.250	0.629	0.054	0.0005	1.1	4.2	13.7			0	0	0	0	0	0	2.96	0.16
9.999	1.807	0.721	0.068	0.0005	1.1	4.2	13.7			0	0	0	0	0	0	3.74	0.25
9.999	2.445	0.805	0.081	0.0006	1.1	4.2	13.7			0	0	0.707	0	0	0.01	4.53	0.37
9.999	3.336	0.901	0.098	0.0006	1.1	4.2	13.7			0	0	0.707	0	0	0.02	5.55	0.54
9.999	4.713	1.020	0.121	0.0007	1.1	4.2	13.7			0	0	0.707	0	0	0.06	6.95	0.84
9.999	7.079	1.174	0.156	0.0008	1.1	4.2	13.7			0	0	1.414	0	0	0.23	9.04	1.41
9.999	11.353	1.374	0.212	0.0009	1.1	4.2	13.7			0.707	0	1.414	0.20	0	0.89	12.19	2.58
9.999	20.318	1.656	0.309	0.0010	1.1	4.2	13.7			0.707	0	11.314	2.16	0	3.33	17.47	5.39
4.999	36.559	1.981	0.454	0.0012	1.1	4.2	13.7			1.414	0.707	11.314	7.73	5.02	7.58	24.70	11.21
3.999	68.557	2.381	0.688	0.0014	1.1	4.2	13.7	1.2	0.12	2.828	0.707	22.627	34.86	24.63	28.33	35.09	24.13
0.949	146.69	2.929	1.141	0.0017	1.1	4.2	13.7	2.4	0.92	5.561	1.414	22.627	40.49	41.32	40.85	52.10	59.42
0.08	307.13	3.516	1.862	0.0019	1.1	4.2	13.7	12.5	9.5	22.627	11.314	45.258	14.56	29.03	18.7	71.59	133.30

Feature	Q	R	V	S	D_{16}	D_{50}	D_{84}	FFC	PDS	τ	ώ
Estimated Q_b	406.436	3.75	2.19	0.0025	1.1	4.2	13.7	30	30	100.73	220.95

Annual series flood frequency curve		Dominant discharge			Partial series flood frequency curve	
$Q_{1.5}$	$Q_{2.44}$	Yang	AW	EH	$Q_{0.9}$	$Q_{2.0}$
89.45	147.96	71.53	84.74	67.15	146	179.5

Table 10 Summary table for Mkomazi Site 4a

%	Q	R	V	S	D_{16}	D_{50}	D_{84}	FFC	PDS	Max Y	Max AW	Max EH	% tran Y	%tran AW	% tran EH	τ	ω
9.999	0.079	0.440	0.009	0.0020	0.35	12	15			0	0	0	0	0	0	8.97	0.08
9.999	1.317	0.614	0.072	0.0021	0.35	12	15			0	0	0	0	0	0.03	12.92	0.93
9.999	1.904	0.663	0.092	0.0021	0.35	12	15			0	0	0	0	0	0.07	14.07	1.29
9.999	2.576	0.704	0.112	0.0021	0.35	12	15			0.354	0	0.01	0	0	0.12	15.03	1.69
9.999	3.515	0.751	0.137	0.0021	0.35	12	15			0.354	0	0.05	0	0	0.21	16.16	2.21
9.999	4.966	0.856	0.169	0.0021	0.35	12	15			0.354	0	0.15	0	0	0.42	18.25	3.09
9.999	7.458	0.980	0.217	0.0022	0.35	12	15			0.707	0.354	0.61	0.35	0.35	1.03	21.37	4.65
9.999	11.961	1.160	0.291	0.0022	0.35	12	15			0.707	0.354	2.25	1.23	1.23	2.63	25.68	7.46
9.999	21.406	1.432	0.414	0.0023	0.35	12	15			1.414	0.707	8.84	6.75	6.75	8.30	32.23	13.34
4.999	38.518	1.759	0.589	0.0023	0.35	12	15			2.828	0.707	15.61	13.41	13.41	14.26	40.56	23.89
3.999	72.230	2.193	0.856	0.0024	0.35	12	15	1.2	0.12	2.828	1.414	41.37	42.76	42.76	42.23	52.20	44.68
0.949	154.55	2.872	1.343	0.0024	0.35	12	15	2.4	0.92	2.828	1.414	16.59	16.59	16.59	17.62	72.07	96.80
0.08	323.58	2.966	2.014	0.0025	0.35	12	15	12.5	8	45.255	22.627	10.15	18.9	18.90	13.07	78.72	158.27

Feature	Q	R	V	S	D_{16}	D_{50}	D_{84}	FFC	PDS	τ	ω
bench	35.05	1.73	0.53	0.0025	0.35	12	15			44.69	23.51
Estimated Q	171.52	2.81	1.45	0.0026	0.35	12	15	3.3	1.25	78.37	113.64
terrace 1	381.94	3.01	2.21	0.0028	0.35	12	15	19	13	88.56	195.33
terrace 2	844.05	3.43	3.01	0.0028	0.35	12	15	39	39	99.31	298.86

Annual series flood frequency curve		Dominant discharge			Partial series flood frequency curve	
$Q_{1.5}$	$Q_{2.44}$	Yang	AW	EH	$Q_{0.9}$	$Q_{2.0}$
94.03	155.670	53.14	57.22	51.68	154	189

Table 11 Summary table for Mkomazi Site 4b

%	Q	R	V	S	D_{16}	D_{50}	D_{84}	FFC	PDS	Max Y	Max AW	Max EH	% tran Y	%tran AW	% tran EH	τ	ω
9.999	0.079	0.333	0.012	0.0020	0.35	12	15			0	0	0.707	0	0	0	7	0.09
9.999	1.317	0.612	0.100	0.0021	0.35	12	15			0	0	1.414	0	0	0.04	13.44	1.35
9.999	1.904	0.675	0.129	0.0021	0.35	12	15			0.354	0	1.414	0.01	0	0.08	14.98	1.93
9.999	2.576	0.731	0.158	0.0021	0.35	12	15			0.354	0	1.414	0.04	0	0.14	16.38	2.59
9.999	3.515	0.778	0.195	0.0021	0.35	12	15			0.707	0.354	2.828	0.11	0.05	0.25	17.59	3.43
9.999	4.966	0.802	0.243	0.0021	0.35	12	15			0.707	0.354	2.828	0.35	0.14	0.44	18.22	4.42
9.999	7.458	0.838	0.310	0.0022	0.35	12	15			0.707	0.707	5.651	1.01	0.53	0.98	19.22	5.96
9.999	11.961	0.920	0.402	0.0022	0.35	12	15			1.414	0.707	22.627	2.92	1.84	2.25	21.40	8.60
9.999	21.406	1.173	0.553	0.0023	0.35	12	15			2.828	0.707	22.627	9	6.87	7.73	28.19	15.59
4.999	38.518	1.498	0.757	0.0023	0.35	12	15			2.828	1.414	22.627	14.58	11.47	12.15	37.25	28.19
3.999	72.230	1.797	1.093	0.0024	0.35	12	15	1.2	0.12	2.828	1.414	45.255	36.44	34.61	34.40	45.92	50.19
0.949	154.55	2.217	1.634	0.0024	0.35	12	15	2.4	0.92	22.627	11.314	90.51	27.51	33	30.22	58.04	94.85
0.08	323.58	2.809	2.368	0.0025	0.35	12	15	12.5	8	45.255	22.627	90.51	8.03	11.50	11.33	76.09	180.19

Feature	Q	R	V	S	D_{16}	D_{50}	D_{84}	FFC	PDS	τ	ω
bench	63.02	1.72	1.03	0.0025	0.35	12	15	1.12	0.1	46.62	47.88
Estimated Q	319.48	2.84	2.27	0.0026	0.35	12	15	11	8	80.18	182.10
terrace 1	532.08	3.39	2.98	0.0028	0.35	12	15	39	39	102.99	307.29
terrace 2	967.62	3.49	4.06	0.0028	0.35	12	15	39	39	103.93	421.85

Annual series flood frequency curve		Dominant discharge			Partial series flood frequency curve	
$Q_{1.5}$	$Q_{2.44}$	Yang	AW	EH	$Q_{0.9}$	$Q_{2.0}$
94.03	155.670	52.07	58.63	54.34	154	189

Table 12 Summary table for Mkomazi Site 5a

%	Q	R	V	S	D_{16}	D_{50}	D_{84}	FFC	PDS	Max Y	Max AW	Max EH	% tran Y	%tran AW	% tran EH	τ	ω
9.999	0.133	1.374	0.003	0.0002	0.18	1.7	15			0	0	0	0	0	0	2.16	0.01
9.999	2.211	1.518	0.045	0.0004	0.18	1.7	15			0	0	0	0	0	0	6.33	0.28
9.999	3.195	1.575	0.062	0.0005	0.18	1.7	15			0	0	0	0	0	0	7.54	0.47
9.999	4.322	1.626	0.081	0.0005	0.18	1.7	15			0	0	1.414	0	0	0.01	8.72	0.70
9.999	5.898	1.684	0.105	0.0006	0.18	1.7	15			0.177	0	1.414	0.01	0	0.03	10.13	1.07
9.999	8.332	1.774	0.141	0.0007	0.18	1.7	15			0.354	0.177	2.828	0.03	0.01	0.07	11.98	1.70
9.999	12.515	1.879	0.199	0.0008	0.18	1.7	15			0.354	0.177	5.651	0.13	0.05	0.22	14.61	2.91
9.999	20.071	2.022	0.293	0.0009	0.18	1.7	15			0.707	0.354	5.651	0.57	0.26	0.69	18.38	5.38
9.999	35.919	2.239	0.466	0.0011	0.18	1.7	15			1.414	0.707	11.314	3.39	1.73	3.27	24.29	11.31
4.999	64.631	2.501	0.733	0.0013	0.18	1.7	15			2.828	1.414	11.314	9.37	4.98	7.23	31.92	23.39
3.999	131.92	2.916	1.246	0.0015	0.18	1.7	15	1.2	0.12	5.651	5.651	22.627	36.40	28	31.12	43.59	54.26
0.949	291.28	3.525	2.159	0.0018	0.18	1.7	15	2.7	0.92	11.314	22.627	45.255	39.96	45.10	46.16	54.54	117.74
0.08	503.13	3.172	3.037	0.0020	0.18	1.7	15	13	9.7	90.51	45.255	45.255	10.15	16.87	11.20	63.83	193.87

Feature	Q	R	V	S	D_{16}	D_{50}	D_{84}	FFC	PDS	τ	ω
bench	114.879	2.75	1.10	0.0005	0.18	1.7	15	1.16	0.09	14.19	15.58
Estimated Q	199.777	2.97	1.67	0.0008	0.18	1.7	15	1.64	0.27	24.53	40.92
terrace 1	630.994	3.22	3.68	0.0035	0.18	1.7	15	36	35	115.80	426.58
terrace 2	1783.64	4.53	6.06	0.0044	0.18	1.7	15	39	39	207.35	1256.73

Annual series flood frequency curve		Dominant discharge			Partial series flood frequency curve	
$Q_{1.5}$	$Q_{2.44}$	Yang	AW	EH	$Q_{0.9}$	$Q_{2.0}$
182.4	293.100	127.19	149.96	132.5	286	346.5

Table 13 Summary table for Mkomazi Site 5b

%	Q	R	V	S	D_{16}	D_{50}	D_{84}	FFC	PDS	Max Y	Max AW	Max EH	% tran Y	%tran AW	% tran EH	τ	ώ
9.999	0.133	0.986	0.004	0.0002	0.18	1.7	15			0	0	0	0	0	0	1.54	0.01
9.999	2.211	1.299	0.048	0.0004	0.18	1.7	15			0	0	0	0	0	0	5.40	0.26
9.999	3.195	1.374	0.065	0.0005	0.18	1.7	15			0	0	0	0	0	0	6.56	0.43
9.999	4.322	1.442	0.083	0.0005	0.18	1.7	15			0	0	1.414	0	0	0.01	7.71	0.64
9.999	5.898	1.519	0.106	0.0006	0.18	1.7	15			0.177	0	1.414	0.01	0	0.03	9.11	0.96
9.999	8.332	1.639	0.138	0.0007	0.18	1.7	15			0.354	0.177	2.828	0.04	0.02	0.08	10.97	1.52
9.999	12.515	1.773	0.189	0.0008	0.18	1.7	15			0.354	0.177	2.828	0.14	0.06	0.22	13.62	2.58
9.999	20.071	1.951	0.270	0.0009	0.18	1.7	15			0.707	0.354	5.651	0.60	0.32	0.70	17.57	4.74
9.999	35.919	2.221	0.414	0.0011	0.18	1.7	15			1.414	0.354	5.651	3.40	1.92	3.27	24.05	9.96
4.999	64.631	2.551	0.633	0.0013	0.18	1.7	15			2.828	0.707	11.314	9.15	5.32	7.23	32.65	20.66
3.999	131.92	3.055	1.048	0.0015	0.18	1.7	15	1.2	0.12	2.828	2.828	22.627	36.63	28.64	31.18	46.05	48.23
0.949	291.28	3.790	1.775	0.0018	0.18	1.7	15	2.7	0.92	22.627	11.314	45.255	39.96	47.03	46.37	60.06	106.59
0.08	503.13	3.307	2.498	0.0020	0.18	1.7	15	13	9.7	45.255	22.627	45.255	10.07	16.69	10.91	66.71	166.62

Feature	Q	R	V	S	D_{16}	D_{50}	D_{84}	FFC	PDS	τ	ώ
Estimated Q_b	131.085	2.94	1.02	0.0005	0.18	1.7	15	1.2	0.12	15.46	15.77
terrace 1	442.324	3.91	2.34	0.0008	0.18	1.7	15	7.7	3.8	33.40	78.13
terrace 2	1172.116	4.04	4.48	0.0028	0.18	1.7	15	39	39	119.19	533.41

Annual series flood frequency curve		Dominant discharge			Partial series flood frequency curve	
$Q_{1.5}$	$Q_{2.44}$	Yang	AW	EH	$Q_{0.9}$	$Q_{2.0}$
182.4	293.100	127.19	149.96	132.50	286	346.5

Table 14 Summary table for Mkomazi Site 6a

%	Q	R	V	S	D_{16}	D_{50}	D_{84}	FFC	PDS	Max Y	Max AW	Max EH	% tran Y	%tran AW	% tran EH	τ	ω
0.999	0.136	0.463	0.008	0.0015	3.8	26	100			0	0	0	0	0	0	6.88	0.05
0.999	2.255	0.648	0.072	0.0017	3.8	26	100			0	0	1.414	0	0	0.01	11.16	0.81
0.999	3.26	0.703	0.095	0.0018	3.8	26	100			0	0	1.414	0	0	0.02	12.52	1.18
0.999	4.41	0.755	0.118	0.0018	3.8	26	100			0	0	2.828	0	0	0.05	13.88	1.63
0.999	6.017	0.815	0.147	0.0019	3.8	26	100			0	0	2.828	0	0	0.10	15.51	2.27
0.999	8.501	0.881	0.187	0.0020	3.8	26	100			0	0	2.828	0	0	0.21	17.45	3.26
0.999	12.767	0.959	0.247	0.0021	3.8	26	100			0.707	0	2.828	0.17	0	0.5	19.98	4.93
0.999	20.476	1.028	0.337	0.0022	3.8	26	100			0.707	0	2.828	0.76	0	1.37	22.79	7.68
0.999	36.644	1.195	0.485	0.0024	3.8	26	100			1.414	0.707	45.255	4.63	3.11	4.75	28.62	13.88
4.999	65.937	1.471	0.697	0.0026	3.8	26	100			2.828	1.414	45.255	12.03	7.94	8.86	38.10	26.57
3.999	134.59	1.879	1.083	0.0028	3.8	26	100	1.2	0.12	2.828	2.828	90.51	39.66	34.31	33.35	53.31	57.70
0.949	297.16	2.423	1.753	0.0030	3.8	26	100	2.4	0.92	2.828	5.651	90.51	34.57	40.95	39.27	75.07	131.59
0.08	513.29	2.894	2.431	0.0032	3.8	26	100	12	9.7	45.255	45.255	181.01	8.17	13.68	11.50	94.60	229.97

Feature	Q	R	V	S	D_{16}	D_{50}	D_{84}	FFC	PDS	τ	ω
bench	80.34	1.54	0.81	0.0040	3.8	26	100			62.24	50.40
Estimated Q	223.05	2.35	1.36	0.0040	3.8	26	100	1.9	0.34	95.80	130.63
terrace 1	908.44	3.35	3.50	0.0040	3.8	26	100	39	-39	137.39	480.85
terrace 2	2661.09	4.94	6.12	0.0040	3.8	26	100	39	-39	205.34	1257.00

Annual series flood frequency curve		Dominant discharge			Partial series flood frequency curve	
$Q_{1.4}$	$Q_{2.44}$	Yang	AW	EH	$Q_{0.9}$	$Q_{2.0}$
186	299	119.89	136.95	119.29	294	354

Table 15 Summary table for Mkomazi Site 6b

%	Q	R	V	S	D_{16}	D_{50}	D_{84}	FFC	PDS	Max Y	Max AW	Max EH	% tran Y	%tran AW	% tran EH	τ	ω
9.999	0.136	0.291	0.028	0.0015	3.8	26	100			0	0	0	0	0	0	4.30	0.12
9.999	2.255	0.300	0.207	0.0017	3.8	26	100			0	0	1.414	0	0	0.02	5.15	1.07
9.999	3.26	0.323	0.252	0.0018	3.8	26	100			0.707	0	2.828	0.02	0	0.04	5.74	1.45
9.999	4.41	0.338	0.293	0.0018	3.8	26	100			0.707	0	2.828	0.05	0	0.06	6.19	1.81
9.999	6.017	0.366	0.339	0.0019	3.8	26	100			0.707	0.707	2.828	0.11	0.08	0.12	6.92	2.35
9.999	8.501	0.410	0.396	0.0020	3.8	26	100			1.414	0.707	2.828	0.32	0.26	0.24	8.06	3.19
9.999	12.767	0.480	0.475	0.0021	3.8	26	100			1.414	0.707	2.828	0.82	0.85	0.48	9.92	4.71
9.999	20.476	0.570	0.587	0.0022	3.8	26	100			2.828	0.707	2.828	2.81	2.47	1.46	12.53	7.35
9.999	36.644	0.690	0.754	0.0024	3.8	26	100			2.828	1.414	5.651	9.34	8.38	4.91	16.35	12.33
4.999	65.937	0.897	0.969	0.0026	3.8	26	100			2.828	2.828	45.255	13.52	12.50	8.85	22.93	22.23
3.999	134.59	1.270	1.349	0.0028	3.8	26	100	1.2	0.12	2.828	2.828	45.255	35.93	33.87	33.04	35.48	47.85
0.049	297.16	1.807	1.992	0.0030	3.8	26	100	2.4	0.92	45.255	22.627	90.510	30.08	31.99	39.21	55.08	109.74
0.08	513.29	2.283	2.632	0.0032	3.8	26	100	12	9.7	90.510	45.255	181.01	7	9.60	11.57	73.36	193.12

Feature	Q	R	V	S	D_{16}	D_{50}	D_{84}	FFC	PDS	τ	ω
bench	266.148	1.84	1.77	0.0040	3.8	26	100	2.3	0.61	73.77	130.45
Estimated Qb	860.244	3.01	3.30	0.0040	3.8	26	100	39	39	122.16	403.12
terrace 1	1659.309	3.65	5.00	0.0040	3.8	26	100	39	39	148.26	740.73

Annual series flood frequency curve		Dominant discharge			Partial series flood frequency curve	
$Q_{1.5}$	$Q_{2.44}$	Yang	AW	EH	$Q_{0.9}$	$Q_{2.0}$
186	299	96.9	100.44	118.16	294	354

Table 16 Summary table for Mkomazi Site 6c

%	Q	R	V	S	D_{16}	D_{50}	D_{84}	FFC	PDS	Max Y	Max AW	Max EH	% tran Y	%tran AW	% tran EH	τ	ω
9.999	0.136	1.075	0.004	0.0015	3.8	26	100			0	0	0	0	0	0	11.50	0.05
9.999	2.255	1.235	0.056	0.0017	3.8	26	100			0	0	1.414	0	0	0.01	17.09	0.95
9.999	3.26	1.266	0.078	0.0018	3.8	26	100			0	0	1.414	0	0	0.02	18.45	1.43
9.999	4.41	1.284	0.101	0.0018	3.8	26	100			0	0	2.828	0	0	0.04	19.57	1.98
9.999	6.017	1.306	0.132	0.0019	3.8	26	100			0	0	2.828	0	0	0.08	20.89	2.76
9.999	8.501	1.334	0.177	0.0020	3.8	26	100			0	0	2.828	0	0	0.19	22.58	4.00
9.999	12.767	1.374	0.247	0.0021	3.8	26	100			0.707	0	2.828	0.12	0	0.45	24.91	6.15
9.999	20.476	1.436	0.358	0.0022	3.8	26	100			1.414	0	5.651	0.78	0	1.39	28.27	10.13
9.999	36.644	1.550	0.555	0.0024	3.8	26	100			2.828	0.707	45.255	5.52	2.14	5.19	33.86	18.78
4.999	65.937	1.688	0.838	0.0026	3.8	26	100			2.828	1.414	45.255	12.07	6.71	9.20	40.79	34.20
3.999	134.59	1.864	1.326	0.0028	3.8	26	100	1.2	0.12	2.828	2.828	90.510	38.81	33.54	33.59	50.38	66.80
0.949	297.16	2.246	2.067	0.0030	3.8	26	100	2.4	0.92	45.255	22.627	90.510	34.68	43.70	38.59	67.79	140.15
0.08	513.29	2.760	2.757	0.0032	3.8	26	100	12	9.7	90.510	45.255	181.01	8.02	13.91	11.23	89.44	246.57

Feature	Q	R	V	S	D_{16}	D_{50}	D_{84}	FFC	PDS	τ	ω
Estimated Q	258.82	2.15	1.89	0.0040	3.8	26	100	2.1	0.54	90.73	171.38
terrace 1	927.435	3.54	3.63	0.0040	3.8	26	100	39	39	152.38	553.31
terrace 2	2328.304	4.66	5.88	0.0040	3.8	26	100	39	39	200.23	1177.88

Annual series flood frequency curve		Dominant discharge			Partial series flood frequency curve	
$Q_{1.5}$	$Q_{2.44}$	Yang	AW	EH	$Q_{0.9}$	$Q_{2.0}$
186	299	117.48	144.86	117.10	294	354

Table 17 Summary table for Mkomazi Site 7a

%	Q	R	V	S	D_{16}	D_{50}	D_{84}	FFC	PDS	Max Y	Max AW	Max EH	% tran Y	%tran AW	% tran EH	τ	ω
9.999	0.144	0.165	0.084	0.0080	8.6	48	220			0	0	1.414	0	0	0	13.18	1.11
9.999	2.389	0.207	0.382	0.0074	8.6	48	220			1.414	0	22.627	0.12	0	0.16	15.25	5.82
9.999	3.453	0.242	0.422	0.0073	8.6	48	220			1.414	0	22.627	0.30	0	0.29	17.53	7.41
9.999	4.672	0.275	0.460	0.0071	8.6	48	220			1.414	0	22.627	0.54	0	0.45	19.63	9.04
9.999	6.374	0.319	0.501	0.0070	8.6	48	220			1.414	0	45.255	0.94	0	0.78	22.35	11.20
9.999	9.006	0.396	0.557	0.0069	8.6	48	220			2.828	0	45.255	2.48	0	1.48	27.15	15.11
9.999	13.526	0.504	0.641	0.0067	8.6	48	220			2.828	0	45.255	5.63	0	3.07	33.62	21.54
9.999	21.693	0.589	0.759	0.0064	8.6	48	220			2.828	0	45.255	12.32	0	6.22	37.83	28.73
9.999	38.821	0.777	0.517	0.0064	8.6	48	220			2.828	0	45.255	7.56	0	10	49.99	46.25
4.999	69.854	1.053	0.634	0.0061	8.6	48	220			2.828	0	90.51	14.17	0	13.71	64.08	73.15
3.999	142.58	1.505	0.739	0.0057	8.6	48	220	1.2	0.12	2.828	0	90.51	30.55	0	32.56	85.88	129.56
0.949	314.82	2.195	0.946	0.0052	8.6	48	220	2.4	0.92	2.828	0	90.51	20.40	0	24.86	115.88	242.09
0.08	543.78	2.767	1.523	0.0047	8.6	48	220	12	9	11.314	1.414	362.03	4.98	100	6.44	132.92	349.70

Feature	Q	R	V	S	D_{16}	D_{50}	D_{84}	FFC	PDS	τ	ω
Estimated Q_b	378.202	2.37	2.28	0.0029	8.6	48	220	4.4	2.1	221.82	504.84
terrace 1	975.531	3.27	3.33	0.0028	8.6	48	220	39	39	93.45	311.56

Annual series flood frequency curve		Dominant discharge			Partial series flood frequency curve	
$Q_{1.5}$	$Q_{2.44}$	Yang	AW	EH	$Q_{0.9}$	Q_{20}
197.1	316.7	68.5	543.79	81.74	310	375

Table 18 Summary table for Mkomazi Site 7b

%	Q	R	V	S	D_{16}	D_{50}	D_{84}	FFC	PDS	Max Y	Max AW	Max EH	% tran Y	%tran AW	% tran EH	τ	ω
9.999	0.144	0.074	0.114	0.0080	8.6	48	220			0	0	0	0	0	0	5.77	0.66
9.999	2.389	0.293	0.203	0.0074	8.6	48	220			0	0	22.627	0	0	0.13	21.29	4.32
9.999	3.453	0.362	0.230	0.0073	8.6	48	220			0	0	22.627	0	0	0.26	25.85	5.95
9.999	4.672	0.394	0.257	0.0071	8.6	48	220			0	0	22.627	0	0	0.40	27.75	7.13
9.999	6.374	0.463	0.287	0.0070	8.6	48	220			0	0	22.627	0	0	0.70	32.03	9.21
9.999	9.006	0.558	0.328	0.0069	8.6	48	220			0	0	22.627	0	0	1.36	37.76	12.38
9.999	13.526	0.659	0.386	0.0067	8.6	48	220			1.414	0	45.255	2.07	0	2.67	43.34	16.74
9.999	21.693	0.826	0.468	0.0064	8.6	48	220			1.414	0	45.255	4.08	0	4.73	52.33	24.50
9.999	38.821	1.078	0.337	0.0064	8.6	48	220			1.414	0	45.255	6.01	0	9.98	68.34	41.19
4.999	69.854	1.432	0.438	0.0061	8.6	48	220			1.414	0	90.51	9.48	0	14.21	86.18	67.93
3.999	142.58	1.932	0.543	0.0057	8.6	48	220	1.2	0.12	2.828	0	90.51	37.61	0	33.89	109.52	121.45
0.949	314.82	2.659	0.736	0.0052	8.6	48	220	2.4	0.92	2.828	0	90.51	36.83	0	25.86	138.98	225.96
0.08	543.78	3.176	1.218	0.0047	8.6	48	220	12	9	2.828	0	181.01	9.95	0	5.82	150.56	316.87

Feature	Q	R	V	S	D_{16}	D_{50}	D_{84}	FFC	PDS	τ	ω
bench	94.005	1.65	0.89	0.0092	8.6	48	220	1.01		151.80	135.85
Estimated Qb	316.341	2.62	1.68	0.0028	8.6	48	220	2.44	0.93	73.74	123.72
terrace 1	1986.07	4.82	3.77	0.0028	8.6	48	220	>39	>39	136.98	517.08

Annual series flood frequency curve		Dominant discharge			Partial series flood frequency curve	
$Q_{1.5}$	$Q_{2.44}$	Yang	AW	EH	$Q_{0.9}$	$Q_{2.0}$
197.1	316.7	125.25	0	86.12	310	375

Table 19 Summary table for Mkomazi Site 8a

%	Q	R	V	S	D_{16}	D_{50}	D_{84}	FFC	PDS	Max Y	Max AW	Max EH	% tran Y	%tran AW	% tran EH	τ	ω
9.999	0.148	0.404	0.027	0.009	13	30	150			0	0	1.414	0	0	0	35.77	0.95
9.999	2.456	0.462	0.318	0.0083	13	30	150			0	0	45.255	0	0	0.21	38.54	12.25
9.999	3.550	0.491	0.426	0.0082	13	30	150			1.414	0	45.255	0.17	0	0.43	40.35	17.18
9.999	4.803	0.519	0.537	0.0081	13	30	150			2.828	1.414	90.51	1.37	0.66	1.27	42.03	22.58
9.999	6.553	0.550	0.679	0.0080	13	30	150			2.828	1.414	90.51	1.21	0.34	1.36	43.90	29.79
9.999	9.258	0.592	0.871	0.0078	13	30	150			2.828	1.414	90.51	2.53	1.01	2.53	46.31	40.32
9.999	13.905	0.649	1.156	0.0076	13	30	150			2.828	2.828	90.51	5.24	3.43	5.24	49.45	57.18
9.999	22.301	0.721	1.576	0.0073	13	30	150			11.314	22.627	181.01	12.52	17.44	11.78	53.06	83.62
9.999	39.909	0.651	1.222	0.0073	13	30	150			2.828	5.651	90.51	15.54	12.7	14.72	47.79	104.50
4.999	71.813	0.594	1.461	0.0070	13	30	150			22.627	11.314	90.51	17.64	21.95	13.28	41.29	108.53
3.999	146.58	0.765	1.463	0.0066	13	30	150	1.2	0.12	22.627	11.314	90.51	26.87	26.47	24.91	50.39	150.46
0.049	323.64	1.293	1.587	0.0061	13	30	150	2.5	0.92	2.828	5.651	181.01	12.83	7.8	19.19	79.47	278.40
0.08	559.03	1.759	2.361	0.0056	13	30	150	12	9.5	45.255	45.255	181.01	4.08	8.13	5.08	99.13	404.22

Feature	Q	R	V	S	D_{16}	D_{50}	D_{84}	FFC	PDS	τ	ω
Estimated Q	275.65	1.20	3.26	0.0040	13	30	150	2.1	0.49	48.69	158.51
terrace 1	1498.06	3.03	5.71	0.0036	13	30	150	39	39	111.71	637.71
terrace 2	2074.55	3.55	6.35	0.0036	13	30	150	39	39	131.81	836.77
terrace 3	3580.09	4.45	7.38	0.0036	13	30	150	39	39	165.83	1224.20

Annual series flood frequency curve		Dominant discharge			Partial series flood frequency curve	
$Q_{1.5}$	$Q_{2.44}$	Yang	AW	EH	$Q_{0.9}$	Q_{20}
202.50	325.60	60.76	61.40	62.15	320	385

Table 20 Summary table for Mkomazi Site 8b

%	Q	R	V	S	D_{16}	D_{50}	D_{84}	FFC	PDS	Max Y	Max AW	Max EH	% tran Y	%tran AW	% tran EH	τ	ω
9.999	0.148	0.206	0.061	0.009	13	30	150			0	0	1.414	0	0	0	18.10	1.11
9.999	2.456	0.351	0.525	0.0083	13	30	150			0	0	45.255	0	0	0.22	29.06	15.25
9.999	3.550	0.391	0.673	0.0082	13	30	150			1.414	0	45.255	0.17	0	0.43	31.94	21.49
9.999	4.803	0.354	0.811	0.0081	13	30	150			2.828	0	45.255	0.51	0	0.72	28.55	23.16
9.999	6.553	0.369	0.963	0.0080	13	30	150			2.828	1.414	90.51	1.22	0.33	1.37	29.25	28.17
9.999	9.258	0.389	1.149	0.0078	13	30	150			2.828	1.414	90.51	2.52	0.99	2.54	30.31	34.82
9.999	13.905	0.405	1.376	0.0076	13	30	150			2.828	2.828	90.51	5.28	3.39	5.27	30.70	42.26
9.999	22.301	0.517	1.679	0.0073	13	30	150			22.627	22.627	181.01	12.77	17.05	11.85	37.87	63.56
9.999	39.909	0.690	1.202	0.0073	13	30	150			2.828	5.651	90.51	15.65	12.41	14.80	50.64	108.98
4.999	71.813	0.876	1.545	0.0070	13	30	150			22.627	22.627	90.51	17.77	24.39	13.36	61.17	170.06
3.999	146.58	1.057	1.793	0.0066	13	30	150	1.2	0.12	22.627	11.314	90.51	27.07	25.88	25.01	69.43	254.16
0.949	323.64	1.129	1.833	0.0061	13	30	150	2.5	0.92	2.828	5.651	181.01	12.92	7.62	19.31	68.52	277.37
0.08	559.03	1.656	2.580	0.0056	13	30	150	12	9.5	45.255	45.255	181.01	4.11	7.94	5.11	92.49	412.17

Feature	Q	R	V	S	D_{16}	D_{50}	D_{84}	FFC	PDS	τ	ω
Estimated Q_c	356.71	1.35	3.67	0.0040	13	30	150	3.3	1.26	53.90	197.91
terrace 1	1594.33	3.14	6.13	0.0036	13	30	150	39	39	116.16	712.19
terrace 2	3369.71	4.50	8.18	0.0036	13	30	150	39	39	168.52	1379.03

Annual series flood frequency curve		Dominant discharge			Partial series flood frequency curve	
$Q_{1.5}$	$Q_{2.44}$	Yang	AW	EH	$Q_{0.9}$	$Q_{2.0}$
202.5	325.6	61.51	62.3	62.69	320	385

Table 21 Summary table for Mkomazi Site 9a

%	Q	R	V	S	D_{16}	D_{50}	D_{84}	FFC	PDS	Max Y	Max AW	Max EH	% tran Y	%tran AW	% tran EH	τ	ω
9.999	1.290	0.444	0.071	0.0040	4.2	60	410			0	0	2.828	0	0	0	20.63	1.47
9.999	3.814	0.547	0.161	0.0046	4.2	60	410			0.354	0	11.314	0.01	0	0.04	26.11	4.21
9.999	5.116	0.579	0.199	0.0047	4.2	60	410			0.354	0	11.314	0.02	0	0.07	27.85	5.54
9.999	6.924	0.629	0.247	0.0047	4.2	60	410			0.707	0	11.314	0.05	0	0.13	30.58	7.54
9.999	9.579	0.691	0.309	0.0047	4.2	60	410			0.707	0	11.314	0.12	0.04	0.25	33.97	10.50
9.999	13.447	0.760	0.390	0.0048	4.2	60	410			1.414	0.354	45.255	0.34	0.10	0.52	37.91	14.78
9.999	20.028	0.846	0.510	0.0049	4.2	60	410			2.828	0.707	45.255	1	0.35	1.18	42.91	21.88
9.999	31.990	0.958	0.692	0.0050	4.2	60	410			2.828	1.414	45.255	3.94	1.23	3.02	49.66	34.37
9.999	55.327	1.078	0.977	0.0050	4.2	60	410			2.828	2.828	90.51	11.40	4.72	8.30	56.10	54.82
4.999	92.686	1.255	1.332	0.0051	4.2	60	410			11.314	2.828	90.51	14.08	6.51	11.48	66.78	88.94
3.999	186.15	1.457	1.953	0.0052	4.2	60	410	1.3	0.13	45.255	22.627	181.01	34.97	34.08	32.66	79.04	154.36
0.040	421.35	1.903	2.968	0.0054	4.2	60	410	2.3	0.6	90.510	90.51	181.01	30.96	46.92	37.55	105.92	314.41
0.08	727.78	2.369	3.905	0.0056	4.2	60	410	6	5.5	181.01	181.01	724.07	3.11	6.05	4.78	136.31	532.29

Feature	Q	R	V	S	D_{16}	D_{50}	D_{84}	FFC	PDS	τ	ω
Estimated Q	117.26	1.44	1.49	0.0058	4.2	60	410	11	0.07	82.30	122.71
terrace 1	1455.22	3.04	5.51	0.0062	4.2	60	410	38	38	188.83	1041.28

Annual series flood frequency curve		Dominant discharge			Partial series flood frequency curve	
$Q_{1.5}$	$Q_{2.44}$	Yang	AW	EH	$Q_{0.9}$	$Q_{2.0}$
255	470	172.01	179.36	139.7	496.5	575.3

Table 22 Summary table for Mkomazi Site 9b

%	Q	R	V	S	D_{16}	D_{50}	D_{84}	FFC	PDS	Max Y	Max AW	Max EH	% tran Y	%tran AW	% tran EH	τ	ω
9.999	1.290	0.444	0.071	0.0040	4.2	60	410			0	0	2.828	0	0	0	20.63	1.47
9.999	3.814	0.547	0.161	0.0046	4.2	60	410			0.354	0	11.314	0.01	0	0.04	26.11	4.21
9.999	5.116	0.579	0.199	0.0047	4.2	60	410			0.354	0	11.314	0.02	0	0.07	27.85	5.54
9.999	6.924	0.629	0.247	0.0047	4.2	60	410			0.707	0	11.314	0.05	0	0.13	30.58	7.54
9.999	9.579	0.691	0.309	0.0047	4.2	60	410			0.707	0.354	11.314	0.12	0.04	0.23	33.97	10.50
9.999	13.447	0.760	0.390	0.0048	4.2	60	410			1.414	0.354	45.255	0.36	0.1	0.51	37.91	14.78
9.999	20.028	0.846	0.510	0.0049	4.2	60	410			2.828	0.707	45.255	1.05	0.33	1.15	42.91	21.88
9.999	31.990	0.958	0.692	0.0050	4.2	60	410			2.828	1.414	45.255	4.14	1.15	2.85	49.66	34.37
9.999	55.327	1.078	0.977	0.0050	4.2	60	410			2.828	2.828	90.510	11.97	9.4	8.11	56.10	54.82
4.999	92.686	1.255	1.332	0.0051	4.2	60	410			5.651	5.651	90.510	8.57	7.42	11.21	66.78	88.94
3.999	186.15	1.457	1.953	0.0052	4.2	60	410	1.3	0.13	45.255	22.627	181.01	36.71	31.75	31.89	79.04	154.36
0.940	421.35	1.903	2.968	0.0054	4.2	60	410	2.3	0.6	90.51	90.51	181.01	30.47	41	34.39	105.92	314.41
0.08	727.78	2.369	3.905	0.0056	4.2	60	410	6	5.5	181.01	724.07	724.07	6.54	13.82	9.41	136.31	532.29

Feature	Q	R	V	S	D_{16}	D_{50}	D_{84}	FFC	PDS	τ	ω
terrace 1	1458.216	3.54	5.23	0.0062	4.2	60	410	38	38	220.23	1151.99

Annual series flood frequency curve		Dominant discharge			Partial series flood frequency curve	
$Q_{1.5}$	$Q_{2.44}$	Yang	AW	EH	$Q_{0.9}$	Q_{20}
255	470	130.1	176.24	139.04	496.5	575.3

Table 23 Summary table for Mkomazi Site 10a

%	Q	R	V	S	D_{16}	D_{50}	D_{84}	FFC	PDS	Max Y	Max AW	Max EH	% tran Y	%tran AW	% tran EH	τ	ω
9.999	1.349	0.532	0.046	0.0020	15	50	400			0	0	0	0	0	0	9.88	0.45
9.999	3.987	0.626	0.112	0.0021	15	50	400			0	0	0.707	0	0	0.01	12.73	1.42
9.999	5.349	0.661	0.141	0.0021	15	50	400			0	0	0.707	0	0	0.03	13.82	1.94
9.999	7.238	0.698	0.177	0.0022	15	50	400			0	0	1.414	0	0	0.07	15.06	2.67
9.999	10.015	0.736	0.225	0.0023	15	50	400			0	0	1.414	0	0	0.14	16.48	3.71
9.999	14.058	0.797	0.288	0.0023	15	50	400			0.707	0	1.414	0.12	0	0.27	18.57	5.34
9.999	20.938	0.860	0.380	0.0025	15	50	400			1.414	0	5.651	0.53	0	0.79	21.02	7.98
9.999	33.444	0.949	0.518	0.0026	15	50	400			1.414	0	22.627	1.90	0	2.17	24.55	12.71
9.999	57.842	1.122	0.729	0.0026	15	50	400			2.828	0.707	45.255	8.13	2.6	6.39	29.04	21.18
4.999	96.809	1.345	0.995	0.0028	15	50	400			2.828	1.414	45.255	11.57	5.39	10.17	37.30	37.12
3.999	194.39	1.747	1.492	0.0030	15	50	400	1.3	0.13	2.828	5.651	90.51	31.57	21.91	36.74	51.70	77.13
0.949	439.51	1.888	2.254	0.0032	15	50	400	2.38	0.60	45.255	45.255	90.51	36.53	51.71	34.34	60.07	135.37
0.08	759.15	2.266	2.815	0.0035	15	50	400	6	6	90.51	45.255	90.51	9.65	18.69	8.88	77.84	219.13

Feature	Q	R	V	S	D_{16}	D_{50}	D_{84}	FFC	PDS	τ	ω
Estimated Q	324.87	1.80	2.41	0.0080	15	50	400	1.8	0.33	144.12	347.08
terrace 1	1156.99	2.67	3.02	0.0050	15	50	400	38	38	132.94	402.12
terrace 2	4297.17	4.41	5.06	0.0043	15	50	400	38	38	190.42	964.21

Annual series flood frequency curve		Dominant discharge			Partial series flood frequency curve	
$Q_{1.5}$	$Q_{2.44}$	Yang	AW	EH	$Q_{0.9}$	$Q_{2.0}$
268	440	155.73	226.02	159	518	600

Table 24 Summary table for Mkomazi Site 10b

%	Q	R	V	S	D_{16}	D_{50}	D_{84}	FFC	PDS	Max Y	Max AW	Max EH	% tran Y	%tran AW	% tran EH	τ	ώ
9.999	1.349	1.349	0.140	0.0020	15	50	400			0	0	0	0	0	0	3.53	0.50
9.999	3.987	3.987	0.202	0.0021	15	50	400			0	0	0.707	0	0	0.02	7.52	1.52
9.999	5.349	5.349	0.229	0.0021	15	50	400			0	0	0.707	0	0	0.03	9.02	2.07
9.999	7.238	7.238	0.263	0.0022	15	50	400			0	0	1.414	0	0	0.07	10.80	2.84
9.999	10.015	10.015	0.307	0.0023	15	50	400			0.707	0	1.414	0.11	0	0.16	12.90	3.95
9.999	14.058	14.058	0.362	0.0023	15	50	400			0.707	0	2.828	0.24	0	0.32	15.43	5.58
9.999	20.938	20.938	0.440	0.0025	15	50	400			1.414	0	5.651	0.83	0	0.73	18.95	8.35
9.999	33.444	33.444	0.558	0.0026	15	50	400			2.828	0	22.627	3.04	0	2.39	23.98	13.37
9.999	57.842	57.842	0.735	0.0026	15	50	400			2.828	0.707	45.255	9.52	4.04	6.83	29.35	21.58
4.999	96.899	96.899	0.962	0.0028	15	50	400			2.828	0.707	45.255	12.85	5.19	10.93	39.68	38.18
3.999	194.39	194.39	1.401	0.0030	15	50	400	1.3	0.13	2.828	5.651	90.510	34.06	29.92	34.48	49.37	69.17
0.949	439.51	439.50	2.022	0.0032	15	50	400	2.38	0.60	45.255	22.627	90.510	31.43	44.44	34.67	64.67	130.75
0.08	759.15	759.15	2.543	0.0035	15	50	400	6	6	90.51	45.255	90.510	7.93	16.41	9.38	80.87	205.62

Feature	Q	R	V	S	D_{16}	D_{50}	D_{84}	FFC	PDS	τ	ώ
Estimated Q	195.34	1.71	1.60	0.0080	15	50	400	1.3	0.13	136.76	218.81
terrace 1	1068.02	2.60	2.97	0.0050	15	50	400	>38	38	129.33	384.05
terrace 2	5154.72	4.91	5.44	0.0043	15	50	400	>38	>38	212.28	1155.08

Annual series flood frequency curve		Dominant discharge			Partial series flood frequency curve	
$Q_{1.5}$	$Q_{2.44}$	Yang	AW	EH	$Q_{0.9}$	$Q_{2.0}$
208	440	142.48	204.96	155.34	518	600

Table 25 Summary table for Mkomazi Site 11

%	Q	R	V	S	D_{16}	D_{50}	D_{84}	FFC	PDS	Max Y	Max AW	Max EH	% tran Y	%tran AW	% tran EH	τ	ω
9.999	1.378	0.197	0.281	0.0080	22	65	160			0	0	11.314	0	0	0.01	15.67	4.41
9.999	4.074	0.313	0.437	0.0078	22	65	160			1.414	0	45.255	0.01	0	0.09	23.87	10.43
9.999	5.465	0.361	0.499	0.0077	22	65	160			1.414	0	90.51	0.02	0	0.16	27.16	13.56
9.999	7.396	0.415	0.576	0.0075	22	65	160			2.828	0	90.51	0.07	0	0.28	30.73	17.70
9.999	10.232	0.478	0.674	0.0074	22	65	160			2.828	1.414	90.51	0.14	0.01	0.50	34.79	23.44
9.999	14.363	0.551	0.797	0.0072	22	65	160			2.828	1.414	181.01	0.26	0.02	0.92	39.21	31.26
9.999	21.394	0.657	0.979	0.0070	22	65	160			2.828	1.414	181.01	0.51	0.04	1.91	45.55	44.57
9.999	34.171	0.806	1.252	0.0068	22	65	160			11.314	5.651	181.01	1.11	0.15	4.51	53.99	67.61
9.999	59.099	0.942	1.680	0.0068	22	65	160			22.627	22.627	181.01	2.83	0.82	12.22	63.47	106.65
4.999	99.006	1.131	2.208	0.0064	22	65	160			45.255	45.255	90.51	3.86	2.03	14.15	72.74	160.63
3.999	199.18	1.406	3.180	0.0061	22	65	160	1.35	0.13	90.51	90.510	362.04	21.18	18.35	37.31	86.27	274.36
0.949	451.61	1.474	4.598	0.0057	22	65	160	2.53	0.60	181.01	727.07	181.01	56.78	62.85	23.24	84.35	387.87
0.08	780.06	1.748	5.618	0.0052	22	65	160	7	5.5	181.01	727.07	362.04	13.24	15.73	4.69	91.74	515.37

Feature	Q	R	V	S	D_{16}	D_{50}	D_{84}	FFC	PDS	τ	ω
bench	246.98	1.38	3.46	0.0195	22	65	160	1.48	0.18	266.30	922.32
Estimated Q.	268.26	1.38	3.75	0.0210	22	65	160	1.51	0.21	287.29	1076.88
terrace 1	854.79	1.77	5.79	0.0250	22	65	160	17	15	438.16	2538.27
terrace 2	3239.36	2.69	9.15	0.0357	22	65	160	38	38	950.93	8701.68

Annual series flood frequency curve		Dominant discharge			Partial series flood frequency curve	
$Q_{1.5}$	$Q_{2.44}$	Yang	AW	EH	$Q_{0.9}$	$Q_{2.0}$
260	450	217.82	280.81	124.63	532.2	616.62

Table 26 Summary table for Mkomazi Site 12

%	Q	R	V	S	D_{16}	D_{50}	D_{84}	FFC	PDS	Max Y	Max AW	Max EH	% tran Y	%tran AW	% tran EH	τ	ω
9.999	1.451	0.307	0.065	0.0007	0.68	3.9	230			0	0	0	0	0	0	2.17	0.14
9.999	4.290	0.459	0.110	0.0010	0.68	3.9	230			0	0	0	0	0	0	4.41	0.48
9.999	5.756	0.527	0.127	0.0011	0.68	3.9	230			0	0	0	0	0	0	5.55	0.71
9.999	7.789	0.604	0.149	0.0012	0.68	3.9	230			0	0	0	0	0	0	6.96	1.04
9.999	10.777	0.694	0.179	0.0013	0.68	3.9	230			0	0	0	0	0	0	8.81	1.57
9.999	15.128	0.798	0.216	0.0014	0.68	3.9	230			0	0	0	0	0	0	11.20	2.42
9.999	22.531	0.927	0.271	0.0016	0.68	3.9	230			0	0	0.354	0	0	0.27	14.59	3.95
9.999	35.988	1.098	0.354	0.0018	0.68	3.9	230			0	0	0.707	0	0	1.13	19.65	6.96
9.999	62.243	1.335	0.486	0.0018	0.68	3.9	230			0.354	00	0.707	3.08	0	3.26	23.92	11.62
4.999	104.27	1.626	0.658	0.0021	0.68	3.9	230			0.707	0	2.828	10.81	0	7.3	33.53	22.06
3.999	209.71	2.026	0.985	0.0023	0.68	3.9	230	1.3	0.13	0.707	0	22.627	38.43	0	29.70	47.06	46.83
0.949	475.33	2.631	1.602	0.0027	0.68	3.9	230	2.38	0.60	0.707	0.354	45.255	37.79	51.35	43.67	70.35	112.69
0.08	821.04	3.141	2.201	0.0031	0.68	3.9	230	6	6	11.314	5.651	45.255	9.88	48.65	14.66	96.09	211.49

Feature	Q	R	V	S	D_{16}	D_{50}	D_{84}	FFC	PDS	τ	ω
Estimated Qb	174.310	1.92	0.90	0.0009	0.68	3.9	230	1.25	0.10	16.28	14.67
terrace 1	597.656	2.94	1.77	0.0015	0.68	3.9	230	2.90	1.13	43.98	77.66
terrace 2	3183.112	4.54	4.72	0.0027	0.68	3.9	230	38	38	120.59	568.85

Annual series flood frequency curve		Dominant discharge			Partial series flood frequency curve	
$Q_{1.5}$	$Q_{2.44}$	Yang	AW	EH	$Q_{0.9}$	$Q_{2.0}$
285	500	206.73	502.47	209.41	560.18	649.01

Table 27 Summary table for Mkomazi Site 13

%	Q	R	V	S	D_{16}	D_{50}	D_{84}	FFC	PDS	Max Y	Max AW	Max EH	% tran Y	%tran AW	% tran EH	τ	ώ
9.999	1.466	0.266	0.128	0.0012	3.2	26	96			0	0	0.354	0	0	0	3.18	0.41
9.999	4.334	0.342	0.247	0.0013	3.2	26	96			0.354	0	0.354	0.03	0	0.03	4.44	1.10
9.999	5.814	0.360	0.290	0.0013	3.2	26	96			0.354	0	1.414	0.05	0	0.07	4.80	1.39
9.999	7.868	0.384	0.359	0.0014	3.2	26	96			0.707	0.354	1.414	0.14	0.17	0.14	5.16	1.85
9.999	10.885	0.349	0.377	0.0014	3.2	26	96			1.414	0.354	1.414	0.25	0.29	0.19	4.95	1.87
9.999	15.280	0.410	0.425	0.0015	3.2	26	96			1.414	0.354	1.414	0.55	0.57	0.40	6.03	2.56
9.999	22.759	0.503	0.490	0.0016	3.2	26	96			1.414	0.354	2.828	1.26	1.20	1	7.76	3.81
9.999	36.352	0.652	0.587	0.0016	3.2	26	96			2.828	0.707	5.651	3.53	3.17	2.53	10.65	6.26
9.999	62.872	0.847	0.738	0.0016	3.2	26	96			2.828	1.414	5.651	9.94	9.51	7.14	13.88	10.25
4.999	105.32	1.100	0.918	0.0018	3.2	26	96			2.828	1.414	11.314	13.53	11.92	12.34	19.24	17.65
3.999	211.34	1.547	1.255	0.0019	3.2	26	96	1.3	0.13	2.828	5.651	22.627	34.95	33.55	14.04	28.67	35.99
0.949	477.94	2.232	1.828	0.0020	3.2	26	96	2.38	0.60	22.627	11.314	90.510	29.33	31.35	50.21	44.56	91.843
0.08	825.54	2.457	2.300	0.0021	3.2	26	96	6	6	45.255	22.627	90.510	6.42	8.27	11.91	53.02	121.96

Feature	Q	R	V	S	D_{16}	D_{50}	D_{84}	FFC	PDS	τ	ώ
Estimated Q	168.835	1.41	1.12	0.0020	3.2	26	96	1.23	0.09	27.79	31.19
terrace 1	674.841	2.46	1.90	0.0025	3.2	26	96	5	3.6	60.86	115.62
terrace 2	4849.854	6.60	4.49	0.0026	3.2	26	96	38	38	172.26	772.82
terrace 3	10163.597	9.10	6.36	0.0026	3.2	26	96	38	38	239.94	1524.90

Annual series flood frequency curve		Dominant discharge			Partial series flood frequency curve	
$Q_{1.5}$	$Q_{2.44}$	Yang	AW	EH	$Q_{0.9}$	$Q_{2.0}$
290	500	146.73	150.74	165.74	563	652.6

Table 28 Summary table for Mhlathuze Site 1 pool virgin

%	Q	R	V	S	D_{16}	D_{50}	D_{84}	FFC	PDS	Max Y	Max AW	Max EH	% tran Y	%tran AW	% tran EH	τ	ω
9.999	0	0	0	0.0070	0.23	0.50	0.90			0	0	0	0	0	0	0	0
9.999	0.506	0.477	0.104	0.0066	0.23	0.50	0.90			0.354	0.177	2.828	0	0	0.08	30.91	3.28
9.999	0.856	0.516	0.153	0.0065	0.23	0.50	0.90			0.354	0.354	2.828	0.03	0.02	0.20	32.91	5.14
9.999	1.280	0.553	0.202	0.0064	0.23	0.50	0.90			0.707	0.354	5.651	0.11	0.05	0.42	34.70	7.16
9.999	1.787	0.588	0.252	0.0064	0.23	0.50	0.90			0.707	0.707	5.651	0.38	0.16	0.77	36.92	9.49
9.999	2.399	0.628	0.304	0.0063	0.23	0.50	0.90			0.707	0.707	5.651	0.81	0.37	1.29	38.79	12.06
9.999	3.258	0.478	0.360	0.0052	0.23	0.50	0.90			1.414	0.707	5.651	1.40	0.81	1.05	24.38	8.90
9.999	4.613	0.466	0.408	0.0060	0.23	0.50	0.90			1.414	0.707	5.651	3.19	1.85	2.25	27.42	11.36
9.999	7.604	0.490	0.465	0.0058	0.23	0.50	0.90			1.414	1.414	5.651	6.69	4.23	4.15	27.86	13.12
4.999	13.416	0.600	0.502	0.0055	0.23	0.50	0.90			1.414	1.414	5.651	6.50	3.95	4.35	32.35	16.44
3.999	29.042	0.994	0.591	0.0051	0.23	0.50	0.90	1.3	0.16	2.828	1.414	5.651	15.09	7.50	13.02	49.71	39.73
0.949	145.27	2.086	0.924	0.0040	0.23	0.50	0.90	2.6	1.07	2.828	1.414	5.651	24.53	12.85	27.28	78.73	73.81
0.08	1020.2	3.049	3.297	0.0028	0.23	0.50	0.90	16	10	2.828	5.651	5.651	41.28	68.21	45.12	83.76	280.26

Feature	Q	R	V	S	D_{16}	D_{50}	D_{84}	FFC	PDS	τ	ω
bench	26.63	0.74	0.74	0.0007	0.23	0.50	0.90	1.28	0.13	5.06	0.39
Estimated Qb	116.42	1.39	1.29	0.0010	0.23	0.50	0.90	2.50	0.77	13.67	1.82

Annual series flood frequency curve		Dominant discharge			Partial series flood frequency curve	
$Q_{1.5}$	$Q_{2.44}$	Yang	AW	EH	$Q_{0.9}$	$Q_{2.0}$
40	105	38.97	62.44	46.91	130	243.60

Table 29 Summary table for Mhlathuze Site 1 riffle virgin

%	Q	R	V	S	D_{16}	D_{50}	D_{84}	FFC	PDS	Max Y	Max AW	Max EH	% tran Y	%tran AW	% tran EH	τ	ώ
9.999	0	0	0	0.0560	0.40	22	35			0	0	0	0	0	0	0	0
9.999	0.506	0.09	0.512	0.0524	0.40	22	35			2.828	1.414	45.255	0.61	0.45	0.09	46.26	3.51
9.999	0.856	0.12	0.574	0.0514	0.40	22	35			2.828	1.414	45.255	1.13	0.83	0.23	60.51	3.71
9.999	1.280	0.149	0.638	0.0505	0.40	22	35			2.828	1.414	45.255	1.84	1.39	0.45	73.82	5.05
9.999	1.787	0.176	0.702	0.0496	0.40	22	35			2.828	2.828	45.255	2.76	2.17	0.79	85.64	6.49
9.999	2.399	0.203	0.765	0.0487	0.40	22	35			2.828	2.828	45.255	3.95	3.22	1.28	96.98	8.03
9.999	3.258	0.234	0.830	0.0477	0.40	22	35			2.828	2.828	45.255	4.38	4.77	2.09	109.50	9.89
9.999	4.613	0.281	0.897	0.0464	0.40	22	35			2.828	5.561	45.255	8.22	7.15	3.63	127.91	12.57
9.999	7.604	0.372	0.991	0.0442	0.40	22	35			2.828	5.561	45.255	13.75	12.32	7.93	161.30	17.59
4.999	13.416	0.492	1.135	0.0414	0.40	22	35			2.828	5.561	45.255	12.59	12.08	9.30	199.82	25.14
3.999	29.942	0.820	1.317	0.0367	0.40	22	35	1.3	0.16	2.828	11.314	45.255	21.45	21.15	25.24	295.22	42.97
0.949	145.27	1.356	1.778	0.0262	0.40	22	35	2.6	1.07	22.627	22.627	45.255	22.04	26.95	31.00	348.52	67.00
0.08	1020.2	4.096	1.765	0.0145	0.40	22	35	16	10	2.828	1.414	45.255	7.27	7.12	17.98	582.64	109.40

Feature	Q	R	V	S	D_{16}	D_{50}	D_{84}	FFC	PDS	τ	ώ
Estimated Qb	64.45	1.434	1.61	0.0090	0.40	22	35	1.80	0.41	126.61	22.46
terrace 1	331.95	3.025	3.02	0.0063	0.40	22	35	6.80	2.62	186.95	64.21
terrace 2	1061.25	4.202	5.80	0.0150	0.40	22	35	16	11	618.32	414.77

Annual series flood frequency curve		Dominant discharge			Partial series flood frequency curve	
$Q_{1.5}$	$Q_{2.44}$	Yang	AW	EH	$Q_{0.9}$	$Q_{2.0}$
40	105	16.06	18.25	29.34	130	243.60

Table 30 Summary table for Mhlathuze Site 1 pool present

%	Q	R	V	S	D_{16}	D_{50}	D_{84}	FFC	PDS	Max Y	Max AW	Max EH	% tran Y	%tran AW	% tran EH	τ	ω
9.999	0	0	0	0.0070	0.23	0.50	0.90			0	0	0	0	0	0	0	0
9.999	0.311	0.448	0.072	0.0067	0.23	0.50	0.90			0.177	0	2.828	0	0	0.10	29.45	0.22
9.999	0.374	0.458	0.083	0.0067	0.23	0.50	0.90			0.177	0	2.828	0	0	0.14	30.10	0.26
9.999	0.440	0.468	0.094	0.0067	0.23	0.50	0.90			0.354	0	2.828	0.01	0	0.18	30.76	0.30
9.999	0.515	0.478	0.106	0.0066	0.23	0.50	0.90			0.354	0.177	2.828	0.02	0.01	0.24	30.95	0.34
9.999	0.597	0.488	0.118	0.0066	0.23	0.50	0.90			0.354	0.177	2.828	0.03	0.02	0.32	31.60	0.39
9.999	0.696	0.499	0.132	0.0066	0.23	0.50	0.90			0.354	0.354	2.828	0.06	0.04	0.42	32.31	0.44
9.999	0.837	0.514	0.151	0.0065	0.23	0.50	0.90			0.354	0.354	2.828	0.10	0.08	0.58	32.78	0.51
9.999	1.215	0.547	0.195	0.0065	0.23	0.50	0.90			0.707	0.354	5.651	0.27	0.21	1.17	34.61	0.70
4.999	2.591	0.638	0.319	0.0062	0.23	0.50	0.90			0.707	0.707	5.651	1.58	1.01	2.16	38.80	1.29
3.999	10.046	0.700	0.485	0.0057	0.23	0.50	0.90	1.45	0.13	1.414	1.414	5.651	12.67	8.97	9.43	39.14	1.43
0.049	69.354	1.405	0.756	0.0045	0.23	0.50	0.90	3.5	0.94	2.828	1.414	5.651	33.24	23.64	28.25	62.02	4.85
0.08	595.12	3.045	1.923	0.0031	0.23	0.50	0.90	18	13	2.828	2.828	5.651	52.01	66.02	57.01	92.60	18.45

Feature	Q	R	V	S	D_{16}	D_{50}	D_{84}	FFC	PDS	τ	ω
bench	26.63	0.74	0.74	0.0007	0.23	0.50	0.90	2.2	0.34	5.06	0.39
Estimated Qb	116.42	1.39	1.29	0.0010	0.23	0.50	0.90	4.3	1.50	13.67	1.82

Annual series flood frequency curve		Dominant discharge			Partial series flood frequency curve	
$Q_{1.5}$	$Q_{2.44}$	Yang	AW	EH	$Q_{0.9}$	Q_{20}
12.5	32	52.12	70.32	44.63	68	152.96

Table 31 Summary table for Mhlathuze Site 1 riffle present

%	Q	R	V	S	D_{16}	D_{50}	D_{84}	FFC	PDS	Max Y	Max AW	Max EH	% tran Y	%tran AW	% tran EH	τ	ώ
0.999	0	0	0	0.0560	0.40	22	35			0	0	0	0	0	0	0	0
0.999	0.311	0.070	0.479	0.0531	0.40	22	35			1.414	1.414	45.255	1.50	1.52	0.17	36.28	1.84
0.999	0.374	0.075	0.489	0.0529	0.40	22	35			1.414	1.414	45.255	1.83	1.85	0.22	38.90	2.01
0.999	0.440	0.083	0.497	0.0526	0.40	22	35			1.414	1.414	45.255	2.15	2.13	0.29	42.90	2.26
0.999	0.515	0.091	0.511	0.0524	0.40	22	35			2.828	1.414	45.255	2.57	2.54	0.37	46.89	2.55
0.999	0.597	0.101	0.526	0.0521	0.40	22	35			2.828	1.414	45.255	3.03	2.95	0.49	51.45	2.88
0.999	0.696	0.110	0.545	0.0518	0.40	22	35			2.828	1.414	45.255	3.63	3.55	0.63	55.71	3.24
0.999	0.837	0.119	0.570	0.0514	0.40	22	35			2.828	1.414	45.255	4.54	4.50	0.85	59.93	3.65
0.999	1.215	0.145	0.627	0.0506	0.40	22	35			2.828	1.414	45.255	7.11	7.22	1.60	72.10	4.85
4.999	2.591	0.210	0.781	0.0484	0.40	22	35			2.828	2.828	45.255	8.93	9.91	2.82	100	8.47
3.999	10.046	0.434	1.032	0.0429	0.40	22	35	1.45	0.13	2.828	5.651	45.255	29.68	35.89	18.76	182.81	20.89
0.949	69.354	1.356	0.848	0.0313	0.40	22	35	3.50	0.94	2.828	1.414	45.255	23.16	18.80	39.37	415.77	38.16
0.08	595.12	4.097	1.029	0.0174	0.40	22	35	18	13	2.828	1.414	45.255	11.85	9.13	34.43	698.29	76.46

Feature	Q	R	V	S	D_{16}	D_{50}	D_{84}	FFC	PDS	τ	ώ
Estimated Qb	64.45	1.434	1.61	0.0090	0.40	22	35	3.5	0.85	126.61	22.46
terrace 1	331.95	3.025	3.02	0.0063	0.40	22	35	10	7.5	186.95	64.21
terrace 2	1061.25	4.202	5.80	0.0150	0.40	22	35	26	17	618.32	414.77

Annual series flood frequency curve		Dominant discharge			Partial series flood frequency curve	
$Q_{1.5}$	$Q_{2.44}$	Yang	AW	EH	$Q_{0.9}$	$Q_{2.0}$
12.5	32	7.81	7.12	28.32	68	152.96

Table 32 Summary table for Mhlathuze Site 2 virgin

%	Q	R	V	S	D_{16}	D_{50}	D_{84}	FFC	PDS	Max Y	Max AW	Max EH	% tran Y	%tran AW	% tran EH	τ	ω
9.999	0	0	0	0.0017	0.40	0.65	1.40			0	0	0	0	0	0	0	0
9.999	0.656	0.064	0.290	0.0018	0.40	0.65	1.40			0.707	0.354	1.414	0.03	0.04	0	1.13	0.03
9.999	1.112	0.093	0.254	0.0018	0.40	0.65	1.40			0.707	0.354	1.414	0.04	0.04	0.01	1.64	0.04
9.999	1.721	0.127	0.243	0.0018	0.40	0.65	1.40			0.707	0.354	1.414	0.06	0.06	0.02	2.24	0.06
9.999	2.469	0.169	0.242	0.0018	0.40	0.65	1.40			0.707	0.354	1.414	0.09	0.10	0.04	3.15	0.08
9.999	3.342	0.220	0.251	0.0019	0.40	0.65	1.40			0.707	0.354	2.828	0.17	0.15	0.07	4.10	0.11
9.999	4.521	0.278	0.266	0.0019	0.40	0.65	1.40			0.707	0.354	2.828	0.32	0.25	0.12	5.18	0.14
9.999	6.354	0.352	0.293	0.0019	0.40	0.65	1.40			0.707	0.707	2.828	0.67	0.63	0.24	6.56	0.20
9.999	10.378	0.479	0.344	0.0020	0.40	0.65	1.40			1.414	0.707	2.828	2.04	2.12	0.69	9.40	0.33
4.999	17.907	0.644	0.419	0.0020	0.40	0.65	1.40			1.414	0.707	2.828	3.23	3.28	0.98	12.64	0.55
3.999	38.388	0.859	0.556	0.0021	0.40	0.65	1.40	1.36	0.15	2.828	1.414	2.828	10.94	11.95	3.28	17.70	1.02
0.949	195.99	1.779	0.918	0.0024	0.40	0.65	1.40	3.50	0.93	2.828	1.414	5.651	31.97	32.13	16.67	41.88	3.98
0.08	1435.3	5.173	1.908	0.0026	0.40	0.65	1.40	15	9.20	2.828	2.828	11.314	50.46	49.23	77.87	131.94	26.46

Feature	Q	R	V	S	D_{16}	D_{50}	D_{84}	FFC	PDS	τ	ω
bench	36.132	0.842	0.54	0.0018	0.40	0.65	1.40	1.04	0.14	14.87	0.84
Top of island	51.213	0.939	0.60	0.0019	0.40	0.65	1.40	1.05	0.21	17.51	1.08
Estimated Q	196.322	1.784	0.91	0.0022	0.40	0.65	1.40	1.14	0.93	38.49	3.64
terrace 1	567.527	3.353	1.30	0.0024	0.40	0.65	1.40	5.5	2.60	78.94	10.68
terrace 2	1006.554	4.424	1.61	0.0024	0.40	0.65	1.40	12	7.50	108.49	18.28

Annual series flood frequency curve		Dominant discharge			Partial series flood frequency curve	
$Q_{1.5}$	$Q_{2.44}$	Yang	AW	EH	$Q_{0.9}$	$Q_{2.0}$
47	118	107.83	104.60	245.92	190	417.38

Table 33 Summary table for Mhlathuze Site 2 present

%	Q	R	V	S	D_{16}	D_{50}	D_{84}	FFC	PDS	Max Y	Max AW	Max EH	% tran Y	%tran AW	% tran EH	τ	ώ
9.999	0	0	0	0.0017	0.40	0.65	1.40			0	0	0	0	0	0	0	0
9.999	0.353	0.044	0.351	0.0018	0.40	0.65	1.40			0.707	0.707	1.414	0.04	0.27	0	0.73	0.03
9.999	0.455	0.051	0.304	0.0018	0.40	0.65	1.40			0.707	0.707	1.414	0.04	0.07	0	0.85	0.03
9.999	0.605	0.066	0.283	0.0018	0.40	0.65	1.40			0.707	0.354	1.414	0.04	0.05	0.01	1.10	0.03
9.999	0.831	0.082	0.275	0.0018	0.40	0.65	1.40			0.707	0.354	1.414	0.06	0.07	0.01	1.37	0.04
9.999	1.115	0.094	0.252	0.0019	0.40	0.65	1.40			0.707	0.354	1.414	0.06	0.06	0.01	1.57	0.04
9.999	1.514	0.118	0.244	0.0019	0.40	0.65	1.40			0.707	0.354	1.414	0.07	0.08	0.02	1.97	0.05
9.999	2.135	0.148	0.241	0.0019	0.40	0.65	1.40			0.707	0.354	1.414	0.12	0.13	0.04	2.61	0.06
9.999	3.522	0.229	0.253	0.0020	0.40	0.65	1.40			0.707	0.354	2.828	0.31	0.28	0.12	4.04	0.11
4.999	6.775	0.367	0.298	0.0020	0.40	0.65	1.40			0.707	0.707	2.828	0.67	0.65	0.24	6.84	0.21
3.999	20.166	0.687	0.438	0.0021	0.40	0.65	1.40	1.5	0.13	1.414	0.707	2.828	5.69	5.85	1.77	13.48	0.61
0.949	136.89	1.528	0.818	0.0024	0.40	0.65	1.40	3.5	0.86	2.828	1.414	5.651	32.01	33.26	14.67	34.48	2.92
0.08	1094.3	4.497	1.715	0.0026	0.40	0.65	1.40	21	13	2.828	2.828	11.314	60.91	59.22	83.1	114.70	20.57

Feature	Q	R	V	S	D_{16}	D_{50}	D_{84}	FFC	PDS	τ	ώ
bench	36.132	0.842	0.54	0.0018	0.40	0.65	1.40	1.32	0.27	14.87	0.84
Top of island	51.213	0.939	0.60	0.0019	0.40	0.65	1.40	1.50	0.37	17.51	1.08
Estimated Q.	196.322	1.784	0.91	0.0022	0.40	0.65	1.40	3.50	1.22	38.49	3.64
terrace 1	567.527	3.353	1.30	0.0024	0.40	0.65	1.40	7.50	4.86	78.94	10.68
terrace 2	1006.554	4.424	1.61	0.0024	0.40	0.65	1.40	14	15	108.49	18.28

Annual series flood frequency curve		Dominant discharge			Partial series flood frequency curve	
$Q_{1.5}$	$Q_{2.44}$	Yang	AW	EH	$Q_{0.9}$	$Q_{2.0}$
20	52	146.01	136.94	305.32	138.50	269.210

Table 34 Summary table for Mhlathuze Site 3 virgin

%	Q	R	V	S	D_{16}	D_{50}	D_{84}	FFC	PDS	Max Y	Max AW	Max EH	% tran Y	%tran AW	% tran EH	τ	ω
9.999	0	0	0	0.0007	0.36	0.68	1.80			0	0	0	0	0	0	0	0
9.999	0.932	0.078	0.359	0.0007	0.36	0.68	1.80			0.707	0.707	0.707	0.03	0.04	0.01	0.54	0.02
9.999	1.491	0.014	0.299	0.0007	0.36	0.68	1.80			0.707	0.707	0.707	0	0	0	0.10	0.03
9.999	2.211	0.199	0.295	0.0007	0.36	0.68	1.80			0.707	0.707	1.414	0.06	0.04	0.04	1.37	0.04
9.999	3.095	0.232	0.296	0.0007	0.36	0.68	1.80			0.654	0.654	1.414	0.09	0.06	0.07	1.59	0.05
9.999	4.112	0.297	0.306	0.0007	0.36	0.68	1.80			0.654	0.654	1.414	0.16	0.09	0.13	2.04	0.06
9.999	5.424	0.369	0.323	0.0007	0.36	0.68	1.80			0.654	0.654	1.414	0.26	0.16	0.22	2.53	0.08
9.999	7.479	0.462	0.353	0.0007	0.36	0.68	1.80			0.707	0.707	2.828	0.54	0.38	0.42	3.17	0.12
9.999	12.236	0.629	0.419	0.0007	0.36	0.68	1.80			0.707	0.707	2.828	1.68	1.26	1.11	4.32	0.19
4.999	21.375	0.817	0.524	0.0080	0.36	0.68	1.80			0.707	0.707	2.828	3.24	2.42	2.07	6.41	0.35
3.999	48.661	1.207	0.736	0.0080	0.36	0.68	1.80	1.3	0.15	1.414	1.414	2.828	13.22	10.36	7.81	9.47	0.72
0.949	245.49	1.588	1.341	0.0080	0.36	0.68	1.80	3.3	0.93	5.651	5.651	5.651	35.51	44.90	21.04	12.46	1.72
0.08	1736.4	4.569	2.337	0.0080	0.36	0.68	1.80	16	9.5	5.651	5.651	5.651	45.21	40.31	67.09	35.86	8.75

Feature	Q	R	V	S	D_{16}	D_{50}	D_{84}	FFC	PDS	τ	ω
Estimated Q	149.398	1.790	1.19	0.0008	0.36	0.68	1.80	2.3	0.61	14.05	1.73
terrace 1	530.994	2.370	1.59	0.0008	0.36	0.68	1.80	4.9	1.89	18.60	3.05
terrace 2	1768.15	4.682	2.40	0.0009	0.36	0.68	1.80	16	11	41.34	10.37

Annual series flood frequency curve		Dominant discharge			Partial series flood frequency curve	
$Q_{1.5}$	$Q_{2.44}$	Yang	AW	EH	$Q_{0.9}$	$Q_{5.0}$
88	168	130.08	153.13	185.18	244	541.79

Table 35 Summary table for Mhlathuze Site 3 present

%	Q	R	V	S	D_{16}	D_{50}	D_{84}	FFC	PDS	Max Y	Max AW	Max EH	% tran Y	%tran AW	% tran EH	τ	$\dot{\omega}$
9.999	0	0	0	0.0007	0.38	0.88	1.60			0	0	0	0	0	0	0	0
9.999	0.429	0.067	0.189	0.0007	0.38	0.88	1.60			2.828	2.828	1.414	0.11	1.80	0.01	0.46	0.03
9.999	0.565	0.069	0.129	0.0007	0.38	0.88	1.60			1.414	2.828	1.414	0.09	0.84	0.01	0.47	0.02
9.999	0.773	0.072	0.109	0.0007	0.38	0.88	1.60			1.414	0.707	1.414	0.07	0.21	0.01	0.49	0.02
9.999	1.088	0.099	0.106	0.0007	0.38	0.88	1.60			0.707	0.354	1.414	0.05	0.04	0.03	0.68	0.02
9.999	1.476	0.141	0.111	0.0007	0.38	0.88	1.60			0.707	0.354	1.414	0.06	0.04	0.03	0.97	0.03
9.999	2.009	0.187	0.118	0.0007	0.38	0.88	1.60			0.707	0.354	1.414	0.08	0.05	0.06	1.28	0.04
9.999	2.837	0.214	0.131	0.0007	0.38	0.88	1.60			0.707	0.354	1.414	0.13	0.09	0.09	1.47	0.04
9.999	4.883	0.341	0.162	0.0007	0.38	0.88	1.60			0.707	0.354	1.414	0.23	0.21	0.27	2.34	0.08
4.999	10.330	0.567	0.242	0.0007	0.38	0.88	1.60			1.414	0.707	2.828	0.90	0.69	0.61	3.89	0.16
3.999	30.714	0.972	0.444	0.0008	0.38	0.88	1.60	1.32	0.41	2.828	1.414	2.828	8.65	6.79	5.01	7.63	0.48
0.949	184.46	1.669	0.864	0.0008	0.38	0.88	1.60	4.3	0.92	2.828	2.828	2.828	38.85	45.32	23.37	13.10	1.72
0.08	1410.4	4.307	1.875	0.0008	0.38	0.88	1.60	22	12	2.828	5.561	5.561	50.78	43.92	70.51	33.80	7.38

Feature	Q	R	V	S	D_{16}	D_{50}	D_{84}	FFC	PDS	τ	$\dot{\omega}$
Estimated Q_c	149.398	1.790	1.19	0.0008	0.36	0.68	1.80	2.62	0.76	14.05	1.73
terrace 1	530.994	2.370	1.59	0.0008	0.36	0.68	1.80	9.5	2.62	18.60	3.05
terrace 2	1768.15	4.682	2.40	0.0009	0.36	0.68	1.80	30	16	41.34	10.37

Annual series flood frequency curve		Dominant discharge			Partial series flood frequency curve	
$Q_{1.5}$	$Q_{2.44}$	Yang	AW	EH	$Q_{0.9}$	$Q_{2.0}$
50	105	154.2	124	228.72	181	376.53

Table 36 Summary table for Mhlathuze Site 4 virgin

%	Q	R	V	S	D_{16}	D_{50}	D_{84}	FFC	PDS	Max Y	Max AW	Max EH	% tran Y	%tran AW	% tran EH	τ	$\acute{\omega}$
9.999	0	0.119	0	0.0009	0.13	0.38	0.88			0	0	0	0	0	0	1.05	0
9.999	1.510	0.217	0.213	0.0009	0.13	0.38	0.88			0.354	0	1.414	0.01	0	0.05	1.92	0.04
9.999	2.275	0.276	0.249	0.0009	0.13	0.38	0.88			0.707	0	1.414	0.04	0	0.11	2.44	0.06
9.999	3.154	0.331	0.285	0.0009	0.13	0.38	0.88			0.707	0.354	1.414	0.12	0.05	0.21	2.92	0.09
9.999	4.201	0.386	0.322	0.0009	0.13	0.38	0.88			0.707	0.707	1.414	0.24	0.12	0.36	3.41	0.11
9.999	5.373	0.438	0.358	0.0009	0.13	0.38	0.88			1.414	0.707	2.828	0.51	0.27	0.59	3.87	0.14
9.999	6.820	0.496	0.397	0.0009	0.13	0.38	0.88			1.414	0.707	2.828	1	0.54	0.94	4.38	0.18
9.999	9.110	0.572	0.453	0.0009	0.13	0.38	0.88			1.414	0.707	2.828	2.03	1.17	1.66	5.05	0.24
9.999	14.170	0.685	0.552	0.0008	0.13	0.38	0.88			2.828	1.414	2.828	4.59	3.26	2.98	5.38	0.31
4.999	23.653	0.783	0.680	0.0008	0.13	0.38	0.88			2.828	1.414	2.828	6.01	5.36	3.50	6.14	0.44
3.999	53.078	1.158	0.922	0.0008	0.13	0.38	0.88	1.3	0.24	2.828	2.828	2.828	18.69	17.71	12.60	9.09	0.87
0.949	263.20	1.452	0.966	0.0008	0.13	0.38	0.88	3.3	1.12	2.828	2.828	2.828	22.69	18.34	18.27	11.40	1.14
0.08	1849.7	3.448	2.702	0.0007	0.13	0.38	0.88	16	13	2.828	11.314	5.651	44.06	53.17	58.73	23.68	6.64

Feature	Q	R	V	S	D_{16}	D_{50}	D_{84}	FFC	PDS	τ	$\acute{\omega}$
bench	77.286	0.882	0.920	0.0009	0.13	0.38	0.88	1.40	0.25	7.79	0.74
Estimated Qb	234.191	1.326	0.998	0.0007	0.13	0.38	0.88	3	0.81	9.11	0.94
terrace 1	1379.600	3.451	2.015	0.0007	0.13	0.38	0.88	13	6.70	23.70	4.95

Annual series flood frequency curve		Dominant discharge			Partial series flood frequency curve	
$Q_{1.5}$	$Q_{2.44}$	Yang	AW	EH	$Q_{0.9}$	$Q_{2.0}$
90	178	51.62	99.82	106.2	257	593.331

Table 37 Summary table for Mhlathuze Site 4 present

%	Q	R	V	S	D_{16}	D_{50}	D_{84}	FFC	PDS	Max Y	Max AW	Max EH	% tran Y	%tran AW	% tran EH	τ	ω
9.999	0	0.119	0	0.0009	0.13	0.38	0.88			0	0	0	0	0	0	1.05	0
9.999	0.657	0.127	0.163	0.0009	0.13	0.38	0.88			0.177	0	1.414	0	0	0.01	1.12	0.02
9.999	0.973	0.164	0.183	0.0009	0.13	0.38	0.88			0	0	1.414	0	0	0.03	1.45	0.03
9.999	1.392	0.206	0.207	0.0009	0.13	0.38	0.88			0.354	0	1.414	0.01	0	0.07	1.82	0.04
9.999	1.870	0.246	0.231	0.0009	0.13	0.38	0.88			0.354	0	1.414	0.03	0	0.12	2.17	0.05
9.999	2.418	0.285	0.256	0.0009	0.13	0.38	0.88			0.707	0	1.414	0.09	0	0.19	2.52	0.07
9.999	3.138	0.330	0.284	0.0009	0.13	0.38	0.88			0.707	0.354	1.414	0.18	0.08	0.32	2.91	0.09
9.999	4.211	0.386	0.323	0.0009	0.13	0.38	0.88			0.707	0.354	2.828	0.39	0.16	0.58	3.41	0.11
9.999	6.698	0.491	0.394	0.0009	0.13	0.38	0.88			1.414	0.707	2.828	1.55	0.89	1.45	4.34	0.18
4.999	12.757	0.661	0.526	0.0008	0.13	0.38	0.88			2.828	1.414	2.828	3.46	2.36	2.48	5.19	0.28
3.999	35.156	0.952	0.789	0.0008	0.13	0.38	0.88	2.3	0.24	2.828	1.414	2.828	15.62	15.57	9.32	7.47	0.62
0.949	202.47	1.381	0.981	0.0008	0.13	0.38	0.88	3.2	1.12	2.828	2.828	2.828	29.14	27.36	21.45	10.84	1.10
0.08	1530.5	3.451	2.235	0.0007	0.13	0.38	0.88	19	13	2.828	5.651	2.828	49.52	53.28	63.88	23.70	5.49

Feature	Q	R	V	S	D_{16}	D_{50}	D_{84}	FFC	PDS	τ	ω
bench	77.286	0.882	0.920	0.0009	0.13	0.38	0.88	1.78	0.35	7.79	0.74
Estimated Qb	234.191	1.326	0.998	0.0007	0.13	0.38	0.88	3.80	1.00	9.11	0.94
terrace 1	1379.600	3.451	2.015	0.0007	0.13	0.38	0.88	19	15	23.70	4.95

Annual series flood frequency curve		Dominant discharge			Partial series flood frequency curve	
$Q_{1.5}$	$Q_{2.44}$	Yang	AW	EH	$Q_{0.9}$	Q_{20}
68	142	104.55	122.02	131.11	210	464.286

Table 38 Summary table for Olifants Site 1

%	Q	v	R	S	D16	D50	D84	FFC	PDS	Max Y	Max AW	Max EH	% tran Y	% tran AW	% tran EH	τ	ώ
9.999	0.047	0.065	0.076	0.0128	21	96	277			0	0	0	0	0	0	10.03	0.65
9.999	0.59	0.309	0.100	0.0125	21	96	277			0.354	0	2.828	0.01	0	0.02	12.99	1.76
9.999	0.336	0.150	0.110	0.0125	21	96	277			0.354	0	2.828	0.02	0	0.03	14.24	2.13
9.999	0.448	0.169	0.120	0.0124	21	96	277			0.354	0.354	2.828	0.04	0.02	0.05	15.46	2.61
9.999	0.663	0.197	0.136	0.0123	21	96	277			0.354	0.354	5.651	0.09	0.05	0.10	17.35	3.42
9.999	1.088	0.242	0.160	0.0121	21	96	277			0.707	0.354	45.255	0.27	0.15	0.23	20.22	4.89
9.999	1.897	0.306	0.190	0.0119	21	96	277			0.707	0.707	45.255	0.77	0.53	0.58	23.59	7.23
9.999	3.504	0.371	0.268	0.0115	21	96	277			1.414	0.707	90.51	2.09	1.3	1.72	31.92	11.85
9.999	7.364	0.553	0.318	0.0111	21	96	277			2.828	0.707	90.51	8.98	6.29	5.84	38.37	21.23
4.999	15.013	0.753	0.410	0.0104	21	96	277			2.828	1.414	181.019	14.07	11.18	9.35	47.56	35.80
3.999	32.792	1.048	0.542	0.0096	21	96	277	1.08	0.12	2.828	2.828	181.019	34.29	31.98	25.62	58.79	61.59
0.949	110.68	1.597	0.916	0.0082	21	96	277	4.1	1.04	11.314	22.627	181.019	29.67	37.68	36.16	80.30	128.26
0.08	361.24	2.126	1.860	0.0069	21	96	277	13	6.6	22.627	22.627	362.039	9.70	10.83	20.31	135.41	287.89

feature	Q	v	R	S	D16	D50	D84	FFC	PDS	τ	ώ
Estimated Qb	61.77	1.45	0.69	0.0090	21	96	277	1.6	0.33	67.39	97.53
terrace 1	755.62	2.73	2.63	0.0069	21	96	277	>64	>64	190.88	522.07
terrace 3	1898.72	3.78	3.19	0.0069	21	96	277	>64	>64	226.63	856.82

Annual series flood frequency curve		Dominant discharge			Partial series flood frequency curve	
$Q_{1.5}$	$Q_{2.33}$	Yang	AW	EH	Q[illegible]	Q[illegible]
53.5	74.5	26.61	31.77	32.44	96.67	178.09

Table 39 Summary table for Olifants Site 2

%	Q	v	R	S	D16	D50	D84	FFC	PDS	Max Y	Max AW	Max EH	% tran Y	% tran AW	% tran EH	τ	ω
9.999	0.518	0.567	0.151	0.015	5	220	520			2.828	1.414	22.627	0.04	0.01	0.01	22.44	12.72
9.999	1.547	0.837	0.219	0.014	5	220	520			2.828	5.651	45.255	0.23	0.06	0.05	27.08	22.67
9.999	2.105	0.941	0.248	0.014	5	220	520			5.651	5.651	362.039	0.09	0.09	0.09	34.35	32.33
9.999	2.794	1.053	0.277	0.014	5	220	520			5.651	5.651	362.039	0.54	0.14	0.16	38.32	40.36
9.999	3.877	1.202	0.312	0.014	5	220	520			11.314	11.314	362.039	0.87	0.24	0.28	43.27	52.00
9.999	5.771	1.413	0.360	0.013	5	220	520			11.314	22.627	362.039	1.52	0.45	0.57	46.32	65.43
9.999	9.109	1.711	0.417	0.013	5	220	520			22.627	45.255	362.039	2.89	0.92	1.26	53.66	91.80
9.999	14.927	2.102	0.495	0.012	5	220	520			45.255	90.51	724.077	5.76	2.01	3.01	58.91	123.83
9.999	26.747	2.697	0.603	0.011	5	220	520			90.51	181.019	724.077	13.05	5.32	8.5	65.84	177.58
4.999	47.229	3.454	0.739	0.011	5	220	520			90.51	1448.15	724.077	14.39	9.56	11.79	80.73	278.83
3.999	94.574	4.722	0.897	0.010	5	220	520	1.2	0.13	181.019	724.077	1448.15	33.98	50.71	31.51	89.48	422.52
0.949	278.45	5.534	1.294	0.008	5	220	520	4.28	0.95	181.019	724.077	1448.15	22.62	28.27	35.18	106.69	590.39
0.08	721.61	4.589	1.453	0.007	5	220	520	30	11	181.019	724.077	724.077	4.03	2.23	7.23	106.14	487.09

feature	Q	v	R	S	D16	D50	D84	FFC	PDS	Max Calibre	τ	ω
Estimated Qb	418.14	3.8	1.10	0.0080	5	220	520	9.2	1.9		107.91	410.20
terrace 1	620.91	4.64	1.24	0.0073	5	220	520	15.8	3.8		98.68	458.20
terrace 2	1245.16	4.13	2.04	0.0073	5	220	520	>64	64		164.45	679.83
terrace 3	2597.88	3.97	3.26	0.0073	5	220	520	>64	64		261.49	1038.56

Annual series flood frequency curve		Dominant discharge			Partial series flood frequency curve	
$Q_{1.5}$	$Q_{2.33}$	Yang	AW	EH	$Q_{1.5}$	$Q_{2.33}$
127	190	19.07	29.06	26.58	273.67	440.053

Table 40 Summary table for Olifants Site 3

%	Q	v	R	S	D16	D50	D84	FFC	PDS	Max Y	Max AW	Max EH	% tran Y	% tran AW	% tran EH	τ	ω
9.999	0.068	0.036	0.217	0.0061	140	250	480			0	0	0	0	0	0	14.36	0.52
9.999	0.220	0.106	0.233	0.0066	140	250	480			0	0	0.707	0	0	0	16.69	1.76
9.999	0.292	0.135	0.239	0.0068	140	250	480			0	0	0.707	0	0	0	17.64	2.38
9.999	0.368	0.165	0.006	0.0068	140	250	480			0	0	1.414	0	0	0.01	18.31	3.01
9.999	0.467	0.201	0.007	0.0069	140	250	480			0	0	1.414	0	0	0.01	19.30	3.89
9.999	0.639	0.260	0.007	0.0071	140	250	480			0.707	0	1.414	0.13	0	0.02	20.60	5.36
9.999	0.993	0.368	0.007	0.0073	140	250	480			0.707	0	1.414	0.11	0	0.06	23.11	8.50
9.999	1.709	0.549	0.008	0.0083	140	250	480			0.707	0	2.828	0.77	0.11	0.21	27.30	14.98
9.999	3.381	0.856	0.009	0.0093	140	250	480			2.828	0.707	2.828	3.79	0.97	1.02	30.42	26.03
4.999	6.808	1.248	0.010	0.0106	140	250	480			2.828	1.414	5.651	6.71	2.05	2.26	45.42	56.70
3.999	15.399	1.843	0.124	0.0124	140	250	480	1.01	0.13	2.828	2.828	11.314	26.67	13.47	12.01	73.21	134.96
0.949	52.411	2.960	0.0158	0.0158	140	250	480	4.2	1.17	22.627	45.255	362.039	35.19	43.45	40.59	158.35	468.71
0.08	186.47	3.896	0.0196	0.0196	140	250	480	8.4	5.35	181.019	362.039	724.077	26.54	39.95	43.80	327.75	1276.8

feature	Q	v	R	S	D16	D50	D84	FFC	PDS	τ	ω
Estimated Qb	160.451	3.777	1.47	0.0192	140	250	480	9.5	4.2	303.38	1145.87
terrace 1	605.061	4.038	2.13	0.0229	140	250	480	>64	>64	499.28	2017.73
terrace 2	889.071	3.716	2.51	0.0238	140	250	480	>64	>64	607.99	2259.78
terrace 3	1295.414	3.335	3.20	0.0247	140	250	480	>64	>64	804.38	2682.76

Annual series flood frequency curve		Dominant discharge			Partial series flood frequency curve	
$Q_{1.5}$	$Q_{2.33}$	Yang	AW	EH	$Q_{0.5}$	$Q_{2.0}$
30.50	40.650	38.59	63.64	63.20	45.936	81.161

Table 41 Summary table for Olifants Site 4

%	Q	v	R	S	D16	D50	D84	FFC	PDS	Max Y	Max AW	Max EH	% tran Y	% tran AW	% tran EH	τ	ω
9.999	0.291	0.114	0.193	0.0033	90	320	500			0	0	0	0	0	0	6.59	0.75
9.999	0.834	0.173	0.251	0.0040	90	320	500			0	0	0	0	0	0	10.63	1.84
9.999	1.111	0.195	0.291	0.0045	90	320	500			0	0	0	0	0	0	13.93	2.71
9.999	1.421	0.217	0.326	0.0046	90	320	500			0	0	0	0	0	0	16.09	3.50
9.999	1.812	0.244	0.362	0.0047	90	320	500			0	0	1.414	0	0	0.08	18.32	4.47
9.999	2.371	0.278	0.397	0.0049	90	320	500			0	0	2.828	0	0	0.24	21.00	5.83
9.999	3.286	0.328	0.457	0.0051	90	320	500			0	0	2.828	0	0	0.48	25.21	8.27
9.999	5.052	0.408	0.459	0.0054	90	320	500			1.414	0	5.651	1.40	0	1.19	26.38	10.76
9.999	9.294	0.520	0.445	0.0060	90	320	500			2.828	0	2.828	8.61	0	2.91	27.82	14.47
4.999	17.391	0.565	0.551	0.0060	90	320	500			2.828	0	5.651	14.19	0	4.19	33.98	19.19
3.999	37.601	0.589	0.942	0.0060	90	320	500	1.2	0.12	2.828	0	45.255	31.25	0	15.20	57.81	34.03
0.949	121.63	0.704	1.462	0.0075	90	320	500	4.95	0.83	2.828	0	181.019	30.13	0	33.35	110.82	78.03
0.08	379.49	0.851	2.802	0.0104	90	320	500	30	9.2	2.828	0	724.077	14.42	0	42.38	293.41	249.83

feature	Q	v	R	S	D16	D50	D84	FFC	PDS	τ	ω
Estimated Qb	80.216	2.770	1.38	0.0104	90	320	500	2.8	0.44	146.23	99.52
terrace 1	551.246	6.176	3.43	0.0104	90	320	500	30	15	359.20	334.28
terrace 2	993.212	7.890	4.26	0.0104	90	320	500	>64	>64	444.22	481.49
terrace 3	1462.110	9.267	5.13	0.0104	90	320	500	>64	>64	534.42	640.78

Annual series flood frequency curve		Dominant discharge			Partial series flood frequency curve	
$Q_{1.5}$	$Q_{2.33}$	Yang	AW	EH	$Q_{2.3}$	$Q_{2.0}$
48.90	73.00	28.49	-	43.31	125.924	191.584

APPENDIX H

RBS AND MILHOUS FOR ALL RIVERS

The following tables contain a number of symbols. The list below explains their meaning.

Q	is discharge in m^3s^{-1}
d	is depth in m
ρ	is the density of the water ($kg.m^{-3}$)
g	is the gravitational acceleration (m/sec^2)
ρ_s	is the density of the sediment ($kg.m^{-3}$)
R	is the hydraulic radius (m)
S	is the slope (m/m)
D_{16}	is the sediment size in millimetres at which 16% of the sediment is finer
D_{50}	is the sediment size in millimetres at which 50% of the sediment is finer
D_{84}	is the sediment size in millimetres at which 84% of the sediment is finer
τ	is the boundary shear stress (N/m^2)
τ_{ci}*	is the critical dimensionless shear stress
τ_{ci}	is the Shield's criterion
τRBS	is the Relative Bed Stability calculated using the shear stress criterion
q_c	is the bankfull unit discharge (m^2s^{-1})
$q_{critical}$	is the critical bankfull discharge
$\acute{\omega}$	is the stream power (Wm^{-2})
RBS_q	is the Relative Bed Stability calculated using the bankfull unit discharge
β	is the Milhous beta value

Table 1 RBS and Milhous for Mkomazi Site 1a

Site	Q	d	ρ	g	ρ_s	R	S	D50	D84	τ	τ_{ci}^*	τ_{ci}	τ RBS	q_c	$q_{critical}$	ω	RBS_n	β
D84																		
1a	0.015	0.317	1000	9.81	2650	0.14	0.0017	5.6	16	2.42	0.0216	5.59	2.3131	1.169	1.976	0.553	3.5731	0.02666
1a	0.246	0.417	1000	9.81	2650	0.22	0.0022	5.6	16	4.66	0.0216	5.59	1.2000	0.919	1.553	0.901	1.7230	0.05138
1a	0.355	0.467	1000	9.81	2650	0.27	0.0023	5.6	16	5.93	0.0216	5.59	0.9429	0.870	1.471	1.061	1.3866	0.06539
1a	0.480	0.513	1000	9.81	2650	0.31	0.0024	5.6	16	7.18	0.0216	5.59	0.7784	0.828	1.400	1.218	1.1498	0.07922
1a	0.655	0.566	1000	9.81	2650	0.36	0.0025	5.6	16	8.72	0.0216	5.59	0.6407	0.784	1.325	1.409	0.9402	0.09623
1a	0.926	0.630	1000	9.81	2650	0.41	0.0026	5.6	16	10.75	0.0216	5.59	0.5200	0.733	1.239	1.665	0.7440	0.11858
1a	1.391	0.715	1000	9.81	2650	0.49	0.0029	5.6	16	13.71	0.0216	5.59	0.4077	0.673	1.137	2.040	0.5572	0.15122
1a	2.230	0.828	1000	9.81	2650	0.59	0.0031	5.6	16	18.13	0.0216	5.59	0.3083	0.603	1.020	2.604	0.3916	0.20002
1a	3.991	0.992	1000	9.81	2650	0.73	0.0036	5.6	16	25.50	0.0216	5.59	0.2192	0.522	0.882	3.553	0.2483	0.28127
1a	7.181	1.191	1000	9.81	2650	0.89	0.0041	5.6	16	35.83	0.0216	5.59	0.1560	0.447	0.755	4.900	0.1541	0.39533
1a	13.467	1.448	1000	9.81	2650	1.09	0.0048	5.6	16	51.12	0.0216	5.59	0.1093	0.376	0.636	6.942	0.0916	0.56401
1a	30.367	1.865	1000	9.81	2650	1.38	0.0058	5.6	16	79.05	0.0216	5.59	0.0707	0.303	0.511	10.867	0.0471	0.87211
1a	69.606	2.413	1000	9.81	2650	1.70	0.0070	5.6	16	117.06	0.0216	5.59	0.0477	0.246	0.416	16.924	0.0246	1.29143
D16																		
Site	Q	d	ρ	g	ρ_s	R	S	D50	D16	τ	τ_{ci}^*	τ_{ci}	τ RBS	q_c	$q_{critical}$	ω	RBS_n	β
1a	0.015	0.317	1000	9.81	2650	0.14	0.0017	5.6	1.8	2.42	0.0996	2.90	1.2010	0.044	0.025	0.553	0.0452	0.02666
1a	0.246	0.417	1000	9.81	2650	0.22	0.0022	5.6	1.8	4.66	0.0996	2.90	0.6230	0.035	0.020	0.901	0.0218	0.05138
1a	0.355	0.467	1000	9.81	2650	0.27	0.0023	5.6	1.8	5.93	0.0996	2.90	0.4896	0.033	0.019	1.061	0.0175	0.06539
1a	0.480	0.513	1000	9.81	2650	0.31	0.0024	5.6	1.8	7.18	0.0996	2.90	0.4041	0.031	0.018	1.218	0.0146	0.07922
1a	0.655	0.566	1000	9.81	2650	0.36	0.0025	5.6	1.8	8.72	0.0996	2.90	0.3327	0.030	0.017	1.409	0.0119	0.09623
1a	0.926	0.630	1000	9.81	2650	0.41	0.0026	5.6	1.8	10.75	0.0996	2.90	0.2700	0.028	0.016	1.665	0.0094	0.11858
1a	1.391	0.715	1000	9.81	2650	0.49	0.0029	5.6	1.8	13.71	0.0996	2.90	0.2117	0.025	0.014	2.040	0.0071	0.15122
1a	2.230	0.828	1000	9.81	2650	0.59	0.0031	5.6	1.8	18.13	0.0996	2.90	0.1601	0.023	0.013	2.604	0.0050	0.20002
1a	3.991	0.992	1000	9.81	2650	0.73	0.0036	5.6	1.8	25.50	0.0996	2.90	0.1138	0.020	0.011	3.553	0.0031	0.28127
1a	7.181	1.191	1000	9.81	2650	0.89	0.0041	5.6	1.8	35.83	0.0996	2.90	0.0810	0.017	0.010	4.900	0.0020	0.39533
1a	13.467	1.448	1000	9.81	2650	1.09	0.0048	5.6	1.8	51.12	0.0996	2.90	0.0568	0.014	0.008	6.942	0.0012	0.56401
1a	30.367	1.865	1000	9.81	2650	1.38	0.0058	5.6	1.8	79.05	0.0996	2.90	0.0367	0.011	0.006	10.867	0.0006	0.87211
1a	69.606	2.413	1000	9.81	2650	1.70	0.0070	5.6	1.8	117.06	0.0996	2.90	0.0248	0.009	0.005	16.924	0.0003	1.29143

Table 2 RBS and Milhous for Mkomazi Site 1b

Site	Q	d	ρ	g	ρ_s	R	S	D50	D84	τ	τ_{ci}^*	τ_{ci}	τ RBS	q_c	$q_{critical}$	ώ	RBS_q	β
D84																		
1b	0.015	0.513	1000	9.81	2650	0.238	0.0017	5.6	16	4.06	0.0216	5.59	1.3753	1.169	1.976	0.894	2.2105	0.04483
1b	0.246	0.761	1000	9.81	2650	0.464	0.0022	5.6	16	9.84	0.0216	5.59	0.5679	0.919	1.553	1.645	0.9437	0.10858
1b	0.355	0.812	1000	9.81	2650	0.511	0.0023	5.6	16	11.37	0.0216	5.59	0.4915	0.870	1.471	1.843	0.7981	0.12546
1b	0.480	0.859	1000	9.81	2650	0.554	0.0024	5.6	16	12.88	0.0216	5.59	0.4340	0.828	1.400	2.037	0.6873	0.14208
1b	0.655	0.911	1000	9.81	2650	0.600	0.0025	5.6	16	14.68	0.0216	5.59	0.3808	0.784	1.325	2.269	0.5837	0.16190
1b	0.926	0.976	1000	9.81	2650	0.658	0.0026	5.6	16	17.08	0.0216	5.59	0.3272	0.733	1.239	2.581	0.4800	0.18845
1b	1.391	1.061	1000	9.81	2650	0.733	0.0029	5.6	16	20.53	0.0216	5.59	0.2722	0.673	1.137	3.029	0.3753	0.22654
1b	2.230	1.173	1000	9.81	2650	0.829	0.0031	5.6	16	25.60	0.0216	5.59	0.2183	0.603	1.020	3.690	0.2764	0.28239
1b	3.991	1.336	1000	9.81	2650	0.985	0.0036	5.6	16	34.60	0.0216	5.59	0.1615	0.522	0.882	4.785	0.1844	0.38173
1b	7.181	1.532	1000	9.81	2650	1.110	0.0041	5.6	16	44.80	0.0216	5.59	0.1247	0.447	0.755	6.304	0.1198	0.49426
1b	13.467	1.784	1000	9.81	2650	1.292	0.0048	5.6	16	60.76	0.0216	5.59	0.0920	0.376	0.636	8.554	0.0744	0.67034
1b	30.367	2.190	1000	9.81	2650	1.570	0.0058	5.6	16	89.78	0.0216	5.59	0.0623	0.303	0.511	12.763	0.0401	0.99046
1b	69.606	2.721	1000	9.81	2650	1.909	0.0070	5.6	16	131.36	0.0216	5.59	0.0425	0.246	0.416	19.081	0.0218	1.44917

D16

Site	Q	d	ρ	g	ρ_s	R	S	D50	D16	τ	τ_{ci}^*	τ_{ci}	τ RBS	q_c	$q_{critical}$	ώ	RBS_q	β
1b	0.015	0.513	1000	9.81	2650	0.238	0.0017	5.6	1.8	4.06	0.0996	2.90	0.7141	0.044	0.025	0.894	0.0280	0.04483
1b	0.246	0.761	1000	9.81	2650	0.464	0.0022	5.6	1.8	9.84	0.0996	2.90	0.2949	0.035	0.020	1.645	0.0119	0.10858
1b	0.355	0.812	1000	9.81	2650	0.511	0.0023	5.6	1.8	11.37	0.0996	2.90	0.2552	0.033	0.019	1.843	0.0101	0.12546
1b	0.480	0.859	1000	9.81	2650	0.554	0.0024	5.6	1.8	12.88	0.0996	2.90	0.2253	0.031	0.018	2.037	0.0087	0.14208
1b	0.655	0.911	1000	9.81	2650	0.600	0.0025	5.6	1.8	14.68	0.0996	2.90	0.1977	0.030	0.017	2.269	0.0074	0.16190
1b	0.926	0.976	1000	9.81	2650	0.658	0.0026	5.6	1.8	17.08	0.0996	2.90	0.1699	0.028	0.016	2.581	0.0061	0.18845
1b	1.391	1.061	1000	9.81	2650	0.733	0.0029	5.6	1.8	20.53	0.0996	2.90	0.1413	0.025	0.014	3.029	0.0048	0.22654
1b	2.230	1.173	1000	9.81	2650	0.829	0.0031	5.6	1.8	25.60	0.0996	2.90	0.1134	0.023	0.013	3.690	0.0035	0.28239
1b	3.991	1.336	1000	9.81	2650	0.985	0.0036	5.6	1.8	34.60	0.0996	2.90	0.0839	0.020	0.011	4.785	0.0023	0.38173
1b	7.181	1.532	1000	9.81	2650	1.110	0.0041	5.6	1.8	44.80	0.0996	2.90	0.0648	0.017	0.010	6.304	0.0015	0.49426
1b	13.467	1.784	1000	9.81	2650	1.292	0.0048	5.6	1.8	60.76	0.0996	2.90	0.0478	0.014	0.008	8.554	0.0009	0.67034
1b	30.367	2.190	1000	9.81	2650	1.570	0.0058	5.6	1.8	89.78	0.0996	2.90	0.0323	0.011	0.006	12.763	0.0005	0.99046
1b	69.606	2.721	1000	9.81	2650	1.909	0.0070	5.6	1.8	131.36	0.0996	2.90	0.0221	0.009	0.005	19.081	0.0003	1.44917

Table 3 RBS and Milhous for Mkomazi Site 1c

Site	Q	d	ρ	g	ρ_s	R	S	D50	D84	τ	τ_{ci}^*	τ_{ci}	τ RBS	q_c	$q_{critical}$	ώ	RBS_q	β
D84																		
1c	0.015	0.567	1000	9.81	2650	0.385	0.0017	5.6	16	6.58	0.0216	5.59	0.8495	1.169	1.976	0.988	2.0003	0.07258
1c	0.246	0.681	1000	9.81	2650	0.487	0.0022	5.6	16	10.33	0.0216	5.59	0.5410	0.919	1.553	1.472	1.0547	0.11398
1c	0.355	0.708	1000	9.81	2650	0.512	0.0023	5.6	16	11.40	0.0216	5.59	0.4903	0.870	1.471	1.606	0.9155	0.12575
1c	0.480	0.733	1000	9.81	2650	0.534	0.0024	5.6	16	12.43	0.0216	5.59	0.4495	0.828	1.400	1.739	0.8052	0.13716
1c	0.655	0.763	1000	9.81	2650	0.560	0.0025	5.6	16	13.70	0.0216	5.59	0.4081	0.784	1.325	1.900	0.6973	0.15110
1c	0.926	0.800	1000	9.81	2650	0.593	0.0026	5.6	16	15.39	0.0216	5.59	0.3632	0.733	1.239	2.115	0.5857	0.16976
1c	1.391	0.851	1000	9.81	2650	0.638	0.0029	5.6	16	17.86	0.0216	5.59	0.3129	0.673	1.137	2.430	0.4679	0.19706
1c	2.230	0.922	1000	9.81	2650	0.699	0.0031	5.6	16	21.57	0.0216	5.59	0.2592	0.603	1.020	2.901	0.3516	0.23791
1c	3.991	1.030	1000	9.81	2650	0.786	0.0036	5.6	16	27.61	0.0216	5.59	0.2025	0.522	0.882	3.689	0.2391	0.30456
1c	7.181	1.168	1000	9.81	2650	0.891	0.0041	5.6	16	35.97	0.0216	5.59	0.1554	0.447	0.755	4.807	0.1571	0.39678
1c	13.467	2.071	1000	9.81	2650	1.448	0.0048	5.6	16	68.12	0.0216	5.59	0.0820	0.376	0.636	9.931	0.0641	0.75155
1c	30.367	2.420	1000	9.81	2650	1.453	0.0058	5.6	16	83.07	0.0216	5.59	0.0673	0.303	0.511	14.101	0.0363	0.91641
1c	69.606	2.861	1000	9.81	2650	1.229	0.0070	5.6	16	84.55	0.0216	5.59	0.0661	0.246	0.416	20.061	0.0207	0.93276
Site	Q	d	ρ	g	ρ_s	R	S	D50	D16	τ	τ_{ci}^*	τ_{ci}	τ RBS	q_c	$q_{critical}$	ώ	RBS_q	β
D16																		
1c	0.015	0.567	1000	9.81	2650	0.385	0.0017	5.6	1.8	6.58	0.0996	2.90	0.4411	0.044	0.025	0.988	0.0253	0.07258
1c	0.246	0.681	1000	9.81	2650	0.487	0.0022	5.6	1.8	10.33	0.0996	2.90	0.2809	0.035	0.020	1.472	0.0133	0.11398
1c	0.355	0.708	1000	9.81	2650	0.512	0.0023	5.6	1.8	11.40	0.0996	2.90	0.2546	0.033	0.019	1.606	0.0116	0.12575
1c	0.480	0.733	1000	9.81	2650	0.534	0.0024	5.6	1.8	12.43	0.0996	2.90	0.2334	0.031	0.018	1.739	0.0102	0.13716
1c	0.655	0.763	1000	9.81	2650	0.560	0.0025	5.6	1.8	13.70	0.0996	2.90	0.2119	0.030	0.017	1.900	0.0088	0.15110
1c	0.926	0.800	1000	9.81	2650	0.593	0.0026	5.6	1.8	15.39	0.0996	2.90	0.1886	0.028	0.016	2.115	0.0074	0.16976
1c	1.391	0.851	1000	9.81	2650	0.638	0.0029	5.6	1.8	17.86	0.0996	2.90	0.1625	0.025	0.014	2.430	0.0059	0.19706
1c	2.230	0.922	1000	9.81	2650	0.699	0.0031	5.6	1.8	21.57	0.0996	2.90	0.1346	0.023	0.013	2.901	0.0044	0.23791
1c	3.991	1.030	1000	9.81	2650	0.786	0.0036	5.6	1.8	27.61	0.0996	2.90	0.1051	0.020	0.011	3.689	0.0030	0.30456
1c	7.181	1.168	1000	9.81	2650	0.891	0.0041	5.6	1.8	35.97	0.0996	2.90	0.0807	0.017	0.010	4.807	0.0020	0.39678
1c	13.467	2.071	1000	9.81	2650	1.448	0.0048	5.6	1.8	68.12	0.0996	2.90	0.0426	0.014	0.008	9.931	0.0008	0.75155
1c	30.367	2.420	1000	9.81	2650	1.453	0.0058	5.6	1.8	83.07	0.0996	2.90	0.0349	0.011	0.006	14.101	0.0005	0.91641
1c	69.606	2.861	1000	9.81	2650	1.229	0.0070	5.6	1.8	84.55	0.0996	2.90	0.0343	0.009	0.005	20.061	0.0003	0.93276

Table 4 RBS and Milhous for Mkomazi Site 2a

Site	Q	d	ρ	g	ρ_s	R	S	D50	D84	τ	τ_{ci}^*	τ_{ci}	τ RBS	q_c	$q_{critical}$	$\bar{\omega}$	RBS_o	β
D84																		
2a	0.025	0.442	1000	9.81	2650	0.221	0.0030	10	45	6.57	0.0157	11.44	1.7417	2.975	6.311	1.335	4.7267	0.04057
2a	0.424	0.640	1000	9.81	2650	0.356	0.0031	10	45	10.69	0.0157	11.44	1.0702	2.931	6.218	1.960	3.1716	0.06603
2a	0.613	0.685	1000	9.81	2650	0.389	0.0031	10	45	11.73	0.0157	11.44	0.9752	2.920	6.195	2.107	2.9395	0.07246
2a	0.830	0.728	1000	9.81	2650	0.420	0.0031	10	45	12.71	0.0157	11.44	0.8999	2.910	6.173	2.246	2.7490	0.07852
2a	1.132	0.777	1000	9.81	2650	0.455	0.0031	10	45	13.82	0.0157	11.44	0.8278	2.898	6.148	2.406	2.5547	0.08536
2a	1.599	0.840	1000	9.81	2650	0.499	0.0031	10	45	15.22	0.0157	11.44	0.7514	2.883	6.116	2.611	2.3423	0.09404
2a	2.402	0.924	1000	9.81	2650	0.556	0.0031	10	45	17.07	0.0157	11.44	0.6700	2.863	6.073	2.893	2.0997	0.10546
2a	3.852	1.041	1000	9.81	2650	0.638	0.0032	10	45	19.76	0.0157	11.44	0.5788	2.836	6.016	3.285	1.8314	0.12208
2a	6.893	1.217	1000	9.81	2650	0.758	0.0032	10	45	23.77	0.0157	11.44	0.4813	2.797	5.934	3.888	1.5262	0.14683
2a	12.404	1.439	1000	9.81	2650	0.908	0.0032	10	45	28.87	0.0157	11.44	0.3961	2.752	5.838	4.666	1.2511	0.17837
2a	23.643	1.749	1000	9.81	2650	1.166	0.0033	10	45	37.77	0.0157	11.44	0.3029	2.697	5.721	5.775	0.9906	0.23331
2a	54.193	2.280	1000	9.81	2650	1.573	0.0034	10	45	52.28	0.0157	11.44	0.2188	2.620	5.558	7.722	0.7198	0.32300
2a	124.217	3.009	1000	9.81	2650	2.051	0.0035	10	45	70.01	0.0157	11.44	0.1634	2.543	5.394	10.470	0.5152	0.43251
D16																		
Site	Q	d	ρ	g	ρ_s	R	S	D50	D16	τ	τ_{ci}^*	τ_{ci}	τ RBS	q_c	$q_{critical}$	$\bar{\omega}$	RBS_o	β
2a	0.025	0.442	1000	9.81	2650	0.221	0.0030	10	2.8	6.57	0.1097	4.97	0.7571	0.046	0.024	1.335	0.0183	0.04057
2a	0.424	0.640	1000	9.81	2650	0.356	0.0031	10	2.8	10.69	0.1097	4.97	0.4652	0.045	0.024	1.960	0.0123	0.06603
2a	0.613	0.685	1000	9.81	2650	0.389	0.0031	10	2.8	11.73	0.1097	4.97	0.4239	0.045	0.024	2.107	0.0114	0.07246
2a	0.830	0.728	1000	9.81	2650	0.420	0.0031	10	2.8	12.71	0.1097	4.97	0.3912	0.045	0.024	2.246	0.0106	0.07852
2a	1.132	0.777	1000	9.81	2650	0.455	0.0031	10	2.8	13.82	0.1097	4.97	0.3598	0.045	0.024	2.406	0.0099	0.08536
2a	1.599	0.840	1000	9.81	2650	0.499	0.0031	10	2.8	15.22	0.1097	4.97	0.3266	0.045	0.024	2.611	0.0091	0.09404
2a	2.402	0.924	1000	9.81	2650	0.556	0.0031	10	2.8	17.07	0.1097	4.97	0.2913	0.044	0.024	2.893	0.0081	0.10546
2a	3.852	1.041	1000	9.81	2650	0.638	0.0032	10	2.8	19.76	0.1097	4.97	0.2516	0.044	0.023	3.285	0.0071	0.12208
2a	6.893	1.217	1000	9.81	2650	0.758	0.0032	10	2.8	23.77	0.1097	4.97	0.2092	0.043	0.023	3.888	0.0059	0.14683
2a	12.404	1.439	1000	9.81	2650	0.908	0.0032	10	2.8	28.87	0.1097	4.97	0.1722	0.043	0.023	4.666	0.0048	0.17837
2a	23.643	1.749	1000	9.81	2650	1.166	0.0033	10	2.8	37.77	0.1097	4.97	0.1316	0.042	0.022	5.775	0.0038	0.23331
2a	54.193	2.280	1000	9.81	2650	1.573	0.0034	10	2.8	52.28	0.1097	4.97	0.0951	0.041	0.022	7.722	0.0028	0.32300
2a	124.217	3.009	1000	9.81	2650	2.051	0.0035	10	2.8	70.01	0.1097	4.97	0.0710	0.039	0.021	10.470	0.0020	0.43251

Table 5 RBS and Milhous for Mkomazi Site 2b

Site	Q	d	ρ	g	ρ_s	R	S	D50	D84	τ	τ_{ci}^*	τ_{ci}	τ RBS	q_c	$q_{critical}$	ώ	RBS_q	β
D84																		
2b	0.025	0.392	1000	9.81	2650	0.286	0.0030	10	45	8.48	0.0157	11.44	1.3490	2.975	6.311	1.185	5.3240	0.05238
2b	0.424	0.576	1000	9.81	2650	0.427	0.0031	10	45	12.83	0.0157	11.44	0.8916	2.931	6.218	1.765	3.5226	0.07925
2b	0.613	0.619	1000	9.81	2650	0.460	0.0031	10	45	13.86	0.0157	11.44	0.8249	2.920	6.195	1.903	3.2549	0.08566
2b	0.830	0.658	1000	9.81	2650	0.489	0.0031	10	45	14.80	0.0157	11.44	0.7729	2.910	6.173	2.029	3.0417	0.09142
2b	1.132	0.704	1000	9.81	2650	0.523	0.0031	10	45	15.89	0.0157	11.44	0.7199	2.898	6.148	2.179	2.8210	0.09815
2b	1.599	0.761	1000	9.81	2650	0.565	0.0031	10	45	17.23	0.0157	11.44	0.6640	2.883	6.116	2.367	2.5843	0.10642
2b	2.402	0.840	1000	9.81	2650	0.621	0.0031	10	45	19.06	0.0157	11.44	0.6002	2.863	6.073	2.629	2.3104	0.11774
2b	3.852	0.947	1000	9.81	2650	0.693	0.0032	10	45	21.46	0.0157	11.44	0.5330	2.836	6.016	2.989	2.0129	0.13256
2b	6.893	1.110	1000	9.81	2650	0.800	0.0032	10	45	25.08	0.0157	11.44	0.4560	2.797	5.934	3.547	1.6731	0.15496
2b	12.404	1.315	1000	9.81	2650	0.921	0.0032	10	45	29.29	0.0157	11.44	0.3905	2.752	5.838	4.263	1.3695	0.18093
2b	23.643	1.600	1000	9.81	2650	1.094	0.0033	10	45	35.41	0.0157	11.44	0.3230	2.697	5.721	5.282	1.0831	0.21878
2b	54.193	2.087	1000	9.81	2650	1.427	0.0034	10	45	47.41	0.0157	11.44	0.2412	2.620	5.558	7.069	0.7862	0.29291
2b	124.217	2.757	1000	9.81	2650	1.950	0.0035	10	45	66.54	0.0157	11.44	0.1719	2.543	5.394	9.592	0.5623	0.41108
D16																		
Site	Q	d	ρ	g	ρ_s	R	S	D50	D16	τ	τ_{ci}^*	τ_{ci}	τ RBS	q_c	$q_{critical}$	ώ	RBS_q	β
2b	0.025	0.392	1000	9.81	2650	0.286	0.0030	10	2.8	8.48	0.1097	4.97	0.5864	0.046	0.024	1.185	0.0206	0.05238
2b	0.424	0.576	1000	9.81	2650	0.427	0.0031	10	2.8	12.83	0.1097	4.97	0.3876	0.045	0.024	1.765	0.0136	0.07925
2b	0.613	0.619	1000	9.81	2650	0.460	0.0031	10	2.8	13.86	0.1097	4.97	0.3586	0.045	0.024	1.903	0.0126	0.08566
2b	0.830	0.658	1000	9.81	2650	0.489	0.0031	10	2.8	14.80	0.1097	4.97	0.3360	0.045	0.024	2.029	0.0118	0.09142
2b	1.132	0.704	1000	9.81	2650	0.523	0.0031	10	2.8	15.89	0.1097	4.97	0.3129	0.045	0.024	2.179	0.0109	0.09815
2b	1.599	0.761	1000	9.81	2650	0.565	0.0031	10	2.8	17.23	0.1097	4.97	0.2886	0.045	0.024	2.367	0.0100	0.10642
2b	2.402	0.840	1000	9.81	2650	0.621	0.0031	10	2.8	19.06	0.1097	4.97	0.2609	0.044	0.024	2.629	0.0089	0.11774
2b	3.852	0.947	1000	9.81	2650	0.693	0.0032	10	2.8	21.46	0.1097	4.97	0.2317	0.044	0.023	2.989	0.0078	0.13256
2b	6.893	1.110	1000	9.81	2650	0.800	0.0032	10	2.8	25.08	0.1097	4.97	0.1982	0.043	0.023	3.547	0.0065	0.15496
2b	12.404	1.315	1000	9.81	2650	0.921	0.0032	10	2.8	29.29	0.1097	4.97	0.1698	0.043	0.023	4.263	0.0053	0.18093
2b	23.643	1.600	1000	9.81	2650	1.094	0.0033	10	2.8	35.41	0.1097	4.97	0.1404	0.042	0.022	5.282	0.0042	0.21878
2b	54.193	2.087	1000	9.81	2650	1.427	0.0034	10	2.8	47.41	0.1097	4.97	0.1049	0.041	0.022	7.069	0.0030	0.29291
2b	124.217	2.757	1000	9.81	2650	1.950	0.0035	10	2.8	66.54	0.1097	4.97	0.0747	0.039	0.021	9.592	0.0022	0.41108

Table 6 RBS and Milhous for Mkomazi Site 2c

Site	Q	d	ρ	g	ρ_s	R	S	D50	D84	τ	τ_{ci}^*	τ_{ci}	τ RBS	q_c	$q_{critical}$	ώ	RBS_o	β
D84																		
2c	0.025	0.316	1000	9.81	2650	0.222	0.0030	10	45	6.58	0.0157	11.44	1.7393	2.975	6.311	0.956	6.6044	0.04063
2c	0.424	0.712	1000	9.81	2650	0.357	0.0031	10	45	10.74	0.0157	11.44	1.0649	2.931	6.218	2.182	2.8498	0.06635
2c	0.613	0.792	1000	9.81	2650	0.430	0.0031	10	45	12.98	0.0157	11.44	0.8813	2.920	6.195	2.435	2.5439	0.08018
2c	0.830	0.864	1000	9.81	2650	0.495	0.0031	10	45	14.97	0.0157	11.44	0.7640	2.910	6.173	2.665	2.3165	0.09249
2c	1.132	0.945	1000	9.81	2650	0.566	0.0031	10	45	17.19	0.0157	11.44	0.6653	2.898	6.148	2.925	2.1016	0.10621
2c	1.599	1.045	1000	9.81	2650	0.652	0.0031	10	45	19.90	0.0157	11.44	0.5749	2.883	6.116	3.250	1.8820	0.12291
2c	2.402	1.175	1000	9.81	2650	0.767	0.0031	10	45	23.53	0.0157	11.44	0.4860	2.863	6.073	3.677	1.6517	0.14539
2c	3.852	1.347	1000	9.81	2650	0.908	0.0032	10	45	28.10	0.0157	11.44	0.4070	2.836	6.016	4.251	1.4152	0.17363
2c	6.893	1.593	1000	9.81	2650	1.092	0.0032	10	45	34.23	0.0157	11.44	0.3341	2.797	5.934	5.090	1.1658	0.21147
2c	12.404	1.888	1000	9.81	2650	1.265	0.0032	10	45	40.24	0.0157	11.44	0.2843	2.752	5.838	6.121	0.9538	0.24858
2c	23.643	2.275	1000	9.81	2650	1.536	0.0033	10	45	49.74	0.0157	11.44	0.2299	2.697	5.721	7.510	0.7617	0.30729
2c	54.193	2.891	1000	9.81	2650	1.793	0.0034	10	45	59.60	0.0157	11.44	0.1919	2.620	5.558	9.793	0.5675	0.36819
2c	124.217	3.675	1000	9.81	2650	2.034	0.0035	10	45	69.41	0.0157	11.44	0.1648	2.543	5.394	12.786	0.4219	0.42879
D16																		
Site	Q	d	ρ	g	ρ_s	R	S	D50	D16	τ	τ_{ci}^*	τ_{ci}	τ RBS	q_c	$q_{critical}$	ώ	RBS_o	β
2c	0.025	0.316	1000	9.81	2650	0.222	0.0030	10	2.8	6.58	0.1097	4.97	0.7560	0.046	0.024	0.956	0.0256	0.04063
2c	0.424	0.712	1000	9.81	2650	0.357	0.0031	10	2.8	10.74	0.1097	4.97	0.4629	0.045	0.024	2.182	0.0110	0.06635
2c	0.613	0.792	1000	9.81	2650	0.430	0.0031	10	2.8	12.98	0.1097	4.97	0.3831	0.045	0.024	2.435	0.0098	0.08018
2c	0.830	0.864	1000	9.81	2650	0.495	0.0031	10	2.8	14.97	0.1097	4.97	0.3321	0.045	0.024	2.665	0.0090	0.09249
2c	1.132	0.945	1000	9.81	2650	0.566	0.0031	10	2.8	17.19	0.1097	4.97	0.2892	0.045	0.024	2.925	0.0081	0.10621
2c	1.599	1.045	1000	9.81	2650	0.652	0.0031	10	2.8	19.90	0.1097	4.97	0.2499	0.045	0.024	3.250	0.0073	0.12291
2c	2.402	1.175	1000	9.81	2650	0.767	0.0031	10	2.8	23.53	0.1097	4.97	0.2113	0.044	0.024	3.677	0.0064	0.14539
2c	3.852	1.347	1000	9.81	2650	0.908	0.0032	10	2.8	28.10	0.1097	4.97	0.1769	0.044	0.023	4.251	0.0055	0.17363
2c	6.893	1.593	1000	9.81	2650	1.092	0.0032	10	2.8	34.23	0.1097	4.97	0.1452	0.043	0.023	5.090	0.0045	0.21147
2c	12.404	1.888	1000	9.81	2650	1.265	0.0032	10	2.8	40.24	0.1097	4.97	0.1236	0.043	0.023	6.121	0.0037	0.24858
2c	23.643	2.275	1000	9.81	2650	1.536	0.0033	10	2.8	49.74	0.1097	4.97	0.1000	0.042	0.022	7.510	0.0029	0.30729
2c	54.193	2.891	1000	9.81	2650	1.793	0.0034	10	2.8	59.60	0.1097	4.97	0.0834	0.041	0.022	9.793	0.0022	0.36819
2c	124.217	3.675	1000	9.81	2650	2.034	0.0035	10	2.8	69.41	0.1097	4.97	0.0716	0.039	0.021	12.786	0.0016	0.42879

Table 7 RBS and Milhous for Mkomazi Site 3a

Site	Q	d	ρ	g	ρ_s	R	S	D50	D84	τ	τ_{ci}^*	τ_{ci}	τ RBS	q_c	$q_{critical}$	$\bar{\omega}$	RBS_n	β
D84																		
3a	0.044	0.426	1000	9.81	2650	0.198	0.0003	4.2	13.7	0.51	0.0197	4.36	8.4841	7.662	13.839	0.113	122.9413	0.00756
3a	1.250	0.879	1000	9.81	2650	0.616	0.0005	4.2	13.7	2.87	0.0197	4.36	1.5182	3.968	7.167	0.418	17.1488	0.04226
3a	1.807	0.970	1000	9.81	2650	0.699	0.0005	4.2	13.7	3.58	0.0197	4.36	1.2167	3.568	6.444	0.507	12.7071	0.05273
3a	2.445	1.054	1000	9.81	2650	0.775	0.0006	4.2	13.7	4.31	0.0197	4.36	1.0121	3.258	5.885	0.598	9.8476	0.06339
3a	3.336	1.150	1000	9.81	2650	0.861	0.0006	4.2	13.7	5.21	0.0197	4.36	0.8364	2.960	5.346	0.710	7.5260	0.07671
3a	4.713	1.271	1000	9.81	2650	0.967	0.0007	4.2	13.7	6.46	0.0197	4.36	0.6751	2.654	4.794	0.865	5.5394	0.09504
3a	7.079	1.433	1000	9.81	2650	1.106	0.0008	4.2	13.7	8.30	0.0197	4.36	0.5257	2.330	4.209	1.096	3.8404	0.12205
3a	11.353	1.654	1000	9.81	2650	1.290	0.0009	4.2	13.7	11.07	0.0197	4.36	0.3939	2.003	3.618	1.448	2.4991	0.16289
3a	20.318	1.982	1000	9.81	2650	1.547	0.0010	4.2	13.7	15.63	0.0197	4.36	0.2790	1.669	3.015	2.042	1.4764	0.22993
3a	36.559	2.390	1000	9.81	2650	1.884	0.0012	4.2	13.7	22.26	0.0197	4.36	0.1959	1.401	2.530	2.879	0.8787	0.32749
3a	68.557	2.932	1000	9.81	2650	2.301	0.0014	4.2	13.7	31.73	0.0197	4.36	0.1374	1.179	2.128	4.122	0.5164	0.46679
3a	146.698	3.772	1000	9.81	2650	2.893	0.0017	4.2	13.7	46.99	0.0197	4.36	0.0928	0.981	1.772	6.247	0.2836	0.69127
3a	307.136	4.838	1000	9.81	2650	3.482	0.0019	4.2	13.7	64.60	0.0197	4.36	0.0675	0.846	1.527	9.148	0.1669	0.95020
D16																		
Site	Q	d	ρ	g	ρ_s	R	S	D50	D16	τ	τ_{ci}^*	τ_{ci}	τ RBS	q_c	$q_{critical}$	$\bar{\omega}$	RBS_n	β
3a	0.044	0.426	1000	9.81	2650	0.198	0.0003	4.2	1.1	0.51	0.1150	2.05	3.9811	0.174	0.089	0.113	0.7926	0.00756
3a	1.250	0.879	1000	9.81	2650	0.616	0.0005	4.2	1.1	2.87	0.1150	2.05	0.7124	0.090	0.046	0.418	0.1106	0.04226
3a	1.807	0.970	1000	9.81	2650	0.699	0.0005	4.2	1.1	3.58	0.1150	2.05	0.5709	0.081	0.042	0.507	0.0819	0.05273
3a	2.445	1.054	1000	9.81	2650	0.775	0.0006	4.2	1.1	4.31	0.1150	2.05	0.4749	0.074	0.038	0.598	0.0635	0.06339
3a	3.336	1.150	1000	9.81	2650	0.861	0.0006	4.2	1.1	5.21	0.1150	2.05	0.3925	0.067	0.034	0.710	0.0485	0.07671
3a	4.713	1.271	1000	9.81	2650	0.967	0.0007	4.2	1.1	6.46	0.1150	2.05	0.3168	0.060	0.031	0.865	0.0357	0.09504
3a	7.079	1.433	1000	9.81	2650	1.106	0.0008	4.2	1.1	8.30	0.1150	2.05	0.2467	0.053	0.027	1.096	0.0248	0.12205
3a	11.353	1.654	1000	9.81	2650	1.290	0.0009	4.2	1.1	11.07	0.1150	2.05	0.1848	0.046	0.023	1.448	0.0161	0.16289
3a	20.318	1.982	1000	9.81	2650	1.547	0.0010	4.2	1.1	15.63	0.1150	2.05	0.1309	0.038	0.019	2.042	0.0095	0.22993
3a	36.559	2.390	1000	9.81	2650	1.884	0.0012	4.2	1.1	22.26	0.1150	2.05	0.0919	0.032	0.016	2.879	0.0057	0.32749
3a	68.557	2.932	1000	9.81	2650	2.301	0.0014	4.2	1.1	31.73	0.1150	2.05	0.0645	0.027	0.014	4.122	0.0033	0.46679
3a	146.698	3.772	1000	9.81	2650	2.893	0.0017	4.2	1.1	46.99	0.1150	2.05	0.0436	0.022	0.011	6.247	0.0018	0.69127
3a	307.136	4.838	1000	9.81	2650	3.482	0.0019	4.2	1.1	64.60	0.1150	2.05	0.0317	0.019	0.010	9.148	0.0011	0.95020

Table 8 RBS and Milhous for Mkomazi Site 3b

Site	Q	d	ρ	g	ρ_s	R	S	D50	D84	τ	τ_{ci}^*	τ_{ci}	τ RBS	q_c	$q_{critical}$	ώ	RBS_q	β
D84																		
3b	0.044	0.534	1000	9.81	2650	0.349	0.0003	4.2	13.7	0.90	0.0197	4.36	4.8238	7.662	13.839	0.141	98.0768	0.01330
3b	1.250	0.793	1000	9.81	2650	0.505	0.0005	4.2	13.7	2.36	0.0197	4.36	1.8509	3.968	7.167	0.377	19.0086	0.03466
3b	1.807	0.850	1000	9.81	2650	0.522	0.0005	4.2	13.7	2.68	0.0197	4.36	1.6277	3.568	6.444	0.444	14.5011	0.03942
3b	2.445	0.904	1000	9.81	2650	0.540	0.0006	4.2	13.7	3.00	0.0197	4.36	1.4532	3.258	5.885	0.513	11.4816	0.04415
3b	3.336	0.968	1000	9.81	2650	0.561	0.0006	4.2	13.7	3.40	0.0197	4.36	1.2824	2.960	5.346	0.598	8.9411	0.05003
3b	4.713	1.048	1000	9.81	2650	0.587	0.0007	4.2	13.7	3.92	0.0197	4.36	1.1131	2.654	4.794	0.714	6.7181	0.05764
3b	7.079	1.160	1000	9.81	2650	0.592	0.0008	4.2	13.7	4.44	0.0197	4.36	0.9819	2.330	4.209	0.887	4.7442	0.06534
3b	11.353	1.315	1000	9.81	2650	0.703	0.0009	4.2	13.7	6.04	0.0197	4.36	0.7223	2.003	3.618	1.151	3.1434	0.08882
3b	20.318	1.554	1000	9.81	2650	0.894	0.0010	4.2	13.7	9.04	0.0197	4.36	0.4826	1.669	3.015	1.601	1.8830	0.13294
3b	36.559	1.863	1000	9.81	2650	1.129	0.0012	4.2	13.7	13.34	0.0197	4.36	0.3269	1.401	2.530	2.244	1.1272	0.19625
3b	68.557	2.289	1000	9.81	2650	1.430	0.0014	4.2	13.7	19.72	0.0197	4.36	0.2212	1.179	2.128	3.218	0.6615	0.29008
3b	146.698	2.980	1000	9.81	2650	1.989	0.0017	4.2	13.7	32.31	0.0197	4.36	0.1350	0.981	1.772	4.935	0.3590	0.47525
3b	307.136	3.898	1000	9.81	2650	2.714	0.0019	4.2	13.7	50.35	0.0197	4.36	0.0866	0.846	1.527	7.371	0.2072	0.74063
D16																		
Site	Q	d	ρ	g	ρ_s	R	S	D50	D16	τ	τ_{ci}^*	τ_{ci}	τ RBS	q_c	$q_{critical}$	ώ	RBS_q	β
3b	0.044	0.534	1000	9.81	2650	0.349	0.0003	4.2	1.1	0.90	0.1150	2.05	2.2635	0.174	0.089	0.141	0.6323	0.01330
3b	1.250	0.793	1000	9.81	2650	0.505	0.0005	4.2	1.1	2.36	0.1150	2.05	0.8685	0.090	0.046	0.377	0.1225	0.03466
3b	1.807	0.850	1000	9.81	2650	0.522	0.0005	4.2	1.1	2.68	0.1150	2.05	0.7638	0.081	0.042	0.444	0.0935	0.03942
3b	2.445	0.904	1000	9.81	2650	0.540	0.0006	4.2	1.1	3.00	0.1150	2.05	0.6819	0.074	0.038	0.513	0.0740	0.04415
3b	3.336	0.968	1000	9.81	2650	0.561	0.0006	4.2	1.1	3.40	0.1150	2.05	0.6018	0.067	0.034	0.598	0.0576	0.05003
3b	4.713	1.048	1000	9.81	2650	0.587	0.0007	4.2	1.1	3.92	0.1150	2.05	0.5223	0.060	0.031	0.714	0.0433	0.05764
3b	7.079	1.160	1000	9.81	2650	0.592	0.0008	4.2	1.1	4.44	0.1150	2.05	0.4608	0.053	0.027	0.887	0.0306	0.06534
3b	11.353	1.315	1000	9.81	2650	0.703	0.0009	4.2	1.1	6.04	0.1150	2.05	0.3390	0.046	0.023	1.151	0.0203	0.08882
3b	20.318	1.554	1000	9.81	2650	0.894	0.0010	4.2	1.1	9.04	0.1150	2.05	0.2265	0.038	0.019	1.601	0.0121	0.13294
3b	36.559	1.863	1000	9.81	2650	1.129	0.0012	4.2	1.1	13.34	0.1150	2.05	0.1534	0.032	0.016	2.244	0.0073	0.19625
3b	68.557	2.289	1000	9.81	2650	1.430	0.0014	4.2	1.1	19.72	0.1150	2.05	0.1038	0.027	0.014	3.218	0.0043	0.29008
3b	146.698	2.980	1000	9.81	2650	1.989	0.0017	4.2	1.1	32.31	0.1150	2.05	0.0633	0.022	0.011	4.935	0.0023	0.47525
3b	307.136	3.898	1000	9.81	2650	2.714	0.0019	4.2	1.1	50.35	0.1150	2.05	0.0406	0.019	0.010	7.371	0.0013	0.74063

Table 9 RBS and Milhous for Mkomazi Site 3c

Site	Q	d	ρ	g	ρ_s	R	S	D50	D84	τ	τ_{ci}^*	τ_{ci}	τ RBS	q_c	$q_{critical}$	ω	RBS_n	β
D84																		
3c	0.044	0.339	1000	9.81	2650	0.122	0.0003	4.2	13.7	0.32	0.0197	4.36	13.8424	7.662	13.839	0.090	154.4926	0.00463
3c	1.250	0.904	1000	9.81	2650	0.629	0.0005	4.2	13.7	2.93	0.0197	4.36	1.4873	3.968	7.167	0.430	16.6746	0.04314
3c	1.807	1.007	1000	9.81	2650	0.721	0.0005	4.2	13.7	3.70	0.0197	4.36	1.1789	3.568	6.444	0.526	12.2402	0.05442
3c	2.445	1.101	1000	9.81	2650	0.805	0.0006	4.2	13.7	4.48	0.0197	4.36	0.9746	3.258	5.885	0.624	9.4273	0.06583
3c	3.336	1.206	1000	9.81	2650	0.901	0.0006	4.2	13.7	5.46	0.0197	4.36	0.7986	2.960	5.346	0.745	7.1766	0.08034
3c	4.713	1.334	1000	9.81	2650	1.020	0.0007	4.2	13.7	6.81	0.0197	4.36	0.6403	2.654	4.794	0.908	5.2778	0.10020
3c	7.079	1.503	1000	9.81	2650	1.174	0.0008	4.2	13.7	8.81	0.0197	4.36	0.4951	2.330	4.209	1.149	3.6616	0.12958
3c	11.353	1.726	1000	9.81	2650	1.374	0.0009	4.2	13.7	11.80	0.0197	4.36	0.3696	2.003	3.618	1.511	2.3949	0.17360
3c	20.318	2.047	1000	9.81	2650	1.656	0.0010	4.2	13.7	16.74	0.0197	4.36	0.2606	1.669	3.015	2.109	1.4295	0.24617
3c	36.559	2.431	1000	9.81	2650	1.981	0.0012	4.2	13.7	23.41	0.0197	4.36	0.1863	1.401	2.530	2.929	0.8639	0.34438
3c	68.557	2.923	1000	9.81	2650	2.381	0.0014	4.2	13.7	32.84	0.0197	4.36	0.1328	1.179	2.128	4.109	0.5180	0.48310
3c	146.698	3.653	1000	9.81	2650	2.949	0.0017	4.2	13.7	47.90	0.0197	4.36	0.0911	0.981	1.772	6.050	0.2928	0.70462
3c	307.136	4.536	1000	9.81	2650	3.516	0.0019	4.2	13.7	65.22	0.0197	4.36	0.0669	0.846	1.527	8.577	0.1780	0.95932
D16																		
Site	Q	d	ρ	g	ρ_s	R	S	D50	D16	τ	τ_{ci}^*	τ_{ci}	τ RBS	q_c	$q_{critical}$	ω	RBS_n	β
3c	0.044	0.339	1000	9.81	2650	0.122	0.0003	4.2	1.1	0.32	0.1150	2.05	6.4955	0.174	0.089	0.090	0.9960	0.00463
3c	1.250	0.904	1000	9.81	2650	0.629	0.0005	4.2	1.1	2.93	0.1150	2.05	0.6979	0.090	0.046	0.430	0.1075	0.04314
3c	1.807	1.007	1000	9.81	2650	0.721	0.0005	4.2	1.1	3.70	0.1150	2.05	0.5532	0.081	0.042	0.526	0.0789	0.05442
3c	2.445	1.101	1000	9.81	2650	0.805	0.0006	4.2	1.1	4.48	0.1150	2.05	0.4573	0.074	0.038	0.624	0.0608	0.06583
3c	3.336	1.206	1000	9.81	2650	0.901	0.0006	4.2	1.1	5.46	0.1150	2.05	0.3747	0.067	0.034	0.745	0.0463	0.08034
3c	4.713	1.334	1000	9.81	2650	1.020	0.0007	4.2	1.1	6.81	0.1150	2.05	0.3005	0.060	0.031	0.908	0.0340	0.10020
3c	7.079	1.503	1000	9.81	2650	1.174	0.0008	4.2	1.1	8.81	0.1150	2.05	0.2323	0.053	0.027	1.149	0.0236	0.12958
3c	11.353	1.726	1000	9.81	2650	1.374	0.0009	4.2	1.1	11.80	0.1150	2.05	0.1734	0.046	0.023	1.511	0.0154	0.17360
3c	20.318	2.047	1000	9.81	2650	1.656	0.0010	4.2	1.1	16.74	0.1150	2.05	0.1223	0.038	0.019	2.109	0.0092	0.24617
3c	36.559	2.431	1000	9.81	2650	1.981	0.0012	4.2	1.1	23.41	0.1150	2.05	0.0874	0.032	0.016	2.929	0.0056	0.34438
3c	68.557	2.923	1000	9.81	2650	2.381	0.0014	4.2	1.1	32.84	0.1150	2.05	0.0623	0.027	0.014	4.109	0.0033	0.48310
3c	146.698	3.653	1000	9.81	2650	2.949	0.0017	4.2	1.1	47.90	0.1150	2.05	0.0427	0.022	0.011	6.050	0.0019	0.70462
3c	307.136	4.536	1000	9.81	2650	3.516	0.0019	4.2	1.1	65.22	0.1150	2.05	0.0314	0.019	0.010	8.577	0.0011	0.95932

Table 10 RBS and Milhous for Mkomazi Site 4a

Site	Q	d	ρ	g	ρ_s	R	S	D50	D84	τ	τ_{ci}^*	τ_{ci}	τ RBS	q_c	$q_{critical}$	ώ	RBS_n	β
D84																		
4a	0.079	0.936	1000	9.81	2650	0.440	0.0020	12	15	8.72	0.0385	9.35	1.0716	0.899	1.005	1.892	0.5309	0.04490
4a	1.317	1.280	1000	9.81	2650	0.614	0.0021	12	15	12.54	0.0385	9.35	0.7454	0.870	0.972	2.665	0.3647	0.06455
4a	1.904	1.359	1000	9.81	2650	0.663	0.0021	12	15	13.64	0.0385	9.35	0.6853	0.863	0.965	2.850	0.3385	0.07022
4a	2.576	1.432	1000	9.81	2650	0.704	0.0021	12	15	14.57	0.0385	9.35	0.6414	0.856	0.958	3.022	0.3168	0.07501
4a	3.515	1.517	1000	9.81	2650	0.751	0.0021	12	15	15.65	0.0385	9.35	0.5970	0.849	0.950	3.226	0.2944	0.08060
4a	4.966	1.624	1000	9.81	2650	0.856	0.0021	12	15	18.01	0.0385	9.35	0.5189	0.841	0.940	3.485	0.2698	0.09272
4a	7.458	1.770	1000	9.81	2650	0.980	0.0022	12	15	20.88	0.0385	9.35	0.4476	0.830	0.928	3.844	0.2413	0.10749
4a	11.961	1.969	1000	9.81	2650	1.160	0.0022	12	15	25.10	0.0385	9.35	0.3723	0.815	0.912	4.343	0.2099	0.12923
4a	21.406	2.270	1000	9.81	2650	1.432	0.0023	12	15	31.64	0.0385	9.35	0.2954	0.796	0.890	5.114	0.1740	0.16290
4a	38.518	2.650	1000	9.81	2650	1.759	0.0023	12	15	39.80	0.0385	9.35	0.2348	0.776	0.867	6.112	0.1419	0.20492
4a	72.230	3.162	1000	9.81	2650	2.193	0.0024	12	15	50.93	0.0385	9.35	0.1835	0.753	0.842	7.486	0.1125	0.26219
4a	154.557	3.971	1000	9.81	2650	2.872	0.0024	12	15	68.85	0.0385	9.35	0.1357	0.727	0.813	9.703	0.0838	0.35445
4a	323.589	5.016	1000	9.81	2650	2.966	0.0025	12	15	73.16	0.0385	9.35	0.1278	0.704	0.787	12.611	0.0624	0.37663
D16																		
Site	Q	d	ρ	g	ρ_s	R	S	D50	D16	τ	τ_{ci}^*	τ_{ci}	τ RBS	q_c	$q_{critical}$	ώ	RBS_n	β
4a	0.079	0.936	1000	9.81	2650	0.440	0.0020	12	0.35	8.72	0.5343	3.03	0.3471	0.003	0.001	1.892	0.0003	0.04490
4a	1.317	1.280	1000	9.81	2650	0.614	0.0021	12	0.35	12.54	0.5343	3.03	0.2414	0.003	0.001	2.665	0.0002	0.06455
4a	1.904	1.359	1000	9.81	2650	0.663	0.0021	12	0.35	13.64	0.5343	3.03	0.2219	0.003	0.001	2.850	0.0002	0.07022
4a	2.576	1.432	1000	9.81	2650	0.704	0.0021	12	0.35	14.57	0.5343	3.03	0.2078	0.003	0.001	3.022	0.0002	0.07501
4a	3.515	1.517	1000	9.81	2650	0.751	0.0021	12	0.35	15.65	0.5343	3.03	0.1934	0.003	0.001	3.226	0.0002	0.08060
4a	4.966	1.624	1000	9.81	2650	0.856	0.0021	12	0.35	18.01	0.5343	3.03	0.1681	0.003	0.001	3.485	0.0001	0.09272
4a	7.458	1.770	1000	9.81	2650	0.980	0.0022	12	0.35	20.88	0.5343	3.03	0.1450	0.003	0.001	3.844	0.0001	0.10749
4a	11.961	1.969	1000	9.81	2650	1.160	0.0022	12	0.35	25.10	0.5343	3.03	0.1206	0.003	0.000	4.343	0.0001	0.12923
4a	21.406	2.270	1000	9.81	2650	1.432	0.0023	12	0.35	31.64	0.5343	3.03	0.0957	0.003	0.000	5.114	0.0001	0.16290
4a	38.518	2.650	1000	9.81	2650	1.759	0.0023	12	0.35	39.80	0.5343	3.03	0.0760	0.003	0.000	6.112	0.0001	0.20492
4a	72.230	3.162	1000	9.81	2650	2.193	0.0024	12	0.35	50.93	0.5343	3.03	0.0594	0.003	0.000	7.486	0.0001	0.26219
4a	154.557	3.971	1000	9.81	2650	2.872	0.0024	12	0.35	68.85	0.5343	3.03	0.0440	0.003	0.000	9.703	0.0000	0.35445
4a	323.589	5.016	1000	9.81	2650	2.966	0.0025	12	0.35	73.16	0.5343	3.03	0.0414	0.003	0.000	12.611	0.0000	0.37663

Table 11 RBS and Milhous for Mkomazi Site 4b

Site	Q	d	ρ	g	ρ_s	R	S	D50	D84	τ	τ_{ci}^*	τ_{ci}	τ RBS	q_c	$q_{critical}$	ώ	RBS_n	β
D84																		
4b	0.079	0.688	1000	9.81	2650	0.333	0.0020	12	15	6.61	0.0385	9.35	1.4145	0.899	1.005	1.391	0.7223	0.03402
4b	1.317	1.037	1000	9.81	2650	0.612	0.0021	12	15	12.50	0.0385	9.35	0.7479	0.870	0.972	2.159	0.4502	0.06434
4b	1.904	1.117	1000	9.81	2650	0.675	0.0021	12	15	13.88	0.0385	9.35	0.6733	0.863	0.965	2.342	0.4118	0.07146
4b	2.576	1.190	1000	9.81	2650	0.731	0.0021	12	15	15.14	0.0385	9.35	0.6173	0.856	0.958	2.512	0.3813	0.07794
4b	3.515	1.275	1000	9.81	2650	0.778	0.0021	12	15	16.24	0.0385	9.35	0.5756	0.849	0.950	2.711	0.3503	0.08359
4b	4.966	1.382	1000	9.81	2650	0.802	0.0021	12	15	16.87	0.0385	9.35	0.5539	0.841	0.940	2.965	0.3170	0.08686
4b	7.458	1.526	1000	9.81	2650	0.838	0.0022	12	15	17.86	0.0385	9.35	0.5233	0.830	0.928	3.314	0.2799	0.09194
4b	11.961	1.724	1000	9.81	2650	0.920	0.0022	12	15	19.90	0.0385	9.35	0.4696	0.815	0.912	3.802	0.2397	0.10246
4b	21.406	2.021	1000	9.81	2650	1.173	0.0023	12	15	25.92	0.0385	9.35	0.3605	0.796	0.890	4.553	0.1955	0.13346
4b	38.518	2.393	1000	9.81	2650	1.498	0.0023	12	15	33.90	0.0385	9.35	0.2757	0.776	0.867	5.519	0.1571	0.17453
4b	72.230	2.894	1000	9.81	2650	1.797	0.0024	12	15	41.73	0.0385	9.35	0.2240	0.753	0.842	6.852	0.1229	0.21485
4b	154.557	3.679	1000	9.81	2650	2.217	0.0024	12	15	53.15	0.0385	9.35	0.1759	0.727	0.813	8.989	0.0904	0.27361
4b	323.589	4.688	1000	9.81	2650	2.809	0.0025	12	15	69.27	0.0385	9.35	0.1349	0.704	0.787	11.786	0.0668	0.35662
D16																		
Site	Q	d	ρ	g	ρ_s	R	S	D50	D16	τ	τ_{ci}^*	τ_{ci}	τ RBS	q_c	$q_{critical}$	ώ	RBS_n	β
4b	0.079	0.688	1000	9.81	2650	0.333	0.0020	12	0.35	6.61	0.5343	3.03	0.4581	0.003	0.001	1.391	0.0004	0.03402
4b	1.317	1.037	1000	9.81	2650	0.612	0.0021	12	0.35	12.50	0.5343	3.03	0.2422	0.003	0.001	2.159	0.0002	0.06434
4b	1.904	1.117	1000	9.81	2650	0.675	0.0021	12	0.35	13.88	0.5343	3.03	0.2181	0.003	0.001	2.342	0.0002	0.07146
4b	2.576	1.190	1000	9.81	2650	0.731	0.0021	12	0.35	15.14	0.5343	3.03	0.2000	0.003	0.001	2.512	0.0002	0.07794
4b	3.515	1.275	1000	9.81	2650	0.778	0.0021	12	0.35	16.24	0.5343	3.03	0.1864	0.003	0.001	2.711	0.0002	0.08359
4b	4.966	1.382	1000	9.81	2650	0.802	0.0021	12	0.35	16.87	0.5343	3.03	0.1794	0.003	0.001	2.965	0.0002	0.08686
4b	7.458	1.526	1000	9.81	2650	0.838	0.0022	12	0.35	17.86	0.5343	3.03	0.1695	0.003	0.001	3.314	0.0002	0.09194
4b	11.961	1.724	1000	9.81	2650	0.920	0.0022	12	0.35	19.90	0.5343	3.03	0.1521	0.003	0.000	3.802	0.0001	0.10246
4b	21.406	2.021	1000	9.81	2650	1.173	0.0023	12	0.35	25.92	0.5343	3.03	0.1168	0.003	0.000	4.553	0.0001	0.13346
4b	38.518	2.393	1000	9.81	2650	1.498	0.0023	12	0.35	33.90	0.5343	3.03	0.0893	0.003	0.000	5.519	0.0001	0.17453
4b	72.230	2.894	1000	9.81	2650	1.797	0.0024	12	0.35	41.73	0.5343	3.03	0.0725	0.003	0.000	6.852	0.0001	0.21485
4b	154.557	3.679	1000	9.81	2650	2.217	0.0024	12	0.35	53.15	0.5343	3.03	0.0570	0.003	0.000	8.989	0.0000	0.27361
4b	323.589	4.688	1000	9.81	2650	2.809	0.0025	12	0.35	69.27	0.5343	3.03	0.0437	0.003	0.000	11.786	0.0000	0.35662

Table 12 RBS and Milhous for Mkomazi Site 5a

Site	Q	d	ρ	g	ρ_s	R	S	D50	D84	τ	τ_{ci}^*	τ_{ci}	τ RBS	q_c	$q_{critical}$	ω	RBS_q	β
D84																		
5a	0.133	2.461	1000	9.81	2650	1.374	0.0002	1.7	15	2.11	0.0098	2.38	1.1284	15.794	46.915	0.385	121.8805	0.07663
5a	2.211	2.757	1000	9.81	2650	1.518	0.0004	1.7	15	6.18	0.0098	2.38	0.3853	5.299	15.741	1.143	13.7686	0.22445
5a	3.195	2.825	1000	9.81	2650	1.575	0.0005	1.7	15	7.34	0.0098	2.38	0.3240	4.546	13.505	1.343	10.0535	0.26692
5a	4.322	2.888	1000	9.81	2650	1.626	0.0005	1.7	15	8.48	0.0098	2.38	0.2807	4.013	11.919	1.535	7.7636	0.30808
5a	5.898	2.960	1000	9.81	2650	1.684	0.0006	1.7	15	9.84	0.0098	2.38	0.2419	3.534	10.498	1.762	5.9565	0.35745
5a	8.332	3.052	1000	9.81	2650	1.774	0.0007	1.7	15	11.72	0.0098	2.38	0.2030	3.077	9.140	2.056	4.4451	0.42602
5a	12.515	3.176	1000	9.81	2650	1.879	0.0008	1.7	15	14.30	0.0098	2.38	0.1664	2.627	7.802	2.465	3.1658	0.51977
5a	20.071	3.346	1000	9.81	2650	2.022	0.0009	1.7	15	18.01	0.0098	2.38	0.1321	2.204	6.546	3.037	2.1551	0.65442
5a	35.919	3.602	1000	9.81	2650	2.239	0.0011	1.7	15	23.87	0.0098	2.38	0.0997	1.801	5.351	3.915	1.3669	0.86763
5a	64.631	3.925	1000	9.81	2650	2.501	0.0013	1.7	15	31.43	0.0098	2.38	0.0757	1.498	4.450	5.028	0.8851	1.14228
5a	131.926	4.426	1000	9.81	2650	2.916	0.0015	1.7	15	43.61	0.0098	2.38	0.0546	1.233	3.662	6.749	0.5426	1.58491
5a	291.284	5.166	1000	9.81	2650	3.525	0.0018	1.7	15	61.81	0.0098	2.38	0.0385	1.032	3.064	9.235	0.3318	2.24629
5a	503.130	5.823	1000	9.81	2650	3.172	0.0020	1.7	15	60.85	0.0098	2.38	0.0391	0.933	2.772	11.385	0.2435	2.21126
D16																		
Site	Q	d	ρ	g	ρ_s	R	S	D50	D16	τ	τ_{ci}^*	τ_{ci}	τ RBS	q_c	$q_{critical}$	ω	RBS_q	β
5a	0.133	2.461	1000	9.81	2650	1.374	0.0002	1.7	0.18	2.11	0.2167	0.63	0.2994	0.021	0.007	0.385	0.0176	0.07663
5a	2.211	2.757	1000	9.81	2650	1.518	0.0004	1.7	0.18	6.18	0.2167	0.63	0.1022	0.007	0.002	1.143	0.0020	0.22445
5a	3.195	2.825	1000	9.81	2650	1.575	0.0005	1.7	0.18	7.34	0.2167	0.63	0.0860	0.006	0.002	1.343	0.0014	0.26692
5a	4.322	2.888	1000	9.81	2650	1.626	0.0005	1.7	0.18	8.48	0.2167	0.63	0.0745	0.005	0.002	1.535	0.0011	0.30808
5a	5.898	2.960	1000	9.81	2650	1.684	0.0006	1.7	0.18	9.84	0.2167	0.63	0.0642	0.005	0.002	1.762	0.0009	0.35745
5a	8.332	3.052	1000	9.81	2650	1.774	0.0007	1.7	0.18	11.72	0.2167	0.63	0.0539	0.004	0.001	2.056	0.0006	0.42602
5a	12.515	3.176	1000	9.81	2650	1.879	0.0008	1.7	0.18	14.30	0.2167	0.63	0.0441	0.003	0.001	2.465	0.0005	0.51977
5a	20.071	3.346	1000	9.81	2650	2.022	0.0009	1.7	0.18	18.01	0.2167	0.63	0.0351	0.003	0.001	3.037	0.0003	0.65442
5a	35.919	3.602	1000	9.81	2650	2.239	0.0011	1.7	0.18	23.87	0.2167	0.63	0.0264	0.002	0.001	3.915	0.0002	0.86763
5a	64.631	3.925	1000	9.81	2650	2.501	0.0013	1.7	0.18	31.43	0.2167	0.63	0.0201	0.002	0.001	5.028	0.0001	1.14228
5a	131.926	4.426	1000	9.81	2650	2.916	0.0015	1.7	0.18	43.61	0.2167	0.63	0.0145	0.002	0.001	6.749	0.0001	1.58491
5a	291.284	5.166	1000	9.81	2650	3.525	0.0018	1.7	0.18	61.81	0.2167	0.63	0.0102	0.001	0.000	9.235	0.0000	2.24629
5a	503.130	5.823	1000	9.81	2650	3.172	0.0020	1.7	0.18	60.85	0.2167	0.63	0.0104	0.001	0.000	11.385	0.0000	2.21126

Table 13 RBS and Milhous for Mkomazi Site 5b

Site	Q	d	ρ	g	ρ_s	R	S	D50	D84	τ	τ_{ci}^*	τ_{ci}	τ RBS	q_c	$q_{critical}$	ώ	RBS_n	β
D84																		
5b	0.133	1.646	1000	9.81	2650	0.986	0.0002	1.7	15	1.51	0.0098	2.38	1.5731	15.794	46.915	0.257	182.2283	0.05497
5b	2.211	2.089	1000	9.81	2650	1.299	0.0004	1.7	15	5.28	0.0098	2.38	0.4504	5.299	15.741	0.866	18.1713	0.19200
5b	3.195	2.184	1000	9.81	2650	1.374	0.0005	1.7	15	6.41	0.0098	2.38	0.3713	4.546	13.505	1.038	13.0041	0.23292
5b	4.322	2.271	1000	9.81	2650	1.442	0.0005	1.7	15	7.52	0.0098	2.38	0.3164	4.013	11.919	1.207	9.8729	0.27330
5b	5.898	2.370	1000	9.81	2650	1.519	0.0006	1.7	15	8.87	0.0098	2.38	0.2682	3.534	10.498	1.411	7.4393	0.32239
5b	8.332	2.493	1000	9.81	2650	1.639	0.0007	1.7	15	10.84	0.0098	2.38	0.2196	3.077	9.140	1.680	5.4419	0.39378
5b	12.515	2.656	1000	9.81	2650	1.773	0.0008	1.7	15	13.50	0.0098	2.38	0.1763	2.627	7.802	2.061	3.7856	0.49045
5b	20.071	2.876	1000	9.81	2650	1.951	0.0009	1.7	15	17.38	0.0098	2.38	0.1370	2.204	6.546	2.611	2.5073	0.63145
5b	35.919	3.199	1000	9.81	2650	2.221	0.0011	1.7	15	23.68	0.0098	2.38	0.1005	1.801	5.351	3.477	1.5390	0.86070
5b	64.631	3.595	1000	9.81	2650	2.551	0.0013	1.7	15	32.06	0.0098	2.38	0.0742	1.498	4.450	4.606	0.9663	1.16509
5b	131.926	4.191	1000	9.81	2650	3.055	0.0015	1.7	15	45.70	0.0098	2.38	0.0521	1.233	3.662	6.390	0.5730	1.66084
5b	291.284	5.040	1000	9.81	2650	3.790	0.0018	1.7	15	66.47	0.0098	2.38	0.0358	1.032	3.064	9.010	0.3401	2.41573
5b	503.130	5.770	1000	9.81	2650	3.307	0.0020	1.7	15	63.43	0.0098	2.38	0.0375	0.933	2.772	11.281	0.2457	2.30516
D16																		
Site	Q	d	ρ	g	ρ_s	R	S	D50	D16	τ	τ_{ci}^*	τ_{ci}	τ RBS	q_c	$q_{critical}$	ώ	RBS_n	β
5b	0.133	1.646	1000	9.81	2650	0.986	0.0002	1.7	0.18	1.51	0.2167	0.63	0.4174	0.021	0.007	0.257	0.0262	0.05497
5b	2.211	2.089	1000	9.81	2650	1.299	0.0004	1.7	0.18	5.28	0.2167	0.63	0.1195	0.007	0.002	0.866	0.0026	0.19200
5b	3.195	2.184	1000	9.81	2650	1.374	0.0005	1.7	0.18	6.41	0.2167	0.63	0.0985	0.006	0.002	1.038	0.0019	0.23292
5b	4.322	2.271	1000	9.81	2650	1.442	0.0005	1.7	0.18	7.52	0.2167	0.63	0.0839	0.005	0.002	1.207	0.0014	0.27330
5b	5.898	2.370	1000	9.81	2650	1.519	0.0006	1.7	0.18	8.87	0.2167	0.63	0.0712	0.005	0.002	1.411	0.0011	0.32239
5b	8.332	2.493	1000	9.81	2650	1.639	0.0007	1.7	0.18	10.84	0.2167	0.63	0.0583	0.004	0.001	1.680	0.0008	0.39378
5b	12.515	2.656	1000	9.81	2650	1.773	0.0008	1.7	0.18	13.50	0.2167	0.63	0.0468	0.003	0.001	2.061	0.0005	0.49045
5b	20.071	2.876	1000	9.81	2650	1.951	0.0009	1.7	0.18	17.38	0.2167	0.63	0.0363	0.003	0.001	2.611	0.0004	0.63145
5b	35.919	3.199	1000	9.81	2650	2.221	0.0011	1.7	0.18	23.68	0.2167	0.63	0.0267	0.002	0.001	3.477	0.0002	0.86070
5b	64.631	3.595	1000	9.81	2650	2.551	0.0013	1.7	0.18	32.06	0.2167	0.63	0.0197	0.002	0.001	4.606	0.0001	1.16509
5b	131.926	4.191	1000	9.81	2650	3.055	0.0015	1.7	0.18	45.70	0.2167	0.63	0.0138	0.002	0.001	6.390	0.0001	1.66084
5b	291.284	5.040	1000	9.81	2650	3.790	0.0018	1.7	0.18	66.47	0.2167	0.63	0.0095	0.001	0.000	9.010	0.0000	2.41573
5b	503.130	5.770	1000	9.81	2650	3.307	0.0020	1.7	0.18	63.43	0.2167	0.63	0.0100	0.001	0.000	11.281	0.0000	2.30516

Table 14 RBS and Milhous for Mkomazi Site 6a

Site	Q	d	ρ	g	ρ_s	R	S	D50	D84	τ	τ_{ci}^*	τ_{ci}	τ RBS	q_c	$q_{critical}$	ω	RBS_n	β
D84																		
6a	0.136	1.003	1000	9.81	2650	0.463	0.0015	26	100	6.78	0.0175	28.37	4.1867	21.735	42.625	1.497	28.4745	0.01610
6a	2.255	1.303	1000	9.81	2650	0.648	0.0017	26	100	11.06	0.0175	28.37	2.5640	18.309	35.907	2.267	15.8423	0.02629
6a	3.260	1.370	1000	9.81	2650	0.703	0.0018	26	100	12.39	0.0175	28.37	2.2899	17.646	34.608	2.463	14.0523	0.02944
6a	4.410	1.432	1000	9.81	2650	0.755	0.0019	26	100	13.71	0.0175	28.37	2.0688	17.075	33.487	2.651	12.6321	0.03258
6a	6.017	1.504	1000	9.81	2650	0.815	0.0019	26	100	15.29	0.0175	28.37	1.8549	16.467	32.295	2.876	11.2297	0.03634
6a	8.501	1.593	1000	9.81	2650	0.881	0.0020	26	100	17.17	0.0175	28.37	1.6520	15.775	30.937	3.165	9.7740	0.04081
6a	12.767	1.713	1000	9.81	2650	0.959	0.0021	26	100	19.61	0.0175	28.37	1.4470	14.951	29.320	3.571	8.2115	0.04658
6a	20.476	1.878	1000	9.81	2650	1.028	0.0022	26	100	22.29	0.0175	28.37	1.2727	14.003	27.461	4.150	6.6166	0.05297
6a	36.644	2.124	1000	9.81	2650	1.195	0.0024	26	100	27.90	0.0175	28.37	1.0167	12.885	25.269	5.056	4.9979	0.06630
6a	65.937	2.431	1000	9.81	2650	1.471	0.0026	26	100	37.02	0.0175	28.37	0.7664	11.850	23.240	6.236	3.7268	0.08795
6a	134.591	2.903	1000	9.81	2650	1.879	0.0028	26	100	51.55	0.0175	28.37	0.5503	10.758	21.099	8.118	2.5990	0.12249
6a	297.169	3.592	1000	9.81	2650	2.423	0.0030	26	100	72.39	0.0175	28.37	0.3919	9.778	19.175	10.939	1.7529	0.17202
6a	513.294	4.197	1000	9.81	2650	2.894	0.0032	26	100	90.96	0.0175	28.37	0.3119	9.238	18.117	13.446	1.3474	0.21613
D16																		
Site	Q	d	ρ	g	ρ_s	R	S	D50	D16	τ	τ_{ci}^*	τ_{ci}	τ RBS	q_c	$q_{critical}$	ω	RBS_n	β
6a	0.136	1.003	1000	9.81	2650	0.463	0.0015	26	3.8	6.78	0.1729	10.64	1.5697	0.161	0.062	1.497	0.0411	0.01610
6a	2.255	1.303	1000	9.81	2650	0.648	0.0017	26	3.8	11.06	0.1729	10.64	0.9613	0.136	0.052	2.267	0.0229	0.02629
6a	3.260	1.370	1000	9.81	2650	0.703	0.0018	26	3.8	12.39	0.1729	10.64	0.8585	0.131	0.050	2.463	0.0203	0.02944
6a	4.410	1.432	1000	9.81	2650	0.755	0.0019	26	3.8	13.71	0.1729	10.64	0.7756	0.126	0.048	2.651	0.0182	0.03258
6a	6.017	1.504	1000	9.81	2650	0.815	0.0019	26	3.8	15.29	0.1729	10.64	0.6954	0.122	0.047	2.876	0.0162	0.03634
6a	8.501	1.593	1000	9.81	2650	0.881	0.0020	26	3.8	17.17	0.1729	10.64	0.6194	0.117	0.045	3.165	0.0141	0.04081
6a	12.767	1.713	1000	9.81	2650	0.959	0.0021	26	3.8	19.61	0.1729	10.64	0.5425	0.111	0.042	3.571	0.0119	0.04658
6a	20.476	1.878	1000	9.81	2650	1.028	0.0022	26	3.8	22.29	0.1729	10.64	0.4771	0.104	0.040	4.150	0.0096	0.05297
6a	36.644	2.124	1000	9.81	2650	1.195	0.0024	26	3.8	27.90	0.1729	10.64	0.3812	0.095	0.036	5.056	0.0072	0.06630
6a	65.937	2.431	1000	9.81	2650	1.471	0.0026	26	3.8	37.02	0.1729	10.64	0.2873	0.088	0.034	6.236	0.0054	0.08795
6a	134.591	2.903	1000	9.81	2650	1.879	0.0028	26	3.8	51.55	0.1729	10.64	0.2063	0.080	0.030	8.118	0.0038	0.12249
6a	297.169	3.592	1000	9.81	2650	2.423	0.0030	26	3.8	72.39	0.1729	10.64	0.1469	0.072	0.028	10.939	0.0025	0.17202
6a	513.294	4.197	1000	9.81	2650	2.894	0.0032	26	3.8	90.96	0.1729	10.64	0.1169	0.068	0.026	13.446	0.0019	0.21613

Table 15 RBS and Milhous for Mkomazi Site 6b

Site	Q	d	ρ	g	ρ_s	R	S	D50	D84	τ	τ_{ci}^*	τ_{ci}	τ RBS	q_c	$q_{critical}$	$\hat{\omega}$	RBS_a	β
D84																		
6b	0.136	2.272	1000	9.81	2650	0.291	0.0015	26	100	4.27	0.0175	28.37	6.6473	21.735	42.625	3.391	12.5697	0.01014
6b	2.255	2.492	1000	9.81	2650	0.300	0.0017	26	100	5.12	0.0175	28.37	5.5422	18.309	35.907	4.334	8.2846	0.01216
6b	3.260	2.546	1000	9.81	2650	0.323	0.0018	26	100	5.70	0.0175	28.37	4.9804	17.646	34.608	4.576	7.5623	0.01353
6b	4.410	2.597	1000	9.81	2650	0.338	0.0019	26	100	6.14	0.0175	28.37	4.6179	17.075	33.487	4.808	6.9654	0.01460
6b	6.017	2.657	1000	9.81	2650	0.366	0.0019	26	100	6.87	0.0175	28.37	4.1306	16.467	32.295	5.081	6.3561	0.01632
6b	8.501	2.734	1000	9.81	2650	0.410	0.0020	26	100	7.99	0.0175	28.37	3.5526	15.775	30.937	5.433	5.6941	0.01897
6b	12.767	2.841	1000	9.81	2650	0.480	0.0021	26	100	9.81	0.0175	28.37	2.8912	14.951	29.320	5.923	4.9504	0.02332
6b	20.476	2.992	1000	9.81	2650	0.570	0.0022	26	100	12.37	0.0175	28.37	2.2940	14.003	27.461	6.612	4.1532	0.02939
6b	36.644	3.225	1000	9.81	2650	0.690	0.0024	26	100	16.12	0.0175	28.37	1.7604	12.885	25.269	7.677	3.2914	0.03829
6b	65.937	3.529	1000	9.81	2650	0.897	0.0026	26	100	22.56	0.0175	28.37	1.2573	11.850	23.240	9.052	2.5674	0.05361
6b	134.591	4.018	1000	9.81	2650	1.270	0.0028	26	100	34.85	0.0175	28.37	0.8141	10.758	21.099	11.237	1.8776	0.08280
6b	297.169	4.773	1000	9.81	2650	1.807	0.0030	26	100	53.99	0.0175	28.37	0.5254	9.778	19.175	14.535	1.3193	0.12830
6b	513.294	5.467	1000	9.81	2650	2.283	0.0032	26	100	71.76	0.0175	28.37	0.3953	9.238	18.117	17.514	1.0344	0.17052
D16																		
Site	Q	d	ρ	g	ρ_s	R	S	D50	D16	τ	τ_{ci}^*	τ_{ci}	τ RBS	q_c	$q_{critical}$	$\hat{\omega}$	RBS_a	β
6b	0.136	2.272	1000	9.81	2650	0.291	0.0015	26	3.8	4.27	0.1729	10.64	2.4922	0.161	0.062	3.391	0.0182	0.01014
6b	2.255	2.492	1000	9.81	2650	0.300	0.0017	26	3.8	5.12	0.1729	10.64	2.0778	0.136	0.052	4.334	0.0120	0.01216
6b	3.260	2.546	1000	9.81	2650	0.323	0.0018	26	3.8	5.70	0.1729	10.64	1.8672	0.131	0.050	4.576	0.0109	0.01353
6b	4.410	2.597	1000	9.81	2650	0.338	0.0019	26	3.8	6.14	0.1729	10.64	1.7313	0.126	0.048	4.808	0.0101	0.01460
6b	6.017	2.657	1000	9.81	2650	0.366	0.0019	26	3.8	6.87	0.1729	10.64	1.5486	0.122	0.047	5.081	0.0092	0.01632
6b	8.501	2.734	1000	9.81	2650	0.410	0.0020	26	3.8	7.99	0.1729	10.64	1.3319	0.117	0.045	5.433	0.0082	0.01897
6b	12.767	2.841	1000	9.81	2650	0.480	0.0021	26	3.8	9.81	0.1729	10.64	1.0840	0.111	0.042	5.923	0.0071	0.02332
6b	20.476	2.992	1000	9.81	2650	0.570	0.0022	26	3.8	12.37	0.1729	10.64	0.8601	0.104	0.040	6.612	0.0060	0.02939
6b	36.644	3.225	1000	9.81	2650	0.690	0.0024	26	3.8	16.12	0.1729	10.64	0.6600	0.095	0.036	7.677	0.0048	0.03829
6b	65.937	3.529	1000	9.81	2650	0.897	0.0026	26	3.8	22.56	0.1729	10.64	0.4714	0.088	0.034	9.052	0.0037	0.05361
6b	134.591	4.018	1000	9.81	2650	1.270	0.0028	26	3.8	34.85	0.1729	10.64	0.3052	0.080	0.030	11.237	0.0027	0.08280
6b	297.169	4.773	1000	9.81	2650	1.807	0.0030	26	3.8	53.99	0.1729	10.64	0.1970	0.072	0.028	14.535	0.0019	0.12830
6b	513.294	5.467	1000	9.81	2650	2.283	0.0032	26	3.8	71.76	0.1729	10.64	0.1482	0.068	0.026	17.514	0.0015	0.17052

Table 16 RBS and Milhous for Mkomazi Site 6c

Site	Q	d	ρ	g	ρ_s	R	S	D50	D84	τ	τ_{ci}^*	τ_{ci}	τ RBS	q_c	$q_{critical}$	$\bar{\omega}$	RBS_q	β
D84																		
6c	0.136	0.716	1000	9.81	2650	1.075	0.0015	26	100	15.74	0.0175	28.37	1.8020	21.735	42.625	1.069	39.8882	0.03741
6c	2.255	0.949	1000	9.81	2650	1.235	0.0017	26	100	21.07	0.0175	28.37	1.3466	18.309	35.907	1.651	21.7518	0.05006
6c	3.260	1.003	1000	9.81	2650	1.266	0.0018	26	100	22.33	0.0175	28.37	1.2706	17.646	34.608	1.803	19.1940	0.05306
6c	4.410	1.054	1000	9.81	2650	1.284	0.0019	26	100	23.32	0.0175	28.37	1.2163	17.075	33.487	1.951	17.1624	0.05542
6c	6.017	1.112	1000	9.81	2650	1.306	0.0019	26	100	24.50	0.0175	28.37	1.1580	16.467	32.295	2.126	15.1884	0.05821
6c	8.501	1.187	1000	9.81	2650	1.334	0.0020	26	100	26.01	0.0175	28.37	1.0908	15.775	30.937	2.358	13.1171	0.06180
6c	12.767	1.288	1000	9.81	2650	1.374	0.0021	26	100	28.10	0.0175	28.37	1.0096	14.951	29.320	2.685	10.9210	0.06677
6c	20.476	1.427	1000	9.81	2650	1.436	0.0022	26	100	31.14	0.0175	28.37	0.9112	14.003	27.461	3.154	8.7078	0.07398
6c	36.644	1.638	1000	9.81	2650	1.550	0.0024	26	100	36.20	0.0175	28.37	0.7836	12.885	25.269	3.899	6.4807	0.08603
6c	65.937	1.905	1000	9.81	2650	1.688	0.0026	26	100	42.47	0.0175	28.37	0.6679	11.850	23.240	4.887	4.7559	0.10092
6c	134.591	2.324	1000	9.81	2650	1.864	0.0028	26	100	51.14	0.0175	28.37	0.5547	10.758	21.099	6.499	3.2465	0.12153
6c	297.169	2.949	1000	9.81	2650	2.246	0.0030	26	100	67.10	0.0175	28.37	0.4228	9.778	19.175	8.981	2.1351	0.15944
6c	513.294	3.507	1000	9.81	2650	2.760	0.0032	26	100	86.75	0.0175	28.37	0.3270	9.238	18.117	11.236	1.6125	0.20612
D16																		
Site	Q	d	ρ	g	ρ_s	R	S	D50	D16	τ	τ_{ci}^*	τ_{ci}	τ RBS	q_c	$q_{critical}$	$\bar{\omega}$	RBS_q	β
6c	0.136	0.716	1000	9.81	2650	1.075	0.0015	26	3.8	15.74	0.1729	10.64	0.6756	0.161	0.062	1.069	0.0576	0.03741
6c	2.255	0.949	1000	9.81	2650	1.235	0.0017	26	3.8	21.07	0.1729	10.64	0.5049	0.136	0.052	1.651	0.0314	0.05006
6c	3.260	1.003	1000	9.81	2650	1.266	0.0018	26	3.8	22.33	0.1729	10.64	0.4764	0.131	0.050	1.803	0.0277	0.05306
6c	4.410	1.054	1000	9.81	2650	1.284	0.0019	26	3.8	23.32	0.1729	10.64	0.4560	0.126	0.048	1.951	0.0248	0.05542
6c	6.017	1.112	1000	9.81	2650	1.306	0.0019	26	3.8	24.50	0.1729	10.64	0.4342	0.122	0.047	2.126	0.0219	0.05821
6c	8.501	1.187	1000	9.81	2650	1.334	0.0020	26	3.8	26.01	0.1729	10.64	0.4089	0.117	0.045	2.358	0.0189	0.06180
6c	12.767	1.288	1000	9.81	2650	1.374	0.0021	26	3.8	28.10	0.1729	10.64	0.3785	0.111	0.042	2.685	0.0158	0.06677
6c	20.476	1.427	1000	9.81	2650	1.436	0.0022	26	3.8	31.14	0.1729	10.64	0.3416	0.104	0.040	3.154	0.0126	0.07398
6c	36.644	1.638	1000	9.81	2650	1.550	0.0024	26	3.8	36.20	0.1729	10.64	0.2938	0.095	0.036	3.899	0.0094	0.08603
6c	65.937	1.905	1000	9.81	2650	1.688	0.0026	26	3.8	42.47	0.1729	10.64	0.2504	0.088	0.034	4.887	0.0069	0.10092
6c	134.591	2.324	1000	9.81	2650	1.864	0.0028	26	3.8	51.14	0.1729	10.64	0.2080	0.080	0.030	6.499	0.0047	0.12153
6c	297.169	2.949	1000	9.81	2650	2.246	0.0030	26	3.8	67.10	0.1729	10.64	0.1585	0.072	0.028	8.981	0.0031	0.15944
6c	513.294	3.507	1000	9.81	2650	2.760	0.0032	26	3.8	86.75	0.1729	10.64	0.1226	0.068	0.026	11.236	0.0023	0.20612

Table 17 RBS and Milhous for Mkomazi Site 7a

Site	Q	d	ρ	g	ρ_s	R	S	D50	D84	τ	τ_{ci}^*	τ_{ci}	τ RBS	q_c	$q_{critical}$	ώ	RBS_o	β
D84																		
7a	0.144	0.644	1000	9.81	2650	0.165	0.0079	48	220	12.73	0.0155	55.20	4.3369	10.991	23.529	5.079	4.6325	0.01638
7a	2.389	0.887	1000	9.81	2650	0.207	0.0074	48	220	14.96	0.0155	55.20	3.6911	11.852	25.373	6.540	3.8797	0.01925
7a	3.453	0.948	1000	9.81	2650	0.242	0.0073	48	220	17.21	0.0155	55.20	3.2082	12.073	25.846	6.875	3.7592	0.02215
7a	4.672	1.005	1000	9.81	2650	0.275	0.0071	48	220	19.27	0.0155	55.20	2.8646	12.283	26.297	7.177	3.6639	0.02480
7a	6.374	1.073	1000	9.81	2650	0.319	0.0070	48	220	21.96	0.0155	55.20	2.5143	12.530	26.826	7.528	3.5636	0.02826
7a	9.006	1.160	1000	9.81	2650	0.396	0.0069	48	220	26.65	0.0155	55.20	2.0715	12.847	27.503	7.959	3.4556	0.03430
7a	13.526	1.282	1000	9.81	2650	0.504	0.0067	48	220	32.95	0.0155	55.20	1.6754	13.282	28.434	8.538	3.3301	0.04241
7a	21.693	1.453	1000	9.81	2650	0.589	0.0064	48	220	37.00	0.0155	55.20	1.4919	13.883	29.721	9.302	3.1949	0.04762
7a	38.821	1.719	1000	9.81	2650	0.777	0.0061	48	220	46.14	0.0155	55.20	1.1964	14.782	31.647	10.405	3.0415	0.05939
7a	69.854	2.068	1000	9.81	2650	1.053	0.0057	48	220	58.65	0.0155	55.20	0.9411	15.886	34.010	11.738	2.8974	0.07549
7a	142.586	2.634	1000	9.81	2650	1.505	0.0052	48	220	76.85	0.0155	55.20	0.7183	17.500	37.465	13.714	2.7319	0.09891
7a	314.822	3.512	1000	9.81	2650	2.195	0.0047	48	220	101.25	0.0155	55.20	0.5452	19.610	41.983	16.518	2.5417	0.13032
7a	543.787	4.324	1000	9.81	2650	2.767	0.0044	48	220	119.04	0.0155	55.20	0.4637	21.212	45.413	18.959	2.3953	0.15321
D16																		
Site	Q	d	ρ	g	ρ_s	R	S	D50	D16	τ	τ_{ci}^*	τ_{ci}	τ RBS	q_c	$q_{critical}$	ώ	RBS_o	β
7a	0.144	0.644	1000	9.81	2650	0.165	0.0079	48	8.6	12.73	0.1499	20.87	1.6398	0.085	0.036	5.079	0.0071	0.01638
7a	2.389	0.887	1000	9.81	2650	0.207	0.0074	48	8.6	14.96	0.1499	20.87	1.3956	0.092	0.039	6.540	0.0059	0.01925
7a	3.453	0.948	1000	9.81	2650	0.242	0.0073	48	8.6	17.21	0.1499	20.87	1.2131	0.093	0.039	6.875	0.0057	0.02215
7a	4.672	1.005	1000	9.81	2650	0.275	0.0071	48	8.6	19.27	0.1499	20.87	1.0832	0.095	0.040	7.177	0.0056	0.02480
7a	6.374	1.073	1000	9.81	2650	0.319	0.0070	48	8.6	21.96	0.1499	20.87	0.9507	0.097	0.041	7.528	0.0054	0.02826
7a	9.006	1.160	1000	9.81	2650	0.396	0.0069	48	8.6	26.65	0.1499	20.87	0.7833	0.099	0.042	7.959	0.0053	0.03430
7a	13.526	1.282	1000	9.81	2650	0.504	0.0067	48	8.6	32.95	0.1499	20.87	0.6335	0.103	0.043	8.538	0.0051	0.04241
7a	21.693	1.453	1000	9.81	2650	0.589	0.0064	48	8.6	37.00	0.1499	20.87	0.5641	0.107	0.045	9.302	0.0049	0.04762
7a	38.821	1.719	1000	9.81	2650	0.777	0.0061	48	8.6	46.14	0.1499	20.87	0.4524	0.114	0.048	10.405	0.0046	0.05939
7a	69.854	2.068	1000	9.81	2650	1.053	0.0057	48	8.6	58.65	0.1499	20.87	0.3559	0.123	0.052	11.738	0.0044	0.07549
7a	142.586	2.634	1000	9.81	2650	1.505	0.0052	48	8.6	76.85	0.1499	20.87	0.2716	0.135	0.057	13.714	0.0042	0.09891
7a	314.822	3.512	1000	9.81	2650	2.195	0.0047	48	8.6	101.25	0.1499	20.87	0.2061	0.152	0.064	16.518	0.0039	0.13032
7a	543.787	4.324	1000	9.81	2650	2.767	0.0044	48	8.6	119.04	0.1499	20.87	0.1753	0.164	0.069	18.959	0.0037	0.15321

Table 18 RBS and Milhous for Mkomazi Site 7b

Site	Q	d	ρ	g	ρ_s	R	S	D50	D84	τ	τ_{ci}^*	τ_{ci}	τ RBS	q_c	$q_{critical}$	ω	RBS_ω	β
D84																		
7b	0.144	0.183	1000	9.81	2650	0.074	0.0079	48	220	5.75	0.0155	55.20	9.5971	10.991	23.529	1.443	16.3024	0.00740
7b	2.389	0.518	1000	9.81	2650	0.293	0.0074	48	220	21.20	0.0155	55.20	2.6034	11.852	25.373	3.819	6.6435	0.02729
7b	3.453	0.597	1000	9.81	2650	0.362	0.0073	48	220	25.74	0.0155	55.20	2.1450	12.073	25.846	4.330	5.9694	0.03312
7b	4.672	0.671	1000	9.81	2650	0.394	0.0071	48	220	27.63	0.0155	55.20	1.9980	12.283	26.297	4.792	5.4876	0.03556
7b	6.374	0.756	1000	9.81	2650	0.463	0.0070	48	220	31.88	0.0155	55.20	1.7317	12.530	26.826	5.304	5.0578	0.04103
7b	9.006	0.866	1000	9.81	2650	0.558	0.0069	48	220	37.55	0.0155	55.20	1.4702	12.847	27.503	5.942	4.6287	0.04833
7b	13.526	1.015	1000	9.81	2650	0.659	0.0067	48	220	43.03	0.0155	55.20	1.2828	13.282	28.434	6.760	4.2061	0.05539
7b	21.693	1.222	1000	9.81	2650	0.826	0.0064	48	220	51.88	0.0155	55.20	1.0640	13.883	29.721	7.824	3.7989	0.06677
7b	38.821	1.537	1000	9.81	2650	1.078	0.0061	48	220	64.01	0.0155	55.20	0.8624	14.782	31.647	9.304	3.4016	0.08239
7b	69.854	1.939	1000	9.81	2650	1.432	0.0057	48	220	79.74	0.0155	55.20	0.6922	15.886	34.010	11.006	3.0901	0.10264
7b	142.586	2.573	1000	9.81	2650	1.932	0.0052	48	220	98.67	0.0155	55.20	0.5594	17.500	37.465	13.396	2.7967	0.12700
7b	314.822	3.527	1000	9.81	2650	2.659	0.0047	48	220	122.67	0.0155	55.20	0.4500	19.610	41.983	16.588	2.5309	0.15788
7b	543.787	4.385	1000	9.81	2650	3.176	0.0044	48	220	136.62	0.0155	55.20	0.4041	21.212	45.413	19.227	2.3620	0.17584
D16																		
Site	Q	d	ρ	g	ρ_s	R	S	D50	D16	τ	τ_{ci}^*	τ_{ci}	τ RBS	q_c	$q_{critical}$	ω	RBS_ω	β
7b	0.144	0.183	1000	9.81	2650	0.074	0.0079	48	8.6	5.75	0.1499	20.87	3.6288	0.085	0.036	1.443	0.0249	0.00740
7b	2.389	0.518	1000	9.81	2650	0.293	0.0074	48	8.6	21.20	0.1499	20.87	0.9844	0.092	0.039	3.819	0.0102	0.02729
7b	3.453	0.597	1000	9.81	2650	0.362	0.0073	48	8.6	25.74	0.1499	20.87	0.8110	0.093	0.039	4.330	0.0091	0.03312
7b	4.672	0.671	1000	9.81	2650	0.394	0.0071	48	8.6	27.63	0.1499	20.87	0.7555	0.095	0.040	4.792	0.0084	0.03556
7b	6.374	0.756	1000	9.81	2650	0.463	0.0070	48	8.6	31.88	0.1499	20.87	0.6548	0.097	0.041	5.304	0.0077	0.04103
7b	9.006	0.866	1000	9.81	2650	0.558	0.0069	48	8.6	37.55	0.1499	20.87	0.5559	0.099	0.042	5.942	0.0071	0.04833
7b	13.526	1.015	1000	9.81	2650	0.659	0.0067	48	8.6	43.03	0.1499	20.87	0.4851	0.103	0.043	6.760	0.0064	0.05539
7b	21.693	1.222	1000	9.81	2650	0.826	0.0064	48	8.6	51.88	0.1499	20.87	0.4023	0.107	0.045	7.824	0.0058	0.06677
7b	38.821	1.537	1000	9.81	2650	1.078	0.0061	48	8.6	64.01	0.1499	20.87	0.3261	0.114	0.048	9.304	0.0052	0.08239
7b	69.854	1.939	1000	9.81	2650	1.432	0.0057	48	8.6	79.74	0.1499	20.87	0.2617	0.123	0.052	11.006	0.0047	0.10264
7b	142.586	2.573	1000	9.81	2650	1.932	0.0052	48	8.6	98.67	0.1499	20.87	0.2115	0.135	0.057	13.396	0.0043	0.12700
7b	314.822	3.527	1000	9.81	2650	2.659	0.0047	48	8.6	122.67	0.1499	20.87	0.1702	0.152	0.064	16.588	0.0039	0.15788
7b	543.787	4.385	1000	9.81	2650	3.176	0.0044	48	8.6	136.62	0.1499	20.87	0.1528	0.164	0.069	19.227	0.0036	0.17584

Table 19 RBS and Milhous for Mkomazi Site 8a

Site	Q	d	ρ	g	ρ_s	R	S	D50	D84	τ	τ_{ci}^*	τ_{ci}	τ RBS	q_c	$q_{critical}$	ω̄	RBS_q	β
D84																		
8a	0.148	0.678	1000	9.81	2650	0.404	0.0089	30	150	35.21	0.0146	35.41	1.0059	5.413	12.105	6.025	2.0091	0.07250
8a	2.456	0.819	1000	9.81	2650	0.462	0.0083	30	150	37.86	0.0146	35.41	0.9355	5.808	12.986	6.836	1.8998	0.07796
8a	3.55	0.856	1000	9.81	2650	0.491	0.0082	30	150	39.61	0.0146	35.41	0.8941	5.908	13.210	7.036	1.8775	0.08157
8a	4.803	0.892	1000	9.81	2650	0.519	0.0081	30	150	41.24	0.0146	35.41	0.8588	6.003	13.423	7.228	1.8571	0.08492
8a	6.553	0.934	1000	9.81	2650	0.550	0.0080	30	150	43.04	0.0146	35.41	0.8228	6.115	13.673	7.445	1.8365	0.08864
8a	9.258	0.990	1000	9.81	2650	0.592	0.0078	30	150	45.36	0.0146	35.41	0.7807	6.257	13.990	7.731	1.8096	0.09341
8a	13.905	1.068	1000	9.81	2650	0.649	0.0076	30	150	48.38	0.0146	35.41	0.7320	6.451	14.425	8.116	1.7774	0.09963
8a	22.301	1.182	1000	9.81	2650	0.721	0.0073	30	150	51.85	0.0146	35.41	0.6831	6.718	15.021	8.663	1.7339	0.10677
8a	39.909	1.362	1000	9.81	2650	0.651	0.0070	30	150	44.45	0.0146	35.41	0.7967	7.113	15.904	9.486	1.6766	0.09154
8a	71.813	1.604	1000	9.81	2650	0.594	0.0066	30	150	38.28	0.0146	35.41	0.9252	7.590	16.973	10.541	1.6101	0.07882
8a	146.584	2.007	1000	9.81	2650	0.765	0.0061	30	150	45.67	0.0146	35.41	0.7755	8.276	18.506	12.209	1.5157	0.09404
8a	323.649	2.654	1000	9.81	2650	1.293	0.0056	30	150	70.56	0.0146	35.41	0.5019	9.151	20.462	14.760	1.3863	0.14530
8a	559.033	3.270	1000	9.81	2650	1.759	0.0052	30	150	90.29	0.0146	35.41	0.3922	9.799	21.911	17.108	1.2807	0.18595

D16

Site	Q	d	ρ	g	ρ_s	R	S	D50	D16	τ	τ_{ci}^*	τ_{ci}	τ RBS	q_c	$q_{critical}$	ω̄	RBS_q	β
8a	0.148	0.678	1000	9.81	2650	0.404	0.0089	30	13	35.21	0.0808	17.00	0.4829	0.138	0.091	6.025	0.0151	0.07250
8a	2.456	0.819	1000	9.81	2650	0.462	0.0083	30	13	37.86	0.0808	17.00	0.4492	0.148	0.098	6.836	0.0143	0.07796
8a	3.55	0.856	1000	9.81	2650	0.491	0.0082	30	13	39.61	0.0808	17.00	0.4293	0.151	0.099	7.036	0.0141	0.08157
8a	4.803	0.892	1000	9.81	2650	0.519	0.0081	30	13	41.24	0.0808	17.00	0.4123	0.153	0.101	7.228	0.0139	0.08492
8a	6.553	0.934	1000	9.81	2650	0.550	0.0080	30	13	43.04	0.0808	17.00	0.3950	0.156	0.103	7.445	0.0138	0.08864
8a	9.258	0.990	1000	9.81	2650	0.592	0.0078	30	13	45.36	0.0808	17.00	0.3748	0.160	0.105	7.731	0.0136	0.09341
8a	13.905	1.068	1000	9.81	2650	0.649	0.0076	30	13	48.38	0.0808	17.00	0.3515	0.165	0.108	8.116	0.0134	0.09963
8a	22.301	1.182	1000	9.81	2650	0.721	0.0073	30	13	51.85	0.0808	17.00	0.3280	0.171	0.113	8.663	0.0130	0.10677
8a	39.909	1.362	1000	9.81	2650	0.651	0.0070	30	13	44.45	0.0808	17.00	0.3825	0.181	0.119	9.486	0.0126	0.09154
8a	71.813	1.604	1000	9.81	2650	0.594	0.0066	30	13	38.28	0.0808	17.00	0.4442	0.194	0.127	10.541	0.0121	0.07882
8a	146.584	2.007	1000	9.81	2650	0.765	0.0061	30	13	45.67	0.0808	17.00	0.3723	0.211	0.139	12.209	0.0114	0.09404
8a	323.649	2.654	1000	9.81	2650	1.293	0.0056	30	13	70.56	0.0808	17.00	0.2410	0.233	0.154	14.760	0.0104	0.14530
8a	559.033	3.270	1000	9.81	2650	1.759	0.0052	30	13	90.29	0.0808	17.00	0.1883	0.250	0.165	17.108	0.0096	0.18595

Table 20 RBS and Milhous for Mkomazi Site 8b

Site	Q	d	ρ	g	ρ_s	R	S	D50	D84	τ	τ_{ci}^*	τ_{ci}	τ RBS	q_c	$q_{critical}$	ω	RBS_q	β
D84																		
8b	0.148	0.440	1000	9.81	2650	0.206	0.0089	30	150	17.99	0.0146	35.41	1.9690	5.413	12.105	3.910	3.0958	0.03704
8b	2.456	0.619	1000	9.81	2650	0.351	0.0083	30	150	28.72	0.0146	35.41	1.2329	5.808	12.986	5.166	2.5136	0.05915
8b	3.55	0.664	1000	9.81	2650	0.391	0.0082	30	150	31.49	0.0146	35.41	1.1247	5.908	13.210	5.458	2.4204	0.06485
8b	4.803	0.707	1000	9.81	2650	0.354	0.0081	30	150	28.17	0.0146	35.41	1.2573	6.003	13.423	5.729	2.3431	0.05801
8b	6.553	0.758	1000	9.81	2650	0.369	0.0080	30	150	28.82	0.0146	35.41	1.2287	6.115	13.673	6.042	2.2629	0.05935
8b	9.258	0.823	1000	9.81	2650	0.389	0.0078	30	150	29.83	0.0146	35.41	1.1872	6.257	13.990	6.427	2.1768	0.06143
8b	13.905	0.915	1000	9.81	2650	0.405	0.0076	30	150	30.21	0.0146	35.41	1.1722	6.451	14.425	6.953	2.0746	0.06222
8b	22.301	1.044	1000	9.81	2650	0.517	0.0073	30	150	37.19	0.0146	35.41	0.9521	6.718	15.021	7.651	1.9631	0.07660
8b	39.909	1.248	1000	9.81	2650	0.690	0.0070	30	150	47.14	0.0146	35.41	0.7513	7.113	15.904	8.692	1.8298	0.09707
8b	71.813	1.515	1000	9.81	2650	0.876	0.0066	30	150	56.46	0.0146	35.41	0.6272	7.590	16.973	9.956	1.7047	0.11627
8b	146.584	1.951	1000	9.81	2650	1.057	0.0061	30	150	63.09	0.0146	35.41	0.5613	8.276	18.506	11.869	1.5592	0.12992
8b	323.649	2.633	1000	9.81	2650	1.129	0.0056	30	150	61.59	0.0146	35.41	0.5750	9.151	20.462	14.643	1.3974	0.12682
8b	559.033	3.269	1000	9.81	2650	1.656	0.0052	30	150	85.00	0.0146	35.41	0.4166	9.799	21.911	17.103	1.2811	0.17505
D16																		
Site	Q	d	ρ	g	ρ_s	R	S	D50	D16	τ	τ_{ci}^*	τ_{ci}	τ RBS	q_c	$q_{critical}$	ω	RBS_q	β
8b	0.148	0.440	1000	9.81	2650	0.206	0.0089	30	13	17.99	0.0808	17.00	0.9454	0.138	0.091	3.910	0.0233	0.03704
8b	2.456	0.619	1000	9.81	2650	0.351	0.0083	30	13	28.72	0.0808	17.00	0.5919	0.148	0.098	5.166	0.0189	0.05915
8b	3.55	0.664	1000	9.81	2650	0.391	0.0082	30	13	31.49	0.0808	17.00	0.5400	0.151	0.099	5.458	0.0182	0.06485
8b	4.803	0.707	1000	9.81	2650	0.354	0.0081	30	13	28.17	0.0808	17.00	0.6037	0.153	0.101	5.729	0.0176	0.05801
8b	6.553	0.758	1000	9.81	2650	0.369	0.0080	30	13	28.82	0.0808	17.00	0.5900	0.156	0.103	6.042	0.0170	0.05935
8b	9.258	0.823	1000	9.81	2650	0.389	0.0078	30	13	29.83	0.0808	17.00	0.5700	0.160	0.105	6.427	0.0164	0.06143
8b	13.905	0.915	1000	9.81	2650	0.405	0.0076	30	13	30.21	0.0808	17.00	0.5628	0.165	0.108	6.953	0.0156	0.06222
8b	22.301	1.044	1000	9.81	2650	0.517	0.0073	30	13	37.19	0.0808	17.00	0.4571	0.171	0.113	7.651	0.0147	0.07660
8b	39.909	1.248	1000	9.81	2650	0.690	0.0070	30	13	47.14	0.0808	17.00	0.3607	0.181	0.119	8.692	0.0137	0.09707
8b	71.813	1.515	1000	9.81	2650	0.876	0.0066	30	13	56.46	0.0808	17.00	0.3011	0.194	0.127	9.956	0.0128	0.11627
8b	146.584	1.951	1000	9.81	2650	1.057	0.0061	30	13	63.09	0.0808	17.00	0.2695	0.211	0.139	11.869	0.0117	0.12992
8b	323.649	2.633	1000	9.81	2650	1.129	0.0056	30	13	61.59	0.0808	17.00	0.2761	0.233	0.154	14.643	0.0105	0.12682
8b	559.033	3.269	1000	9.81	2650	1.656	0.0052	30	13	85.00	0.0808	17.00	0.2000	0.250	0.165	17.103	0.0096	0.17505

Table 21 RBS and Milhous for Mkomazi Site 9a

Site	Q	d	ρ	g	ρ_s	R	S	D50	D84	τ	τ_{ci}^*	τ_{ci}	τ RBS	q_c	$q_{critical}$	ω	RBS_n	β
D84																		
9a	1.290	0.915	1000	9.81	2650	0.444	0.0045	60	410	19.59	0.0117	77.79	3.9712	52.502	137.243	4.112	33.3778	0.02017
9a	3.814	1.053	1000	9.81	2650	0.547	0.0046	60	410	24.75	0.0117	77.79	3.1424	51.017	133.360	4.855	27.4699	0.02549
9a	5.116	1.101	1000	9.81	2650	0.579	0.0047	60	410	26.41	0.0117	77.79	2.9451	50.525	132.075	5.120	25.7950	0.02720
9a	6.924	1.157	1000	9.81	2650	0.629	0.0047	60	410	28.98	0.0117	77.79	2.6840	49.979	130.648	5.433	24.0469	0.02984
9a	9.579	1.226	1000	9.81	2650	0.691	0.0047	60	410	32.17	0.0117	77.79	2.4178	49.352	129.008	5.822	22.1574	0.03313
9a	13.447	1.308	1000	9.81	2650	0.760	0.0048	60	410	35.88	0.0117	77.79	2.1682	48.654	127.185	6.289	20.2241	0.03694
9a	20.028	1.418	1000	9.81	2650	0.846	0.0049	60	410	40.56	0.0117	77.79	1.9177	47.790	124.925	6.931	18.0232	0.04177
9a	31.990	1.573	1000	9.81	2650	0.958	0.0050	60	410	46.84	0.0117	77.79	1.6605	46.728	122.151	7.842	15.5772	0.04823
9a	55.327	1.794	1000	9.81	2650	1.078	0.0051	60	410	54.03	0.0117	77.79	1.4397	45.460	118.835	9.166	12.9654	0.05563
9a	92.686	2.050	1000	9.81	2650	1.255	0.0052	60	410	64.43	0.0117	77.79	1.2073	44.279	115.748	10.725	10.7923	0.06634
9a	186.151	2.491	1000	9.81	2650	1.457	0.0054	60	410	77.15	0.0117	77.79	1.0082	42.771	111.805	13.440	8.3186	0.07944
9a	421.352	3.187	1000	9.81	2650	1.903	0.0056	60	410	104.13	0.0117	77.79	0.7470	41.217	107.745	17.777	6.0609	0.10722
9a	727.789	3.795	1000	9.81	2650	2.369	0.0057	60	410	132.13	0.0117	77.79	0.5887	40.337	105.443	21.581	4.8859	0.13604
D16																		
Site	Q	d	ρ	g	ρ_s	R	S	D50	D16	τ	τ_{ci}^*	τ_{ci}	τ RBS	q_c	$q_{critical}$	ω	RBS_n	β
9a	1.290	0.915	1000	9.81	2650	0.444	0.0045	60	4.2	19.59	0.2895	19.68	1.0048	0.054	0.014	4.112	0.0035	0.02017
9a	3.814	1.053	1000	9.81	2650	0.547	0.0046	60	4.2	24.75	0.2895	19.68	0.7950	0.053	0.014	4.855	0.0029	0.02549
9a	5.116	1.101	1000	9.81	2650	0.579	0.0047	60	4.2	26.41	0.2895	19.68	0.7451	0.052	0.014	5.120	0.0027	0.02720
9a	6.924	1.157	1000	9.81	2650	0.629	0.0047	60	4.2	28.98	0.2895	19.68	0.6791	0.052	0.014	5.433	0.0025	0.02984
9a	9.579	1.226	1000	9.81	2650	0.691	0.0047	60	4.2	32.17	0.2895	19.68	0.6117	0.051	0.014	5.822	0.0023	0.03313
9a	13.447	1.308	1000	9.81	2650	0.760	0.0048	60	4.2	35.88	0.2895	19.68	0.5486	0.050	0.013	6.289	0.0021	0.03694
9a	20.028	1.418	1000	9.81	2650	0.846	0.0049	60	4.2	40.56	0.2895	19.68	0.4852	0.050	0.013	6.931	0.0019	0.04177
9a	31.990	1.573	1000	9.81	2650	0.958	0.0050	60	4.2	46.84	0.2895	19.68	0.4201	0.048	0.013	7.842	0.0016	0.04823
9a	55.327	1.794	1000	9.81	2650	1.078	0.0051	60	4.2	54.03	0.2895	19.68	0.3643	0.047	0.012	9.166	0.0014	0.05563
9a	92.686	2.050	1000	9.81	2650	1.255	0.0052	60	4.2	64.43	0.2895	19.68	0.3055	0.046	0.012	10.725	0.0011	0.06634
9a	186.151	2.491	1000	9.81	2650	1.457	0.0054	60	4.2	77.15	0.2895	19.68	0.2551	0.044	0.012	13.440	0.0009	0.07944
9a	421.352	3.187	1000	9.81	2650	1.903	0.0056	60	4.2	104.13	0.2895	19.68	0.1890	0.043	0.011	17.777	0.0006	0.10722
9a	727.789	3.795	1000	9.81	2650	2.369	0.0057	60	4.2	132.13	0.2895	19.68	0.1490	0.042	0.011	21.581	0.0005	0.13604

Table 22 RBS and Milhous for Mkomazi Site 9b

Site	Q	d	ρ	g	ρ_s	R	S	D50	D84	τ	τ_{ci}^*	τ_{ci}	τ RBS	q_c	$q_{critical}$	ώ	RBS_{ω}	β
D84																		
9b	1.290	0.567	1000	9.81	2650	0.567	0.0045	60	410	25.00	0.0117	77.79	3.1120	52.502	137.243	2.548	53.8637	0.02574
9b	3.814	0.742	1000	9.81	2650	0.742	0.0046	60	410	33.56	0.0117	77.79	2.3179	51.017	133.360	3.421	38.9835	0.03455
9b	5.116	0.803	1000	9.81	2650	0.803	0.0047	60	410	36.63	0.0117	77.79	2.1234	50.525	132.075	3.734	35.3677	0.03772
9b	6.924	0.872	1000	9.81	2650	0.872	0.0047	60	410	40.17	0.0117	77.79	1.9365	49.979	130.648	4.095	31.9063	0.04136
9b	9.579	0.955	1000	9.81	2650	0.955	0.0047	60	410	44.49	0.0117	77.79	1.7483	49.352	129.008	4.535	28.4450	0.04581
9b	13.447	1.052	1000	9.81	2650	1.052	0.0048	60	410	49.64	0.0117	77.79	1.5671	48.654	127.185	5.060	25.1359	0.05111
9b	20.028	1.182	1000	9.81	2650	1.182	0.0049	60	410	56.67	0.0117	77.79	1.3726	47.790	124.925	5.777	21.6248	0.05835
9b	31.990	1.361	1000	9.81	2650	1.361	0.0050	60	410	66.58	0.0117	77.79	1.1684	46.728	122.151	6.786	17.9991	0.06855
9b	55.327	1.611	1000	9.81	2650	1.611	0.0051	60	410	80.76	0.0117	77.79	0.9631	45.460	118.835	8.233	14.4341	0.08316
9b	92.686	1.896	1000	9.81	2650	1.896	0.0052	60	410	97.31	0.0117	77.79	0.7993	44.279	115.748	9.920	11.6684	0.10020
9b	186.151	2.375	1000	9.81	2650	2.375	0.0054	60	410	125.73	0.0117	77.79	0.6187	42.771	111.805	12.816	8.7235	0.12946
9b	421.352	3.108	1000	9.81	2650	3.108	0.0056	60	410	170.06	0.0117	77.79	0.4574	41.217	107.745	17.335	6.2154	0.17510
9b	727.789	3.732	1000	9.81	2650	3.732	0.0057	60	410	208.18	0.0117	77.79	0.3737	40.337	105.443	21.221	4.9689	0.21435

Site	Q	d	ρ	g	ρ_s	R	S	D50	D16	τ	τ_{ci}^*	τ_{ci}	τ RBS	q_c	$q_{critical}$	ώ	RBS_q	β
D16																		
9b	1.290	0.567	1000	9.81	2650	0.567	0.0045	60	4.2	25.00	0.2895	19.68	0.7874	0.054	0.014	2.548	0.0057	0.02574
9b	3.814	0.742	1000	9.81	2650	0.742	0.0046	60	4.2	33.56	0.2895	19.68	0.5865	0.053	0.014	3.421	0.0041	0.03455
9b	5.116	0.803	1000	9.81	2650	0.803	0.0047	60	4.2	36.63	0.2895	19.68	0.5372	0.052	0.014	3.734	0.0037	0.03772
9b	6.924	0.872	1000	9.81	2650	0.872	0.0047	60	4.2	40.17	0.2895	19.68	0.4899	0.052	0.014	4.095	0.0033	0.04136
9b	9.579	0.955	1000	9.81	2650	0.955	0.0047	60	4.2	44.49	0.2895	19.68	0.4423	0.051	0.014	4.535	0.0030	0.04581
9b	13.447	1.052	1000	9.81	2650	1.052	0.0048	60	4.2	49.64	0.2895	19.68	0.3965	0.050	0.013	5.060	0.0026	0.05111
9b	20.028	1.182	1000	9.81	2650	1.182	0.0049	60	4.2	56.67	0.2895	19.68	0.3473	0.050	0.013	5.777	0.0023	0.05835
9b	31.990	1.361	1000	9.81	2650	1.361	0.0050	60	4.2	66.58	0.2895	19.68	0.2956	0.048	0.013	6.786	0.0019	0.06855
9b	55.327	1.611	1000	9.81	2650	1.611	0.0051	60	4.2	80.76	0.2895	19.68	0.2437	0.047	0.012	8.233	0.0015	0.08316
9b	92.686	1.896	1000	9.81	2650	1.896	0.0052	60	4.2	97.31	0.2895	19.68	0.2022	0.046	0.012	9.920	0.0012	0.10020
9b	186.151	2.375	1000	9.81	2650	2.375	0.0054	60	4.2	125.73	0.2895	19.68	0.1565	0.044	0.012	12.816	0.0009	0.12946
9b	421.352	3.108	1000	9.81	2650	3.108	0.0056	60	4.2	170.06	0.2895	19.68	0.1157	0.043	0.011	17.335	0.0007	0.17510
9b	727.789	3.732	1000	9.81	2650	3.732	0.0057	60	4.2	208.18	0.2895	19.68	0.0945	0.042	0.011	21.221	0.0005	0.21435

Table 23 RBS and Milhous for Mkomazi Site 10a

Site	Q	d	ρ	g	ρ_s	R	S	D50	D84	τ	τ_{ci}^*	τ_{ci}	τ RBS	q_c	$q_{critical}$	ώ	RBS_q	β
D84																		
10a	1.349	0.906	1000	9.81	2650	0.532	0.0019	50	400	9.83	0.0105	67.96	6.9143	133.855	378.599	1.708	221.6723	0.01214
10a	3.987	1.019	1000	9.81	2650	0.626	0.0021	50	400	12.63	0.0105	67.96	5.3808	121.456	343.529	2.095	163.9669	0.01561
10a	5.349	1.061	1000	9.81	2650	0.661	0.0021	50	400	13.71	0.0105	67.96	4.9581	117.691	332.881	2.244	148.3646	0.01694
10a	7.238	1.110	1000	9.81	2650	0.698	0.0022	50	400	14.93	0.0105	67.96	4.5533	113.697	321.583	2.421	132.8430	0.01844
10a	10.015	1.171	1000	9.81	2650	0.736	0.0023	50	400	16.31	0.0105	67.96	4.1667	109.320	309.205	2.645	116.9060	0.02015
10a	14.058	1.244	1000	9.81	2650	0.797	0.0023	50	400	18.36	0.0105	67.96	3.7016	104.713	296.174	2.920	101.4331	0.02269
10a	20.938	1.346	1000	9.81	2650	0.860	0.0025	50	400	20.75	0.0105	67.96	3.2749	99.342	280.983	3.311	84.8533	0.02564
10a	33.444	1.492	1000	9.81	2650	0.949	0.0026	50	400	24.24	0.0105	67.96	2.8032	93.219	263.663	3.885	67.8650	0.02996
10a	57.842	1.706	1000	9.81	2650	1.122	0.0028	50	400	30.64	0.0105	67.96	2.2184	86.506	244.676	4.749	51.5224	0.03785
10a	96.899	1.962	1000	9.81	2650	1.345	0.0030	50	400	39.05	0.0105	67.96	1.7402	80.779	228.478	5.806	39.3522	0.04826
10a	194.392	2.418	1000	9.81	2650	1.747	0.0032	50	400	54.78	0.0105	67.96	1.2406	74.117	209.635	7.727	27.1304	0.06769
10a	439.509	3.168	1000	9.81	2650	1.888	0.0035	50	400	63.99	0.0105	67.96	1.0621	67.911	192.080	10.946	17.5483	0.07906
10a	759.150	3.850	1000	9.81	2650	2.266	0.0036	50	400	80.24	0.0105	67.96	0.8470	64.649	182.854	13.900	13.1551	0.09915
D16																		
Site	Q	d	ρ	g	ρ_s	R	S	D50	D16	τ	τ_{ci}^*	τ_{ci}	τ RBS	q_c	$q_{critical}$	ώ	RBS_q	β
10a	1.349	0.906	1000	9.81	2650	0.532	0.0019	50	15	9.83	0.1045	25.38	2.5820	0.972	0.532	1.708	0.3117	0.01214
10a	3.987	1.019	1000	9.81	2650	0.626	0.0021	50	15	12.63	0.1045	25.38	2.0094	0.882	0.483	2.095	0.2306	0.01561
10a	5.349	1.061	1000	9.81	2650	0.661	0.0021	50	15	13.71	0.1045	25.38	1.8515	0.855	0.468	2.244	0.2086	0.01694
10a	7.238	1.110	1000	9.81	2650	0.698	0.0022	50	15	14.93	0.1045	25.38	1.7003	0.826	0.452	2.421	0.1868	0.01844
10a	10.015	1.171	1000	9.81	2650	0.736	0.0023	50	15	16.31	0.1045	25.38	1.5560	0.794	0.435	2.645	0.1644	0.02015
10a	14.058	1.244	1000	9.81	2650	0.797	0.0023	50	15	18.36	0.1045	25.38	1.3823	0.760	0.416	2.920	0.1426	0.02269
10a	20.938	1.346	1000	9.81	2650	0.860	0.0025	50	15	20.75	0.1045	25.38	1.2230	0.721	0.395	3.311	0.1193	0.02564
10a	33.444	1.492	1000	9.81	2650	0.949	0.0026	50	15	24.24	0.1045	25.38	1.0468	0.677	0.371	3.885	0.0954	0.02996
10a	57.842	1.706	1000	9.81	2650	1.122	0.0028	50	15	30.64	0.1045	25.38	0.8284	0.628	0.344	4.749	0.0725	0.03785
10a	96.899	1.962	1000	9.81	2650	1.345	0.0030	50	15	39.05	0.1045	25.38	0.6498	0.587	0.321	5.806	0.0553	0.04826
10a	194.392	2.418	1000	9.81	2650	1.747	0.0032	50	15	54.78	0.1045	25.38	0.4633	0.538	0.295	7.727	0.0382	0.06769
10a	439.509	3.168	1000	9.81	2650	1.888	0.0035	50	15	63.99	0.1045	25.38	0.3966	0.493	0.270	10.946	0.0247	0.07906
10a	759.150	3.850	1000	9.81	2650	2.266	0.0036	50	15	80.24	0.1045	25.38	0.3163	0.469	0.257	13.900	0.0185	0.09915

Table 24 RBS and Milhous for Mkomazi Site 10b

Site	Q	d	ρ	g	ρ_s	R	S	D50	D84	τ	τ_{ci}^*	τ_{ci}	τ RBS	q_c	$q_{critical}$	ώ	RBS_n	β
D84																		
10b	1.349	0.414	1000	9.81	2650	0.190	0.0019	50	400	3.52	0.0105	67.96	19.3305	133.855	378.599	0.780	485.1089	0.00434
10b	3.987	0.609	1000	9.81	2650	0.371	0.0021	50	400	7.48	0.0105	67.96	9.0869	121.456	343.529	1.252	274.3552	0.00924
10b	5.349	0.677	1000	9.81	2650	0.433	0.0021	50	400	8.97	0.0105	67.96	7.5728	117.691	332.881	1.432	232.5182	0.01109
10b	7.238	0.754	1000	9.81	2650	0.502	0.0022	50	400	10.74	0.0105	67.96	6.3287	113.697	321.583	1.644	195.5646	0.01327
10b	10.015	0.847	1000	9.81	2650	0.578	0.0023	50	400	12.82	0.0105	67.96	5.3023	109.320	309.205	1.913	161.6256	0.01584
10b	14.058	0.956	1000	9.81	2650	0.666	0.0023	50	400	15.33	0.0105	67.96	4.4321	104.713	296.174	2.244	131.9904	0.01895
10b	20.938	1.102	1000	9.81	2650	0.780	0.0025	50	400	18.82	0.0105	67.96	3.6111	99.342	280.983	2.711	103.6411	0.02325
10b	33.444	1.302	1000	9.81	2650	0.932	0.0026	50	400	23.80	0.0105	67.96	2.8555	93.219	263.663	3.390	77.7685	0.02941
10b	57.842	1.584	1000	9.81	2650	1.138	0.0028	50	400	31.09	0.0105	67.96	2.1863	86.506	244.676	4.409	55.4906	0.03841
10b	96.899	1.904	1000	9.81	2650	1.433	0.0030	50	400	41.60	0.0105	67.96	1.6335	80.779	228.478	5.634	40.5509	0.05141
10b	194.392	2.441	1000	9.81	2650	1.673	0.0032	50	400	52.45	0.0105	67.96	1.2957	74.117	209.635	7.800	26.8748	0.06481
10b	439.509	3.266	1000	9.81	2650	2.036	0.0035	50	400	69.00	0.0105	67.96	0.9850	67.911	192.080	11.284	17.0217	0.08525
10b	759.150	3.970	1000	9.81	2650	2.354	0.0036	50	400	83.36	0.0105	67.96	0.8153	64.649	182.854	14.333	12.7574	0.10300
D16																		
Site	Q	d	ρ	g	ρ_s	R	S	D50	D16	τ	τ_{ci}^*	τ_{ci}	τ RBS	q_c	$q_{critical}$	ώ	RBS_n	β
10b	1.349	0.414	1000	9.81	2650	0.190	0.0019	50	15	3.52	0.1045	25.38	7.2186	0.972	0.532	0.780	0.6822	0.00434
10b	3.987	0.609	1000	9.81	2650	0.371	0.0021	50	15	7.48	0.1045	25.38	3.3933	0.882	0.483	1.252	0.3858	0.00924
10b	5.349	0.677	1000	9.81	2650	0.433	0.0021	50	15	8.97	0.1045	25.38	2.8279	0.855	0.468	1.432	0.3270	0.01109
10b	7.238	0.754	1000	9.81	2650	0.502	0.0022	50	15	10.74	0.1045	25.38	2.3633	0.826	0.452	1.644	0.2750	0.01327
10b	10.015	0.847	1000	9.81	2650	0.578	0.0023	50	15	12.82	0.1045	25.38	1.9801	0.794	0.435	1.913	0.2273	0.01584
10b	14.058	0.956	1000	9.81	2650	0.666	0.0023	50	15	15.33	0.1045	25.38	1.6551	0.760	0.416	2.244	0.1856	0.01895
10b	20.938	1.102	1000	9.81	2650	0.780	0.0025	50	15	18.82	0.1045	25.38	1.3485	0.721	0.395	2.711	0.1457	0.02325
10b	33.444	1.302	1000	9.81	2650	0.932	0.0026	50	15	23.80	0.1045	25.38	1.0663	0.677	0.371	3.390	0.1094	0.02941
10b	57.842	1.584	1000	9.81	2650	1.138	0.0028	50	15	31.09	0.1045	25.38	0.8164	0.628	0.344	4.409	0.0780	0.03841
10b	96.899	1.904	1000	9.81	2650	1.433	0.0030	50	15	41.60	0.1045	25.38	0.6100	0.587	0.321	5.634	0.0570	0.05141
10b	194.392	2.441	1000	9.81	2650	1.673	0.0032	50	15	52.45	0.1045	25.38	0.4838	0.538	0.295	7.800	0.0378	0.06481
10b	439.509	3.266	1000	9.81	2650	2.036	0.0035	50	15	69.00	0.1045	25.38	0.3678	0.493	0.270	11.284	0.0239	0.08525
10b	759.150	3.970	1000	9.81	2650	2.354	0.0036	50	15	83.36	0.1045	25.38	0.3044	0.469	0.257	14.333	0.0179	0.10300

Table 25 RBS and Milhous for Mkomazi Site 11

Site	Q	d	ρ	g	$ρ_s$	R	S	D50	D84	τ	$τ_{ci}$*	$τ_{ci}$	τ RBS	q_c	$q_{critical}$	ώ	RBS_q	β
D84																		
11	1.378	0.338	1000	9.81	2650	0.197	0.0081	65	160	15.66	0.0240	62.04	3.9618	6.631	10.404	2.732	3.8077	0.01488
11	4.074	0.497	1000	9.81	2650	0.313	0.0078	65	160	23.84	0.0240	62.04	2.6019	6.933	10.877	3.861	2.8173	0.02266
11	5.465	0.551	1000	9.81	2650	0.361	0.0077	65	160	27.11	0.0240	62.04	2.2884	7.042	11.049	4.221	2.6176	0.02577
11	7.396	0.613	1000	9.81	2650	0.415	0.0075	65	160	30.67	0.0240	62.04	2.0227	7.170	11.249	4.621	2.4343	0.02915
11	10.232	0.688	1000	9.81	2650	0.478	0.0074	65	160	34.70	0.0240	62.04	1.7878	7.326	11.493	5.088	2.2588	0.03298
11	14.363	0.776	1000	9.81	2650	0.551	0.0072	65	160	39.08	0.0240	62.04	1.5872	7.510	11.783	5.613	2.0993	0.03715
11	21.394	0.893	1000	9.81	2650	0.657	0.0070	65	160	45.28	0.0240	62.04	1.3700	7.759	12.174	6.274	1.9404	0.04304
11	34.171	1.054	1000	9.81	2650	0.806	0.0068	65	160	53.45	0.0240	62.04	1.1605	8.099	12.707	7.127	1.7830	0.05081
11	59.099	1.280	1000	9.81	2650	0.942	0.0064	65	160	59.42	0.0240	62.04	1.0439	8.565	13.438	8.234	1.6321	0.05648
11	99.006	1.536	1000	9.81	2650	1.131	0.0061	65	160	67.80	0.0240	62.04	0.9150	9.071	14.231	9.387	1.5161	0.06444
11	199.182	1.968	1000	9.81	2650	1.406	0.0057	65	160	78.31	0.0240	62.04	0.7921	9.850	15.454	11.174	1.3831	0.07444
11	451.614	2.629	1000	9.81	2650	1.474	0.0052	65	160	75.26	0.0240	62.04	0.8243	10.861	17.041	13.679	1.2458	0.07153
11	780.063	3.190	1000	9.81	2650	1.748	0.0049	65	160	84.40	0.0240	62.04	0.7350	11.562	18.139	15.698	1.1556	0.08022
D16																		
Site	Q	d	ρ	g	$ρ_s$	R	S	D50	D16	τ	$τ_{ci}$*	$τ_{ci}$	τ RBS	q_c	$q_{critical}$	ώ	RBS_q	β
11	1.378	0.338	1000	9.81	2650	0.197	0.0081	65	22	15.66	0.0961	34.21	2.1847	0.338	0.197	2.732	0.0720	0.01488
11	4.074	0.497	1000	9.81	2650	0.313	0.0078	65	22	23.84	0.0961	34.21	1.4348	0.353	0.206	3.861	0.0533	0.02266
11	5.465	0.551	1000	9.81	2650	0.361	0.0077	65	22	27.11	0.0961	34.21	1.2619	0.359	0.209	4.221	0.0495	0.02577
11	7.396	0.613	1000	9.81	2650	0.415	0.0075	65	22	30.67	0.0961	34.21	1.1154	0.366	0.213	4.621	0.0460	0.02915
11	10.232	0.688	1000	9.81	2650	0.478	0.0074	65	22	34.70	0.0961	34.21	0.9859	0.374	0.217	5.088	0.0427	0.03298
11	14.363	0.776	1000	9.81	2650	0.551	0.0072	65	22	39.08	0.0961	34.21	0.8753	0.383	0.223	5.613	0.0397	0.03715
11	21.394	0.893	1000	9.81	2650	0.657	0.0070	65	22	45.28	0.0961	34.21	0.7555	0.396	0.230	6.274	0.0367	0.04304
11	34.171	1.054	1000	9.81	2650	0.806	0.0068	65	22	53.45	0.0961	34.21	0.6399	0.413	0.240	7.127	0.0337	0.05081
11	59.099	1.280	1000	9.81	2650	0.942	0.0064	65	22	59.42	0.0961	34.21	0.5757	0.437	0.254	8.234	0.0309	0.05648
11	99.006	1.536	1000	9.81	2650	1.131	0.0061	65	22	67.80	0.0961	34.21	0.5045	0.462	0.269	9.387	0.0287	0.06444
11	199.182	1.968	1000	9.81	2650	1.406	0.0057	65	22	78.31	0.0961	34.21	0.4368	0.502	0.292	11.174	0.0261	0.07444
11	451.614	2.629	1000	9.81	2650	1.474	0.0052	65	22	75.26	0.0961	34.21	0.4545	0.554	0.322	13.679	0.0236	0.07153
11	780.063	3.190	1000	9.81	2650	1.748	0.0049	65	22	84.40	0.0961	34.21	0.4053	0.589	0.343	15.698	0.0218	0.08022

Table 26 RBS and Milhous for Mkomazi Site 12

Site	Q	d	ρ	g	ρ_s	R	S	D50	D84	τ	τ_{ci}^*	τ_{ci}	τ RBS	q_c	$q_{critical}$	ώ	RBS_o	β
D84																		
12	1.451	0.922	1000	9.81	2650	0.307	0.0007	3.9	230	2.16	0.0026	9.65	4.4710	172.460	1324.404	0.661	2004.866	0.03420
12	4.290	1.130	1000	9.81	2650	0.459	0.0010	3.9	230	4.40	0.0026	9.65	2.1944	121.904	936.161	1.104	848.2845	0.06968
12	5.756	1.201	1000	9.81	2650	0.527	0.0011	3.9	230	5.51	0.0026	9.65	1.7510	110.565	849.082	1.280	663.4653	0.08732
12	7.789	1.282	1000	9.81	2650	0.604	0.0012	3.9	230	6.91	0.0026	9.65	1.3976	99.971	767.722	1.495	513.6513	0.10940
12	10.777	1.378	1000	9.81	2650	0.694	0.0013	3.9	230	8.74	0.0026	9.65	1.1049	89.772	689.406	1.769	389.8124	0.13838
12	15.128	1.491	1000	9.81	2650	0.798	0.0014	3.9	230	11.10	0.0026	9.65	0.8698	80.354	617.080	2.113	292.0905	0.17578
12	22.531	1.640	1000	9.81	2650	0.927	0.0016	3.9	230	14.44	0.0026	9.65	0.6685	70.782	543.566	2.602	208.8699	0.22871
12	35.988	1.844	1000	9.81	2650	1.098	0.0018	3.9	230	19.41	0.0026	9.65	0.4972	61.373	471.315	3.324	141.8122	0.30749
12	62.243	2.127	1000	9.81	2650	1.335	0.0021	3.9	230	27.11	0.0026	9.65	0.3561	52.543	403.501	4.404	91.6223	0.42942
12	104.272	2.445	1000	9.81	2650	1.626	0.0023	3.9	230	37.18	0.0026	9.65	0.2596	46.007	353.308	5.700	61.9855	0.58889
12	209.711	2.976	1000	9.81	2650	2.026	0.0027	3.9	230	53.29	0.0026	9.65	0.1811	39.329	302.029	7.980	37.8461	0.84412
12	475.339	3.778	1000	9.81	2650	2.631	0.0031	3.9	230	79.06	0.0026	9.65	0.1221	33.883	260.200	11.573	22.4826	1.25243
12	821.039	4.451	1000	9.81	2650	3.141	0.0033	3.9	230	101.37	0.0026	9.65	0.0952	31.283	240.238	14.642	16.4072	1.60585
D16																		
Site	Q	d	ρ	g	ρ_s	R	S	D50	D16	τ	τ_{ci}^*	τ_{ci}	τ RBS	q_c	$q_{critical}$	ώ	RBS_o	β
12	1.451	0.922	1000	9.81	2650	0.307	0.0007	3.9	0.68	2.16	0.1528	1.68	0.7792	0.028	0.012	0.661	0.0175	0.03420
12	4.290	1.130	1000	9.81	2650	0.459	0.0010	3.9	0.68	4.40	0.1528	1.68	0.3824	0.020	0.008	1.104	0.0074	0.06968
12	5.756	1.201	1000	9.81	2650	0.527	0.0011	3.9	0.68	5.51	0.1528	1.68	0.3052	0.018	0.007	1.280	0.0058	0.08732
12	7.789	1.282	1000	9.81	2650	0.604	0.0012	3.9	0.68	6.91	0.1528	1.68	0.2436	0.016	0.007	1.495	0.0045	0.10940
12	10.777	1.378	1000	9.81	2650	0.694	0.0013	3.9	0.68	8.74	0.1528	1.68	0.1926	0.014	0.006	1.769	0.0034	0.13838
12	15.128	1.491	1000	9.81	2650	0.798	0.0014	3.9	0.68	11.10	0.1528	1.68	0.1516	0.013	0.005	2.113	0.0026	0.17578
12	22.531	1.640	1000	9.81	2650	0.927	0.0016	3.9	0.68	14.44	0.1528	1.68	0.1165	0.011	0.005	2.602	0.0018	0.22871
12	35.988	1.844	1000	9.81	2650	1.098	0.0018	3.9	0.68	19.41	0.1528	1.68	0.0867	0.010	0.004	3.324	0.0012	0.30749
12	62.243	2.127	1000	9.81	2650	1.335	0.0021	3.9	0.68	27.11	0.1528	1.68	0.0621	0.008	0.004	4.404	0.0008	0.42942
12	104.272	2.445	1000	9.81	2650	1.626	0.0023	3.9	0.68	37.18	0.1528	1.68	0.0452	0.007	0.003	5.700	0.0005	0.58889
12	209.711	2.976	1000	9.81	2650	2.026	0.0027	3.9	0.68	53.29	0.1528	1.68	0.0316	0.006	0.003	7.980	0.0003	0.84412
12	475.339	3.778	1000	9.81	2650	2.631	0.0031	3.9	0.68	79.06	0.1528	1.68	0.0213	0.005	0.002	11.573	0.0002	1.25243
12	821.039	4.451	1000	9.81	2650	3.141	0.0033	3.9	0.68	101.37	0.1528	1.68	0.0166	0.005	0.002	14.642	0.0001	1.60585

Table 27 RBS and Milhous for Mkomazi Site 13

Site	Q	d	ρ	g	ρ_s	R	S	D50	D84	τ	τ_{ci}^*	τ_{ci}	τ RBS	q_c	$q_{critical}$	ω	RBS_o	β
D84																		
13	1.466	0.862	1000	9.81	2650	0.266	0.0012	26	96	3.15	0.0180	28.02	8.8906	25.954	49.872	1.040	47.9717	0.00749
13	4.334	0.994	1000	9.81	2650	0.342	0.0013	26	96	4.40	0.0180	28.02	6.3659	23.641	45.427	1.303	34.8635	0.01046
13	5.814	1.042	1000	9.81	2650	0.360	0.0013	26	96	4.76	0.0180	28.02	5.8914	22.938	44.077	1.403	31.4108	0.01130
13	7.868	1.099	1000	9.81	2650	0.384	0.0014	26	96	5.23	0.0180	28.02	5.3615	22.191	42.642	1.524	27.9732	0.01242
13	10.885	1.169	1000	9.81	2650	0.349	0.0014	26	96	4.91	0.0180	28.02	5.7036	21.373	41.070	1.677	24.4933	0.01167
13	15.280	1.253	1000	9.81	2650	0.410	0.0015	26	96	5.98	0.0180	28.02	4.6839	20.511	39.413	1.865	21.1375	0.01422
13	22.759	1.370	1000	9.81	2650	0.503	0.0016	26	96	7.68	0.0180	28.02	3.6494	19.505	37.479	2.132	17.5764	0.01825
13	36.352	1.537	1000	9.81	2650	0.652	0.0016	26	96	10.50	0.0180	28.02	2.6685	18.356	35.272	2.525	13.9667	0.02495
13	62.872	1.781	1000	9.81	2650	0.847	0.0018	26	96	14.55	0.0180	28.02	1.9258	17.096	32.850	3.118	10.5347	0.03458
13	105.325	2.072	1000	9.81	2650	1.100	0.0019	26	96	20.03	0.0180	28.02	1.3990	16.019	30.781	3.845	8.0061	0.04760
13	211.342	2.586	1000	9.81	2650	1.547	0.0020	26	96	30.28	0.0180	28.02	0.9254	14.765	28.371	5.161	5.4972	0.07196
13	477.941	3.428	1000	9.81	2650	2.232	0.0021	26	96	47.05	0.0180	28.02	0.5956	13.594	26.122	7.365	3.5469	0.11180
13	825.538	4.188	1000	9.81	2650	2.457	0.0022	26	96	53.97	0.0180	28.02	0.5193	12.979	24.939	9.378	2.6595	0.12824

D16																		
Site	Q	d	ρ	g	ρ_s	R	S	D50	D16	τ	τ_{ci}^*	τ_{ci}	τ RBS	q_c	$q_{critical}$	ω	RBS_o	β
13	1.466	0.862	1000	9.81	2650	0.266	0.0012	26	3.2	3.15	0.1950	10.10	3.2048	0.158	0.055	1.040	0.0533	0.00749
13	4.334	0.994	1000	9.81	2650	0.342	0.0013	26	3.2	4.40	0.1950	10.10	2.2947	0.144	0.050	1.303	0.0387	0.01046
13	5.814	1.042	1000	9.81	2650	0.360	0.0013	26	3.2	4.76	0.1950	10.10	2.1237	0.140	0.049	1.403	0.0349	0.01130
13	7.868	1.099	1000	9.81	2650	0.384	0.0014	26	3.2	5.23	0.1950	10.10	1.9326	0.135	0.047	1.524	0.0311	0.01242
13	10.885	1.169	1000	9.81	2650	0.349	0.0014	26	3.2	4.91	0.1950	10.10	2.0560	0.130	0.046	1.677	0.0272	0.01167
13	15.280	1.253	1000	9.81	2650	0.410	0.0015	26	3.2	5.98	0.1950	10.10	1.6884	0.125	0.044	1.865	0.0235	0.01422
13	22.759	1.370	1000	9.81	2650	0.503	0.0016	26	3.2	7.68	0.1950	10.10	1.3155	0.119	0.042	2.132	0.0195	0.01825
13	36.352	1.537	1000	9.81	2650	0.652	0.0016	26	3.2	10.50	0.1950	10.10	0.9619	0.112	0.039	2.525	0.0155	0.02495
13	62.872	1.781	1000	9.81	2650	0.847	0.0018	26	3.2	14.55	0.1950	10.10	0.6942	0.104	0.037	3.118	0.0117	0.03458
13	105.325	2.072	1000	9.81	2650	1.100	0.0019	26	3.2	20.03	0.1950	10.10	0.5043	0.097	0.034	3.845	0.0089	0.04760
13	211.342	2.586	1000	9.81	2650	1.547	0.0020	26	3.2	30.28	0.1950	10.10	0.3336	0.090	0.032	5.161	0.0061	0.07196
13	477.941	3.428	1000	9.81	2650	2.232	0.0021	26	3.2	47.05	0.1950	10.10	0.2147	0.083	0.029	7.365	0.0039	0.11180
13	825.538	4.188	1000	9.81	2650	2.457	0.0022	26	3.2	53.97	0.1950	10.10	0.1872	0.079	0.028	9.378	0.0030	0.12824

Table 28 RBS and Milhous for Mhlathuze Site 1 pool virgin flow

Site	Q	d	ρ	g	ρ_s	R	S	D50	D84	τ	τ_{ci}^*	τ_{ci}	τ RBS	q_c	$q_{critical}$	ώ	RBS_a	β
D84																		
1vP	0.000	0.600	1000	9.81	2650	0.000	0.0070	0.5	0.9	0.00	0.0298	0.43	ERR	0.003	0.004	4.200	0.0010	0.00000
1vP	0.506	0.874	1000	9.81	2650	0.477	0.0066	0.5	0.9	31.08	0.0298	0.43	0.0140	0.003	0.005	5.796	0.0008	3.83994
1vP	0.856	0.945	1000	9.81	2650	0.516	0.0065	0.5	0.9	33.08	0.0298	0.43	0.0131	0.004	0.005	6.177	0.0008	4.08746
1vP	1.280	1.013	1000	9.81	2650	0.553	0.0064	0.5	0.9	34.92	0.0298	0.43	0.0124	0.004	0.005	6.523	0.0007	4.31510
1vP	1.787	1.079	1000	9.81	2650	0.588	0.0064	0.5	0.9	36.64	0.0298	0.43	0.0119	0.004	0.005	6.850	0.0007	4.52755
1vP	2.399	1.145	1000	9.81	2650	0.628	0.0063	0.5	0.9	38.56	0.0298	0.43	0.0113	0.004	0.005	7.172	0.0007	4.76408
1vP	3.258	1.224	1000	9.81	2650	0.478	0.0062	0.5	0.9	28.88	0.0298	0.43	0.0150	0.004	0.005	7.541	0.0007	3.56842
1vP	4.613	1.328	1000	9.81	2650	0.466	0.0060	0.5	0.9	27.55	0.0298	0.43	0.0158	0.004	0.005	8.007	0.0007	3.40387
1vP	7.604	1.509	1000	9.81	2650	0.490	0.0058	0.5	0.9	27.91	0.0298	0.43	0.0156	0.004	0.005	8.768	0.0006	3.44866
1vP	13.416	1.769	1000	9.81	2650	0.600	0.0055	0.5	0.9	32.50	0.0298	0.43	0.0134	0.004	0.006	9.774	0.0006	4.01595
1vP	29.942	2.268	1000	9.81	2650	0.994	0.0051	0.5	0.9	49.27	0.0298	0.43	0.0088	0.005	0.006	11.464	0.0006	6.08766
1vP	145.270	3.958	1000	9.81	2650	2.006	0.0040	0.5	0.9	78.61	0.0298	0.43	0.0055	0.006	0.008	15.807	0.0005	9.71363
1vP	1020.298	8.563	1000	9.81	2650	3.049	0.0028	0.5	0.9	84.10	0.0298	0.43	0.0052	0.009	0.012	24.073	0.0005	10.39115
D16																		
Site	Q	d	ρ	g	ρ_s	R	S	D50	D16	τ	τ_{ci}^*	τ_{ci}	τ RBS	q_c	$q_{critical}$	ώ	RBS_a	β
1vP	0.000	0.600	1000	9.81	2650	0.000	0.0070	0.5	0.23	0.00	0.0775	0.29	ERR	0.000	0.000	4.200	0.0001	0.00000
1vP	0.506	0.874	1000	9.81	2650	0.477	0.0066	0.5	0.23	31.08	0.0775	0.29	0.0093	0.000	0.000	5.796	0.0001	3.83994
1vP	0.856	0.945	1000	9.81	2650	0.516	0.0065	0.5	0.23	33.08	0.0775	0.29	0.0087	0.000	0.000	6.177	0.0001	4.08746
1vP	1.280	1.013	1000	9.81	2650	0.553	0.0064	0.5	0.23	34.92	0.0775	0.29	0.0083	0.000	0.000	6.523	0.0000	4.31510
1vP	1.787	1.079	1000	9.81	2650	0.588	0.0064	0.5	0.23	36.64	0.0775	0.29	0.0079	0.000	0.000	6.850	0.0000	4.52755
1vP	2.399	1.145	1000	9.81	2650	0.628	0.0063	0.5	0.23	38.56	0.0775	0.29	0.0075	0.000	0.000	7.172	0.0000	4.76408
1vP	3.258	1.224	1000	9.81	2650	0.478	0.0062	0.5	0.23	28.88	0.0775	0.29	0.0100	0.000	0.000	7.541	0.0000	3.56842
1vP	4.613	1.328	1000	9.81	2650	0.466	0.0060	0.5	0.23	27.55	0.0775	0.29	0.0105	0.001	0.000	8.007	0.0000	3.40387
1vP	7.604	1.509	1000	9.81	2650	0.490	0.0058	0.5	0.23	27.91	0.0775	0.29	0.0103	0.001	0.000	8.768	0.0000	3.44866
1vP	13.416	1.769	1000	9.81	2650	0.600	0.0055	0.5	0.23	32.50	0.0775	0.29	0.0089	0.001	0.000	9.774	0.0000	4.01595
1vP	29.942	2.268	1000	9.81	2650	0.994	0.0051	0.5	0.23	49.27	0.0775	0.29	0.0059	0.001	0.000	11.464	0.0000	6.08766
1vP	145.270	3.958	1000	9.81	2650	2.006	0.0040	0.5	0.23	78.61	0.0775	0.29	0.0037	0.001	0.001	15.807	0.0000	9.71363
1vP	1020.298	8.563	1000	9.81	2650	3.049	0.0028	0.5	0.23	84.10	0.0775	0.29	0.0034	0.001	0.001	24.073	0.0000	10.39115

Table 29 RBS and Milhous for Mhlathuze Site 1 pool present-day flow

Site	Q	d	ρ	g	ρ_s	R	S	D50	D84	τ	τ_{ci}^*	τ_{ci}	τ RBS	q_c	$q_{critical}$	ω̂	RBS_o	β
D84																		
1pP	0.000	0.600	1000	9.81	2650	0.000	0.0070	0.5	0.9	0.00	0.0298	0.43	ERR	0.003	0.004	4.200	0.0010	0.00000
1pP	0.311	0.821	1000	9.81	2650	0.448	0.0067	0.5	0.9	29.49	0.0298	0.43	0.0147	0.003	0.005	5.508	0.0008	3.64345
1pP	0.374	0.839	1000	9.81	2650	0.458	0.0067	0.5	0.9	30.03	0.0298	0.43	0.0145	0.003	0.005	5.607	0.0008	3.71009
1pP	0.440	0.857	1000	9.81	2650	0.468	0.0067	0.5	0.9	30.57	0.0298	0.43	0.0142	0.003	0.005	5.706	0.0008	3.77683
1pP	0.515	0.876	1000	9.81	2650	0.478	0.0066	0.5	0.9	31.10	0.0298	0.43	0.0140	0.003	0.005	5.809	0.0008	3.84238
1pP	0.597	0.894	1000	9.81	2650	0.488	0.0066	0.5	0.9	31.62	0.0298	0.43	0.0137	0.004	0.005	5.905	0.0008	3.90726
1pP	0.696	0.915	1000	9.81	2650	0.499	0.0066	0.5	0.9	32.19	0.0298	0.43	0.0135	0.004	0.005	6.017	0.0008	3.97778
1pP	0.837	0.942	1000	9.81	2650	0.514	0.0065	0.5	0.9	32.97	0.0298	0.43	0.0132	0.004	0.005	6.160	0.0008	4.07399
1pP	1.215	1.003	1000	9.81	2650	0.547	0.0065	0.5	0.9	34.63	0.0298	0.43	0.0125	0.004	0.005	6.473	0.0007	4.27916
1pP	2.591	1.164	1000	9.81	2650	0.638	0.0062	0.5	0.9	39.04	0.0298	0.43	0.0111	0.004	0.005	7.260	0.0007	4.82362
1pP	10.046	1.628	1000	9.81	2650	0.700	0.0057	0.5	0.9	38.98	0.0298	0.43	0.0111	0.004	0.006	9.241	0.0006	4.81626
1pP	69.354	3.020	1000	9.81	2650	1.405	0.0045	0.5	0.9	62.04	0.0298	0.43	0.0070	0.005	0.007	13.593	0.0005	7.66515
1pP	595.123	6.871	1000	9.81	2650	3.045	0.0031	0.5	0.9	92.57	0.0298	0.43	0.0047	0.008	0.011	21.294	0.0005	11.43836
D16																		
Site	Q	d	ρ	g	ρ_s	R	S	D50	D16	τ	τ_{ci}^*	τ_{ci}	τ RBS	q_c	$q_{critical}$	ω̂	RBS_o	β
1pP	0.000	0.600	1000	9.81	2650	0.000	0.0070	0.5	0.23	0.00	0.0775	0.29	ERR	0.000	0.000	4.200	0.0001	0.00000
1pP	0.311	0.821	1000	9.81	2650	0.448	0.0067	0.5	0.23	29.49	0.0775	0.29	0.0098	0.000	0.000	5.508	0.0001	3.64345
1pP	0.374	0.839	1000	9.81	2650	0.458	0.0067	0.5	0.23	30.03	0.0775	0.29	0.0096	0.000	0.000	5.607	0.0001	3.71009
1pP	0.440	0.857	1000	9.81	2650	0.468	0.0067	0.5	0.23	30.57	0.0775	0.29	0.0094	0.000	0.000	5.706	0.0001	3.77683
1pP	0.515	0.876	1000	9.81	2650	0.478	0.0066	0.5	0.23	31.10	0.0775	0.29	0.0093	0.000	0.000	5.809	0.0001	3.84238
1pP	0.597	0.894	1000	9.81	2650	0.488	0.0066	0.5	0.23	31.62	0.0775	0.29	0.0091	0.000	0.000	5.905	0.0001	3.90726
1pP	0.696	0.915	1000	9.81	2650	0.499	0.0066	0.5	0.23	32.19	0.0775	0.29	0.0090	0.000	0.000	6.017	0.0001	3.97778
1pP	0.837	0.942	1000	9.81	2650	0.514	0.0065	0.5	0.23	32.97	0.0775	0.29	0.0088	0.000	0.000	6.160	0.0001	4.07399
1pP	1.215	1.003	1000	9.81	2650	0.547	0.0065	0.5	0.23	34.63	0.0775	0.29	0.0083	0.000	0.000	6.473	0.0000	4.27916
1pP	2.591	1.164	1000	9.81	2650	0.638	0.0062	0.5	0.23	39.04	0.0775	0.29	0.0074	0.000	0.000	7.260	0.0000	4.82362
1pP	10.046	1.628	1000	9.81	2650	0.700	0.0057	0.5	0.23	38.98	0.0775	0.29	0.0074	0.001	0.000	9.241	0.0000	4.81626
1pP	69.354	3.020	1000	9.81	2650	1.405	0.0045	0.5	0.23	62.04	0.0775	0.29	0.0047	0.001	0.000	13.593	0.0000	7.66515
1pP	595.123	6.871	1000	9.81	2650	3.045	0.0031	0.5	0.23	92.57	0.0775	0.29	0.0031	0.001	0.001	21.294	0.0000	11.43836

Table 30 RBS and Milhous for Mhlathuze Site 1 riffle virgin flow

Site	Q	d	ρ	g	$ρ_s$	R	S	D50	D84	τ	$τ_{ci}$*	$τ_{ci}$	τ RBS	q_c	$q_{critical}$	ώ	RBS_n	β
D84																		
1VC	0.000	0.000	1000	9.81	2650	0	0.0056	22	25	0.00	0.0411	16.65	ERR	0.618	0.659	0.000	ERR	0.00000
1VC	0.506	0.318	1000	9.81	2650	0.09	0.0053	22	25	4.70	0.0411	16.65	3.5399	0.653	0.696	1.694	0.4111	0.01321
1VC	0.856	0.363	1000	9.81	2650	0.12	0.0053	22	25	6.18	0.0411	16.65	2.6928	0.664	0.708	1.907	0.3711	0.01736
1VC	1.280	0.401	1000	9.81	2650	0.149	0.0052	22	25	7.58	0.0411	16.65	2.1978	0.674	0.718	2.078	0.3455	0.02128
1VC	1.787	0.435	1000	9.81	2650	0.176	0.0051	22	25	8.83	0.0411	16.65	1.8849	0.684	0.729	2.226	0.3274	0.02481
1VC	2.399	0.468	1000	9.81	2650	0.203	0.0051	22	25	10.06	0.0411	16.65	1.6557	0.694	0.739	2.363	0.3129	0.02824
1VC	3.258	0.505	1000	9.81	2650	0.234	0.0050	22	25	11.42	0.0411	16.65	1.4586	0.706	0.752	2.511	0.2995	0.03206
1VC	4.613	0.551	1000	9.81	2650	0.281	0.0049	22	25	13.44	0.0411	16.65	1.2390	0.722	0.769	2.686	0.2864	0.03774
1VC	7.604	0.624	1000	9.81	2650	0.372	0.0047	22	25	17.20	0.0411	16.65	0.9680	0.749	0.799	2.941	0.2716	0.04831
1VC	13.416	1.019	1000	9.81	2650	0.492	0.0045	22	25	21.72	0.0411	16.65	0.7665	0.789	0.841	4.586	0.1834	0.06100
1VC	29.942	1.476	1000	9.81	2650	0.82	0.0041	22	25	33.38	0.0411	16.65	0.4988	0.864	0.921	6.125	0.1504	0.09375
1VC	145.270	3.057	1000	9.81	2650	1.356	0.0034	22	25	44.68	0.0411	16.65	0.3726	1.095	1.167	10.269	0.1137	0.12548
1VC	1020.298	7.509	1000	9.81	2650	4.096	0.0025	22	25	99.55	0.0411	16.65	0.1673	1.540	1.642	18.604	0.0882	0.27956

D16																		
Site	Q	d	ρ	g	$ρ_s$	R	S	D50	D16	τ	$τ_{ci}$*	$τ_{ci}$	τ RBS	q_c	$q_{critical}$	ώ	RBS_n	β
1VC	0.000	0.000	1000	9.81	2650	0	0.0056	22	0.4	0.00	0.7438	4.82	ERR	0.001	0.000	0.000	ERR	0.00000
1VC	0.506	0.318	1000	9.81	2650	0.09	0.0053	22	0.4	4.70	0.7438	4.82	1.0238	0.001	0.000	1.694	0.0001	0.01321
1VC	0.856	0.363	1000	9.81	2650	0.12	0.0053	22	0.4	6.18	0.7438	4.82	0.7788	0.001	0.000	1.907	0.0001	0.01736
1VC	1.280	0.401	1000	9.81	2650	0.149	0.0052	22	0.4	7.58	0.7438	4.82	0.6357	0.001	0.000	2.078	0.0001	0.02128
1VC	1.787	0.435	1000	9.81	2650	0.176	0.0051	22	0.4	8.83	0.7438	4.82	0.5452	0.001	0.000	2.226	0.0001	0.02481
1VC	2.399	0.468	1000	9.81	2650	0.203	0.0051	22	0.4	10.06	0.7438	4.82	0.4789	0.001	0.000	2.363	0.0001	0.02824
1VC	3.258	0.505	1000	9.81	2650	0.234	0.0050	22	0.4	11.42	0.7438	4.82	0.4219	0.001	0.000	2.511	0.0001	0.03206
1VC	4.613	0.551	1000	9.81	2650	0.281	0.0049	22	0.4	13.44	0.7438	4.82	0.3584	0.001	0.000	2.686	0.0001	0.03774
1VC	7.604	0.624	1000	9.81	2650	0.372	0.0047	22	0.4	17.20	0.7438	4.82	0.2800	0.002	0.000	2.941	0.0001	0.04831
1VC	13.416	1.019	1000	9.81	2650	0.492	0.0045	22	0.4	21.72	0.7438	4.82	0.2217	0.002	0.000	4.586	0.0000	0.06100
1VC	29.942	1.476	1000	9.81	2650	0.82	0.0041	22	0.4	33.38	0.7438	4.82	0.1443	0.002	0.000	6.125	0.0000	0.09375
1VC	145.270	3.057	1000	9.81	2650	1.356	0.0034	22	0.4	44.68	0.7438	4.82	0.1078	0.002	0.000	10.269	0.0000	0.12548
1VC	1020.298	7.509	1000	9.81	2650	4.096	0.0025	22	0.4	99.55	0.7438	4.82	0.0484	0.003	0.000	18.604	0.0000	0.27956

Table 31 RBS and Milhous for Mhlathuze Site 1 riffle present-day flow

Site	Q	d	ρ	g	ρ_s	R	S	D50	D84	τ	τ_{ci}^*	τ_{ci}	τ RBS	q_c	$q_{critical}$	$\acute{\omega}$	RBS_o	β
D84																		
1pC	0.000	0.000	1000	9.81	2650	0.000	0.0056	22	25	0.00	0.0411	16.65	ERR	0.618	0.659	0.000	ERR	0.00000
1pC	0.311	0.282	1000	9.81	2650	0.070	0.0054	22	25	3.70	0.0411	16.65	4.5042	0.646	0.688	1.518	0.4534	0.01038
1pC	0.374	0.295	1000	9.81	2650	0.075	0.0054	22	25	3.95	0.0411	16.65	4.2194	0.648	0.691	1.582	0.4368	0.01108
1pC	0.440	0.308	1000	9.81	2650	0.083	0.0053	22	25	4.35	0.0411	16.65	3.8261	0.651	0.694	1.646	0.4215	0.01222
1pC	0.515	0.320	1000	9.81	2650	0.091	0.0053	22	25	4.75	0.0411	16.65	3.5025	0.654	0.697	1.704	0.4089	0.01335
1pC	0.597	0.332	1000	9.81	2650	0.101	0.0053	22	25	5.26	0.0411	16.65	3.1673	0.656	0.700	1.762	0.3972	0.01476
1pC	0.696	0.345	1000	9.81	2650	0.110	0.0053	22	25	5.70	0.0411	16.65	2.9201	0.659	0.703	1.823	0.3855	0.01601
1pC	0.837	0.361	1000	9.81	2650	0.119	0.0053	22	25	6.14	0.0411	16.65	2.7136	0.663	0.707	1.898	0.3726	0.01723
1pC	1.215	0.396	1000	9.81	2650	0.145	0.0052	22	25	7.39	0.0411	16.65	2.2542	0.672	0.717	2.056	0.3485	0.02074
1pC	2.591	0.477	1000	9.81	2650	0.210	0.0050	22	25	10.37	0.0411	16.65	1.6064	0.697	0.742	2.400	0.3094	0.02911
1pC	10.046	0.668	1000	9.81	2650	0.434	0.0046	22	25	19.64	0.0411	16.65	0.8478	0.768	0.818	3.082	0.2655	0.05516
1pC	69.354	2.174	1000	9.81	2650	1.356	0.0037	22	25	49.71	0.0411	16.65	0.3350	0.972	1.036	8.124	0.1275	0.13960
1pC	595.123	5.857	1000	9.81	2650	4.097	0.0027	22	25	108.20	0.0411	16.65	0.1539	1.403	1.496	15.767	0.0949	0.30384
D16																		
Site	Q	d	ρ	g	ρ_s	R	S	D50	D16	τ	τ_{ci}^*	τ_{ci}	τ RBS	q_c	$q_{critical}$	$\acute{\omega}$	RBS_o	β
1pC	0.000	0.000	1000	9.81	2650	0.000	0.0056	22	0.4	0.00	0.7438	4.82	ERR	0.001	0.000	0.000	ERR	0.00000
1pC	0.311	0.282	1000	9.81	2650	0.070	0.0054	22	0.4	3.70	0.7438	4.82	1.3027	0.001	0.000	1.518	0.0001	0.01038
1pC	0.374	0.295	1000	9.81	2650	0.075	0.0054	22	0.4	3.95	0.7438	4.82	1.2203	0.001	0.000	1.582	0.0001	0.01108
1pC	0.440	0.308	1000	9.81	2650	0.083	0.0053	22	0.4	4.35	0.7438	4.82	1.1066	0.001	0.000	1.646	0.0001	0.01222
1pC	0.515	0.320	1000	9.81	2650	0.091	0.0053	22	0.4	4.75	0.7438	4.82	1.0130	0.001	0.000	1.704	0.0001	0.01335
1pC	0.597	0.332	1000	9.81	2650	0.101	0.0053	22	0.4	5.26	0.7438	4.82	0.9161	0.001	0.000	1.762	0.0001	0.01476
1pC	0.696	0.345	1000	9.81	2650	0.110	0.0053	22	0.4	5.70	0.7438	4.82	0.8446	0.001	0.000	1.823	0.0001	0.01601
1pC	0.837	0.361	1000	9.81	2650	0.119	0.0053	22	0.4	6.14	0.7438	4.82	0.7848	0.001	0.000	1.898	0.0001	0.01723
1pC	1.215	0.396	1000	9.81	2650	0.145	0.0052	22	0.4	7.39	0.7438	4.82	0.6520	0.001	0.000	2.056	0.0001	0.02074
1pC	2.591	0.477	1000	9.81	2650	0.210	0.0050	22	0.4	10.37	0.7438	4.82	0.4646	0.001	0.000	2.400	0.0001	0.02911
1pC	10.046	0.668	1000	9.81	2650	0.434	0.0046	22	0.4	19.64	0.7438	4.82	0.2452	0.002	0.000	3.082	0.0001	0.05516
1pC	69.354	2.174	1000	9.81	2650	1.356	0.0037	22	0.4	49.71	0.7438	4.82	0.0969	0.002	0.000	8.124	0.0000	0.13960
1pC	595.123	5.857	1000	9.81	2650	4.097	0.0027	22	0.4	108.20	0.7438	4.82	0.0445	0.003	0.000	15.767	0.0000	0.30384

Table 32 RBS and Milhous for Mhlathuze Site 2 virgin flow

Site	Q	d	ρ	g	ρ_s	R	S	D50	D84	τ	τ_{ci}^*	τ_{ci}	τ RBS	q_c	$q_{critical}$	ω	RBS_q	β
D84																		
2V	0.000	0.000	1000	9.81	2650	0	0.0017	0.65	1.4	0.00	0.0263	0.60	ERR	0.031	0.046	0.000	ERR	0.00000
2V	0.656	0.181	1000	9.81	2650	0.064	0.0018	0.65	1.4	1.12	0.0263	0.60	0.5315	0.029	0.043	0.323	0.1337	0.10659
2V	1.112	0.232	1000	9.81	2650	0.093	0.0018	0.65	1.4	1.65	0.0263	0.60	0.3610	0.029	0.043	0.420	0.1014	0.15693
2V	1.721	0.285	1000	9.81	2650	0.127	0.0018	0.65	1.4	2.28	0.0263	0.60	0.2609	0.029	0.042	0.523	0.0803	0.21710
2V	2.469	0.338	1000	9.81	2650	0.169	0.0019	0.65	1.4	3.08	0.0263	0.60	0.1937	0.028	0.041	0.627	0.0660	0.29249
2V	3.342	0.390	1000	9.81	2650	0.22	0.0019	0.65	1.4	4.05	0.0263	0.60	0.1471	0.028	0.041	0.732	0.0558	0.38518
2V	4.521	0.450	1000	9.81	2650	0.278	0.0019	0.65	1.4	5.19	0.0263	0.60	0.1149	0.027	0.040	0.856	0.0471	0.49292
2V	6.354	0.528	1000	9.81	2650	0.352	0.0019	0.65	1.4	6.67	0.0263	0.60	0.0894	0.027	0.040	1.020	0.0388	0.63394
2V	10.378	0.665	1000	9.81	2650	0.479	0.0020	0.65	1.4	9.30	0.0263	0.60	0.0641	0.026	0.038	1.317	0.0292	0.88440
2V	17.907	0.860	1000	9.81	2650	0.644	0.0020	0.65	1.4	12.90	0.0263	0.60	0.0462	0.025	0.037	1.756	0.0212	1.22612
2V	38.388	1.232	1000	9.81	2650	0.859	0.0021	0.65	1.4	18.03	0.0263	0.60	0.0331	0.024	0.035	2.636	0.0134	1.71395
2V	195.995	2.655	1000	9.81	2650	1.779	0.0024	0.65	1.4	41.38	0.0263	0.60	0.0144	0.021	0.031	6.295	0.0050	3.93259
2V	1435.327	6.781	1000	9.81	2650	5.173	0.0026	0.65	1.4	132.44	0.0263	0.60	0.0045	0.019	0.028	17.697	0.0016	12.58809
D16																		
Site	Q	d	ρ	g	ρ_s	R	S	D50	D16	τ	τ_{ci}^*	τ_{ci}	τ RBS	q_c	$q_{critical}$	ω	RBS_q	β
2V	0.000	0.000	1000	9.81	2650	0	0.0017	0.65	0.4	0.00	0.0632	0.41	ERR	0.005	0.004	0.000	ERR	0.00000
2V	0.656	0.181	1000	9.81	2650	0.064	0.0018	0.65	0.4	1.12	0.0632	0.41	0.3650	0.004	0.004	0.323	0.0109	0.10659
2V	1.112	0.232	1000	9.81	2650	0.093	0.0018	0.65	0.4	1.65	0.0632	0.41	0.2479	0.004	0.003	0.420	0.0083	0.15693
2V	1.721	0.285	1000	9.81	2650	0.127	0.0018	0.65	0.4	2.28	0.0632	0.41	0.1792	0.004	0.003	0.523	0.0066	0.21710
2V	2.469	0.338	1000	9.81	2650	0.169	0.0019	0.65	0.4	3.08	0.0632	0.41	0.1330	0.004	0.003	0.627	0.0054	0.29249
2V	3.342	0.390	1000	9.81	2650	0.22	0.0019	0.65	0.4	4.05	0.0632	0.41	0.1010	0.004	0.003	0.732	0.0046	0.38518
2V	4.521	0.450	1000	9.81	2650	0.278	0.0019	0.65	0.4	5.19	0.0632	0.41	0.0789	0.004	0.003	0.856	0.0038	0.49292
2V	6.354	0.528	1000	9.81	2650	0.352	0.0019	0.65	0.4	6.67	0.0632	0.41	0.0614	0.004	0.003	1.020	0.0032	0.63394
2V	10.378	0.665	1000	9.81	2650	0.479	0.0020	0.65	0.4	9.30	0.0632	0.41	0.0440	0.004	0.003	1.317	0.0024	0.88440
2V	17.907	0.860	1000	9.81	2650	0.644	0.0020	0.65	0.4	12.90	0.0632	0.41	0.0317	0.004	0.003	1.756	0.0017	1.22612
2V	38.388	1.232	1000	9.81	2650	0.859	0.0021	0.65	0.4	18.03	0.0632	0.41	0.0227	0.004	0.003	2.636	0.0011	1.71395
2V	195.995	2.655	1000	9.81	2650	1.779	0.0024	0.65	0.4	41.38	0.0632	0.41	0.0099	0.003	0.003	6.295	0.0004	3.93259
2V	1435.327	6.781	1000	9.81	2650	5.173	0.0026	0.65	0.4	132.44	0.0632	0.41	0.0031	0.003	0.002	17.697	0.0001	12.58809

Table 33 RBS and Milhous for Mhlathuze Site 2 present-day flow

Site	Q	d	ρ	g	ρ_s	R	S	D50	D84	τ	τ_{ci}^*	τ_{ci}	τ RBS	q_c	$q_{critical}$	$\tilde{\omega}$	RBS_q	β
D84																		
2P	0.000	0.000	1000	9.81	2650	0	0.0017	0.65	1.4	0.00	0.0263	0.60	ERR	0.031	0.046	0.000	ERR	0.00000
2P	0.353	0.135	1000	9.81	2650	0.044	0.0018	0.65	1.4	0.76	0.0263	0.60	0.7825	0.030	0.044	0.238	0.1839	0.07239
2P	0.455	0.153	1000	9.81	2650	0.051	0.0018	0.65	1.4	0.89	0.0263	0.60	0.6720	0.030	0.044	0.271	0.1607	0.08429
2P	0.605	0.174	1000	9.81	2650	0.066	0.0018	0.65	1.4	1.15	0.0263	0.60	0.5163	0.030	0.043	0.310	0.1396	0.10972
2P	0.831	0.203	1000	9.81	2650	0.082	0.0018	0.65	1.4	1.44	0.0263	0.60	0.4125	0.029	0.043	0.365	0.1178	0.13732
2P	1.115	0.233	1000	9.81	2650	0.094	0.0018	0.65	1.4	1.67	0.0263	0.60	0.3571	0.029	0.043	0.422	0.1010	0.15862
2P	1.514	0.269	1000	9.81	2650	0.118	0.0018	0.65	1.4	2.11	0.0263	0.60	0.2820	0.029	0.042	0.491	0.0858	0.20090
2P	2.135	0.316	1000	9.81	2650	0.148	0.0018	0.65	1.4	2.68	0.0263	0.60	0.2223	0.028	0.042	0.584	0.0713	0.25482
2P	3.522	0.400	1000	9.81	2650	0.229	0.0019	0.65	1.4	4.23	0.0263	0.60	0.1410	0.028	0.041	0.753	0.0542	0.40178
2P	6.775	0.544	1000	9.81	2650	0.367	0.0019	0.65	1.4	6.98	0.0263	0.60	0.0854	0.027	0.039	1.054	0.0374	0.66300
2P	20.166	0.910	1000	9.81	2650	0.687	0.0021	0.65	1.4	13.86	0.0263	0.60	0.0430	0.025	0.037	1.871	0.0197	1.31724
2P	136.895	2.242	1000	9.81	2650	1.528	0.0023	0.65	1.4	34.78	0.0263	0.60	0.0171	0.022	0.032	5.202	0.0062	3.30540
2P	1094.274	5.968	1000	9.81	2650	4.497	0.0026	0.65	1.4	113.95	0.0263	0.60	0.0052	0.019	0.029	15.416	0.0019	10.83076
D16																		
Site	Q	d	ρ	g	ρ_s	R	S	D50	D16	τ	τ_{ci}^*	τ_{ci}	τ RBS	q_c	$q_{critical}$	$\tilde{\omega}$	RBS_q	β
2P	0.000	0.000	1000	9.81	2650	0	0.0017	0.65	0.4	0.00	0.0632	0.41	ERR	0.005	0.004	0.000	ERR	0.00000
2P	0.353	0.135	1000	9.81	2650	0.044	0.0018	0.65	0.4	0.76	0.0632	0.41	0.5374	0.005	0.004	0.238	0.0150	0.07239
2P	0.455	0.153	1000	9.81	2650	0.051	0.0018	0.65	0.4	0.89	0.0632	0.41	0.4615	0.005	0.004	0.271	0.0131	0.08429
2P	0.605	0.174	1000	9.81	2650	0.066	0.0018	0.65	0.4	1.15	0.0632	0.41	0.3545	0.005	0.004	0.310	0.0114	0.10972
2P	0.831	0.203	1000	9.81	2650	0.082	0.0018	0.65	0.4	1.44	0.0632	0.41	0.2833	0.004	0.004	0.365	0.0096	0.13732
2P	1.115	0.233	1000	9.81	2650	0.094	0.0018	0.65	0.4	1.67	0.0632	0.41	0.2452	0.004	0.003	0.422	0.0082	0.15862
2P	1.514	0.269	1000	9.81	2650	0.118	0.0018	0.65	0.4	2.11	0.0632	0.41	0.1936	0.004	0.003	0.491	0.0070	0.20090
2P	2.135	0.316	1000	9.81	2650	0.148	0.0018	0.65	0.4	2.68	0.0632	0.41	0.1527	0.004	0.003	0.584	0.0058	0.25482
2P	3.522	0.400	1000	9.81	2650	0.229	0.0019	0.65	0.4	4.23	0.0632	0.41	0.0968	0.004	0.003	0.753	0.0044	0.40178
2P	6.775	0.544	1000	9.81	2650	0.367	0.0019	0.65	0.4	6.98	0.0632	0.41	0.0587	0.004	0.003	1.054	0.0031	0.66300
2P	20.166	0.910	1000	9.81	2650	0.687	0.0021	0.65	0.4	13.86	0.0632	0.41	0.0295	0.004	0.003	1.871	0.0016	1.31724
2P	136.895	2.242	1000	9.81	2650	1.528	0.0023	0.65	0.4	34.78	0.0632	0.41	0.0118	0.003	0.003	5.202	0.0005	3.30540
2P	1094.274	5.968	1000	9.81	2650	4.497	0.0026	0.65	0.4	113.95	0.0632	0.41	0.0036	0.003	0.002	15.416	0.0002	10.83076

Table 34 RBS and Milhous for Mhlathuze Site 3 virgin flow

Site	Q	d	ρ	g	ρ_s	R	S	D50	D84	τ	τ_{ci}^*	τ_{ci}	τ RBS	q_c	$q_{critical}$	$\tilde{\omega}$	RBS_n	β
D84																		
3V	0.000	0.000	1000	9.81	2650	0	0.0007	0.68	1.8	0.00	0.0228	0.66	ERR	0.123	0.199	0.000	ERR	0.00000
3V	0.932	0.327	1000	9.81	2650	0.0788	0.0007	0.68	1.8	0.55	0.0228	0.66	1.2001	0.120	0.195	0.234	0.8329	0.05021
3V	1.491	0.398	1000	9.81	2650	0.0143	0.0007	0.68	1.8	0.10	0.0228	0.66	6.5807	0.119	0.194	0.286	0.6772	0.00916
3V	2.211	0.468	1000	9.81	2650	0.199	0.0007	0.68	1.8	1.41	0.0228	0.66	0.4706	0.118	0.193	0.338	0.5700	0.12806
3V	3.095	0.539	1000	9.81	2650	0.232	0.0007	0.68	1.8	1.65	0.0228	0.66	0.4017	0.118	0.192	0.391	0.4900	0.15000
3V	4.112	0.606	1000	9.81	2650	0.297	0.0007	0.68	1.8	2.12	0.0228	0.66	0.3124	0.117	0.191	0.442	0.4317	0.19288
3V	5.424	0.680	1000	9.81	2650	0.369	0.0007	0.68	1.8	2.65	0.0228	0.66	0.2503	0.117	0.190	0.498	0.3809	0.24078
3V	7.479	0.777	1000	9.81	2650	0.462	0.0007	0.68	1.8	3.34	0.0228	0.66	0.1987	0.116	0.188	0.572	0.3291	0.30327
3V	12.236	0.953	1000	9.81	2650	0.629	0.0007	0.68	1.8	4.59	0.0228	0.66	0.1445	0.114	0.186	0.709	0.2626	0.41712
3V	21.375	1.201	1000	9.81	2650	0.817	0.0008	0.68	1.8	6.04	0.0228	0.66	0.1098	0.113	0.184	0.905	0.2027	0.54885
3V	48.661	1.690	1000	9.81	2650	1.207	0.0008	0.68	1.8	9.12	0.0228	0.66	0.0728	0.110	0.179	1.301	0.1378	0.82818
3V	245.495	3.307	1000	9.81	2650	1.588	0.0008	0.68	1.8	12.52	0.0228	0.66	0.0530	0.105	0.171	2.658	0.0643	1.13760
3V	1736.416	7.449	1000	9.81	2650	4.569	0.0008	0.68	1.8	37.52	0.0228	0.66	0.0177	0.100	0.163	6.236	0.0262	3.40883
D16																		
Site	Q	d	ρ	g	ρ_s	R	S	D50	D16	τ	τ_{ci}^*	τ_{ci}	τ RBS	q_c	$q_{critical}$	$\tilde{\omega}$	RBS_n	β
3V	0.000	0.000	1000	9.81	2650	0	0.0007	0.68	0.36	0.00	0.0702	0.41	ERR	0.011	0.008	0.000	ERR	0.00000
3V	0.932	0.327	1000	9.81	2650	0.0788	0.0007	0.68	0.36	0.55	0.0702	0.41	0.7405	0.011	0.008	0.234	0.0333	0.05021
3V	1.491	0.398	1000	9.81	2650	0.0143	0.0007	0.68	0.36	0.10	0.0702	0.41	4.0605	0.011	0.008	0.286	0.0271	0.00916
3V	2.211	0.468	1000	9.81	2650	0.199	0.0007	0.68	0.36	1.41	0.0702	0.41	0.2904	0.011	0.008	0.338	0.0228	0.12806
3V	3.095	0.539	1000	9.81	2650	0.232	0.0007	0.68	0.36	1.65	0.0702	0.41	0.2479	0.011	0.008	0.391	0.0196	0.15000
3V	4.112	0.606	1000	9.81	2650	0.297	0.0007	0.68	0.36	2.12	0.0702	0.41	0.1928	0.010	0.008	0.442	0.0173	0.19288
3V	5.424	0.680	1000	9.81	2650	0.369	0.0007	0.68	0.36	2.65	0.0702	0.41	0.1544	0.010	0.008	0.498	0.0152	0.24078
3V	7.479	0.777	1000	9.81	2650	0.462	0.0007	0.68	0.36	3.34	0.0702	0.41	0.1226	0.010	0.008	0.572	0.0132	0.30327
3V	12.236	0.953	1000	9.81	2650	0.629	0.0007	0.68	0.36	4.59	0.0702	0.41	0.0891	0.010	0.007	0.709	0.0105	0.41712
3V	21.375	1.201	1000	9.81	2650	0.817	0.0008	0.68	0.36	6.04	0.0702	0.41	0.0677	0.010	0.007	0.905	0.0081	0.54885
3V	48.661	1.690	1000	9.81	2650	1.207	0.0008	0.68	0.36	9.12	0.0702	0.41	0.0449	0.010	0.007	1.301	0.0055	0.82818
3V	245.495	3.307	1000	9.81	2650	1.588	0.0008	0.68	0.36	12.52	0.0702	0.41	0.0327	0.009	0.007	2.658	0.0026	1.13760
3V	1736.416	7.449	1000	9.81	2650	4.569	0.0008	0.68	0.36	37.52	0.0702	0.41	0.0109	0.009	0.007	6.236	0.0010	3.40883

Table 35 RBS and Milhous for Mhlathuze Site 3 present-day flow

Site	Q	d	ρ	g	ρ_s	R	S	D50	D84	τ	τ_{ci}^*	τ_{ci}	τ RBS	q_c	$q_{critical}$	ώ	RBS_n	β
D84																		
3V	0.000	0.000	1000	9.81	2650	0	0.0007	0.68	1.8	0.00	0.0228	0.66	ERR	0.123	0.199	0.000	ERR	0.00000
3V	0.932	0.327	1000	9.81	2650	0.0788	0.0007	0.68	1.8	0.55	0.0228	0.66	1.2001	0.120	0.195	0.234	0.8329	0.05021
3V	1.491	0.398	1000	9.81	2650	0.0143	0.0007	0.68	1.8	0.10	0.0228	0.66	6.5807	0.119	0.194	0.286	0.6772	0.00916
3V	2.211	0.468	1000	9.81	2650	0.199	0.0007	0.68	1.8	1.41	0.0228	0.66	0.4706	0.118	0.193	0.338	0.5700	0.12806
3V	3.095	0.539	1000	9.81	2650	0.232	0.0007	0.68	1.8	1.65	0.0228	0.66	0.4017	0.118	0.192	0.391	0.4900	0.15000
3V	4.112	0.606	1000	9.81	2650	0.297	0.0007	0.68	1.8	2.12	0.0228	0.66	0.3124	0.117	0.191	0.442	0.4317	0.19288
3V	5.424	0.680	1000	9.81	2650	0.369	0.0007	0.68	1.8	2.65	0.0228	0.66	0.2503	0.117	0.190	0.498	0.3809	0.24078
3V	7.479	0.777	1000	9.81	2650	0.462	0.0007	0.68	1.8	3.34	0.0228	0.66	0.1987	0.116	0.188	0.572	0.3291	0.30327
3V	12.236	0.953	1000	9.81	2650	0.629	0.0007	0.68	1.8	4.59	0.0228	0.66	0.1445	0.114	0.186	0.709	0.2626	0.41712
3V	21.375	1.201	1000	9.81	2650	0.817	0.0008	0.68	1.8	6.04	0.0228	0.66	0.1098	0.113	0.184	0.905	0.2027	0.54885
3V	48.661	1.690	1000	9.81	2650	1.207	0.0008	0.68	1.8	9.12	0.0228	0.66	0.0728	0.110	0.179	1.301	0.1378	0.82818
3V	245.495	3.307	1000	9.81	2650	1.588	0.0008	0.68	1.8	12.52	0.0228	0.66	0.0530	0.105	0.171	2.658	0.0643	1.13760
3V	1736.416	7.449	1000	9.81	2650	4.569	0.0008	0.68	1.8	37.52	0.0228	0.66	0.0177	0.100	0.163	6.236	0.0262	3.40883
D16																		
Site	Q	d	ρ	g	ρ_s	R	S	D50	D16	τ	τ_{ci}^*	τ_{ci}	τ RBS	q_c	$q_{critical}$	ώ	RBS_n	β
3V	0.000	0.000	1000	9.81	2650	0	0.0007	0.68	0.36	0.00	0.0702	0.41	ERR	0.011	0.008	0.000	ERR	0.00000
3V	0.932	0.327	1000	9.81	2650	0.0788	0.0007	0.68	0.36	0.55	0.0702	0.41	0.7405	0.011	0.008	0.234	0.0333	0.05021
3V	1.491	0.398	1000	9.81	2650	0.0143	0.0007	0.68	0.36	0.10	0.0702	0.41	4.0605	0.011	0.008	0.286	0.0271	0.00916
3V	2.211	0.468	1000	9.81	2650	0.199	0.0007	0.68	0.36	1.41	0.0702	0.41	0.2904	0.011	0.008	0.338	0.0228	0.12806
3V	3.095	0.539	1000	9.81	2650	0.232	0.0007	0.68	0.36	1.65	0.0702	0.41	0.2479	0.011	0.008	0.391	0.0196	0.15000
3V	4.112	0.606	1000	9.81	2650	0.297	0.0007	0.68	0.36	2.12	0.0702	0.41	0.1928	0.010	0.008	0.442	0.0173	0.19288
3V	5.424	0.680	1000	9.81	2650	0.369	0.0007	0.68	0.36	2.65	0.0702	0.41	0.1544	0.010	0.008	0.498	0.0152	0.24078
3V	7.479	0.777	1000	9.81	2650	0.462	0.0007	0.68	0.36	3.34	0.0702	0.41	0.1226	0.010	0.008	0.572	0.0132	0.30327
3V	12.236	0.953	1000	9.81	2650	0.629	0.0007	0.68	0.36	4.59	0.0702	0.41	0.0891	0.010	0.007	0.709	0.0105	0.41712
3V	21.375	1.201	1000	9.81	2650	0.817	0.0008	0.68	0.36	6.04	0.0702	0.41	0.0677	0.010	0.007	0.905	0.0081	0.54885
3V	48.661	1.690	1000	9.81	2650	1.207	0.0008	0.68	0.36	9.12	0.0702	0.41	0.0449	0.010	0.007	1.301	0.0055	0.82818
3V	245.495	3.307	1000	9.81	2650	1.588	0.0008	0.68	0.36	12.52	0.0702	0.41	0.0327	0.009	0.007	2.658	0.0026	1.13760
3V	1736.416	7.449	1000	9.81	2650	4.569	0.0008	0.68	0.36	37.52	0.0702	0.41	0.0109	0.009	0.007	6.236	0.0010	3.40883

Table 36 RBS and Milhous for Mhlathuze Site 4 virgin flow

Site	Q	d	ρ	g	ρ_s	R	S	D50	D84	τ	τ_{ci}*	τ_{ci}	τ RBS	q_c	$q_{critical}$	ῶ	RBS_n	β
D84																		
4v	0.000	0.310	1000	9.81	2650	0.119	0.0009	0.88	1.6	1.05	0.0296	0.77	0.7299	0.078	0.105	0.279	0.3746	0.07376
4v	1.510	0.607	1000	9.81	2650	0.217	0.0009	0.88	1.6	1.87	0.0296	0.77	0.4103	0.080	0.107	0.533	0.2016	0.13123
4v	2.275	0.670	1000	9.81	2650	0.276	0.0009	0.88	1.6	2.37	0.0296	0.77	0.3242	0.080	0.108	0.585	0.1845	0.16609
4v	3.154	0.729	1000	9.81	2650	0.331	0.0009	0.88	1.6	2.82	0.0296	0.77	0.2715	0.081	0.109	0.634	0.1712	0.19829
4v	4.201	0.789	1000	9.81	2650	0.386	0.0009	0.88	1.6	3.28	0.0296	0.77	0.2339	0.081	0.109	0.683	0.1597	0.23021
4v	5.373	0.847	1000	9.81	2650	0.438	0.0009	0.88	1.6	3.71	0.0296	0.77	0.2070	0.081	0.110	0.730	0.1501	0.26013
4v	6.820	0.911	1000	9.81	2650	0.496	0.0009	0.88	1.6	4.18	0.0296	0.77	0.1836	0.082	0.110	0.782	0.1409	0.29329
4v	9.110	0.997	1000	9.81	2650	0.572	0.0009	0.88	1.6	4.79	0.0296	0.77	0.1601	0.082	0.111	0.851	0.1303	0.33628
4v	14.170	1.155	1000	9.81	2650	0.685	0.0008	0.88	1.6	5.68	0.0296	0.77	0.1350	0.083	0.112	0.976	0.1148	0.39878
4v	23.653	1.383	1000	9.81	2650	0.783	0.0008	0.88	1.6	6.41	0.0296	0.77	0.1196	0.084	0.114	1.154	0.0985	0.45004
4v	53.078	1.876	1000	9.81	2650	1.158	0.0008	0.88	1.6	9.27	0.0296	0.77	0.0828	0.087	0.117	1.530	0.0763	0.65054
4v	263.205	3.617	1000	9.81	2650	1.452	0.0008	0.88	1.6	11.06	0.0296	0.77	0.0694	0.091	0.123	2.808	0.0439	0.77627
4v	1849.764	8.531	1000	9.81	2650	3.448	0.0007	0.88	1.6	24.95	0.0296	0.77	0.0307	0.097	0.131	6.294	0.0207	1.75185

D16

Site	Q	d	ρ	g	ρ_s	R	S	D50	D16	τ	τ_{ci}*	τ_{ci}	τ RBS	q_c	$q_{critical}$	ῶ	RBS_n	β
4v	0.000	0.310	1000	9.81	2650	0.119	0.0009	0.88	0.38	1.05	0.0810	0.50	0.4742	0.009	0.006	0.279	0.0211	0.07376
4v	1.510	0.607	1000	9.81	2650	0.217	0.0009	0.88	0.38	1.87	0.0810	0.50	0.2665	0.009	0.006	0.533	0.0114	0.13123
4v	2.275	0.670	1000	9.81	2650	0.276	0.0009	0.88	0.38	2.37	0.0810	0.50	0.2106	0.009	0.006	0.585	0.0104	0.16609
4v	3.154	0.729	1000	9.81	2650	0.331	0.0009	0.88	0.38	2.82	0.0810	0.50	0.1764	0.009	0.006	0.634	0.0097	0.19829
4v	4.201	0.789	1000	9.81	2650	0.386	0.0009	0.88	0.38	3.28	0.0810	0.50	0.1519	0.009	0.006	0.683	0.0090	0.23021
4v	5.373	0.847	1000	9.81	2650	0.438	0.0009	0.88	0.38	3.71	0.0810	0.50	0.1345	0.009	0.006	0.730	0.0085	0.26013
4v	6.820	0.911	1000	9.81	2650	0.496	0.0009	0.88	0.38	4.18	0.0810	0.50	0.1193	0.009	0.006	0.782	0.0079	0.29329
4v	9.110	0.997	1000	9.81	2650	0.572	0.0009	0.88	0.38	4.79	0.0810	0.50	0.1040	0.010	0.006	0.851	0.0073	0.33628
4v	14.170	1.155	1000	9.81	2650	0.685	0.0008	0.88	0.38	5.68	0.0810	0.50	0.0877	0.010	0.006	0.976	0.0065	0.39878
4v	23.653	1.383	1000	9.81	2650	0.783	0.0008	0.88	0.38	6.41	0.0810	0.50	0.0777	0.010	0.006	1.154	0.0056	0.45004
4v	53.078	1.876	1000	9.81	2650	1.158	0.0008	0.88	0.38	9.27	0.0810	0.50	0.0538	0.010	0.007	1.530	0.0043	0.65054
4v	263.205	3.617	1000	9.81	2650	1.452	0.0008	0.88	0.38	11.06	0.0810	0.50	0.0451	0.011	0.007	2.808	0.0025	0.77627
4v	1849.764	8.531	1000	9.81	2650	3.448	0.0007	0.88	0.38	24.95	0.0810	0.50	0.0200	0.011	0.007	6.294	0.0012	1.75185

Table 37 RBS and Milhous for Mhlathuze Site 4 present-day flow

Site	Q	d	ρ	g	ρ_s	R	S	D50	D84	τ	τ_{ci}*	τ_{ci}	τ RBS	q_c	$q_{critical}$	ω	RBS_n	β
D84																		
4p	0.000	0.310	1000	9.81	2650	0.119	0.0009	0.88	1.6	1.05	0.0296	0.77	0.7299	0.078	0.105	0.279	0.3746	0.07376
4p	0.657	0.511	1000	9.81	2650	0.127	0.0009	0.88	1.6	1.10	0.0296	0.77	0.6955	0.079	0.106	0.452	0.2355	0.07741
4p	0.973	0.552	1000	9.81	2650	0.164	0.0009	0.88	1.6	1.42	0.0296	0.77	0.5404	0.079	0.107	0.487	0.2196	0.09962
4p	1.392	0.596	1000	9.81	2650	0.206	0.0009	0.88	1.6	1.78	0.0296	0.77	0.4318	0.080	0.107	0.524	0.2049	0.12469
4p	1.870	0.638	1000	9.81	2650	0.246	0.0009	0.88	1.6	2.11	0.0296	0.77	0.3628	0.080	0.108	0.559	0.1928	0.14840
4p	2.418	0.680	1000	9.81	2650	0.285	0.0009	0.88	1.6	2.44	0.0296	0.77	0.3142	0.080	0.108	0.594	0.1821	0.17137
4p	3.138	0.728	1000	9.81	2650	0.33	0.0009	0.88	1.6	2.82	0.0296	0.77	0.2723	0.081	0.109	0.633	0.1714	0.19771
4p	4.211	0.789	1000	9.81	2650	0.386	0.0009	0.88	1.6	3.28	0.0296	0.77	0.2339	0.081	0.109	0.683	0.1597	0.23020
4p	6.698	0.906	1000	9.81	2650	0.491	0.0009	0.88	1.6	4.14	0.0296	0.77	0.1854	0.082	0.110	0.778	0.1415	0.29043
4p	12.757	1.115	1000	9.81	2650	0.661	0.0008	0.88	1.6	5.49	0.0296	0.77	0.1396	0.083	0.112	0.945	0.1183	0.38575
4p	35.156	1.602	1000	9.81	2650	0.952	0.0008	0.88	1.6	7.71	0.0296	0.77	0.0995	0.085	0.115	1.323	0.0870	0.54127
4p	202.479	3.236	1000	9.81	2650	1.381	0.0008	0.88	1.6	10.60	0.0296	0.77	0.0723	0.091	0.122	2.532	0.0483	0.74428
4p	1530.548	7.835	1000	9.81	2650	3.451	0.0007	0.88	1.6	25.08	0.0296	0.77	0.0306	0.096	0.130	5.804	0.0224	1.76047
Site	Q	d	ρ	g	ρ_s	R	S	D50	D16	τ	τ_{ci}*	τ_{ci}	τ RBS	q_c	$q_{critical}$	ω	RBS_n	β
D16																		
4p	0.000	0.310	1000	9.81	2650	0.119	0.0009	0.88	0.38	1.05	0.0810	0.50	0.4742	0.009	0.006	0.279	0.0211	0.07376
4p	0.657	0.511	1000	9.81	2650	0.127	0.0009	0.88	0.38	1.10	0.0810	0.50	0.4519	0.009	0.006	0.452	0.0133	0.07741
4p	0.973	0.552	1000	9.81	2650	0.164	0.0009	0.88	0.38	1.42	0.0810	0.50	0.3511	0.009	0.006	0.487	0.0124	0.09962
4p	1.392	0.596	1000	9.81	2650	0.206	0.0009	0.88	0.38	1.78	0.0810	0.50	0.2805	0.009	0.006	0.524	0.0116	0.12469
4p	1.870	0.638	1000	9.81	2650	0.246	0.0009	0.88	0.38	2.11	0.0810	0.50	0.2357	0.009	0.006	0.559	0.0109	0.14840
4p	2.418	0.680	1000	9.81	2650	0.285	0.0009	0.88	0.38	2.44	0.0810	0.50	0.2041	0.009	0.006	0.594	0.0103	0.17137
4p	3.138	0.728	1000	9.81	2650	0.33	0.0009	0.88	0.38	2.82	0.0810	0.50	0.1769	0.009	0.006	0.633	0.0097	0.19771
4p	4.211	0.789	1000	9.81	2650	0.386	0.0009	0.88	0.38	3.28	0.0810	0.50	0.1519	0.009	0.006	0.683	0.0090	0.23020
4p	6.698	0.906	1000	9.81	2650	0.491	0.0009	0.88	0.38	4.14	0.0810	0.50	0.1204	0.009	0.006	0.778	0.0080	0.29043
4p	12.757	1.115	1000	9.81	2650	0.661	0.0008	0.88	0.38	5.49	0.0810	0.50	0.0907	0.010	0.006	0.945	0.0067	0.38575
4p	35.156	1.602	1000	9.81	2650	0.952	0.0008	0.88	0.38	7.71	0.0810	0.50	0.0646	0.010	0.006	1.323	0.0049	0.54127
4p	202.479	3.236	1000	9.81	2650	1.381	0.0008	0.88	0.38	10.60	0.0810	0.50	0.0470	0.010	0.007	2.532	0.0027	0.74428
4p	1530.548	7.835	1000	9.81	2650	3.451	0.0007	0.88	0.38	25.08	0.0810	0.50	0.0199	0.011	0.007	5.804	0.0013	1.76047

Table 38 RBS and Milhous for Olifants Site 1

Site	Q	d	ρ	g	ρ_s	R	S	D50	D84	τ	τ_{ci}^*	τ_{ci}	τ RBS	q_c	$q_{critical}$	ω	RBS_q	β
D84																		
1	0.047	0.165	1000	9.81	2650	0.076	0.0126	96	277	9.40	0.0214	96.09	10.2244	9.183	15.599	2.075	7.5166	0.00605
1	0.259	0.264	1000	9.81	2650	0.1	0.0124	96	277	12.12	0.0214	96.09	7.9269	9.390	15.951	3.264	4.8871	0.00780
1	0.336	0.284	1000	9.81	2650	0.11	0.0123	96	277	13.27	0.0214	96.09	7.2404	9.440	16.036	3.491	4.5928	0.00854
1	0.448	0.307	1000	9.81	2650	0.12	0.0122	96	277	14.39	0.0214	96.09	6.6764	9.503	16.142	3.759	4.2946	0.00926
1	0.663	0.343	1000	9.81	2650	0.136	0.0121	96	277	16.16	0.0214	96.09	5.9468	9.604	16.314	4.150	3.9306	0.01040
1	1.086	0.393	1000	9.81	2650	0.16	0.0119	96	277	18.74	0.0214	96.09	5.1286	9.761	16.581	4.690	3.5355	0.01206
1	1.897	0.459	1000	9.81	2650	0.19	0.0117	96	277	21.80	0.0214	96.09	4.4089	9.990	16.969	5.362	3.1648	0.01403
1	3.504	0.543	1000	9.81	2650	0.268	0.0114	96	277	29.86	0.0214	96.09	3.2178	10.320	17.530	6.173	2.8397	0.01922
1	7.364	0.668	1000	9.81	2650	0.318	0.0108	96	277	33.84	0.0214	96.09	2.8393	10.864	18.455	7.243	2.5480	0.02178
1	15.013	0.813	1000	9.81	2650	0.41	0.0102	96	277	41.22	0.0214	96.09	2.3315	11.581	19.672	8.334	2.3606	0.02652
1	32.792	1.010	1000	9.81	2650	0.542	0.0095	96	277	50.36	0.0214	96.09	1.9081	12.648	21.485	9.564	2.2465	0.03241
1	110.682	2.007	1000	9.81	2650	0.916	0.0081	96	277	72.91	0.0214	96.09	1.3179	15.042	25.551	16.288	1.5687	0.04692
1	361.246	3.287	1000	9.81	2650	1.86	0.0068	96	277	124.28	0.0214	96.09	0.7732	18.300	31.085	22.391	1.3883	0.07998
D16																		
Site	Q	d	ρ	g	ρ_s	R	S	D50	D16	τ	τ_{ci}^*	τ_{ci}	τ RBS	q_c	$q_{critical}$	ω	RBS_q	β
1	0.047	0.165	1000	9.81	2650	0.076	0.0126	96	21	9.40	0.1304	44.32	4.7158	0.192	0.090	2.075	0.0432	0.00605
1	0.259	0.264	1000	9.81	2650	0.1	0.0124	96	21	12.12	0.1304	44.32	3.6562	0.196	0.092	3.264	0.0281	0.00780
1	0.336	0.284	1000	9.81	2650	0.11	0.0123	96	21	13.27	0.1304	44.32	3.3395	0.197	0.092	3.491	0.0264	0.00854
1	0.448	0.307	1000	9.81	2650	0.12	0.0122	96	21	14.39	0.1304	44.32	3.0794	0.198	0.093	3.759	0.0247	0.00926
1	0.663	0.343	1000	9.81	2650	0.136	0.0121	96	21	16.16	0.1304	44.32	2.7429	0.200	0.094	4.150	0.0226	0.01040
1	1.086	0.393	1000	9.81	2650	0.16	0.0119	96	21	18.74	0.1304	44.32	2.3655	0.204	0.095	4.690	0.0203	0.01206
1	1.897	0.459	1000	9.81	2650	0.19	0.0117	96	21	21.80	0.1304	44.32	2.0335	0.209	0.098	5.362	0.0182	0.01403
1	3.504	0.543	1000	9.81	2650	0.268	0.0114	96	21	29.86	0.1304	44.32	1.4842	0.215	0.101	6.173	0.0163	0.01922
1	7.364	0.668	1000	9.81	2650	0.318	0.0108	96	21	33.84	0.1304	44.32	1.3096	0.227	0.106	7.243	0.0146	0.02178
1	15.013	0.813	1000	9.81	2650	0.41	0.0102	96	21	41.22	0.1304	44.32	1.0753	0.242	0.113	8.334	0.0136	0.02652
1	32.792	1.010	1000	9.81	2650	0.542	0.0095	96	21	50.36	0.1304	44.32	0.8801	0.264	0.123	9.564	0.0129	0.03241
1	110.682	2.007	1000	9.81	2650	0.916	0.0081	96	21	72.91	0.1304	44.32	0.6079	0.314	0.147	16.288	0.0090	0.04692
1	361.246	3.287	1000	9.81	2650	1.86	0.0068	96	21	124.28	0.1304	44.32	0.3566	0.382	0.179	22.391	0.0080	0.07998

Table 39 RBS and Milhous for Olifants Site 2

Site	Q	d	ρ	g	ρ_s	R	S	D50	D84	τ	τ_{ci}^*	τ_{ci}	τ RBS	q_c	$q_{critical}$	ώ	RBS_n	β
D84																		
2	0.518	0.305	1000	9.81	2650	0.151	0.0143	220	520	21.13	0.0246	207.43	9.8173	20.568	31.622	4.355	7.2612	0.00593
2	1.547	0.434	1000	9.81	2650	0.219	0.0138	220	520	29.62	0.0246	207.43	7.0032	21.367	32.850	5.978	5.4952	0.00832
2	2.105	0.479	1000	9.81	2650	0.248	0.0136	220	520	33.11	0.0246	207.43	6.2644	21.677	33.327	6.514	5.1164	0.00930
2	2.794	0.524	1000	9.81	2650	0.277	0.0134	220	520	36.49	0.0246	207.43	5.6842	22.005	33.831	7.038	4.8070	0.01025
2	3.877	0.582	1000	9.81	2650	0.312	0.0132	220	520	40.39	0.0246	207.43	5.1359	22.442	34.502	7.681	4.4918	0.01134
2	5.771	0.661	1000	9.81	2650	0.36	0.0129	220	520	45.47	0.0246	207.43	4.5618	23.068	35.465	8.514	4.1653	0.01277
2	9.109	0.766	1000	9.81	2650	0.417	0.0125	220	520	50.96	0.0246	207.43	4.0706	23.937	36.802	9.536	3.8594	0.01431
2	15	0.897	1000	9.81	2650	0.495	0.0119	220	520	57.99	0.0246	207.43	3.5767	25.094	38.580	10.711	3.6019	0.01629
2	26.747	1.081	1000	9.81	2650	0.603	0.0113	220	520	66.61	0.0246	207.43	3.1140	26.803	41.207	12.175	3.3845	0.01871
2	47.229	1.297	1000	9.81	2650	0.739	0.0105	220	520	76.35	0.0246	207.43	2.7167	28.889	44.414	13.665	3.2503	0.02144
2	94.574	1.621	1000	9.81	2650	0.897	0.0096	220	520	84.40	0.0246	207.43	2.4576	32.079	49.318	15.547	3.1721	0.02370
2	278.456	2.651	1000	9.81	2650	1.294	0.0081	220	520	103.34	0.0246	207.43	2.0073	38.547	59.263	21.582	2.7459	0.02902
2	721.615	4.156	1000	9.81	2650	1.453	0.0070	220	520	99.86	0.0246	207.43	2.0771	45.605	70.114	29.114	2.4083	0.02804
D16																		
Site	Q	d	ρ	g	ρ_s	R	S	D50	D16	τ	τ_{ci}^*	τ_{ci}	τ RBS	q_c	$q_{critical}$	ώ	RBS_n	β
2	0.518	0.305	1000	9.81	2650	0.151	0.0143	220	5	21.13	0.6363	51.49	2.4371	0.019	0.003	4.355	0.0007	0.00593
2	1.547	0.434	1000	9.81	2650	0.219	0.0138	220	5	29.62	0.6363	51.49	1.7385	0.020	0.003	5.978	0.0005	0.00832
2	2.105	0.479	1000	9.81	2650	0.248	0.0136	220	5	33.11	0.6363	51.49	1.5551	0.020	0.003	6.514	0.0005	0.00930
2	2.794	0.524	1000	9.81	2650	0.277	0.0134	220	5	36.49	0.6363	51.49	1.4111	0.021	0.003	7.038	0.0004	0.01025
2	3.877	0.582	1000	9.81	2650	0.312	0.0132	220	5	40.39	0.6363	51.49	1.2750	0.021	0.003	7.681	0.0004	0.01134
2	5.771	0.661	1000	9.81	2650	0.36	0.0129	220	5	45.47	0.6363	51.49	1.1325	0.022	0.003	8.514	0.0004	0.01277
2	9.109	0.766	1000	9.81	2650	0.417	0.0125	220	5	50.96	0.6363	51.49	1.0105	0.023	0.003	9.536	0.0004	0.01431
2	14.927	0.897	1000	9.81	2650	0.495	0.0119	220	5	57.99	0.6363	51.49	0.8879	0.024	0.004	10.711	0.0003	0.01629
2	26.747	1.081	1000	9.81	2650	0.603	0.0113	220	5	66.61	0.6363	51.49	0.7730	0.025	0.004	12.175	0.0003	0.01871
2	47.229	1.297	1000	9.81	2650	0.739	0.0105	220	5	76.35	0.6363	51.49	0.6744	0.027	0.004	13.665	0.0003	0.02144
2	94.574	1.621	1000	9.81	2650	0.897	0.0096	220	5	84.40	0.6363	51.49	0.6101	0.030	0.005	15.547	0.0003	0.02370
2	278.456	2.651	1000	9.81	2650	1.294	0.0081	220	5	103.34	0.6363	51.49	0.4983	0.036	0.005	21.582	0.0003	0.02902
2	721.615	4.156	1000	9.81	2650	1.453	0.0070	220	5	99.86	0.6363	51.49	0.5156	0.043	0.006	29.114	0.0002	0.02804

Table 40 RBS and Milhous for Olifants Site 3

Site	Q	d	ρ	g	ρ_s	R	S	D50	D84	τ	τ_{ci}^*	τ_{ci}	τ RBS	q_c	$q_{critical}$	ω	RBS_n	β
D84																		
3	0.068	0.364	1000	9.81	2650	0.22	0.0055	250	480	11.79	0.0285	221.46	18.7917	52.819	73.188	2.011	36.3961	0.00291
3	0.22	0.391	1000	9.81	2650	0.23	0.0055	250	480	12.66	0.0285	221.46	17.4890	52.653	72.958	2.163	33.7253	0.00313
3	0.292	0.400	1000	9.81	2650	0.24	0.0055	250	480	12.99	0.0285	221.46	17.0463	52.598	72.882	2.218	32.8616	0.00321
3	0.368	0.409	1000	9.81	2650	0.24	0.0055	250	480	13.29	0.0285	221.46	16.6648	52.547	72.812	2.269	32.0847	0.00328
3	0.467	0.420	1000	9.81	2650	0.25	0.0056	250	480	13.62	0.0285	221.46	16.2650	52.490	72.732	2.330	31.2158	0.00336
3	0.639	0.436	1000	9.81	2650	0.26	0.0056	250	480	14.14	0.0285	221.46	15.6613	52.405	72.614	2.423	29.9647	0.00349
3	0.993	0.464	1000	9.81	2650	0.28	0.0056	250	480	15.04	0.0285	221.46	14.7231	52.265	72.421	2.586	28.0033	0.00372
3	2	0.510	1000	9.81	2650	0.30	0.0056	250	480	16.49	0.0285	221.46	13.4292	52.056	72.131	2.852	25.2924	0.00408
3	3.381	0.592	1000	9.81	2650	0.30	0.0056	250	480	16.71	0.0285	221.46	13.2495	51.727	71.675	3.327	21.5445	0.00413
3	6.808	0.715	1000	9.81	2650	0.40	0.0057	250	480	22.00	0.0285	221.46	10.0649	51.305	71.090	4.051	17.5473	0.00544
3	15.399	0.936	1000	9.81	2650	0.55	0.0057	250	480	30.79	0.0285	221.46	7.1934	50.704	70.257	5.362	13.1031	0.00761
3	52.411	1.534	1000	9.81	2650	0.94	0.0058	250	480	53.59	0.0285	221.46	4.1322	49.630	68.769	8.950	7.6837	0.01324
3	186.472	2.785	1000	9.81	2650	1.56	0.0060	250	480	91.19	0.0285	221.46	2.4286	48.458	67.145	16.603	4.0442	0.02253
D16																		
Site	Q	d	ρ	g	ρ_s	R	S	D50	D16	τ	τ_{ci}^*	τ_{ci}	τ RBS	q_c	$q_{critical}$	ω	RBS_n	β
3	0.068	0.364	1000	9.81	2650	0.22	0.0055	250	140	11.79	0.0675	153.02	12.9847	8.320	6.226	2.011	3.0962	0.00291
3	0.22	0.391	1000	9.81	2650	0.23	0.0055	250	140	12.66	0.0675	153.02	12.0846	8.294	6.206	2.163	2.8690	0.00313
3	0.292	0.400	1000	9.81	2650	0.24	0.0055	250	140	12.99	0.0675	153.02	11.7787	8.285	6.200	2.218	2.7955	0.00321
3	0.368	0.409	1000	9.81	2650	0.24	0.0055	250	140	13.29	0.0675	153.02	11.5151	8.277	6.194	2.269	2.7294	0.00328
3	0.467	0.420	1000	9.81	2650	0.25	0.0056	250	140	13.62	0.0675	153.02	11.2388	8.268	6.187	2.330	2.6555	0.00336
3	0.639	0.436	1000	9.81	2650	0.26	0.0056	250	140	14.14	0.0675	153.02	10.8216	8.255	6.177	2.423	2.5491	0.00349
3	0.993	0.464	1000	9.81	2650	0.28	0.0056	250	140	15.04	0.0675	153.02	10.1734	8.233	6.161	2.586	2.3822	0.00372
3	2	0.510	1000	9.81	2650	0.30	0.0056	250	140	16.49	0.0675	153.02	9.2793	8.200	6.136	2.852	2.1516	0.00408
3	3.381	0.592	1000	9.81	2650	0.30	0.0056	250	140	16.71	0.0675	153.02	9.1551	8.148	6.097	3.327	1.8328	0.00413
3	6.808	0.715	1000	9.81	2650	0.40	0.0057	250	140	22.00	0.0675	153.02	6.9547	8.081	6.048	4.051	1.4927	0.00544
3	15.399	0.936	1000	9.81	2650	0.55	0.0057	250	140	30.79	0.0675	153.02	4.9705	7.987	5.977	5.362	1.1147	0.00761
3	52.411	1.534	1000	9.81	2650	0.94	0.0058	250	140	53.59	0.0675	153.02	2.8552	7.818	5.850	8.950	0.6537	0.01324
3	186.472	2.785	1000	9.81	2650	1.56	0.0060	250	140	91.19	0.0675	153.02	1.6781	7.633	5.712	16.603	0.3440	0.02253

Table 41 RBS and Milhous for Olifants Site 4

Site	Q	d	ρ	g	ρ_s	R	S	D50	D84	τ	τ_{ci}^*	τ_{ci}	τ RBS	q_c	$q_{critical}$	ώ	RBS_n	β
D84																		
4	0.291	0.487	1000	9.81	2650	0.193	0.0033	320	500	6.25	0.0329	266.48	42.6502	99.918	124.898	1.607	77.7163	0.00121
4	0.834	0.641	1000	9.81	2650	0.251	0.0040	320	500	9.85	0.0329	266.48	27.0557	80.551	100.689	2.564	39.2704	0.00190
4	1.111	0.691	1000	9.81	2650	0.291	0.0045	320	500	12.85	0.0329	266.48	20.7437	70.596	88.246	3.110	28.3793	0.00248
4	1.421	0.737	1000	9.81	2650	0.326	0.0046	320	500	14.71	0.0329	266.48	18.1141	68.880	86.100	3.390	25.3967	0.00284
4	1.812	0.785	1000	9.81	2650	0.362	0.0047	320	500	16.69	0.0329	266.48	15.9656	67.241	84.051	3.690	22.7810	0.00322
4	2.371	0.843	1000	9.81	2650	0.397	0.0049	320	500	19.08	0.0329	266.48	13.9639	64.174	80.218	4.131	19.4199	0.00368
4	3.286	0.918	1000	9.81	2650	0.445	0.0051	320	500	22.26	0.0329	266.48	11.9691	61.362	76.703	4.682	16.3832	0.00430
4	5	1.027	1000	9.81	2650	0.457	0.0054	320	500	24.21	0.0329	266.48	11.0073	57.557	71.947	5.546	12.9732	0.00467
4	9.294	1.204	1000	9.81	2650	0.459	0.0060	320	500	27.02	0.0329	266.48	9.8634	51.151	63.938	7.224	8.8508	0.00522
4	17.391	1.464	1000	9.81	2650	0.551	0.0060	320	500	32.43	0.0329	266.48	8.2166	51.151	63.938	8.784	7.2790	0.00626
4	37.601	2.016	1000	9.81	2650	0.942	0.0060	320	500	55.45	0.0329	266.48	4.8061	51.151	63.938	12.096	5.2859	0.01070
4	121.635	3.284	1000	9.81	2650	1.462	0.0075	320	500	107.57	0.0329	266.48	2.4773	39.839	49.799	24.630	2.0219	0.02077
4	379.494	5.279	1000	9.81	2650	2.802	0.0104	320	500	285.87	0.0329	266.48	0.9322	27.625	34.531	54.902	0.6290	0.05519
D16																		
Site	Q	d	ρ	g	ρ_s	R	S	D50	D16	τ	τ_{ci}^*	τ_{ci}	τ RBS	q_c	$q_{critical}$	ώ	RBS_n	β
4	0.291	0.487	1000	9.81	2650	0.193	0.0033	320	90	6.25	0.1094	159.31	25.4978	7.631	4.047	1.607	2.5180	0.00121
4	0.834	0.641	1000	9.81	2650	0.251	0.0040	320	90	9.85	0.1094	159.31	16.1749	6.152	3.262	2.564	1.2724	0.00190
4	1.111	0.691	1000	9.81	2650	0.291	0.0045	320	90	12.85	0.1094	159.31	12.4013	5.391	2.859	3.110	0.9195	0.00248
4	1.421	0.737	1000	9.81	2650	0.326	0.0046	320	90	14.71	0.1094	159.31	10.8293	5.260	2.790	3.390	0.8229	0.00284
4	1.812	0.785	1000	9.81	2650	0.362	0.0047	320	90	16.69	0.1094	159.31	9.5448	5.135	2.723	3.690	0.7381	0.00322
4	2.371	0.843	1000	9.81	2650	0.397	0.0049	320	90	19.08	0.1094	159.31	8.3481	4.901	2.599	4.131	0.6292	0.00368
4	3.286	0.918	1000	9.81	2650	0.445	0.0051	320	90	22.26	0.1094	159.31	7.1556	4.686	2.485	4.682	0.5308	0.00430
4	5	1.027	1000	9.81	2650	0.457	0.0054	320	90	24.21	0.1094	159.31	6.5806	4.396	2.331	5.546	0.4203	0.00467
4	9.294	1.204	1000	9.81	2650	0.459	0.0060	320	90	27.02	0.1094	159.31	5.8967	3.906	2.072	7.224	0.2868	0.00522
4	17.391	1.464	1000	9.81	2650	0.551	0.0060	320	90	32.43	0.1094	159.31	4.9121	3.906	2.072	8.784	0.2358	0.00626
4	37.601	2.016	1000	9.81	2650	0.942	0.0060	320	90	55.45	0.1094	159.31	2.8732	3.906	2.072	12.096	0.1713	0.01070
4	121.635	3.284	1000	9.81	2650	1.462	0.0075	320	90	107.57	0.1094	159.31	1.4810	3.042	1.613	24.630	0.0655	0.02077
4	379.494	5.279	1000	9.81	2650	2.802	0.0104	320	90	285.87	0.1094	159.31	0.5573	2.110	1.119	54.902	0.0204	0.05519